ISSN 2542-1565

Vol. 16 2023 No. 01

GEOGRAPHY ENVIRONMENT SUSTAINABILITY

Special issue «LARGE RIVERS HYDROLOGY AND HYDROGEOCHEMESTRY»

«The journal GEOGRAPHY, ENVIRONMENT, SUSTAINABILITY was founded in 2008 by Russian Geographical Society, the Lomonosov Moscow State University Geography Department, and the Russian Academy of Sciences Institute of Geography. Since that time the journal publishes **4 issues per year**, containing original research papers and reviews. The journal issues are open source and distributed through subscriptions, library exchanges of leading universities, and via the website through the world»

FOUNDERS OF THE JOURNAL: Russian Geographical Society, Faculty of Geography, Lomonosov Moscow State University and Institute of Geography of the Russian Academy of Sciences

The journal is published with financial support of the Russian Geographical Society.

The journal is registered in Federal service on supervision of observance of the legislation in sphere of mass communications and protection of a cultural heritage. The certificate of registration: ПИ № ФС77-67752, 2016, December 21.

PUBLISHER
Russian Geographical Society
Moscow, 109012 Russia
Novaya ploshchad, 10, korp. 2
Phone 8-800-700-18-45
E-mail: press@rgo.ru
www.rgo.ru/en

EDITORIAL OFFICE
Lomonosov Moscow State University
Moscow 119991 Russia
Leninskie Gory, 1,
Faculty of Geography, 1806a
Phone 7-495-9391552
Fax 7-495-9391552
E-mail: ges-journal@geogr.msu.ru
www.ges.rgo.ru

DESIGN
Layout designer: Tereshkin Anton
Moscow, 115088,
26 Simonovsky Val str., bldg. One
Phone: +7 (903) 108-04-44
E-mail: smile.tai@gmail.com

DOI prefix: 10.24057

Format A4 (210x297mm)

"GEOGRAPHY, ENVIRONMENT, SUSTAINABILITY" is the only original English-language journal in the field of geography and environmental sciences published in Russia. It is supposed to be an outlet from the Russian-speaking countries to Europe and an inlet from Europe to the Russian-speaking countries regarding environmental and Earth sciences, geography and sustainability. The main sections of the journal are the theory of geography and ecology, the theory of sustainable development, use of natural resources, natural resources assessment, global and regional changes of environment and climate, social-economical geography, ecological regional planning, sustainable regional development, applied aspects of geography and ecology, geoinformatics and ecological cartography, ecological problems of oil and gas sector, nature conservations, health and environment, and education for sustainable development.

OPEN ACCESS POLICY. "GEOGRAPHY, ENVIRONMENT, SUSTAINABILITY" is an open access journal. All articles are made freely available to readers immediately upon publication. Our open access policy is in accordance with the Budapest Open Access Initiative (BOAI) definition - it means that articles have free availability on the public internet, permitting any users to read, download, copy, distribute, print, search, or link to the full texts of these articles, crawl them for indexing, pass them as data to software, or use them for any other lawful purpose, without financial, legal, or technical barriers other than those inseparable from gaining access to the internet itself.

Date of publication: March 31st, 2023.

EDITORIAL BOARD

EDITORIAL OFFICE

CONTENTS

RESEARCH PAPER

SPATIOTEMPORAL TRENDS AND VARIABILITY ANALYSIS OF RAINFALL AND TEMPERATURE OVER BENIN METROPOLITAN REGION, EDO STATE, NIGERIA

Verere S. Balogun[1], Emmanuel Ekpenkhio[1*], Beauty Ebena[1]

[1]Department of Geography and Regional Planning, Faculty of Social Sciences, University of Benin, PMB 1154, Benin City, Nigeria

***Corresponding author:** aigbounited@gmail.com

Received: January 3rd, 2022 / Accepted: February 15th, 2023 / Published: March 31st, 2023

https://DOI-10.24057/2071-9388-2022-001

ABSTRACT. Rainfall and temperature are the two major climatic variables affecting humans and the environment. Hence, it is essential to study rainfall and temperature variability over urban areas. This study focused on analyzing the spatiotemporal trends and variability of rainfall and temperature over Benin metropolitan region, Nigeria. Time series analysis was used to determine temporal trends in rainfall as well as minimum and maximum atmospheric temperatures over a study period of 30 years (1990 to 2019). Analysis of variance was used to understand spatiotemporal variations of climatic elements among the spatial units (urban core, intermediate and peripheral areas). Land surface temperature (LST) and land use/land cover (LULC) classes of the study area were analyzed from Landsat TM Imagery of 2020. Results revealed a decreasing trend for rainfall and increasing trend for minimum and maximum atmospheric temperatures in all the spatial units. Rainfall distribution and temperature among the spatial units were statistically insignificant; however, significant temporal decadal variations were noticed for minimum and maximum air temperatures. This investigation provided valuable information for assessing changes in rainfall and temperature and concluded that the study area is becoming warmer; an indication of global warming and climate change.

KEYWORDS: Benin metropolitan region, climate change, rainfall, spatiotemporal, temperature, trend, variability

CITATION: Balogun V. S., Ekpenkhio E., Ebena B. (2023). Spatiotemporal Trends And Variability Analysis Of Rainfall And Temperature Over Benin Metropolitan Region, Edo State, Nigeria. Geography, Environment, Sustainability, 1(16), 6-15
https://DOI-10.24057/2071-9388-2022-001

Conflict of interests: The authors reported no potential conflict of interest.

INTRODUCTION

Climate change and variability is acknowledged today by a large part of the scientific community as a global phenomenon with diverse impacts on the environment, society and economy (Bayable et al. 2021; Wang et al. 2018; Birkmann & Mechler 2015; Tierney et al. 2013; IPCC 2007). Natural and anthropogenic factors are responsible for the devastating climate change through the emission of greenhouse gases. Infact, climate change is becoming a serious threat to sustainable development. Several studies (Niyongendak et al. 2020; Niang et al. 2014; IPCC 2014; IPCC 2007) have reported increases in the intensity and frequency of weather events. Globally, empirical data have shown that temperature has been on the rise since the late 19th century, with the last three decades been warmer than all previous decades (Hartmann et al. 2013). Per decade global temperature has been projected to increase by between 0.2 to 0.5°C, but rainfall variability differs from one region to another (IPCC 2007).

Trends in climate offer a general idea of noticeable changes within historical climatic data and throw up concerns regarding extreme weather events. The study of climate change focuses on the changes in climatic elements like rainfall and temperature, hence, the variability of these elements is of immense significance. Climatic variability across spatial and temporal dimensions are usually detected from the analysis of long-term observational data of specific climatic elements collected over an average period of not less than thirty years (Asfaw et al. 2018; Rahmstorf et al. 2017). The World Meteorological Organization (WMO 2016) considered the period 2011 to 2015 as the warmest on record since modern observations began in the late 1800s. Intergovernmental Panel on Climate Change (IPCC 2007) argued that the global climate has changed rapidly with approximately 0.7°C increase in mean temperature within the last century. But, the rate of climate change varies significantly among regions and this may be due to the varying land use/land cover types with different surface albedo, carbon cycle and evapotranspiration affecting the climate in different ways (Fatema & Chakrabart 2020; Snyder et al. 2004; Meissner et al. 2003). While temperature and rainfall may decrease over time in a given area, the trend at another locale may be the reverse (Adelekan 2011). This means that local climatic changes may not align with the overall regional or continental pattern of climate fluctuations. Consequently, the evidences and effects of climate change vary over space and time.

The effects of climate change are prominent in developing countries that are mainly dependent on climate driven economic sectors (Ongoma & Chen 2017).

Due to anthropogenic forcing, the 21st century warming will be strong in Africa (IPCC 2013). Urban spaces in developing societies are seen as hot spots to the effects of climate change due in part to the emerging industrial and commercial activities, high population density and infrastructures that are major emitters of greenhouse gases. Within this context, urban areas are expected to be significantly exposed to the impacts of climate change such as increased variability in temperature and rainfall (Dodman 2009). Additionally, IPCC (2013) stated that in most parts of sub-Sahara Africa, rainfall amount is expected to decline while rainfall variability is likely to increase. Specifically in Nigeria, the impacts of climate change will be felt in various climatic elements, especially rainfall and temperature. Therefore, it is anticipated that climate change may cause fluctuations in rainfall and temperature trends which can be intensified or weakened. Increase in temperature can cause incidents of heat waves, heat related sicknesses and even death in affected areas. Also, as the earth's temperature increases the rate of cloud formation and evapotranspiration increases and as a result, the rate of rainfall also increases (Ali-Rahmani et al. 2016). This could equally lead to a corresponding increase in the frequency of floods. Therefore, assessing the trends and variability of climatic indicators is a requirement for characterizing the features of climate change and adopting mitigation and adaptation strategies against the adverse impacts of climate change. Furthermore, there is the need to understand the past and current climatic trends in order to take up-to-date decisions in various planning processes such as producing renewable energy like solar and hydro energy as well as management of water resources. Therefore, studies for characterizing the fluctuations and trends of some climate factors are important and urgent.

There has been much recent scientific interest in climatic trends and variability. Several studies have been carried out at different spatiotemporal scales and in different parts of the world. For example, Ma (2021) studied the recent changes in temperature and precipitation of the summer and autumn seasons over Fujian Province, China and revealed an upward trend in both temperature and precipitation over a period of forty-eight years. Ekwueme & Agunwamba (2021) in examining trend analysis and variability of air temperature and rainfall in the regional river basins of southeastern Nigeria for the period 1922 to 2008 observed negative trend for rainfall in the study areas except for Owerri and Awka. For air temperature, they reported positive trend for all the study sites. Edokpa (2020) investigated variability in the long-term trends of rainfall and temperature over southern Nigeria and found no significant increasing/decreasing trend in monthly, seasonal and annual rainfall, with a decadal sequence of alternately increasing and decreasing rainfall trend. Niyongendako et al. (2020) examined trend and variability analysis of rainfall and extreme temperatures in Burundi and reported high monthly and inter-annual variability of rainfall and significant increasing trend for both minimum and maximum temperatures. Wani et al. (2017) carried out an assessment of trends and variability of rainfall and temperature for the district of Mandi in Himachal Pradesh, India and found that the annual minimum and maximum temperatures for the period of 30 years indicated an increasing trend but the amount of annual rainfall did not show any significant trend.

Other inquiries on climatic trends and variability include spatiotemporal variability and trends of rainfall and its association with Pacific Ocean sea surface temperature in west Harerge zone, eastern Ethiopia (Bayable et al. 2021); trends and variability of temperature and evaporation over the African continent: relationships with precipitation (Onyutha 2021); trends in climate variables (temperature and rainfall) and local perceptions of climate change in Lamu, Kenya (Yvonne et al. 2020); rainfall variability and trend analysis in Makurdi metropolis, Benue State, Nigeria (Aho et al. 2019); temporal and spatial variability of temperature and precipitation over East Africa from 1951 to 2010 (Ongoma & Chen 2017); descriptive analysis of rainfall and temperature trends over Akure, Nigeria (Ogunrayi et al. 2016); analysis of rainfall and temperature variability over Nigeria (Akinsanola & Ogunjobi 2014); climate variation assessment based on rainfall and temperature in Ibadan, southwestern, Nigeria (Egbinola & Amobichukwu 2013); changing rainfall and anthropogenic-induced flooding: impacts and adaptation strategies in Benin City, Nigeria (Atedhor et al. 2011) and others.

Therefore, our contribution in this study is to analyze the spatiotemporal trends and variability of rainfall and temperature from 1990 to 2019 over the Benin metropolitan region, as it is relatively the least studied area during the study period; creating a comparative dearth of current knowledge vis-a-vis other areas of the country and the world. Also, prior studies in the study area (Okhakhu 2016; Atedhor et al. 2011) did not show the trends and spatial variability of rainfall and temperature within and among the urban core, intermediate and peripheral areas respectively. Up till now, no investigation has revealed the land surface temperature and land use/land cover classes of the study area. This investigation centers on localized climate change assessment based on rainfall and temperature variations in order to understand the current climatic trends in the study area. This study will serve as a basis for current climate change mitigation and adaptation strategies in the study area. The outcome of this research will help to deepen the scientific and quantitative knowledge of climatic trends and variability and provide up-to-date empirical evidence on climate change, if any, in the study area. Thus, the specific objectives of the study were to (i) determine the temporal trends in rainfall and temperature in the spatial units, (ii) ascertain significant spatial variations in rainfall and temperature among the spatial units (iii) determine significant temporal variations in rainfall and temperature among the spatial units, and (iv) evaluate the current land surface temperature and land use/land cover classes of the study area.

MATERIALS AND METHODS

Study area

Benin metropolitan region which is made up of Oredo, Egor, Ikpoba-Okha and the urbanized parts of Ovia North-East and Uhunmwode Local Government Areas of Edo State (Balogun & Onokerhoraye 2017) is among the fastest growing ancient cities in Nigeria (Nkeki & Asikhia 2019). Benin metropolitan region is confined within Latitudes 6° 16′ and 6° 33′ N and Longitudes 5° 31′ and 5° 45′ E (Fig. 1). Its territorial coverage is approximately 1,318 km^2 with 166 km in the perimeter and situated on a fairly flat land, about 78 m above sea level (Asikhia & Nkeki 2013). Urbanization processes and other associated land use/land cover developments have partitioned the region into three major spatial units; the urban core, intermediate and peripheral areas (Nkeki & Asikhia 2019).

Benin metropolitan region is underlain by sedimentary formation of the Miocene-Pleistocene-age often referred to as the Benin formation (Odemerho 1988). It is located in the humid lowland tropical rainforest belt of Nigeria and

experiences the typical rainforest zone climate of southern Nigeria which belongs to the Af category of Koppen's climatic classification scheme. The rainy season begins in March and ends in October. The area experiences a total average of 120 rainy days annually and could reach up to 140 rainy days in some years (Ugwa et al. 2016). Rainfalls are of high intensity and usually of double maxima with a little dry spell in August (Atedhor et al. 2011). The city is well drained by two major rivers; Ikpoba river, which drains the northeast of the city, and Ogba river, which drains the southwest of the city. The vegetation is predominantly the evergreen rainforest while urban developments have drastically reduced the vegetation.

Data collection and analyses

Monthly atmospheric temperature (minimum and maximum) and rainfall data for 30 years (1990 to 2019) over the urban core, intermediate and peripheral areas of the Benin metropolitan region were obtained from the Climatic Research Unit (CRU) Global Climate Dataset website. The climatic data points and locations of climatic data extraction points are shown in Figure 2 and Table 1 respectively. Land surface temperature (LST) map and land use/land cover classes data were analyzed from Landsat TM Imagery (2020) downloaded from the United State Geological Survey (USGS) website.

Data on rainfall and atmospheric temperature for 30 years (1990 to 2019) were analyzed for temporal trends using the time series analytical technique (Terence, 2006). Analysis of variance was used to understand the spatiotemporal variations of rainfall and temperature that exists among the urban core, intermediate and peripheral areas. Other statistical parameters like the mean, range and coefficient of variation of the climatic data were also computed. All statistical analyses were carried out using SPSS version 21 and Microsoft Excel. Results of the statistical analyses of temperature and rainfall were depicted using graphical and tabular methods.

RESULTS AND DISCUSSION

Trend analysis of rainfall

Rainfall and temperature are the foremost climatic variables that influence human well-being and crops production. (Ogunrayi et al. 2016). A 30 year time series analysis of the rainfall dataset as shown in Figures 3, 4 and 5 indicated an insignificant negative (decreasing) trend at $p > 0.05$ for rainfall amounts received in the urban core, intermediate and peripheral areas. The trend of rainfall was -3.458 mm per annum ($R^2 = 0.0435$) in the urban core, -3.3689 mm per annum ($R^2 = 0.0417$) in the intermediate and -3.4617 mm per annum ($R^2 = 0.0424$) in the periphery. This result suggests that rainfall has been on the decline over the study period.

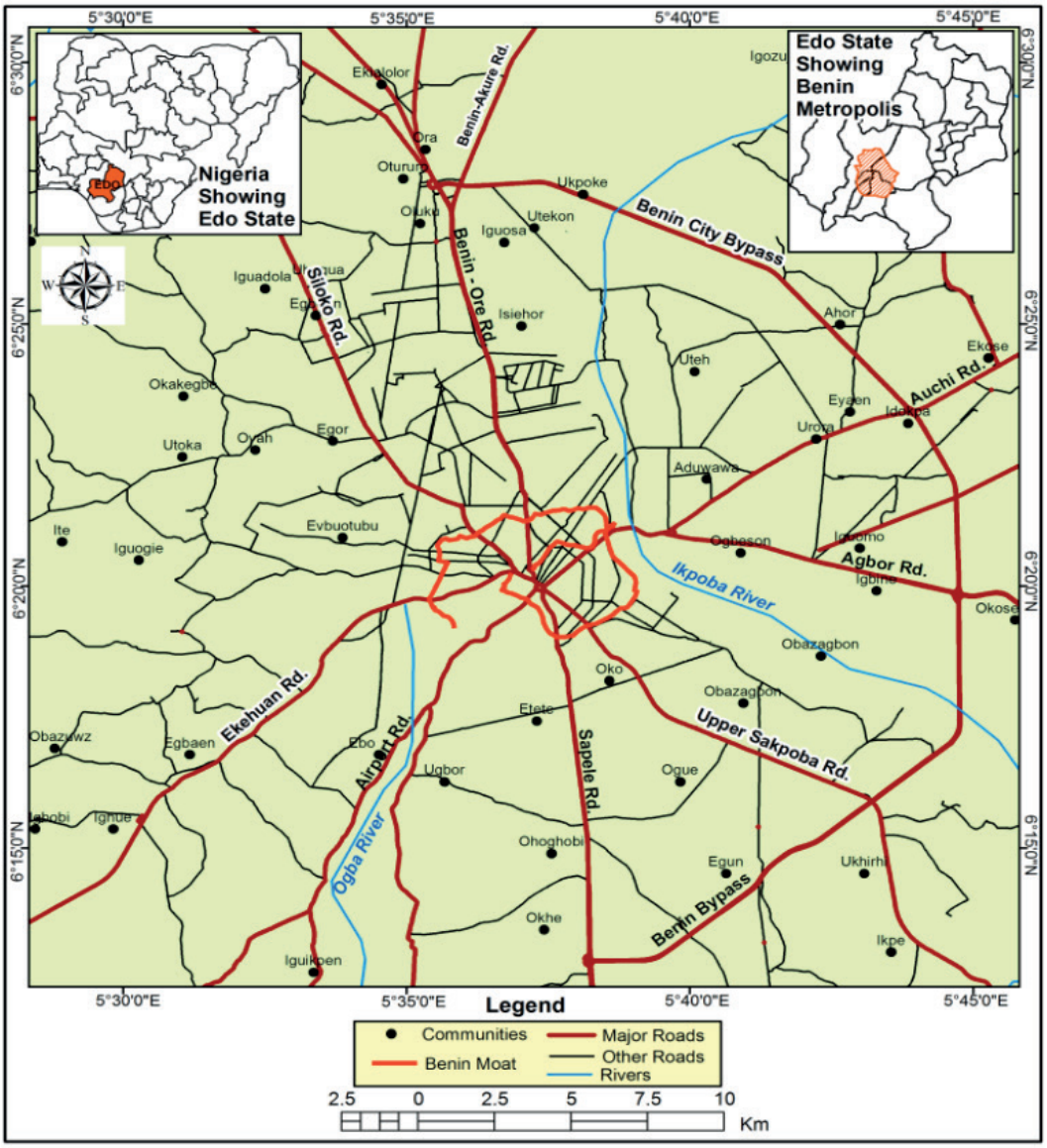

Fig. 1. Benin metropolitan region (Compiled using Google Earth Imagery, 2021)

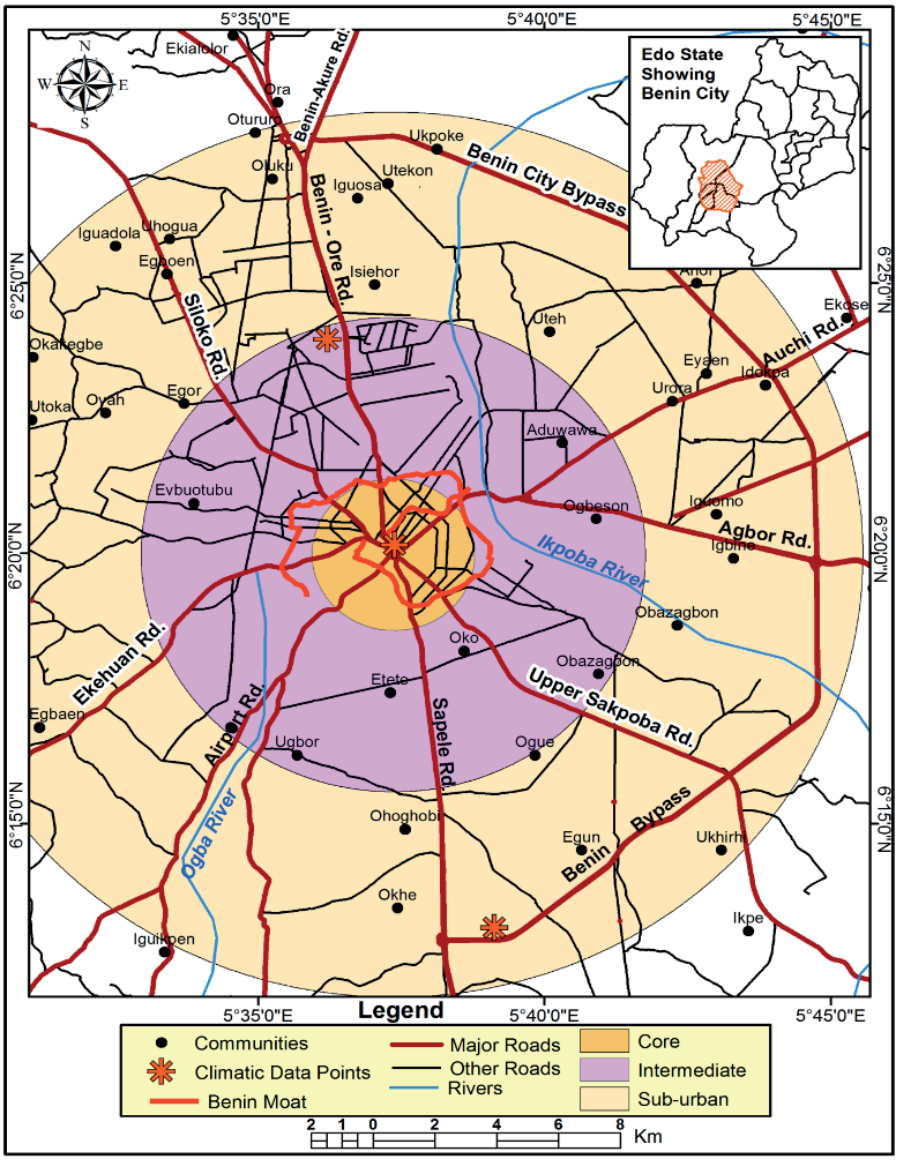

Fig. 2. Benin metropolitan region showing climatic data points (Compiled using open street map database, 2021)

Table 1. Geographical location of climatic data extraction points

S/No.	Description	Spatial unit	GPS coordinates
1	Paved surface near King's Square	Urban core	6° 20′ 9.60″ N, 5° 37′ 22.80″ E
2	Open field near Film House opposite Ekosodin road	Intermediate	6° 24′ 18.00″ N, 5° 35′ 23.99″ E
3	Bush fallow by Sapele road near Benin bye-pass	Periphery	6° 13′ 4.79″ N, 5° 39′ 7.20″ E

In the urban core, the highest rainfall amount (2338.00 mm) was recorded in 1991 and the lowest rainfall (1718.10 mm) was observed in 1993. Whereas in the intermediate area, the highest rainfall (2303.85 mm) was recorded in 1991 while the lowest rainfall (1681.2 mm) occurred in 1993. For the peripheral area, the highest rainfall (2386.3 mm) was experienced in 1991 and the lowest rainfall (1772.0 mm) occurred in 1993. From the results, the total rainfall amount during the study period was characterized by one distinct peak in 1991. This implies that 1991 was the wettest year during the period under study. Also the result shows that precipitation amounts were highest over the periphery (2386.3 mm) compared to the urban core and intermediate areas during the period under evaluation. The rainfall trend contradicts the work of Edokpa (2020) who detected no significant increasing/decreasing trend in monthly, seasonal and annual rainfall over the south-south region of Nigeria.

Trend analysis of atmospheric temperature

In analyzing the trend of minimum air temperature in the study area, Figures 6, 7 and 8 revealed an insignificant positive (increasing) trend for this climatic parameter ($p > 0.05$). In the urban core, intermediate and peripheral areas, minimum temperature was increasing at rates of 0.033°C ($R^2 = 0.588$), 0.033°C ($R^2 = 0.587$) and 0.033°C ($R^2 = 0.590$) per annum respectively. For changes in the maximum air temperature, Figures 9, 10 and 11 also indicated insignificant positive (increasing) trend at $p > 0.05$ in all the spatial units. Like minimum air temperature, maximum air temperature was increasing at rates of 0.027°C per annum ($R^2 = 0.043$) in the urban core, 0.028°C per annum ($R^2 = 0.547$) in the intermediate and 0.027°C per annum ($R^2 = 0.546$) in the periphery. This infers that the minimum and maximum air temperatures were increasing over the study period especially as there was decadal variability (Table 3). The annual average maximum temperature of the region was characterized by

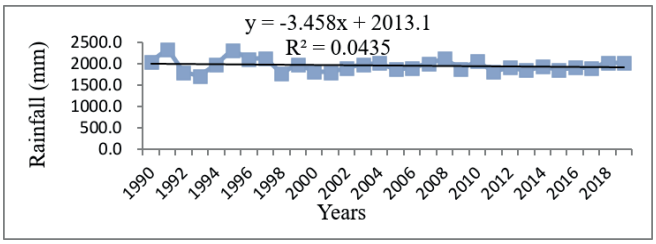

Fig. 3. Annual rainfall trend in urban core area (1990–2019)

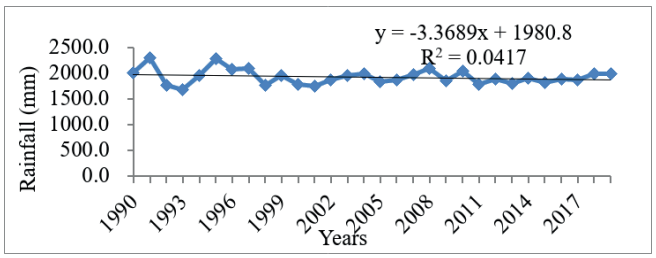

Fig. 4. Annual rainfall trend in intermediate area (1990–2019)

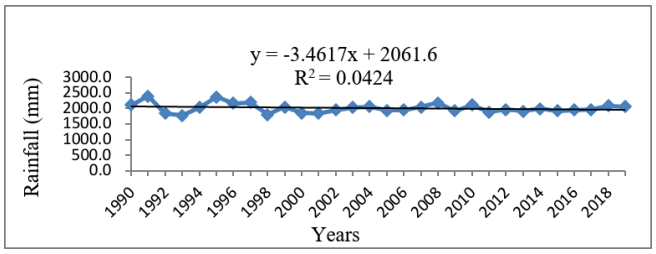

Fig. 5. Annual rainfall trend in peripheral area (1990–2019)

two distinct peaks across all spatial units (Fig. 9, 10 and 11); one in 2016 and the other in 2017. This shows that these years were the warmest years within the period under study. The overall increase in temperature may be due to the ongoing global warming, coupled with other factors such as land use and land cover changes. Generally, this connotes that there has been a surge in temperature in the study area, that is, the study area has become warmer. This warming may have negative implications on the physiological comfort and health of people in the area. The outcome on temperature trends across the study area is consistent with the findings of Ongoma & Chen (2017). Similarly, other studies (Ragatoa et al. 2018; Eresanya et al. 2018; Amadi et al. 2014) have shown a rising trend in air temperature across Nigeria.

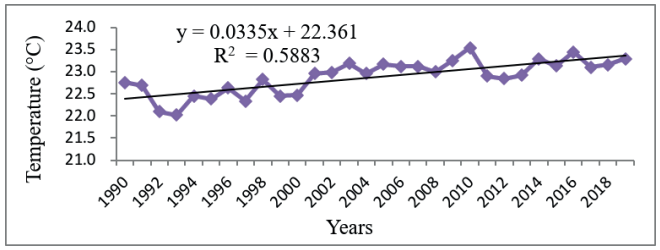

Fig. 6. Average minimum air temperature trend in urban core area (1990–2019)

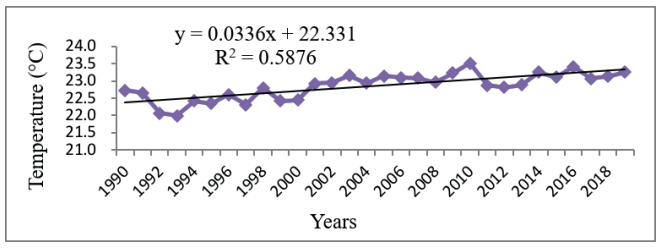

Fig. 7. Average minimum air temperature trend in intermediate area (1990–2019)

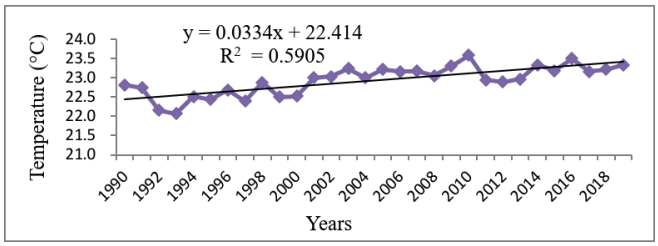

Fig. 8. Average minimum air temperature trend in peripheral area (1990–2019)

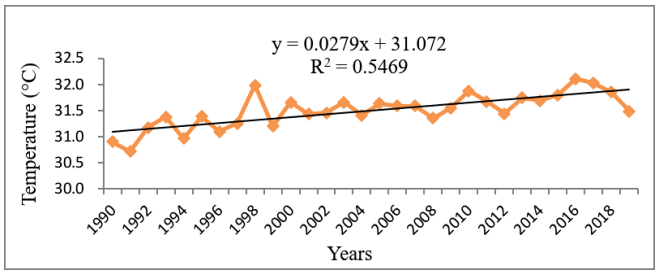

Fig. 9. Average maximum air temperature trend in urban core area (1990–2019)

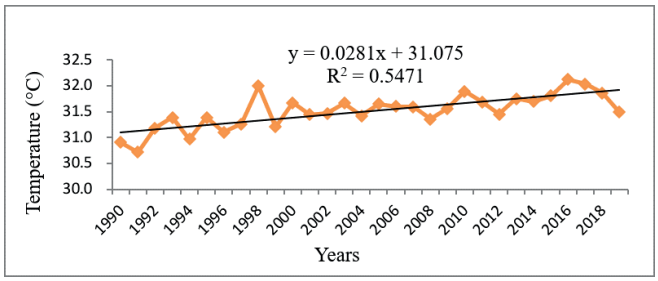

Fig. 10. Average maximum air temperature trend in intermediate area (1990–2019)

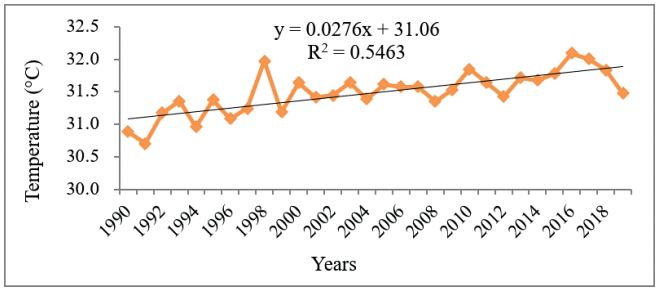

Fig. 11. Average maximum air temperature trend in peripheral area (1990–2019)

Spatiotemporal variability of rainfall and temperature

The distribution of total annual rainfall and atmospheric temperatures (minimum and maximum) of the different spatial units from 1990 to 2019 are presented in Table 2. Results indicated no marked variation of total rainfall among the urban core, intermediate and peripheral areas. This denotes that rainfall is fairly evenly distributed between the spatial units. However, the peripheral area received the greatest amount of rainfall during this period varying from 1772.03 to 2386.25 mm with mean value of 2007.97 mm over. This result differs from that of Egbinola & Amobichukwu (2013) who found that rainfall in Ibadan was highly variable. Although estimates of minimum air temperature was slightly higher in the peripheral area with values varying from 22.07 to 23.58 mm and mean value of 22.93°C, the values recorded for maximum air temperature were similar across the spatial units. The analysis of temperature data revealed non-significant variation ($p > 0.05$) among the spatial units. This implies that there were no marked changes in temperature across the spatial units that make up the Benin metropolitan region between 1990 and 2019.

Table 2. Spatial variations of climatic elements (1990–2019)

Urban core				Intermediate				Periphery				
Range	Mean	Std	CV (%)	Range	Mean	Std	CV (%)	Range	Mean	Std	CV (%)	p-value
Total annual rainfall (mm)												
1718.13 - 2337.95	1959.46	145.96	7.45	1681.19 - 2303.85	1928.53	145.20	7.53	1772.03 - 2386.25	2007.97	147.92	7.37	0.11
Annual average minimum air temperature (°C)												
22.02 - 23.53	22.88	0.38	1.68	21.99 - 23.51	22.85	0.38	1.69	22.07 - 23.58	22.93	0.38	1.67	0.71
Annual average maximum air temperature (°C)												
30.72 - 32.11	31.50	0.33	1.05	30.71 - 32.12	31.51	0.33	1.06	30.70 - 32.09	31.49	0.32	1.04	0.96

Temporal decadal variations of rainfall and temperature are presented in Table 3. The results show that there was non-significant ($p > 0.05$) decline in total rainfall amounts received in the urban core, intermediate and peripheral areas per decade. This connotes a consistent decrease in rainfall amount over the various spatial units during the period under investigation. Thus, it could be opined that the study area is becoming drier. This result is not surprising as minimum and maximum air temperatures have been on the increase over the same period (Table 3).

Atmospheric temperatures varied significantly with time for both the minimum and maximum air temperatures (Table 3). The result indicated a significant ($p < 0.05$) increase in minimum and maximum atmospheric temperatures per decade during the study period. This suggests that temperature over the study region is becoming warmer. Population boom and other associated land use/land cover changes may be attributed for the surge in minimum and maximum temperatures in the study area. The urban core area recorded decadal higher mean values for maximum air temperature compared to the intermediate and peripheral areas. Human activities and prevalence of hard, dry surfaces such as buildings, side-walks, roads, parking lots etc., in the urban core area which provide less shade and moisture than natural landscapes may have contributed to the observed higher temperatures. This finding indicates that the urban heat island phenomenon is in force in the study region as exemplified by the work of Efe & Eyefia (2014) and connotes clear evidences of global warming and climate change. This result aligns with the works of Oguntude et al. (2012), Atedhor et al. (2011) and Odjugo (2010) which reported separately clear indications of warming.

The urban heat island effect caused through urbanization processes such as reduced natural landscapes, increased industrial and commercial activities, urban material properties, metabolic heat as

Table 3. Temporal decadal variations of climatic elements from 1990–1999, 2000–2009 and 2010–2019 respectively

Climatic elements and spatial units	1990 - 1999				2000 - 2009				2010 - 2019				
	Range	Mean	Std	CV (%)	Range	Mean	Std	CV (%)	Range	Mean	Std	CV (%)	p-value
Total annual rainfall in urban core area (mm)	1718.13 - 2337.95	2020.36	213.88	10.59	1793.57 - 2121.63	1929.34	100.77	5.22	1819.49 - 2061.73	1928.68	81.04	4.20	0.27
Total annual rainfall in intermediate area (mm)	1681.19 - 2303.85	1988.44	210.54	10.59	1758.92 - 2087.37	1899.77	101.38	5.34	1784.59 - 2034.89	1897.38	85.72	4.52	0.28
Total annual rainfall in peripheral area (mm)	1772.03 - 2386.25	2069.31	218.80	10.57	1843.52 - 2178.01	1975.81	102.41	5.18	1874.36 - 2109.35	1978.80	76.63	3.87	0.28
Annual average minimum air temperature in urban core area (°C)	22.02 - 22.82	22.46	0.26	1.20	22.47 - 23.25	23.16	0.22	1.01	22.84 - 23.52	23.16	0.23	1.01	0.00*
Annual average minimum air temperature in intermediate area (°C)	21.99 - 22.79	22.43	0.26	1.20	22.44 - 23.22	22.99	0.22	0.96	22.80 - 23.51	23.13	0.23	1.01	0.00*
Annual average minimum air temperature in peripheral area (°C)	22.07 - 22.87	22.51	0.26	1.19	22.52 - 23.29	23.06	0.21	0.95	22.89 - 23.58	23.21	0.23	1.00	0.00*
Annual average maximum air temperature in urban core area (°C)	30.72 - 31.98	31.21	0.34	1.11	31.35 - 31.66	31.53	0.11	0.35	31.44 - 32.11	31.77	0.21	0.67	0.00*
Annual average maximum air temperature in intermediate area (°C)	30.72 - 31.99	31.20	0.34	1.11	31.35 - 31.66	31.53	0.11	0.36	31.44 - 32.12	31.77	0.21	0.67	0.00*
Annual average maximum air temperature in peripheral (°C)	30.70 - 31.97	31.19	0.34	1.10	31.35 - 31.64	31.52	0.10	0.35	31.42 - 32.09	31.75	0.21	0.66	0.00*

well as urban geometry have altered the urban energy balance in the Benin metropolitan region. Therefore, the thermal, hydrological and aerodynamic properties of the studied region have been altered resulting in higher local temperatures over time. Atmospheric temperatures (minimum and maximum) significantly increased per decade during the study period. This urban heat island effect has potential consequences for weather/climatic, human and environmental conditions. High atmospheric temperature may increase vulnerability to heat related morbidity and mortality (Luber & McGeehin 2008) and affect the energy demand and efficiency of the urban population. These temperature anomalies observed is an indication of warming over the study region.

Current land surface temperature and land use/land cover classes

The land surface temperature is a crucial climate variable for climate change assessment and is a tool for understanding energy balance over the earth surface (James & Mundia 2014). The current land surface temperature of Benin metropolitan region ranged from 23.02 to 33.00°C. The highest value of land surface temperature tends to concentrate along the development corridor from the urban core through the intermediate to the peripheral areas (Fig. 12). The driving factors of emerging commercial activities, high population density and increased built-up areas amongst others which are major emitters of greenhouse gases and alter the thermal, hydrological and aerodynamic properties along this corridor of development could be responsible for the high land surface temperature recorded. Thus, the development corridor can be seen as the zone of rapid urbanization. The undeveloped peripheral areas had lower land surface temperature as depicted by green and yellow shades (Fig. 12) as well as less built up areas (Fig. 13).

CONCLUSIONS

The spatiotemporal trends and variability analysis of rainfall and temperature (1990–2019) over Benin metropolitan region, Nigeria has been examined and provides valuable insights on the spatial and temporal trends of rainfall and temperature in the region. During this period, linear trend line revealed negative (decreasing) trend in total rainfall amounts in the study area and positive (increasing) trend in minimum and maximum

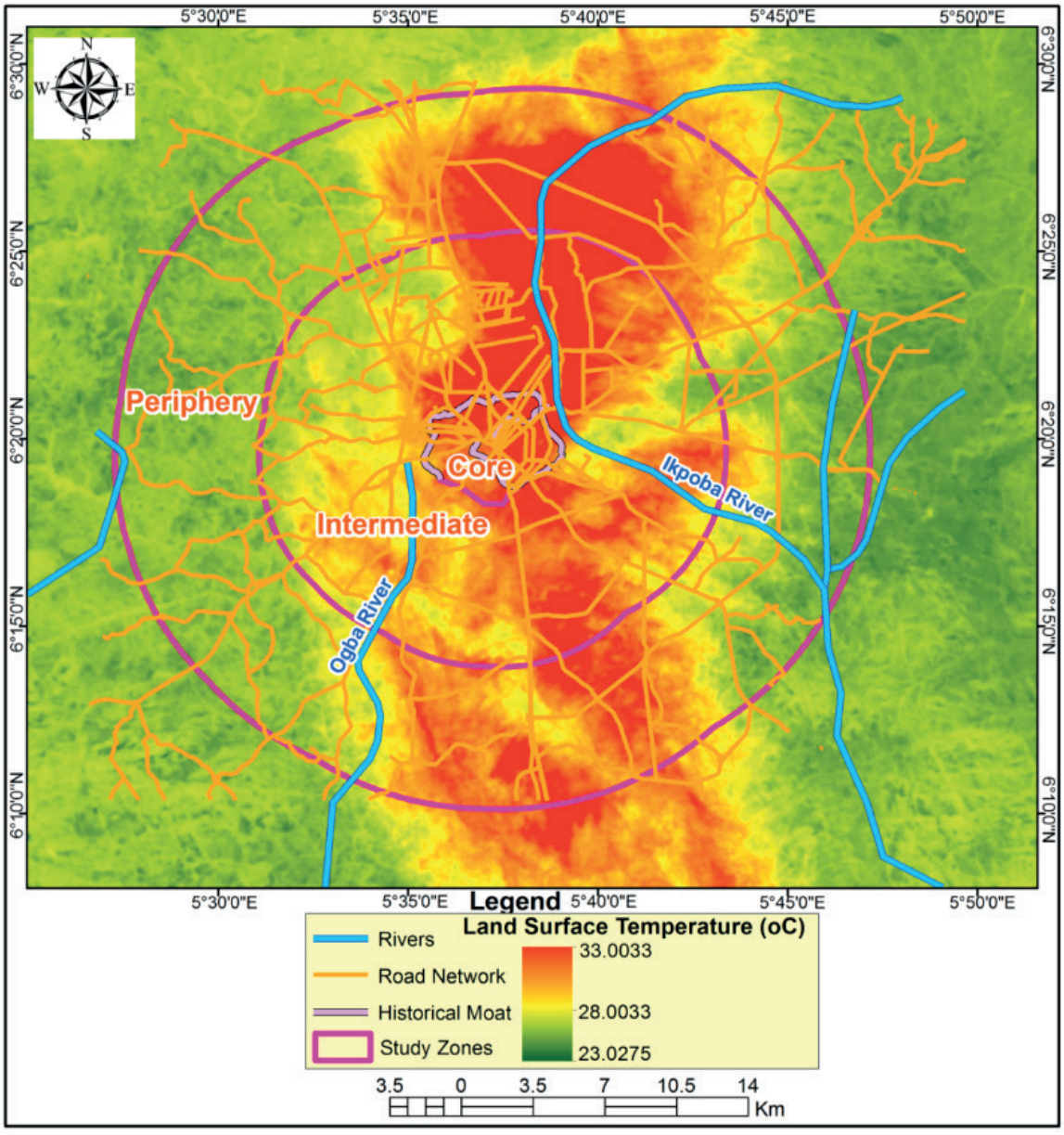

Fig. 12. Benin metropolitan region showing land surface temperature (January, 2020)
Source: Analyzed from Landsat TM Imagery, downloaded from the United State Geological Survey website

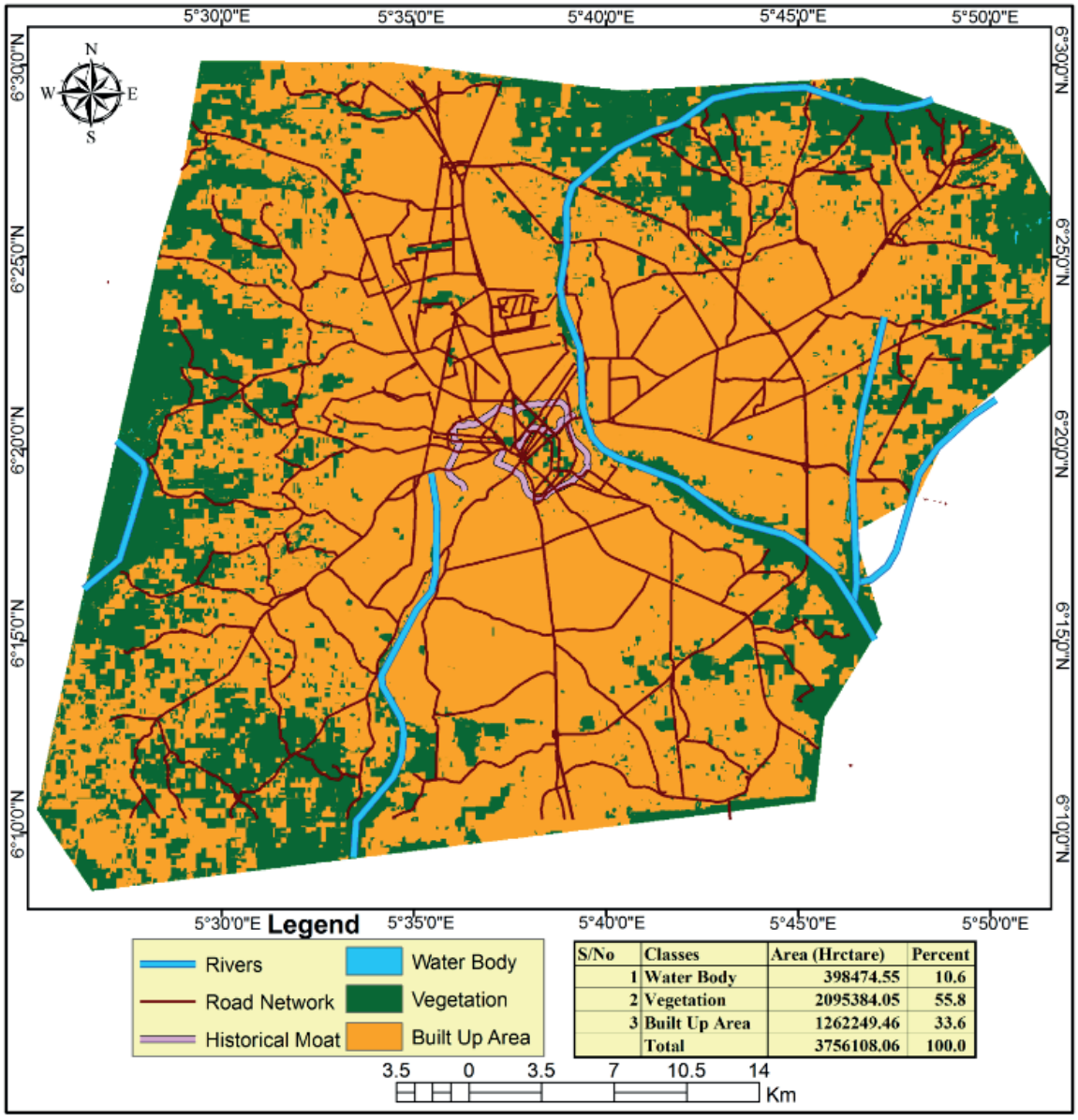

S/No	Classes	Area (Hrctare)	Percent
1	Water Body	398474.55	10.6
2	Vegetation	2095384.05	55.8
3	Built Up Area	1262249.46	33.6
	Total	3756108.06	100.0

Fig. 13. Benin metropolitan region showing land use/land cover classes (2020)
Source: Analyzed from Landsat TM Imagery, downloaded from the United State Geological Survey website

air temperatures indicating warming throughout the study period. Variability analysis showed that atmospheric temperatures significantly varied per decade across the three spatial units with a surge in mean atmospheric temperatures per decade indicating warming. Landsat TM imagery reported higher land surface temperature along the corridor of development. This indicated that global warming and climate change has occurred in the study area. Also, the significant rise in temperature could create shifts in the cropping season thereby reducing yield. It was recommended that qualitative climatic data should be made available and accessible especially from weather stations for easy analysis in order to improve climate change forecasting capacity in the study area.

REFERENCES

Adelekan I.O. (2011). Climate change, weather extremes and society: The Seventeenth Faculty Lecture, Department of Geography, University of Ibadan, 4-19.

Aho I.M., Akpen G.D. & Ojo O.O. (2019). Rainfall variability and trend analysis in Makurdi metropolis, Benue State, Nigeria. Nigerian Journal of Engineering, 26(2), 17-24.

Akinsanola A.A. & Ogunjobi K.O. (2014). Analysis of rainfall and temperature variability over Nigeria. Global Journal of Human Social Science, 14(3), 1-18.

Ali-Rahmani S.E., Brahim C. & Abdelkader B. (2016). Groundwater recharge estimation in semi-arid zone: a study case from the region of Djelfa, Algeria. Applied Water Science, 7(5), 2255-2265, DOI: 10.1007/s13201-016-0399-y.

Amadi S.O., Udo S.O. & Ewona L.O. (2014). Trends and variations of monthly mean minimum and maximum temperature data over Nigeria for the period 1950-2012, International Journal of Pure and Applied Physics, 2(4), 1-27, DOI: 10.9790/4861-07413141.

Asfaw A., Simane B., Hassen A. & Bantider A. (2018) Variability and time series trend analysis of rainfall and temperature in north central Ethiopia: a case study in Woleka sub-basin. Weather and Climate Extremes, 19, 29-41, DOI: 10.1016/j.wace.2017.12.002.

Asikhia M.O. & Nkeki F.N. (2013). Polycentric employment growth and the community behavior in Benin Metropolitan Region, Nigeria. Journal of Geography and Geology 5(2), 1-17, DOI: 10.5539/jgg.v5n2p1.

Atedhor G.O., Odjugo P.A.O. & Uriri A.E. (2011). Changing rainfall and anthropogenic-induced flooding: Impacts and adaptation strategies in Benin City, Nigeria. Journal of Geography and Regional Planning, 4(1), 42-52, DOI: 10.5897/JGRP.9000030.

Balogun T.F. & Onokerhoraye A.G. (2017). Spatio-temporal growth of Benin City, Nigeria and its implications for access to infrastructure. Journal of Geography and Geology, 9(2), 11-23, DOI: 10.5539/jgg.v9n2p11.

Bayable G., Amare G., Alemu G. & Gashaw T. (2021). Spatiotemporal variability and trends of rainfall and its association with Pacific Ocean Sea surface temperature in West Harerge Zone, Eastern Ethiopia. Environmental Systems Research, 10(7), 1-21, DOI: 10.1186/s40068-020-00216-y.

Birkmann J. & Mechler R. (2015). Advancing climate adaptation and risk management. New insights, concepts, and approaches: what have we learned from the SREX and the AR5 processes? Climatic Change, 133(1), 1-6, DOI: 10.1007/s10584-015-1515-y.

Dodman D. (2009) Blaming cities for climate change: an analysis of urban greenhouse gas emissions inventories. Environmental and Urbanization, 21(1), 85-201, DOI: 10.1177/0956247809103016.

Edokpa D.A. (2020). Variability in the long-term trends of rainfall and temperature over southern Nigeria. Journal of Geography Meteorology and Environment, 3(1), 15-41.

Efe S.I. & Eyefia O.A. (2014). Urban warming in Benin City, Nigeria. Atmospheric and Climate Sciences, 4, 241-252, DOI: 10.4236/acs.2014.42027.

Egbinola C.N. & Amobichukwu A.C. (2013). Climate variation assessment based on rainfall and temperature in Ibadan, south-western, Nigeria. Journal of Environment and Earth Science, 3(11), 32-45.

Ekwueme B.N. & Agunwamba C.J. (2021). Trend analysis and variability of air temperature and rainfall in Regional River Basins. Civil Engineering Journal, 7(5), 816-826, DOI: 10.28991/cej-2021-03091692.

Eresanya E.O., Ajayi V.O., Daramola M.T. & Balogun R. (2018) Temperature extremes over selected stations in Nigeria. Physical Science International Journal, 20(1), 1-10, DOI: 10.9734/PSIJ/2018/34637.

Fatema S. & Chakrabarty A. (2020). Land use/land cover change with impact on land surface temperature: a case study of Mkda planning area, West Bengal, India. Geography, Environment, Sustainability, 13(4), 43-53, DOI-10.24057/2071-9388-2020-62.

Hartmann D.J., Klein G., Tank A.M.G., Rusticucci M., Alexander L.V., Bronnimann S., Charabi Y.A.R., Dentener F.J., Dlugokencky E.J., Easterling D.R., Kaplan A. Soden B.J., Thorne P.W., Wild M. & Zhai P. (2013). Observations: atmosphere and surface. In: Stocker T.F., Qin D., Plattner G.K., Tignor M., Allen S.K., Boschung J., Nauels A., Xia Y., Bex V., Midgley P.M. (eds) Climate change 2013: the physical science basis. Contribution of Working Group I to the Fifth Assessment Report of the Intergovernmental Panel on Climate Change. Cambridge University Press, Cambridge, 159-254.

Intergovernmental Panel on Climate Change (IPCC) (2007). Climate Change 2007 – The Physical Science Basis Contribution of Working Group I to the Fourth Assessment Report of the IPCC. Cambridge University Press, Cambridge.

Intergovernmental Panel on Climate Change (IPCC) (2013). The physical science basis. Contribution of Working Group I to the Fifth Assessment Report of the Intergovernmental Panel on Climate Change (Stocker T.F., Qin D., Plattner G.K., Tignor M., Allen S.K., Boschung J., Nauels A., Xia Y., Bex V., Midgley P.M., Eds.). Cambridge University Press, Cambridge, United Kingdom and New York, NY, USA, 1535.

Intergovernmental Panel on Climate Change (IPCC) (2014). Climate Change (2014) the Physical Science Basis Working Group I Contribution to the Fifth Assessment Report of the Intergovernmental Panel on Climate Change. Cambridge University Press, Cambridge, UK and New York, USA.

James M.M. & Mundia C.N. (2014). Dynamism of land use changes on surface temperature in Kenya: a case study of Nairobi City. International Journal of Science and Research, 3(4), 38-41, DOI: 10.1002/ldr.702.

Luber G. & McGeehin M. (2008). Climate change and extreme heat events. American Journal of Preventive Medicine, 35(5), 429-35, DOI: 10.1016/j.amepre.2008.08.021.

Ma Z., Guo Q. Yang F. Chen H., Li W., Lin L. & Zheng C. (2021). Recent changes in temperature and precipitation of the summer and autumn seasons over Fujian Province, China. Water, 13, 1-15, DOI: 10.3390/w13141900.

Meissner K., Weaver A., Matthews H. & Cox P. (2003). The role of land surface dynamics in glacial inception: a study with the UVic earth system model. Climate Dynamics, 21, 515-537, DOI: 10.1007/s00382-003-0352-2.

Niang I., Ruppel O.C., Abdrabo M.A., Essel A., Lennard C., Padgham J. & Urquhart P. (2014). Africa. In: Barros V.R., Field C.B., Dokken D.J., Mastrandrea M.D., Mach K. J., Bilir T.E., Chatterjee M., Ebi K.L., Estrada Y.O., Genova R.C., Girma B., Kissel E.S., Levy A.N., MacCracken S., Mastrandrea P.R. & White L.L. (eds) Climate change 2014: impacts, adaptation and vulnerability. Part B: regional aspects. Contribution of Working Group II to the Fifth Assessment Report of the Intergovernmental Panel on Climate Change. Cambridge University Press, Cambridge, 1199-1265.

Niyongendako M., Lawin A.E., Manirakiza C. & Lamboni B. (2020). Trend and variability analysis of rainfall and extreme temperatures in Burundi. International Journal of Environment and Climate Change, 10(6), 36-51, DOI: 10.9734/ijecc/2020/v10i630203.

Nkeki F.N. & Asikhia M.O. (2019). Modelling the Impact of residential location preference on travel mode choice in Benin metropolitan region. Nigerian Research Journal of Engineering and Environmental Sciences, 4(1), 131-142.

Odemerho F.O. (1988). Benin City: A Case Study of Urban Flood Problems. In Sada P.O. & Odemerho F.O. (Eds). Environmental Issues and Management in Nigerian Development, Evans Brothers, Ibadan.

Odjugo P.A.O. (2010). General overview of climate change impacts in Nigeria. Journal of Human Ecology, 29(1), 47-55, DOI: 10.1080/09709274.2010.11906248.

Ogunrayi O.A., Akinseye F.M., Goldberg V. & Bernhofer C. (2016). Descriptive analysis of rainfall and temperature trends over Akure, Nigeria. Journal of Geography and Regional Planning, 9(11), 195-202, DOI: 10.5897/JGRP2016.0583.

Oguntunde P.G., Abiodun B.J., Gunnar L. (2012). Spatial and temporal temperature trends in Nigeria, 1901-2000. Meteorology and Atmospheric Physics, 118, 95-105, DOI: 10.1007/s00703-012-0199-3.

Okhakhu P.A. (2016). Assessment of the urban climate of Benin City, Nigeria. Journal of Environment and Earth Science, 6(1), 131-143.

Okoro S.P.A., Aighewi I.T. & Osagie C.O. (2000). Effects of selected monoculture plantation species on the humid tropical soils of southern Nigeria. Indian Journal of Agricultural Sciences, 70(2), 105-109.

Ongoma V. & Chen H. (2017). Temporal and spatial variability of temperature and precipitation over East Africa from 1951 to 2010. Meteorology and Atmospheric Physics, 129, 131-144, DOI: 10.1007/s00703-016-0462-0.

Onyutha C. (2021). Trends and variability of temperature and evaporation over the African continent: relationships with precipitation. Atmósfera, 34(3), 267-287, DOI: 10.20937/ATM.52788.

Ragatoa D.S., Ogunjobi K.O., Okhimamhe A.A., Francis S.D. & Adet L. (2018). A trend analysis of temperature in selected stations in Nigeria using three different approaches, Open Access Library Journal, 5, e4371, DOI: 10.4236/oalib.1104371.

Rahmstorf S., Foster G. & Cahill N. (2017). Global temperature evolution: recent trends and some pitfalls, Environmental Research Letters, 12(5), 1-7, DOI: 10.1088/1748-9326/aa6825.

Snyder P.K., Delire C. & Foley J.A. (2004). Evaluating the influence of different vegetation biomes on the global climate. Climate Dynamics, 23, 279-302, DOI: 10.1007/s00382-004-0430-0.

Terence C.M. (2006). Modelling current trends in Northern Hemisphere temperatures. International Journal of Climatology, 26(7), 867-884, DOI: 10.1002/joc.1286.

Tierney J.E., Smerdon J.E., Anchukaitis K.J., Seager R. (2013). Multidecadal variability in East African hydroclimate controlled by the Indian Ocean. Nature, 493(7432), 389-392, DOI: 10.1038/nature11785.

Ugwa I.K., Umweni A.S. & Bakare A.O. (2016). Properties and agricultural potentials of kulfo series for rubber cultivation in a humid lowland area of southwestern Nigeria. International Journal of Agriculture and Rural Development, 19(2), 2488-2795.

Wang Y., You W., Fan J., Jin M., Wei X. & Wang, Q. (2018). Effects of subsequent rainfall events with different intensities on runoff and erosion in a coarse soil. Catena, 170, 100-107, DOI:10.1016/J.CATENA.2018.06.008.

Wani J.M., Sarda V.K. Jain S.K. (2017). Assessment of trends and variability of rainfall and temperature for the district of Mandi in Himachal Pradesh, India. Slovak Journal of Civil Engineering, 25(3), 15-22, DOI: 10.1515/sjce-2017-0014

World Meteorological Organization (WMO) (2016). Hotter, drier, wetter. Face the future, Bulletin, 65(1), 64.

Yvonne M. Ouma G. Olago D. Opondo M. (2020). Trends in climate variables (temperature and rainfall) and local perceptions of climate change in Lamu, Kenya. Geography, Environment, Sustainability, 13(3), 102-109, DOI: 10.24057/2071-9388-2020-24.

RESEARCH PAPER

HOLOCENE POPULATION OF AMBROSIA ON SOUTH OF RUSSIAN FAR EAST

Valentina B. Bazarova[1*], Marina S. Lyashchevskaya[1], Ekaterina P. Kudryavtseva[1], Yana V. Piskareva[2], Yelena V. Astashenkova[2]

[1]Pacific Geographical Institute, Far Eastern Branch of the Russian Academy of Sciences, Radio St., 5, 690041, Vladivostok, Russia

[2]Institute of History, Archaeology and Ethnography of the Peoples of the Far East, Far Eastern Branch of the Russian Academy of Sciences, Pushkinskaya St., 89, 690000, Vladivostok, Russia

***Corresponding author:** bazarova@tigdvo.ru

Received: August 15th, 2022 / Accepted: February 15th, 2023 / Published: March 31st, 2023

https://DOI-10.24057/2071-9388-2022-123

ABSTRACT. *Ambrosia artemisiifolia* first appeared on the Eurasian continent in the 18th century. In the south of the Russian Far East *Ambrosia* first appeared in the middle Holocene. The presence of its pollen in the sediments on west of the lacustrine Khanka Plain is correlated with the appearance of early men. The presence of *Ambrosia* pollen in Holocene deposits can be considered as an indicator of ancient agriculture in the south of the Russian Far East. The interval from the 19th century to the 1960s is marked by a complete absence of *Ambrosia* in this region. On boundary of early Holocene and middle Holocene population of ragweed existed on eastern part of Eurasia simultaneously and independently from Northern America population. The modern isolated centre of the *Ambrosia* expansion in the south of the Russian Far East began later than the 1960s – 1970s. The modern secondary settling of this species in the east and west parts of Eurasia formed independently. The ranges of the species in China, Japan, the Korean Peninsula, and the south of the Russian Far East also formed independently.

KEYWORDS: *Ambrosia* pollen, distribution in Holocene deposits, ancient agriculture, Russian Far East

CITATION: Bazarova V. B., Lyashchevskaya M. S., Kudryavtseva E. P., Piskareva Y. V., Astashenkova Y. V. (2023). Holocene Population Of Ambrosia On South Of Russian Far East. Geography, Environment, Sustainability, 1(16), 16-25
https://DOI-10.24057/2071-9388-2022-123

ACKNOWLEDGEMENTS: This work was supported by the Ministry of Education and Science of the Russian Federation (state task # 075-01032-22-02).

Conflict of interests: The authors reported no potential conflict of interest.

INTRODUCTION

Ragweed attributed to the Asteraceae family was first described by Carl Linnaeus in the 18th century. The *Ambrosia* genus is native to the North American continent and includes 40 – 43 species (Basset and Terasmae 1962; Vascular plants … 1992; Flora of China … 2011). Although the native range of *Ambrosia artemisiifolia* is restricted to North America, it has colonized temperate regions of the world, including continental Europe, where it has greatly increased in range and abundance since the mid-20th century. It naturalized and frequently form part of the flora in almost all European countries and some countries in the East Asia. This a noxious invasive species is an important weed in agriculture and a source of highly allergenic pollen. The importance placed on *A. artemisiifolia* is reflected by the number of international projects that have now been launched by the European Commission and the increasing number of publications (Smith et al. 2013). Currently, the *Ambrosia* species is widespread globally. The *A. artemisiifolia* first appeared on the Eurasian continent in the 18th century, which is when this species was first introduced in Europe, and has been continued spreading since (Genton et al. 2005). The earliest French herbarium records of the *A. artemisiifolia* were of specimens found in botanical gardens, revealing its presence during the 18th century in at least three botanical gardens and at least five gardens during the first half of the 19th century (Chauvel et al. 2006). In 1902, ragweed invasion had already occurred in Italy (Mandrioli et al. 1998), and in 1907, it reached the Ponnonian part of Romania (Csontos et al. 2010). In Russia, the ragweed was first recorded in 1918 at the Stavropol experimental station (Mar'yushkina 1986). To date, *Ambrosia artemisiifolia* occurs throughout European Russia, reaching as far north as 60°41′ N. The species is widespread in China, Japan, the Korean Peninsula, and in the south of the Russian Far East. In Japan, this plant was introduced at the beginning of the Meiji Era in the 1860s–1870s (Kato and Ohbayashi 2008). In China, *A. artemisiifolia* was first introduced in the 1930s and has since spread from the south to the north (Qin et al. 2014; Zhou et al. 2017). On the Korean Peninsula, *Ambrosia artemisiifolia* and *A. trifida* are thought to have been introduced during the Korean War (1950–1953) when the United Nations forces led by the United States joined South Korea in the conflict (Lee and Oh 1974; Kim and Kil 2016). The first sighting of *Ambrosia* in Primorye, which is south of the Russian Far East, was published in 1966 (Pimenov et al. 1966). In that same year, this species was included in the regional flora (Voroshilov 1966). Its expansion over the Russian Far East

region over its first 20 years has been analyzed thoroughly (Nedoluzhko 1984; Aistova et al. 2014; Vinogradova et al. 2020). By the early 21st century, the species was found to have formed two large ranges on the Eurasian continent, western and eastern.

The first information on the presence of *Ambrosia* pollen in buried deposits of the southern Far East was published in the 1990s. Two cultural layers dated to the Holocene were excavated on the Khanka Plain (the first and second halves of the second millennium BC) (Verkhovskaya and Yesipenko 1993). The same species was found in the sediment of the northern coast of Talmi Lake and lagoonal deposits in Boisman Bay, south of Primorye (5.3 – 4.5 ka BP) (Verkhovskaya and Kundyshev 1993, 1995). New data concerning fossil *Ambrosia* pollen were obtained by studying the sedimentary sequences on the western coasts of Khanka Lake (south of the Russian Far East).

In this research, paleogeography- and ecology-based approaches are being used to address the questions of (a) distribution of *Ambrosia* on southern Far East of Russia in Holocene, and (b) how presence of pollen of *Ambrosia* in Holocene records correlates with Neolithic archaeological traditions. As a first step towards answering these questions we studied fossil Ambrosia pollen in Holocene records of southern Far East, and the second step we analyzed the ecological features of *Ambrosia*, and the third step we analyzed spatial and temporal appearance of Neolithic ancient agriculture on this area.

SETTING

There is a high accumulative plain in western Khanka Plain. The beds of the Melgunovka and Komissarovka rivers cut through this plain, and flow into the western part of Khanka Lake.

The climate of the Khanka Plain is under the control of two interacting atmospheric regions as the baric pressure gradient changes its direction twice a year. In the winter, westerlies are dominant, and severe frosts are common. In the summer, air masses move from the ocean to the continent. The most intense cyclonic activity occurs from June to August. The mean annual temperature varies from 3.8 °C in the west to 2.4 °C in the east of the plain, and the annual rainfall is 520 mm in the west of the region and 660 mm in the east. Note that regional winters have moderate snowfall and unstable snow cover.

The vegetation of the Khanka Plain consists of steppified open forests of mongolian oak (*Quercus mongolica Fisch*. ex *Ledeb*.), dahurian birch (*Betula dahurica* Pall.), and thickets of lespedeza and hazel associated with grass and herb steppe meadows. Meadow and mountain steppes occupy more than 30% of the area. These steppes are widespread in the western plain and are less common on the eastern coast of Khanka Lake. Oak forests with pine (*Pinus funebris* Kom.) are found in the low mountains of the northwest, including the steep coasts of Khanka Lake. The ground layer in the forests with steep slopes includes mostly steppe plant communities that are typically dominated by tansy (*Tanacetum boreale* Fisch. ex DC.). There are also communities with feather grass (*Stipa baicalensis* Roshev.) and those consisting of grass, sedges, and herbs. Sagebrush occurs in several plant communities. The southern and eastern coasts of Khanka Lake, as well as river floodplains, host meadows overgrown with small-reed (*Calamagrostis*), sedge- and herb-reed meadows, and grass swamps. The mountain margins of the lake catchment, particularly in the east, are covered with coniferous broadleaf forests of Korean pine (*Pinus koraiensis* Siebold et Zucc.) (Kurentsova 1962; Kolesnikov 1969).

An approximate assessment shows, that currently the *Ambrosia artemisiifolia* occupies more than 300,000 hectares in Primorye, including fields occupied by soybeans (223 thousand hectares), different levels roadsides, vegetable gardens, and settlement wastelands. During the last 12 – 15 years, some arable lands were neglected, and associations with *Artemisia, Sonchus*, and *Cirsium* (Asteraceae family) have occupied these places. *Ambrosia artemisiifolia* absents in these associations. Meanwhile, in freshly ploughed fields, this species primarily dominates in the first two years, whereas in old abandoned arable land, the species disappears in 2–3 years.

MATERIALS AND METHODS

To address the research goals, newly obtained palynological and radiocarbon data from the Holocene floodplains, beach ridge deposits, and deposits of archaeological sites were examined. The new data regarding fossil *Ambrosia* pollen were obtained by studying the sedimentary sequences on the western coasts of Khanka Lake (south of the Russian Far East). Further, the data obtained by previous researchers were also employed (Fig. 1).

Subfossil pollen assemblages were recovered from superficial samples taken from genetically different materials (silt, soil, sand, and moss). Samples 1 – 3, 6 – 7, 10 – 13, and 15 were taken from the eastern part of the Khanka Plain, and samples 4 – 5, 8 – 9, and 14 – from western part (Fig. 2). The samples were collected in June of 2004, which is before the common ragweed flowering. This species begins to bloom in the second half of July, and its seeds mature in mid-September. Deposits on the studied sections were presented with floodplain loams and sands, soils, and lacustrine sands.

Pollen analysis. The sampling technique involved cleaning the wall of the section and collecting samples from the top to the bottom. This approach eliminated samples contaminated with modern pollen as much as possible. The samples for the pollen analyses were taken at intervals of 2 cm from records of Melgunovka River flood plain, and Komissarovka River floodplain deposits, and of 5 cm from records of beach ridge and of the Novoselishche settlement deposits. Pollen was extracted according to a routine procedure as follows: samples are treated using the standard NaOH (10%) method (Sladkov 1967), and pollen grains are concentrated using the heavy liquid flotation method (Pokrovskaya 1966). The saturation of all samples by pollen and spores was sufficient for an adequate statistical calculation of the pollen distribution in the sediments. In the subfossil samples the largest amount of *Ambrosia* pollen found reached 504 grains, and the least was 4 grains. The total amount of collected pollen in the Melgunovka section was 310 – 600 grains, that in the Komissarovka section was 103 – 669 grains, the total in the section of the sandy beach ridge was 167 – 709 grains, and that in the Novoselishche settlement section was 186-249 grains.

The percentage of palynomorphs in the three groups, represented by arboreal pollen (AP), non-arboreal pollen (NAP), and spores, was estimated for each sample, wherein it was assumed that the total amount of the main genera pollen was counted as a percentage within each group, and the total amount in each group was 100%. We used the TILIA program (Grimm 1992) to construct pollen diagrams. The fossil common ragweed pollen was identified by species, wherein it was found that the pollen corresponds

to characteristics of *Ambrosia artemisiifolia* (Meier-Melikyan et al. 2004).

Radiocarbon dates. The ages of the studied deposits are based on radiocarbon dating obtained from the V.B. Sobolev's Institute of Geology and Mineralogy, Siberian Branch of RAS (SOAN; Novosibirsk, Russia), and Tomsk Regional Centre, Siberian Branch of RAS (IMKES; Tomsk, Russia). The samples were cleaned with acid/alkali/acid (Arslanov 1987), and the activity was measured via liquid scintillation counting using Quantulus 1220 (PerkinElmer) spectrometry-radiometry. The conventional ages were converted to calibrated ages using the radiocarbon age calibration program CALPAL_A (Weninger et al. 2002) (Table 1).

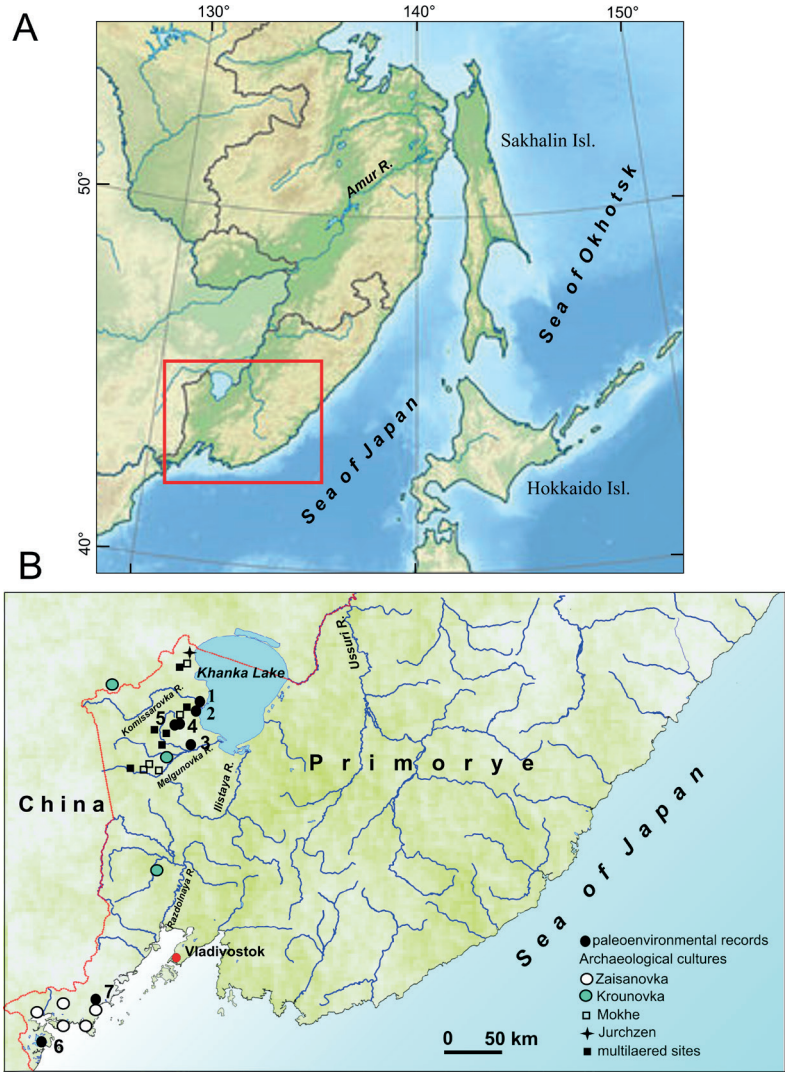

Fig. 1. Map of the studied area (A) and location of the archaeological sites and paleoenvironmental records (B): 1 – Komissarovka River floodplain deposits, 2 - the beach ridge deposits, 3 - Melgunovka River floodplain deposits, 4 - deposits of the Novoselishche settlement; 5 – Novoselishche settlement (Verkhovskaya and Esipenko, 1993), 6 - deposits of Talmi Lake, 7 - lagoonal deposits of Boisman Bay (Verkhovskaya and Kundyshev, 1995)

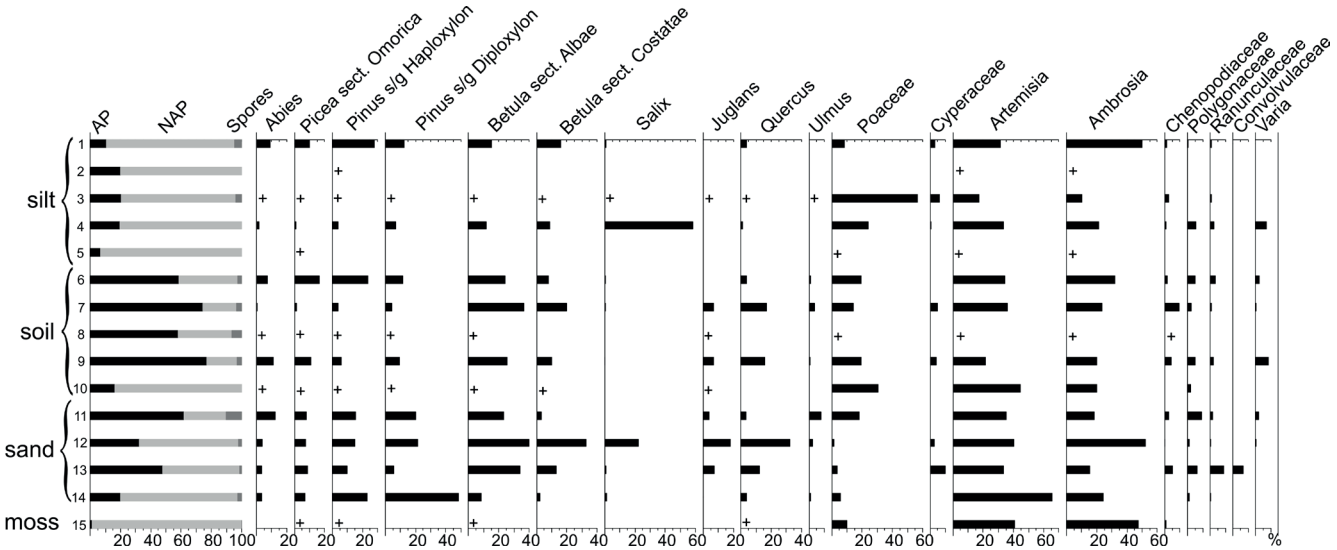

Fig. 2. Pollen diagram of the subfossil deposits on the Khanka Plain

Table 1. Radiocarbon dates

Lab. number	Depth, cm	Material	Date ^{14}C yrs BP	Cal. yrs AD/BC
Section of Melgunovka R. flood plain deposits				
SOAN-9007	10-12	humus loam	370±40	1536±68 AD
SOAN-9008	41-42	humus loam	2190±55	265±79 BC
SOAN-9009	56-58	humus loam	3830±120	2279±170 BC
SOAN-9010	63-65	humus loam	4710±100	3495±111 BC
SOAN-9011	70-72	humus loam	5690±120	4551±130 BC
SOAN-9012	98-100	humus loam	7920±135	6878±177 BC
Section of Komissarovka R. flood plain deposits				
SOAN-9017	10-12	soil	550±50	1367±46 AD
SOAN-9018	40-42	humus loam	1135±45	892±63 AD
Section of the beach ridge at Komissarovka R. mouth				
SOAN-5891	12-17	humus sand	290±50	1577±63 AD
SOAN-5892	27-32	humus sand	545±56	1369±46 AD
Section of the moat from Novoselishche settlement				
IMKES-1575	38-40	charcoal	1535±90	507±85 AD

RESULTS

Subfossil Ambrosia pollen. An analysis of the subfossil pollen spectra revealed that forest landscapes were best presented in the samples of mud left by floods, the forest-steppe environments were best recognizable in the soil samples, and floodplain communities were most easily found in the sandy samples. An abundance (10% – 52%) of *Ambrosia* pollen was found in all the samples (Fig. 2). In particular, the greatest proportion appears in the mud and sand samples in the western part of Khanka Lake, while a somewhat smaller amount was found in the soil samples. The data of other specialists shown, the herbs identified in the subfossil pollen assemblages were mostly Asteraceae throughout the Khanka Plain, wherein the proportion of *Ambrosia* pollen reached, at most, 9% (Petrenko et al. 2009). In the 1970s, subfossil pollen assemblages were studied in sediments of different genesis (fluvial, lacustrine, swamp, and soils) sampled in the eastern, southern, and western parts of the Khanka Plain. None of these samples contained *Ambrosia* pollen (Aleshinskaya and Shumova 1978).

Ambrosia pollen in Melgunovka River floodplain deposits. In the section of deposits studied on the Melgunovka River floodplain (44°34′ N, 132°04′ E, total thickness of 108 cm) there is an alluvial horizon of fine sand at a depth of 28 – 41 cm, in which occasional grains of *Ambrosia* pollen occur in the lower part of the horizon (36 – 38 cm). A calibrated 14C date of 265 ± 79 years BC (4th – 3rd centuries BC) was obtained from the underlying humified loam (depth of 41 – 42 cm) (Table 1). Therefore, the sand with *Ambrosia* pollen cannot be older than the third century BC (Fig. 3). The first minor peak of *Ambrosia* (8.4%) appears at 18 – 20 cm, which is in the lower part of the silty sand horizon dated to the Mediaeval Climatic Optimum. The pollen assemblages at that time were dominated (in the NAP group) by *Artemisia* (up to 45%) with a considerable proportion of the Poaceae (up to 24%), while the participation of the Cyperaceae and hygrophytic plants was lower than that in the underlying Subatlantic deposits. Moving upward, beginning at a depth of 36 – 38 cm, *Ambrosia* pollen is continually present in all the samples. The second peak is documented in the upper part of the humified loam deposited on the floodplain at the time of the Little

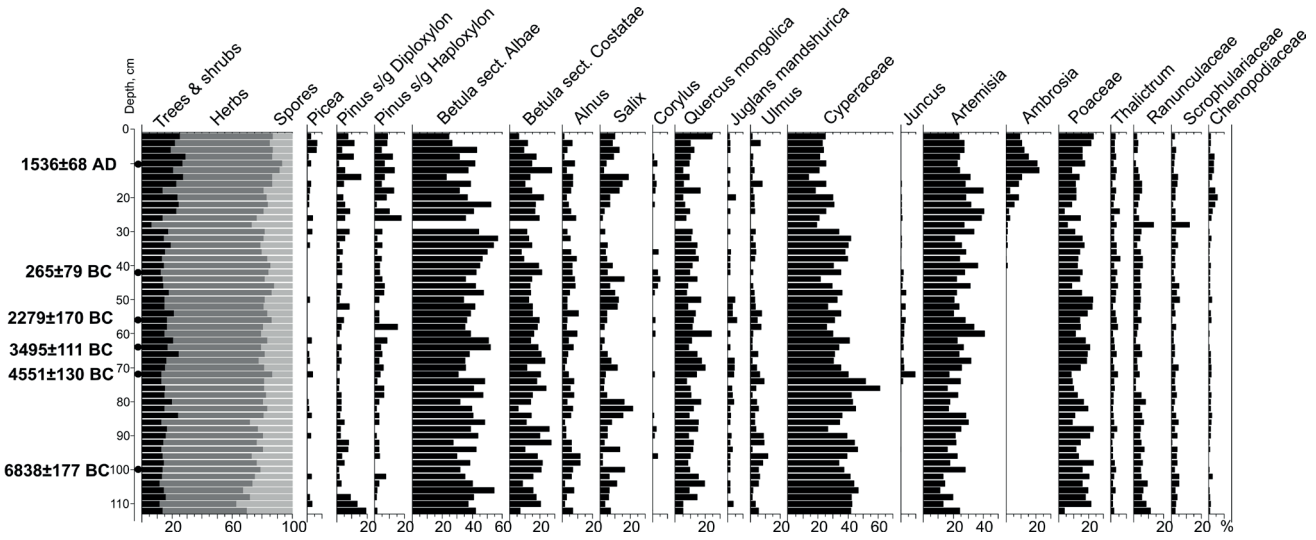

Fig. 3. Pollen diagrams of the Melgunovka River floodplain deposits

Ice Age, which was confirmed by the calibrated ^{14}C date of 1536 ± 68 years AD, which corresponds to the 15th – 16th centuries (Table 1). At this time, the mean annual temperature was approximately 1 °C lower than the current mean annual temperature (Bazarova et al. 2014). This cooling was also accompanied by reduced rainfall. Further, note that the same interval is distinguished by an increased amount of synanthropic plants (*Urtica*).

Ambrosia pollen in Komissarovka River floodplain deposits. Single grains of *Ambrosia* pollen were found in the floodplain deposits of the Komissarovka River (44°50′ N, 132°02′ E) (Bazarova et al. 2018b), which have a total thickness of 60 cm, wherein the *Ambrosia* pollen appears in the 52 – 54 cm interval (Fig. 4). The same horizon revealed the presence of single grains of synanthropic plants (*Urtica* and *Plantago*) in the pollen spectra. The nearest calibrated ^{14}C date of 892 ± 63 years AD (the 9th –10th centuries) was obtained for a sample of the overlying humified loam (40 – 42 cm). Supposedly, *Ambrosia* pollen first appeared in the floodplain deposits of the Komissarovka River in the 5th – 6th centuries. This period was marked by short-term cooling and an insignificant decrease in moisture supply. From the 52 – 54 cm interval and upward, *Ambrosia* pollen presents in every sample. The first peak was recorded in the deposits accumulated on the floodplain at the Medieval Climatic Optimum (the 9th – 10t^{h} centuries). Over the course of the subsequent 3rd or 4th centuries, the warm and relatively humid conditions changed to cooler and drier conditions. The second peak of the species occurred in the soil horizon formed during the Little Ice Age, which occurred during the 14th – 15th centuries (1367 ± 46 years AD) (Table 1). The pollen assemblages at this time are dominated by *Artemisia* (up to 60%), and various forb and herbs were also abundant (up to 59%). The peaks of *Urtica* and *Plantago* are synchronous with the maximum peak of *Ambrosia*.

Ambrosia pollen in sandy beach ridge deposits. The pollen was found in a sandy beach ridge section exposed at a depth of 75 cm near the Komissarovka River mouth (44°50′ N, 132°01′ E). The age of the ridge is estimated to be approximately 1 ka years AD (Bazarova et al. 2008). The *Ambrosia* grains were first found near the base of the sequence, dating back to the Mediaeval Climatic Optimum. In addition, the pollen appeared in the deposits attributed to the Little Ice Age (1369 ± 46 years AD, 1577 ± 63 years AD) (Table 1). In the pollen spectra, *Artemisia* was dominant, Poaceae and Asteraceae were present, and the apophyte pollen, *Urtica*, was occasionally found (Fig. 5).

Ambrosia pollen in Novoselishche settlement deposits. The archaeological site of the Novoselishche settlement is located on top of a gentle hill to the west of Khanka Lake. Samples for this section were obtained by cleaning the moat wall surrounding the settlement (44°39′ N, 131° 50′ E). The total thickness of the deposits is 55 cm, and *Ambrosia* pollen appears in the spectra beginning at a depth of 40 cm. In addition, Asteraceae, Ranunculaceae, *Artemisia*, and Poaceae pollen were found. Further, a large amount of *Urtica* pollen and other ruderal plant pollen (*Cannabis sativa* and Cichoriaceae) were presented (Fig. 6). The radiocarbon date was obtained using the charcoal located at a depth of 38 – 40 cm (507 ± 85 years AD) (Table 1). The pollen assemblages studied in each section strongly suggest that the steppe and forest-steppe landscapes on the Khanka Plain formed during the second half of the Holocene.

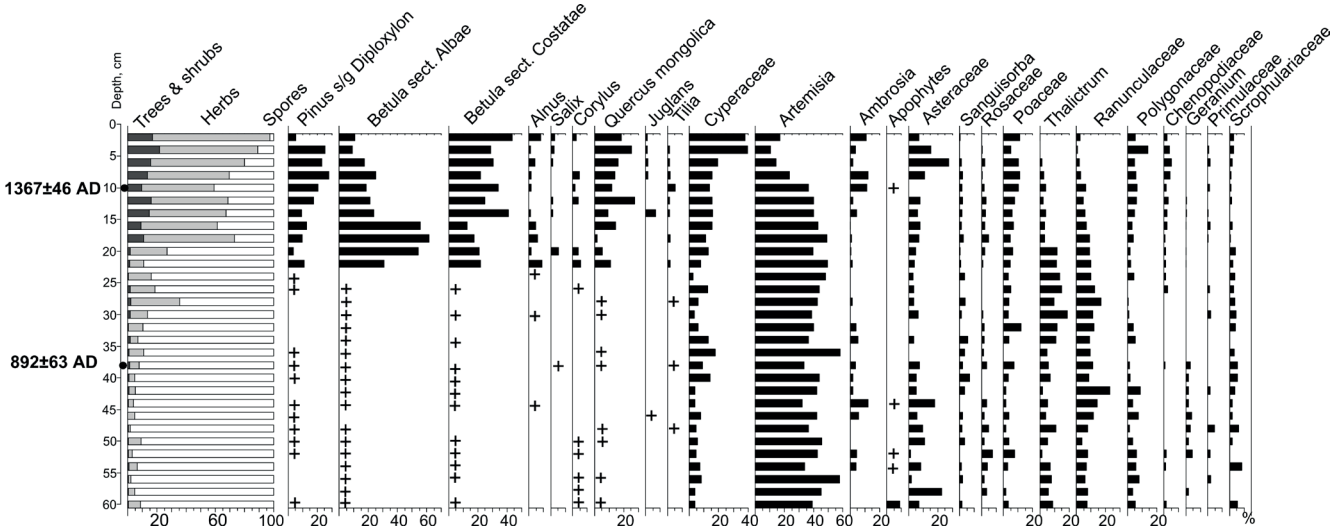

Fig. 4. Pollen diagrams of the Komissarovka River floodplain deposits

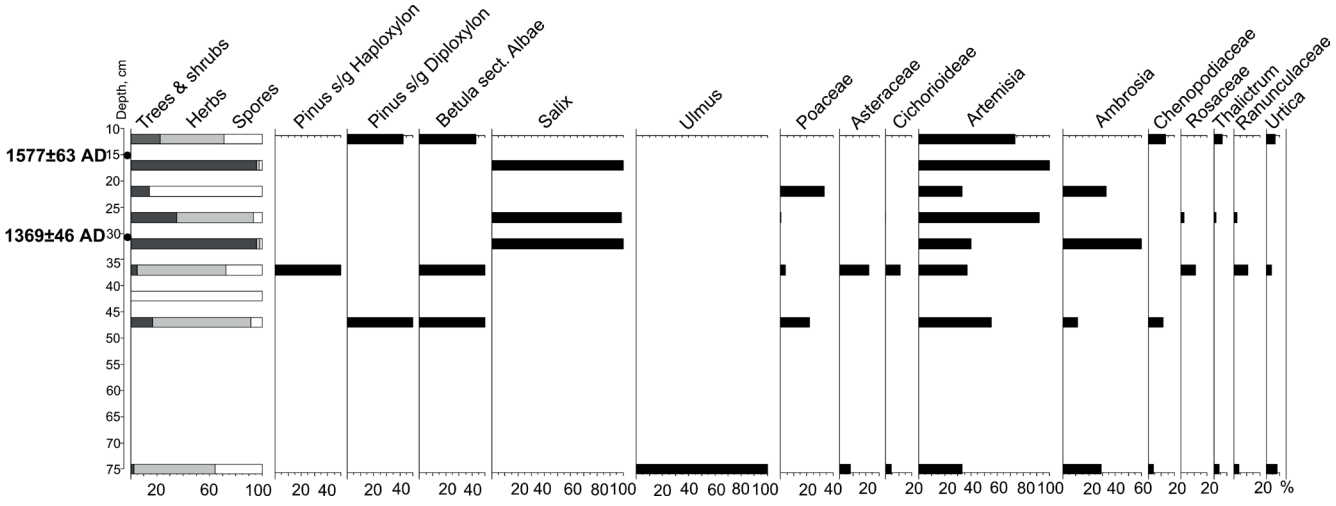

Fig. 5. Pollen diagrams of the beach ridge at the Komissarovka River mouth

DISCUSSION

Ecological features of Ambrosia artemisiifolia. There are two modern distribution ranges of *Ambrosia artemisiifolia* in Russia and adjacent countries (Nadtochii and Budrevskaya 2003). *Ambrosia artemisiifolia* is a heliophyte. Phenological observations show that, at latitudes – 40° – 50° N, common ragweed seed maturation occurs in September when the average temperature remains above 15 °C (Reznik 2009). In Siberia and northern Russia, as the average temperature in September is below 15 °C (8 – 11 °C) (https://ru.climate-data.org/location/459/), the species distribution is primarily limited by climatic conditions. The identification of separate plants or small ragweed parterres is possible in the case of alien seeds (Reznik 2009). *Ambrosia artemisiifolia* colonizes a wide range of habitats, such as cultivated fields, disturbed grasslands, roadsides, and riparian and ruderal habitats, if two conditions are fulfilled: (1) enough availability of seed and (2) soil disturbance (Ziska et al. 2006; Skjøth et al. 2010). Compared to other ruderal species, the ecological characteristics of ragweed have only its inherent differences.

In the Russian Far East, *Ambrosia artemisiifolia* is found in various habitats, both wet and dry, suggesting it can endure temporary excessive moisture even though it does not occur in wetlands. Its seeds require open unsodden places for germination, meaning they usually inhabit arable farmlands, kitchen gardens, fallow lands, roadsides, railroad embankments, and dumping grounds. The species is widely distributed along linear constructions disturbing the natural vegetation, such as wood-transport roads, main highways, and oil and gas pipelines. Note that the plant may occur even at a considerable distance from settlements. As *Ambrosia* seeds are currently abundant, they begin to grow on fallows in the first year, and along pipelines only 1 or 2 years after operation. Further, there is no species penetration in natural undisturbed communities (Kudryavtseva et al. 2018).

Ambrosia artemisiifolia pollen is easily recognizable as it is different not only from the pollen of other composite tribes but also from close species of the Ambrosieae tribe. N. Verkhovskaya and L. Yesipenko (1993) compared the *Ambrosia* pollen from the buried sediments with reference specimens of the present-day *Ambrosia trifida* L., *A. artemisiifolia* L., *A. dumosa* (A. Gray) Payne, and *A. ilicifolia* L., and established that the fossil pollen is morphologically similar to that of *A. artemisiifolia*

We have received picture of the pollen grain (Fig. 7) from records of the Khanka Plain using microscope Axio Imager A2 Zeizz (x400), and have determined its morphological characteristics. The pollen grain has spherical shape, its diameter is 21.5-22 µm, polar axis (P) is 23.0 µm, equatorial diameter (E) is 24.0 µm, and P/E=0.96. The contour of grains is finely toothed. Grain surface is covered by thorns, its height is about 1.7 µm. They closely adjoin to each other, almost touching the bases. The distance between the thorn peaks is about 3 µm. Comparison of the measured parameters with the morphological data from atlas (Meier-Melikyan et al. 2004) allow assume that fossil *Ambrosia* pollen from records of the Khanka Plain correspond to the characteristics of *Ambrosia artemisiifolia*.

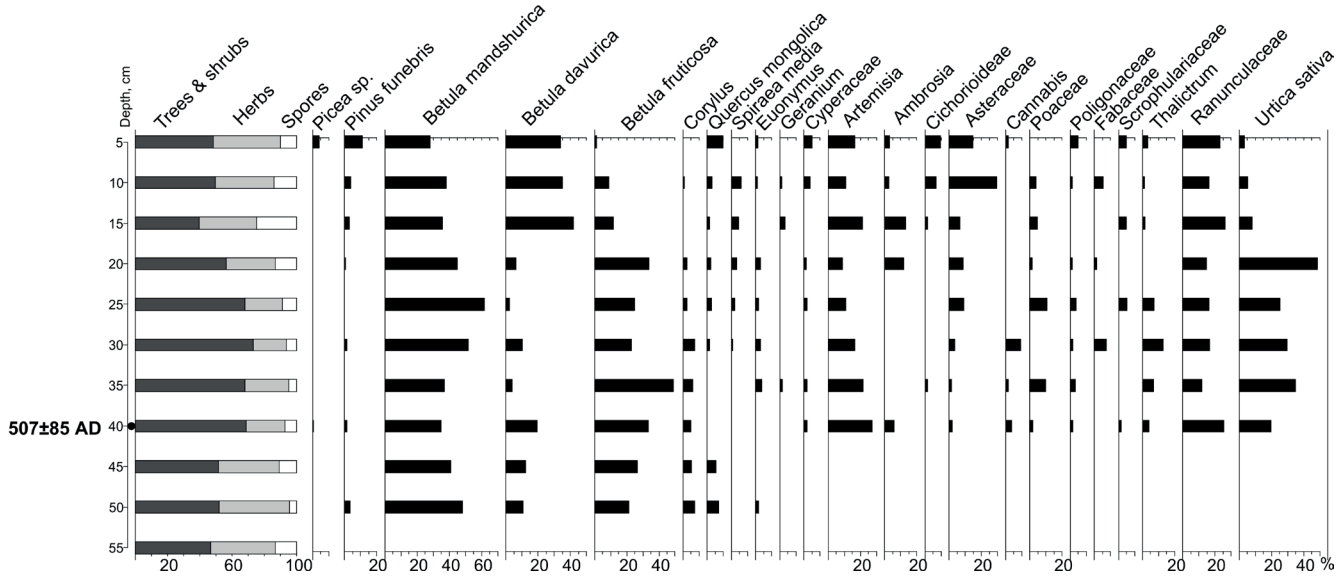

Fig. 6. Pollen diagrams of the moat deposits on archaeological site of the Novoselishche settlement

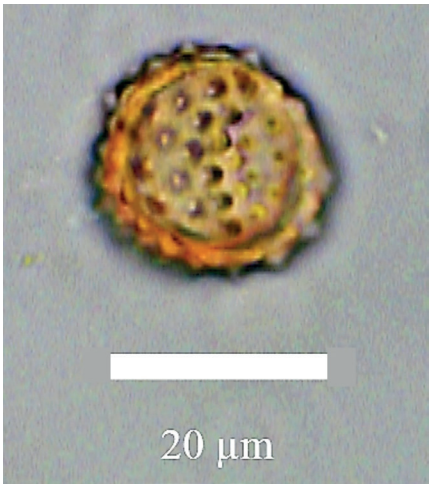

Fig. 7. Pollen grain of the *Ambrosia* artemisiifolia

Spatial and temporal correlations fossil Ambrosia pollen and Neolithic archaeological cultures. A records of pollen assemblages are one of the most common proxies employed to detect the impact of human activities on the environment. In particular, the presence of *Urtica, Plantago, Ambrosia*, Cichoriaceae, Caryophillaceae, Ranunculaceae, and *Polygonium* pollen in the sediments is evidence of human habitation in this area. These species, which are related to synanthropic (apophytes) plants, grow in the vicinity of dwellings, roadsides, and disturbed lands, and thus, indicators of human habitation (Li et al. 2008; Behre 1981).

The first information on the presence of *Ambrosia* pollen in buried deposits of the southern Russian Far East was published in the 1990s (Verkhovskaya and Yesipenko 1993; Verkhovskaya and Kundyshev 1993, 1995). Two cultural layers dated to the Holocene were excavated on the Khanka Plain in the vicinity of the Novoselishche village. The lower layer was attributed to the Final Neolithic (the first half of the 2nd millennium BC), and the upper layer was attributed to the early Bronze Age (the second half of the 2nd millennium BC). In the lower cultural layer, *Ambrosia* dominated the pollen assemblages in the NAP group (47.1% – 55.5%) (Verkhovskaya and Yesipenko 1993). Single grains of *Ambrosia* were found in the sand and gravel deposits of an old beach ridge on the northern coast of Talmi Lake and lagoonal deposits in Boisman Bay (south of Primorye). These deposits were formed at the end of the Holocene optimum (5.3 – 4.5 ka years BP). The climate changes at this time resulted in a reduction of forested areas and an expansion of forest-steppe communities in the south of Primorye (Verkhovskaya and Kundyshev 1993, 1995).

During 5.5-3.5 ka years BP the Zaisanovka cultural tradition became widespread in Primorye (Lyashchevskaya et al. 2022). A new population arrived with a new economic system – agriculture in the middle Holocene (Vostretsov 2005; Sergusheva 2013, and references therein). The earliest of them settled in the southern and western Primorye (Moreva et al. 2002). Apparently, they are associated with the first migration wave, which came from Manchuria through the Razdolnaya River valley. The middle stage (4.2-4.0 ka years BP) of this culture development is represented by the sites located on the coast of Peter the Great Gulf, which were likely a result of the next migration wave along the valley of the Tumannaya River (Krutykh 2012). The final stage of this culture (4.0-3.3 ka years BP) is represented by the group of sites located near Lake Khanka (Klyuev et al. 2002). One of the causes of the rapid expansion of *Ambrosia* could be the population growth in the south of the Russian Far East during the late Holocene. The ecological properties of common ragweed and a comparison of the obtained data with archaeological materials indicated that the presence of *Ambrosia* pollen in the Holocene deposits can use as an indicator of ancient agriculture in the south of the Russian Far East. The fossil pollen from our records is morphologically similar to *Ambrosia artemisiifolia*.

On western part of the Khanka Plain the first men appeared in paleometal epoch. The *Ambrosia* pollen appeared in deposits west of the Khanka Plain can be correlated with regional colonization by early men of this territory. For example, in the Melgunovka River floodplain, *Ambrosia* pollen was found in deposits accumulated in the 3rd century BC. Between the 4th – 3rd centuries BC and the 2nd–3rd century AD the continental part of Primorye was settled by people of the Krounovka Culture. The archaeological sites confined to the regions west of the Khanka Plain belong to the Khanka group of the Krounovka Culture. The archaeological materials of this time suggest they were advanced agricultural communities (Krounovka I … 2004; Sergusheva 2007; Vostretsov 2013).

In the floodplain sequence at the Komissarovka River mouth, *Ambrosia* pollen was identified in sediments dating back to the 5th – 6th centuries AD. This period was marked by cooling and reduced humidity, which contributed to an increase in the steppe area of the Khanka Plain (Bazarova et al. 2018a). The archaeological sites at this time are mostly related to the Mokhe culture (Tungusic and Manchur people), which was first mentioned in literature dating back to the 5th – 7th centuries AD. At this time, the Mokhe culture first appeared in the Manchuria, Primorye, and the Amur River basin. There are several territorial-chronological groups, including the Khanka group. Settlements near Khanka Lake were positioned in small valleys or on mountain slopes. The population was engaged in agriculture, hunting, and livestock farming (Klyuev et al. 2002; Piskareva 2013; Sergusheva 2018; Piskareva et al. 2019).

The pollen diagram of the Komissarovka River floodplain displays a peak of this species in the layers corresponding to the Mediaeval Climatic Optimum (Fig. 4). The grains of *Ambrosia* pollen were found in the deposits of a beach ridge not far from the Komissarovka River mouth, in sands datable to that event (Fig. 5). At this time (the 8th – 10th centuries AD), the Bohai State existed in the Manchuria territory and the northern Korean Peninsula. The Bohai settlements were mostly confined to fertile lands in the valleys of the Razdolnaya, Ilistaya, and other rivers, primarily in their middle and lower reaches. *Ambrosia* pollen was found in the pollen spectra from the cultural layer of the Starorechenskoe settlement (7th – 10th centuries AD) in the valley of the Razdolnaya River (Razzhigaeva et al. 2020). The majority of the Bohai settlements were concentrated in places favourable for agriculture (State of Bokhai …, 1994). The climate characteristics during the Mediaeval Climatic Optimum were higher than those currently, and therefore were beneficial not only for agriculture but also cattle breeding.

The pollen diagrams of the floodplain sequences of the Melgunovka and Komissarovka rivers show two peaks of *Ambrosia* pollen and a distinct gap between them, wherein the latter peak belongs to deposits dated from the 13th to the late 14th century. However, deposits of the same age in the beach ridge near the Komissarovka River mouth were devoid of *Ambrosia* pollen. According to archaeological materials, the Bohai State collapsed in the 10th century, and shortly after, the Jurchzhen Golden Empire (1115 – 1234) ceased to exist. The absence of any states and settlements from the 14th century suggests a desolation of the territory (State of the Bokhai … 1994).

Fossil Ambrosia pollen in Holocene deposits of adjacent and other territories. The pollen diagram of the deposits studied in the Yangtze River delta shows the presence of occasional *Ambrosia* grains in layers dated to 8320 ± 170 years BP, and approximately 4 ka years BP (Liu and Qiu 1994). By 8.5 ka years BP ago, more prehistoric societies with rice remains occurred in the middle and lower Yangzi Basin (Lu 2006; Jiang and Li L. 2006; Long et al. 2021; and references therein). Recent systematic archaeobotanical research conducted in the Lower Yangtze region revealed rice domestication is a very long process, which probably started 10–8 ka years BP (Fuller et al. 2009). In the south of the Korean Peninsula (the Paju-Unjeong area) oldest *Ambrosia* pollen was found in deposits dated 8425 – 7520 cal. years BP. Then it was found in deposits dated to the end of the middle and beginning of the late Holocene

(4700 – 2170 cal. years BP) (Yi 2011). Comparable data were obtained by other authors, revealing that single grains of *Ambrosia* were recovered from deposits dated to 8 – 4.5 ka years BP on the Korean Peninsula (Evstigneeva and Naryshkina 2013). Humans have been influencing Chinese landscape for thousands of years (Zhao and Piperno 2000; Cohen 2011; Betts et al. 2014). Thus, the appearance of the ragweed on south of the Russian Far East was most likely related to the first contacts, general widening, and the gradual migration of humans from China and Korea.

In North America (New England) ragweed pollen was found in found in sediments dated 10-8 ka years BP (Faison et al., 2006; Oswald et al., 2018, 2020).

Before present the palaeobotanical data for eastern Asia were insufficient to draw a conclusion regarding the absence of certain historic plants. In general, the floras of eastern Eurasia and North America are very similar in their evolution, and a species comparison provided proof of their resemblance. Considering this connection, it is conceivable to suggest existing of second centre (Asian) of the *Ambrosia* in China during the past millennia. Obtained new data allow us suppose that in eastern part of Eurasia ragweed population existed simultaneously and independently from Northern America population on boundary of early Holocene and middle Holocene.

Probably, a further increase of the average annual temperature in the south of Russian Far East will lead to shift of the *Ambrosia* population boundary to the north along the Middle and Lower Amur basin, on the territory of the Amur Region and the Khabarovsk Territory. In China, projections of potential distribution under future climate change scenarios suggest further expansion of the *Ambrosia artemisiifolia* and *A. trifida* to ecologically friendly the southeastern coastal regions, to northern Taiwan and to the Beijing-Tianjin-Tangshan region of northern China (Qin et al. 2014).

Atmospheric conditions affect the release of anemophilic pollen, and the timing and extent are depended by climate change. Simulations using pollen emission model and future climate data show that higher temperatures at the end of the century shift the start of spring emissions 10–40 days earlier, and summer/autumn weeds and grasses 5–15 days later and lengthen the duration of the pollen season. Observational data suggest that many taxa are projected to have higher pollen production at higher temperatures (e.g., late-flowering *Ulmus*, Cupressaceae, *Ambrosia,* Poaceae). Phenological shifts depend on the temperature response of individual taxa, with convergence in some regions and divergence in others. Temperature and precipitation alter daily pollen emission maxima by −35 to 40% and increase the annual total pollen emission by 16–40% due to changes in phenology and temperature-driven pollen production. Increasing atmospheric CO_2 may increase pollen production, and doubling production in conjunction with climate increases end-of-century emissions up to 200% (Zhang and Steiner 2022).

Currently, the *Ambrosia* species is widespread globally. It naturalized and frequently form part of the flora in almost all European countries and some countries in the East Asia. Steps are being taken to reduce further geographical expansion and limit increases in population densities of the plant in order to protect agriculture and the allergic population. This is particularly important when one considers possible range shifts, changes in flowering phenology and increases in the amount of pollen that could be brought about by changes in climate.

CONCLUSIONS

An analysis of the obtained data allowed to take answers on the questions of this research.

In the south of the Russian Far East, *Ambrosia* appeared in the middle Holocene (Verkhovskaya and Yesipenko 1993; Verkhovskaya and Kundyshev 1993, 1995). The new data presented in this study confirm that it did not occur earlier than the second half of the middle Holocene in the south of the Russian Far East.

The presence of *Ambrosia* pollen in the middle and late Holocene sediment suggests that this species is an extinct archeophytes. Further, our data suggest that an origin centre of the common ragweed distribution existed in the east of Eurasia long before of 18th century. In eastern Asia the oldest deposits with *Ambrosia* pollen dated to 8320 ± 170 years BP were found in the Yangtze River delta (Liu and Qiu 1994). In central China (Ren, 2000) and the Korean Peninsula (Yi 2011; Evstigneeva and Naryshkina 2013) *Ambrosia* pollen was found in deposits of the middle Holocene. An analysis of the pollen assemblages recorded the presence of *Ambrosia* in layers formed over an extended period.

Comparison of the obtained pollen records with archaeological materials indicated that the presence of *Ambrosia* pollen in the Holocene deposits has good spatial and temporal correlation with Neolithic agriculture in the south of the Russian Far East.

From the 19th century to the 1960s, *Ambrosia* was practically absent in the south of the Russian Far East. The reasons for this absence remain unknown. The absence of *Ambrosia* pollen in the subfossil pollen spectra of the Khanka Plain (Aleshinskaya and Shumova 1978) supports the conclusion that the modern isolated population of the *Ambrosia* expansion in the south of the Russian Far East occurred later than the 1960s – 1970s. On adjacent areas modern populations of this plant appeared before. In Japan it was introduced in the 1860s – 1870s (Kato and Ohbayashi 2008). In Chine, *Ambrosia artemisiifolia* was first introduced in the 1930s (Qin et al. 2014; Zhou et al. 2017), and finally, in the Korean portion, *Ambrosia artemisiifolia* and *A. trifida* were introduced at the beginning of the 1950s (Lee and Oh 1974; Kim and Kil 2016). We did not find data regarding the distribution of this plant in the Chinese and Korean territories from the 19th century to the 1930s. We believe that the modern secondary settling of this species in the east and west of Eurasia formed independently. The ranges in China, Japan, the Korean Peninsula, and the south of the Russian Far East also formed independently.

Currently *Ambrosia artemisiifolia* become naturalized and frequently forms part of the flora. Simulation forecast show that higher temperatures at the end of the century can lead to phenological shifts and pollen emission. Increasing atmospheric CO_2 also may increase pollen production.

REFERENCES

Aistova E.V., Bezborodov V.G., Gus'kova E.V. and Rogatnykh D.Yu. (2014). Formation of trophic relations of native leaf-beetle species (Coleoptera, Chrysomelidae) with Ambrosia artemisiifolia (Asteraceae) in Primorskii krai of Russia. Zoologicheskii Zhurnal. 93, 960-966 (in Russian).

Aleshinskaya Z.V. and Shumova G.M. (1978). Subfossil pollen spectra of the Khanka Plain. In: Grichuk, M.P., Korotkii, A.M. (Eds.), Pollen studies on Far East. DVNTs Press, Vladivostok, 60-66 (in Russian).

Arslanov Kh.A. (1987). Radiocarbon: Geochemistry and Geochronology. Leningrad state university, Leningrad (in Russian).

Basset I.J. and Terasmae J. (1962). Ragweeds, Ambrosia species in Canada and their history in postglacial time. Canadian Journal of Botany. 40, 141-150, DOI: 10.1139/b62-015.

Bazarova V.B., Mokhova L.M., Orlova L.A. and Belyanin P.S. (2008). Variation of the Lake Khanka Level in the Late Holocene, Primorye. Russian Journal of Pacific Geology. 2, 82-86 (in Russian).

Bazarova V.B., Grebennikova T.A. and Orlova L.A. (2014). Natural-Environment Dynamics Within the Amur Basin During the Neoglacial. Geography and Natural Resources. 35(3), 275-283.

Bazarova V.B., Lyashchevskaya M.S., Makarova, T.R. Makarevich, R.A. and Orlova, L.A. (2018a). Holocene overbank deposition in the drainage basin of Lake Khanka. Russian Geology and Geophysics, 59, 410-1418, DOI: 10.15372/GiG20181102.

Bazarova V.B., Lyashchevskaya M.S., Makarova T.R. and Orlova L.A. (2018b). Environments of the middle-late Holocene sedimentation in river floodplains of the Prikhanka Plain (southern Far East). Russian Journal of Pacific Geology, 37, 94-105, DOI: 10.1134/S1819714018060106.

Behre K-E. (1981). The interpretation of anthropogenic indicators in pollen diagram. In: Pollen et Spores, 23, 225-245.

Betts A., Jia P. and Dodson J. (2014). The origins of wheat in China and potential pathways for its introduction: A review. Quaternary International. 348, 158-168, DOI: 10.1016/j.quaint.2013.07.044.

Chauvel B., Dtssant F., Cardinal-Legrand C. and Bretagnolle F. (2006). The historical spread of Ambrosia artemisiifolia L. in France from herbarium records. Journal of Biogeography. 6, 665-673, DOI: 10.1111/j.1365-2699.2005.01401.x.

Cohen D.J. (2011). The Beginnings of Agriculture in China. A Multiregional View. Current Anthropology, 52, 273-293, DOI: 10.1086/659965

Csontos P., Vitalos, S.M., Barina, Z. and Kiss I. (2010). Early distribution and spread of Ambrosia artemisiifolia in Central and Eastern Europe. Botanica Hevletica. 120, 75-78, DOI: 10.1007/s00035-010-0072-2.

Evstigneeva T.A. and Naryshkina N.N. (2013). Mid-Holocene Vegetation and Environments on the Northeast coast of Korean Peninsula. Botanica Pacifica. A Journal of plant science and conservation. 2, 27-34.

Faison E.K., Foster D.R. Oswald W.W., Hansen B.C.S. and Doughty E. (2006). Early Holocene openlands in southern New England. Ecology, 87(10), 2537-2547.

Flora of China (Asteraceae). (2011). Science Press (Beijing) and Missouri Botanical Garden Press (St. Louis).

Fuller D., Qin L., Zheng Y., Zhao Z., Chen X., Hosoya L.A. and Sun G.P. (2009). The Domestication Process and Domestication Rate in Rice: Spikelet Bases from the Lower Yangtze. Science, 323(5921) 1607-1610, DOI: 10.1126/science.1166605.

Genton B., Shykoff A. and Giraud T. (2005). High genetic diversity in French invasive populations of common ragweed, Ambrosia artemisiifolia, as a result of multiple sources of introduction. Molecular Ecology (Chichester). 14, 4275-4285.

Grimm E.S. (1992). TILIA and TILIA GRAPH: pollen spreadsheed and graphic program, in: 8th International Palynjlogical Congress. Program and Abstracts. Aixen-Provence, France, 56.

Kato A. and Ohbayashi N. (2008). Insect Communities Associated with an Invasive Plant the Common Ragweed, Ambrosia artemisiifolia L. in Western Japan. Japanese Journal of Environmental Entomology and Zoology. 19, 125 -132.

Kim Ch-G. and Kil J. (2016). Allien flora of Korean Peninsula. Biological Invasions. 18, 1843-1852, DOI: 10.1007/s10530-016-1124-3.

Klyuev N.A., Sergusheva Ye.A. and Verkhovskaya N.B. (2002). Agriculture on final Neolithic (by data of the Novoselishche-4 site). In: Bolotin D.P., Zabiyako A.P. (Eds.), Traditional culture in Eastern Asia. Amurskii State University, Blagoveshchensk, 102-126 (in Russian).

Kolesnikov B.P. (1969). Vegetation. In: Gerasimov I.P. (Ed.), Southern part of the Far East. Nauka, Moscow, 206-250 (in Russian).

Krounovka 1 site in Primorye, Russia. Report of excavation in 2002 and 2003. 2004. In: Komoto M. and Kumamoto O.H. (Eds.), Study of Environmental Change of Early Holocene and the Prehistoric Subsistence System in Far East Asia, Shimoda Print Co. Ltd.

Krutykh Ye.B. (2012). Zaisanovskaya archaeological culture: the problem of interpretation. Russia and the Pacific. 1, 139-154 (in Russian).

Kudryavtseva E.P., Bazarova V.B., Lyashchevskaya M.S. and Mokhova L.M. (2018). Common ragweed (Ambrosia artemisiifolia): the present-day distribution and the presence in the Holocene deposits of Primorskii Krai (south of the Russian Far East). Komarov readings, LXVI, 125-146 (in Russian).

Kurentsova G.A. (1962). Vegetation of the Khanka Plain and surround areas. AN SSSR Press, Moscow-Leningrad (in Russian).

Lee Y.N. and Oh Y.C. (1974). Korean of naturalized plants (1). Korean Journal of Life Sciences. 12, 25-31.

Jiang L. and Li L. (2006). New evidence for the origins of sedentism and rice domestication in the Lower Yangzi River, China. Antiquity 80(308), 355-361.

Li Y-Y., Zhow L-P. and Cui H-T. (2008). Pollen indicators as human activity. Chinese Science Bulletin. 53, 1281-1293.

Liu K-B. and Qiu H-L. (1994). Late Holocene pollen records of vegetation changes in China: climate or human disturbance? Terrestrial, Atmospheric and Oceanic Sciences. 5, 393-410.

Long T., Chen H., Leipe C., Wagner M. and Tarasov P. (2022). Modelling the chronology and dynamics of the spread of Asian rice from ca. 8000 BCE to 1000 CE. Quaternary International. 623, 101-109, DOI: 10.1016/j.quaint.2021.11.016.

Lu T.L-D. (2006). The Occurrence of Cereal Cultivation in China. Asian Perspectives. 45(2), 130-158.

Lyashchevskaya M.S., Bazarova V.B., Dorofeeva N.A. and Leipe C. (2022). Late Pleistocene–Holocene environmental and cultural changes in Primorye, southern Russian Far East: A review. Quaternary International, 623, 68-82, DOI: 10.1016/j.quaint.2022.02.010.

Mandrioli P., Di Cecco M. and Andina G. (1998). Ragweed pollen: the air allergen is spreading in Italy. Aerobiologia. 14, 13-20.

Mar'yushkina V.Ya. (1986). Ambrosia artemisiifolia and basis of biological control. Naukova dumka, Kiev (in Russian).

Meier-Melikyan N.R., Bovina I.Yu., Kosenko Ya.V., Poleva S.V., Severova E.E., Tekleva M.V. and Tokarev P.I. (2004). Atlas of aster pollen grains (Asteraceae). Pollen morphology and development of Asteraceae family species sporoderma. Comradeship of scientific publications KMK, Moscow (in Russian).

Moreva O.L., Popov A.N. and Fukuda M. (2002). Ceramics with rope ornament in the Neolithic of Primorye. Vladivostok. In: Kradin N.N. (Ed.), Archaeology and cultural anthropology of the Far East and Central Asia, 57-67 (in Russian).

Nadtochii I.N. and Budrevskaya I.F. (2003). Agroecological maps of the Russia and adjacent countries. Ambrosia artemisiifolia L. http://www.agroatlas.ru/ru/content/weeds/Ambrosia_artemisiifolia/map/index.html (accessed 23 October 2003).

Nedoluzhko V.A. (1984). The distribution of Ambrosia artemisiifolia (Asteraceae) in the Prymorskii region. Botanicheskii zhurnal. 69, 527-529 (in Russian).

Oswald W.W., Foster D.R., Shuman B.N., Doughty E.D., Faison E.K., Hall B.R., Hansen B.C. S., Lindbladh M., Marroquin A. and Truebe, S.A. (2018). Subregional variability in the response of New England vegetation to postglacial climate change. Journal of Biogeography. 45, 2375-2388, DOI: 10.1111/jbi.13407.

Oswald W. W., Foster D.R., Shuman B.N., Chilton E.S., Doucette D.L. and Duranleau D. L. (2020). Conservation implications of limited Native American impacts in pre-contact New England. Nature Sustainability. 3, 241-246, DOI: 10.1038/s41893-019-0466-0.

Petrenko T.I., Mikishin Yu.A. and Belyanina N.I. (2009). Subfossil pollen complex of the Khanka Plain, Primorye. Natural and technical sciences, 4, 162-171(in Russian).

Pokrovskaya I.M. (1966). Methods of paleopollen studies. In: Pokrovskaya I.M. (Ed.), Paleopalynology. Nedra, Leningrad, 29-60 (in Russian).

Pimenov M.G., Khokhryakov A.P. and Pimenova R.Ye. (1966). Floristic records from Southern Primorye. Bulletin of Main Botanical Garden. 63, 78-79 (in Russian).

Piskareva Ya.V. (2013). New investigation results of the Mokhe culture in Primorye. Bulletin of Tomskii State University. History. 2, 80-85 (in Russian).

Piskareva Ya.V., Sergusheva Ye.A., Dorofeeva N.A., Lyashchevskaya M.S. and Sharyi-ool M.O. (2019). Economy of early-middle centuries people in Primorye (on data of Mokhe archaeological culture). Bulletin of archaeology anthropology and ethnography. 1, 25-36 (in Russian).

Qin Z., Ditommaso A., Wu R.S. and Huang H.Y, (2014). Potential distribution of two Ambrosia species in China under projected climate change. Weed Research. 54, 520-53, DOI: 10.1111/wre.12100.

Razzhigaeva N.G., Ganzei L.A., Grebennikova T.A., Kornyushenko T.V., Ganzey K.S., Kudryavtseva E.P., Gridasova I.V., Klyuev N.A. and Prokopets, S.D. (2020). The ratio of natural and anthropogenic factors in the development of the landscapes of the Razdolnaya River, Primorye. Izvestiya RAS. Seriya Geographical. 84, 246-258, DOI: 10.31857/S2587556620020119.

Ren G. (2000). Decline of the mid- to late Holocene forests in China: climatic change or human impact? Journal of Quaternary Science. 15, 273-281. https://doi.org/10,1002 / (SICI) 1099-1417 (200003) 15: 33.3.CO; 2-U.

Reznik S.Ya. (2009). Factors determining geographic ranges and population densite of common ragweed Ambrosia artemisiifolia L. (Asteraceae) and ragweed leaf beetle Zygogramma suturalis F. (Coleoptera, Chrysomelidae). Bulletin zaschity rastenii. 2, 20-28 (in Russian).

Sergusheva Ye.A. (2007). Early agriculture in the Primorye on data of the Krounovka 1 settlement. Bulletin of Novosibirsk State University. History, Philology. 6, 94-103 (in Russian).

Sergusheva Ye.A. (2013). Dynamics of agriculture in late neolithic of Primorye on archaeobotanical data. Vestnik arheologii, antropologii i etnografii. 1(4), 25-36 (in Russian).

Sergusheva Ye.A. (2018). Agriculture on south of the Far East in the early Middle Ages: archaeobotanical studies on Sinelnikovo-1 settlement. Bulletin of ancient technology laboratories. 14, 83-97 (in Russian).

Skjøth A.S., Smith M., Šikoparija B., Stach A., Myszkowska D., Kasprzyk I., Radisic P., Stjepanovic B., Hrga I., Apatini D., Maguyar D., Pálgy A. and Ianovici N. (2010). A method for producing airborne pollen source inventories: an example of Ambrosia (ragweed) on the Pannonian Plain. Argic for Meteorology. 150, 1203-1210.

Sladkov A.M. (1967). Introduction on pollen analysis. Nauka, Moscow (in Russian).

Smith M., Cecchi L., Skjøth C.A., Karrer G. and Šikoparija B. (2013). Common ragweed: A threat to environmental health in Europe. Environment International. 61, 115-126, DOI: 10.1016/j.envint.2013.08.005

State of the Bokhai (698-926 years) and tribes of the Russian Far East, 1994. Nauka, Moscow (in Russian).

Vascular plants of the Soviet Far East. Asteraceae V. 6. 1992. Nauka, St.-Petersburg (in Russian).

Verkhovskaya N.B. and Kundyshev A.S. (1993). Environment of southern Primorye during Neolithic and early Iron century. Bulletin of FEB RAS. 1, 18-26 (in Russian).

Verkhovskaya N.B. and Kundyshev A.S. (1995). Vegetation of Peter the Great Bay coast in the optimum of the Holocene. In: Kuzmin Ya.V. (Ed.), Complex studies of Holocene deposit sections on Peter the Great Bay coast (Sea of Japan). Bagira-Press, Moscow, 8-17 (in Russian).

Verkhovskaya N.B. and Yesipenko L.P. (1993). The time of the Ambrosia artemisiifolia (Asteraceae) appearance in the south of the Russian Far East. Botanicheskii zhurnal. 78, 94-101 (in Russian).

Vinogradova Yu.K., Aistova E.V., Antonova L.A., Chernyagina O.A., Chubar E.A., Darman G.F., Devyatova E.A., Khoreva M.G., Kotenko O.V., Marchuk, E.A., Nikolin E.G., Prokopenko S.V., Kudryavtseva E.P. and Krestov P.V. (2020). Invasive plants and flora of the Russian Far East: the checklist and comments. Botanica Pacifica. A Journal of plant science and conservation. 9, 103-129, DOI: 10.17581/ bp.2020.09107.

Voroshilov V.N. (1966). Flora of the Soviet Far East. Nauka, Moscow (in Russian).

Vostretsov Yu.Ye. (2005). The Interaction of Marine and Agricultural Adaptations in the Basin of the Sea of Japan. Dalnauka, Vladivostok. In: Andreeva Zh.V. (Ed.), The Russian Far East in Prehistory and the Middle Ages: discoveries, problems, hypotheses, 159-186 (in Russian).

Vostretsov Yu.Ye. (2013). Ecological factors of cultural dynamics formation on coastal zone of Eastern Asia in the paleometal epoch. Bulletin of FEB RAS. 1, 109-116 (in Russian).

Weninger B., Jöris O. and Danzeglocke U. (2002). Cologne radiocarbon calibration and paleoclimate research package. CALPAL_A (Advanced) in the Ghost of Edinburgh Edition, Universal zu Kuln, Institut fur Ur-und Fruhgeschichte, Radiocarbon Laboratory. Weyertal 125, D-50923. Kuln, 2005. http://www/calpal-online.de/cgi-bin/quickcal.pl

Yi S. (2011). Holocene vegetation responses to East Asian monsoonal changes in South Korea. In: Blanco J., Kheradmand H. (Eds.), Climate change – Geophysical Foundation and ecological effects. Publisher inTech, Rijeka, 157-178.

Zhang Y., Steiner A.L. (2022). Projected climate-driven changes in pollen emission season length and magnitude over the continental United States. Nat. Commun. 13, 1234, DOI: 10.1038/s41467-022-28764-0.

Zhao Z. and Piperno D. (2000). Late Pleistocene/Holocene environments in the middle Yangtze River valley, China, and rice (Oryza sativa l.) domestication: the phytolith evidence. Geoarchaeology: An International Journal. 15(2), 203-225.

Zhou Z. Wan F. and Guo J. (2017). Common ragweed Ambrosia artemisiifolia L. In: Wan F, Jian M, Zhan A (Eds.), Biological invasions and its management in China, V. 2. Springer Science+Business Media B.V., Dordrecht, 99-109.

Ziska L.H., George K. and Frenz D.A. (2006). Establishment and persistence of common ragweed (Ambrosia artemisiifolia L.) in disturbed soil as a function of an urban–rural macro-environment. Global Change Biology, 12, 1-9, DOI: 10.1111/j.1365-2486.2006.01264.x.

RESEARCH PAPER

REGIONAL PATTERNS OF THIRD-LEVEL DIGITAL INEQUALITY IN RUSSIA: AN ANALYSIS OF GOOGLE TRENDS DATA

Olga Yu. Chereshnia[1*], Marina V. Gribok[1]
[1]Lomonosov Moscow State University, Faculty of Geography, Leninskie Gory, 1, Moscow, 119991, Russia
***Corresponding author:** chereshnia.o@geogr.msu.ru
Received: June 28th, 2022 / Accepted: February 15th, 2023 / Published: March 31st, 2023
https://DOI-10.24057/2071-9388-2022-107

ABSTRACT. Digital inequality extends beyond mere access to technology. This study explores the concept of third-level digital inequality, which describes the situation where individuals or communities have access to technology and the Internet, have required skills, but still struggle to use it effectively. However, there is currently a lack of data and methods for assessing third-level digital inequality. To address this gap, this study aimed to evaluate it on a regional scale by analyzing the popularity of Google search queries. In proposed method, the data are categorized into three groups: everyday services, education, science, and technology, and entertainment. On this basis authors calculated the index of Internet usage efficiency. The study's findings revealed the territorial patterns of digital inequality in the constituent entities of the Russian Federation. Regions in North Caucasus and Siberia showed low Internet usage efficiency, while regions in the Urals and Central Russia had high Internet usage efficiency. The study's methodology is quick, cost-effective, and easy to implement, but it also has limitations. The method only considers the popularity of certain search queries and does not consider the frequency or duration of internet usage, or the specific websites or services accessed, and does not consider individual-level factors that may influence internet usage patterns. The authors emphasize the importance of addressing not only differences in Internet access but also the lack of technology skills, digital literacy, and motivation among certain groups. They conclude that public policies aimed at enhancing internet skills can reduce digital inequality and improve the quality of life of the population.

KEYWORDS: digital inequality, digital divide, Google Trends, Russian regions

CITATION: Chereshnia O. Yu., Gribok M. V. (2022). Regional Patterns Of Third-Level Digital Inequality In Russia: An Analysis Of Google Trends Data. Geography, Environment, Sustainability, 1(16), 26-35
https://DOI-10.24057/2071-9388-2022-107

ACKNOWLEDGEMENTS: The study was funded by the Russian Science Foundation, grant No. 21-77-00024.

Conflict of interests: The authors reported no potential conflict of interest.

INTRODUCTION

Data in digital form has become a critical factor in the production of goods and services across all sectors of society, including economic, cultural, and other human activities. According to the International Telecommunication Union (2019) and Internet World Stats (2022), the number of Internet users has increased fivefold in the last 17 years, from 1 billion in 2005 to 5.1 billion in early 2022.

At first, it was considered that the Internet would bridge the inequalities between people in accessing information and would eventually allow it to be distributed without restriction, thereby ensuring equal access to education and new opportunities for every segment of the world's population. However, the problem of uneven access to digital technologies by different social groups remains. Research on this subject was made at the end of the 1990s. Researchers found that in the United States, the highest degree of Internet accessibility was observed among groups that had access to better education and higher incomes (Hoffman and Novak 1998; Strover 1999). As information technology has become ubiquitous, the problem of unequal access has become more pronounced. The adoption of new digital technologies is often not evenly distributed across social groups or geographic areas. The spread of new technologies, including digital ones, between countries and regions, generally follows the classical laws of innovation diffusion (Zemtsov and Baburin 2017). Unequal distribution of technology infrastructure, such as access to the Internet, computers, and other digital devices was called Digital divide.

According to the Organization for Economic Development (OECD), "Digital divide" refers to the gap between individuals, households, businesses, and geographic areas at different socio-economic levels regarding their opportunities to access information and communication technologies (ICTs) and use them for a variety of activities (OECD, 2001). That is, the digital divide is "the inequality between the 'haves' and the 'have-nots', differentiated through dichotomous measures of access to information technology. This is the interpretation that most researchers rely on, e.g. (Novak and Hoffman 2000; Wilhelm and Thierer 2000; Norris 2001).

Digital inequality, on the other hand, is a broader concept. It encompasses the digital divide and complements it with other factors affecting the use of technologies by people who have formal access to them. Inequality manifests itself in, for example, unequal distribution of Internet skills (e.g.

ability to search for information), and in the use of the Internet not only for entertainment or social networking (Van Deursen and Helsper 2015). Current research identifies three levels of digital inequality:

- The first level is the inequality in physical or economic access to technology;
- The second level is the inequality of usage skills;
- The third level is the unequal distribution of opportunities for tangible outcomes in real life (employment, education, political participation, etc.) due to patterns of technology use (Du et al. 2021; Van Dijk 2012).

Third-level digital inequality refers to a situation where an individual or community has access to technology and the internet, as well as the necessary skills and knowledge to use it, but is still unable to effectively use it to access useful services and resources. Third-level digital inequality can have several different causes, including social and cultural factors, such as a lack of awareness or understanding of the benefits of using technology, or a lack of support or guidance in using it. It may also be caused by technological or infrastructure issues, such as slow or unreliable internet connections, or a lack of relevant content or resources.

Overall, third-level digital inequality represents a deeper and more complex challenge than first- or second-level digital inequality, as it requires addressing not just access and skills, but also attitudes, behaviors, and the design and delivery of services.

The digital inequality can persist even after the digital divide has been bridged and there is almost equal access to technology. This is a problem in both high-income countries (Hargittai and Hinnant 2008; Peter and Valkenburg 2006) and low-income ones (Drori 2010; ITU 2011).

Digital inequality can have significant consequences for sustainable development, as it can limit individuals' and communities' ability to access information, communicate, and participate in economic, social, and cultural activities. This can lead to a range of negative outcomes, including reduced economic opportunities, social isolation, and limited access to education and health services. Digital inequality is a key consideration in several of the United Nations Sustainable Development Goals (SDGs), including Goal 9 (Industry, Innovation, and Infrastructure), Goal 10 (Reduced Inequalities), and Goal 17 (Partnerships for the Goals). Efforts to reduce digital inequality and promote sustainable development therefore require a multi-faceted approach that involves both the public and private sectors, as well as civil society and international organizations.

Research on the first-level digital inequality (the digital divide itself) and the second-level digital inequality is nowadays often published not only abroad but also in Russia (Avraamova and Vershinskaya 2001; Yudina 2020; Gladkova et al. 2020).

Most papers on the digital divide in Russia approach the topic mainly from a technological perspective, i.e. the gap between those who have and those who do not have access to digital technologies, and analyze the many factors that influence this divide. There is enough statistical information to estimate the first two levels of inequality, but it should be acknowledged that methodological approaches to collecting federal statistical data on the specifics of ICT use in Russia do not allow a full assessment of the third level of digital inequality. The problem of a lack of data is also described in the work (Zemtsov et al. 2022) in which the authors studied the issue of digital inequality through the prism of the diffusion of innovations concept. To assess the third level of digital inequality, the authors were able to select only one indicator - the share of the online sector in trade.

The authors estimate that Russia has a high level of Internet connectivity, but relatively low indicators of digital skills and use of Internet technology to improve living standards and quality of life. At the same time, evaluating the effectiveness of the use of the Internet by the public as a crucial information and communication network is becoming increasingly important. "Those who function better digitally and participate more fully in digital social life enjoy a competitive advantage" (Robinson et al. 2015), which can lead to increasing social inequalities.

Markers of social status, such as income and education, are found to affect the quality of Internet use. People with higher social status are more likely to have access to the Internet and use it more effectively (Witte and Mannon 2010). Educated and affluent users will become even better at realising their potential, while people with low income and education will fall further and further behind in using digital technology effectively, falling victim to fraud, cybercrime, receiving unfavourable or imposed services, etc. According to Hargittai and Hsieh (2013), social inequalities would decrease if people with lower social status used the Internet in more useful ways.

In this paper, the authors set out to develop and test a methodology for measuring the third level of the digital inequality, suitable for research at the regional level, namely the use of the Internet to produce tangible results in real life through access to technology.

There is currently no generally accepted methodology for assessing the third level of the digital inequality. While official statistics, such as broadband access or the proportion of the population using the Internet to interact with public authorities, are collected for the first and second level assessments, difficulties arise in assessing the effectiveness of digital technologies in improving quality of life. The main question before us, then, is not whether people use the Internet, but how people use it and, ultimately, with what benefit to real life.

Most of the existing studies on the third level of the digital inequality use a sociological approach. Surveys investigate existing factors such as education, interests or social connections, determine how people interpret new technologies such as the Internet (Zillien 2009) and how they integrate them into their daily lives. However, the more common internet-based surveys are affected by the digital inequality. Representativeness is a key issue: differences in connectivity, skills and use of social media are directly linked to the level of digital inequality (Robinson et al. 2015).

For country-level studies, a computerized telephone survey is currently considered the most reliable. For example, the Media Change and Innovation Division of the Institute of Mass Communication and Media Research at the University of Zurich conducted three nationally representative surveys — in 2011 (Latzer et al. 2012), 2013 (Latzer et al. 2013) and 2015 (Latzer et al. 2015). The surveys used telephone interviews, which also made it possible to interview non-Internet users. Samples were drawn based on age, gender, region and employment. However, these kinds of surveys are complicated by the complexity of their organization and the cost of conducting the survey. There is little comparability with other countries, as survey standards may differ.

With the development of communication studies, the use of techniques such as text mining and network analysis in the study of the digital inequality is spreading (Berry et al. 2011).

Traditional survey-based analysis remains fundamental to research on the digital inequality, and new methods of

big data analysis face many challenges, but nevertheless they promise valuable additional information and are likely to be used more frequently in future research. Internet services, including search engines and social media, have made vast amounts of previously unavailable or unrecorded data available to researchers (Boyd and Crawford 2012). New possibilities for content analysis of Internet resources, search engine analysis and social media analysis have emerged. However, working with such data still has several limitations. Major platforms whose data analysis would be as representative as possible (e.g., Facebook and Twitter) restrict access to their data. Their user agreements limit content collection and transactional data is rarely shared with researchers (Boyd and Crawford 2012).

As can be seen from the papers examples, there is currently an acute lack of methodologies that can quickly, inexpensively (social surveys are one of the most expensive methods of researching the digital inequality) and consistently portray a spatial picture of the third-level digital inequality.

MATERIALS AND METHODS

In this paper, we demonstrate the testing of our developed method for spatial estimation of the third level of digital inequality on a regional scale by analyzing the popularity of Google search queries. We have chosen this search engine because it is the most popular in the world (92% of market in September 2020 according to Search Engine Market Share Worldwide (2022) and in Russia (55,5% according to LiveInternet Site Rating (2022). Tools for analyzing and visualizing search engine statistics are provided by the free online service Google Trends. Data from this service is increasingly being used in various fields of science. In recent years, many papers have been published that use Google Trends to explore public interest in certain socially relevant topics. For example, environmental protection (McCallum and Bury 2014) or unemployment (Yurevich and Akhmadeyev 2021). The service is also used to make predictions ranging from the spread of epidemics (Sulyok et al. 2021) to the results of presidential elections (Granka 2013).

Google Trends works as follows: entering a query (a single word or a group of words) into the search bar, the service generates a report on the search activity in Google for this query, which includes information on the dynamics of popularity of the query in the world or in the selected country during a selected period of time since 2004, as well as the rating of countries or regions of the selected country by the level of popularity of the query. The popularity of a query in Google Trends is a relative value that describes the share of a given query among all search queries for a selected period in a selected territory.

Some queries are recognized by Google Trends as topics. According to the service's support description (https://support.google.com/trends/), topics are the result of an automated classification of thematically related queries in all languages. For example, the most closely related queries to the topic of State Services in Russia are "gosuslugi", "гос услуги","услуги","госуслуги". Information on queries related to a given topic is also contained in the report. The State Services topic report for the period 2016 to 2020 is shown as an example in Figure 1. For each element of the report, tables with data on the constituent entities of the Russian Federation are available for downloading in CSV format (except for the Republic of Crimea and Sevastopol, as they are attributed to Ukraine in the Google database). The language of the report can be any language and depends on the user settings. In our case, English is selected, and the topic names are also in English, although, as mentioned above, they include queries in all the languages available on Google.

For the purposes of this study, we identified three categories of search query topics corresponding to users' areas of interest associated with different types of digital use and impact on quality of life. It is assumed that users' search queries reflect their main patterns of Internet use. People with higher education and income are more likely to use information technology for information, education, work and career purposes, while people with lower education and income mainly use apps for entertainment, chatting, social networking or simple communication (Zillien and Hargittai 2009; Tsetsi and Reins 2017). Van Deursen and Helsper (2015) analyzed papers on Internet use and identified the main categories of positive use:

- economic use associated with trade;
- economic use associated with labour;
- social use;
- use for educational purposes;
- use for political purposes;
- use of public institutions;
- use of medical facilities.

Other data supports this assumption, for example showing that people with higher levels of education benefit more economically, institutionally, and educationally from the Internet than less educated users.

Based on the research described above, we have divided Google users' search queries into conditionally positive and conditionally negative queries. The former reflect the effective use of digital technologies with a positive impact on the quality of life of the population. The latter point out that the use of the Internet does not have a tangible positive effect in real life (Hargittai and Hsieh 2013). For example, people who use modern technology only for entertainment purposes do not get any additional opportunities to improve their education and quality of life. Three categories of searches are thus distinguished:

- **Category 1 Everyday Services** describes the ability to use the Internet to access popular services such as banking, transport, government services, shopping and delivery of goods. It can be assumed that the higher the search interest of the queries in this category, the higher the effectiveness of the use of the Internet in this field.
- **Category 2 Education, Science and Technology,** describes the possibility of using the Internet for education and new knowledge, primarily in the fields of science and technology. We assume that the higher the search interest of the queries in this category, the higher the effectiveness of the use of the Internet in this field.
- **Category 3 Entertainment** describes the ability to use the Internet for recreational purposes: searching for films and TV series, music, video games. According to our assumption, the higher effectiveness of Internet usage may be indicated by lower values of the level of search interest in the topics of this category of queries. We have treated this category of queries as conditionally negative, as research (Van Deursen and Helsper 2018; Van Dijk, 2020) suggest that a high proportion of time on the Internet spent on entertainment reduces the effectiveness of users' use of the Internet.

Table 1 presents the query topics that we have included in the highlighted categories. Each category is made up of four component topics. In doing so, the Marketplace topic includes 4 search topics relating to popular goods delivery services. The topics were selected primarily according to their meaning, considering which are the most popular

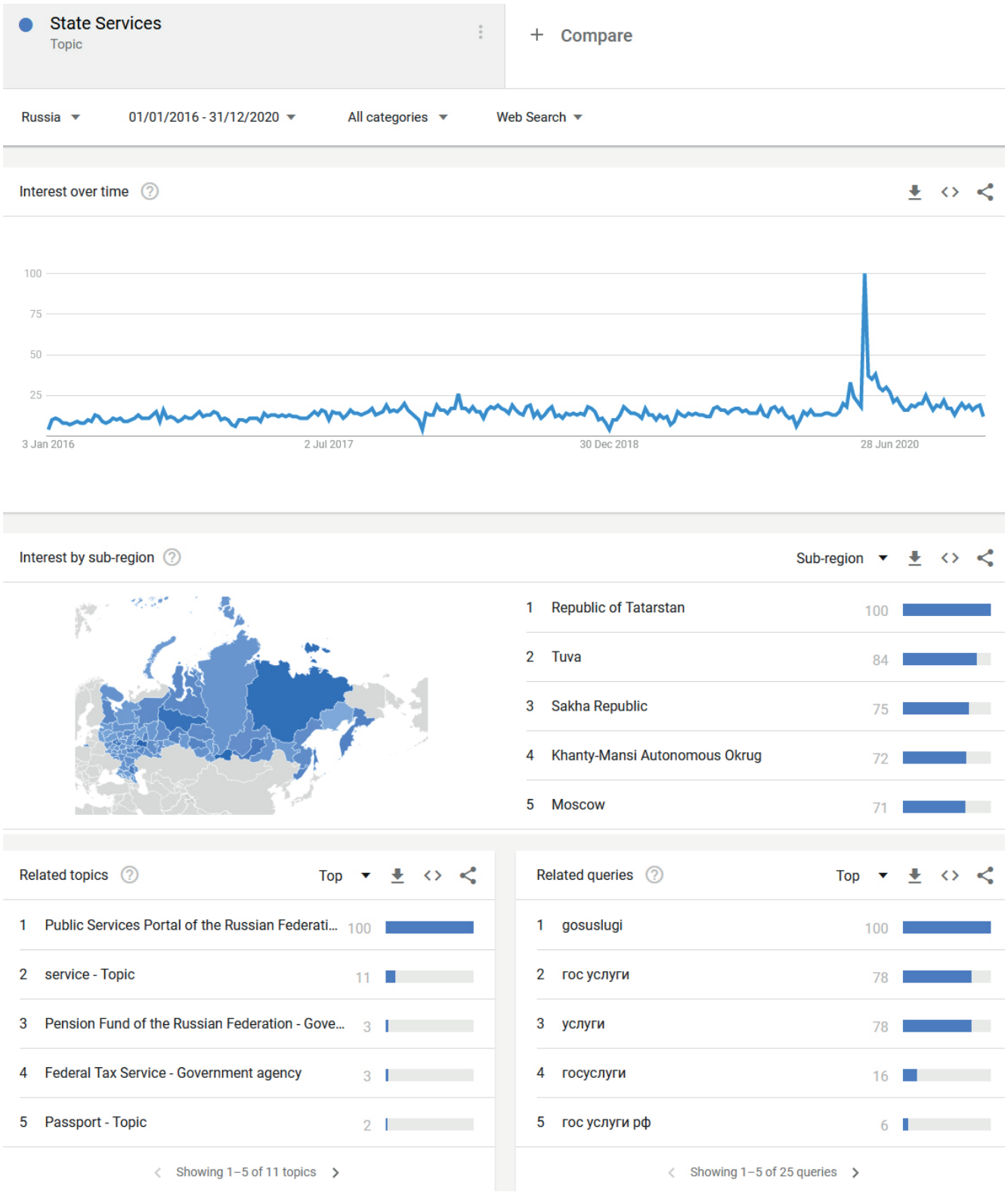

Fig. 1. Screenshot of Google Trends report on "State Services" topic

queries related to the topic, as well as the level of popularity of the topic. If the number of queries from a region is too low, statistics for that region are not calculated in Google Trends — as, for example, for the Nenets and Chukotka regions in Figure 1.

The data on search interest in all the selected topics is consolidated into a table which forms the basis for further calculations. The rows of the table correspond to the names of the constituent entities of the Russian Federation and the columns to the values of the search interest, ranging from 0 to 1. The data is collected for 2016 to 2020. Where the Google Trends report does not include data for a region due to a low number of queries, it was manually assigned the lowest available search interest value for that topic.

Three indices of search interest in each of the three thematic categories, as well as an overall index of Internet usage efficiency, were calculated based on the values obtained.

To calculate the indices of search interest in each of the three thematic categories, as well as an overall index of Internet usage efficiency, normalization (Tikunov 1997, p. 83-85) of the values obtained was carried out using formula (1):

$$\widehat{X}ij = \frac{\left| x_{ij} - \overset{o}{x}_j \right|}{\left| {}_{max/min}x_j - \overset{o}{x}_j \right|} \quad (1)$$

$$i = 1, 2, 3, \ldots, n;$$

$$j = 1, 2, 3, \ldots, m$$

where $\overset{o}{x}$ are the worst of all encountered values (for each indicator), i.e. the lowest values of search interest for category 1 and 2 topics and the highest for category 3 topics; ${}_{max/min}x$ are the values of the indicators that are most different from $\overset{o}{x}$; n is the number of territorial units (regions of Russia) under study; *m* is the number of indicators (search topics) used for the calculations (m = 4). The purpose of this normalization is translating each search interest indicator from the Google Trends report into a deviation from a given best or worst value. The resulting normalization values are restricted to a range of 0 to 1. The evaluation indices for each query category are calculated as the arithmetic average of the four normalized values included in the respective categories.

The resulting indices of search interest by thematic category were also reduced to an overall integral index of Internet usage efficiency by calculating a simple average.

RESULTS

Table 2 lists the constituent entities of the Russian Federation with maximum and minimum values of the revealed level of search interest in the studied thematic categories (let us remind that the calculations were carried out for 83 constituent entities of the Russian Federation without the Republic of Crimea and Sevastopol). Some regions appear in this table more than once. Thus, the Republic of Tatarstan is in the top 5 for search interest in "Everyday Services" and "Education, Science and Technology", while the Republics of Ingushetia and Dagestan were outsiders in the same categories, but leaders in category No. 3 "Entertainment". Moscow was among the leaders in terms of searches for services and facilities, but in last place in terms of search interest in entertainment.

In order to illustrate the results of the calculation, we also made a map illustrating the values of the integral index of Internet usage efficiency by users from different regions (Figure 2).

Table 1. Google Trends query categories selected for regional analysis of the digital inequality

Query categories	Topics in Google Trends		Popular requests from Russian users
1. Everyday Services	State Services		gosuslugi, гос услуги, услуги, госуслуги, гос услуги рф, гос услуги личный кабинет, мфц
	Transport		транспорт, транспорт онлайн, общественный транспорт, яндекс транспорт, transport, транспортные компании, как доехать
	Bank		банк, банки, сбербанк, онлайн банк
	Marketplace	Delivery	доставка, доставка еды, доставка цветов, доставка суши, пицца, delivery
		Ozon.ru	озон, ozon, озон ру, озон магазин, азон, промокод озон
		Wildberries	вайлдберриз, wildberries, вайлдберис
		AliExpress	алиэкспресс, aliexpress, алиэкспресс на русском, али
2. Education, Science and Technology	Education		образование, сетевой город образование, веб образование, электронное образование
	Technology		технологии, технология, technology, информационные технологии, новые технологии
	Research		исследования, исследование, research, методы исследования, исследовать, маркетинговые исследования, научные исследования, клинические исследования
	Science		наука, science, философия, научные статьи, экономика, министерство науки
3. Entertainment	Film		фильм, фильмы, смотреть фильм, кино, фильм онлайн, смотреть фильм онлайн, скачать фильм
	Game		игры, игра, играть, скачать игру, онлайн игры, играть онлайн, игры бесплатно
	Television series		сериал, сериалы, смотреть сериал, турецкий сериал, сериалы онлайн, русские сериалы
	Music		музыка, скачать музыку, слушать музыку, music, скачать музыку бесплатно

Table 2. Constituent entities of the Russian Federation with the highest and lowest levels of search interest on Google for topics in the selected categories

Query categories	Highest level of search interest	Lowest level of search interest
1. Everyday Services	1. Republic of Tatarstan 2. Perm Krai 3. Moscow 4. Republic of Karelia 5. Udmurt Republic	79. Republic of Dagestan 80. Primorsky Krai 81. Chechen Republic 82. Karachay-Cherkessia Republic 83. Republic of Ingushetia
2. Education, Science and Technology	1. Republic of Sakha (Yakutia) 2. Republic of Tatarstan 3. Tyumen region 4. Republic of Komi 5. Republic of Tyva	79. Krasnodar Krai 80. Republic of Dagestan 81. Karachay-Cherkessia Republic 82. Murmansk region 83. Republic of Ingushetia
3.Entertainment	1. Chechen Republic 2. Republic of Ingushetia 3. Republic of Dagestan 4. Kabardino-Balkaria Republic 5. Republic of North Ossetia-Alania	79. Moscow region 80. Nizhny Novgorod region 81. Leningrad region 82. Saint-Petersburg 83. Moscow

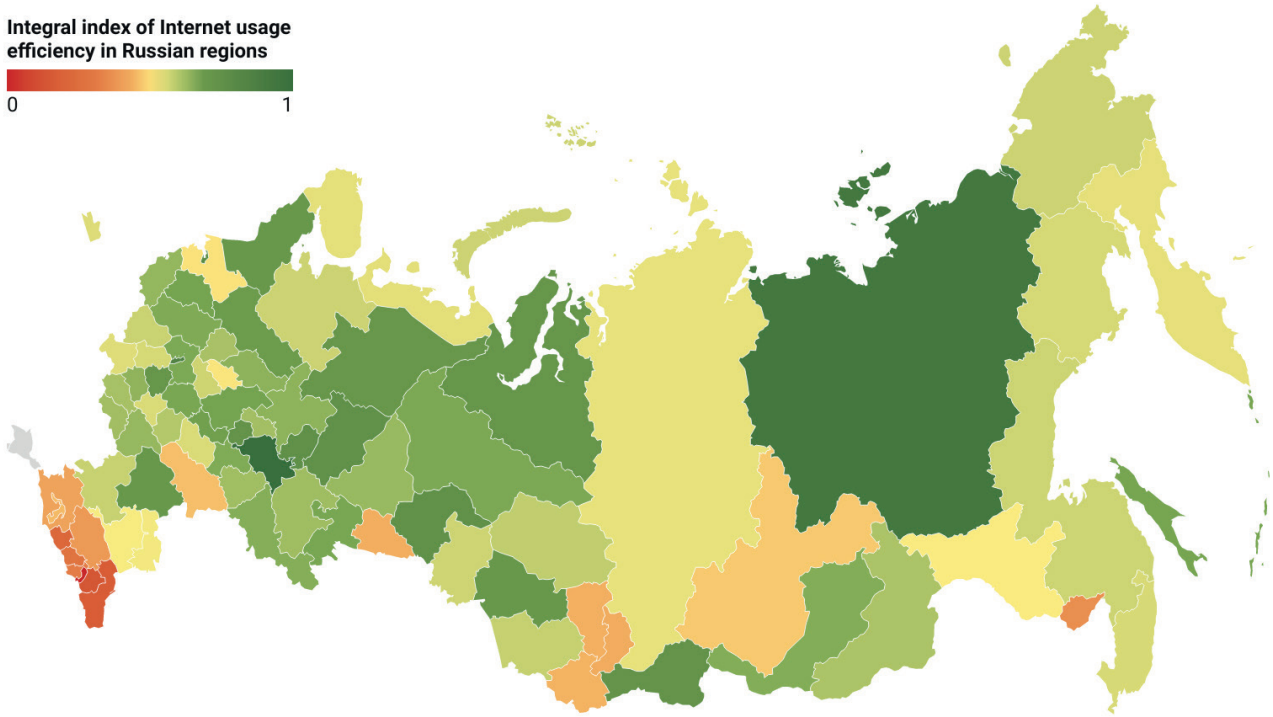

Fig. 2. Integral Index of Internet usage efficiency in Russian regions

As can be seen from the map, there are some geographical patterns in the people's use of the Internet. First of all, we see the regions in the North Caucasus for which the lowest Internet usage efficiency was identified. Search queries in this group of regions gravitate mainly towards the entertainment topics, which indirectly indicates that the Internet is little used for economically and socially useful activities.

We also found rather low Internet usage efficiency in the Siberian regions. Here, users are mostly uninterested in education and science topics and do not demonstrate a high level of use of online services. At the same time, the entertainments search rate is above average.

The Far East regions are the most diverse in terms of the resulting integral index. Here are regions with both very low (Jewish Autonomous Region) and very high (Yakutia) Internet usage efficiency.

The regions of the Urals and Central Russia demonstrate high Internet usage efficiency. Here people most often search for useful services, information for education and science. The only exception is the Kurgan region.

To verify the validity of the methodology developed, it was necessary to assess whether it reflected the correlation between Internet usage efficiency and educational attainment and income levels found in other studies of digital inequality listed before. To do this, we built two scatter diagrams. The first (Figure 3) shows on the vertical axis the share of the population with higher education (based on the 2010 census, as newer data is not available) and the second (Figure 4) shows the average per capita income for 2016-2020. Source of data in both cases was the Rosstat website rosstat.gov.ru. The horizontal axis in both diagrams shows the calculated integral index of Internet usage efficiency. The size of the circles, each corresponding to a constituent entity of the Russian Federation, is proportional to the population size.

As we can see, in both cases the scatter diagrams appear to extend from the lower left to the upper right corner of the diagram, indicating a possible direct correlation between the indicators under investigation.

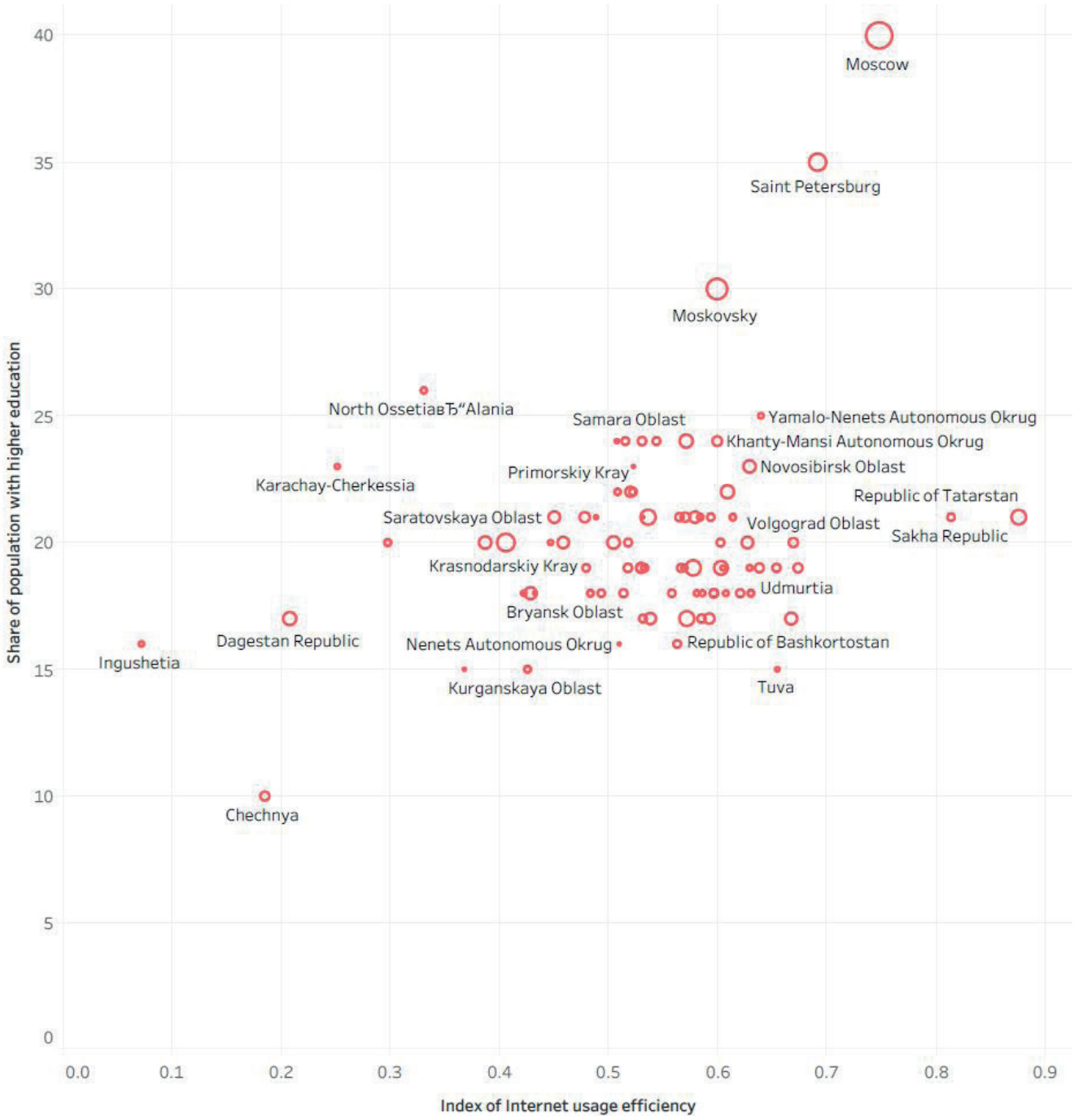

Fig. 3. Distribution of Internet usage efficiency and share of population with higher education by constituent entities of the Russian Federation

The uppermost points in Figure 3 (Moscow, Moscow region and St. Petersburg) are characterized by high levels of educational attainment and Internet usage efficiency. The Republics of Ingushetia, Chechnya, and Dagestan, on the other hand, are characterized by low Internet usage efficiency, combined with a low proportion of people with higher education.

Figure 4 highlights the sparsely populated oil and gas producing regions with high average per capita incomes: Yamalo-Nenets, Nenets, and Chukotka Autonomous Districts. They combine very high revenues with medium Internet usage efficiency. Another group of locations is in the Far East: Sakhalin Region, Magadan Region, and Kamchatka Krai. Here higher average per capita income is combined with a high cost of living, and the Internet usage efficiency index is medium. The Republics of Tatarstan and Sakha (Yakutia) have high rates of Internet usage efficiency and medium level of income. The republics of the North Caucasus are characterized by both low income and low Internet usage efficiency.

DISCUSSION

Research on the geography of digital inequality is currently limited and in need of further methodological development. The study of digital inequality cannot be limited to simply examining differences in Internet access between different population groups. It is also important to consider the inequalities caused by certain groups' lack of skills in using modern technology and applying it to improve their standard of living and quality of life. Digital inequality can have significant consequences for social and economic mobility, as well as for social cohesion and democratic participation. It is crucial for policy makers, businesses, and other stakeholders to address these issues and work towards reducing digital inequality.

Differences in specific online activities — learning, receiving services, having fun — are mainly explained by users' interests, as well as available online skills, which, in turn, depend on social standing. Differences in the purposes

Fig. 4. Distribution of Internet usage efficiency average living wage adjusted income by constituent entities of the Russian Federation

for which the Internet is used tend to further exacerbate social inequalities. People who use modern technology only for entertainment purposes do not get any additional opportunities to improve their education and quality of life (e.g., to improve their health by getting timely medical advice online, which is especially relevant in a pandemic). The study reveals territorial aspects of Internet usage patterns at the level of constituent entities of the Russian Federation, expressed in differences in Google search interest in the topics we selected as digital inequality markers.

The values of the calculated integral index of Internet usage efficiency were mapped. We demonstrated that the Internet usage efficiency indicator is likely to have a direct correlation with the income level of the population and the level of education, which is consistent with the known global research on the digital inequality.

This method has several benefits. First, it is quick and easy to implement. By using Google Trends, researchers can easily access and analyze large amounts of data on internet search patterns. Second, it is cost-effective, as it does not require expensive phone surveys or other resources to collect data. Finally, it can be used to compare internet usage patterns across different regions, making it useful for international comparisons. However, it is important to note that this method does have limitations.

Relying on Google Trends data may introduce bias, as not all internet users use Google as their search engine. This means that the results may not accurately represent the internet usage patterns of the entire population. The method only considers the popularity of certain search queries and does not consider the frequency or duration of internet usage, or the specific websites or services accessed. The method only considers internet usage at a regional level and does not consider individual-level factors that may influence internet usage patterns, such as age, education, or income.

CONCLUSIONS

The study demonstrates the potential for spatial estimation of third-level digital inequality by analyzing Google search queries. The results revealed geographical patterns in Internet usage efficiency in the constituent entities of the Russian Federation, with regions in North Caucasus and Siberia showing low efficiency and regions in the Urals and Central Russia showing high efficiency. The study highlights the importance of not only considering differences in Internet access, but also the lack of skills in using technology among certain groups.

The method used in this study has several benefits, including its speed, cost-effectiveness, and ease of implementation. However, it is important to note that the method has limitations and may introduce bias by relying on Google Trends data.

The findings of this study have important implications for public policy, businesses, and other stakeholders in addressing digital inequality. The study recommends that efforts to reduce digital inequality should not be limited to providing equal access to the Internet but should also include measures to improve digital literacy and the potential for users to realize their full potential online.

The study's results and methodology can contribute to the development of the Russian scientific community's understanding of digital inequality and its spatial characteristics. Further research is needed to refine the methodology and expand its application to other regions and countries. The study provides valuable insights into the geography of digital inequality and can inform the development of targeted interventions to reduce this inequality and promote digital inclusion for all.

REFERENCES

Avraamova E. and Vershinskaya O. (2001). Home computer as a resource of socio-economic adaptation. Information Society, 5, 44-49 (in Russian).

Berry J., Poortinga Y., Breugelmans S., Chasiotis A. and Sam D. (Eds.) (2011). Cross-cultural psychology. Cambridge, UK: Cambridge University Press., 652, DOI: 10.1017/cbo9780511974274.

Boyd D. and Crawford K. (2012). Crititcal questions for big data: Provocations for a cultural, technological, and scholarly phenomenon. Information, Communication & Society, 15(5), 662-679, DOI: 10.1080/1369118x.2012.678878.

Drori G. (2010). Globalization and technology divides: Bifurcation of policy between the "digital divide" and the "innovation divide". Sociological Inquiry, 80(1), 63-91.

Du H., Zhou N., Cao H., Zhang J., Chen A. and King R. (2021). Economic Inequality is Associated with Lower Internet Use: A Nationally Representative Study. Social Indicators Research, 155(3), 789-803, DOI:10.1007/s11205-021-02632-8.

Gladkova A., Vartanova E. and Ragnedda M. (2020). Digital divide and digital capital in multiethnic Russian society. Journal of Multicultural Discourses 15(2), 126-147, DOI: 10.1080/17447143.2020.1745212.

Granka L. (2013). Using online search traffic to predict US presidential elections. PS: Political Science & Politics, 46(2), 271-279.

Hargittai E. and Hinnant A. (2008). Digital inequality: Differences in young adults' use of the Internet. Communication Research, 35(5), 602-621.

Hargittai E. and Hsieh Y. (2013). Digital inequality. The Oxford handbook of Internet studies. Oxford, UK: Oxford University Press. 129-150, DOI: 10.1093/oxfordhb/9780199589074.013.0007.

Hoffman D. and Novak T. (1998). Bridging the Racial Divide on the Internet. Science, 280(5362), 390-391.

International Telecommunication Union (2019). Measuring digital development: Facts and figures 2019. Geneva: ITU Publications, 2019. 11 p. [online] Available at: https://www.itu.int/en/ITU-D/Statistics/Documents/facts/FactsFigures2019_r1.pdf [Accessed 25 Apr. 2022].

Internet World Stats (2022). [online] Available at: https://www.internetworldstats.com/stats.htm [Accessed 25 Apr. 2022].

ITU. Measuring the information society. (2011). Geneva: [online] Available at: http://www.itu.int/en/ITU-D/Statistics/Pages/publications/mis2011.aspx [Accessed 25 Apr. 2022].

Latzer M., Just N., Metreveli S. and Saurwein F. (2012). Internetverbreitung und digitale Bruchlinien in der Schweiz [Internet diffusion and digital divides in Switzerland]. World Internet Project – Switzerland 2011 Report, University of Zurich, Zurich, Switzerland. (in German).

Latzer M., Just N., Metreveli S. and Saurwein F. (2013). Internetverbreitung und digitale Bruchlinien in der Schweiz [Internet diffusion and digital divides in Switzerland]. World Internet Project – Switzerland 2013 Report, University of Zurich, Zurich, Switzerland. (in German).

Latzer M., Büchi M. and Just N. (2015). Internetverbreitung und digitale Bruchlinien in der Schweiz [Internet diffusion and digital divides in Switzerland]. World Internet Project – Switzerland 2015 Report, University of Zurich, Zurich, Switzerland. (in German).

LiveInternet Site Rating (2022). [online] Available at: http://www.liveinternet.ru/stat/ru/searches.html?slice=ru;period=week [Accessed 11 Apr. 2022] (in Russian).

McCallum M. and Bury G. (2014). Public interest in the environment is falling: a response to Ficetola (2013). Biodiversity and conservation, 23(4), 1057-1062.

Norris P. (2001). Digital divide: civic engagement, information poverty, and the Internet worldwide. New York: Cambridge University Press, 303 p.

Novak T. and Hoffman D. (2000). Bridging the Digital Divide: The Internet of Race on Computer Access and Internet Use. [online] Available at: http://www2000.ogsm.vanderbilt.edu/digital.divide.html [Accessed 11 Apr. 2022].

OECD, Understanding the Digital Divide (2001). [online] Available at: http://www.oecd.org/dataoecd/38/57/1888451.pdf [Accessed 11 Apr. 2022].

Peter J., and Valkenburg P. (2006). Adolescents' Internet use: Testing the "disappearing digital divide" versus the "emerging digital differentiation" approach. Poetics, 34(4-5), 293-305.

Robinson L., Cotten,S., Ono H., Quan-Haase A., Mesch G., Chen W., et al. (2015). Digital inequalities and why they matter. Information, Communication & Society, 18(5), 569-582, DOI:10.1080/1369118x.2015.1012532.

Search Engine Market Share Worldwide. (2022). StatCounter Global Stats [online] Available at: https://gs.statcounter.com/search-engine-market-share. [Accessed 11 Apr. 2022].

Strover S. (1999). Rural Internet Connectivity. Columbia, MO: Rural Policy Research Institute. 19.

Sulyok M., Ferenci T. and Walker M. (2021). Google Trends Data and COVID–19 in Europe: Correlations and model enhancement are European wide. Transboundary and Emerging Diseases, 68(4), 2610-2615.

Tikunov V.S. (1997). Modeling in cartography. Moscow: MSU Publishing House, 405. (in Russian).

Tsetsi E. and Reins S. (2017). Smartphone Internet access and use: Extending the digital divide and usage gap. Mobile Media & Communication, 5(3), 239-255, DOI: 10.1177/2050157917708329.

Van Dijk J. (2012). The evolution of the digital divide: The digital divide turns to inequality of skills and usage. Digital enlightenment yearbook. Amsterdam: IOS Press, 57-75.

Van Deursen A. and Helsper E. (2015). The third-level digital divide: Who benefits most from being online? Communication and information technologies annual, 10, 29-52. [online] Available at: http://doc.utwente.nl/97634/1/CH002.pdf [Accessed 11 Apr. 2022].

Van Deursen A. and Helsper E. (2018). Collateral benefits of Internet use: Explaining the diverse outcomes of engaging with the Internet. New Media & Society, 20(7), 2333-2351, DOI: 10.1177/1461444817715282.

Van Dijk J. (2020). The Digital Divide. Cambridge UK, Medford MA USA: Polity Press. 208.

Wilhelm A. and Thierer A. (2000). Should Americans be Concerned about the Digital Divide? Insight on the News, 16(33), 40-42.

Witte J. and Mannon S. (2010). The Internet and social inequalities. New York, NY: Routledge. 192.

Yudina M. (2020). The impact of digitalization on social inequality. Standard of living of the population of the regions of Russia, 16(1), 97-108. (in Russian with English summary), DOI: 10.19181/lsprr.2020.16.1.10.

Yurevich M. and Akhmadeev D. (2021). Possibilities of forecasting the unemployment rate based on the analysis of query statistics (in search engines). Terra Economicus. 19(3), 53-64. (in Russian with English summary), DOI: 10.18522/2073-6606-2021-19-3-53-64.

Zemtsov S.P. and Baburin V.L. (2017). Modeling of diffusion of innovation and typology of Russian regions: a case study of cellular communication. Izvestiya Rossiiskoi Akademii Nauk. Seriya Geograficheskaya, 4, 17-30. (in Russian with English summary), DOI: 10.7868/S0373244417100024.

Zemtsov S.P., Demidova K.V. and Kichaev D.Yu. (2022). Internet diffusion and interregional digital divide in Russia: trends, factors, and the influence of the pandemic. Baltic Region, 14(4), 57-78, DOI: 10.5922/2079-8555-2022-4-4.

Zillien N and Hargittai E. (2009). Digital distinction: Status–specific types of internet usage. Social Science Quarterly, 90(2), 74-291, DOI: 10.1111/j.1540-6237.2009.00617.

Zillien N. (2009). Digitale Ungleichheit: Neue Technologien und alte Ungleichheiten in der Informations-und Wissensgesellschaft [Digital inequality: new technologies and old inequalities in the information and knowledge society]. Wiesbaden, Germany: Springer, 2nd ed. (in German).

RESEARCH PAPER

HUMAN-INDUCED LANDSCAPE ALTERATION IN THE COASTAL REGULATION ZONE OF GOA, INDIA, FROM 2000 TO 2017

Tanvi Deshpande[1*], Sudhakar Pardeshi[2]

[1] Assistant Professor in Geography incl. EVS, Rosary College of Commerce & Arts, Navelim, Margao, Goa, India.

[2] Professor, Department of Geography, Savitribai Phule Pune University, Pune, Maharashtra, India.

***Corresponding author:** tanvi@rosarycollege.org

Received: August 10th, 2021 / Accepted: February 15th, 2023 / Published: March 31st, 2023

https://DOI-10.24057/2071-9388-2021-093

ABSTRACT. In Goa, the tourism industry is the major cornerstone of the economy. With the increasing number of tourists along the coastal areas, more tourism-related infrastructure is emerging within the Coastal Regulation Zone. The sensitive and fragile coastal zones are being covered by concrete structures and the coastal environment becomes vulnerable to degradation. The objective of the paper was to study the changes in landuse and landcover in the Coastal Regulation Zone of Salcete taluka using remote sensing data and geospatial techniques. To fulfill the objective, both primary and secondary data were used. Primary data was based on personal observations and field visits while secondary data consisted of topographic maps, LANDSAT 7 ETM, and LANDSAT 8 satellite images, which were processed and analyzed using ArcGIS 10.3, ERDAS IMAGINE 2014, SAGA (System for Automated Geoscientific Analyses) and MS Excel. From the landuse and landcover analysis for a period of 17 years (2000-2017), it was found that the land cover within the CRZ underwent a tremendous change with the increase in tourism activity and related infrastructure. The analysis revealed that the agricultural area has decreased, whereas built-up areas, barren land, and vegetation area increased. The change detection analysis using SAGA software allowed to understand the conversion between different classes. The study revealed that the increasing number of tourists and tourism activities along the Salcete Coast is deteriorating the environmental setup and disturbing the inherent coastal landscape.

KEYWORDS: Coastal Regulation Zone (CRZ), Landuse and landcover (LULC), Salcete

CITATION: Deshpande T., Pardeshi S. (2023). Human-Induced Landscape Alteration in the Coastal Regulation Zone of Goa, India, from 2000 to 2017. Geography, Environment, Sustainability, 1(16), 36-44
https://DOI-10.24057/2071-9388-2021-093

ACKNOWLEDGEMENTS: My sincere thanks to the Department of Geography, Savitribai Phule Pune University, and to Ms. Pallavi Kulkarni, Ms. Ashwini Lanke, Mr. Vishal Doke for their support received during the completion of this work.

Conflict of interests: The authors reported no potential conflict of interest.

INTRODUCTION

A coastal zone is an area of interface between the land and the sea (Panigrahi and Mohanty 2012). Coastal zones are the most biologically productive regions and form an important component of the global biosystem (Yagouband Kolam 2006). Coastal zones have a high environmental, economic, and social value (Ramesh and Vel 2011). Moreover, the coasts have played an eminent role in economic growth over the years, but over-dependence and various human activities have led to the unsustainable management of coastal ecosystems (Chinnasamy and Parikh 2020).

In recent times, human interference in coastal areas has increased, leading to the major degradation of the fragile coastal environment. Approximately 50% of the world's population resides in coastal zones which puts them under very high stress from population growth, pollution, and over-exploitation of resources (Shi et al. 2001). Zahedi (2008) observed that with the ever-increasing pressure on the coastal belt, and as more people are moving towards the coast, the conditions of beaches are worsening. The population growth along the Indian coasts is also rapidly rising, resulting in a negative impact on land due to the spread of built-up areas, settlements, and recreational facilities (Kaliraj et al. 2017). Development along the coasts is taking place in an uncoordinated and unsustainable manner thereby degrading the coastal environment (Panigrahi and Mohanty 2012).

The Ministry of Environment and Forests (MoEF) passed legislation called the Coastal Regulation Zone (CRZ) notification issued under the Environment Protection Act of 1986. The 2011 notification defines the CRZ as the area from the high tide line (HTL) to 500 m on the landward side, and from the HTL to 100 m or width of the creek, whichever is less, on the landward side of tidally-influenced water bodies connected to the sea (Coastal Regulation Zone (CRZ) Notification, 2011). There are four categories of CRZ, namely CRZ I (Ecologically Sensitive Area), CRZ II (Built-up areas), CRZ III (Rural areas), and CRZ IV territorial waters and tidally-influenced water bodies (Chouhan et al. 2017).

The main purpose of issuing the CRZ notification was to control and minimize the increasing anthropogenic activities and protect the coastal environment from hap-hazardous development and human interference (Mascarenhas 1999).

However, Nayak (2017) stated that coastal regulation has undergone immense changes over the last 25 years, mostly due to incorrect interpretation of the High Tide Line and conflicting laws of the State and Central governments.

Goa, a small coastal State located on the western coast of India is known worldwide as a tourist destination because of its scenic nature and cultural hospitality. Tourism is the fastest-growing industry in the State and is also the backbone of the State's economy. According to the Department of Tourism, Government of Goa website (2018), in the year 1985, 775,212 tourists (682,545 domestic and 92,667 foreign) visited Goa, which increased to 7,785,693 (6,895,234 domestic and 890,459 foreign) in 2017. To provide tourists with basic recreational facilities, many coastal zones in Goa were encroached upon by unplanned built-up areas. With the rise in tourism, many eco-sensitive zones were disturbed and most of the land is under reclamation for recreational purposes.

The present study was carried out with the aim to understand the human-induced landscape alteration in the Coastal Regulation Zone of Salcete taluka. The objective of the paper was to study the changes in land use and land cover in this area using remote sensing data and geospatial techniques.

Landuse and landcover conversion refers to the process of transformation of land cover to land use and change in land use from one type to another due to natural or anthropogenic activities (Kaliraj et al. 2017). Butt et al. (2015) stated that it is essential to study and analyze these changes to better understand the relationship between human activities and natural phenomena. The factors influencing land use and land cover changes should be studied in order to understand and assess environmental impacts and plan for sustainable development (Waiyasusri and Chotpantarat 2022). According to Berlanga-Robles and Ruiz-Luna (2011), landuse and landcover changes are responsible for a 35-50% loss of coastal wetlands. Landuse and landcover change detection has become a necessity for developing efficient strategies for managing natural resources, monitoring environmental changes, and planning policies in various coastal areas (Muttitanon and Tripathi 2005; Kaul and Ingle 2012; Islam et al. 2016).

Remote sensing and Geographic Information Systems (GIS) provide efficient tools for ecosystem and socio-economic management (Haque and Basak 2017). Misra and Balaji (2015) stated that these tools provide a unique opportunity for building information sources and supporting decision-making activities for various coastal zone applications. Remote sensing data is a very useful source of information as it provides up-to-date and complete coverage of any area and is proven to be useful in assessing and monitoring land use and landcover changes (Muttitanon and Tripathi 2005). In order to manage and protect the coastal environment from further exploitation, landuse and landcover changes must be studied.

Study Area

This study focused on the coastal areas of Salcete taluka, which is a sub-division of the South Goa district in the Indian state of Goa. Salcete taluka is located at 15° 12′ 44.82″ N and 74° 4′ 23.628″ E, and its coastal area occupies about 27 km of straight continuous beach strip and numerous sand dunes along the Arabian Sea, with Utorda beach in the north and Betul Beach at the mouth of the Sal River in the south. The Salcete taluka consists of ten major beaches, namely Utorda, Majorda, Betalbatim, Colva, Sernabatim, Benaulim, Varca, Cavelossim, Mobor, and Betul, along with other small beaches such as Carmona and Fatrade (Fig. 1).

Compared to the coastal region of North Goa, the beaches of South Goa are less exploited. However, with the increasing tourism trend and popularity of the destination, exploitation is likely to increase at a tremendous rate in the coming years. Therefore, the coastal area of Salcete taluka was selected to understand its present coastal environmental issues.

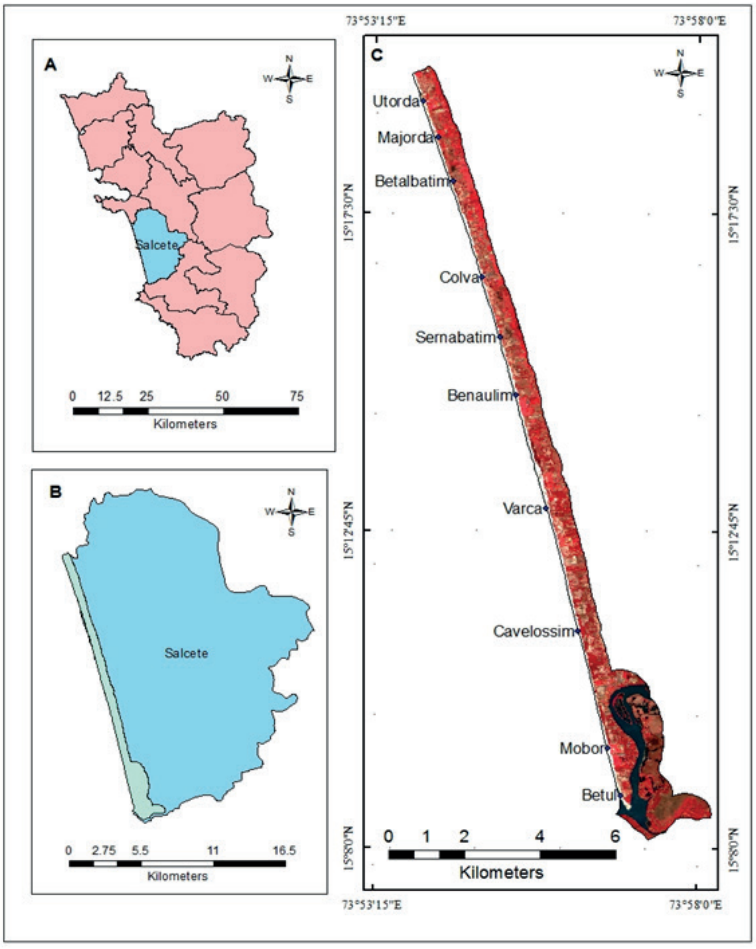

Fig. 1. Location of the study area

MATERIALS AND METHODS

The present study required digital spatial data, which was processed using ArcGIS 10.3, SAGA (System for Automated Geoscientific Analyses), and ERDAS IMAGINE 2014 software. Most of the present study was based on secondary data, particularly the satellite images of LANDSAT 7 ETM and LANDSAT 8 of the year 2000 and 2017 with a 30 m resolution, as well as Survey of India (SOI) topographic maps of 1:50,000 scale. LANDSAT satellite images were used to classify and map landcover changes using geospatial techniques. The change detection was carried out using ERDAS IMAGINE 2014 and SAGA software. Fig. 2 represents the detailed methodology chart, which was followed to carry out the study. LANDSAT images were downloaded from the United States Geological Survey (USGS) website. Table 1 displays the data derived and used for the analysis.

The toposheets were georeferenced to extract the high tide line and use it for creating a buffer of 500 m, which demarcates the extent of the Coastal Regulation Zone of Salcete taluka.

Image processing and stacking were done in ERDAS IMAGINE 2014 software. The images were classified into seven classes, namely sand, agricultural land, barren land, vegetation, water bodies, fallow land, and built-up areas. The spectral signature files were developed for each class to be later used for image classification. The analysis of landuse and landcover changes was performed using the Supervised Classification method with training samples for a more accurate result. Supervised Classification requires preceding knowledge of the study area and involves choosing representative training pixels from a pre-defined classification scheme that will be used with a decision rule (Misra et al. 2015).

Maximum Likelihood Classifier (MLC) algorithm was employed to identify the land cover types in ERDAS IMAGINE 2014. This technique works with the hypothesis of assigning each pixel to the class for which it has the maximum likelihood probability (Ayele et al. 2018). Accuracy assessment, or validation, now has become an integral constituent in incorporating remotely sensed data (Congalton 2001). The results of the land use and land cover change analysis, produced using the Supervised Classification method, are presented with the Overall Accuracy and Kappa coefficients. The values obtained from the accuracy assessment performed using ERDAS IMAGINE validated the output of landuse and landcover classification. For both time periods, more than 75% accuracy was achieved. The data from classified images was processed and analyzed using Microsoft Excel, which included the calculation of the area for each class and preparation of graphs for comparison and understanding of the changes.

SAGA software was used to detect the changes. SAGA offers a large number of scientific methods and tools for processing remote sensing data, including geometrical preprocessing and spectral filtering techniques, supervised and unsupervised classification algorithms, as well as methods for change detection and segmentation for object-oriented image analysis (Conrad et al. 2015). The classified images were given as input in SAGA to identify the changes. The results were mapped using GIS.

Table 1. Data sources and the derived data

Sr. no.	Data source	Data derived
1.	SOI toposheet 48 E/15 , 48 E/16 (1:50,000)	High tide line
2.	LANDSAT 8 image (March, 2017) LANDSAT 7 ETM (March, 2000)	LULC, Change detection using SAGA software

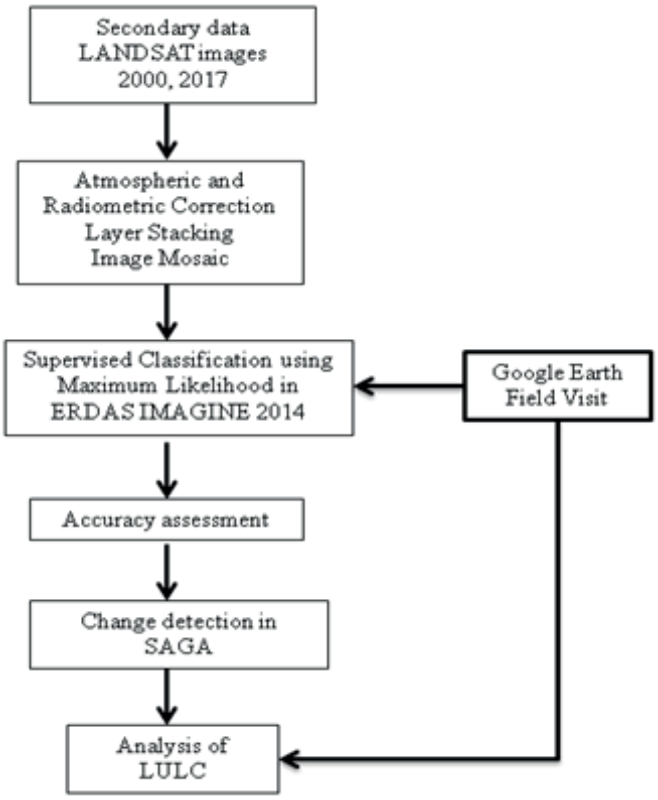

Fig. 2. Methodology Chart

RESULT AND DISCUSSION

Landuse and landcover analysis

Landuse and landcover are dynamic in nature and are affected by both natural and human factors (Dewan et al. 2010). The study of landuse and landcover allows to understand the impact of human interference in the coastal environment. With the increase in the need and greed of human beings, the rate of environmental exploitation has also increased. According to Fabbri (1998), coastal zones have been exploited by man to a greater extent for the growth of industry, resource extraction, tourism, and urbanization, which led to the flourishing of coastal economies.

The unplanned and hap-hazardous development of the tourism industry leads to negative land use and land cover transformations resulting in ecological imbalance and degradation (Saha and Paul 2020). Similar problems have been observed along the coastal region of Salcete taluka with the increase in tourism and development activities. Most of the development activities are directly related to tourism and alter the existing state of landuse and landcover in the coastal region. After all, coastal tourism is growing at a very rapid rate, and so is the hap-hazardous and unplanned development.

The land use and land cover change analysis is incomplete without the accuracy assessment of the classified image (MohanRajan et al. 2020). The result of the accuracy assessment for the classified LANDSAT images showed an overall accuracy of 95.65% and 96.67%, and an overall Kappa coefficient of 0.94 and 0.95 for the years 2000 and 2017, respectively. Remote sensing has given the opportunity to study the dynamics of long-term change in landuse and land cover (Rahman et al. 2017). The long-term change assessment of the coastal regulation zone of Salcete taluka was performed using LANDSAT images for a period of 17 years, from 2000 to 2017. Fig. 3 represents the land use and land cover maps based on supervised classification for these years, while the area distribution for each class is presented in Table 2.

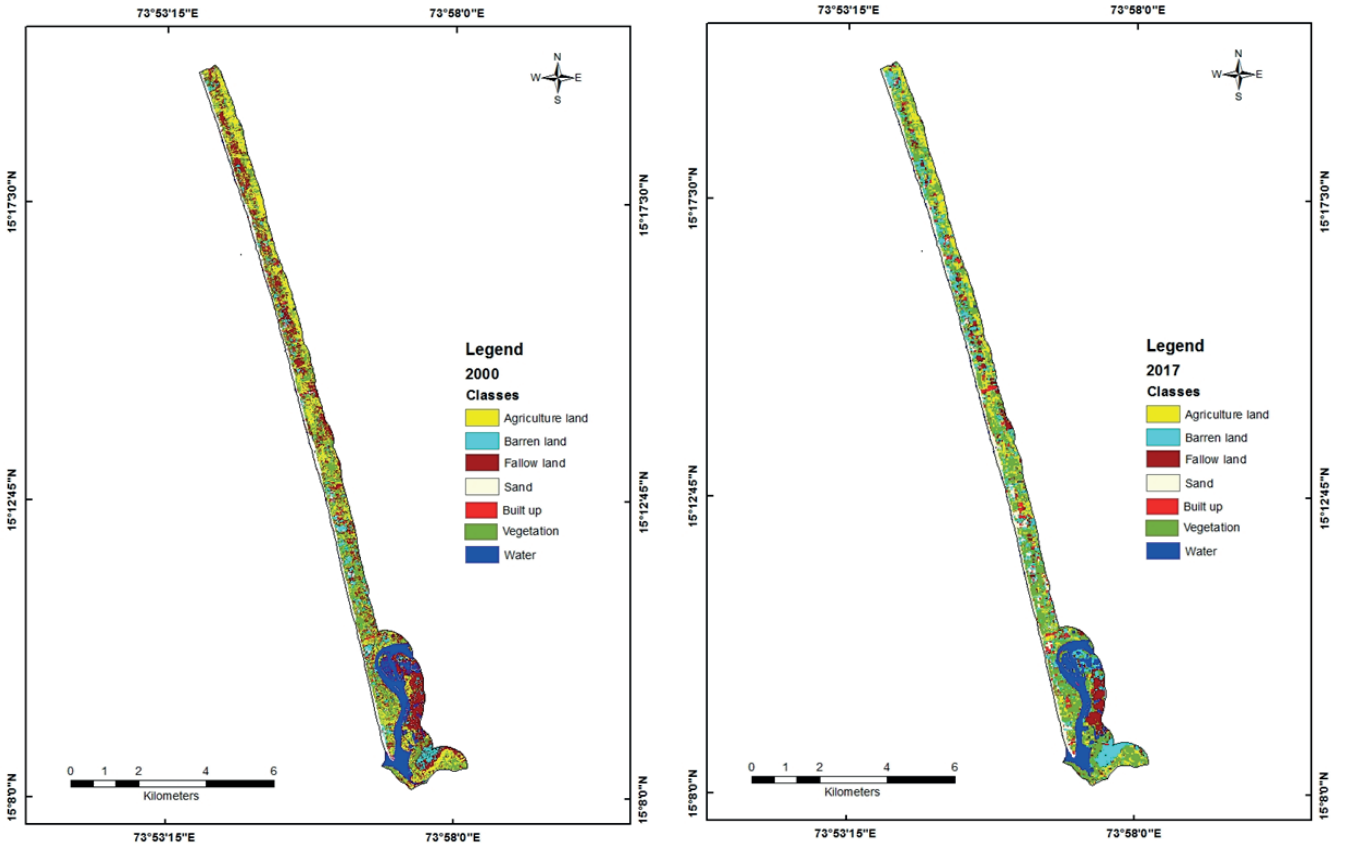

Fig. 3. Land use and land cover maps of 2000 and 2017

Table 2. Land use and land cover data for the years 2000 and 2017

Classes	2000 Area (km^2)	2000 Area%	2017 Area (km^2)	2017 Area%	Change difference (%)
Agricultural land	2.99	17.18	1.73	9.94	-7.24
Barren land	3.21	18.45	3.35	19.25	0.8
Fallow land	1.49	8.56	1.72	9.89	1.33
Sand	1.26	7.24	1.29	7.41	0.17
Built-up area	0.39	2.24	0.59	3.39	1.15
Vegetation	6.29	36.15	6.99	40.17	4.02
Water	1.77	10.17	1.73	9.94	-0.23
Total	17.40	100	17.40	100	-

From the analysis of supervised classification data, it was found that land features underwent tremendous changes under the impact of both natural and anthropogenic factors. The comparative analysis of the years 2000 and 2017 presented in Fig. 4 shows that there was a decrease in agricultural land (from 17.18% in 2000 to 9.94% in 2017) and consequently an increase in fallow land from 8.56% in 2000 to 9.89% in 2017. The drastic change in the area of agricultural land can be highly associated with the changes in the occupational patterns amongst the locals as many of them gave their lands for the development of tourist infrastructure and got involved in tourism activities themselves.

Infrastructure development is the base of the tourism industry. It usually gets boosted to attract more tourists, and when a place gets popularized, to accommodate more tourists, even more large-scale infrastructure development takes place. A similar development pattern is observed in the coastal region of Salcete taluka, with Colva, Benaulim, Majorda, and Cavelosim being the most crowded beaches, receiving a large number of visitors every year. With the increasing tourism activity, built-up areas in the forms of resorts, beach shacks, restaurants, recreational parks, parking spaces, etc. increased from 2.24% in 2000 to 3.39 % in 2017. Various permanent and temporary structures were established on the sand dunes, such as roads, resorts, hotels, parks, etc.

There was also an increase in the area of barren land. In the year 2000, barren land covered 18.45% of the area, which increased up to 19.25% by 2017. However, there has been a small amount of change for sand (7.24% in 2000 and 7.41% in 2017) and water (10.17 % in 2000 to 9.94 % in 2017). On the contrary, the area of vegetation has increased from 6.29 km^2 to 6.99 km^2. The increase in vegetation can be attributed to the growth of mangroves in the inter-tidal zone of the Sal River. Small-scale sand bars have formed at the mouth of the Sal River, which is dominated by mangrove vegetation. An increase in the area under vegetation can also be associated with the development of a commercial coconut plantation. Also, vegetation is grown for recreational purposes along the 5-star properties situated in the beach area. According to our personal perception and the perception of locals, land utilization pattern has changed over the years towards recreational purpose.

Field observation also helped in studying and interpreting the changes along the coast of Salcete taluka. From field observation, it was noticed that coastal sand dunes were removed or flattened for the construction of beach shacks/ restaurants. These structures became a source of litter, as can be seen on the beaches of Colva, Benaulim, etc. The beaches are losing their intrinsic value. Mass tourism and the development of tourist infrastructure are the major contributors towards increasing coastal degradation in Salcete taluka.

Change detection using SAGA software

Balasaraswathi and Srinivasalu (2016) stated that studying changes in the coastal environment is necessary for coastal planners to provide efficient management and planning of the region. SAGA GIS is open-source and easy-to-use software (Gašparović et al. 2019). SAGA software was used to detect the changes in the CRZ of Salcete taluka from 2000 to 2017. Supervised classification of images from the years 2000 and 2017 was given as input for class-wise change detection. Change detection using SAGA facilitated the study of changes in landuse and landcover classes. The land use and land cover change is shown in Table 3, while Fig. 5 provides a graphical representation of the changes that occurred over a period of 17 years.

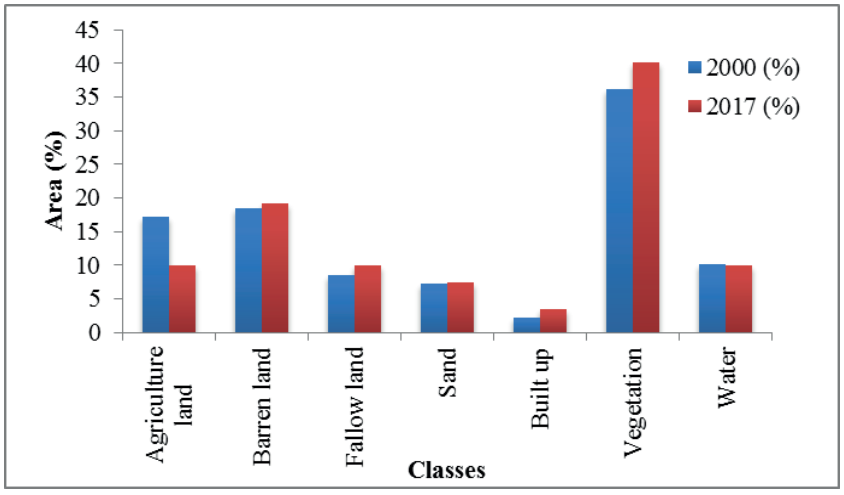

Fig. 4. Change in the area (in %) of different classes from the year 2000 to 2017

Table 3. LULC Change Detection Matrix for 2000-2017 (Area in km^2)

LULC Classes	Agricultural land	Barren land	Built-up area	Fallow land	Sand	Vegetation	Water
Agricultural land	0.28	0.03	0.03	0.05	0	0.2	0
Barren land	0.18	0.51	0.47	0.26	0.02	0.42	0.1
Built-up area	0	0	1.2	0	0	0	0
Fallow land	0.13	0.11	0.48	0.68	0.2	0.32	0.4
Sand	0.15	0.58	0.43	0.08	1.69	0.43	0.35
Vegetation	0.82	0.41	0.44	0.29	0.31	3.42	0.39
Water	0	0	0	0	0.42	0.31	0.81

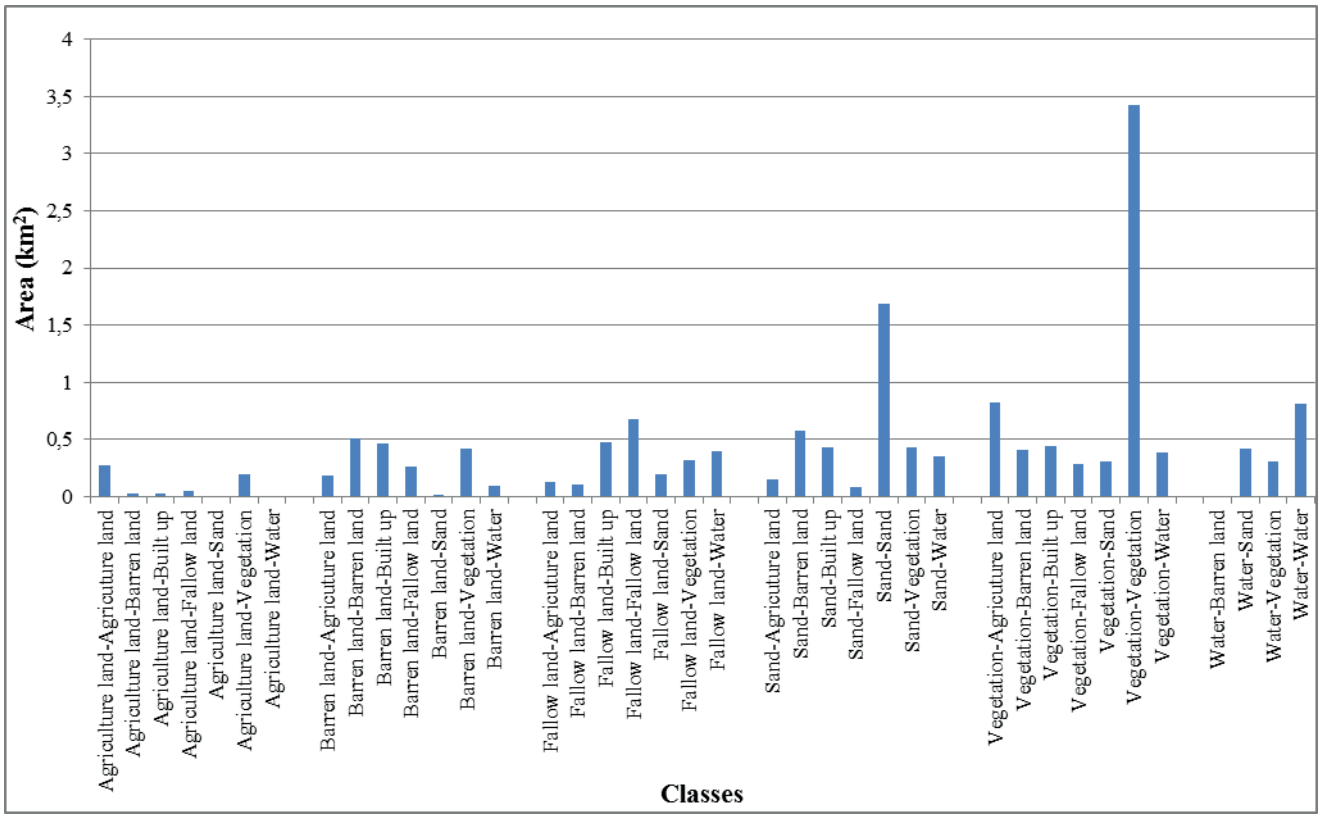

Fig. 5. Representation of LULC changes from 2000 to 2017

Fig.6 represents the change map of the Salcete Taluka CRZ region over a period of 17 years. The area under agricultural land underwent minor changes. First of all, agricultural land became less present in the coastal region due to the shift in the economic and occupational patterns (agrarian to tourism) amongst the local people. People living in coastal regions are mostly dependent upon the tourism industry and the majority of people work in other countries. Hence, agricultural activity is limited. However, 0.2 km^2 of the agricultural land was converted into other classes, primarily vegetation. The conversion of agricultural land into fallow land, sand, water, barren land, and built-up area was negligible.

It was also found that a major part of the barren land was converted into built-up areas (0.47 km^2), which can be attributed to the development of infrastructure to support tourism activities. 0.42 km^2 of land was converted to vegetation, as in some regions barren land became utilized for coconut farms or recreation. Meanwhile, the changes from barren land to other classes, such as agricultural land, fallow land, water, and sand, are much lower. The conversion of fallow land into water (0.4 km^2) can be associated with aquaculture activity. In many areas, especially near Betul, there is an increase in aquaculture activities due to the increasing demand for fish in the resorts and other restaurants situated in the coastal region. The conversion of fallow land into built-up areas (0.48 km^2) might be attributed to the increase in the number of houses and tourist-related infrastructure. This indicates the shifting of occupation from agriculture to the tourism industry as many local people are involved in it directly or indirectly.

Large areas of sand were converted into barren land (0.58 km^2) and vegetation (0.43 km^2). The conversion of the land under sand into vegetation can be associated with the growth of mangroves at the mouth of the Sal River. Furthermore, lawns were developed by hotels and resorts located along the coastal area for recreational purposes. In addition, sand dunes present in the coastal area were covered by different types of coastal vegetation, such as Casurina, Spinifex and *Ipomea*. 0.35 km^2 of the area under sand was converted into water which can be attributed to the increase in aquaculture activities in the coastal villages of Betul, Cavelossim, Assolna, etc. The increase in built-up area (0.43 km^2) was due to the growth in tourist infrastructure on the beach.

Vegetation cover was also converted to agricultural land (0.82 km^2), particularly in the most northern part of the study area, in the village of Utorda. It is a very common scenario in coastal areas, where people sell or give away agricultural land for development purposes and convert the land under natural vegetation for agricultural use. The area under vegetation was also converted into built-up land (0.44 km^2) for the development of tourism-related infrastructure. 0.41 km^2, 0.29 km^2, and 0.31 km^2 of land were converted into barren land, fallow land, and sand. 0.39 km^2 of vegetation area was converted into water, which can be associated with aquaculture activities. 0.42 km^2 of water were converted into sand, which is partially represented by a sand bar formed at the mouth of the River Sal. There was also an increase in riverine vegetation such as mangroves, which relates to the conversion of water to vegetation (0.31 km^2).

Limitations and Suggestions

There are a few limitations associated with the present work. First of all, there are no proper records of the infrastructure development taking place in the coastal zone as some of the constructions are illegal. 30 meters spatial resolution of LANDSAT images is also a drawback as land use cannot be identified in detail. Also, there is a lack of data regarding the number of tourists visiting a beach per day in order to study the human pressure on the ecosystem. However, there are also a few suggestions for solving the existing problems related to human interference. Firstly, there is a need for adequate monitoring of hap-hazardous activities and strict implementation of the CRZ rules and regulations to encounter rising environmental

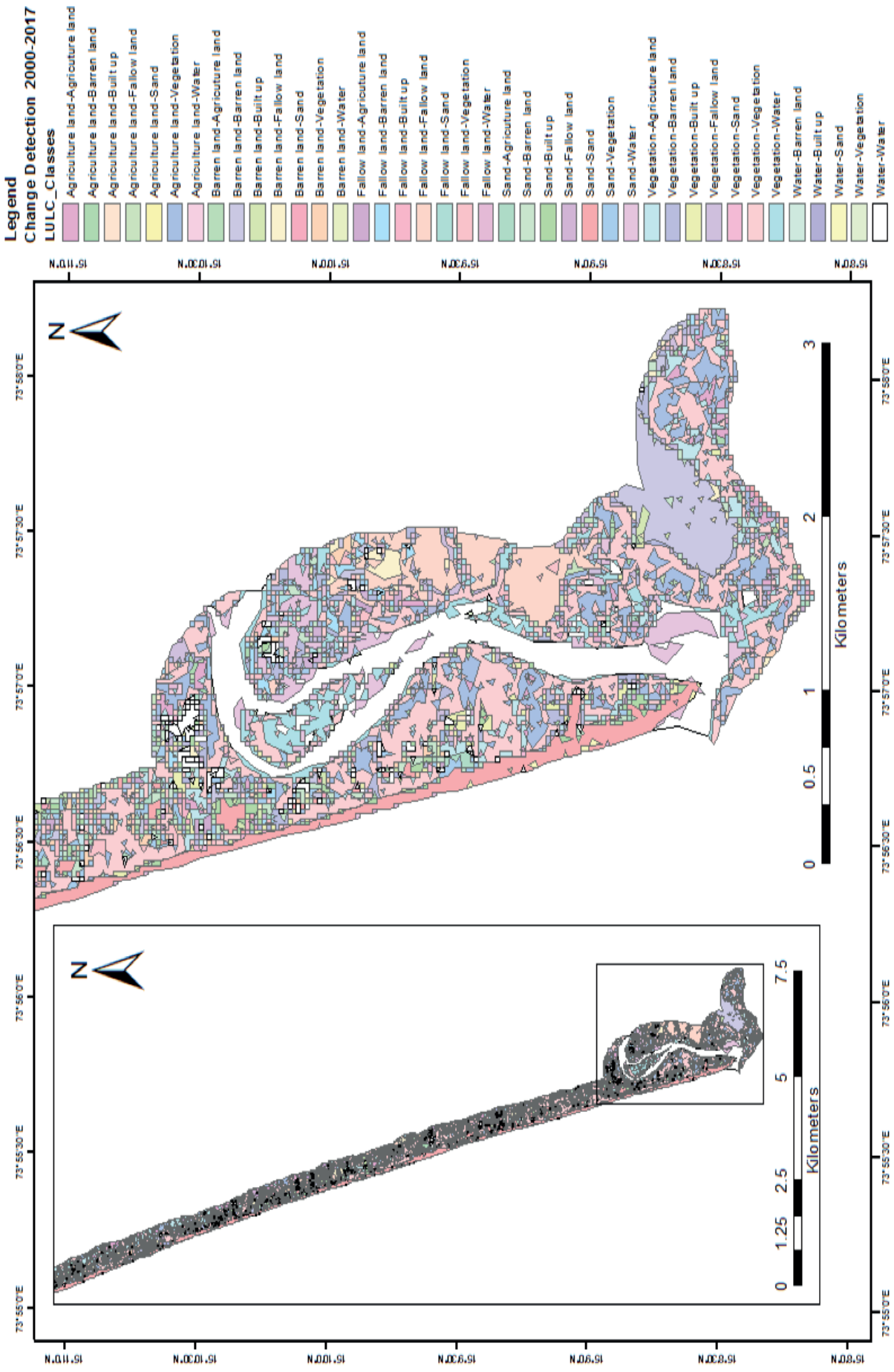

Fig. 6. Change detection map for a period of 17 years

problems. Secondly, looking at the mass tourism taking place along the coastal regions and violations of the CRZ, the government can come up with alternative tourism plans such as eco-tourism, wildlife tourism, rural tourism, agro-tourism, etc. to divert tourist flow to the interior regions of Goa which will boost the local economy and reduce pressure on the coastal environment. Thirdly, the development of sustainable and eco-friendly structures can be promoted in the coastal zones.

CONCLUSION

From the analysis, it was found that the area divided into different classes underwent tremendous change under the impact of both natural and anthropogenic factors. An extensive transformation within the CRZ of Salcete taluka took place over a period of 17 years. The results of the accuracy assessment of the classified LANDSAT images for the years 2000 and 2017 showed an overall accuracy of 95.65% and 96.67%, respectively. From the results of supervised classification for long-term changes, it was found that the area of agricultural land has decreased much higher compared to other classes, which might be attributed to the change in the perspective of locals due to the expansion of tourism.

On the other hand, vegetation, barren land, fallow land, and built-up land showed an increase in the area, while sand and water area remained the same. The agricultural land decreased by 7.24%, whereas barren land, fallow land, sand, built-up area, and vegetation increased by 0.8%, 1.33%, 0.17%, 1.15%, and 4.02%, respectively. From the change detection in the Salcete taluka coastal area, it was found that the area of agricultural land has decreased, whileother land classes showed an increasing pattern. The change detection analysis using SAGA software allowed to understand conversion between different classes. However, the limitations of the study included the spatial resolution of LANDSAT images (30 meters), which does not allow for detailed mapping of land use, while insufficient records of development activities and tourists visiting the beach on a daily/monthly/yearly basis limit the study of human interference.

Looking at the increasing mass tourism along the coast of Goa and increasing human interference in the fragile coastal ecosystem, this study can be useful for reducing further damage and raising awareness. Moreover, it showed that the authorities should constantly monitor any forms of illegal activity taking place in coastal zones. Strict rules and regulations need to be developed to protect coastal zones from further human interference. Awareness needs to be created amongst the locals and tourists for protecting the coastal environment. Sustainable development and sustainable tourism need to be promoted and practiced to avoid any further damage. The government can come up with alternative tourism plans such as eco-tourism, wildlife tourism, rural tourism, agro-tourism, etc. to divert tourist flow to the interior regions of Goa which will boost the local economy and reduce pressure on the coastal environment.

REFERENCES

Ayele G. Tebeje A. Demissie S. Belete M. Jemberrie M. Teshome W. Mengistu D.and Teshale E. (2018). Time Series Land Cover Mapping and Change Detection Analysis Using Geographic Information System andRemote Sensing, Northern Ethiopia. Air, Soil and Water Research,11, 1–18, https://doi.org/10.1177/1178622117751603.

Balasaraswathi P. and Srinivasalu S. (2016).Change detection analysis of coastal zone features in Cuddalore District, Tamil Nadu using Remote Sensing and GIS techniques. Journal of Applied Geology and Geophysics, 4 (5), 01-08, DOI: 10.9790/0990-0405020108.

Berlanga-Robles C. and Ruiz-Luna A. (2011). Integrating Remote Sensing Techniques, Geographical Information Systems (GIS), and Stochastic Models for Monitoring Land Use and Land Cover (LULC) Changes in the Northern Coastal Region of Nayarit, Mexico. GIScience& Remote Sensing, 48 (2), 245–263, DOI: 10.2747/1548-1603.48.2.245.

Butt A. Shabbir R. Ahmad S. and Aziz N. (2015) Land use change mapping and analysis usingRemote Sensing and GIS: A case study of Simly watershed, Islamabad, Pakistan. The Egyptian Journal of Remote Sensing and Space Sciences, 18, 251-259.

Chinnasamy P. and Parikh A. (2020).Remote sensing- based assessment of Coastal Regulation Zones in India: a case study of Mumbai, India. Environment, Development and Sustainability, 23(11), 1-20, DOI:10.1007/s10668-020-00955-z.

Chouhan H. Parthasarathy D. and Pattanaik S. (2017). Urban development, environmental vulnerability and CRZ violations in India: impacts on fishing communities and sustainability implications in Mumbai coast. Environment, Development and Sustainability, 19(3), 971–985, DOI:10.1007/s10668-016-9779-6.

Congalton R. (2001). Accuracy assessment and validation of remotely sensed and other spatial information. International Journal of Wildland Fire, 10, 321-328, DOI:10.1071/WF01031.

Conrad O. Bechtel B. Bock M. Dietrich H. Fischer E. Gerlitz L. Wehberg J. Wichmann V. and Böhner J. (2015).System for Automated Geoscientific Analyses (SAGA) v. 2.1.4. Geoscientific Model Development, 8, 1991-2007, DOI:10.5194/gmd-8-1991-2015.

Coastal Regulation Zone (CRZ) Notification 2011, (2011). Coastal Regulation Zone Notification Ministry of Environment and Forests (Department of Environment, Forests and Wildlife). Available at: http://www.indiaenvironmentportal.org.in/content/321917/coastal-regulation-zone-crz-notification-2011/ [Accessed 20 Dec. 2017].

Department of Tourism, Government of Goa, (2018). Department of Tourism, Government of Goa, India - Tourist Arrivals. Available at: https://www.goatourism.gov.in/tourist-arrival-statistics/[Accessed 02 Jan. 2018].

Dewan A. Yamaguchi Y. and Rahman M. (2010). Dynamics of land use/cover changes and the analysis of landscape fragmentation in Dhaka Metropolitan, Bangladesh. Geo Journal, 77, 315–330, DOI:10.1007/s10708-010-9399-x .

Fabbri K. (1998).A methodology for supporting decision making in integrated coastal zone management. Ocean & Coastal Management, 39, 51-62.

Gašparović M. Zrinjski M. andGudelj M. (2019). Automatic cost-effective method for land cover classification (ALCC). Computers, Environment and Urban Systems, 76, 1–10, https://doi.org/10.1016/j.compenvurbsys.2019.03.001.

Haque I. andBasak R. (2017). Land cover change detection using GIS and remote sensing techniques: A spatio-temporal study on Tanguar Haor, Sunamganj, Bangladesh. The Egyptian Journal of Remote Sensing and Space Sciences, 20(2), 251–263, DOI: 10.1016/j.ejrs.2016.12.003.

Islam R. Miah G. and Inoue Y. (2016). Analysis of land use and land cover changes in the coastal area of Bangladesh using LANDSAT imagery. Land Degradation & Development, 27(4), 899–909, DOI: 10.1002/ldr.2339.

Kaliraj S. Chandrasekar N. Ramachandran K. Srinivas Y. and Saravanan S. (2017). Coastal land use and land cover change and transformations of Kanyakumari coast, India using remote sensing and GIS. The Egyptian Journal of Remote Sensing and Space Sciences, 20 (2), 169-185, DOI:10.1016/j.ejrs.2017.04.003.

Kaul H. and Ingle S. (2012). Land use land cover classification and change detection using high resolution temporal satellite data. Journal of Environment, 1(4), 146-152.

Mascarenhas A. (1999). The Coastal Regulation Zone of Goa: Oceanographic, environmental and societal perspectives. Current Science, 77(12), 1598-1605.

Misra A. and Balaji R. (2015).A study on the shoreline changes and Land-use/ land-cover along the South Gujarat coastline. Procedia Engineering, 116, 381-389, DOI:10.1016/j.proeng.2015.08.311.

Misra A. ManiMurali R. and Vethamony P. (2015).Assessment of the Land-Use/Land-Cover (LULC) and Mangrove changes along the Mandovi- Zuari Estuarine complex of Goa, India. Arab Journal of Geosciences. 8, 267-279.

MohanRajan S. Loganathan A. and Manoharan P. (2020). Survey on Land Use/Land Cover (LU/LC) change analysis in remote sensing and GIS environment: Techniques and Challenges. Environmental Science and Pollution Research, 27, 29900–29926, https://doi.org/10.1007/s11356-020-09091-7.

Muttitanon W. and Tripathi N. (2005). Land use/land cover changes in the coastal zone of Ban Don Bay, Thailand using LANDSAT 5 TM data. International Journal of Remote Sensing, 26(11),2311–2323, https://doi.org/10.1080/01431160512331326666.

Nayak S. (2017). Coastal zone management in India – present status and future needs. Geo-spatial Information Science, 20 (2), 174-183, DOI: 10.1080/10095020.2017.1333715.

Panigrahi J. and Mohanty P. (2012). Effectiveness of the Indian coastal regulation zones provisions for coastal zone management and its evaluation using SWOT analysis. Ocean & Coastal Management, 65, 34-50, DOI:10.1016/j.ocecoaman.2012.04.023.

Rahman M. Tabassum F. Rasheduzzaman M. Saba H. Sarkar L. Ferdous J. Uddin Z. and Islam Z. (2017). Temporal dynamics of land use/land cover change and its prediction using CA-ANN model for southwestern coastal Bangladesh. Environmental Monitoring and Assessment, 189, 565, DOI: 10.1007/s10661-017-6272-0.

Ramesh D. and Vel A. (2011).Methodology of Integrated Coastal Zone Management Plan Preparation-Case Study of Andaman Islands, India. Journal of Environmental Protection, 2(6), 750-760, DOI: 10.4236/jep.2011.26087.

Saha J. and Paul S. (2020). An insight on land use and land cover change due to tourism growth in coastal area and its environmental consequences from West Bengal, India. Spatial Information Research, DOI:10.1007/s41324-020-00368-0.

Shi C. Hutchinson S. Yu L. and Xu S. (2001). Towards a sustainable coast: an integrated coastal zone management framework for Shanghai, People's Republic of China. Ocean & Coastal Management, 44(5-6), 411-427.

Waiyasusri, K. and Chotpantarat, S. (2022). Spatial Evolution of Coastal Tourist City Using the Dyna-CLUE Model in Koh Chang of Thailand during 1990–2050. ISPRS International Journal of Geo-Information 11, 49. https://doi.org/10.3390/ijgi11010049

Yagoub M. and Kolam G. (2006). Monitoring Coastal Zone Land Use and Land Cover Changes of Abu Dhabi Using Remote Sensing. Journal of the Indian Society of Remote Sensing, 34 (1), 57-68.

Zahedi S. (2008). Tourism impact on coastal environment. Environmental Problems in CoastalRegions, VII 99, 45-57, DOI:10.2495/CENV080051.

RESEARCH PAPER

THE SOCIAL EQUITY OF PUBLIC GREEN OPEN SPACE ACCESSIBILITY: THE CASE OF SOUTH TANGERANG, INDONESIA

Hernand Bagaskara Kurniawan[1*], Muhammad Sani Roychansyah[1]
[1]Department of Architecture and Planning, Universitas Gadjah Mada, Yogyakarta, Indonesia
***Corresponding author:** hernandbagaskara@ugm.mail.ac.id
Received: August 17th, 2022 / Accepted: February 15th, 2023 / Published: March 31st, 2023
https://DOI-10.24057/2071-9388-2022-124

ABSTRACT. Public Green Open Space (PGOS) is widely known to provide many benefits for the well-being of urban community, especially the socially vulnerable. Achieving equitable PGOS access is crucial for the sustainability and livability of cities. This study aims to 1) observe the accessibility of PGOS and 2) investigate the social equity of PGOS access in South Tangerang, Indonesia. This study employed network-based accessibility analysis through GIS and constructed a green space access index at urban village level to observe the accessibility of PGOS for urban residents. Furthermore, statistical correlation tests were conducted to examine the social equity of PGOS access against socio-demographic variables. The spatiality of equity was explored by using Bivariate Moran's I. The results found that in South Tangerang, PGOS access is unequal, showing 61.2% of residential areas being underserved. This study also found that PGOS access is higher in elite private neighborhoods. Furthermore, statistical tests showed that PGOS access is inequitable for the low-income group. As for the elderly and population density, PGOS access was found to be equitable. However, no correlation was found between children and PGOS access. Additionally, causes of inequality and inequity in PGOS access and its implications are further discussed. This study addresses several key policy implications for urban planners and specifically for the government of South Tangerang such as the need to reform PGOS planning & policy and developing alternative funding for PGOS.

KEYWORDS: accessibility, equality, equity, GIS, public green open space

CITATION: Kurniawan H. B., Roychansyah M. S. (2023). The Social Equity Of Public Green Open Space Accessibility: The Case Of South Tangerang, Indonesia. Geography, Environment, Sustainability, 1(16), 45-54
https://DOI-10.24057/2071-9388-2022-124

ACKNOWLEDGEMENTS: The authors would very much like to thank the reviewers for their valuable input for the improvement of this article. The authors would also like to thank Dhimas Bayu Anindito, Yori Herwangi, Luthfi Muhamad Iqbal and many more of those who have contributed to giving insights and who have helped the authors improve the research.

Conflict of interests: The authors reported no potential conflict of interest.

INTRODUCTION

Public Green Open Space (hereafter: PGOS) such as park and urban forest, has long been considered a vital resource for the urban community's health that is constantly experiencing the negative effect of the intense urban activity and development (Satterthwaite 1993). Prior research findings have indicated the significance of PGOS in which it provides many essential benefits for urban dwellers' well-being (Chiesura 2004; Coombes et al. 2010; Ward Thompson et al. 2012; Krefis et al. 2018). PGOS stimulates physical & social activities and establishes interaction with nature which leads to the improvement of the urban community's quality of life, overall health, and social cohesion (Ward Thompson et al. 2012; Holt et al. 2019; Dushkova & Ignatieva 2020; Rigolon et al. 2021; Sharifi et al. 2021). The significance of PGOS benefits is particularly relevant and evident in the context of the recent health crisis, the pandemic of Covid-19 (Marconi et al. 2022; Noszczyk et al. 2022). Noszczyk et al. (2022) revealed that PGOS eases the negative effect of pandemic crisis on urban population.

Accessibility to PGOS as represented by distance is one of the main factors that influences its use and further has an implication on how the urban community can derive benefit from the PGOS optimally, besides its size, quality, and quantity (Coombes et al. 2010; Haq 2011; S. Feng et al. 2019; Zhan et al. 2021). Empirically, Coombes et al. (2010) and Toftager et al. (2011) found that the closer urban residents live to PGOS, the more likely they visit PGOS regularly to exercise, therefore obtaining better health conditions. Consequently, urban residents having different degree of PGOS accessibility may experience different health outcomes which leads to health and quality of life disparity (Rigolon et al. 2021; Sharifi et al. 2021).

PGOS service should be prioritized in areas where the demand is highest, often associated with social vulnerability such as proportion of the vulnerable (e.g. children, the elderly, & the low income group) and population density (Lee & Hong 2013; Yuan et al. 2017; Pham & Labbé 2018; Wolff & Haase 2019; Geneletti et al. 2022). This is due to numerous reasons. Children & the elderly have mobility limitation which restricts them to go long distance and as for the low-income group, they have limitation in financial resource to afford private facilities to carry out exercise and recreation (Romero 2005; Maas et al. 2008; Boone et al. 2009; Reyes et al. 2014). Thus, they have a greater need for nearby public recreation facilities, especially one which enables them to interact with nature (Rigolon et al. 2021). Past empirical research findings suggest that the aforementioned vulnerable group may obtain greater benefit from PGOS than the non-vulnerable (Takano 2002; Feng & Astell-Burt 2017; Twohig-

Bennett & Jones 2018; Rigolon et al. 2021; Geneletti et al. 2022). As for population density, higher population density is often associated with higher urban stress and potential overcrowding of green space use (Wolff & Haase 2019; Liu et al. 2020).

The concept of the spatial match between service level and the social demand is widely known as social equity (Yuan et al. 2017). Social equity is further understood as having two dimensions: 1) horizontal equity, which concerns about the condition of which everyone has the same access to resource (equality) and 2) vertical equity which concerns about the quality of being fair and considers different need and demand of social group in regard to receiving access to resource (access to resource is distributed proportionately) (Boone et al. 2009; Yuan et al. 2017; He et al. 2020). Achieving social equity in the context of urban infrastructure such as PGOS has been recognized as a crucial aspect of sustainable and resilient urban development (Zhou & Wang 2011; Wolch et al. 2014; Meerow et al. 2019; Zheng et al. 2020; Chen et al. 2020; Li et al. 2021). Thus, the study to evaluate the social equity of PGOS accessibility is considered important (Rigolon 2016; Li et al. 2021). Findings of such a study could inform the decision makers to further mitigate the negative impact of which PGOS inequity exists (Rigolon et al. 2021; Xu et al. 2022). Recently, there has been an increasing number of research focused on evaluating the equity of PGOS accessibility in various cities, of which most studies found that the non-vulnerable such as those with higher Socio-Economic Status (SES) tend to have better access to PGOS than the vulnerable (Tan & Samsudin 2017; Yuan et al. 2017; Chen et al. 2020; He et al. 2020; Sharifi et al. 2021; Herreros-Cantis & McPhearson 2021). However, the issue of equity in PGOS in the context of developing countries is still relatively less explored (Chen et al. 2020; Du et al. 2020).

Based on the previous discussions, using the case of South Tangerang, Indonesia, this study aims to 1) observe the accessibility of PGOS and 2) investigate the social equity of PGOS access to understand whether the access is distributed in line with social demand. South Tangerang, Indonesia makes an ideal case study for the topic of green space equity for several reasons. First, South Tangerang is a suitable representation of a city undergoing adverse spatial segregation in Indonesia, indicated by the existence of a number of massive-sized elite settlement areas built by private developers termed as new town (Apriyanto et al. 2015; Winarso et al. 2015). Secondly, South Tangerang aspires to be an equitable, livable, and sustainable city, a condition that's currently on progress to be achieved through the long-term development plan of South Tangerang City (RPJPD 2005-2025). Such vision implies that equitable access to basic public resources such as green space should be fulfilled, therefore increasing the urgency for a PGOS equity study to be conducted. In addition, South Tangerang is one of municipalities within Jakarta Metropolitan Region (Jabodetabek) which has extreme urbanization rate with annual population growth reaching 6.87% (Saifullah et al. 2018). This may impact the availability and distribution of PGOS in South Tangerang. The result of this study is expected to add discussion to the existing studies of green space equity as results are often contextual in which it varies along different geographical areas, cultures, and cities with different development histories (He et al. 2020; Sharifi et al. 2021).

To achieve the objectives set out, this study goes through two steps. First step is accessibility analysis which is done through network analysis in Geographic Information System (GIS). This study incorporated residential land use in the accessibility analysis to identify the optimality of PGOS service for urban residents. Previous studies rarely consider the residential land use variable to assess urban community's accessibility level to green space, rather only focus on administrative boundary alone (He et al. 2020; Mushkani & Ono 2021). Furthermore, this study advanced the accessibility analysis by constructing index of PGOS accessibility at urban village (kelurahan) administrative level to observe the PGOS service in quantitative measure. Secondly, to understand the equity of PGOS access, this study assessed the association between PGOS accessibility and the socio-demographic variables by employing Spearman correlation test. This study further explored the spatiality of the association by using Bivariate Local Indicator of Spatial Association (BiLISA). The socio-demographic variables which are considered in this study are the vulnerable (children, the elderly, and the low-income group) and the population density as previously discussed.

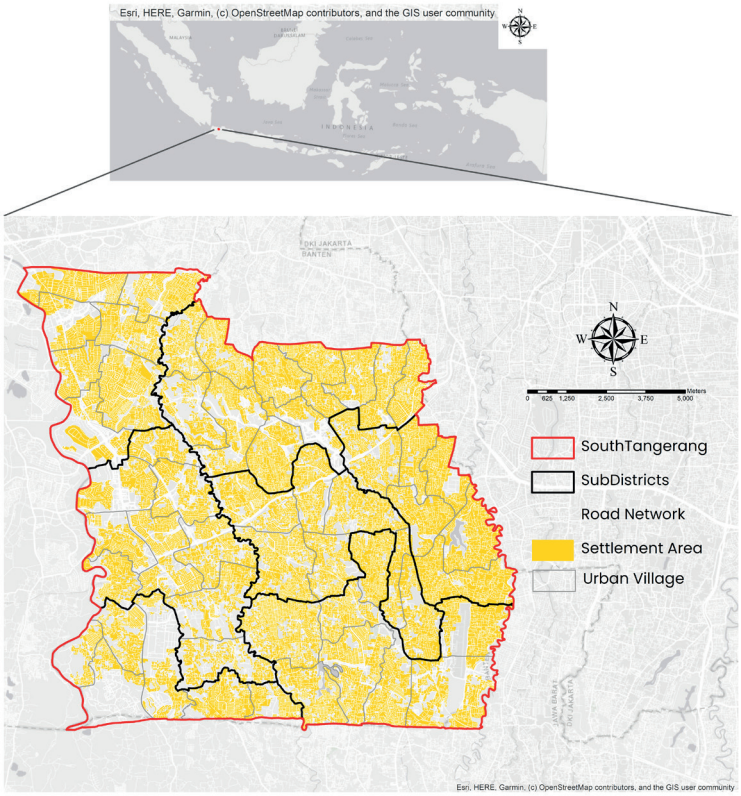

Fig. 1. South Tangerang City

Data Source: The Development Planning Board of South Tangerang

STUDY AREA

The study area is South Tangerang City located in Banten, Indonesia. South Tangerang is part of the highly urbanized Jakarta Metropolitan Region. South Tangerang City is 147.19Km^2 in size, consisting of 54 urban villages with seven sub-districts (administrative level above urban village: kecamatan), namely Setu, Ciputat, East Ciputat, Serpong, North Serpong, Pamulang, and Pondok Aren. In 2021, based on data provided by Agency of Population and Civil Registration, South Tangerang City has 1.3 million population with its density of 10.484 population/Km^2. It is evident that low-income population is aggregating in the urban outskirts (Agency of Population and Civil Registration, 2021), quite possibly due to the low housing prices in urban fringe as argued by Covington (2015). The affluent group generally reside in areas known as kota mandiri or new towns (massive-sized elite housing developed by private sector) (Winarso et al., 2015). There are 3 developers that develop new towns in South Tangerang, namely Bumi Serpong Damai (hereafter: BSD), Bintaro, and Alam Sutera (Firman 2004). The existence of new towns in South Tangerang City has been studied by many to have produced spatial segregation, especially regarding how access to facilities and infrastructure is distributed such as PGOS (Firman 2004; Winarso et al. 2015; Roitman & Recio 2020). South Tangerang has been experiencing various environmental problems, mostly caused by its rapid urban development and lack of green space such as Urban Heat Island and poor air quality (Andriarsi 2021; Prastiwi 2022).

MATERIALS AND METHODS

In this study, PGOS is referred to as public parks and urban forest (human-modified green space), following the definition of PGOS by Du et al. (2020) & Sharifi et al. (2021). Human-modified green space is an urban green infrastructure developed and managed by the government (Sharifi et al. 2021). This study acquired the PGOS data (in shapefile) from OpenStreetMap since access to PGOS spatial database from government officials was unavailable. Furthermore, OpenStreetMap was chosen as the data source because it's open source and its data completeness is reliable for researcher and policymaker (Barrington-Leigh & Millard-Ball 2017; Wibowo et al. 2021). It was identified that there are 128 PGOS in South Tangerang as of 2021. Furthermore, this study also collected the data of PGOS entrance distribution which would be used to model accessibility in the network analysis, by using Google Street View (GSV). GSV was used as it is cost-effective, safety, time-efficient, and reliable to audit built environment (Biljecki & Ito 2021; Haddad et al. 2021) and considering the restricted outdoor activities due to Covid-19 pandemic during data survey.

Network data was obtained from OpenStreetMap as a basis data for accessibility analysis. Administrative boundary at urban village level and the data of residential land use in 2018 were obtained from The Agency of City Development Planning South Tangerang. Both data respectively will be used for accessibility analysis. Specifically for residential land use, this study argues that by considering residential land use for the accessibility analysis, it will provide better accuracy in assessing the PGOS accessibility to urban residents. Furthermore, since the latest data of residential land use beyond 2018 was unavailable for the analysis, this study assumes that residential land use pattern in 2018 remains the same in 2021. Other than that, this study also obtained data of boundary of new town from the private developer's website (BSD: www.bsdcitycommercial.com, Alam Sutera: alam-sutera.com, Bintaro: www.jayaproperty.com) to compare PGOS accessibility based on housing type. Socio-demographic data in 2021 at urban village level was obtained from the Agency of Population and Civil Registration which comprises of population based on age and low-income group. The data will be used in correlation analysis against the PGOS accessibility level to justify social equity.

Examining the Green Space Accessibility

To examine the PGOS accessibility (the equality of service), network analysis method was employed. Network analysis method was chosen since it measures the service coverage of an object based on actual road network, therefore accurately representing accessibility or proximity towards the object of interest. The PGOS accessibility was measured in network analyst tool in ArcGIS 10.3, based on 800 meters distance or 10 minutes' walk, a distance most residents are willing to walk for (Du et al. 2020; He et al. 2020). The result of this analysis is PGOS accessibility coverage which was then intersected against the residential land use in South Tangerang City. Based on the previous analysis, Green Space Accessibility Index (hereafter: GSAI) was constructed to observe varying accessibility (service) level among urban villages in quantitative measure. GSAI was also used in the correlation analysis against the socio-demographic variables. In constructing the accessibility index, this study followed Tan & Samsudin (2017) specified below.

$$Green\ Space\ Accessibility\ Index\ (GSAI) = \frac{Gc}{rA}$$

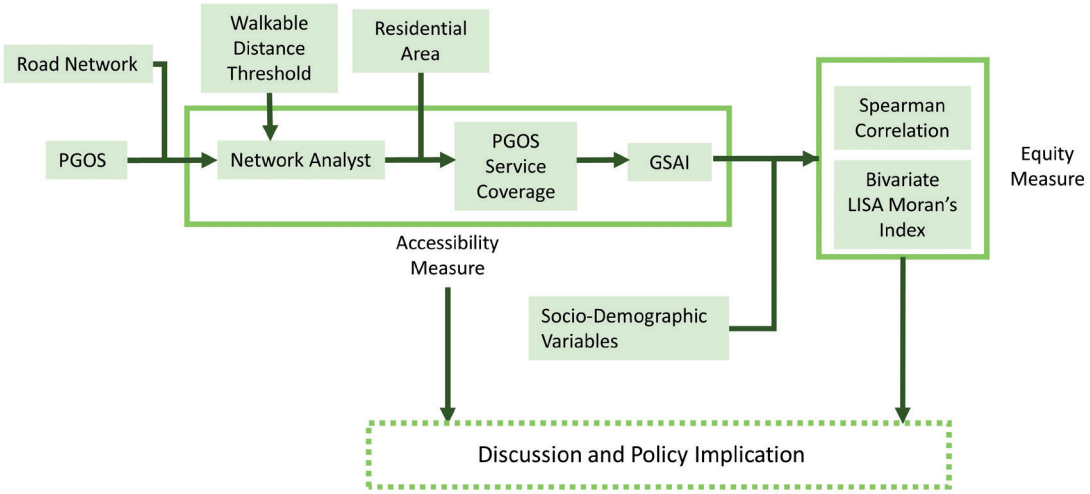

Fig. 2. Methodology Flow

Gc is defined as PGOS coverage over residential area (in Ha) in an urban village, divided by rA which denotes the total residential area (in Ha) in an urban village. Gc considers all PGOS service which covers residential area within the same urban village. It was done to reduce the potential issue of boundary effects encountered when assessing green space service coverage at administrative unit (Zhou & Kim 2013; Tan & Samsudin 2017). GSAI allows to better understand whether urban village has enough green space service covering the residential area, providing urban residents sufficient access to PGOS (within walkable distance). Furthermore, this study classified the GSAI results of 54 urban villages using Jenks method in ArcGIS 10.3 into 5 classes: very low (0-0.12), low (0.13-0.3), moderate (0.31-0.47), high (0.48-0.69), and very high (0.70-0.96).

Analyzing Socio-Demographic Conditions

Socio-demographic data was analyzed at the level of urban village using simple quantitative analysis on the low-income group, the elderly, and the children respectively. Other than that, this study also conducted population density analysis. Prior to analyzing the socio-demographic data, this study classified each socio-demographic character. Firstly, as the data provided by Development Planning Board of South Tangerang already classified low-income population based on Ministerial Decree of Ministry of Social Affairs No 88/HUK/2021, this study only calculates the proportion of the low-income group at urban village. As for the elderly, this study classified the elderly as those who are aged over 60, following the definition from The Law of The Republic Indonesia on Elderly Welfare Number 13 of 1998. As for the children, this study followed He et al. (2020) which stated that children are those who are aged between 0-14. After classifying the demographic characteristic, this study calculates the proportion of each group and the population density.

$$Proportion\ of\ children\ at\ urban\ village\ i = \frac{Number\ of\ Children_i}{Total\ population_i}$$

$$Proportion\ of\ the\ elderly\ at\ urban\ village\ i = \frac{Number\ of\ Elderly_i}{Total\ population_i}$$

$$Proportion\ of\ low\ income\ group\ at\ urban\ village\ i = \frac{Number\ of\ Low-Income_i}{Total\ population_i}$$

$$Population\ density\ at\ urban\ village\ i = \frac{Population_i}{Subdistrict\ area_i}$$

Analyzing Social Equity in Green Space Access

To examine the social equity in PGOS access, this study employed two statistical methods following Zhu et al. (2022). Firstly, the non-spatial statistics correlation analysis was conducted with the Spearman correlation test between GSAI and socio-demographic variables: low-income group, the elderly, children, and population density. The non-spatial correlation test was conducted in SPSS 20.0. The result of the test is an index ranging from -1 to 1 which indicates the correlation's strength and direction. Secondly, the spatial correlation was analyzed using Bivariate Local Indicator Spatial Autocorrelation (BiLISA) Moran's I in Geoda Software. BiLISA Moran's I was used to observe the spatiality of the correlation across study area (at the urban village level) between GSAI and the socio-demographic variables. Talen & Anselin (1998) and Anselin (1995) stated that using BiLISA approach is best when investigating spatial associations between accessibility and socio-economic variables. BiLISA uses Moran's Index for each urban village in South Tangerang with the formula as follows:

$$I_i = Z_i \sum_j W_{ij} Z_j$$

Where Z_i and Z_j respectively are GSAI and socio-demographic variables used in this study, W_{ij} denotes neighborhood weight matrix where sum of j across each row i equals 1. The result of the BiLISA analysis is a spatial correlation map showing areas of different clusters: High-High, High-Low, Low-High, and Low-Low. Low-High indicator means that the socio-demographic variable shows low value while GSAI is high (spatial mismatch), relative to other areas in the case study and vice versa for High-Low. As for the areas marked with High-High and Low-Low indicates equity which implies that PGOS service level (GSAI) is in line with the social demand level (socio-demographic variables). Lastly, this study also reported the results of Global Moran's Index of spatial association which produces spatial correlation index with a value ranging from -1 to 1 indicating similar meaning to the index of non-spatial correlation test (Sharifi et al. 2021).

RESULTS

Public Green Open Space Accessibility

Based on the calculation, PGOS per capita (M^2/capita) in South Tangerang is only 0.387, lower than the standard mandated by the World Health Organization (WHO) of 9M^2/capita. Further on the accessibility analysis (see figure 3), this study found that the PGOS service does not cover a large area of South Tangerang City. Specifically, calculation results showed that PGOS accessibility has only covered 38.8% of the residential area, leaving 61.2% residential area being underserved in South Tangerang. There's only 694,650 population being served by PGOS in 2021 which leaves 48.7% population with very poor access (>800 m) to PGOS. In this analysis, it was found that the pattern of PGOS service coverage tends to agglomerate in certain parts of South Tangerang.

Furthermore, this study calculated the GSAI for each urban village in which the result of GSAI analysis can be observed in Figure 4. Average GSAI from 54 urban villages is 0.37 and the median is 0.35 which suggests that green space service is sub-optimal in many urban villages, covering very small residential area. The lowest value of GSAI is 0 and the highest is 0.95 out of maximum 1 (100% coverage of green space/PGOS). From the result, it was found that there are 5 urban villages with 0 (zero) GSAI indicating that the urban villages are entirely isolated from any PGOS service within walkable distance. Urban residents living in those urban villages may have to put relatively greater effort to access PGOS.

Based on the Jenks classification, GSAI shows 9 urban villages classified as having very high index and 15 urban villages classified as having very low index. The spatial pattern of urban villages with high to very high GSAI aggregates in certain parts of the city such as in the north-eastern and south area. As seen in the chart of urban villages with different GSAI classification (figure 4), most urban villages in South Tangerang have relatively poor access to PGOS. They are urban villages with GSAI classification of Very Low to Low GSAI, amounting up to 46.29% or 25 urban villages of total urban villages as opposed to urban villages with GSAI classified as High to Very High amounting to only 31.48%. Based on both the PGOS service coverage analysis and GSAI calculation, this study confirms that the PGOS accessibility in South Tangerang shows inequality. This

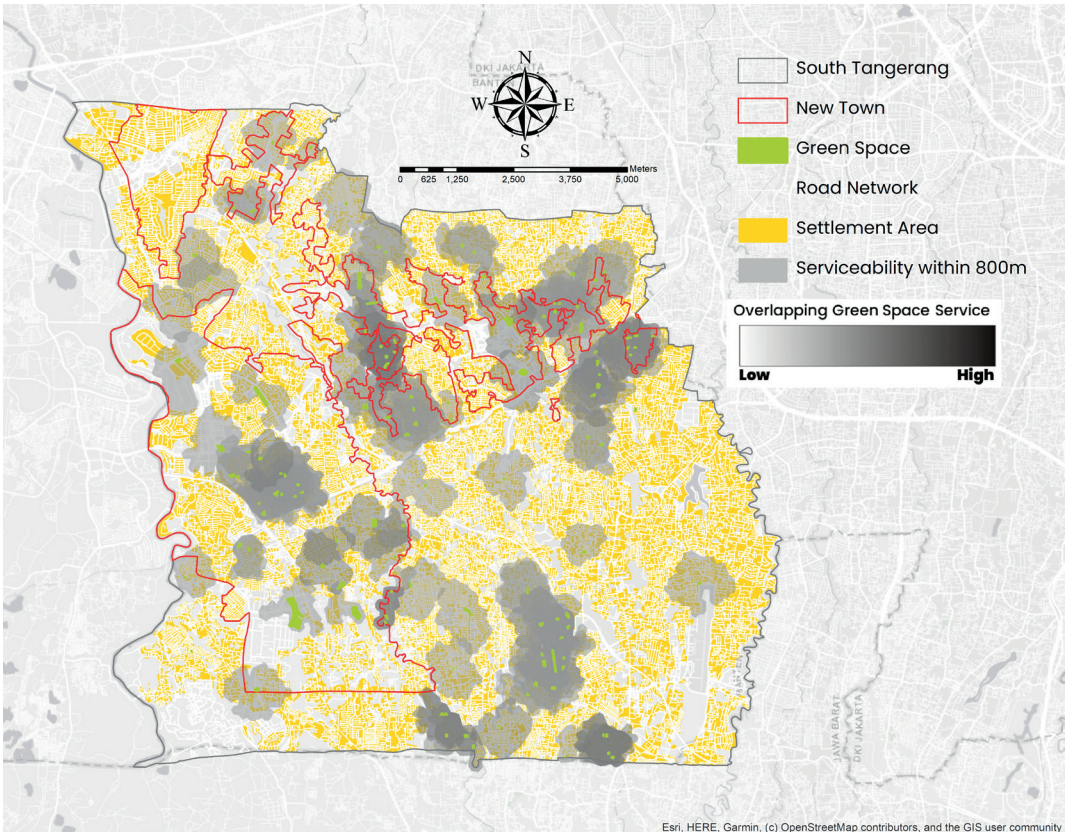

Fig. 3. The spatial accessibility of public green open space

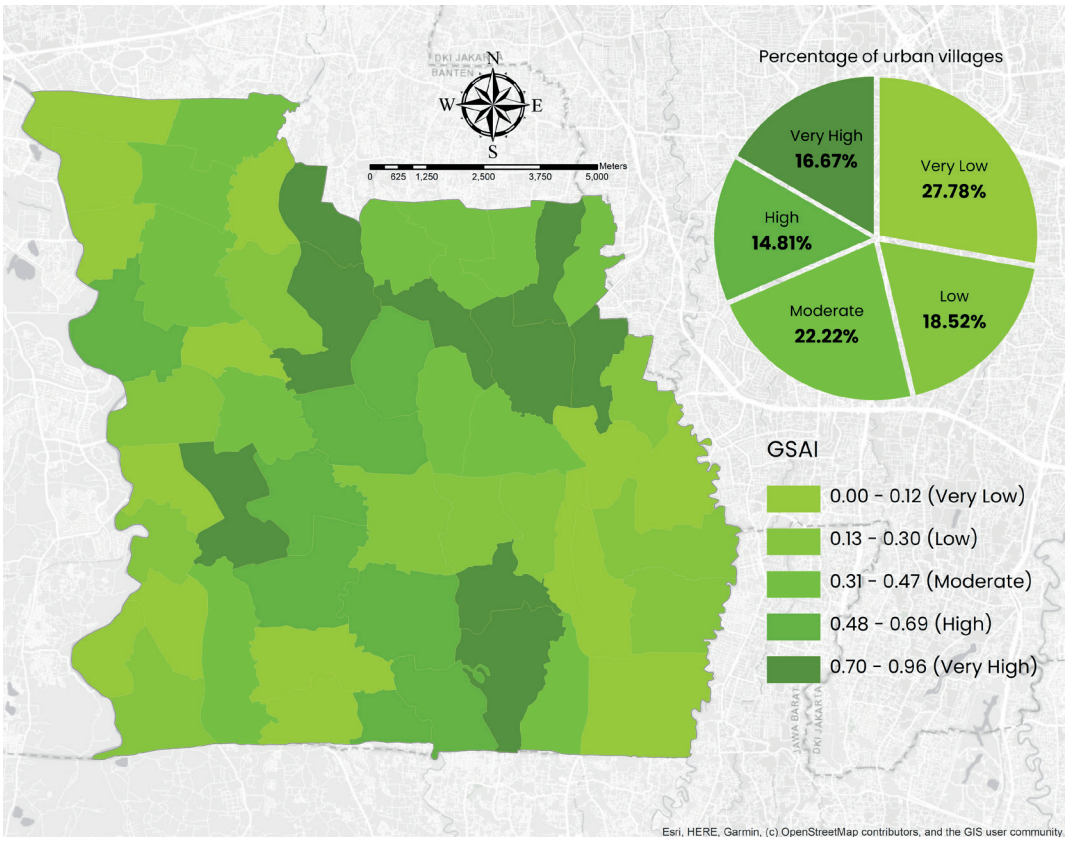

Fig. 4. Spatial distribution of GSAI and percentage of urban village based on GSAI

study also found that new town has more land allocated to PGOS. The coverage of public green space service is also higher in new town of 42.11% than the coverage of PGOS service outside of new town, which only amounts up to 33.5%.

Association Between Green Space Access and Socio-Demographic Variables

The results of the Spearman correlation statistics are presented in table 1. First, the result of the test on low-income and GSAI variable revealed a significant ($P<0.01$) negative correlation. It implies that areas with higher proportion of the low-income group generally have poor

PGOS access (implying inequity). As for the correlation test result of GSAI against the proportion of children, the study found no correlation with index showing 0 value. This study reports a positive Spearman correlation of the proportion of elderly and population density against GSAI, meaning that PGOS access level is generally in line with the demand from the perspective of population density and the elderly.

Furthermore, the spatial pattern of the association between socio-demographic characteristics and GSAI is identified through BiLISA analysis (see figure 5). The BiLISA result for low-income group and GSAI yields an interesting finding: Low-High clusters are prevalent with the Global Moran's index value showing negative spatial correlation. From the perspective of the BiLISA test, urban villages with few numbers of the low income group have higher PGOS accessibility which indicates spatial mismatch of demand & supply and thus an indication of inequity. As for spatial correlation analysis of the proportion of children & GSAI, the spatial association is positive, albeit very weak at 0.065. Furthermore, the result of BiLISA on the proportion of the elderly and population density against GSAI both revealed positive correlation with dominating clusters of High-High and Low-Low. Lastly, all the cluster maps from BiLISA analysis indicate a similar pattern in which the urban center to southwestern area generally show no statistically significant spatial association (clusters shaded in grey) between GSAI and socio-demographic variables.

DISCUSSION

PGOS Accessibility and Its Implication on Social Equity

The inequality of PGOS access in South Tangerang found in this research is consistent to previous studies in many cities (Tan & Samsudin 2017; Chen et al. 2020; Fasihi & Parizadi 2020; Mushkani & Ono 2021; Sharifi et al. 2021). Figure 3 shows that the urban fringe (the southwestern, northwestern & southeastern area) has relatively low PGOS access, possibly implying that urban fringe residents lack opportunities to public recreation facilities. In addition, this article also found many areas with overlapping PGOS service as can be seen in Figure 3. Interestingly, PGOS access tends to be relatively better in private elite neighborhood (new town) such as BSD and Bintaro (an exception for Alam Sutera in the northwestern part of South Tangerang, as many of its vacant land areas are still undeveloped). This study's finding further adds to the discussion of which neighborhoods built by private developers offers a better opportunity to facilities and infrastructures such as green space than public housing (Firman 2004; Tan & Samsudin 2017; Roitman & Recio 2020). It should be clarified that green space in new town is made publicly accessible through The Law No. 1/2011 concerning Housing and Residential Areas and Regulation of The Ministry of Home Affairs of the Republic of Indonesia No. 9/2009, imposed to private developers. The regulations imply the obligation that private housing developers need to fulfill regarding

Table 1. Results of Correlation Test

			Green Space Access Index
Spearman	Low-Income Group	Correlation Coeff.	-0.388**
	Children		0.000
	The Elderly		0.179
	Population Density		0.255

(Note: ** means that the correlation is significant at P<0.01 (2-tailed)

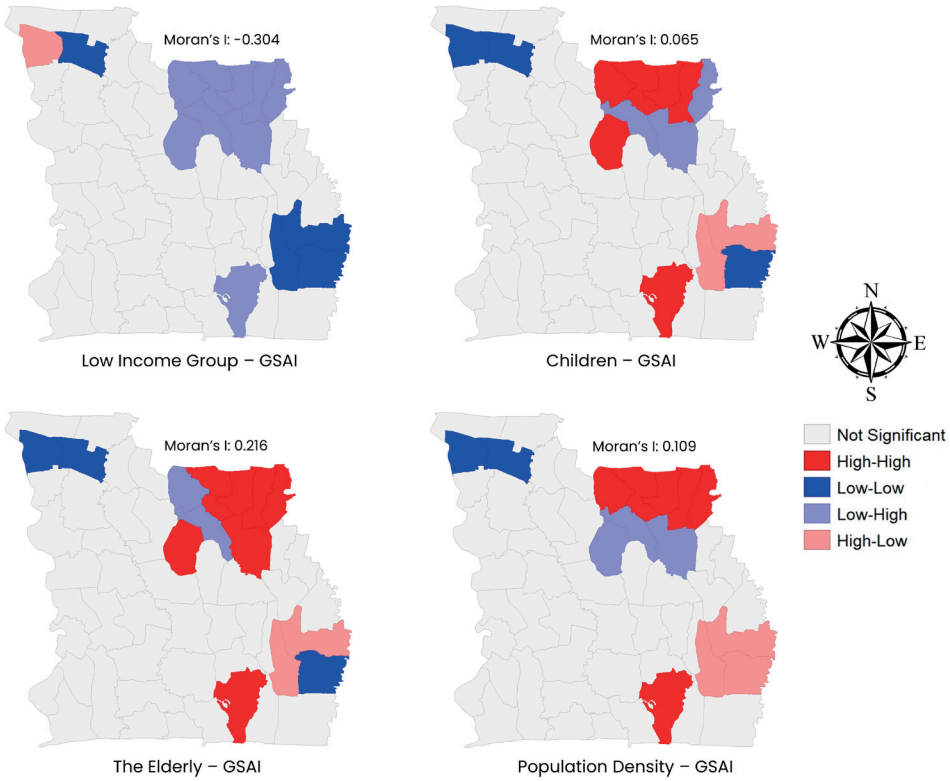

Fig. 5. Spatial distribution of GSAI and percentage of urban village based on GSAI

the provision of facilities & infrastructure and the delegation of the ownership and management responsibility to the town government.

In terms of social equity (the vertical dimension of equity), this study revealed that PGOS access is inequitable for the low-income group in South Tangerang, confirmed by the Spearman and BiLISA results. Here this study argues several reasons which contribute to the formation of dominant cluster of Low-High in the northeastern area of South Tangerang (see figure 5 for low-income vs GSAI). Firstly, the existence of new town Bintaro in the cluster contributes to the high GSAI since green space in Bintaro area has been extensively developed by the private developer. In addition, as Firman (2004) and Winarso et al. (2015) maintain, most occupants of the new town are generally considered elites with high income and social status, resulting in the cluster of very few low-income residents in the area. This finding is also similar with an abundance of prior studies regarding how neighborhoods with dominant affluent group tend to have better green space access, leaving the low income group with poor access to PGOS (Tan & Samsudin 2017; Yuan et al. 2017; Chen et al. 2020; He et al. 2020; Sharifi et al. 2021). The low income having poor access to PGOS can exacerbate their health issues and lead to intergenerational health problems (Sharifi et al. 2021). Regarding children and GSAI, correlation analysis results shows a zero value on Spearman index and a very weak Moran's Index. This article argues that the findings suggest unpatterned equity, a term usually used to describe when there is no apparent systematic relationship between the service of public resource and the socio-demographic variable (in this case, GSAI and the children proportion), as found in the studies of Wilson et al. (2004), Abercrombie et al. (2008), and Maroko et al. (2009). As for correlation of GSAI between proportion of the elderly and population density, it was identified that they indicate equity, albet not significant at 0.179 and 0.255. However, although supply of PGOS service is generally in line with the demand of population density and the elderly, some areas still need to be paid attention to increase green space, especially as suggested in BiLISA result, regarding clusters of High-Low which implies high demand with relatively low supply.

Factors Affecting PGOS Accessibility Pattern and Its Equity

This study argues that the causes of inequity (both in horizontal and vertical dimensions) in PGOS access is contextual. For example, in Ilam City – Iran, the disparity in the distribution of PGOS is mainly caused by the socio-cultural process of the ancient community affecting the early development of the city, followed by the cost and ownership factors of land (Fasihi & Parizadi 2020). Chen et al. (2020) in their study revealed that inequity in PGOS access in Shanghai – China is caused by the urban spatial restructuring policy of which industrial areas were relocated to the urban outskirts causing the massive decrease in green space while later the urban center received intensive PGOS development. Furthermore, green gentrification has also contributed to inequity (Chen et al. 2020). Meanwhile, in the context of South Tangerang – Indonesia, lack of considerations on spatial accessibility and socio-demographic aspect in the PGOS planning & policy may contribute to shaping the inequitable pattern of green space. PGOS planning & policy in South Tangerang (also in most cities in Indonesia) only focuses on the quantitative standard of 30% green space ratio of urban area (overlooking spatial and socio-demographic aspect) which refers to The Law No. 26/2007 concerning Spatial Planning. Tan & Samsudin (2017) argued that ignorance of spatial accessibility measures in PGOS planning contributes to the disparity of PGOS access. Moreover, in terms of PGOS planning, fine spatial scale also matters to be considered (Tan & Samsudin 2017). In addition, according to The Strategic Planning of Agency of Building and Spatial Planning 2016-2021 of South Tangerang, the limited city fiscal budget hinders the optimal development of PGOS, which this study argues, may also manifest into the disparity of PGOS access as observed in Figure 3 & 4. Furthermore, this article argues that the existence of new towns also created the imbalance of PGOS availability between new town areas and areas outside of new town, producing inequitable outcome. Private housing developers intensively develop social infrastructures or amenities such as PGOS in the residential area they develop (new town in this context) for the intention to increase the marketability and attractiveness of the residences they sell. The sufficiency of social infrastructure such as PGOS is in fact one of the primary reasons for people to reside in new town (Firman 2004).

PGOS Accessibility Effect on Distribution of Social & Health Benefits

PGOS provides diverse Ecosystem Services (ES) which benefit the urban residents. Compared to other types of ES, cultural services are provided in greater amounts by PGOS (Milcu et al. 2013; Chang et al. 2017). Cultural services of PGOS include recreation, physical activities facilitation, aesthetic, and spiritual which lead to the well-being (mental and physical health) benefits of the urban community (Chan et al. 2011; Daniel et al. 2012). Researchers argue that the optimality of benefits received by urban residents through ES are associated with distance (Chang et al. 2017; Herreros-Cantis & Mcphearson 2021). Especially for cultural services of PGOS since they can only be obtained in-situ. Evidently, this is because the further residents reside from PGOS, the less willingness they grow to visit PGOS regularly to do physical activities and recreation (Neuvonen 2007; Toftager et al. 2011; Wang et al. 2019), in line with the concept of *distance decay* (Tan & Samsudin 2017). This argument is further supported by empirical studies in cities of Indonesia. Widyahantari & Rudiarto (2019) in the context of Bandung, indicated that urban residents tend to prefer to visit PGOS that is located within walkable distance (easy access). Additionally, other studies taking the context of various cities of Indonesia reported outcomes of being distanced from PGOS (and consequently its ES), that the further urban residents reside from PGOS to an extent where distance is no longer walkable (>1 km), they show worse health such as higher risk of getting Acute Respiratory Infections (Nurimani and Suyud 2016; Wicaksono et al. 2021) and worse quality of life (Danurdara et al. 2019). Previous discussions imply that the inequality of PGOS access in South Tangerang that the study found may affect how PGOS benefits are derived and further may negatively impact the health equity of urban residents (Rigolon et al. 2021). Furthermore, the issue of health inequity may be further exacerbated when it is the vulnerable who get sub-optimal access to PGOS. That is, because green space has greater protective effects and social return to the vulnerable, such as low-income group, than the non-vulnerable (Rigolon et al. 2021; Sharifi et al. 2021).

The importance of good PGOS accessibility is even more amplified during the recent health crisis, the Covid-19 pandemic (Grima et al. 2020; Marconi et al. 2022).

Many recent studies have exemplified the significance of ease of access to PGOS in creating resilient community against health crisis, of which these studies also imply the increasing need for good access of PGOS during pandemic (Grima et al. 2020; Poortinga et al. 2021; Marconi et al. 2022; Noszczyk et al. 2022). Noszczyk et al. (2022) in his research revealed that mental health benefit during the pandemic is related to several factors, one of them is close access to PGOS. Noszczyk et al. (2022) also found that 75% of their respondents believe visiting PGOS during pandemic helps decrease stress level. Access to PGOS is beneficial to help combat the exacerbated depression during pandemic (Grima et al. 2020). Other researchers, Poortinga et al. (2021), reported that people living more than 10 minutes of walk show poorer health than those living closer to PGOS (<5 mins) during and after the first peak of Covid-19 pandemic.

CONCLUSIONS AND POLICY IMPLICATIONS

This study concludes that access to PGOS in South Tangerang hasn't achieved equity both in the horizontal dimension and vertical dimension. PGOS access is unequal for its residents, with 48.7% of population still residing in areas with very poor green space access and only 38.8% residential areas are covered by walkable green space service radius. It was found that PGOS service coverage tends to agglomerate in elite private housing area (new town). Furthermore, on the social equity (vertical dimension) implications, South Tangerang City has not yet provided green space equitably for low-income group indicated by the statistical analysis results of Spearman & Moran's Index, showing significant negative index. As for the children, this study found unpatterned equity as result of correlation tests revealed no discernable association. Furthermore, on the elderly and population density, PGOS is equitable with index from Spearman correlation showing positive value and the spatial association test result showing clusters which indicate equity being dominant. Furthermore, South Tangerang adds to the list of many cities in the world that still has not yet provided equitable green space access for the low-income group, such as Singapore, Ilam, and Melbourne. This acts as evidence that providing green space access that is equitable is a great challenge faced by many cities in many countries in the world. Findings of this study also imply that South Tangerang has not yet fulfilled its development goal of becoming a just and sustainable city.

This article addresses a few key policy implications derived from the findings. Firstly, this article suggests that there's a need to reform PGOS planning and policy in which spatial accessibility measure and aspect of socio-demographic (e.g., the vulnerable) should be taken into account as parameters and be prioritized. As discussed before, using quantitative measure alone in PGOS planning is simply insufficient as it neglects the spatial factor and socio-demographic characteristics (demand determinant as argued by Yuan et al. 2017). Secondly, as lack of funding and limited fiscal capacity is deemed as the main factor in the sub-optimal development of PGOS, this article argues that the town government should consider other types of alternative PGOS funding such as Tax Increment Financing (TIF), Transfer of Development Rights (TDR), and Development Charges. For instance of TIF application, the increased value of property affected by PGOS (Zygmunt & Gluszak 2015; Czembrowski & Kronenberg 2016; Engström & Gren, 2017) can be captured through TIF of which proceeds can be used to refinance the development of PGOS. Thirdly, the government should put more focus on developing PGOS for future PGOS planning (without compromising the quality matter of PGOS) in the residential area of the urban outskirts as that part of the town is relatively the most underserved in terms of PGOS service. In the case where land availability is low but still underserved by PGOS, the government can consider developing pocket parks. Lastly, this article also suggests that PGOS availability and its distribution should be regularly monitored and evaluated by the town government.

REFERENCES

Abercrombie L.C., Sallis J.F., Conway T.L., Frank L.D., Saelens B.E., & Chapman J.E. (2008). Income and Racial Disparities in Access to Public Parks and Private Recreation Facilities. American Journal of Preventive Medicine, 34(1), 9-15, DOI: 10.1016/j.amepre.2007.09.030.

Agency of Building and Spatial Planning of South Tangerang. (2018). The Strategic Planning of Agency of Building and Spatial Planning 2016-2021 of South Tangerang. South Tangerang: Agency of Building and Spatial Planning.

Andriarsi M.K. (2021). Air Pollution in South Tangerang is The Highest in Indonesia (in Bahasa Indonesia with English Summary). [online] Available at: https://databoks.katadata.co.id/datapublish/2021/03/10/polusi-udara-tangerang-selatan-tertinggi-di-indonesia [Accessed 22 Oct. 2022]

Anselin L. (1995). Local Indicators of Spatial Association-LISA. Geographical Analysis, 27(2), 93-115, DOI: 10.1111/j.1538-4632.1995.tb00338.x.

Apriyanto H., Eriyatno E., Rustiadi E., & Mawardi I. (2015). STATUS BERKELANJUTAN KOTA TANGERANG SELATAN-BANTEN DENGAN MENGGUNAKAN KEY PERFORMANCE INDICATORS (Sustainable Status of South Tangerang City-Banten Using Key Performance Indicators). Jurnal Manusia Dan Lingkungan, 22(2), 260, DOI: 10.22146/jml.18750.

Barrington-Leigh C., & Millard-Ball A. (2017). The world's user-generated road map is more than 80% complete. PLOS ONE, 12(8), e0180698, DOI: 10.1371/journal.pone.0180698.

Biljecki F., & Ito K. (2021). Street view imagery in urban analytics and GIS: A review. Landscape and Urban Planning, 215, 104217, DOI: 10.1016/j.landurbplan.2021.104217.

Boone C.G., Buckley G.L., Grove J.M., & Sister C. (2009). Parks and People: An Environmental Justice Inquiry in Baltimore, Maryland. Annals of the Association of American Geographers, 99(4), 767-787, DOI: 10.1080/00045600903102949.

Chan K.M.A., Goldstein J., Satterfield T., Hannahs N., Kikiloi K., Naidoo R., … Woodside U. (2011). Cultural services and non-use values. In P. Kareiva, H. Tallis, T. H. Ricketts, G. C. Daily, & S. Polasky (Eds.), Natural Capital (pp. 206–228). Oxford: Oxford University Press, DOI: 10.1093/acprof:oso/9780199588992.003.0012

Chang J., Qu Z., Xu R., Pan K., Xu B., Min Y., … Ge Y. (2017). Assessing the ecosystem services provided by urban green spaces along urban center-edge gradients. Scientific Reports, 7(1), 11226, DOI: 10.1038/s41598-017-11559-5.

Chen Y., Yue W., & La Rosa D. (2020). Which communities have better accessibility to green space? An investigation into environmental inequality using big data. Landscape and Urban Planning, 204, 103919, DOI: 10.1016/j.landurbplan.2020.103919.

Chiesura A. (2004). The role of urban parks for the sustainable city. Landscape and Urban Planning, 68(1), 129-138, DOI: 10.1016/j.landurbplan.2003.08.003

Coombes E., Jones A.P., & Hillsdon M. (2010). The relationship of physical activity and overweight to objectively measured green space accessibility and use. Social Science & Medicine, 70(6), 816-822, DOI: 10.1016/j.socscimed.2009.11.020

Covington K.L. (2015). Poverty Suburbanization: Theoretical Insights and Empirical Analyses. Social Inclusion, 3(2), 71-90, DOI: 10.17645/si.v3i2.120.

Czembrowski P., & Kronenberg J. (2016). Hedonic pricing and different urban green space types and sizes: Insights into the discussion on valuing ecosystem services. Landscape and Urban Planning, 146, 11-19, DOI: 10.1016/j.landurbplan.2015.10.005.

Daniel T.C., Muhar, A., Arnberger, A., Aznar, O., Boyd, J. W., Chan, K. M. A., … von der Dunk, A. (2012). Contributions of cultural services to the ecosystem services agenda. Proceedings of the National Academy of Sciences, 109(23), 8812-8819, DOI: 10.1073/pnas.1114773109

Danurdara P., Suryanto & Gravitiani E. (2019). A STATEGICAL ANALYSIS OF GREEN OPEN SPACE' MANAGEMENT AND THE RELATION TO PUBLIC MENTAL HEALTH' OPPORTUNITIES. International Journal of Economics, Business and Management Research, 3(07), 55-66.

Du X., Zhang X., Wang H., Zhi X., & Huang J. (2020). Assessing Green Space Potential Accessibility through Urban Artificial Building Data in Nanjing, China. Sustainability, 12(23), 9935, DOI: 10.3390/su12239935.

Dushkova D., Ignatieva M. (2020). New trends in urban environmental health research: from geography of diseases to therapeutic landscapes and healing gardens. GEOGRAPHY, ENVIRONMENT, SUSTAINABILITY, Volume 13(1), DOI: 10.24057/2071-9388-2019-99

Engström G., & Gren A. (2017). Capturing the value of green space in urban parks in a sustainable urban planning and design context: Pros and cons of hedonic pricing. Ecology and Society, 22(2), art21, DOI: 10.5751/ES-09365-220221.

Fasihi H., & Parizadi T. (2020). Analysis of spatial equity and access to urban parks in Ilam, Iran. Journal of Environmental Management, 260, 110122, DOI: 10.1016/j.jenvman.2020.110122.

Feng S., Chen L., Sun R., Feng Z., Li J., Khan M.S., & Jing, Y. (2019). The Distribution and Accessibility of Urban Parks in Beijing, China: Implications of Social Equity. International Journal of Environmental Research and Public Health, 16(24), 4894, DOI: 10.3390/ijerph16244894.

Feng X., & Astell-Burt T. (2017). Do greener areas promote more equitable child health? Health & Place, 46, 267-273, DOI: 10.1016/j.healthplace.2017.05.006.

Firman T. (2004). New town development in Jakarta Metropolitan Region: A perspective of spatial segregation. Habitat International, 20.

Geneletti D., Cortinovis C., & Zardo L. (2022). Simulating crowding of urban green areas to manage access during lockdowns. Landscape and Urban Planning, 219, 104319, DOI: 10.1016/j.landurbplan.2021.104319.

Grima N., Corcoran W., Hill-James C., Langton B., Sommer H., & Fisher B. (2020). The importance of urban natural areas and urban ecosystem services during the COVID-19 pandemic. PLOS ONE, 15(12), e0243344, DOI: 10.1371/journal.pone.0243344.

Haddad M., Christman Z., Pearsall H., & Sanchez M. (2021). Using Google Street View to Examine Urban Context and Green Amenities in the Global South: The Chilean Experience. Frontiers in Sustainable Cities, 3, 684231, DOI: 10.3389/frsc.2021.684231.

Haq S. Md. A. (2011). Urban Green Spaces and an Integrative Approach to Sustainable Environment. Journal of Environmental Protection, 02(05), 601-608, DOI: 10.4236/jep.2011.25069.

He S., Wu Y., & Wang L. (2020). Characterizing Horizontal and Vertical Perspectives of Spatial Equity for Various Urban Green Spaces: A Case Study of Wuhan, China. Frontiers in Public Health, 8, 10, DOI: 10.3389/fpubh.2020.00010.

Herreros–Cantis P., & McPhearson T. (2021). Mapping supply of and demand for ecosystem services to assess environmental justice in New York City. Ecological Applications, 31(6), DOI: 10.1002/eap.2390.

Holt E., Lombard Q., Best N., Smiley-Smith S., & Quinn J. (2019). Active and Passive Use of Green Space, Health, and Well-Being amongst University Students. International Journal of Environmental Research and Public Health, 16(3), 424, DOI: 10.3390/ijerph16030424.

Krefis A., Augustin M., Schlünzen K., Oßenbrügge J., & Augustin, J. (2018). How Does the Urban Environment Affect Health and Well-Being? A Systematic Review. Urban Science, 2(1), 21, DOI: 10.3390/urbansci2010021.

Lee G., & Hong I. (2013). Measuring spatial accessibility in the context of spatial disparity between demand and supply of urban park service. Landscape and Urban Planning, 119, 85-90, DOI: 10.1016/j.landurbplan.2013.07.001.

Li Z., Fan Z., Song Y., & Chai Y. (2021). Assessing equity in park accessibility using a travel behavior-based G2SFCA method in Nanjing, China. Journal of Transport Geography, 96, 103179, DOI: 10.1016/j.jtrangeo.2021.103179.

Liu J., Huang S., Li G., Zhao J., Lu W., & Zhang Z. (2020). High housing density increases stress hormone- or disease-associated fecal microbiota in male Brandt's voles (Lasiopodomys brandtii). Hormones and Behavior, 126, 104838, DOI: 10.1016/j.yhbeh.2020.104838.

Maas J., Verheij R.A., Spreeuwenberg P., & Groenewegen P.P. (2008). Physical activity as a possible mechanism behind the relationship between green space and health: A multilevel analysis. BMC Public Health, 8(1), 206, DOI: 10.1186/1471-2458-8-206.

Marconi P.L., Perelman P.E., & Salgado V.G. (2022). Green in times of COVID-19: Urban green space relevance during the COVID-19 pandemic in Buenos Aires City. Urban Ecosystems, 25(3), 941-953, DOI: 10.1007/s11252-022-01204-z.

Maroko A.R., Maantay J.A., Sohler N.L., Grady K.L., & Arno P.S. (2009). The complexities of measuring access to parks and physical activity sites in New York City: A quantitative and qualitative approach. International Journal of Health Geographics, 8(1), 34, DOI: 10.1186/1476-072X-8-34.

Meerow S., Pajouhesh P., & Miller T.R. (2019). Social equity in urban resilience planning. Local Environment, 24(9), 793-808, DOI: 10.1080/13549839.2019.1645103.

Milcu A.I., Hanspach J., Abson D., & Fischer J. (2013). Cultural Ecosystem Services: A Literature Review and Prospects for Future Research. Ecology and Society, 18(3), art44, DOI: 10.5751/ES-05790-180344.

Ministry of Home Affairs. (2009). Regulation of The Ministry of Home Affairs of the Republic of Indonesia No. 9/2009. Indonesia: Ministry of Home Affairs.

Ministry of Social Affairs. (2021). Ministerial Decree of Ministry of Social Affairs of Indonesia No 88/HUK/2021. Indonesia: Ministry of Social Affairs

Mushkani R.A., & Ono H. (2021). Spatial Equity of Public Parks: A Case Study of Kabul City, Afghanistan. Sustainability, 13(3), 1516, DOI: 10.3390/su13031516.

Neuvonen M., Sievänen T., Tönnes S., & Koskela T. (2007). Access to green areas and the frequency of visits – A case study in Helsinki. Urban Forestry & Urban Greening, 6(4), 235-247, DOI: 10.1016/j.ufug.2007.05.003.

Noszczyk T., Gorzelany J., Kukulska-Kozieł A., & Hernik J. (2022). The impact of the COVID-19 pandemic on the importance of urban green spaces to the public. Land Use Policy, 113, 105925, DOI: 10.1016/j.landusepol.2021.105925.

Nurimani A.F., & Utomo S.W. (2016). Public Green Open Spaces and Acute Respiratory Infection in Population at Jagakarsa Distric 2016 (in Bahasa Indonesia with English summary). Master Thesis, Department of Environmental Health, University of Indonesia.

Pham T.-T.-H., & Labbé D. (2018). Spatial Logic and the Distribution of Open and Green Public Spaces in Hanoi: Planning in a Dense and Rapidly Changing City. Urban Policy and Research, 36(2), 168-185, DOI: 10.1080/08111146.2017.1295936.

Poortinga W., Bird N., Hallingberg B., Phillips R., & Williams D. (2021). The role of perceived public and private green space in subjective health and wellbeing during and after the first peak of the COVID-19 outbreak. Landscape and Urban Planning, 211, 104092, DOI: 10.1016/j.landurbplan.2021.104092.

Prastiwi A.D. (2022). URBAN HEAT ISLAND DI KOTA TANGERANG SELATAN. Jurnal Geosaintek, 8(2), 182, DOI: 10.12962/j25023659.v8i2.11721.

Reyes M., Páez A., & Morency C. (2014). Walking accessibility to urban parks by children: A case study of Montreal. Landscape and Urban Planning, 125, 38-47, DOI: 10.1016/j.landurbplan.2014.02.002.

Rigolon A. (2016). A complex landscape of inequity in access to urban parks: A literature review. Landscape and Urban Planning, 153, 160-169, DOI: 10.1016/j.landurbplan.2016.05.017.

Rigolon A., Browning M.H.E.M., McAnirlin O., & Yoon H. (Violet). (2021). Green Space and Health Equity: A Systematic Review on the Potential of Green Space to Reduce Health Disparities. International Journal of Environmental Research and Public Health, 18(5), 2563, DOI: 10.3390/ijerph18052563.

Roitman S., & Recio R.B. (2020). Understanding Indonesia's gated communities and their relationship with inequality. Housing Studies, 35(5), 795-819, DOI: 10.1080/02673037.2019.1636002.

Romero A.J. (2005). Low-income neighborhood barriers and resources for adolescents' physical activity. Journal of Adolescent Health, 36(3), 253-259, DOI: 10.1016/j.jadohealth.2004.02.027.

Saifullah K., Barus B., & Rustiadi E. (2017). Spatial modelling of land use/cover change (LUCC) in South Tangerang City, Banten. IOP Conference Series: Earth and Environmental Science, 54, 012018, DOI: 10.1088/1755-1315/54/1/01201.

Satterthwaite, D. (1993). The impact on health of urban environments. Environment and Urbanization, 5(2), 87–111, DOI: 10.1177/095624789300500208.

Sharifi F., Nygaard A., Stone W.M., & Levin I. (2021). Accessing green space in Melbourne: Measuring inequity and household mobility. Landscape and Urban Planning, 207, 104004, DOI: 10.1016/j.landurbplan.2020.104004.

Takano T. (2002). Urban residential environments and senior citizens' longevity in megacity areas: The importance of walkable green spaces. Journal of Epidemiology & Community Health, 56(12), 913-918, DOI: 10.1136/jech.56.12.913.

Talen E., & Anselin L. (1998). Assessing Spatial Equity: An Evaluation of Measures of Accessibility to Public Playgrounds. Environment and Planning A: Economy and Space, 30(4), 595-613, DOI: 10.1068/a300595.

Tan P.Y., & Samsudin R. (2017). Effects of spatial scale on assessment of spatial equity of urban park provision. Landscape and Urban Planning, 158, 139-154, DOI: 10.1016/j.landurbplan.2016.11.001.

The Law of The Republic Indonesia on Elderly Welfare Number 13 of 1998.

The Law No. 1/2011 concerning Housing and Residential Areas of The Republic of Indonesia.

Toftager M., Ekholm O., Schipperijn J., Stigsdotter U., Bentsen P., Grønbæk M., … Kamper-Jørgensen F. (2011). Distance to Green Space and Physical Activity: A Danish National Representative Survey. Journal of Physical Activity and Health, 8(6), 741-749, DOI: 10.1123/jpah.8.6.741.

Twohig-Bennett C., & Jones A. (2018). The health benefits of the great outdoors: A systematic review and meta-analysis of greenspace exposure and health outcomes. Environmental Research, 166, 628-637, DOI: 10.1016/j.envres.2018.06.030.

Wang H., Dai X., Wu J., Wu X., & Nie X. (2019). Influence of urban green open space on residents' physical activity in China. BMC Public Health, 19(1), 1093, DOI: 10.1186/s12889-019-7416-7.

Ward Thompson C., Roe J., Aspinall P., Mitchell R., Clow A., & Miller D. (2012). More green space is linked to less stress in deprived communities: Evidence from salivary cortisol patterns. Landscape and Urban Planning, 105(3), 221-229, DOI: 10.1016/j.landurbplan.2011.12.015.

Wibowo B., Aditya R., & Harianto T. (2021). Harnessing open data and technology for the study of accessibility: The case of Indonesia's capital site candidate. Spatium, (46), 46-53, DOI: 10.2298/SPAT2146046W.

Wicaksono M.A.A., Simangunsong N.I., & Suharto B.B. (2021). Pengaruh Jarak terhadap Persepsi Sehat Penghuni Perumahan Kecamatan Tebet Jakarta Selatan. Jurnal Lanskap Indonesia, 13(1), 13-18, DOI: 10.29244/jli.v13i1.33321.

Widyahantari R., & Rudiarto I. (2019). Evaluation of Thematic Parks in Bandung City Based on Spatial Equity Perspective. KnE Social Sciences, DOI: 10.18502/kss.v3i21.5002.

Wilson D.K., Kirtland K.A., Ainsworth B.E., & Addy C.L. (2004). Socioeconomic status and perceptions of access and safety for physical activity. Annals of Behavioral Medicine, 28(1), 20-28, DOI: 10.1207/s15324796abm2801_4.

Winarso H., Hudalah D., & Firman T. (2015). Peri-urban transformation in the Jakarta metropolitan area. Habitat International, 49, 221-229, DOI: 10.1016/j.habitatint.2015.05.024.

Wolch J. R., Byrne J., & Newell J.P. (2014). Urban green space, public health, and environmental justice: The challenge of making cities 'just green enough.' Landscape and Urban Planning, 125, 234-244, DOI: 10.1016/j.landurbplan.2014.01.017.

Wolff M., & Haase D. (2019). Mediating Sustainability and Liveability—Turning Points of Green Space Supply in European Cities. Frontiers in Environmental Science, 7, 61, DOI: 10.3389/fenvs.2019.00061.

Xu C., Chen G., Huang Q., Su M., Rong Q., Yue W., & Haase D. (2022). Can improving the spatial equity of urban green space mitigate the effect of urban heat islands? An empirical study. Science of The Total Environment, 841, 156687, DOI: 10.1016/j.scitotenv.2022.156687.

Yuan Y., Xu J., & Wang Z. (2017). Spatial Equity Measure on Urban Ecological Space Layout Based on Accessibility of Socially Vulnerable Groups—A Case Study of Changting, China. Sustainability, 9(9), 1552, DOI: 10.3390/su9091552.

Zhan P., Hu G., Han R., & Kang Y. (2021). Factors Influencing the Visitation and Revisitation of Urban Parks: A Case Study from Hangzhou, China. Sustainability, 13(18), 10450, DOI: 10.3390/su131810450.

Zheng Z., Shen W., Li Y., Qin Y., & Wang L. (2020). Spatial equity of park green space using KD2SFCA and web map API: A case study of zhengzhou, China. Applied Geography, 123, 102310, DOI: 10.1016/j.apgeog.2020.102310.

Zhou X., & Kim J. (2013). Social disparities in tree canopy and park accessibility: A case study of six cities in Illinois using GIS and remote sensing. Urban Forestry & Urban Greening, 12(1), 88-97, DOI: 10.1016/j.ufug.2012.11.004.

Zhou X., & Wang Y.-C. (2011). Spatial–temporal dynamics of urban green space in response to rapid urbanization and greening policies. Landscape and Urban Planning, 100(3), 268-277, DOI: 10.1016/j.landurbplan.2010.12.013.

Zhu Z., Li J., & Chen Z. (2022). Green space equity: Spatial distribution of urban green spaces and correlation with urbanization in Xiamen, China. Environment, Development and Sustainability, DOI: 10.1007/s10668-021-02061-0.

Zygmunt R., & Gluszak M. (2015). Forest proximity impact on undeveloped land values: A spatial hedonic study. Forest Policy and Economics, 50, 82-89, DOI: 10.1016/j.forpol.2014.07.005.

RESEARCH PAPER

INVENTORY OF LANDSLIDES TRIGGERED BY HURRICANE MATTHEWS IN GUANTÁNAMO, CUBA

Georgui B. Pospehov[1], Yusmira Savón[1*], Ricardo Delgado[2], Enrique A. Castellanos[3], Arisleydis Peña[4]

[1] Saint Petersburg Mining University. 21-Ya Liniya Vasil'yevskogo Ostrova, 2, St Petersburg, 199106.

[2] Delegation of the Ministry of Science, Technology and Environment, Ahogados e/ 12 y 13 north. No. 14. Guantánamo, Cuba.

[3] Ministry of Energy and Mines, Ave. Salvador Allende #666, Centro Habana, La Habana, Cuba.

[4] Institute of Meteorology. Meteorological Center of Guantánamo. 13 North # 14 e/ 1 y el 2 west, Reparto Caribe, Guantánamo, Cuba.

***Corresponding author:** yusmirasvaciano@gmail.com

Received: September 16th, 2022 / Accepted: February 15th, 2023 / Published: March 31st, 2023

https://DOI-10.24057/2071-9388-2022-133

ABSTRACT. Hurricane Matthew affected the eastern region of Cuba from October 4th to 5th causing large damages and numerous landslides. This research presents an inventory of landslides triggered by the hurricane. Visual interpretation of satellite images of moderate resolution from Sentinel 2A instrument and localized higher resolution satellite images provided by PlanetScope, as well as field research were the main sources of information. The resulting landslide inventory was compared with other landslide factors such as slope, geology, and soil deep and composition from maps at a scale of 1:100 000. Data recorded by 1-hour rain gauges and 24-hour rain gauge was also analyzed in order to identify rainfall thresholds for the occurrence of landslides during the Hurricane Matthew influence in the study region. A total of 619 landslides were identified and classified as rockslide, rockfall or debris flows. The research found the slope was not as important factor as the type of rock. Most of landslides were located in areas of green shale of volcanic and vulcanoclastic rocks and rocks of the ophiolitic complex formed by ancient remnants of oceanic crust. The accumulate rainfall threshold estimated for the event was between 178-407 mm/day.

KEYWORDS: Landslide inventory, Hurricane Matthew, Rainfall Threshold, Guantánamo

CITATION: Pospehov G. B., Savón Y., Delgado R., Castellanos E. A., Peña A. (2023). Inventory Of Landslides Triggered By Hurricane Matthews In Guantánamo, Cuba. Geography, Environment, Sustainability, 1(16), 55-63
https://DOI-10.24057/2071-9388-2022-133

Conflict of interests: The authors reported no potential conflict of interest.

INTRODUCTION

Landslides are very dangerous geomorphological phenomena that cause damage to social infrastructure, making it ineffective, and to economic infrastructure, contributing to a decrease in productivity, hence the importance of their study and prediction (Kutepova 2012). These phenomena are closely linked to the physical-mechanical properties of the rock masses, which determine the degree of deformation of these (Gospodarikov 2010; Gusev 2016; Pospehov et al. 2018; Trushko and Protosenya 2019) and also to conditioning factors such as the type of rock, topography, soil characteristics, hydrogeology (Dashko 2018; Kutepova 2012), the rain among others.

A significant part of the methodologies for landslide risk assessment includes as a fundamental input, detailed information on the previous occurrence of landslides in the study area (Dai et al. 2001; Ayalew and Yamagishi 2005). Which strengthen the case for comprehensive landslide inventories as requirement to quantify both landslide hazards and risks (van Westen et al. 2008). Research on landslide inventories has been conducted at global (Brown et al. 1992), as well as nation or regional levels (Guzzetti et al. 1994 and Marcelino et al. 2009).

Landslides induced by tropical cyclones are a significant threat to lives and property in the Caribbean basing (Bertinelli, Mohan, and Strobl 2016). Furthermore, due to the global climate trends, the frequency and intensity of those atmospheric phenomena are bound to increase (Kleptsova et al. 2021). Such increases in tropical cyclone activity pose increasing risks even for extra tropical areas usually considered outside their reach (Ranson et al. 2014). These conditions require frequent updating of landslide inventories in order to gain better comprehension of the landslide hazards and risks.

The island of Cuba is the largest of the Caribbean region with 109 884 km^2. Its eastern region is the most prone to the occurrence of landslides, due to the abundance of mountainous areas with steep slopes. Most of landslides are associated with meteorological events such as tropical cyclones or prolonged periods of rain (Castellanos and van Westen 2008). Landslide hazard, vulnerability and risk assessments carried out in Guantánamo province as part of the national effort to improve disaster management, among other research (Castellanos and van Westen 2007) concluded that rainfall is the most important triggering factor for landslide events in the area.

The year 2016 was very active from the meteorological point of view for the easternmost region of Cuba due to several events that caused heavy rainfall. In the proposed study area there were 19 heavy rainfall events (more than 100 mm in 24 hours) recorded by the rain gauge network

maintained by the Institute of Meteorology and the Institute of Hydraulic Resources. Two months recorded the heaviest rainfall: April with five heavy rainfall events accumulating 863.3 mm and October with 12 heavy rainfall events accumulating 2448.6 mm. In this work we present the inventory of landslides triggered by hurricane Matthew as it passed through the eastern part of Cuba.

The landslide inventory was carried out for the period from August 2016 to January 2017. The main source of information for this inventory were before and after the event Sentinel 2A satellite images from MSI instrument operated by the European Space Agency (ESA). Moderate resolution (10 m per pixel) true color and false color near-infrared images were generated from level 1C products. Images dates, identifiers and cloud percentage are shown in Table 1. Before and after hurricane images provided by PlanetScope were also used for the areas where the occurrence of landslides was more frequent. PlanetScope images have a mean resolution of 3 m per pixel of which true color and false color near infrared scenes were used. Scene dates, identifiers and cloud percentage are shown in Table 1.

As can be seen in the Table 1, Sentinel images covered the period before and after the hurricane from August 30, 2016 to January 1, 2017. These images covered the entire study area. PlanetScope images were used in an area of 5 000 km^2 in total. The selection of scenes was conditioned by the cloud percentage, which interferes with the visual analysis by the selected period in which there was no episodes of intense rains that could cause landslides unrelated to the hurricane.

The limits of the study area were defined taking into account the frame of topographic sheets at 1:10 000 scale. High-resolution post event satellite images provided by free internet providers Google and Microsoft were used as additional source of information.

The study area was divided into 183 squares of 5 x 5 km and a visual interpretation was made using true color, false color infrared and Normalized Difference Vegetation Index (NDVI) scenes to enhance the discrimination of areas with vegetation coverage. Each square was examined and searched looking for vegetation loss and soil and rocks exposed after the hurricane and for typical landslide fans and features. Points were draw near the center of suspected landslides for further review.

After the visual interpretation phase, field visits were made to selected locations in the study area for the purpose of checking and direct identification of landslides. Some of the fieldwork was focused to confirm areas of possible occurrence of landslide events. Several fieldwork routes were traced through the towns and roads affected by the hurricane.

Once the landslide inventory was completed, spatial analysis was used to preliminarily identify the main environmental factors associated with landslides in the area. These analyzes comprise maps of elevations and slopes derived from a digital elevation model (DEM) with a resolution of 25 m per pixel, where the slope in degrees and the elevation in meters above sea level were analyzed. The vertical uncertainty DEM is in a range of 10 m. Likewise, the geological map at a scale of 1:100 000 from the Institute of Geology and Paleontology and the soil parameters (soil depth and texture) at a scale of 1:100 000 from the Institute of Soils of Cuba were included in the analysis.

In order to better understand the behavior of the rain as a triggering factor, the precipitation data from 1-hour rain gauge stations operated by INSMET and 24-hour rain gauge stations operated by INRH. Data was collected for the year 2016 and for October 2016. Analysis of rainfall thresholds that contributed to the occurrence of landslides during the passage of Hurricane Matthew was carried out, taking into account accumulated rainfall data.

The expression for threshold (Th) calculations proposed by (Stedinger et al. 1993) was used in this research. This expression excludes high and low values that are far from the central tendency of the sample:

$$Th = X^{-} \pm k_n S_y \quad (1)$$

where X^{-} and S_y are the mean and standard deviations of the logarithms of accumulated rainfall peaks, excluding previously detected outliers, and k_n is a critical value for the sample size n whose data points deviate significantly from the trend of the remaining data. Its expression is the following

$$k_n = -0.9043 + 3.345\sqrt{\log n} - 0.40461\log n \quad (2)$$

For normal data, the largest observation will exceed $X^{-} \pm k_n S_y$ with a probability of only 10 percent; therefore, the equation is a one-sided test for outliers with a significance level of 10 percent, for a normal distribution; k_n values are tabulated for samples n > 150

For this expression, low outliers are generally valid observations, but because the logarithms of the observed rainfall accumulation peaks are used to fit a two-parameter distribution with a generalized coefficient of deviation, one or more unusual values may distort the entire fitted frequency

Table 1. Satellite images used in the landslide inventory after the passage of Hurricane Matthew on October 4, 2016

Satellite image	Date/Time	Cloud Percentage
Sentinel 2A	2016-08-30 T15:36:22.026Z	36.68
Sentinel 2A	2016-09-19 T15:36:12.026Z	6.60
Sentinel 2A	2016-10-09 T15:36:12.026Z	40.77
Sentinel 2A	2017-01-07 T15:36:01.026Z	9.81
PlanetScope	2016-10-22 T08:07:49Z	11
PlanetScope	2016-10-19 T14:31:14+00:00	6
PlanetScope	2016-10-19 T14:31:15+15:00:00	14
PlanetScope	2016-10-19 T14:31:16+00:00	6
PlanetScope	2016-10-19 T14:31:17+00:00	4
PlanetScope	2016-10-19 T14:31:18+00:00	0

distribution. Therefore, detection of such values is important, and fitted distributions should be compared graphically with the data to detect problems (Stedinger et al. 1993).

Study area

The area of influence of Hurricane Matthew is located in the eastern of Cuba (Fig. 1). Low mountains with less 600 meters above sea level (masl) predominate in this area. There are also some relatively isolated heights not exceeding 1200 masl. Coastal plains and small intra-mountains alluvial valleys surrounded by steep slopes are the most common flat areas in the region (Figure 1a).

The study area is complex from the lithological and structural point of view. It is composed of the rocky complexes of the Cretaceous basement, with rocks of the metamorphic complex, mainly sericite and albite schists and andesite-basaltic lavas. The layers are finely stratified and rocks of the ophiolitic complex have a high degree of fracturing. There are also rocks of the Paleogene volcanic island arc with predominance of tuffs. To a lesser degree, there are rocks of the Neogene-Quaternary coverage composed mainly by the alternation of sandstones, lutite, calcareous lutite and biodetritic limestones (Iturralde-Vinent 1998). The marine terraces are composed of bioclastic and biogenic limestone, calcareous sandstone generated by a combination of recent movements of the earth's crust with the cycles of sea levels due to glaciations stand out in the coastal area. The mountain ranges in the area represent one of the most extensive and well-preserved forest ecosystems in the Antilles.

Matthew Hurricane

Hurricane Matthew, which hit the northeast of the island of Cuba, originated as a tropical storm from a strong tropical wave south of the Lesser Antilles in the early morning of September 28, 2016, reaching category 5 on the Saffir - Simpson scale on October 2 in the warm waters of the eastern Caribbean. It made landfall in Cuban territory on October 4 approximately at 6:00 p.m. in local time near Punta Caleta (20°07'00" N, 74°30'10" W), on the south coast as a category 4 in Saffir-Simpson scale (Ballester and Rubiera 2016) as shown in Figure 1b.

Hurricane Matthew has been the most intense recorded in this region of Cuba and caused damage to agriculture, communications infrastructure, electricity, water supply services, roads and homes in the affected communities. Total economic losses were estimated at 2,430.8 million pesos, of which 24.1 million were spent on prevention measures, 388.5 million on home reconstruction, 70.1 million on equipment, 519.5 million in the agriculture and 81.9 million in goods and services, according to data from the National Statistics Office. It should be noted that the data available on hurricane damage in Cuba is generally not differentiated by cause, which makes it difficult to identify the proportion of those losses caused by landslides.

Figure 2a presents the accumulated rainfall of the stations during the year 2016. It is notable the increase in the accumulated precipitation recorded in stations d1, h6, h3, d2 and d3 in October, coinciding with the occurrence of hurricane Matthew. Gauges d1, d6 and h3 recorded the highest accumulated rainfall in the year in this time period totaling 2309.2 mm; 2217.3 mm and 1690.6 mm in the year respectively.

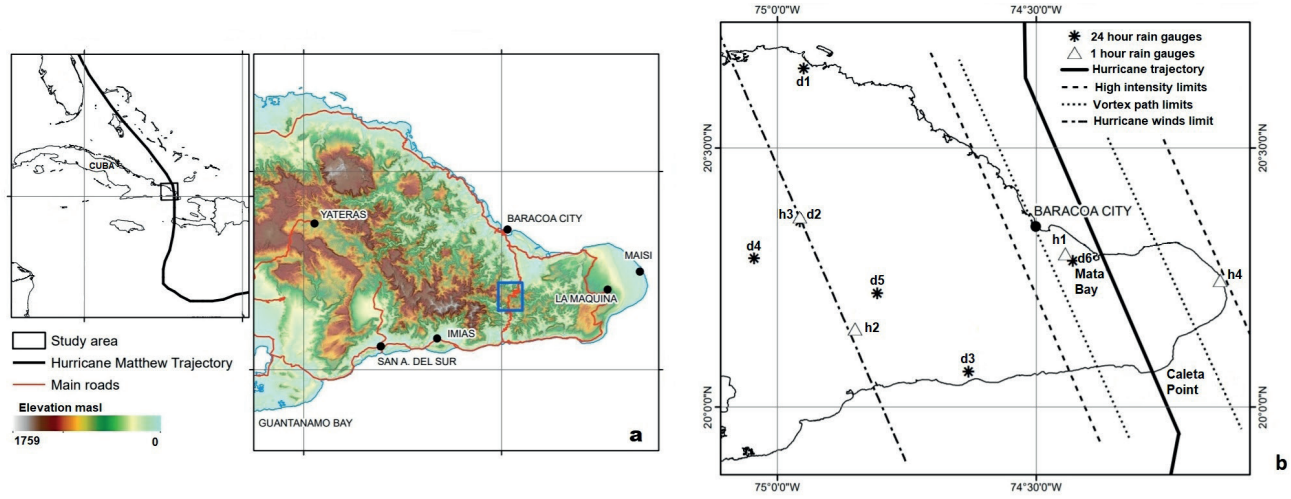

Fig. 1. a) Location of Study Area, hurricane Matthew track and elevation. b) Affected zone of hurricane Matthew and rain gauge location (after Ballester and Rubiera, 2016; and Steward 2017). The blue box in 1a correspond to the photos of Figure 3.

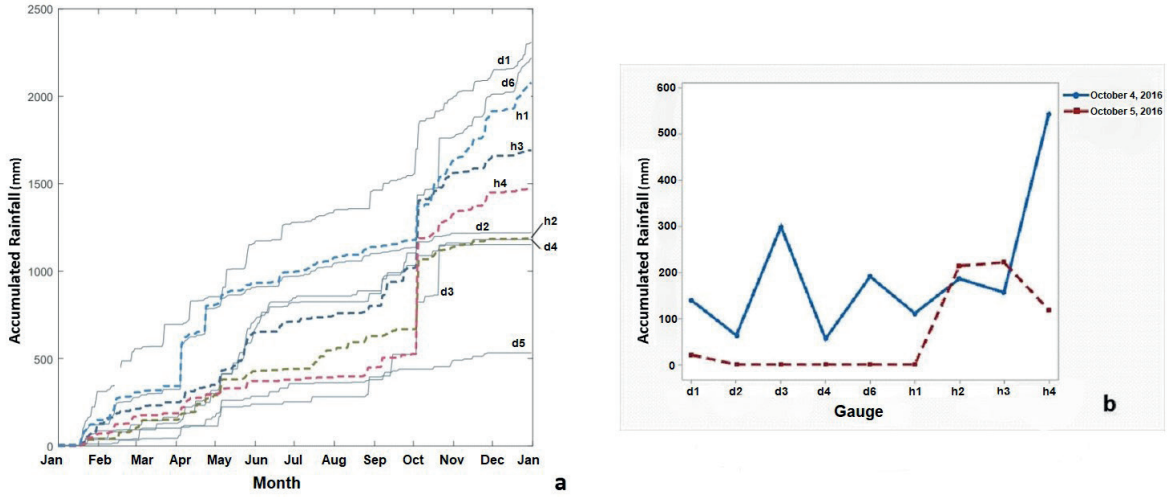

Fig. 2. a) Accumulated rainfall recorded by 1-hour (dashed line) and 24-hour (straight line) rain gauge stations in 2016. b) Accumulated rainfall recorded by each gauge on October 4th and 5th

The highest accumulated rainfall due to Hurricane Matthew was recorded by gauges h4, h2 and h3 (located in Figure 1b). October 4th was the day of highest precipitation in the entire area affected by the hurricane as shown in (Figure 2b). The heavy rainfalls associated with the hurricane and its feeding bands were very intense, specifically on the days of Hurricane Matthew. Rainfall peaked on the day 4 in the gauges h4 and d3 and on the day 5 in gauges h2 and h3. It must be noted that several gauges ceased to operate after October 4th due to the hurricane damages to equipment and infrastructure.

Results and discussion

The inventory carried out in the study area found 619 landslide events associated to Hurricane Matthew. Those landslides were identified taking into the time frame, selecting only recent material movement with loss of the soil layer. The vast majority of those landslide events were shallow landslides. The Figure 3 shows typical landslide examples among those selected.

The identified landslides were classified according to Keefer and Wilson (1989) as rockslides, debris flows and rockfalls. Rockfalls and debris flows corresponding accounted to 86 % of identified landslide events and concentrated at the north and center of the study area as shows Figure 4a. Rockfalls were only identified in the southern part of the study area near marine terraces, which is consistent with previous research (Castellanos & Van Westen, 2008) see Figure 4a.

Fig. 3. Landslide photos taken on 27.11.2016 during fieldwork. Photo location in the blue box in figure 1a

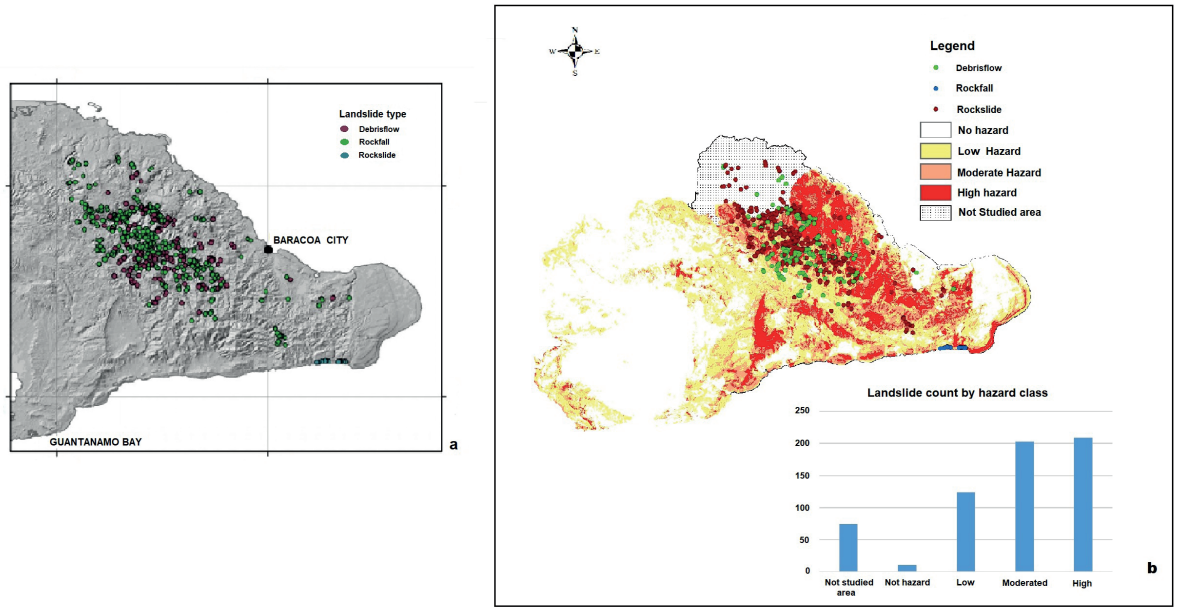

Fig. 4. Landslides triggered by hurricane Matthew. a) Landslide inventory on the relief map and b) Landslides inventory on the hazard map (Castellanos & van Westen, 2008)

Comparing the new inventory of landslides with a previous landslide hazard map for Guantanamo province (Castellanos & Van Westen 2008), 75% of landslide events occurred in area classified as of moderated and high landslide hazard (202 and 209 events respectively) while only 23% (123 events) were located in areas classified as low hazard areas and 2% in not hazard areas (Figure 4 b). Landslides outside the landslide hazard map were not taken into account. This result validates the rationale under the cited research and offers insight into better addressing the hazard mapping in the region.

The spatial analysis of the relation between the landslide inventory and geographical and geological factors found that slope angle is very important component of the conditioning factors as mentioned by Aristazabal and Gómez (2007) and Aristizabal and Yokota (2006). This research found no noticeable difference in slope angle in rockslide and debris flow events. The highest occurrence of landslides was at slope angles between 25 – 42°. Identified rockfall-type events were tightly concentrated near the marine terrace system. This terrace system has a slope angle in general greater than 74° (see Figure 5a). Debris flows and rockslides were triggered by hurricane Matthew mostly between 200 - 500 masl, while rockfall events were identified at heights lower than 45 masl, in the lower level of the terrace system near the shoreline.

Most of rockslide-type landslides were generated in materials composed by green schists of volcanic and vulcanoclastic rocks and rocks of the ophiolitic complex constituted by ancient remains of oceanic crust as shown in Figure 5c. Within its composition predominate harzburguites, lherzolites and serpentinized dunites of the Cretaceous Lower-Upper and Middle Jurassic as show Table 2. These are the oldest rocks in the study area and present different degrees of weathering and high deformation. Debris flows mostly occurred in rocks from the Middle Jurassic ophiolitic complex and in magmatic rocks and to a lesser degree in rocks composed of green schists of volcanic and vulcanoclastic rocks of Cretaceous age. Rockfalls were concentrated in the Maya formation composed of organodetritic and organogenic limestones from the Upper Pliocene-Upper Pleistocene and the Jaimanitas formation composed of carcified biodetritic limestone from the Upper Pleistocene (Table 2).

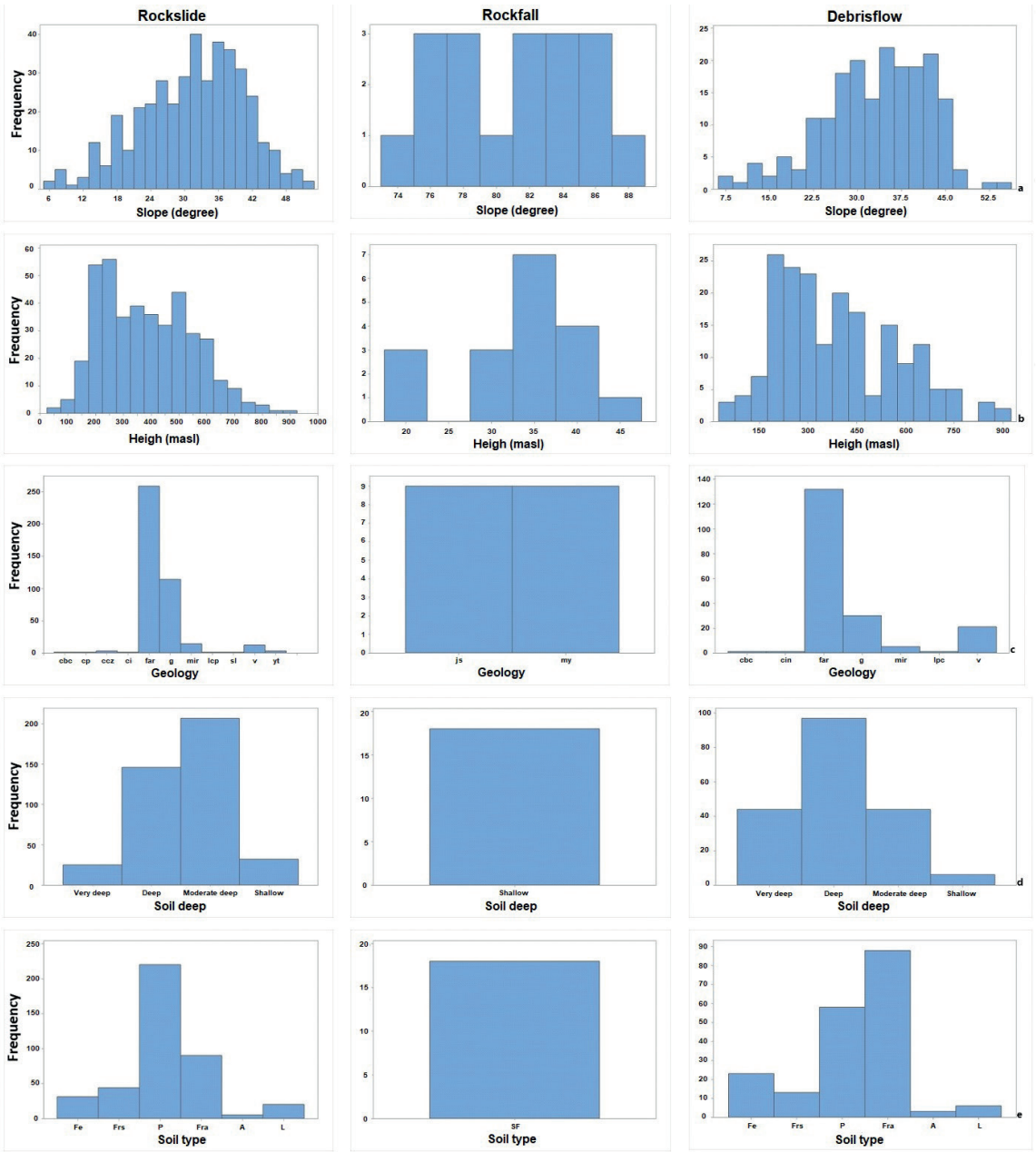

Fig. 5. Distribution landslide types taking into account the slope in degrees (a), height in masl (b), rock formations (c) geology (see table 2), soil depth (d) and soil type (e) where: Fe are ferritic soils; Fr fersialitic; P brown soils; Fra ferralitic soils; To alitic soils; L latosolic soils and IF soils in formation

Table 2. Relation of landslide occurrence with rock types

Unit name	Rock type	Age	Landslide type		
			rockslide	debrisflow	rockfall
Ofiolitic Complex (g)	Rocks of the ophiolitic association: harzburguites, lherzolites, serpentinized dunites	Middle jurassic	114	30	
Magmatic rocks (v)	Undifferentiated gabbroids, gabbros, and diabases		12	21	
Formation La Farola (far)	Green schists of volcanic and vulcanoclastic rocks	Lower Cretaceous- Upper Cretaceous	259	132	
Formation La Picota (lpc)	polymythic conglomerates interspersed with polymythic sandstones	Upper Cretaceous	1	1	
Formation Capdevila (cp)	conglomerates with sandstones and siltstones	Lower Eocene	1		
Formation Castillo de los Indios (cin)	volcanic rocks mainly tuffs	Lower-Middle Eocene		1	
Formation Miranda (mir)	conglomerates of tuff, tuff, and marl	Lower-Middle Eocene	14	5	
Formation San Luis (sl)	Stratifications of polymictic sandstones, siltstones, marls	Middle Eocene- Upper Eocene	1		
Formation Yateras (yt)	biodetritic limestones alternated with biogenic limestones	Upper Oligocene	3		
Member Cilindro (ci)	Polymictic conglomerates with lenticular stratification and sometimes crossed, weakly cemented, with sandstone lenses, containing lignite. The matrix is polymictic sandstone, containing carbonate.	Upper Oligocene- Lower basal Miocene	1		
Formation Cabacú (cbc)	Gravelite, sandstones and siltstones	Upper Oligocene- Lower basal Miocene	1	1	
Formation Cabo Cruz (ccz)	Biodetritic limestones	Middle Miocene- Upper Miocene	3		
Formation Jaimanita	Massive biodetritic limestones, generally karst, very fossiliferous.	Upper Pleistocene.			9
Formation Maya (my)	Marine Deposits, Organodetritic and Organogenic Limestones.	Upper Pliocene-Upper Pleistocene			9

Other factors conditioning the occurrence of landslide events were considered, such as the depth and type of soil. According to the soil classification of the Cuban Soil Institute, 1973, in the study area Ferritic, Ferralitic, Fersialitic and Brown soils are common, which overlie ultrabasic and basic rocks with intense alteration and a high content of clay minerals.

A total of 358 of identified landslide events occurred over moderately deep soils (210) and in deep soils (148) with depth ranges from 20-50 cm to 50-100 cm respectively (Figure 4d). These figures are consistent with the predominance of shallow landslides. Regarding rockfall events, its distribution was on areas of shallow layers of soils in formation with less than 20 cm. A high number of rockslides were identified in areas of brown soils (53%) with a clay loam and sandy texture followed by ferralitic soils (17%) with a sandy loam and clay loam texture. However, debris flows had a predominance in Ferralitic soils (46%) over Brown soils (31%) (Figure 5e).

Rain thresholds after Hurricane Matthew

The assessment of the relationship between landslides and rainfall during and immediately after the hurricane influence was one of the main goals of this study. After accounting for the spatial location and the radius of influence of the rain gauges, the research found that most of the landslides were concentrated in the areas affected by intense rainfall. Such findings confirm the relationship of the occurrence of landslides with intense rainfall found by other authors (Lumb 1975; Garland and Oliver 1993; Kay and Chen 1995; Finlay et al. 1997; Crosta 1998, 2003; Guzzetti 1998; Crozier 1999; Dai et al. 2001; Aleotti 2004; Dikshit et al. 2019; Sarkar and Dorji 2019).

The behavior of the accumulated (24 h) daily rainfall (AR) associated with the days of Hurricane Matthew influence over the study area (October 4th, 5th and 6th), the accumulated antecedent rainfall (AAR) for 3 and 15 days and the accumulated total over those days (Figure 6) were compared with the landslide inventory. This research found the majority of landslides were located near areas of significant rainfall accumulated. As can be seen in the Figure 6, the daily rainfall accumulations on day 6 (Figure 6c) and the previous rainfall accumulations for 3 and 15 days (Figure 6d and 6e) are not significant for the area, reporting values below 30 mm/d.

The definition of empirical or statistical thresholds is an excellent indicator for landslide forecast since it allows the association of the probability of landslide events with established weather forecast models. Accordingly, thresholds are important elements for designing landslide early warning systems along with other conditioning factors which may increase their effectiveness. To calculate the rainfall thresholds after the passage of Hurricane Matthew, the records of 10 mountain rain gauges located in the area were analyzed (see fig 1) and the existence of rain gauges with rainfall records that deviated from the accumulated rainfall trend in the period of the hurricane's passage. For the establishment of the rainfall thresholds, minimum accumulated rainfalls of 0.8-50 mm and maximum accumulated rainfalls of 250-520 mm were analyzed. The computed thresholds for accumulated rainfall corresponding to day 4 are shown in Figure 7. The maximum threshold in which the highest percentage of landslide events occurs (88%) is between 355 mm and 178 mm. In the case of day 5, the maximum calculated threshold (82% of landslide events) was 407 mm and the minimum threshold 118 mm. The standard deviation is significantly higher for the rainfall records on day 5 due to the number of measurements with zero rainfall data, mostly by equipment failures, which creates higher uncertainty for the thresholds on this day (Figure 7d).

The thresholds for the combination of AR and AAR of 3 days were discarded because AR of less than 30 mm which is below intense rainfall accumulates.

This research found little evidence of influence of antecedent accumulated rainfall in landslide occurrence. The accumulated rainfall on October 4th and 5th are mostly the triggering factors of most landslides. The minimum thresholds calculated on these days could be indicative of the amount of rainfall above which the probabilities of occurrence of landslide events may drastically increase. These threshold values, along other conditioning factors, may be the foundation for setting up an early warning system for landslides in the region.

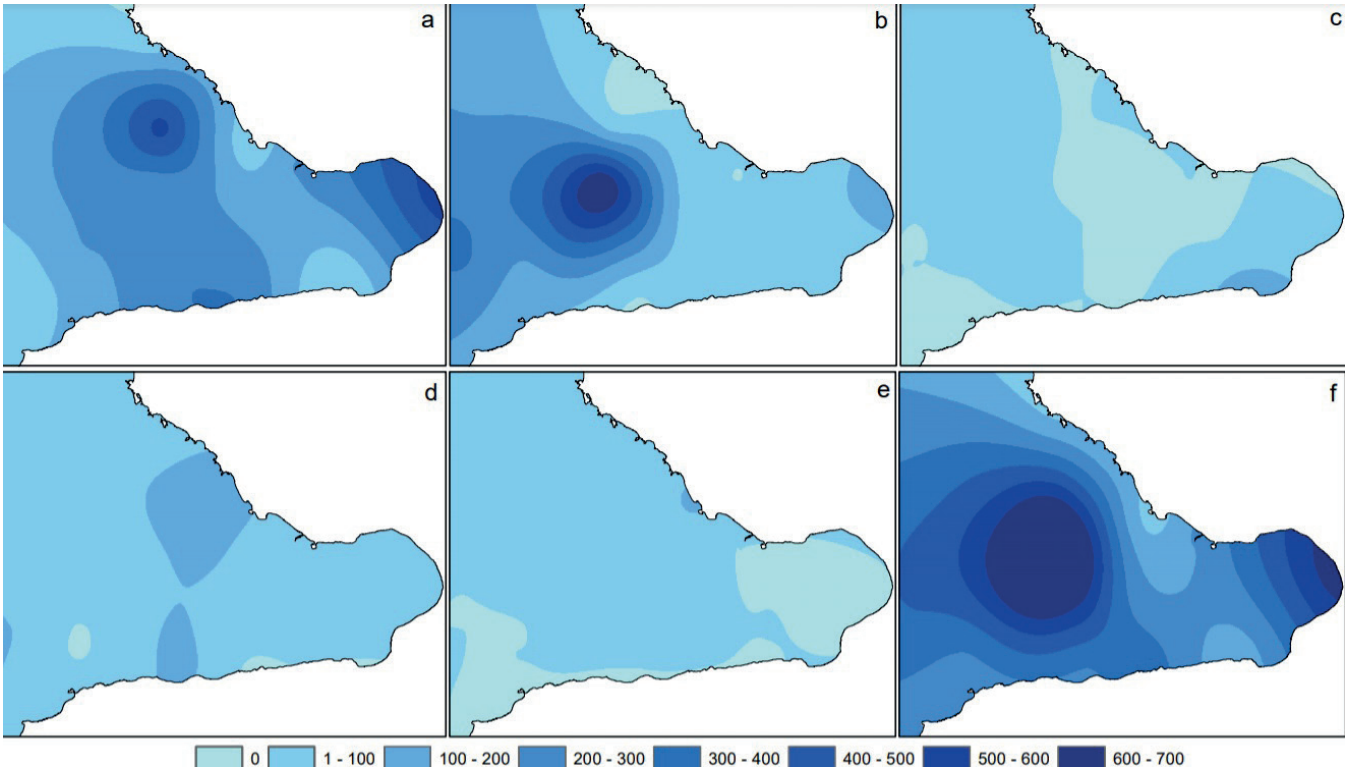

Fig. 6. Rainfall associated to Matthew hurricane and before (mm): a) October 4, 2016; b) October 5, 2016; c) October 6, 2016; d) accumulated rainfall 3 days before; e) accumulated rainfall 15 days before; f) Accumulated rainfall days 4, 5 and 6 October 2016

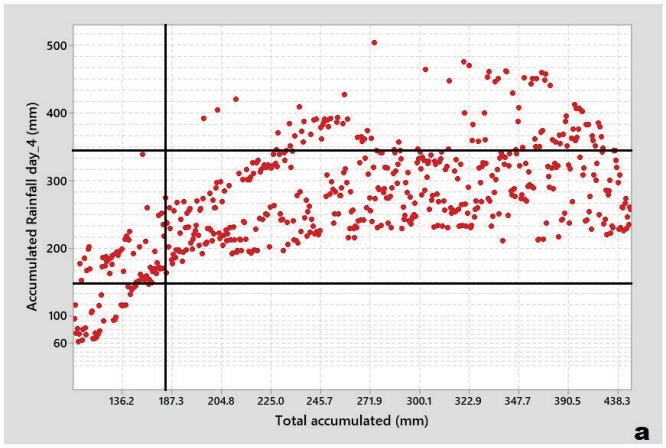

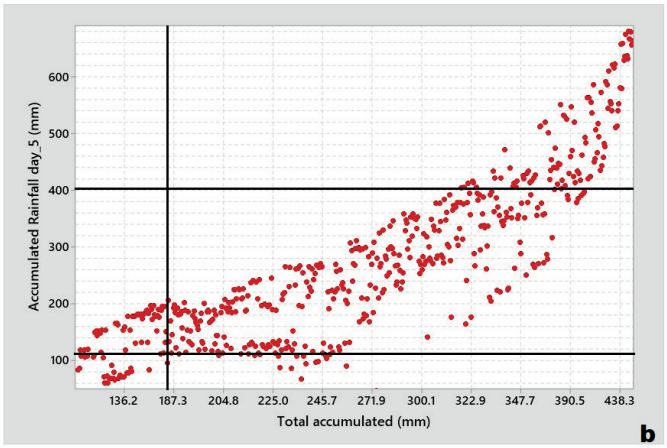

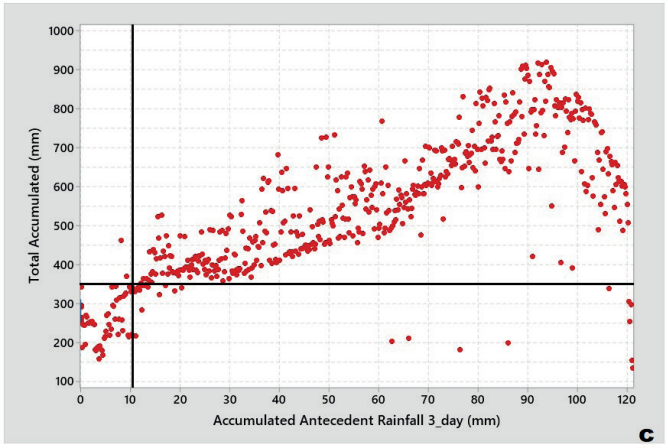

Statistics

Variable	Mean	St.Dev	Median	Mode	Value mode
AR_4	271.16	81.28	268.72	271.41	4
AR_5	262.73	144.31	236.23	0	8
TA	533.89	177.00	522.69	700.83	4
AAR 3_day	26.357	15.491	23.660	0	7

d

Fig. 7. Rainfall thresholds triggering landslides for Hurricane Matthew in the study area: a) rainfall threshold day 4; b) rainfall threshold day 5; c) rainfall threshold calculated considering 3 days of antecedent rainfall; d) statistics for accumulated rainfall and accumulated rainfall antecedents, where AR is the accumulated daily rainfall for day 4 (AR_4) and for day 5 (AR_5). TA is total accumulated rainfall throughout the passage of the hurricane. AAR 3_day is accumulated of antecedent rainfall for three days

CONCLUSIONS

Hurricane Matthew affected Guantánamo province in Eastern Cuba triggering 619 landslides as interpreted by satellite images and fieldwork. The majority of the landslides found were rockslides that occurred in the north-central part of the study area with a small amount of debrisflows and rockfalls. The areas with higher rainfall overlapped with highest landslide occurrence, except for intra mountain valleys, which is in accordance with the nature of the event. Most of the landslides identified were triggered on high and moderated hazard zones for the hazard map from previous research.

Slope angle does not seem to represent a factor as important as the rock type in the area, since many landslides occurred in slopes lower than 45°. Debrisflow occurred mostly on deep ferralitic soils and rockslides on moderately deep brown soils. Most of landslides were located in green schists of volcanic and vulcanoclastic rocks, as well as rocks of the ophiolitic association: harzburguites, lherzolites and serpentinized dunites.

Rainfall thresholds causing landslides during the passage of Hurricane Matthew are between 178-407 mm/d. The accumulated antecedent rainfall was not significant for the establishment of thresholds.

This landslide inventory contributes to previous efforts in reducing landslide risk in the mountain areas of Guantánamo province and are the base to updating landslide susceptibility and hazard maps in the region.

REFERENCES

Aleotti P. (2004). A warning system for rainfall-induced shallow failures. Engineering Geology, 73, 247-265, DOI:10.1016/j.enggeo.2004.01.007.

Aristizábal E. and Gómez J. (2007). Inventario de emergencias y desastres en el Valle de Aburrá. originados por fenómenos naturales y antrópicos en el periodo 1880-2007. Gestión y Ambiente, 10(2),17-30, https://revistas.unal.edu.co/index.php/gestion/article/view/1409.

Ariztizábal E. and Yokota S. (2006). Geomorfología aplicada a la ocurrencia de deslizamientos en el valle de aburra. DYNA, 73(149), 05-16. https://revistas.unal.edu.co/index.php/dyna/article/view/807.

Ayalew L. and Yamagishi H. (2005). The application of GISbased logistic regression for landslide susceptibility mapping in the Kakuda-Yahiko Mountains, Central Japan. Geomorphology, 65, 15-31, DOI:10.1016/j.geomorph.2004.06.010.

Ballester M. and Rubiera J. (2016). Summary of cyclone season 2016 in North Atlantic, Institute of Meteorology (INSMET), Ministry of Science, Technology and Environment, Cuba, http://www.insmet.cu/asp/genesis.asp?TB0=PLANTILLAS&TB1=TEMPORADA&TB2=/Temporadas/temporada2016.html#home.

Bertinelli L., Mohan P. and Strobl E. (2016). Hurricane Damage Risk Assessment in the Caribbean: An Analysis Using Synthetic Hurricane Events and Nightlight Imagery. Ecological Economics, 124, 135-144, DOI:10.1016/j.ecolecon.2016.02.004.

Brown W.M., Cruden D.M. and Denison J.S. (1992). The directory of the world landslide inventory. USGS Open File Report 92 (427), 239.

Castellanos E.A. and Van Westen C.J. (2007). Generation of a landslide risk index map for Cuba using spatial multi-criteria evaluation. Landslides, 4, 311-325, DOI:10.1007/s10346-007-0087-y.

Castellanos E.A. and Van Westen C.J. (2008). Qualitative landslide susceptibility assessment by multicriteria analysis: A case study from San Antonio del Sur, Guantánamo, Cuba, Geomorphology, 94(3-4), 453-466, DOI:10.1016/j.geomorph.2006.10.038.

Crosta G.B. (1998). Regionalization of rainfall thresholds: an aid to landslide hazard evaluation. Environmental Geology, 35, 131-145, DOI:10.1007/s002540050300.

Crozier M.J. (1999). Prediction of rainfall-triggered landslide: a test of antecedent water status model. Earth surface processes and landforms, 24, 825-833, DOI:10.1002/(SICI)1096-9837(199908)24:9<825::AID-ESP14>3.0.CO;2-M.

Dai F., Lee C., Li J., and Xu Z.W. (2001). Assessment of landslide susceptibility on the natural terrain of Lantau Island, Hong Kong. Environmental Geology, 40, 381-391, DOI:10.1007/s002540000163.

Dashko R.E. and Kotiukov P.V. (2018). Fractured clay rocks as a surrounding medium of underground structures: The features of geotechnical and hydrogeological assessment. Saint Petersburg, 1, 241–248, https://onepetro.org/ISRMEUROCK/proceedings-abstract/EUROCK18/All-EUROCK18/ISRM-EUROCK-2018-025/446888.

Dikshit A., Sarkar R., Pradhan B., Acharya S. and Dorji K. (2019). Estimating Rainfall Thresholds for Landslide Occurrence in the Bhutan Himalayas. Water 11, 1616, DOI: 10.3390/w11081616.

Finlay P.J., Fell R. and Maguire P.K. (1997). The relationship between the probability of landslide occurrence and rainfall. Canadian Geotechnical Journal, 36, 811–824, DOI:10.1139/t97-047.

Garland G.G. and Oliver M.J. (1993). Predicting landslides from rainfall in a humid, sub-tropical region. Geomorphology, 8, 165-173, DOI:10.1016/0169-555X(93)90035-Z.

Gospodarikov A.P., and Zatsepin M.A. (2010). Mathematical modeling of stress-strain state of the mined seam deposits. Journal of Mining Institute, 187, 47, https://pmi.spmi.ru/index.php/pmi/article/view/6623.

Gusev V.N. (2016). Forecasting safe conditions for developing coal bed suites under aquifers on the basis of geomechanics of technogenic water conducting fractures. Journal of Mining Institute, 221, 638, DOI:10.18454/pmi.2016.5.638.

Guzzetti F. (1998). Hydrological triggers of diffused landsliding. Environmental Geology, 2(35), 78-79.

Guzzetti F., Cardinalli M., and Reichenbach P. (1994.) The AVI project: a bibliographical and archive inventory of landslides and floods in Italy. Environmental Management, 18, 623-633, DOI: 10.1007/BF02400865.

Iturralde-Vinent M.A. (1998). Sinopsis de la Constitución Geológica de Cuba». Acta geológica hispánica, 33, 9-56, https://www.raco.cat/index.php/ActaGeologica/article/view/75545.

Kay J.N. and Chen T. (1995). Rainfall-landslide relationship for Hong Kong. Proceeding ICE. Geotechnical Engineering 113, 117-118, DOI: 10.1680/igeng.1995.27592.

Kleptsova O.S., Dijkstra H.A., van Westen R.M., van der Boog C.G., Katsman C.A., James R.K., Bouma T.J., Klees R., Riva E.M., Slobbe D.C., Zijlema M. and Pietrzak J.D. (2021). Impacts of Tropical Cyclones on the Caribbean Under Future Climate Conditions. Journal of Geophysical Research: Oceans, 126(9), e2020JC016869, DOI:10.1029/2020JC016869.

Kutepova N.A., Kutepov Y.I., and Shabarov A.N. (2012). Engineering-geological ensuring for safety of mining work in water-inundated solid mass. Journal of Mining Institute, 197, 197. извлечено от https://pmi.spmi.ru/index.php/pmi/article/view/5991.

Kutepova N.A., Kutepov Y.I., & Shabarov A.N. (2012). The monitoring of hidrogeomehanical processes during the flooding of Angero-Sudgensk mines. Journal of Mining Institute, 197, 215, https://pmi.spmi.ru/index.php/pmi/article/view/5994.

Lumb P. (1975). Slope failure in Hong Kong. Quarterly Journal Engineering Geologist, 8, 31–65, DOI: 10.1144/GSL.QJEG.1975.008.01.02.

Marcelino E.V., Fromaggio A.R. and Maeda E.E. (2009). Landslide inventory using image fusion techniques in Brazil, International Journal of Applied Earth Observation and Geoinformation, 11, 181-191, DOI: 10.1016/j.jag.2009.01.003.

Pospehov G.B., Straupnik I.A. and Pankratov K.V. (2018). Geoengineering researches for the restoration of the lands disturbed by mining. 14th Conference and Exhibition on Engineering and Mining Geophysics, vol. 2018, № 137600, 1-5, DOI: 10.3997/2214-4609.201800528.

Ranson M., Kousky C., Ruth M., Jantarasami L., Crimmins A. and Tarquinio L. (2014). Tropical and Extratropical Cyclone Damages under Climate Change. Climatic Change, 127(2), 227-41, DOI: 10.1007/s10584-014-1255-4.

Sarkar R. and Dorji K. (2019). Determination of the Probabilities of Landslide Events—A Case Study of Bhutan. Hidrology, 6(2), 52, DOI: 10.3390/hydrology6020052.

Stedinger J.R. (1993). Frequency analysis of extreme events. In: Maidment DR (ed) Handbook of Hydrology. McGraw-Hill: New York., 18.1-18.66.

Trushko V.L., and Protosenya A.G. (2019). Prospects of geomechanics development in the context of new technological paradigm. Journal of Mining Institute, 236, 162, DOI: 10.31897/pmi.2019.2.162.

Van Westen C.J., Castellanos E.A. and Kuriakose S.L. (2008). Spatial data for landslide susceptibility, hazard and vulnerability assessment: an overview. Engineering Geology, 102(3-4), 112-131, https://www.sciencedirect.com/science/article/abs/pii/S0013795208001786.

RESEARCH PAPER

SETTLEMENT DEVELOPMENT BASED ON ENVIRONMENTAL CARRYING CAPACITY IN BATU CITY, INDONESIA

Agung Witjaksono[1], Ardiyanto Maksimillianus Gai[1]*, Rizka Rahma Maulida[1]

[1]Urban and Regional Planning Department, Malang National Institute of Technology, Bendungan Sigura-gura Street 2, Malang, 65145, Indonesia

***Corresponding author:** ardiyanto_maksimilianus@lecturer.itn.ac.id

Received: January 31th, 2022 / Accepted: February 15th, 2023 / Published: March 31st, 2023

https://DOI-10.24057/2071-9388-2022-018

ABSTRACT. The increase in population and demand for settlement facilities and infrastructure affects the attractiveness of Batu city (Indonesia) and has a significant impact on the environmentWe perform spatial mapping of the environmental carrying capacity in developing settlements using the overlay-geoprocessing method. This method is based on unit indicators such as slope, morthology, soil type, elevation, and potential for disasters for obtaining the data on land capability, land suitability, and settlement development plans. Land capability analysis shows that slope, morthology and altitude are the main factors for attributing moderate, low, and poor development capability. The land capability unit shows the areas with slope steepness and land morthology that are not appropriate for intensively developing areas. Batu City areas of moderate, low, and poor development capacity cover 13,365.14 ha, 3193.04 ha, and 2858.07 ha. We also demonstrate that there is about 2,363 ha of unsuitable land use with poor land capability and 3,784.28 ha of land can be developed for settlement. Using this approach we determine saturation point in the residential area plan, because the environmental impact will increase if no threshold is given for residential development.

KEYWORDS: settlement development, carrying capacity, tourism, geoprocessing, GIS

CITATION: Witjaksono A., Gai A. M., Maulida R. R. (2022). Settlement Development Based On Environmental Carrying Capacity In Batu City, Indonesia. Geography, Environment, Sustainability, 1(16), 64-72
https://DOI-10.24057/2071-9388-2022-018

Conflict of interests: The authors reported no potential conflict of interest.

INTRODUCTION

Tourism is one of the drivers of sustainability, that recognized as a viable method of developing a region with abundant resources (jeong et al. 2014). Sustainable tourism indicators provide essential guidance for decision-making in developing priority strategies that are necessary for resource allocation with medium and long-term planning (Ristić et al. 2019). The guidance is essential because tourism development assists the local economy and puts more pressure on natural resources, local culture and ecological conditions, affecting the sustainability of tourism areas (Świąder et al. 2020; Wang et al. 2020). Furthermore, cities demonstrate less impressive spatial and physical characteristics as well as social sustainability, which is an important factor in the community's livability (Eizenberg & Jabareen 2017; Neamțu 2012).

The habitability of a community is unachievable when environmental problems such as floods, droughts, groundwater pollution, ecological diseases, and waste occur (Widodo et al. 2015). Furthermore, deteriorating water quality, possible epidemics, and urban disturbances can pose policy threats to sustainable urban growth (Roy et al. 2021). Hence, environmental carrying capacity is essential to support the development and improve the quality of life. Settlements development is related to the land's carrying capacity, which contains two main components: the availability of natural resource potential and environmental bearing capacity. It is essential because humans must be placed in safe residential spaces (Andersen et al. 2020). Other research proved that unlimited population and settlement growth would cause environmental damage. So it is necessary to improve the quality of human settlements in the future (Świąder et al. 2020).

One factor requiring improvement is water resources. It is a determinant that must be considered for sustainable development, especially in the housing business due to the increasing population. It is also imperative to consider this issue in implementing tourism because water is one of the components of environmental carrying capacity in the tourism and social sectors.

A development plan should be based on the carrying capacity of both land and water as water carrying capacity includes land locations that can potentially maintain water reserves in the soil. In previous studies, there has been little discussion about the carrying capacity of water (Widodo et al. 2015) and a paradigm shift is needed to explain modern urban-related changes (Zgheib et al. 2020). In addition, a theoretical foundation will allow to accommodate the environmental carrying capacity paradigm in the form of regional policies (Fan et al. 2017; Su & Yu 2020).

Batu City is a mountainous area flanked by several mountains, such as Panderman, Anjasmoro, and Arjuno.

It has an area of 19,908.72 ha, divided into three sub-districts (Batu, Junrejo, Bumiaji) and 24 villages. The total population in Batu Sub-district is 213,046 people, with a growth rate of 1.14 from 2010 to 2020[1]. As a tourism city, Batu experienced an increase in the number of tourists by 30.4% in 2019. This also promoted the growth of tourism objects, lodging, and restaurant facilities. As a result, the number of hotels in Batu City in 2020 increased by 45.27%[2]. Tourism development will lead to the increasing number of residents of Batu City on productive land, which can cause various impacts due to land changes, including an increase in the risk of flooding and landslides that cause a decrease in the land carrying capacity.

Most Batu City is located on sloping terrain with a land slope of 25-40%. Geographically, it is placed in the uppermost part of the Brantas River, where water resources are abundant. However, the spring water discharge is decreasing due to encroachment on the protected forest with an area of ± 5,900 ha used for plantations and settlements. In addition, the reduced area becomes congested by roads, causing longer water seepage. It was also proven that dense settlements cause longer runoff absorption time (Kumar et al. 2021). As a result, Batu City is easily flooded because the sustainability of environmental functions and the environmental carrying capacity were not considered in development planning, especially in settlement areas.

The increasing tourism activities in Batu City impact housing needs, relying heavily on natural resources. To ensure that its development continues to maintain the natural cycle, consideration of the location and natural conditions of the city is highly suggested. Research on the carrying capacity of resources and the environment has shifted from theory to practice and from single-factor studies to multi-factor analysis. The sustainability criteria on a regional scale provide an evaluation of the carrying capacity, which can be used as a scientific basis for planning (Zhou et al. 2020). This study aims to map the settlement development plan based on the land's carrying capacity with the main component being the carrying capacity of water.

MATERIAL AND METHODS

This research used mosaics of high-resolution space images (QuickBird, Landsat) available on map services. Through global measurements from satellites, mapping can include the dynamical aspects of the Earth's surface. Synoptic and long-term satellite monitoring of the Earth provides time series data sets made in a highly consistent manner facilitating surface analysis for change detection. Image interpretation is the process of studying images by recognizing and assessing objects. The operation phases needed for the object recognition seen in the image are as follows: detection is object recognition with essential characteristics of the sensor; identification is to characterize objects using reference data; interpretation is to collect more accurate details. Object recognition is an integral part of image interpretation. For this purpose, the image identity and object type are essential during the problem-solving analysis (Saing et al. 2021).

Object characteristics in the image can be used to recognize objects referred to by interpretation elements. satellite image analysis can be done using several approaches, one of which is a GIS program that has been commonly used. The present use of GIS is restricted to geographic and computational areas but has expanded to other fields (Maguire 1991), including agriculture, economics, mathematics, regional, and urban spatial planning. Several analytical methods and tools have been implemented using GIS. The classification application (Wijaya 2015) is the most widely used. Some GIS definitions; each manual or analytical method is used to store and modify the geographically referenced data (Aronoff 1989); the institution component represents the infrastructure organizational framework integrated with the database assistance, experience, and financing continuously over time. Also, a comprehensive framework geographically model (Koshkariov et al. 1989); a decision support system that requires the integration of spatial reference data in the handling of problems; a management information system type that enables general information to appear on maps (Saing et al. 2021).

To support environmental carrying capacity analysis, the overlay-geoprocessing method was applied using GIS software. The analysis requires more than one layer to be physically stacked to be analyzed visually. These layers are analyzed using the intersect feature to obtain spatial data slices that will form new map information.

This research has two outputs. First, it shows the suitability of the land's carrying capacity for the settlement plan in the city planning document. Second, it shows the direction of settlement development based on the carrying capacity related to water resources, building cover ratio, and building height from the city planning document.

Land carrying capacity is an important component because a mismatch between land use and land capability accelerates productivity (Tscharntke et al. 2012). Other research shows that land capability can be estimated by calculating the area's carrying capacity (D'Amour et al. 2017; Hixon 2008).

There were three stages of overlay-geoprocessing analysis (Fig.1). First, the maps of layers, like slope, morthology, elevation, soil type, and disaster vulnerability were used as unit indicators to analyze the land capability. Second, an analysis of conformity with the settlement plan in Batu City was carried out using the results of the land carrying capacity study and the settlement development plan based on the city planning document as unit indicators. Third, research on the indicators of the carrying capacity of water resources, land cover ratio, and building height was carried out. The land cover ratio and building height indicators were obtained from urban planning documents. Meanwhile, the carrying capacity of water resources was acquired from environmental feasibility documents.

RESULTS

In this study, the results of the analysis are divided into three parts: land capability analysis, land suitability analysis, and analysis of settlement development plans.

Land Capability Analysis

Calculation of the settlement land capability was carried out by analyzing carrying capacity through the following units:

• Slope. The land slope analysis based on the decree of the Indonesian minister of forestry in 1980 (Qibthia et al. 2019). The land slope factor affects the land capability analysis by determining the land function as shown in Table 1.

[1] *Batu City Population Development in 2021*
[2] *Batu City Tourism Development in 2021*

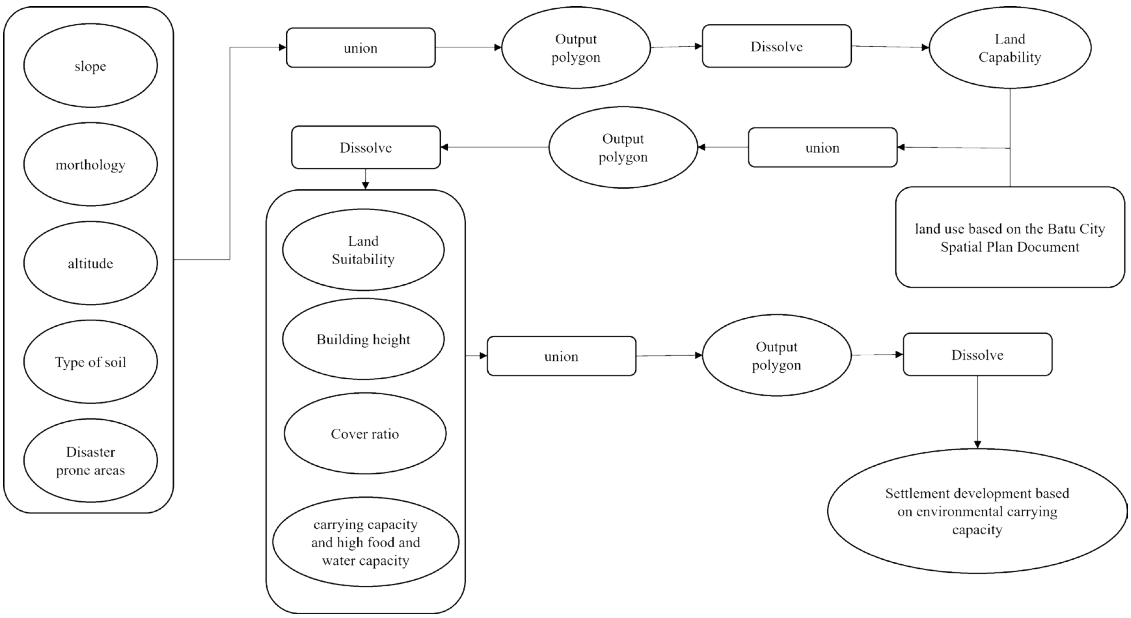

Fig. 1. Flowchart on the overlay layers

Table 1. Types of Land Use and Land Area of Batu City Land Use Plans that are not suitable with Land Capability

Slopes (%)	Classification	Area (ha)
0-8	Flat	2,207.21
8-15	Gentle	2,223.73
15-25	Sloping	1,799.37
25-40	Steep	4,529.85
>40	Very Steep	4,493.33

• MorthologyMorthology.
Morthological characteristics are sorting out the shape of the landscape nature/morthology of the region and/or area planning that can be developed according to its function. The geographical landscape is represented by hills and mountains, with an altitude of + 800 meters above sea level.
• Altitude
Based on the altitude, Batu City is classified into 6 (six) classes that the geomorthological mapping presented below refers to to the system developed by Verstappen (1967, 1968) and Van Zuidam (1968, 1975) based on experiences in tropical regions such as Indonesia and Latin America. The classification includes the following classes:
– 1. 600-1000 meters ASL with an area of 6,019.21 ha .
– This area covers three sub-districts: firstly, Batu Sub-District, which includes Sidomulyo Village, Temas, Sisir, Malik, and Sumberejo Village, and a small part of Oro-Oro Ombo, Pesanggrahan, and Songgokerto Village, Junrejo Sub-district, which includes Junrejo, Torongrejo, Pendem, Beji, Mojorejo, Dadaprejo, and parts of Tlekung village, and Bumiaji Sub-District, which includes a small number of villages.
– 2. 1000-1500 meters ASL with an area of 6.493,64 ha
The area at this altitude covers most of the villages in Bumiaji and Batu Sub-Districts, including the Songgokerto, Oro-Oro Ombo, and Pesanggrahan Villages and a small part of Tlekung Village in the Junrejo Sub-District area.
– 3. 1500-2000 meters ASL with an area of 4.820,40 ha
The area at this altitude includes small parts of Tlekung Village, Junrejo Sub-District, and Oro-Oro Ombo and Pesanggarahan Villages, especially around Mount Panderman, Mount Bokong, and Mount Punukwari. Meanwhile, in Bumiaji Sub-District, almost all villages are located at this altitude, especially the ones near Mount Rawung, Mount Tunggangan, and Mount Pusungkutuk.
– 4. 2000-2.500 meters ASL with an area of 1789,81 ha
The area at this altitude is relatively small and covers the territory around Mount Srandil and at the end of Oro Oro Ombo Village in Batu Sub-District, which borders Wagir Sub-District. For Bumiaji Sub-District, this altitude includes Mount Anjasamoro and a small part of the Giripurno, Bumiaji, Sumbergondo, and Torongrejo Villages.
– 5. 2.500-3000 meters ASL with an area of 707,32 ha
The area at this altitude covers a small number of villages located in the Bumiaji Sub-District regions bordering the Prigen Sub-District.
– 6. 3000 meters ASL with an area of 78.29 ha.
The area at this altitude includes several villages in Bumiaji Sub-District, around Mount Arjuno (Sourgondo Village), Mount Kembar, and Welirang (Tulungrejo Village).
• Type of soil
Land capability analysis is based on soil type factors according to different erosion sensitivity depending on the criteria and classification . It based on the decree of the Indonesian minister of forestry in 1980 (Qibthia et al. 2019) (Table 2).
• Disaster-prone areas
Batu City is flanked by several mountains, including Panderman, Anjasmoro, and Arjuno. Therefore, there is a volcanic disaster-prone area in Bumiaji Sub-District. Based on the results of the land capability assessment based on the units of slope, morthology, elevation, soil type, and disaster-prone areas, we obtained the following result . Slope, morthology, and altitude influence moderate, low, and poor development capability. The land capability unit

Table 2. Type of Soils Classification

Type of Soil	Classification	Area (ha)
Alluvial	not vulnerable	239.86 ha in Batu Sub-District, 199.93 ha in Junrejo, and 376.48 ha in Bumiaji Sub-District
Latosol/Inceptisols	less vulnerable	covers an area of 889.31 ha in Batu Sub-District, 741.25 ha in Junrejo Sub-District, and 1395.81 ha in Bumiaji Sub-District
Brown forest soil/ultisols	a bit vulnerable	covers an area of 260.34 ha, 217.00 ha, and 408.61 ha in Batu, Junrejo, and Bumiaji Sub-District
Androsol, Laterit, Grumusol, Podsol, Podsolic	vulnerable	1,831.04 ha in Batu Sub-District, 1,526.19 ha in Junrejo Sub-District, and 2,873.89 ha in Bumiaji Sub-District
Regosol, Litosol, Organosol, Rensina	very vulnerable	-

shows the areas with slope steepness and land morthology that are not appropriate for intensively developing areas. The areas of moderate, low, and poor development capacity cover 13,365.14 ha, 3193.04 ha, and 2858.07 ha, respectively.Existing land use in areas with moderate development capability consists of built-up land uses, such as industry, offices, trade and services, public facilities, tourism, urban forests, fisheries, permanent production forests, and horticulture. Land use types corresponding to low development capacity include horticultural areas, protected forests, permanent production forests, tourism, trade and services, housing, and urban forests. Finally, land use at poor development capacity consists of public facilities, horticulture, protected forest, permanent production forest, tourism, trade and housing services, and urban forest.

Based on the results of land capability analysis and the existing use, it is necessary to adjust the land use based on the Batu City Spatial Plan, especially the areas corresponding to tourism, housing, and trade in regions with insufficient land capacity.

Land Suitability Analysis

In this section, a suitability analysis is carried out based on the results of the land capability analysis (Fig.2) and the map of the Batu City land use plan. This analysis aims to show how well the land use plan matches the land's capability. Based on the results of the GIS overlay, some land use types were found to be unsuitable for the land capability in Batu City. Types and areas that are not suitable are shown in Table 3.

Table 3. Types of Land Use and Land Area of Batu City Land Use Plans that are not suitable with Land Capability

Land Capability	Land Use	Land area (ha)
Moderate	Public and Social Facilities	185.15
	Tourism	440.73
	Trade and Services	550.29
	Offices	34.44
	Defense and security	65.85
	Housing area	2,924.97
	Industry	13.15
	Farm	43.04
	Transportation	0.95
Low	Tourism	16.74
	Trade and Services	0.03
	Housing area	3.53
Poor	Public Facilities and Social Facilities	1.30
	Tourism	0.10
	Trade and services	0.003
	Housing area	0.96
Total		4,281.233

Based on the results of the suitability analysis (Fig.3), unsuitable land use types covered 4258.57 ha of land characterized by moderate capability. That is because the available land in Batu City is only of average capability, and all urban activity centers, offices, trade, and settlements, are located there. Also, there is 20.3 ha of unsuitable land use at low land capability and 2,363 ha of unsuitable land use at poor land capability. It is due to the development of tourism areas accompanied by the need for trade and settlements around them. Residential areas that exist on land with low land capability generally function as hotels, guest houses, or homestays for tourists.

Sustainable Development Analysis

This section presents the analysis of unit indicators from the results of land suitability assessment, land cover ratio plans, building height plans, and directions for carrying capacity and high food and water capacity in Batu City. This analysis aims to show a plan based on the unit indicators from the previous section (Fig.3 and develop a plan that considers the carrying capacity of water. The plans of the cover ratio and building height (Fig. a and b) were obtained from the city planning document, while the direction of carrying capacity and high food and water capacity in Batu City (Fig.c) was based on environmental city documents.

The land cover ratio (Fig.a) shows the recommended land cover for each house plot based on land slope, morthology, and soil type indicators. The recommended building height (Fig.b) shows the maximum building height in the area based on land slope and soil type indicators. The carrying capacity and high food and water capacity (Fig.c) indicate the areas with the potential to have high food and water reserves. The recommendations are based on areas with increased productivity and the maximum amount of sustainable water extraction per year.

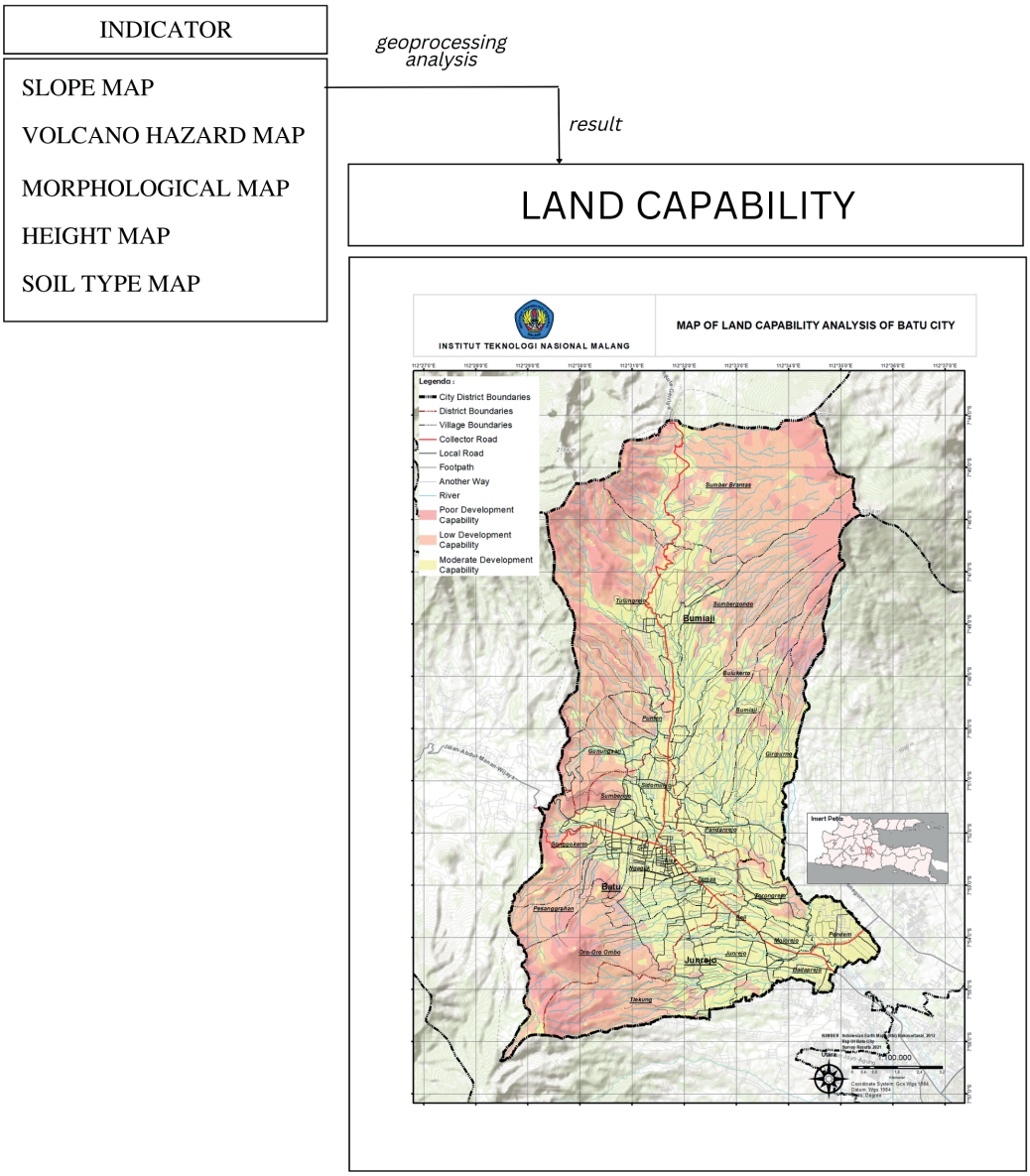

Fig. 2. Land Capability Analysis Using 5 Indicators (Slope, Morthology, Soil Type, Height, Volcano Hazard) in Batu City

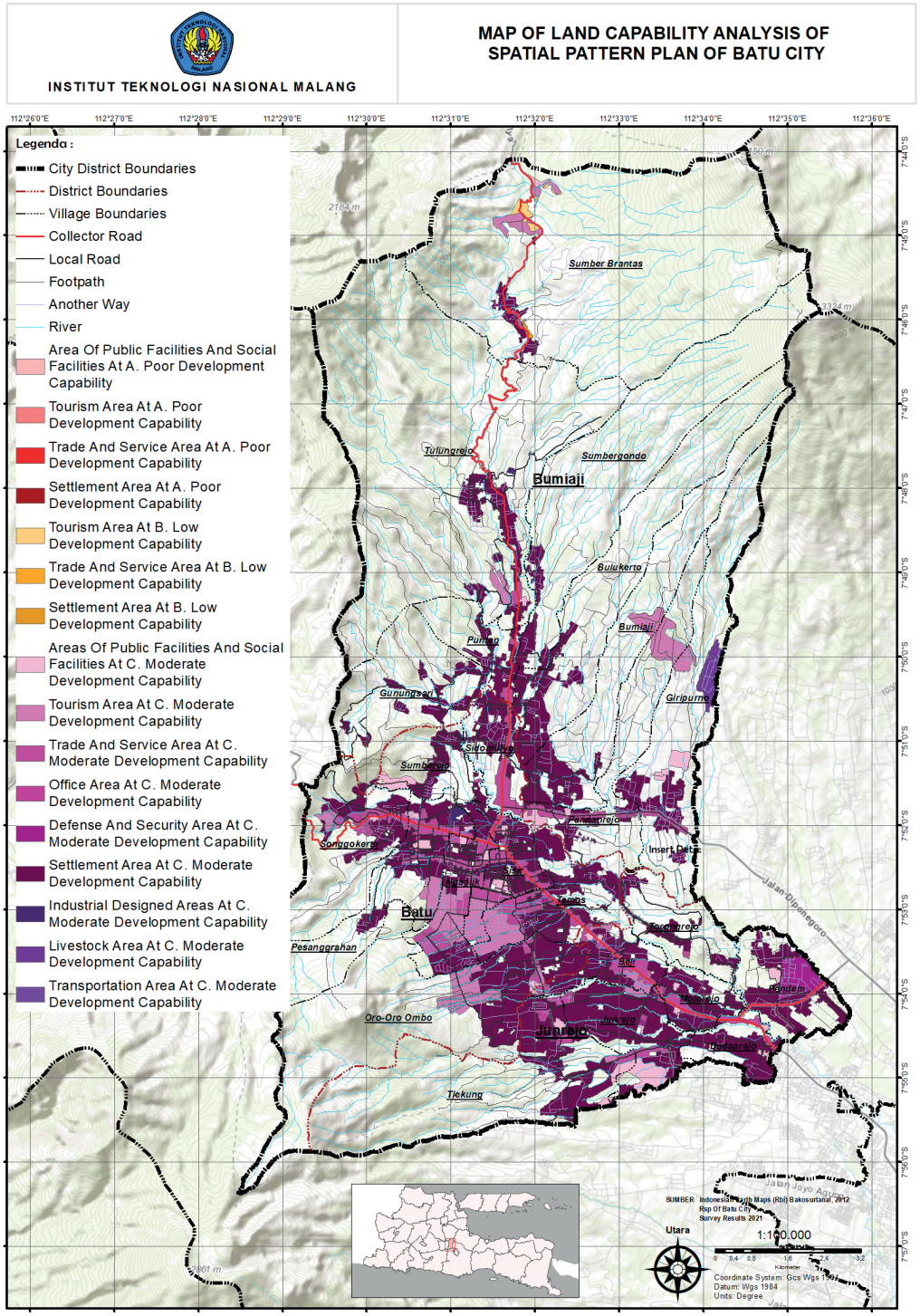

Fig. 3. Suitability Analysis of Land Capability and the Land Use Plan of Batu City

Figure d presents the results of combining 3 indicators shown in Fig. d . These results show that 3,784.28 ha of land can be used in Batu City as a residential area when considering water carrying capacity indicators. The highest land availability is observed in Junrejo sub-district. In Fig. d, it can also be seen that most of the recommended land is characterized by moderate land capability and is located in the city activity center.

DISCUSSION

The role of environmental carrying capacity is to provide an overview of the maximum limit that can be sustained by nature. In urban development, its role is vital amid economic and population growth issues. Sustainable development plans integrate economic and social challenges to maintain the balance of nature (Świąder et al. 2020). It is expected for a growing city to have an upper threshold for urban development at a certain carrying capacity point.

Batu City does not have an upper threshold because physical development is carried out massively, even in areas with low land capacity. In contrast, the environmental carrying capacity is a comprehensive reform that coordinates economic development and environmental protection (Su & Yu 2020), especially in cities in mountainous areas. The dilemma is to maximize the use of natural resources with reducing the risk of natural damage.

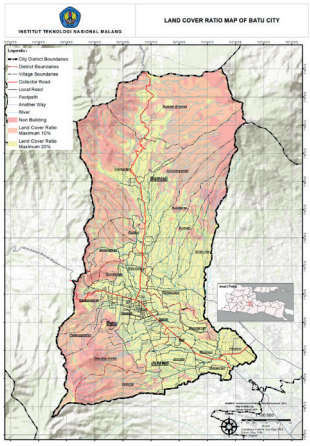

Fig. 4a

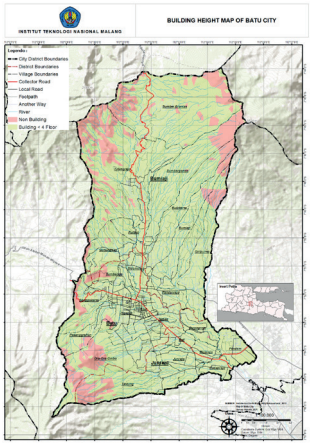

Fig. 4b

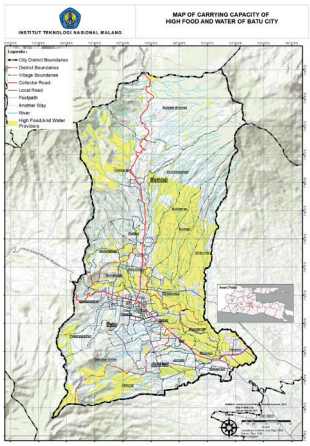

Fig. 4c

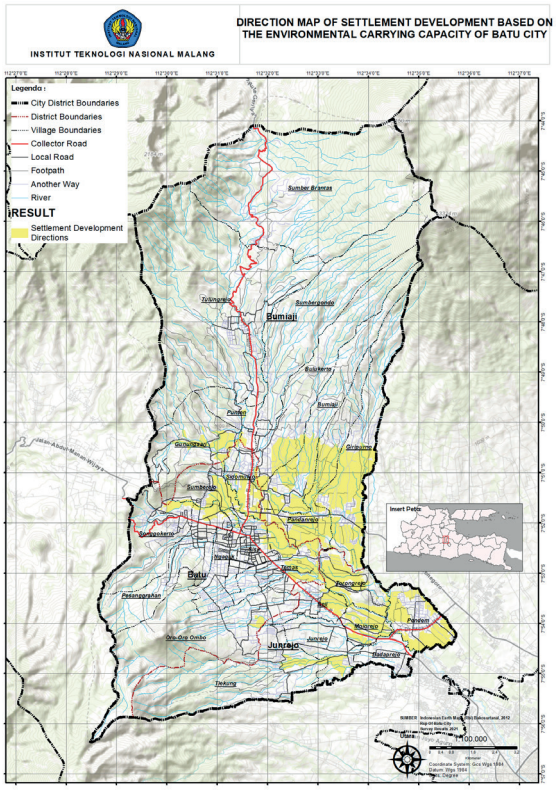

Fig. 4d

Fig. 4. Settlement Development Plan of Batu City

CONCLUSION

The results showed that most of the land in Batu City was characterized by medium capacity of 13,365.14 ha, of which 4,258.57 ha was not suitable for land use. At low land capability, the total area of unsuitable land use is 2,383.3 ha. Spatial analysis showed that the development of residential areas should be directed at the land with a medium capacity of 3,784.28 ha.

The high attractiveness of the city for tourism requires establishing policies and setting the threshold for the city's capacity. In addition, Batu City is located upstream, where its watershed has an impact on other cities in the vicinity, which is another reason for setting a city-carrying capacity threshold. If this is not done, the increase in the number of residents in Batu City as an upstream and tourist city will significantly impact the environment and threaten the city's sustainability.

In future studies, the settlement area plan that considers the environmental carrying capacity can be developed. In addition, it is necessary to develop indicators for environmental policies for urban areas in the upstream regions, including indicators for determining residential areas.

REFERENCES

Andersen, C. E., Ohms, P., Rasmussen, F. N., Birgisdóttir, H., Birkved, M., Hauschild, M., and Ryberg, M. (2020). Assessment of absolute environmental sustainability in the built environment. Building and Environment, 171, DOI: 10.1016/j.buildenv.2019.106633.

Aronoff, S. (1989). Geographic information systems: A management perspective. Geocarto International, 4(4), 58, DOI: 10.1080/10106048909354237.

Bjørn, A., Margni, M., Roy, P.-O., Bulle, C., and Hauschild, M. Z. (2016). A proposal to measure absolute environmental sustainability in life cycle assessment. Ecological Indicators, 63, 1–13, DOI: https://doi.org/10.1016/j.ecolind.2015.11.046.

Chapman, E. J., and Byron, C. J. (2018). The flexible application of carrying capacity in ecology. Global Ecology and Conservation, 13, 1–12, DOI: 10.1016/j.gecco.2017.e00365.

Chen, D., Zhou, Q., and Yu, L. (2020). Response of resources and environment carrying capacity under the evolution of land use structure in Chongqing Section of the Three Gorges Reservoir Area. Journal of Environmental Management, 274, 111169, DOI: https://doi.org/10.1016/j.jenvman.2020.111169.

D'Amour, C. B., Reitsma, F., Baiocchi, G., Barthel, S., Güneralp, B., Erb, K. H., Haberl, H., Creutzig, F., and Seto, K. C. (2017). Future urban land expansion and implications for global croplands. Proceedings of the National Academy of Sciences of the United States of America, 114(34), 8939–8944, DOI: 10.1073/pnas.1606036114.

Doe, B., Peprah, C., and Chidziwisano, J. R. (2020). Sustainability of slum upgrading interventions: Perception of low-income households in Malawi and Ghana. Cities, 107, DOI: 10.1016/j.cities.2020.102946.

Eizenberg, E., and Jabareen, Y. (2017). Social sustainability: A new conceptual framework. Sustainability (Switzerland), 9(1), DOI: 10.3390/su9010068.

Fan, J., Zhou, K., and Wang, Y. F. (2017). Basic points and progress in technical methods of early-warning of the national resource and environmental carrying capacity (V 2016). Progress in Geography, 36(3), 266–276,

Gaisie, E., Han, S. S., and Kim, H. M. (2021). Complexity of resilience capacities: Household capitals and resilience outcomes on the disaster cycle in informal settlements. International Journal of Disaster Risk Reduction, 60, DOI: 10.1016/j.ijdrr.2021.102292.

Hixon, M. A. (2008). Carrying Capacity (B. B. T.-E. of E. (Second E. Fath, Ed.; pp. 258–260). Elsevier, DOI: https://doi.org/10.1016/B978-0-444-63768-0.00468-6.

Jeong, J. S., García-Moruno, L., Hernández-Blanco, J., and Jaraíz-Cabanillas, F. J. (2014). An operational method to supporting siting decisions for sustainable rural second home planning in ecotourism sites. Land Use Policy, 41, 550–560, DOI: https://doi.org/10.1016/j.landusepol.2014.04.012.

Jia, K., Qiao, W., Chai, Y., Feng, T., Wang, Y., and Ge, D. (2020). Spatial distribution characteristics of rural settlements under diversified rural production functions: A case of Taizhou, China. Habitat International, 102, DOI: 10.1016/j.habitatint.2020.102201.

Khaled Al Shawabkeh, R., Alobaidat, E., Ibraheem Alhaddad, M., and Alzouby, A. M. (2022). The role of social infrastructure services in developing the city centre planning: A framework for delivering sustainable cities in Jordan. Ain Shams Engineering Journal, 13(6), 101800, DOI: https://doi.org/10.1016/j.asej.2022.101800.

Koshkariov, A. V., Tikunov, V. S., and Trofimov, A. M. (1989). The current state and the main trends in the development of geographical information systems in the U.S.S.R. International Journal of Geographical Information Systems, 3(3), 257–272, DOI: 10.1080/02693798908941512.

Kumar, A., Pramanik, M., Chaudhary, S., and Negi, M. S. (2021). Land evaluation for sustainable development of Himalayan agriculture using RS-GIS in conjunction with analytic hierarchy process and frequency ratio. Journal of the Saudi Society of Agricultural Sciences, 20(1), 1–17, DOI: 10.1016/j.jssas.2020.10.001.

Li, R. min, Yin, Z. qiang, Wang, Y., Li, X. lei, Liu, Q., and Gao, M. meng. (2018). Geological resources and environmental carrying capacity evaluation review, theory, and practice in China. China Geology, 1(4), 556–565, DOI: 10.31035/cg2018050.

Liu, X., Pei, T., Zhou, C., Du, Y., Ma, T., Xie, C., and Xu, J. (2018). A systems dynamic model of a coal-based city with multiple adaptive scenarios: A case study of Ordos, China. Science China Earth Sciences, 61(3), 302–316, DOI: 10.1007/s11430-016-9077-5.

Maguire, D. J. (1991). An Overview and Definition of GIS. In: Maguire, D.J., Goodchild, M.F. and Rhind, D.W., Eds., Geographical Information Systems: Principles and Applications. Wiley, Hoboken, Vol. 1, 9-,

Neamţu, B. (2012). Measuring the social sustainability of urban communities: The role of local authorities. Transylvanian Review of Administrative Sciences, 37, 112–127,

Parikh, P., Bisaga, I., Loggia, C., Georgiadou, M. C., and Ojo-Aromokudu, J. (2020). Barriers and opportunities for participatory environmental upgrading: Case study of Havelock informal settlement, Durban. City and Environment Interactions, 5, DOI: 10.1016/j.cacint.2020.100041.

Qibthia, N. D. M. Al, Rostian, T. S., and ... (2019). Land Use Analysis Based on Land Capacity in Ciptagelar Adat Village and Surrounding in The Special Zone of Halimun Salak National Park (Analisis Penggunaan Lahan Berdasarkan Kemampuan Lahan Pada Kampung Adat Ciptagelar Dan Sekitarnya Di Zona Khusus Taman Gunung Halimun Salak). Prosiding Seminar Nasional Cendekiawan Ke 5, 1–7, http://trijurnal.lemlit.trisakti.ac.id/index.php/semnas/article/view/5729

Ristić, D., Vukoičić, D., and Milinčić, M. (2019). Tourism and sustainable development of rural settlements in protected areas - Example NP Kopaonik (Serbia). Land Use Policy, 89, DOI: 10.1016/j.landusepol.2019.104231.

Roy, S., Bose, A., Singha, N., Basak, D., and Chowdhury, I. R. (2021). Urban waterlogging risk as an undervalued environmental challenge: An Integrated MCDA-GIS based modeling approach. Environmental Challenges, 4, DOI: 10.1016/j.envc.2021.100194.

Saing, Z., Djainal, H., and Deni, S. (2021). Land use balance determination using satellite imagery and geographic information system: case study in South Sulawesi Province, Indonesia. Geodesy and Geodynamics, 12(2), 133–147, DOI: 10.1016/j.geog.2020.11.006.

Sevegnani, F., Giannetti, B. F., Agostinho, F., and Almeida, C. M. V. B. (2017). Assessment of municipal potential prosperity, carrying capacity and trade. Journal of Cleaner Production, 153, 425–434, DOI: https://doi.org/10.1016/j.jclepro.2016.11.018.

Su, Y., and Yu, Y. (2020). Dynamic early warning of regional atmospheric environmental carrying capacity. Science of The Total Environment, 714, 136684, DOI: https://doi.org/10.1016/j.scitotenv.2020.136684.

Świąder, M., Lin, D., Szewrański, S., Kazak, J. K., Iha, K., van Hoof, J., Belčáková, I., and Altiok, S. (2020). The application of ecological footprint and biocapacity for environmental carrying capacity assessment: A new approach for European cities. Environmental Science and Policy, 105, 56–74, DOI: 10.1016/j.envsci.2019.12.010.

Tscharntke, T., Clough, Y., Wanger, T. C., Jackson, L., Motzke, I., Perfecto, I., Vandermeer, J., and Whitbread, A. (2012). Global food security, biodiversity conservation and the future of agricultural intensification. Biological Conservation, 151(1), 53–59, DOI: https://doi.org/10.1016/j.biocon.2012.01.068.

Tsiaras, E., Papadopoulos, D. N., Antonopoulos, C. N., Papadakis, V. G., and Coutelieris, F. A. (2020). Planning and assessment of an off-grid power supply system for small settlements. Renewable Energy, 149, 1271–1281, DOI: 10.1016/j.renene.2019.10.118.

Wang, J., Huang, X., Gong, Z., and Cao, K. (2020). Dynamic assessment of tourism carrying capacity and its impacts on tourism economic growth in urban tourism destinations in China. Journal of Destination Marketing & Management, 15, 100383, DOI: https://doi.org/10.1016/j.jdmm.2019.100383.

Widodo, B., Lupyanto, R., Sulistiono, B., Harjito, D. A., Hamidin, J., Hapsari, E., Yasin, M., and Ellinda, C. (2015). Analysis of Environmental Carrying Capacity for the Development of Sustainable Settlement in Yogyakarta Urban Area. Procedia Environmental Sciences, 28(SustaiN 2014), 519–527, DOI: 10.1016/j.proenv.2015.07.062.

Wijaya, N. (2015). Deteksi Perubahan Penggunaan Lahan Dengan Citra Landsat Dan Sistem Informasi Geografis: Studi Kasus Di Wilayah Metropolitan Bandung, Indonesia. Geoplanning: Journal of Geomatics and Planning, 2(2), DOI: 10.14710/geoplanning.2.2.82-92.

Zgheib, T., Giacona, F., Granet-Abisset, A. M., Morin, S., and Eckert, N. (2020). One and a half century of avalanche risk to settlements in the upper Maurienne valley inferred from land cover and socio-environmental changes. Global Environmental Change, 65(March), 102149, DOI: 10.1016/j.gloenvcha.2020.102149.

Zhang, B., Su, S., Zhu, Y., and Li, X. (2020). An LCA-based environmental impact assessment model for regulatory planning. Environmental Impact Assessment Review, 83, DOI: 10.1016/j.eiar.2020.106406.

Zhou, L., Dang, X., Sun, Q., and Wang, S. (2020). Multi-scenario simulation of urban land change in Shanghai by random forest and CA-Markov model. Sustainable Cities and Society, 55, DOI: 10.1016/j.scs.2020.102045.

RESEARCH PAPER

BIODIVERSITY OF BRYOPHYTE OF PHOTIC ZONES OF CAVES IN THE KUTUK TRACT (SOUTHERN URAL, BASHKIRIA)

Svetlana E. Mazina[1,2,3*], Ekaterina V. Kozlova[2], Anton S. Fedorov[2], Shamil R. Abdullin[4]

[1] Research and technical centre of radiation-chemical safety and hygiene FMBA of Russian Federation, str. Schukinskaya, 40, 123182, Moscow, Russian Federation

[2] Peoples Friendship University of Russia (RUDN University), Miklukho-Maklaya str. 6, 117198, Moscow, Russian Federation

[3] Federal State Budgetary Educational Institution of Higher Education "State University of Land Use Planning" Kazakov str. 15,105064, Moscow, Russian Federation

[4] Federal Scientific Center of the East Asia Terrestrial Biodiversity, Far Eastern Branch of Russian Academy of Sciences, Vladivostok, Prospekt 100-letiya Vladivostoku 159/1, 690022, Vladivostok, Russia.

***Corresponding author:** conophytum@mail.ru

Received: May 18th, 2022 / Accepted: February 15th, 2023 / Published: March 31st, 2023

https://DOI-10.24057/2071-9388-2022-093

ABSTRACT. This article presents results of a study of bryophytes in seven caves of the Kutuk tract of the National Park «Bashkiria» of the Republic of Bashkortostan, including the largest cave in Bashkiria – Kutuk-Sumgan.

Fifty-five bryophytes species were found in the studied caves. The dominant species in all caves was *Timmia bavarica*. The species composition of bryophytes of each cave is unique. Among identified bryophytes species 23, species were found only in one cave, and 11 species in 2 caves. During our survey, we found 31 species in Kutuk-Sumgan Cave, 21 species in Kutuk-2 and Kutuk-3 caves, 19 species in Kutuk-4 caves, 18 species in Vintovaya and Zigzag caves and 14 species in Kutuk-1 cave.

Using the Jaccard and Phi-squared similarity indices, we revealed the stability of the bryoflora of the caves in different years and show its changes. Changes in the composition and structure of mosses in the Kutuk tract may be caused by mechanical influences. Benchmark similarity analysis allowed us to determine the influence of entrance morphology and glaciation in the photic zone of the caves on the composition of bryophytes.

Using the Kutuk tract caves as an example, it is shown that in the primary analysis of the bryoflora, when selecting a characteristic cave, up to 40% of the total species composition of the caves can be identified in a single cave. The current study of Kutuk tract caves shows that identification of the primere analyses of bioflora permits identification of up to 40% of species composition of an individual cave.

Three criteria for selecting a characteristic cave were identified: size of the photic zone and morphology of the entrance, diversity of habitats, and the least degree of disturbance.

KEYWORDS: Cave, photic zone, mosses, Kutuk-Sumgan, bryophytes

CITATION: Mazina S. E., Kozlova E. V., Fedorov A. S., Abdullin S. R. (2023). Biodiversity Of Bryophyte Of Photic Zones Of Caves In The Kutuk Tract (Southern Ural, Bashkiria). Geography, Environment, Sustainability, 1(16), 73-85
https://DOI-10.24057/2071-9388-2022-093

ACKNOWLEDGEMENTS: The authors thank Dr. Baisheva Elvira Zakiryanovna for confirmation of the identification of some species, Gainutdinov Ildar Almazovich for collecting samples and providing data, Loginov Vladimir Anatolievich and Samsonov Vasily Borisovich for their help in preparing this article.

Conflict of interests: The authors reported no potential conflict of interest.

INTRODUCTION

Karst caves are the most vulnerable part of karst ecosystems due to various anthropogenic influences (Neill et al. 2004; Parise et al. 2009; Zhang and Zhu 2012; Simões et al. 2014). In the recent years the number of studies of the biodiversity of karst caves is constantly increasing. However, in many regions caves remain poorly studied, for example, in the Republic of Bashkortostan (South Ural, Russia). Of particular interest is the biota of the habitats of the cave entrance zones, which have several unique features. Unusual climatic conditions and high humidity (Northup and Lavoie 2001; Williams 2008), the presence of environmental gradients (Mulec et al. 2008), habitat diversity (Mulec et al. 2008; Novak et al. 2012; Czerwik-Marcinkowska 2013), the proven microrefugial role of the cave entrances as ecotones (Monro et al. 2018), determine the high biodiversity of phototrophs realized in small volumes of subterranean cavity entrances. The most popular are studies of species adaptations to cave environments, relationships and competition within populations and communities, features of reproductive strategies, the habitat-forming potential of cave biota, biodiversity formation, and the conservation value of cave

photic zones (Serena and Meluzzi 1997; Pentecost and Zhaohui 2001; Tao et al. 2015; Monro et al. 2018; Puglisi et al. 2019).

The discrete and distant location of different cave entrances determines the disjunct range of species in the entrance zones of the caves. In addition, the adaptability to certain specific conditions, low reproductive potential, and small population sizes increase the probability of extinction, including habitat loss (Bichuette and Trajano 2010).

The low diversity of mosses in karst caves, the relationship of species composition with the microhabitat and the possibility of using mosses as indicators of the plant diversity of caves were revealed (Ren et al. 2021).

Participation of bryophytes in communities is related to cave humidity and increases in the presence of water flows (Popkova and Mazina 2019; Mazina et al. 2020). Generally, bryophyte of cave habitats diversity decreases southwards and in dryer caves (Mazina and Popkova 2017; Kozlova et al. 2019; Popkova et al. 2019; Popkova and Mazina 2020). Evidence from the caves of Montenegro, located in a small area, shown the low similarity of species composition of bryophytes explained by the peculiarities of morphology of cave entrance zones, without analyzing their disturbance (Kozlova et al. 2019; Kozlova and Mazina, 2020). Ren et al. (2021) indicated that the diversity of bryophytes and the number of individuals decreased with various disturbances, liverworts disappeared with drought-tolerant species prevailed. At the same time, the authors highlight the heterogeneity of the habitat as a factor influencing the diversity of plants in caves.

There are several problems in assessing the floristic composition of cave entrance sites. Considering the diversity of biotopes in the photic zones of caves, the question arises of the influence of the morphological features of the entrance on the species composition. For specially protected nature conservation areas, a constant task is to monitor the state of ecosystems in order to determine the dynamics of their development and timely identify negative changes. Inventory of cave flora is complicated by their inaccessibility. Therefore, it is relevant to determine the required minimum of studied objects to obtain objective information about biodiversity of bryophytes in caves within a relatively small and quite homogeneous territory. Comparison of the similarity of bryophytes in the photic cave zones can provide an answer to the question of how many entrances need to be investigated for the initial assessment of bryophytes cave biodiversity; whether there are characteristic objects and what are the criteria for their selection; what percentage of the flora is found in each cave, and whether these data can be extrapolated to other caves.

The objectives of the study were defined as follows. First, to determine the species composition of bryophytes in the entrance photic zones of the Kutuk tract caves. Second, to compare the species composition and species structure depending on the morphology of the entrance zone. As a third point, the most significant (characteristic) cave types for biodiversity assessment were identified.

MATERIALS AND METHODS

Objects of study

The Kutuk tract is located in the watershed area of the Belaya and Nugush rivers between the Yamantau and Kibiz ridges, on the western slope of the Southern Urals. Administratively, the Kutuk tract is located in Meleuz District of the Republic of Bashkortostan on the territory of the «Bashkiria» National Park (Fig. 1).

The caves of the Kutuk tract are divided into two groups according to their position in relief and determining conditions of their development – riverine or interfluves. Caves of riverine environment are horizontal, slightly descending, dry or with insignificant often seasonal watercourses, confined to the sides of gorges or dry riverbeds. All surveyed caves belong to the caves of interfluves environment; are collectors of karst waters and participate in the formation of the modern underground flow; most of them begin with unwalled shafts of the area (Golubev et al. 1976).

The caves of the Kutuk tract are embedded in gray massive limestones of the Viseian Stage of the Lower Carboniferous (Abdrakhmanov et al. 2002; Kamalov and Chvanov 2014). In the period of floods and rains the entrance shafts of the caves are ponors.

Kutuk-Sumgan Cave (53°0′2″N 56°45′5″E) is 9860 m long, 134 m deep, 52260 m^2 area, 350000 m^3 volume, amplitude 134 m, the lower floors of the cave are flooded. The cave is located at the confluence of Uluklansky and Sumgansky arroyo, confined to faults and zone of intense tectonic fracturing, at a depth of 130 m from the surface the underground river runs along the bottom of the cavity. The entrance zone is a vertical shaft, 116 m deep and 10x20 m in diameter in the upper part, and its mouth is 9.0x4.5 m. At a depth of 60 meters there is a horizontal platform covered with firn. From this platform passages, lead to the labyrinth galleries of the middle tier, which are hypsometrically confined to the level of the ancient (Upper

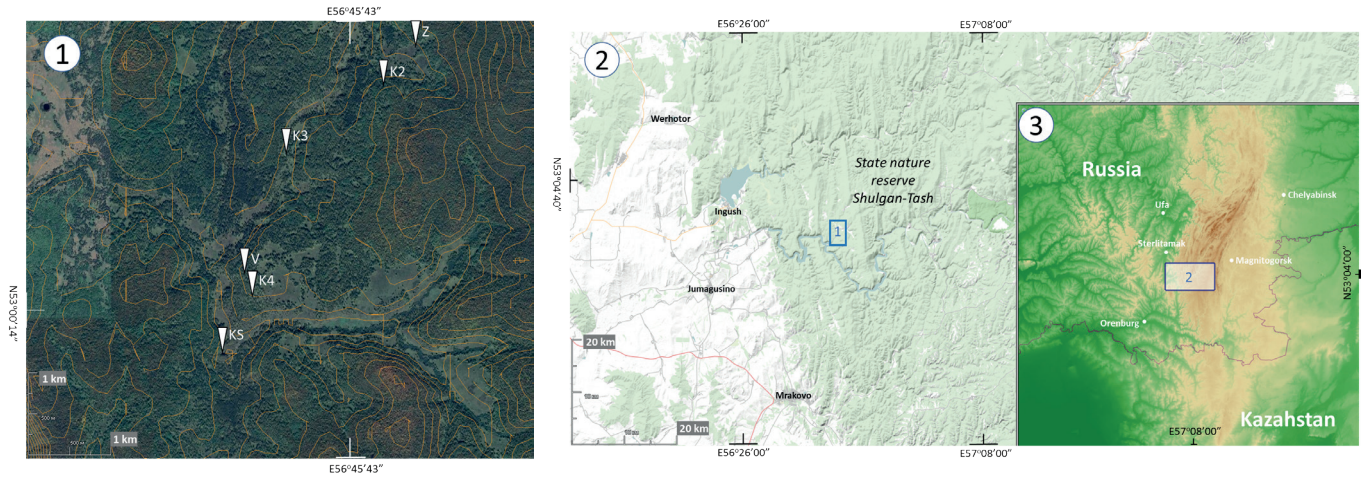

Fig. 1. Location of the explored caves in the Kutuk tract, Republic of Bashkortostan. KS – Kutuk-Sungan, K1 – Kutuk-1, K2 – Kutuk-2, K3 – Kutuk-3, K4 – Kutuk-4, V – Vintovaya, Z – Zigzag. Font: http://earth.google.com. 2022

Pliocene) terrace of the Belaya river valley above floodplain. The walls of the shaft are mostly flat, but in places they act as canopies[1] (Golubev et al. 1976; Kamalov and Chvanov 2014). The walls of the shaft contain ice and snow-ice masses, which provide constant drips and streams along the cave walls, the intensity of water flows varying in different seasons. Snow-ice masses and blocks of ice periodically fall, which leads to fragmentary destruction of the cavity vegetation cover, represented mainly by mosses. Kutuk-1 cave (Ice cave) is located 2.8 km to the north of the Kutuk-Sumgan cave at the base of the limestone wall of the right side of the dryland. The cave is horizontal, with a sloping cavity (main entrance angle 15-20º), consists of two halls-grottoes of 50x70 m and 20x30 m and side passages with the stream. The total length of the cave is 520 meters, it is iced during the whole year. The entrance area of the cave is an inclined icy descent with various sintered ice forms (Bogdanovich 1969). From the entrance to the central part of the largest grotto of the cave, there is a blanket of perennial ice. In the center of the grotto is a clay scree, frozen in some places, in the marginal part of the glacier clay, covers the ice with a layer up to 0.5 m (Kadebskaya and Stepanov 2016).

Kutuk-2 cave (Stalactite cave) is located 2.5 kilometers north of the Kutuk-Sumgan cave. The total length of the passages of Kutuk-2 is 2050 meters, with the amplitude of 110 meters. The length of the accessible part of the cave is 970 meters. The entrance zone is unwalled shafts of 12.5 meters in depth, at the bottom of which opens collapsing grotto, in the north-western part begins a gallery with dry and watered side tributaries. The gallery is blocked by two siphons and is going westward with the deepening of strata. It ends at a depth of 70-80 m with pebble siphons. In the southern part of the avalanche grotto another gallery with a stream goes to the southwest. This gallery is overlapped by a siphon at a depth of 110 m and has a narrow passage to the main part of the cave (Golubev et al. 1976). In winter seasonal glaciation forms in the entrance zone of the cave (Kadebskaya and Stepanov 2016).

Kutuk-3 is located in the Uluklansky log, two hundred meters south of the Kutuk-1 cave in the dry valley. The entrance part has the form of a rectangular sinkhole, at the bottom of which there is 8 meters long inclined (45°) ledge, leading to the descent into the 40 m deep mine. From the entrance to the bottom of the well there is an extended tongue-shaped glacier. At the end of the cave there is more than 50 m long inclined gallery, which is blocked up with blocks. The total depth of the cave is 65 m, at a depth of 61 m it impassably narrows. The walls of the entrance zone are covered with hydrogenous ice (Golubev et al. 1976).

Kutuk-4 cave is 1869 m long, 155 m deep, has 6728 m^2 area, 50500 m^3 volume, and 155 m amplitude. The cave is located on the left slope of Uluklansky log, 0.4 km north of Kutuk-Sumgan cave with an excess of 25 m above the entrance of the latter. The entrance to the cave is in the form of unwalled shafts, 10 m deep, which opens into a hall with ice. Flora is located on the walls of the shaft, on the shelves and at the bottom of the hall, mostly in areas that are not occupied by ice and snow-ice masses. At the bottom of the well, there are clastic and rubble deposits, which are the result of frost weathering. At the entrance part of the cave perennial ice is to be found. This ice field can reach a length of 300 m and a width of 6 m. The formation of the ice was caused by meltwater coming in the spring mainly through the entrance. The main part of the cave consists of the inclined (15°) meander gallery with a length of over 1800 m running along the dip of limestone beds, perpendicular to the extension of Uluklan valley. At a depth of 100-110 m from the entrance side tributaries flow into the main gallery. The cave is watered; the stream is fed by the glacier of the near-entrance part and by infiltration water[2] (Bogdanovich 1969; Kadebskaya and Stepanov 2016).

The Vintovaya cave is located in the thalweg of the Uluklan valley, 0.6 km to the north of the Kutuk-Sumgan cave. Its entrance is located at the base of the rock outcrop in a small funnel. From this tunnel a low passage follows to a steeply dipping (30°) high meandergallery, which is about 1 m wide. This meander gallery is developing in the direction of the dipping layers. It impassably narrows at a depth of 60 m, 270 m from the entrance. A small stream flows in the cave (Golubev et al. 1976).

Zigzag cave is 150 m deep, 2500 m long, has volume of 37900 m^3, is located in the side of the sinkhole, 800 m to the northeast of Kutukskaya-2 cave. The cave forms zigzag meander galleries which are ending with siphons. The mentioned galleries contain an underground river with the flow rate of 50-25 l/sec flows. At a depth of 110 m, the cave cuts through the contact zone of limestones and dolomites. The entrance is represented by two holes about 1.5 m in diameter, which follows to the inclined gallery. In the entrance zone a watercourse can be formed periodically in the form of a stream (Golubev et al. 1976). The cave maps are shown in Fig. 2, the photic zone of the caves in Fig. 3.

Methods

The bryophyte samples were collected in photic zones of caves-entrance sites illuminated by natural sunlight. For vertical shafts entrances, the beginning of the cave was marked out below the surface level. For inclined entrances, the beginning of the cave was determined by lowering the vertical line from the ceiling to the floor inside the cave. Most caves were processed in: May and November 2010; January, March and June 2012; August and November 2016. Samples from cave Zigzag were collected 5.2010, 11.2010, 6.2012, 11.2016. Samples from cave Vintovaya were collected 11.2010, 6.2012, 11.2016. At the sampling points, temperature and humidity were measured with electronic thermometers with an accuracy of 1ºC, 1%.

Samples in the caves were taken from each visually distinguishable tuft of mosses in sterile containers or paper envelopes and provided with a description of the habitat. Collected mosses were dried and soaked in water again before determining. The determination was carried out by observation of anatomical and morphological features using light microscopy. The following treatments were used for the identification: Ignatov and Ignatova (2003–2004), Abramov and Volkova (1998), Shlyakov (1981), Savich and Ladyzhenskaya (1936). Part of the specimens was brought to the herbarium of the Ufa Institute of Biology of the Russian Academy of Sciences. The rest are kept by Gainutdinov I.A. and in the collection of Mazina S.E. Several identifications were confirmed by E.Z. Baisheva (Ufa Branch of the Russian Academy of Sciences).

The nomenclature follows Ignatov et al. (2006) for mosses and Konstantinova et al. (2009) for liverworts.

The participation of species in the community was assessed by the proportion of the species in the sample. Only samples collected in 2016 were analyzed using the

[1] *https://speleoatlas.ru/caves/sumgan-13153*

[2] *https://speleoatlas.ru/caves/kutukskaya-4-17432*

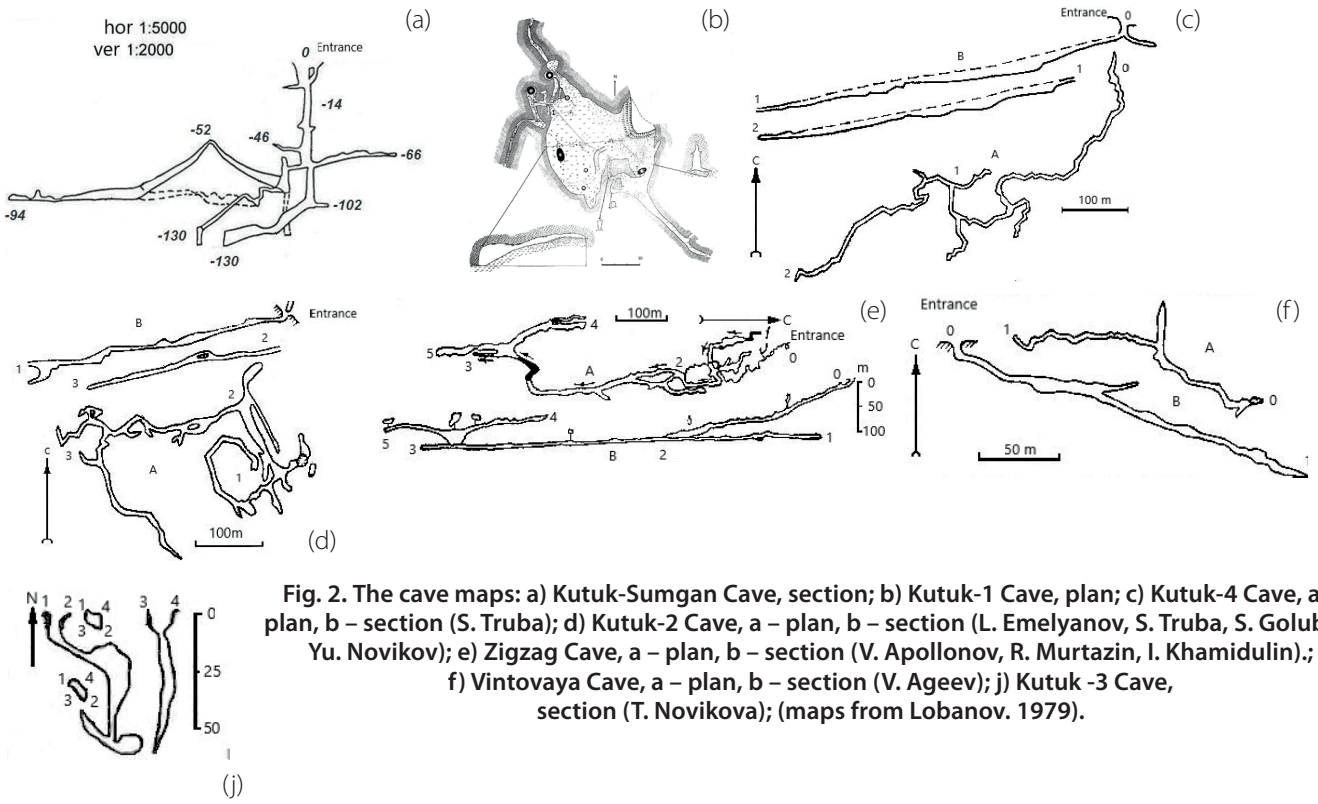

Fig. 2. The cave maps: a) Kutuk-Sumgan Cave, section; b) Kutuk-1 Cave, plan; c) Kutuk-4 Cave, a – plan, b – section (S. Truba); d) Kutuk-2 Cave, a – plan, b – section (L. Emelyanov, S. Truba, S. Golubev, Yu. Novikov); e) Zigzag Cave, a – plan, b – section (V. Apollonov, R. Murtazin, I. Khamidulin).; f) Vintovaya Cave, a – plan, b – section (V. Ageev); j) Kutuk -3 Cave, section (T. Novikova); (maps from Lobanov. 1979).

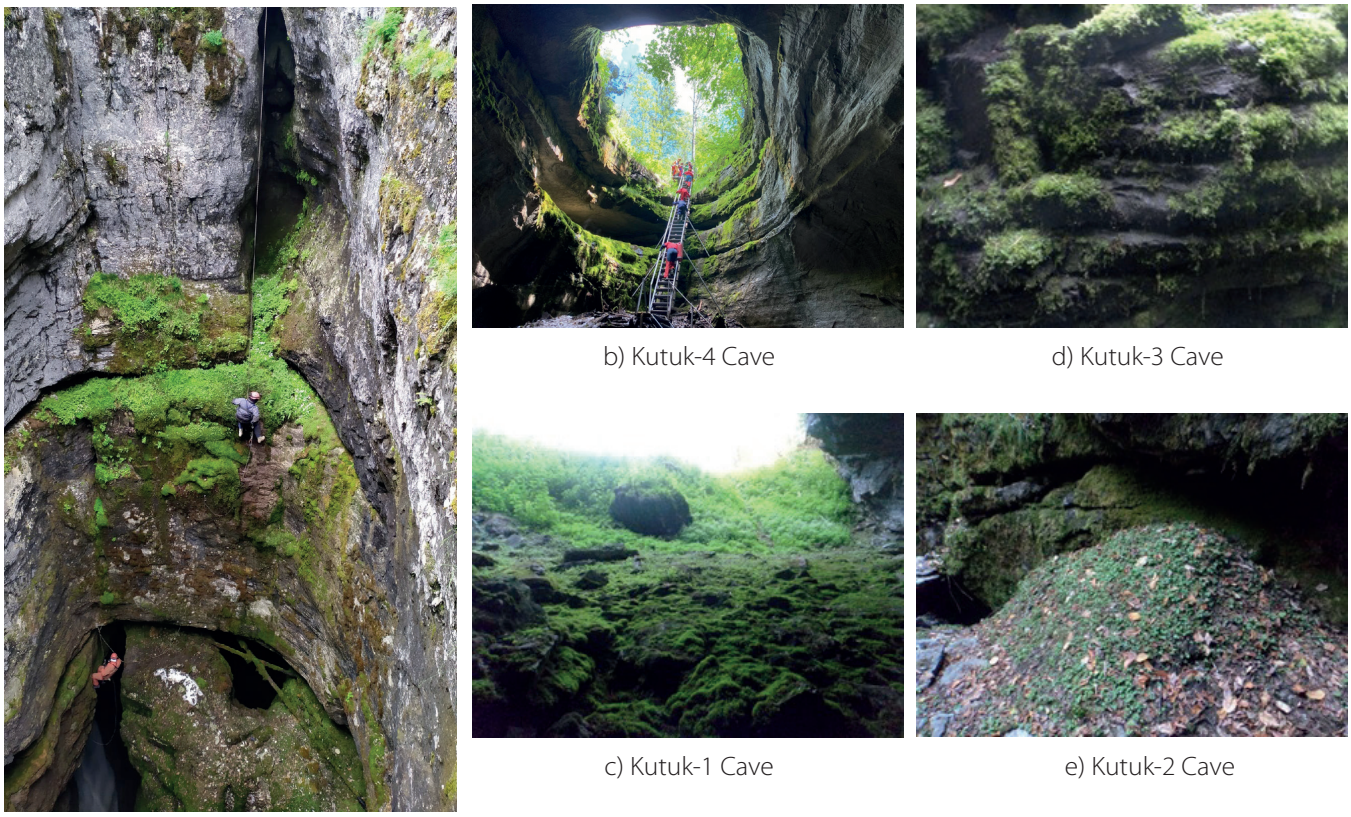

a) Kutuk-Sumgan Cave

b) Kutuk-4 Cave

d) Kutuk-3 Cave

c) Kutuk-1 Cave

e) Kutuk-2 Cave

Fig. 3. The photic zone of the Caves. Photo from Pozdnyakova L., Asylguzhin A., Dmitrieva S., Gainutdinov I.

projective coverage of species. A 5-point scale – analogue of the Brown-Blanquet scale (Braun-Blanquet 1964) was used. Were 1 – the number of organisms is small (up to single), organisms are sparse or with little coverage up to 5%; 2 – the number of organisms is large coverage is from 5 to 25%; 3 – with any number of organisms coverage is from 25 to 50%; 4 – with any number of organisms coverage is from 50 to 75%; 5 – with any number of organisms the coverage is more than 75%. Relative participation was defined as the ratio of the participation of a species to the total participation of all moss species in the photic zone of the cave (as a percentage), the species with the greatest participation were considered to be dominants. The relative occurrence of species was calculated as the ratio of the sum of samples in which the species was detected to the total occurrence of all species (as a percentage).

The Jaccard Index was used to assess the similarity of the species structure. It was calculated on the basis of the occurrence of species (Jaccard 1901, Schmidt 1980). The Phi-square coefficient, which was calculated based on

species occurrence and used to estimate species structure (Byul and Cefel, 2005). The values determined for parallel samples were used as a similarity standard (Maksimov 1984). In accordance with the methodological approach described in the works of Maximov and Kuznetsova (2013) as well as Pichugina and Mazina (2020) the Jaccard index from 0.4 to 1 and the Phi-square index from 0 to 0.6 were chosen as reference values of similarity. The proximity of the cave flora was calculated using square Euclidean distance (Spencer 2013) and Ward method (Blashfield and Aldenderfer 1978). The contribution of each cave to the total composition of the flora was calculated as the ratio of the number of identified species in one cave to the total number of species as a percentage. Statistical processing of the data was carried out using MS Excel, IBM SPSS Statistics 26.

RESULTS AND DISCUSSION

In the studied caves, 55 species of bryophytes and 6 liverworts species were found. The list of species and the distribution of species by caves are presented in Appendix 1.

The number of bryophyte species varied from cave to cave (Appendix 1). In the largest Kutuk-Sumgan cave, 31 species were found; 21 species in Kutuk-2 and Kutuk-3; 19 species in Kutuk-4; 18 species in Vintovaya and Zigzag caves; 14 species in Kutuk-1. The entrances of Kutuk-Sumgan, Kutuk-2, Kutuk-4, Kutuk-3 caves are vertical shafts with snow-ice masses at the bottom and walls. Kutuk-1 has an entrance in the form of an inclined icy descent. The Vintovaya and Zigzag caves are small sloping entrances without glaciation, having clay deposits. The smallest number of species was found in a cave with a sloping ice entrance Kutuk-1. The shafts caves are the richest in terms of the abundance and diversity of bryophytes.

The temperature in the inlet zones of the cave shafts during the sampling period in winter in the upper parts was close to the surface temperature, and in the bottom parts it was from -3 to +2˚C. In summer, the temperature in the shafts was 7-12˚C and in Kutuk-Sumgan cave in the upper part was 4-14˚C. In the caves with horizontal entrances, the temperature was -4 to +7˚C in winter and 7-14˚C in summer. In Kutuk-1 cave, winter temperature was -12 to -5˚C, and in summer from -2 to 4˚C. Humidity in all caves was close to 100%.

In all caves with shafts entrances, the moss layer was well pronounced and constituted 60 to 90% of the surface on clay sediments or soil-like bodies. On limestone blocks, the projective cover was lower, about 20 to 40%. In caves with inclined entrances, areas with moss cover were located within the well-lit zone at the very beginning of the cave, mostly on clay deposits, discretely, occupying 20-30% of the area.

The calculated relative participation indexes showed that *Timmia bavarica* dominated in the photic zones of all caves. In Kutuk-Sumgan Cave the subdominants were *Distichium capillaceum, Brachythecium rotaeanum, Brachytheciastrum velutinum;* in Kutuk-2 *Distichium capillaceum, Plagiomnium medium;* in Kutuk-3 *Distichium capillaceum, Plagiomnium medium, Brachythecium rotaeanum, Hylocomium splendens;* Kutuk-4 *Cratoneuron filicinum, Brachytheciastrum velutinum, Brachythecium rivulare;* in Kutuk-1 *Brachythecium salebrosum, Distichium capillaceum, Brachytheciastrum velutinum, Pohlia cruda;* in Spiral *Campylidium sommerfeltii, Hylocomium splendens, Plagiomnium medium, Orthothecium strictum;* in Zigzag *Distichium capillaceum, Brachythecium glareosum, Sciuro-hypnum curtum, Plagiomnium medium.*

Among the dominant and subdominant species *Timmia bavarica, Distichium capillaceum, Brachythecium glareosum, Pohlia cruda,* and *Orthothecium strictum* belonged to species growing on carbonate rocks and limestone. Among all the species found in the caves, only one, *Rhynchostegium arcticum*, is included in the Red Data Book of the Republic of Bashkortostan (Mirkin 2011).

Only two species of *Brachytheciastrum velutinum* and *Timmia bavarica* were found in all studied caves, and species of *Distichium capillaceum* and *Marchantia polymorpha* were found in six caves. Twenty-three species were found in only one cave and 11 species in two caves. That is, 41% of the cave flora of bryophyte of the Kutuk tract's bryophyte flora are species found only in one cave, with the highest number of such species (6) in the Kutuk-Sumgan Cave. The contribution to the total cave flora of the tract differed between caves (Appendix 2), and ranged from 23 to 41%. The highest contribution to the cave bryophyte species composition was in the cave with the largest entrance zone Kutuk-Sumgan.

Information on the bryoflora of Bashkiria National Park is given in (Flora… 2010), but we did not find any information on cave species in it. In addition to the species listed in the current paper, cave surveys have also revealed species: *Serpoleskea confervoides, Rhynchostegium murale, Rhizomnium punctatum, Plagiothecium denticulatum, Orthothecium strictum, Loeskypnum badium, Pohlia wahlenbergii, Dichodontium pellucidum.*

The reference similarity of bryophytes of the entrance zones during the study period (2010-2016 years) was revealed only in Zigzag and Vintovaya caves, and the similarity of the structure only in Zigzag cave. These caves have small, inclined entrances without glaciation. The most frequent deviations from the reference similarity are noted in caves with large, failed entrances with large amounts of glaciation, such as Kutuk-4 and Kutuk-Sumgan. In most caves composition of bryophytes was similar. In assessing similarity, it is noticeable that the species structure varies more than the species composition (Table 1).

Most of the studied caves have an entrance in the form of a shaft, at the bottom of which accumulations of ice are formed and persist all year round. In winter, snow and ice fall into the well. In spring and summer, ice formations melt on the walls of the well and water flows down. Open entrances collect streams of water during precipitation and the snowmelt season. In addition to water and ice, trees and biota can also fall into cave wells.

Opened shaft cave entrances are more accessible to new species. The mechanical effect of water and ice leads to the removal of part of the fouling from the walls and the flat of the well. Tree trunks overgrown with mosses and soil collapses enter the cave, so the biota may include species that are not characteristic of growing on the host rock (limestone).

There are extremely few data in the literature on the stability of entrance zone communities. For algal biofilms, seasonal changes in species composition in caves in eastern Serbia were determined (Popović et al. 2019), whereas other caves are characterized by stability of entrance zone communities within the cave (Popkova et al. 2019; Kozlova et al. 2019). Apparently, changes in the bryoflora in the caves of the Kutuk tract are related to the morphology of the entrances and reflect disturbances associated with the impact of snow-ice masses.

We analyzed similarity indexes (Jaccard and Phi-square) between the caves and calculated the percentage of occurrence of reference similarity during the studied period (Appendix 2). The species structure of bryophytes in Kutuk-2

and Zigzag caves is most similar, and the species composition is similar in Kutuk-2 and Zigzag, Kutuk-Sumgan and Zigzag, and Kutuk-3 and Kutuk-Sumgan caves. Benchmark similarity is most often revealed for bryophytes within the same cave. Caves with shaft entrances during the study period showed reference similarity to each other. The Zigzag and Vintovaya caves stand out, the latter having bryoflora significantly different from other caves. Both of these caves have small entrance areas without permanent glaciation. The bryoflora of the Kutuk-1 cave, which also has an inclined entrance, but with permanent glaciation, is not so different from caves with shaft entrances. In other words, the presence of permanent snow-ice masses or glaciation in the entrance zone affects the composition of bryophytes. Consequently, while selecting objects for the inventory of bryoflora of caves, we can recommend investigating caves with different types of entrances and taking into account the presence of ice or snow-ice masses in the entrance zone of the cave.

For comparison of species composition of studied caves a cluster analysis was carried out, which showed similar results for cave proximity. The Ward method provided meaningful clasterisation. Moreover, it is possible to apply statistical criteria to the clustering results. According to the dendric diagram (Fig. 4) from the 7th clasterisation level (9 clusters) the correlation between cluster and sampling place (cave) is revealed.

Pearson coefficient 0.025 ($\alpha < 0.05$). If at the first six levels of clustering there was no separation which correlates with the sampling site, then there are some other factors that affect the species structure of communities. There is an error of experiment, selection or determination. However, if a correlation is found at the seventh and subsequent levels, then it can be assumed that there are at least 9 significant parameters or combinations of parameters that are directly related to the characteristics of the cave. The exact number of parameters is a controversial thesis, due to a high variability of natural ecosystems.

Our observations are consistent with data on the caves in Montenegro, where the morphology of the entrance zone affects the species composition of phototrophs (Kozlova et al. 2019). It can be assumed that large cave entrances, as in Kutuk-Sumgan Cave, have more diverse habitats, which affects biodiversity. This fact can be confirmed by the studies of Monro et al. (2018) and Ren et al. (2021) in caves in China.

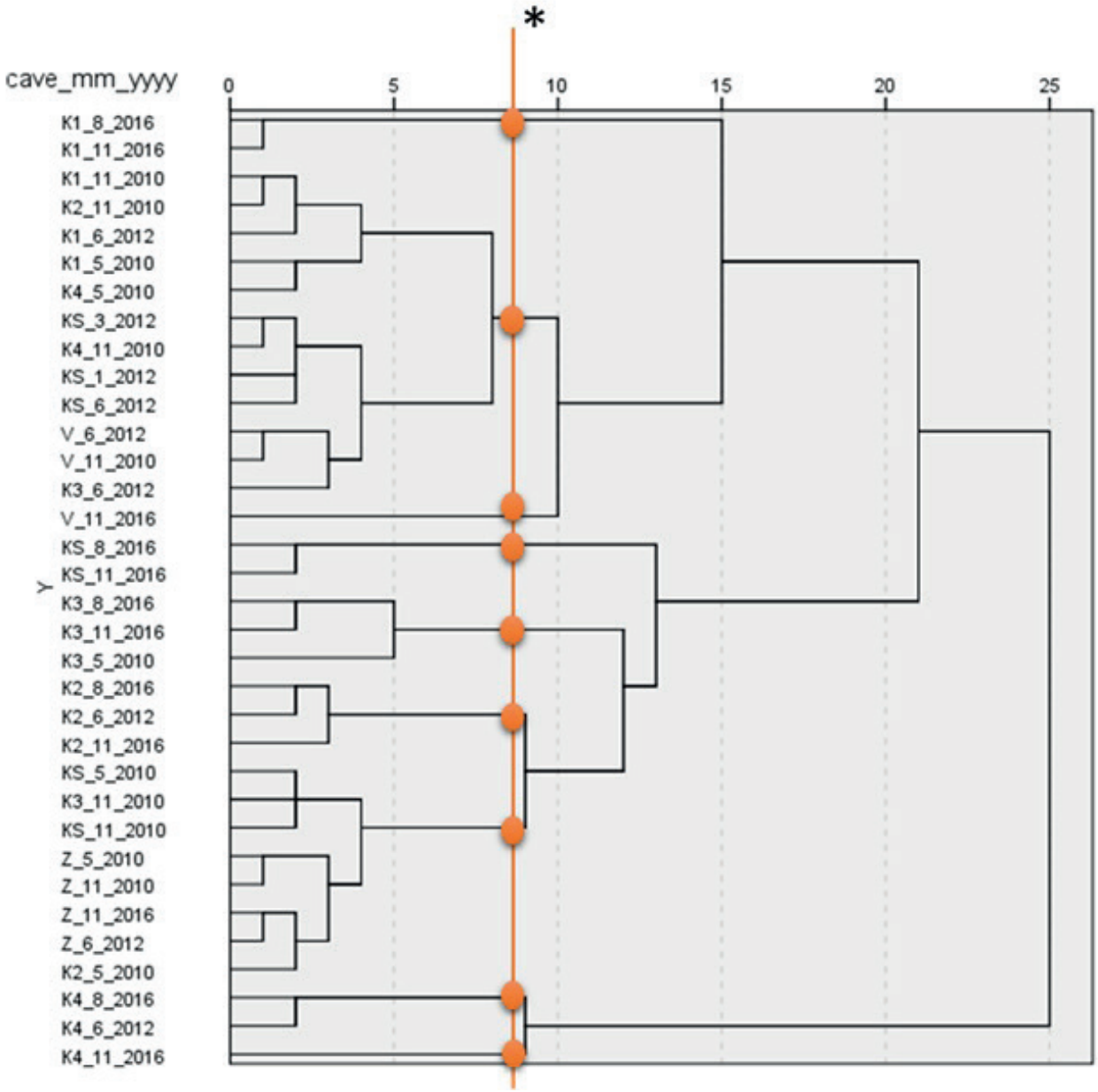

Fig. 4. Hierarchy cluster analyses of the cave bryophyte species structure. Ward method and the square of Euclidian distance were applied. KS – Kutuk-Sungan, K1 – Kutuk-1, K2 – Kutuk-2, K3 – Kutuk-3, K4 – Kutuk-4, V – Vintovaya, Z – Zigzag. The date of sampling was also taken into account. * – from the 7th clasterisation level (9 clusters) the correlation between cluster number and sampling place is reveled. Pearson coefficient 0.025 ($\alpha < 0.05$)

CONCLUSIONS

A study of biodiversity of bryophytes in the caves of the Kutuk tract was carried out for the first time.

The study revealed the stability of the species composition and species structure of moss caves in different years. At the same time, the species composition differed less. The caves with small inclined entrances were the most stable.

Changes in the bryoflora of the photic zones of caves can be related to disturbances, in this case mechanical, due to falling snow and ice, water flows, human actions when passing through the wells with climbing equipment, and the number of species is related to the size of the photic zone, glaciation and habitat diversity. When selecting caves for biodiversity assessment, caves with different morphological entrances should be included in the study, their degree of disturbance should be assessed, selecting among the caves with similar entrance sites the least disturbed ones.

Analysis of bryophytes of the photic zone of the single characteristic cave can reveal up to 40% of the bryoflora of caves situated around.

Instability of cave bryoflora can be an indicator of disturbance, which is convenient to use to assess negative influences or natural processes.

REFERENCES

Abdrakhmanov R.F., Martin V.I., Popov V.G., Rozhdestvenskiy A.P., Smirnov A.I. and Travkin A.I. (2002). Karst of Bashkortostan. UFA: Informreklama (UFA), (In Russian).

Abramov I.I. and Volkova L.A. (1998). Identifier of leafy mosses of Karelia, (In Russian).

Bichuette M.E. and Trajano E. (2010). Conservation of subterranean fishes. In Trajano E, Bichuette ME, Kapoor BG, editors. Biology of Subterranean Fishes. Enfield: Science Publishers, 65-80.

Blashfield R.K., and Aldenderfer M.S.. (1978). The literature on cluster analysis. Multivariate behavioral research 13(3), 271-295.

Bogdanovich E.D. (1969). Caves of the Kutuk tract. In: Karst issues, Perm, (In Russian).

Braun-Blanquet J. (1964). Pflanzensoziologie: Grundzüge der Vegetationsskunde 3rd ed. Berlin: Springer-Verlag, DOI: 10.1007/978-3-7091-8110-2.

Byuhl A. and Tsefel P. (2005). SPSS: The Art of Information Processing. Analysis of statistical data and recovery of hidden patterns. DiaSoft, (In Russian).

Czerwik–Marcinkowska J. (2013). Observations on aerophytic cyanobacteria and algae from ten caves in the Ojców National Park. Acta Agrobotanica, 66(1), 39-52.

Golubev S.I., Lobanov Yu.E., Truba S.B., Novikova T.D. and Zagidulin M.T. (1976). Caves of the Kutuk tract in Bashkiria. In: Caves, Collection of scientific papers, Perm: Perm State University. 16, 79-87, (In Russian).

Ignatov M.S., O.M. Afonina, E.A. Ignatova, A. Abolina, T.V. Akatova, E. Z. Baisheva, L.V. Bardunov, E.A. Baryakina, O.A. Belkina, A.G. Bezgodov, M.A. Boychuk, V.Ya. Cherdantseva, I.V. Czernyadjeva, G.Ya. Doroshina, A.P. Dyachenko, V.E. Fedosov, I.L. Goldberg, E.I. Ivanova, I. Jukoniene, L. Kannukene, S.G.Kazanovsky, Z.Kh. Kharzinov, L.E. Kurbatova, A.I.Maksimov, U.K. Mamatkulov,V. A. Manakyan, O.M. Maslovsky, M.G. Napreenko, T. N. Otnyukova, L.Ya. Partyka, O.Yu. Pisarenko, N.N. Popova, G.F. Rykovsky, D.Ya. Tubanova, G.V. Zheleznova and V.I. Zolotov. (2006). Check-list of mosses of East Europe and North Asia. Arctoa, 15, 1–130.

Ignatov M.S. and Ignatova E.A. (2003). Flora of mosses of the middle part of European Russia. Vol. 1. Sphagnaceae-Hedwigiaceae. M.: KMK.1-608. Ignatov M.S., Ignatova E.A. (2004). Flora of mosses of the middle part of European Russia. Vol. 2. Fontinalaceae-Amblystegiaceae. M.: KMK.609-944, (In Russian).

Flora and vegetation of Bashkiria National Park (syntaxonomy, Anthropogenic dynamics, ecological zoning) / Edited by B.M. Mirkin. – Ufa: Academy of Sciences of RB, Gilem, 2010, 512.

Jaccard P. (1901). Distribution de la flore alpine dans le Bassin des Drouceset dans quelques regions voisines. Bulletin de la Société Vaudoise desSciences Naturelles, 37(140), 241-272.

Kadebskaya O.I. and Stepanov Yu.I. (2016). Characteristics of ice and cryogenic minerals in the caves of the Kutuk tract (Bashkortostan). Geology, Geography and Global Energy, 2(61), 30-39, (In Russian).

Kamalov V.G. and Chvanov M.A. (2014). The Sumgan Gap: History of Development. In: Caves. Collection of scientific works, Perm: Perm State University. 37, 181-188, (In Russian).

Konstantinova N.A., Bakalin V.A., Andreeva E.N., Bezgodov A.G., Borovichev E.A., Dulin M.V., Mamontov Y.S. (2009). List of liverworts (Marchantiophyta) of Russia. Arctoa, 18, 1-64, (In Russian).

Kozlova E.V. and Mazina S.E. (2020). Mosaicity of phytocenoses of photic zones on the example of caves. Montenegro Problems of Regional Ecology, 1, 27-33, (In Russian), DOI: 10.24411/1728-323X-2020-11027.

Kozlova E.V., Mazina S.E. and Pešić V. (2019). Biodiversity of phototrophs in illuminated entrance zones of seven caves in Montenegro. Ecologica Montenegrina, 20, 24-39, DOI: 10.37828/em.2019.20.3.

Lobanov Y. (1979). Ural Caves Sverdlovsk. Sredne-Uralsky Book Publishers, 173.

Maksimov V.N. (1984). Metrological properties of similarity indices (in application to biological analysis of water quality). Complex assessments of surface water quality. L.: Gidrometeoizdat, 77-84, (In Russian).

Maksimov V.N. and Kuznetsova N.A. (2013). Benchmark similarity: use in comparing the composition and structure of communities. M.: KMK (In Russian).

Mazina S.E., Popkova A.V., Zvolinski V.P. and Yuzbekov A.K. (2020). Biodiversity and productivity of phototrophic communities from the illuminated cave zone with high content of CO2. Cave and Karst Science, 47(3), 131-137.

Mazina S.E. and Popkova A.V. (2017). Communities of the lighted zone of hypogean monastic cells of the rock monastery «Dormition of God's Mother», the reserve Old Orhey. South of Russia: ecology, development, 12, 4(45), 138-146, (In Russian), DOI: 10.18470/1992-1098-2017-4-138-146.

Mirkin B.M. (2011). Red Book of the Republic of Bashkortostan: in 2 vols. T. 1: Plants and fungi. Ufa: MediaPrint, 384. (In Russian).

Monro A.K., Bystriakova N., Fu L., Wen F. and Wei Y. (2018). Discovery of a diverse cave flora in China. PLoS ONE 13, e0190801, DOI: 10.1371/journal.pone.0190801.

Mulec J. (2008). Microorganisms in hypogen: examples from Slovenian karst caves. Acta Carsologica, 37(1), 153-160, DOI: 10.3986/ac.v37i1.167.

Neill H., GutieÂrrez M. and Aley T. (2004). Influences of agricultural practices on water quality of Tumbling Creek cave stream in Taney County, Missouri. Environ Geology, 45, 550-559.

Northup D.E., and Lavoie K.H. (2001). Geomicrobiology of caves: a review. Geomicrobiol Journal, 18, 199-222, DOI: 10.1080/01490450152467750.

Novak T., Perc M., Lipovsek S. and Janžekovič F. (2012). Duality of terrestrial subterranean fauna. International Journal of Speleology, 41(2), 181-188, DOI: 10.5038/1827-806X.41.2.5.

Parise M., De Waele J. and Gutierrez F. (2009). Current perspectives on the environmental impacts and hazards in karst. Environ Geol., 58. 2,5-237, DOI: 10.1007/s00254-008-1608-2.

Pentecost A. and Zhaohui, Z. (2001). The distribution of plants in Scoska Cave, North Yorkshire, and their relationship to light intensity, 1256.

Pichugina E.K. and Mazina S.E. (2020). An approach to the analysis of communities of fouling in photic zones of caves and lamp flora. Natural Sciences: current issues and social challenges. Materials of the III International Scientific-Practical Conference, 300-304, (In Russian).

Popkova A., Mazina S. and Lashenova T. (2019). Phototrophic communities of Ahshtyrskaya Cave in the condition of artificial light. Ecologica Montenegrina, 23, 8-19, DOI: 10.37828/em.2019.23.2.

Popkova A.V. and Mazina S.E. (2019). Microbiota of Hypogean Habitats in Otap Head Cave. Environmental Research, Engineering and Management, 75 (3).

Popkova A.V. and Mazina S.E. (2020). Biodiversity of phototrophic communities of Simon Kananit Grotto. Ecology of urbanized territories, 2, 56-61, (In Russian), DOI: 10.24411/1816-1863-2020-12056.

Popović S., Krizmanić J., Vidaković D., Jakovljević O., Trbojević I., Predojević D., Vidović M. and Subakov Simić G. (2020). Seasonal dynamics of cyanobacteria and algae in biofilm from the entrance of two caves. Geomicrobiology Journal, 37(4), 315-326, DOI: 10.1080/01490451.2019.1700322.

Puglisi M., Privitera M., Minissale P. and Costa R. (2019). Diversity and ecology of the bryophytes in the cave environment: a study on the volcanic and karstic caves of Sicily. Plant Biosystems-An International Journal Dealing with all Aspects of Plant Biology, 153(1), 134-146, DOI: 10.1080/11263504.2018.1478903.

Gabriel R., Pereira F.E., Borges P.A. and Constância, J.P. (2008). Indicators of conservation value of Azorean caves based on its bryophyte flora at cave entrances. In XI International Symposium on Vulcanospeleology, 114-118.

Ren H., Wang F., Ye W., Zhang Q., Han T., Huang Y., Chu G., Hui D. and Guo Q. (2021). Bryophyte diversity is related to vascular plant diversity and microhabitat under disturbance in karst caves. Ecological Indicators, 120, 106947, DOI: 10.1016/j.ecolind.2020.106947.

Savich L.I. and Ladyzhenskaya K.I. (1936). Identifier of hepatic mosses of the north of the European part of the USSR. Leningrad: Proceedings of the Acad. of Sciences of the USSR (In Russian).

Schmidt V.M. (1980). Statistical methods in comparative floristics. L.: Publishing house of Leningrad State University (In Russian).

Serena F. and Meluzzi C. (1997). Species assemblages and light trend in the zoning of Tana di Casteltendine (Lucca-Italy) entrance. Mém Biospéol, 24, 183-190.

Shlyakov R.N. (1981). The hepatic mosses of the North of the USSR, Vol. 4. Hepatic mosses: Jungermanniaceae-Scapanii. L.: Nauka, 221. (In Russian).

Simòes M.H., Souza-Silva M. and Ferreira R.L. (2014). Cave invertebrates in northwestern Minas Gerais state, Brazil: endemism, threats and conservation priorities. Acta Carsologica, 43, DOI: 159-174 10.3986/ac.v43i1.577.

Spencer N.H. (2013). Essentials of Multivariate Data Analysis, CRC Press, 95.

Tao J.J., Qi Q.W., Kang M. and Huang, H.W. (2015). Adaptive Molecular Evolution of PHYE in Primulina, a karst cave plant. PLoS ONE, 10(6), e0127821, DOI: 10.1371/journal.pone.0127821.

Williams P. (2008). Karst Landscapes and Caves on the World Heritage List. In Williams P, editor. World heritage caves and karst. Gland: IUCN, 5-8.

Zhang Y.H., Zhu D.H. (2012). Large Karst Caves Distribution and Development in China. J Guilin Univer Tech., 32(1), 20-28.

Table 1. Similarity of the species structure and species composition of bryophytes in the caves in different years

Sampling date		Kutuk-1						Kutuk-2				
		5. 2010	11. 2010	6. 2012	8. 2016	11. 2016		5. 2010	11. 2010	6. 2012	8. 2016	11. 2016
			Jaccard						Jaccard			
5.2010			**0,60**	0,30	0,25	0,23			**0,36**	**0,44**	**0,69**	**0,61**
11.2010	PHI	**0,46**		**0,50**	**0,42**	**0,38**	PHI	0,64		0,27	0,33	0,29
6.2012		0,62	**0,44**		**0,69**	**0,64**		0,58	0,62		**0,59**	**0,53**
8.2016		0,62	**0,53**	**0,42**		**0,92**		**0,47**	**0,53**	**0,41**		**0,88**
11.2016		0,62	**0,54**	**0,43**	**0,14**			**0,50**	0,59	**0,47**	**0,28**	
Sampling date		Kutuk-3						Kutuk-4				
		5. 2010	11. 2010	6. 2012	8. 2016	11. 2016		5. 2010	11. 2010	6. 2012	8. 2016	11. 2016
			Jaccard						Jaccard			
5.2010			**0,45**	**0,36**	**0,50**	**0,37**			**0,67**	0,30	**0,40**	0,27
11.2010	PHI	0,63		**0,42**	**0,46**	**0,41**	PHI	**0,51**		0,18	0,27	0,19
6.2012		0,69	**0,50**		**0,47**	**0,42**		0,57	0,72		**0,42**	0,29
8.2016		**0,53**	0,55	0,55		**0,71**		0,57	0,68	**0,48**		**0,64**
11.2016		0,57	**0,48**	**0,52**	**0,31**			0,65	0,72	0,61	**0,46**	
Sampling date		Zigzag						Vintovaya				
		5.2010	11.2010	6.2012	11.2016			11.2010		6.2012	11.2016	
			Jaccard							Jaccard		
5.2010			**0,91**	**0,64**	**0,60**			-		-	-	
11.2010	PHI	**0,26**		**0,60**	**0,56**					**0,62**	**0,35**	
6.2012		**0,46**	**0,45**		**0,69**		PHI	**0,38**			**0,53**	
11.2016		**0,46**	**0,49**	**0,40**				0,62		**0,48**		
Sampling date		Kutuk-Sumgan										
		5.2010	11.2010	1.2012	3.2012		6.2012	8.2016		11.2016		
			Jaccard									
5.2010	PHI		**0,50**	**0,42**	0,23		**0,38**	0,32		0,25		
11.2010		**0,42**		0,31	0,18		**0,37**	**0,38**		0,31		
1.2012		0,69	0,69		**0,36**		**0,56**	**0,47**		**0,38**		
3.2012		0,77	0,77	0,61			**0,41**	0,29		0,23		
6.2012		0,62	0,65	**0,46**	**0,55**			**0,50**		**0,41**		
8.2016		0,60	**0,56**	**0,49**	0,65		**0,50**			**0,78**		
11.2016		0,64	0,63	0,57	0,69		0,58	**0,34**				

Appendix 1. List of bryophytes cave species of the Kutuk tract

	Relative occurrence								Relative participation (abundance)							
	Total	V	Z	K1	K2	K3	K4	KS	Total	V	Z	K1	K2	K3	K4	KS
Abietinella abietina (Hedw.) M.Fleisch.	0,80	-	-	-	-	-	-	3,23	0,39	-	-	-	-	-	-	1,74
Barbilophozia barbata (Schmidel ex Schreb.) Loeske	0,53	-	-	-	1,61	-	-	1,08	0,05	-	-	-	0,16	-	-	0,12
Barbula convoluta Hedw.	1,33	2,86	-	6,98	-	-	-	1,08	1,12	0,74	-	6,02	-	-	-	1,16
Brachytheciastrum velutinum (Hedw.) Ignatov & Huttunen	5,84	5,71	2,08	11,63	3,23	3,64	12,20	5,38	6,17	4,46	1,22	9,83	2,45	1,74	15,61	7,08
Brachythecium glareosum (Bruch ex Spruce) Bruch et al.	3,71	-	8,33	-	6,45	3,64	-	4,30	4,15	-	10,95	-	7,35	2,61	-	6,15
Brachythecium mildeanum (Schimp.) Schimp.	2,65	-	2,08	-	1,61	7,27	2,44	3,23	2,52	-	1,22	-	2,45	6,97	2,93	2,44
Brachythecium rivulare Bruch et al.	0,80	-	-	-	-	-	7,32	-	1,08	-	-	-	-	-	8,00	-
Brachythecium rotaeanum De Not.	5,31	8,57	8,33	-	-	9,09	2,44	7,53	4,77	7,44	6,20	-	-	9,32	1,95	7,83
Brachythecium salebrosum (F.Weber & D.Mohr) Bruch et al	3,18	5,71	-	11,63	6,45	-	-	1,08	3,51	4,91	-	15,45	5,72	-	-	0,58
Brachythecium sp.1	0,53	-	-	-	-	-	-	2,15	0,26	-	-	-	-	-	-	1,16
Brachythecium sp.2	0,80	-	-	4,65	-	-	2,44	-	0,92	-	-	6,02	-	-	0,98	-
Brachythecium albicans (Hedw.) Bruch et al.	0,53	-	-	-	3,23	-	-	-	0,26	-	-	-	1,63	-	-	-
Brachythecium rutabulum (Hedw.) Bruch et al.	2,12	-	-	2,33	6,45	1,82	-	2,15	1,01	-	-	1,20	3,27	0,87	-	0,87
Bryoerythrophyllum recurvirostrum (Hedw.) P.C.Chen	2,65	5,71	4,17	-	6,45	-	-	2,15	1,45	2,98	3,65	-	3,27	-	-	1,16
Calliergonella lindbergii (Mitt.) Hedenäs	0,27	2,86	-	-	-	-	-	-	0,26	2,98	-	-	-	-	-	-
Campylidium sommerfeltii (Myrin) Ochyra	0,80	8,57	-	-	-	-	-	-	0,91	10,27	-	-	-	-	-	-
Chilocyphus sp.	0,27	-	-	-	-	1,82	-	-	0,03	-	-	-	-	0,17	-	-
Conocephalum conicum (L.) Underw.	0,80	5,71	-	-	-	1,82	-	-	0,53	4,46	-	-	-	0,87	-	-
Cratoneuron filicinum (Hedw.) Spruce	2,12	-	-	-	-	-	9,76	4,30	3,13	-	-	-	-	-	15,90	4,35
Cyrtomnium hymenophylloides (Hueb.) Nyh. Ex T. Kop.	0,27	-	-	-	-	1,82	-	-	0,26	-	-	-	-	1,74	-	-
Dichodontium pellucidum (Hedw.) Schimp.	0,27	2,86	-	-	-	-	-	-	0,13	1,49	-	-	-	-	-	-
Distichium capillaceum (Hedw.) Bruch et al.	7,16	-	8,33	11,63	8,06	9,09	4,88	6,45	8,84	-	12,41	12,14	11,44	10,45	3,22	9,11
Encalypta sp.	0,80	-	2,08	4,65	-	-	-	-	0,66	-	1,22	4,01	-	-	-	-

Encalypta rhaptocarpa Schwägr.	0,53	-	-	-	-	3,64	-	-	0,26	-	-	-	-	1,74	-	-
Eurhynchiastrum pulchellum (Hedw.) Ignatov & Huttunen	0,53	-	-	-	-	-	-	2,15	0,26	-	-	-	-	-	-	1,16
Hygroamblystegium humile (P. Beauv.) Vanderpoorten	0,53	-	-	-	-	-	2,44	1,08	0,26	-	-	-	-	-	0,98	0,58
Hygrohypnum luridum (Hedw.) Jenn.	1,06	-	-	-	-	3,64	4,88	-	0,78	-	-	-	-	3,48	1,95	-
Hylocomium splendens (Hedw.) Bruch et al.	2,12	8,57	-	-	-	5,45	-	2,15	2,60	9,52	-	-	-	9,06	-	1,74
Leiocolea heterocolpos (Thed. ex C.Hartm.) H.Buch	0,27	2,86	-	-	-	-	-	-	0,39	4,46	-	-	-	-	-	-
Loeskypnum badium (Hartm.) H.K.G.Paul	0,80	-	-	-	1,61	-	4,88	-	0,66	-	-	-	0,82	-	3,90	-
Marchantia polymorpha L.	7,16	-	8,33	9,30	6,45	7,27	9,76	7,53	4,94	-	6,08	4,01	4,90	5,23	5,85	6,15
Mnium marginatum (Dicks.) P.Beauv.	4,51	-	4,17	6,98	6,45	5,45	-	5,38	4,47	-	3,65	3,01	6,54	6,97	-	6,96
Orthothecium strictum Lorentz	2,65	8,57	4,17	-	-	-	7,32	2,15	2,31	8,33	3,65	-	-	-	4,88	2,32
Plagiochila porelloides (Torr. ex Nees) Lindenb.	0,27	-	-	-	-	-	-	1,08	0,01	-	-	-	-	-	-	0,06
Plagiomnium ellipticum (Brid.) T. Kop.	0,27	-	-	-	-	-	-	1,08	0,39	-	-	-	-	-	-	1,74
Plagiomnium medium (Bruch et al.) T.J.Kop.	5,31	8,57	8,33	-	8,06	9,09	-	3,23	5,60	9,38	8,52	-	10,46	10,02	-	2,90
Plagiomnium rostratum (Schrad.) T.J.Kop.	2,65	2,86	-	6,98	-	1,82	-	5,38	2,57	2,68	-	7,02	-	0,87	-	5,68
Plagiothecium cavifolium (Brid.) Iwats.	0,27	-	-	-	-	-	-	1,08	0,13	-	-	-	-	-	-	0,58
Plagiothecium denticulatum (Hedw.) Bruch et al.	1,06	-	-	-	4,84	-	-	1,08	0,92	-	-	-	3,27	-	-	1,74
Plagiothecium sp.	0,27	-	-	-	-	-	2,44	-	0,53	-	-	-	-	-	3,90	-
Pohlia cruda (Hedw.) Lindb.	3,18	-	8,33	6,98	4,84	1,82	-	1,08	2,88	-	4,87	8,22	6,29	0,87	-	0,58
Pohlia wahlenbergii (Web. Et Mohr)	0,27	-	2,08	-	-	-	-	-	0,13	-	1,22	-	-	-	-	-
Ptilium crista-castrensis (Hedw.) De Not.	0,27	-	-	-	-	-	-	1,08	0,13	-	-	-	-	-	-	0,58
Rhizomnium punctatum (Hedw.) T.J.Kop.	0,80	5,71	-	-	-	-	2,44	-	0,53	4,46	-	-	-	-	0,98	-
Rhynchostegium arcticum (I.Hagen) Ignatov & Huttunen	1,06	-	2,08	-	-	-	-	3,23	0,53	-	1,22	-	-	-	-	1,74
Rhynchostegium murale (Hedw.) Bruch et al.	0,27	2,86	-	-	-	-	-	-	0,13	1,49	-	-	-	-	-	-
Rhytidiadelphus triquetrus (Hedw.) Warnst.	0,27	-	-	-	-	-	2,44	-	0,26	-	-	-	-	-	1,95	-
Sanionia uncinata (Hedw.) Loeske	1,59	-	-	2,33	-	7,27	2,44	-	1,73	-	-	1,00	-	7,14	3,90	-

Sciuro-hypnum curtum (Lindb.) Ignatov	2,65	-	8,33	-	1,61	-	-	5,38	2,19	-	9,98	-	0,82	-	-	4,35
Sciuro-hypnum populeum (Hedw.) Ignatov et Huttunen	0,53	-	-	-	1,61	1,82	-	-	0,39	-	-	-	0,82	1,74	-	-
Sciuro-hypnum reflexum (Starke) Ignatov & Huttunen	2,39	-	8,33	-	6,45	-	2,44	-	2,22	-	7,54	-	4,90	-	4,59	-
Serpoleskea confervoides (Brid.) Loeske	3,18	-	2,08	4,65	4,84	-	4,88	4,30	2,25	-	1,22	4,01	4,25	-	1,95	2,84
Stereodon vaucheri (Lesq.) Lindb. ex Broth.	0,53	2,86	-	-	1,61	-	-	-	0,39	1,49	-	-	1,63	-	-	-
Taxiphyllum wissgrillii (Garov.) Wijk & Margad.	0,53	-	-	-	-	3,64	-	-	0,53	-	-	-	-	3,48	-	-
Timmia bavarica Hessl.	8,75	8,57	8,33	9,30	8,06	9,09	12,20	7,53	16,20	18,45	15,21	18,05	17,57	14,63	16,59	14,56

V – Vintovaya, Z – Zigzag, K1 – Kutuk-1, K2 – Kutuk-2, K3 – Kutuk-3, K4 – Kutuk-4, KS – Kutuk-Sungan

Appendix 2. Percentage of reference similarity in the analyzed samples

Entrance morphology		Small sloping				Inclined icy descent		Shafts							
		Vintovaya		Zigzag		Kutuk-1		Kutuk-2		Kutuk-3		Kutuk-4		Kutuk-Sumgan	
				Jaccard											
		%	n**	%	n	%	n	%	n	%	n	%	n	%	n
Vintovaya		100\66*	3	0	12	0	15	0	15	13	15	0	15	0	21
Zigzag	PHI	0	12	100\100	6	0	20	80	20	45	20	10	20	54	28
Kutuk-1		0	15	0	20	70\70	10	36	25	12	25	16	25	20	35
Kutuk-2		0	15	65	20	24	25	70\80	10	12	25	8	25	34	35
Kutuk-3		0	15	25	20	0	25	16	25	100\80	10	12	25	43	35
Kutuk-4		7	15	5	20	8	25	8	25	12	25	40\50	10	11	35
Kutuk-Sumgan		0	21	32	28	0	35	17	35	17	35	29	35	62\48	21

*Jakkard/PHI-square, **n- number of combinations.

RESEARCH PAPER

SPATIAL VARIATION OF FEATURE DENSITY IN MULTISCALE TOPOGRAPHIC DATA

Timofey E. Samsonov[1*], Olga P. Yakimova[2], Daniil A. Potemkin[2] and Olga A. Guseva[3]

[1] Lomonosov Moscow State University, Faculty of Geography, Leninskiye Gory 1, 119234, Moscow, Russia

[2] Demidov Yaroslavl State University, Faculty of Mathematics, Souyznaya str. 144, 150008, Yaroslavl, Russia

[3] Demidov Yaroslavl State University, Faculty of Biology and Ecology, Matrosova lane 9, 150057, Yaroslavl, Russia

***Corresponding author:** tsamsonov@geogr.msu.ru

Received: August 17th, 2022 / Accepted: February 15th, 2023 / Published: March 31st, 2023

https://DOI-10.24057/2071-9388-2022-127

ABSTRACT. Digital topographic maps are created in a series of scales from large to small, and the underlying spatial data is commonly organized as a multiscale database consisting of several levels of detail (LoDs). Spatial density of features (or spatial objects) in such database varies both between LoDs (coarser levels are less densely populated with features) and within each LoD (feature density changes over the area). While the former type of density variation is caused by generalization, the latter one is mainly conditioned by geographic location and its properties, such as landscape complexity or fraction of urban areas. Since topographic database LoDs are derived using different data sources and generalization techniques, there is a need for a method that can help with automated evaluation of resulting feature density in terms of its appropriateness for the specified location and level of detail. This paper provides such method by uncovering dependencies between the location properties and the density of spatial data in multiscale topographic database. Changes in feature density are modeled as a function of spatial (landscape complexity and terrain ruggedness) and non-spatial (land cover types ratio) measures estimated via independent data sources. Resulting model predicts how much higher or lower is the expected spatial density of features over the area in comparison to the average density for the LoD. This information can be used further to assess the fitness of the data to the desired level of detail of the topographic map.

KEYWORDS: level of detail; topographic data; spatial databases; multiscale mapping

CITATION: Samsonov T. E., Yakimova O. P., Potemkin D. A. and Guseva O. A. (2023). Spatial variation of feature density in multiscale topographic data. Geography, Environment, Sustainability, 1(16), 86-102
https://DOI-10.24057/2071-9388-2022-127

ACKNOWLEDGEMENTS: The part of the study on vector features and land cover analysis was funded by Russian Foundation for Basic Research (RFBR) according to the research project 18-07-01459-a. The work of Timofey Samsonov on density of terrain features has been funded by Russian Science Foundation (RSF) grant No 19-77-00071.

Conflict of interests: The authors reported no potential conflict of interest.

INTRODUCTION

Spatial data for topographic mapping are commonly derived at multiple levels of detail (LoDs) which comprise a multiscale topographic database (Jones and Abraham 1986; Kilpeläinen 2000). Official standards for topographic map compilation are essentially definitions of level of detail which correspond to a specific map scale (Military Topographic Service 1978, 1980, 1985). The standards prescribe multiple rules for selection and generalization of features (spatial objects), as well as precision of their representation. Hence, LoD cannot be easily defined as one number such as scale, and definitions vary significantly. Meng and Forberg (2007) describe LoD as an arbitrary milestone in scale-space continuum which corresponds to a certain degree of generalization. Lemmens (2011) understands LoD as a combination of resolution and the amount of spatial, temporal and semantic detail. Ruas and Bianchin (2002) conceptualize LoD of a spatial database as a combination of the conceptual schema of the data, the semantic resolution, the geometric resolution, the geometric precision, and the granularity. In many cases an LoD can be effectively defined as a specific combination of elements which have a particular size or granularity. This approach is used in 3D city modeling (Kolbe, Gröger, and Plümer 2005; Biljecki, Ledoux, and Stoter 2016), where each level of detail is defined by a specific set of building elements. Samsonov (2022) identified the typical granularity of terrain features selected for small-scale cartographic relief presentation, which is 5-6 mm at mapping scale.

Since rules for LoD derivation can be quite sophisticated, the differences and inconsistencies in LoD can be inferred using the machine learning methods (Touya and Brando-Escobar 2013). In a pursuit of a universal and effective approach to LoD estimation raster analysis methods are developed as well. In particular, a detail resolution method by Cheng et al. (2017) is based on calculation of a rasterized line coalescence. The similar approach can be applied to describe the legibility of individual spatial features (Cheng, Liu, and Zhang 2021).

The notion of LoD can be also traced through the literature on cartographic generalization (or generalization of spatial data). In particular, formalized LoD-based representations are widespread in surface (especially TIN-

based) modeling where the precision of the resulting LoD is defined by simple metric criteria such as vertical error (de Floriani, Marzano, and Puppo 1996). The similar criteria usually expressed in terms of distances, areas or point densities are used in geometric simplification of lines (Douglas and Peucker 1973; Visvalingam and Whyatt 1993; Li and Openshaw 1992), polygons (Buchin et al. 2016; Haunert and Wolff 2010) or in point selection (Töpfer and Pillewizer 1966). Since the LoD is itself a complex notion, its reduction during generalization most probably should be expressed as a combination of multiple characteristics. Such approach was tested by Samsonov and Yakimova (2020), where the authors achieved a similar change in level of detail by joint alteration of Modified Hausdorff Distance and the number of line bends.

Despite a steady interest in the detail-related issues in geographical information science, such investigations remain quite rare. At the same time, one of the most critical requirements for spatial data used in analysis or mapping is the appropriate level of detail or degree of generalization. Heterogeneous natural conditions produce different spatial patterns, some of which can be characterized as a complex interplay of different land cover types and underlying surface (Phillips 1999). Specifically, mountainous areas are characterized by complex terrain, and therefore tend to require denser representation of relief (Imhof 1982). Economically developed, especially urban areas, are characterized by complex configuration of spatial elements (Batty 2013). Topographic maps respond to this by denser patterns of spatial features. From a cartographic point of view, the question arises how much this density should variate over the area, and is there any way to determine if the data underlying the topographic map is appropriate for the selected level of detail and location. To date, no formalized methods have been developed for this purpose. To bring the problem closer to solution we developed a new approach which considers the *relative feature density* – i.e., how much denser the features are over the selected area in relation to the average density for the whole LoD. This property is modeled as a function of location properties which are expressed in a number of spatial (landscape complexity and terrain ruggedness) and non-spatial (ratio between various land cover types) measures estimated via independent detailed data sources.

The rest of the paper is organized into five sections. In the Materials and Methods section, we introduce the notion of relative feature density and then conceptualize our approach to model it as a function of location properties. Experimental work subsection sheds the light on topographic and land cover data used for the case study, as well as their preprocessing needed to construct the desired model. In the Results section we demonstrate how our approach can be effectively used to improve the prediction of LoD based on feature density. Limitations of the approach are settled in the Discussion section. Finally, the main insights gained during the research are summarized in the Conclusion.

MATERIALS AND METHODS

General formulation

The aim of the developed method is to model the relationships that exist between the geographic location and density of features in topographic data. For the sake of brevity, we will use the term density to name the feature density, unless other type of density is explicitly defined. The flowchart of the method in general form is represented in Fig. 1.

We start from some abstract density measure d calculated for each training data fragment (Fig. 1a). Since the expected value of d varies with LoD over the same area, we divide it by the mean $\overline{d}$ for that LoD to obtain the relative density $\hat{d}$(Fig. 1b):

$$\hat{d} = d / \overline{d}$$

Relative density shows how much denser is the LoD fragment in relation to the average density over the whole LoD. Relative density is then modeled as a function of location properties:

$$g\left(\hat{d}_i\right) = \sum\nolimits_j \beta_{ij} f\left(l_j\right) + \varepsilon$$

where $\hat{d}_i$ is i-th relative density measure, l_j is the value of j-th location property, ε is a free term, g and f are linearizing transformation functions specific to the pair of $\hat{d}_i$ and l_j, and β_{ij} are the coefficients. *While building the model, we expect that spatial distribution of the relative density is similar for all LoDs.* Therefore, relative densities are merged into one sample (Fig. 1c) and then used in model fitting with location properties extracted for the same areas (Fig. 1d).

For any new topographic data fragment with known values of l_j the relative density $\hat{d}_i$ can be predicted as $\hat{d}_i = g^{-1}\left(\sum_j \beta_{ij}(l_j) + \varepsilon\right)$ (Fig. 1e). Let's assume that the model is $\ln\left(\hat{d}+1\right) = 0.74\ln\left(l_i+1\right) + 0.2$ and $l_1 = 2$ for the new data. Then the predicted feature density will be $\hat{d}_1 = e^{0.74\ln 3 + 0.2} - 1 \approx 1.753$ times higher at that location than $\overline{d}_1$ (the mean for whole LoD).

Having the actual density d_i for the new data fragment and its predicted relative value $\hat{d}_i$, we can obtain a *normalized density* (Fig. 1f):

$$\tilde{d}_1 = d_i / \hat{d}_i$$

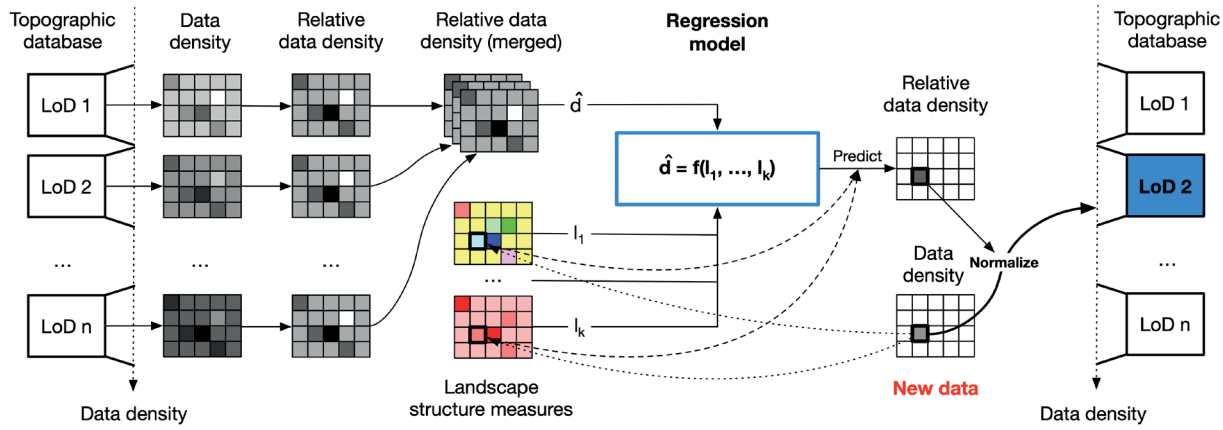

Fig. 1. The flowchart of the method

If the specific implementation of the model (2) is effective, then $\tilde{d}_i$ should be equal to the $\bar{d}_i$ of the desired LoD for well-prepared data. It is expected that for the real-world cases there will be some difference between these values. If the densities (or their transformed values) are distributed normally, then *Z*-score can be used to measure the difference in a statistical way:

$$z_i = \frac{\tilde{d}_i - \bar{d}_i}{s_i}$$

where s_i is a standard deviation of *i*-th density measure.

Finally, it is important not only to calculate the difference, but also to assess its ability to differentiate LoDs effectively. It is expected that for any fragment of k-th LoD its Z-score calculated against its own mean and standard deviation is smaller than a Z-score calculated against the mean and standard deviation of any other LoD (Fig. 1g):

$$\left|z_i^k\right| < \left|z_i^m\right|,\ m \neq k$$

This hypothesis is the main objective tested in the experimental part of our work.

Specific implementation

For this study points, lines and intersections were selected as features which densities are modeled. The corresponding density measures are calculated as follows:

• *Point density* (d_p). Each spatial data feature is converted to the point features. For linear and polygonal features their vertices are extracted. The total number of resulting points is divided by the area covered by the data.

• *Line density* (d_L). The total length of all linear features and the total perimeter of polygonal features are summed and then divided by the area covered by the data.

• *Intersection density* (d_I). An overlay of all linear features and borders of polygonal features is computed. Resulting geometry is set to be point geometry – it means that all intersections between linear and polygonal layers are derived. The number of intersections is divided by the area covered by the data.

While point and line density characterize the total abundance of spatial data that cover the area, intersection density encodes the complexity of topological relations between the features in the database: more intersections indicate more complex pattern of the features.

Location properties act as density predictors. Two groups of measures were considered for this purpose:

• *Non-spatial measures* describe general properties of location and do not account for the shape and spatial pattern of geographic objects that cover the area. Specifically, we use the ratios occupied by different land cover classes such as water, forest, urban and others.

• *Spatial measures* characterize the location through geometry and shape of geographic features that cover the area. For this we used the landscape complexity measures (joint entropy, contagion index, fractal dimension) and terrain ruggedness indices described below.

Joint entropy describes the overall complexity of the landscape pattern (Nowosad and Stepinski 2019):

$$joinet = -\sum_{i=1}^{K}\sum_{j=1}^{K} p_{ij}\log_2 p_{ij}$$

where p_{ij} is probability that *i*-th and *j*-th class are observed in neighboring raster cells, and *K* is the total number of land cover classes.

Contagion index is calculated in a similar way (Riitters et al. 1996):

$$contag = 1 + \frac{\sum_{i=1}^{K}\sum_{j=1}^{K} p_{ij}\ln p_{ij}}{2\ln K}\ \#$$

but accounts for the number of classes. *contag* describes the probability of two random cells belonging to the same class.

Perimeter-Area Fractal Dimension measures the complexity of landscape patches shape and is calculated as (Burrough 1981):

$$pacfac = \frac{2}{\beta}$$

where β is the slope of the regression of landscape patch area A_i against the patch perimeter P_i for all *n* patches in the landscape:

$$\sum_{i=1}^{n} \ln A_i = a + \beta \sum_{i=1}^{n} \ln P_i$$

The value of *pafrac=1* if patches are simple (squares, circles) and for irregular shapes with high fractal dimension.

Terrain ruggedness index is essentially a vertical distance between the central cell of a moving window and its surrounding cells calculated in a raster digital elevation model (Riley, De Gloria, and Elliot 1999):

$$tri = \sqrt{\sum_{i=-1}^{1}\sum_{j=-1}^{1}\left(z_{ij} - z_{00}\right)^2}$$

where z_{00} is a central cell of the floating window.

Data preparation

Experimental evaluation of the method was performed on multiscale topographic database with 3 levels of detail corresponding to 1:200 000, 1:500 000 and 1:1 000 000 mapping scales (referred further as 200, 500 and 1000 LoDs). The database represents layers of digital Russian topographic maps of the corresponding scales which were compiled by The Federal Service for State Registrations, Cadaster and Cartography (Rosreestr) using the generalization of larger-scale maps. Each LoD is represented in Esri geodatabase storage format and contains 47/47/40 layers for 200/500/1000 LoD respectively. The layers in each LoD are grouped into eight feature datasets inside each geodatabase: administrative (3/2/2 layers), economy (7/9/6 layers), geodesy (3/3/2 layers), hydrography (11/11/10 layers), relief (5/5/5 layers), settlements (6/5/4 layers), transport (6/6/6 layers) and vegetation/ground (6/6/5 layers). The number of layers slightly differ between LoDs because some types of objects are removed or added between scales.

33 sample fragments centered on settlements located in different geographic conditions were extracted from each level of detail, resulting in 99 data fragments in total. Each fragment was clipped by 100×100 km rectangle, and then projected into Lambert Azimuthal Equal Area Projection with corresponding center. This projection was selected because it allows each fragment to cover the similar area. The ratio between different land cover types is also correct, while other distortions are negligible within the extent of each fragment. The map of sample fragments' locations is represented in Fig. 2. Samples were divided into training and testing groups, which is explained later in the Experimental work section. The possible difference in feature density between fragments can be judged from Fig. 3. It can be clearly seen that highly urbanized Moscow fragment is characterized by significantly higher feature density at each LoD.

To describe the location, we used external data sources derived independently of topographic data, with better detail and generated without cartographic generalization. The main data source is Copernicus Global Land Cover (CGLC) (Buchhorn et al. 2020), which is a recent high-quality 100 m resolution global raster dataset obtained

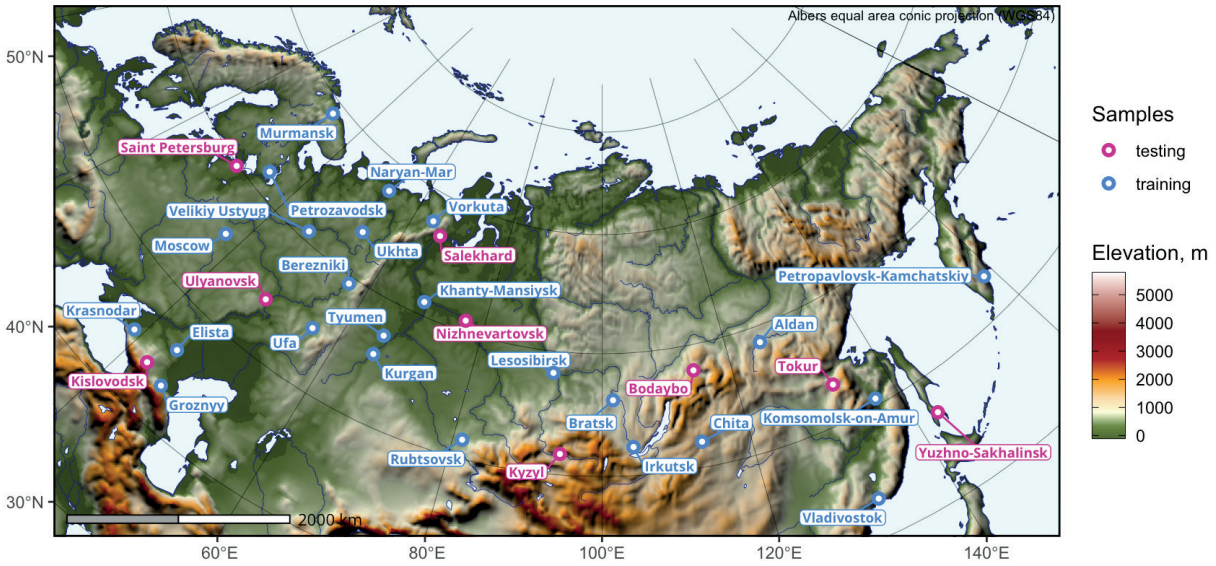

Fig. 2. Locations of sample fragments

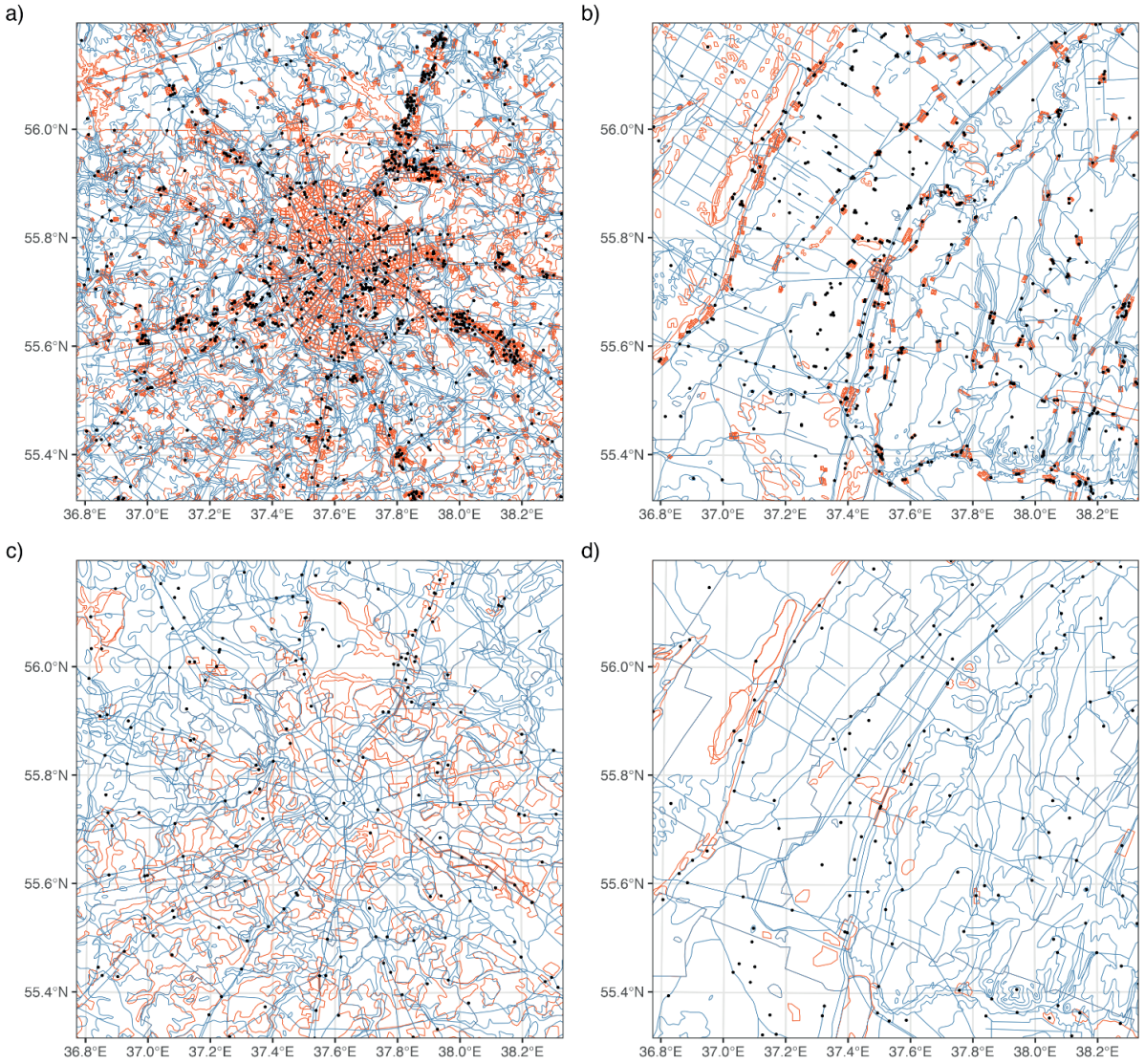

Fig. 3. Example renderings of 500 and 1000 database LoDs for two fragments: (a) Moscow, 500 LoD; (b) Rubtsovsk, 500 LoD, (c) Moscow, 1000 LoD; (d) Rubtsovsk, 1000 LoD. Point, linear and polygon features are shown by black, blue and red color correspondingly. Each fragment is 100 per 100 km. Lambert Azimuthal Equal Area Projection

by classification of satellite imagery. From this dataset 33 fragments were extracted which cover the same area and have the same projection as samples from the database. All land cover extracts are represented in Appendix Fig. A.1.–A.3. with colors according to the official CGLC legend in Appendix Table A.1. which includes 23 classes. These figures illustrate the variety of landscapes selected for the case study, which corresponds to initial selection of fragments. In particular, there are fragments with few (e.g. Aldan, Tokur) and large (e.g. Irkutsk, Tyumen, Saint Petersburg) number of land cover classes. The fragments can also be characterized by small (e.g. Komsomolsk-on-

Amur, Naryan-Mar) or large (e.g. Elista, Rubtsovsk) size of land cover patches. There is also a clear distinction between mostly natural (e.g. Lesosibirsk, Ukhta) and urban/agricultural (e.g. Ufa, Ulyanovsk) landscapes.

Before calculating the location property measures CGLC data was reclassified to a smaller number of classes. This preprocessing step was performed to avoid redundancy in the data in cases where land cover is significantly more detailed than topographic in terms of classes. In particular, all closed forest classes (111–116) and open forest classes (121–126) were merged in just two classes: *cforest* (closed forest) and *oforest* (open forest), which corresponds to differentiation applied in topographic databases under the study. Similarly, open sea (20) and permanent water bodies (80) were merged into one *water class*. Additionally, no input (0), bare (60), snow (70) and moss (100) classes were excluded from the case study, since they occupy a negligible area on most of the fragments. Resulting 8-class land cover classification in addition to open forest, closed forest and water, included the initial classes *shrubs* (20), *grass* (30), *crops* (40), *urban* (50), and *wetland* (90).

To estimate terrain ruggedness, we used GMTED_2010 global raster digital elevation model with resolution 7.5 arc seconds (approximately 140 m on 50°N latitude).

Since 100 m land cover does not adequately reproduce linear objects, we additionally used independent data on drainage and road density. Drainage network data was obtained from newest MERIT Hydro-Vector database (Lin et al. 2021) which was derived globally at 3 arc second resolution (approximately 60 m on 50°N latitude). Thus, land cover, terrain and drainage density data sources have ~100 m spatial resolution. Additionally, road density was averaged from GRIP database Meijer et al. (2018) with 5 arc minute resolution (approximately 6 km on 50°N latitude), which was refined using the official Russian road length statistics for municipalities (Russian Federal State Statistics Service 2021).

Experimental work

For modeling purposes 24 fragments (73% of total number) were used as training subset, and 9 fragments (27% of total number) were used as test subset, which is close to the commonly accepted 70/30 ratio. These subsets were formed to have the comparable variety of landscape types in both of them.

For each sample fragment $d_{P'}$ d_L and d_I were calculated as variables to be modeled. For training subset, the mean value of each measure was calculated, and relative densities $\hat{d}_{P'}$ $\hat{d}_L$ and $\hat{d}_I$ were obtained by division of raw values on corresponding means.

Based on our CGLC reclassification, we calculated the ratio of each fragment's area occupied by each land cover class. *contag*, *pafrac* and *joinent* measures were calculated based on CGLC data. *tri* measure was calculated from GMTED2010 extracts. *roads* and *rivers* variables are the densities of road and drainage network correspondingly aggregated from GRIP and MERIT Hydro-Vector datasets for each database sample as a total length divided by fragment area (10 000 km^2).

Since the initial set of calculated predictors consists of 14 variables, we continued with principal component analysis (PCA) of their values aimed at reduction of dimensions to a smaller number. Before applying PCA the variables were log-transformed, centered at zero and scaled to unit variance. Log transformation was performed in a form $In\left(l_j+1\right)$, where l_j is the value of location property. The term +1 is used to exclude possibility of transforming $l_j=0$ into-∞.

After performing the PCA, we fitted the following model to each relative density measure:

$$In\left(\hat{d}_i+1\right)=\sum\nolimits_j \beta_{ij} PC_j+\varepsilon_i$$

Z-scores for all obtained results were calculated and assessed for their effectiveness in differentiating the results. Extraction and counting of database objects for density estimation was performed using MapAnalyzer QGIS plugin written in Python programming language (Yakimova et al. 2021). All remaining analytical calculations, including PCA, building the regression model and performing the statistical tests were programmed in *R* language, including the l*andscapemeterics R* package by Hesselbarth et al. (2019).

RESULTS

Raw density analysis

We begin our analysis of the training subset from visualization of probability density estimates for raw density variables (Fig. 4). Each variable in each scale has lognormal distribution, which is supplemented by all p-values of Shapiro-Wilk test for log-transformed variables being greater than 0.05. This allows us to apply Z-scores in further analysis.

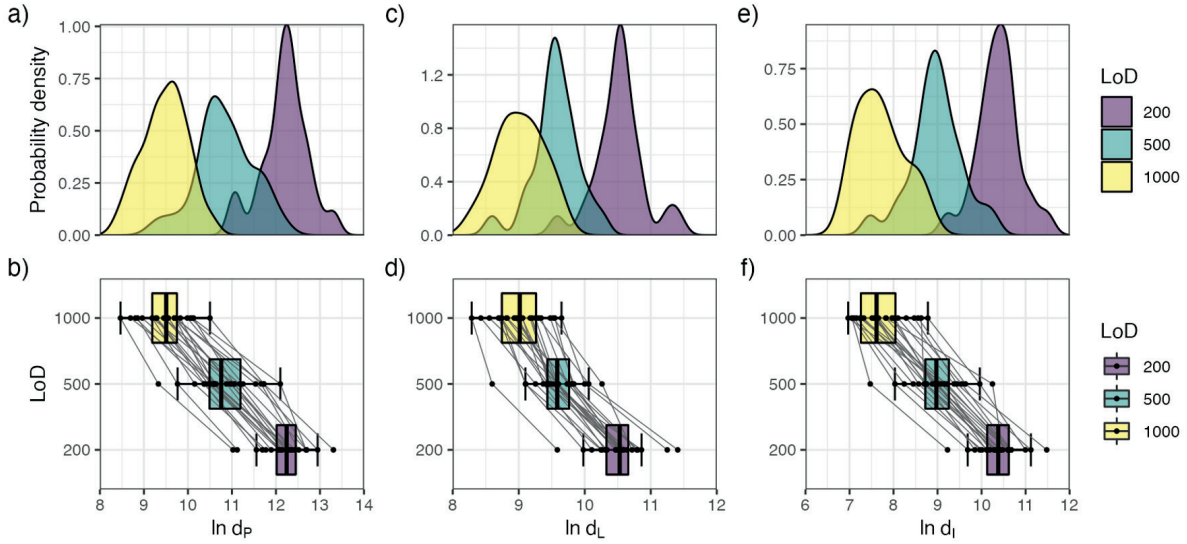

Fig. 4. Distributions of feature density across LoDs: (a-b) point density, (c-d) line density, (e-f) intersection density

As can be seen from lines connecting LoDs of each fragment in Fig. 4, raw densities decrease systematically when the level of detail is decreased correspondingly. This observation is also true for the median values across all fragments. However, distributions overlap significantly. To test whether each of the training fragments can be unmistakably attributed to its level of detail using the density measures, we calculate *Z*-scores and then compare them across all levels. We have the mean and standard deviation of *i*-th density measure at *j*-th level of detail $d_{ij} = d_i(L_j)$. Then for each combination $d_{ikm} = d_i(L_k, F_m)$ of *i*-th density measure calculated at *k*-th level of detail and *m*-th fragment ($3_i x 3_k x 24_m = 216$ combinations in total) *Z*-scores are derived against distribution of each d_{ij}. Expectation is that absolute value of *Z*-score should be minimal when *k=j*, i.e., when *Z*-score of a density measure value is calculated against the mean and standard deviation of its own LoD. If this is true, then raw density measures can be used to assess the suitability of the data fragment for inclusion into the LoD.

Results of *Z*-scores calculation are presented in Fig. 5a, where the rows correspond to d_{km} and the columns correspond to d_{ij}. All values are grouped in *3x3* matrices which correpond to one group of calculations. *Z*-scores for density measures against their own distributions are located on the antidiagonal of each matrix. Therefore, if results meet expectations, these scores should have smallest absolute values in each row of the matrix (colored with blue color).

Fig. 5. Z-scores for density characteristics (training fragments): (a) feature density; (b) normalized feature density. Each row is a unique combination of fragment and level of detail. Each column is a unique combination of feature density measure and level of detail

Fig. 5a indicates that for fragments out of there are cases where expectation is not realized. In particular, for 17% of all d_{ikm} combinations (37 out of 216) the smallest absolute value of Z-score is obtained against another LoD. It means that each 6-th fragment is statistically closer to another LoD in terms of feature density due to it being significantly lower or greater than the mean for its own LoD. For example, Rubtsovsk is located in plain and dry mostly homogeneous sparsely populated landscape, and its database LoDs 200 and 500 are more similar in terms of feature density to the average LoD fragment of 500 and 1000 LoD correspondingly.

Such significant variability in feature density poses a question, whether it is determined by the properties of its geographic location and can be predicted. To answer this question, we apply the method presented in the current paper.

Principle component analysis

PCA results of the derived models are summarized in Fig. 6, Fig. 7, and Fig. 8. According to Fig. 6 the first two PCs explain 53.3% of the total variance, while most of the variance (96%) is explained by the first eight PCs, which were selected for further analysis.

The quality of each PC and variable contributions can be assessed from Fig. 7. In particular, PC1 is formed mainly by *joinent* and *contag* landscape metrics, as well as both types of *forest*, which most probably describes a variability in forest patterns. PC2 is dominated by *pafrac, shrubs, crops* and *roads*. PC3 is formed by *tri, cforest, grass* and *wetland* predictors. PC4 is strongly contributed by *rivers* and *tri*. PC5 is dominated by *tri, grass* and *water*, while PC6 is formed mainly by *pafrac, contag* and *water* variables. PC7 is comprised mainly by *oforest, urban, crops, roads* and *rivers* predictors. Finally, PC8 has significant contributions from *pafrac, contag, tri, shrubs, wetland, crops, roads* and *rivers*. Every variable contributed significantly to at least one PC, while most of them contribute significantly to 2-3 PCs.

It is notable that, despite the expectation, the fraction of urban areas does not contribute as significant as other location properties to any specific PC. However, it is the only location property which contributes equally to the most important PCs 1-2, which results in significant contribution overall analyzed further.

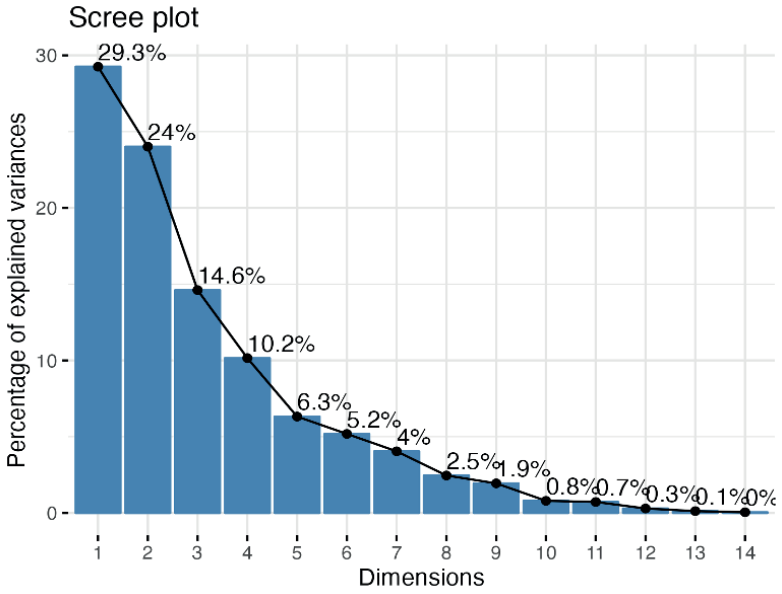

Fig. 6. Fraction of total variance explained by each principal component (scree plot)

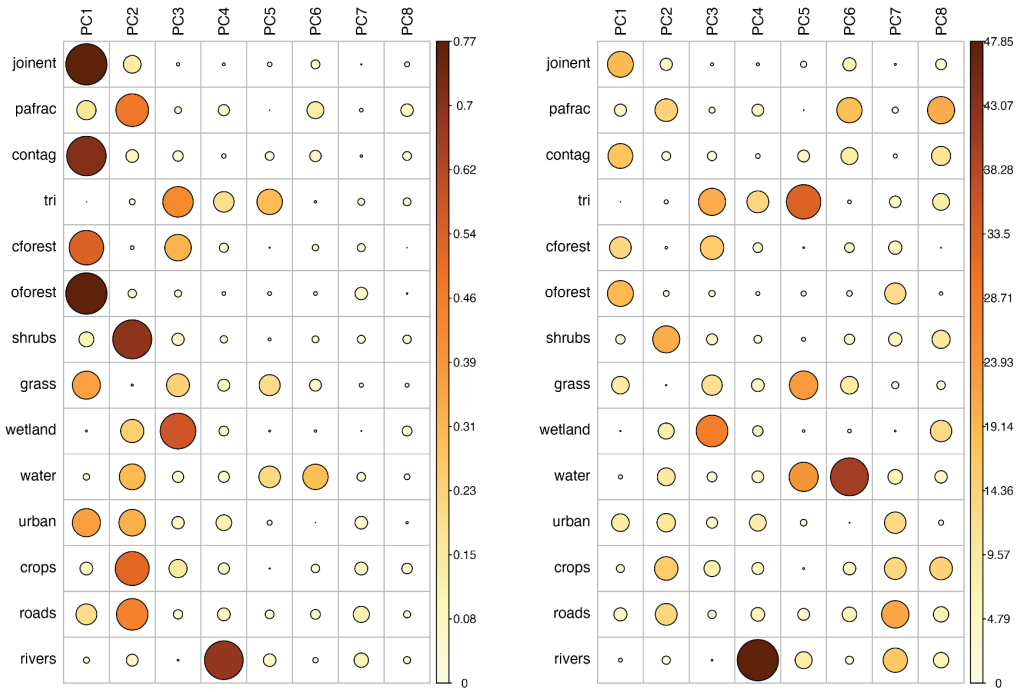

Fig. 7. Principal component analysis summary: (left) quality of representation, *cos*²; (right) variable contributions

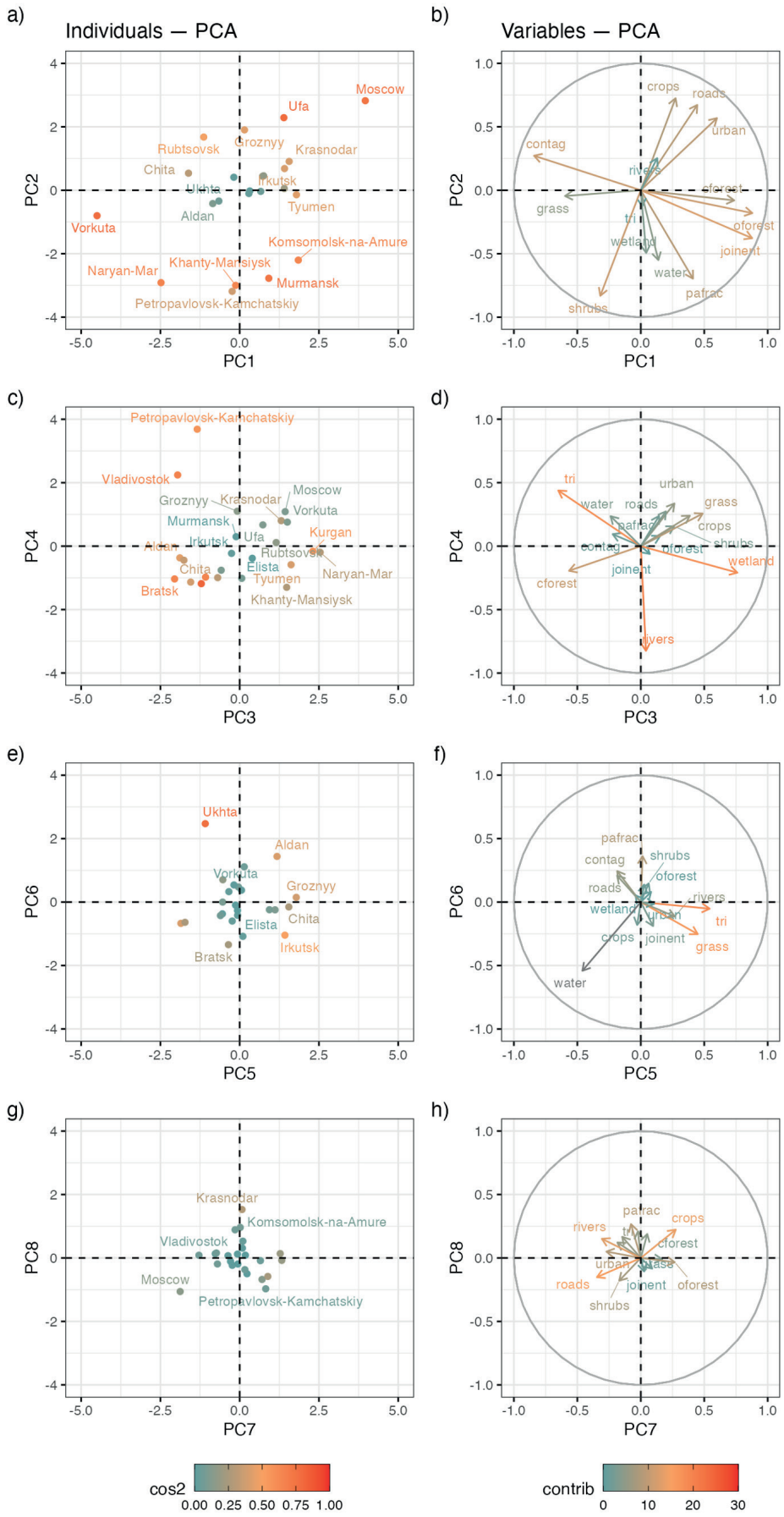

Fig. 8. Principal component analysis details: (a,c,e,g) graph of individuals; (b,d,f,h) graph of variables

Fig. 8 exposes the details of PCA in terms of how the fragments and variable contributions are distributed along first eight PC dimensions. From Fig. 8a we see clearly that the PCs 1–2 differentiate urban/agricultural areas (upper right quarter) and mostly natural ones with lots of forest (lower left quarter). Fig. 8b reveals that fragments are arranged from mountains (left part) to planes (right part) and from less (upper part) to more (lower part) developed river network by PCs 3–4. On Fig. 8c we see mainly differentiation on the ratio of large water bodies by PCs

5-6 with near-water fragments located in lower left quarter of the plot. Finally, the contribution of PCs 7-8 on Fig. 8d on fragment differentiation is less distinct. The graphs of variables represented in Fig. 8b,d,f,h supplement our conclusions with contribution vectors of each PC.

Normalized feature density

The summary of the model for each relative density measure is presented in Table 1. As we see, PCs 1-5 and 7 contribute significantly to regression on $\widehat{d}_P$ and $\widehat{d}_{L'}$ while only PCs 1, 4 and 7 exhibit significant influence on $\widehat{d}_I$. PCs 6 and 8 have neglegible effect on the result in all regressions. These relations between principal components and modeled relative density measures can be assessed visually from Fig. 9 and Fig. 10. In particular, trend lines for PCs 6 and 8 have less explicit slope, which indicates a weak correlation with relative features density.

The derived regression model allows calculation of normalized densities $\tilde{d}_i = d_i / \widehat{d}_{i'}$ which account for landscape heterogeneity and reduce densities to their expected values for corresponding LoD. Distributions of normalized densities can be assessed from Fig. 11. Comparing to raw densities in Fig. 4 it can be seen that normalized distributions have higher kurtosis and intersect less than for raw densities, which means that they their populations can potentially be separated more easily based on Z-scores.

To check this hypothesis, we calculated Z-scores of normalized values against the mean and standard deviation of raw values. Results are presented in Fig. 5b. Now only for 4.6% of all d_{ikm} (10 out of 216) the smallest absolute value

Table 1. Summary of relative feature density regression models

PC***	Points ($\ln\widehat{d}_P$)			Lines ($\ln\widehat{d}_L$)			Intersections ($\ln\widehat{d}_I$)		
	Beta	95% CI**	*p-value	Beta	95% CI	p-value	Beta	95% CI	p-value
Intercept	0.66	0.63, 0.70	•••	0.67	0.64, 0.69	•••	0.66	0.62, 0.71	•••
PC1	0.02	0.00, 0.04	•	0.02	0.01, 0.03	••	0.04	0.02, 0.06	•••
PC2	–0.08	–0.10, –0.06	•••	–0.04	–0.05, –0.02	•••	–0.02	–0.05, 0.00	°
PC3	–0.04	–0.06, –0.01	••	–0.03	–0.05, –0.02	•••	0.01	–0.02, 0.05	°
PC4	0.08	0.05, 0.11	•••	0.04	0.02, 0.06	•••	0.09	0.06, 0.13	•••
PC5	0.05	0.02, 0.09	••	0.07	0.05, 0.10	•••	0.03	–0.02, 0.08	°
PC6	0.01	–0.04, 0.05	°	0.01	–0.02, 0.04	°	0.04	–0.02, 0.09	°
PC7	–0.13	–0.18, –0.08	•••	–0.07	–0.10, –0.03	•••	–0.13	–0.19, –0.06	•••
PC8	0.00	–0.06, 0.06	°	–0.02	–0.07, 0.02	°	–0.01	–0.09, 0.07	°

* p-values: ••• < 0.001, •• < 0.01, • < 0.05, ° ≥ 0.05
** CI – confidence interval, *** PC – principal component

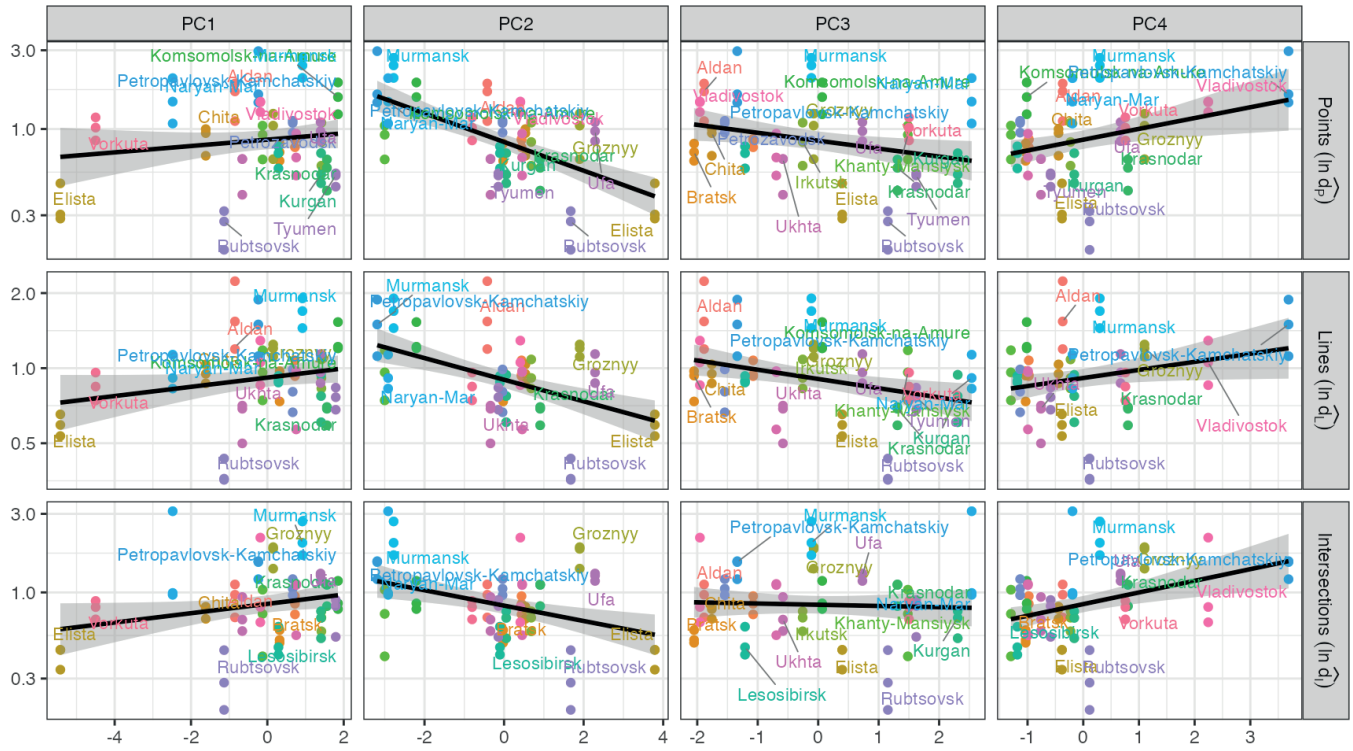

Fig. 9. Relationships of relative feature density with principal components 1-4

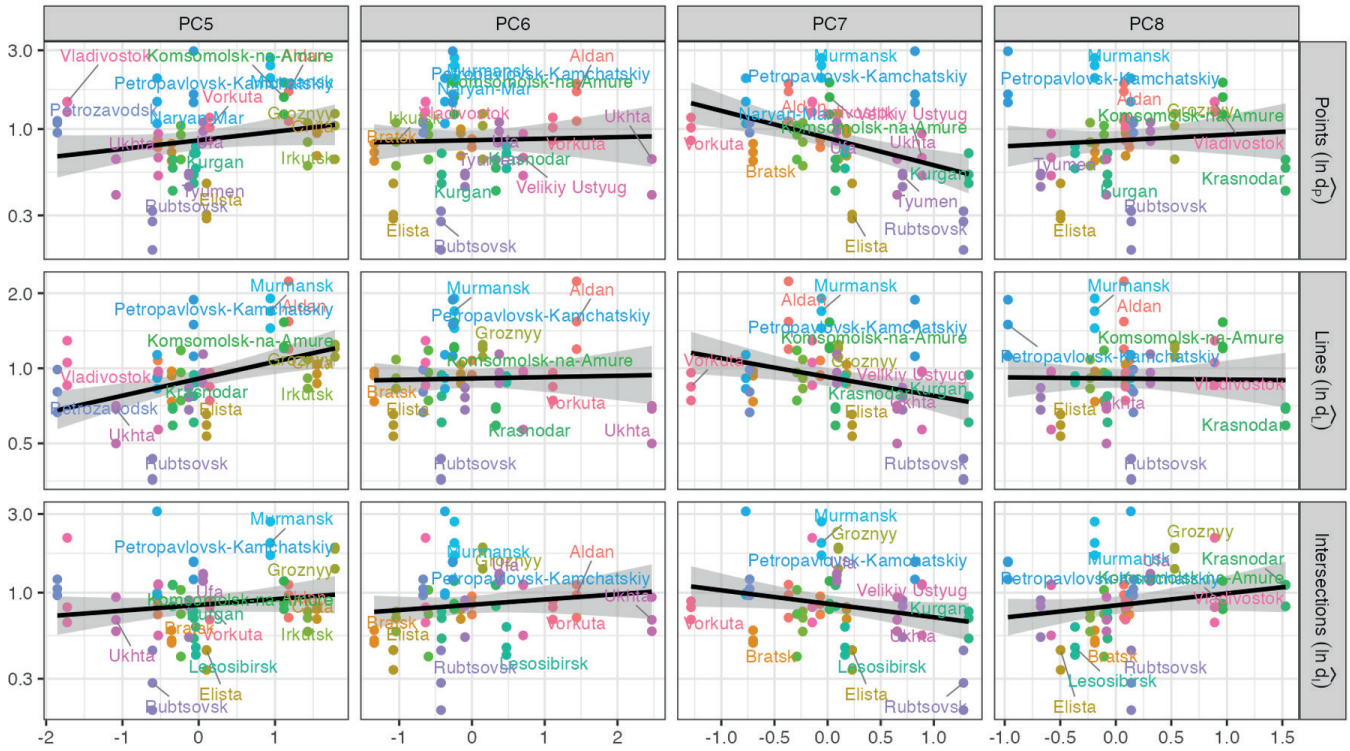

Fig. 10. Relationships of relative feature density with principal components 5-8

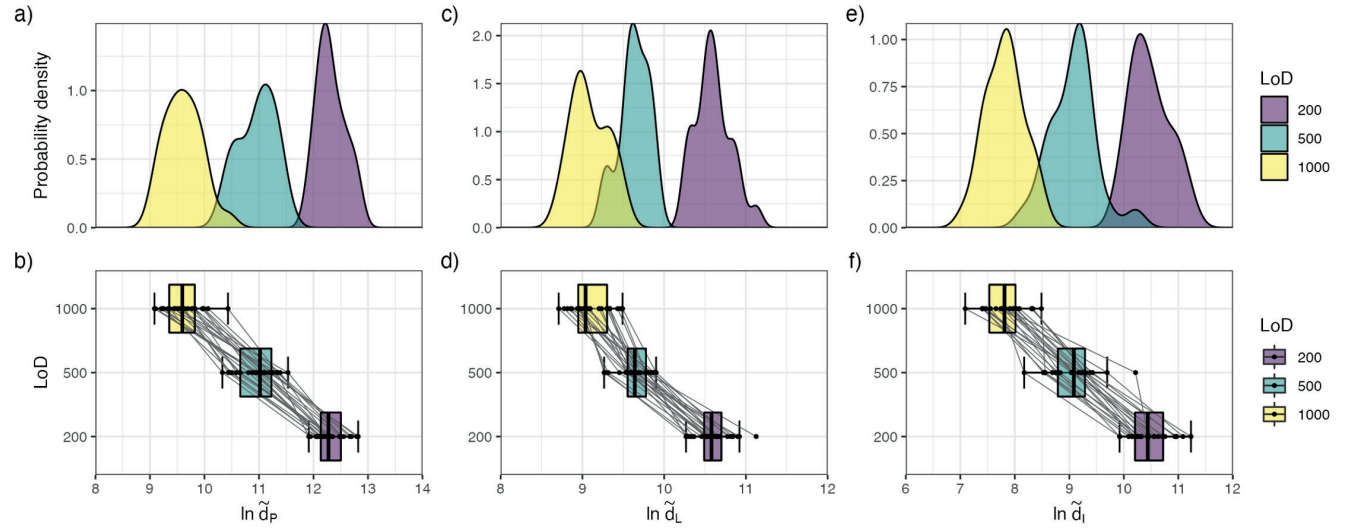

Fig. 11. Distributions of normalized feature density across scales: (a-b) point density; (c-d) line density; (e-f) intersection density

of Z-score is obtained against another LoD. This result means that the error of identifying the most appropriate LoD is significantly reduced after processing with our method, and approximately 95% of training dataset can be recognized correctly.

The robustness of the developed approach was assessed by using the derived PCA transform and regression model to predict relative density for 9 testing fragments ($3_i x 3_k x 9_m = 81$ combinations in total). As can be seen from Fig. 12, our approach improves the error of LoD recognition from 12.3% (10 out of 81) to 2.5% (2 out of 81), which is a significant gain in precision. As in the case of the training dataset, more than 95% of the total samples were related to the true LoD after density normalization.

DISCUSSION

The developed model has several potential applications. First, if a topographic data misses metadata about its level of detail or the most appropriate scale of visualization, the model can be used to predict the most proper level of detail of the data. Second, it can be used as a preliminary means of judging if two topographic databases covering different areas have similar level of detail and can be essentially merged into one database. Third, it is useful to evaluate the results of collaborative generalization during which multiple areas are generalized using different algorithms (Touya, Duchêne, and Ruas 2010). A ratio between feature densities which naturally reflects the difference in landscape structures, is an indicator of good generalization. It must be stressed, however, that all these potential applications need practical assessment of their effectiveness.

There are several limitations of the presented results which need to be overcome in future improvements. The current study is based on the experimental sample which now consists of 33 database fragments. The modest sample size and the fact that fragments do not cover all possible varieties of landscapes may potentially limit the effectiveness of the derived PCs and regression model. In

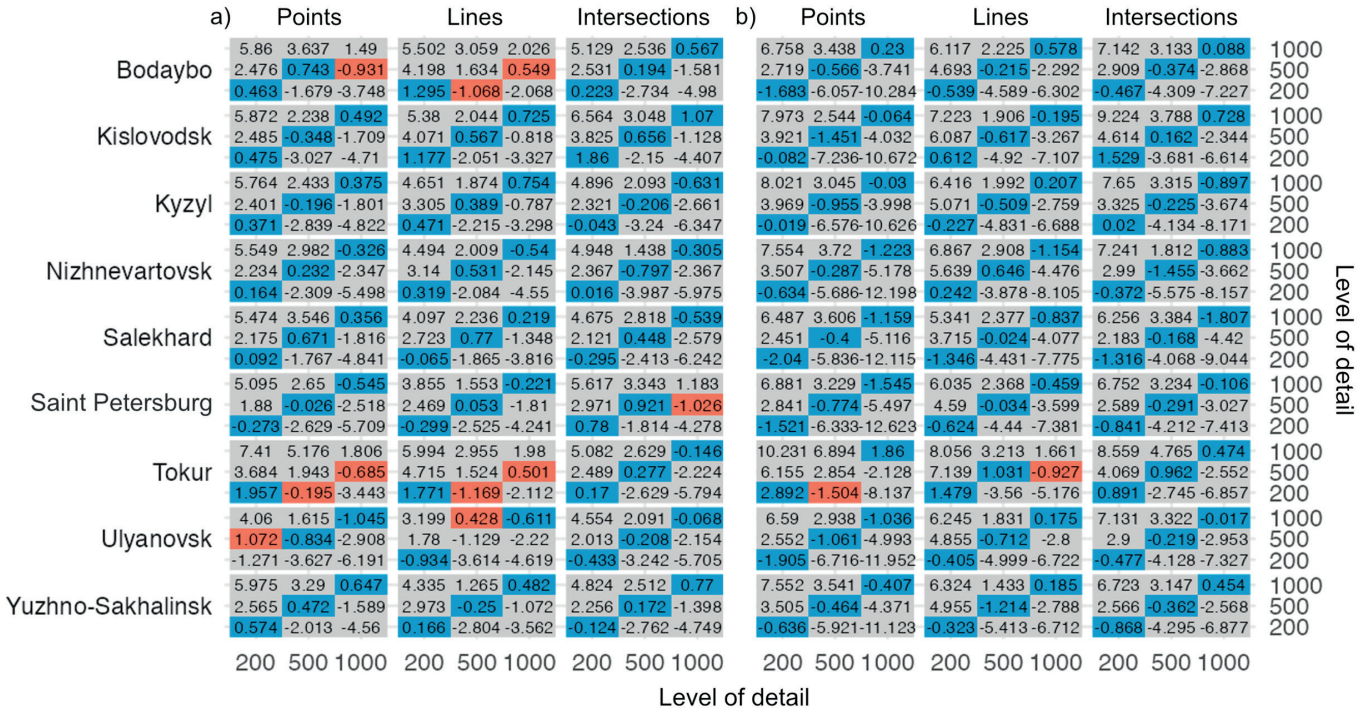

Fig. 12. Z-scores for density characteristics (testing fragments): (a) feature density; (b) normalized feature density. Each row is a unique combination of fragment and level of detail. Each column is a unique combination of feature density measure and level of detail

particular, expected (mean) value of each density measure will change if the sample is extended to include additional fragments. A reasonable way to improve the current result is to subdivide the total area covered by a spatial database product by the grid of similar fragments, and perform model construction and testing based on the total amount of fragments. Since the area of Russia is approximately $1.7 \times 10^7 km^2$, and the area of each fragment is $10^4 km^2$, this will result in approximately 1700 fragments. This amount can be increased multiple times by extracting smaller portions of data (i.e. 50x50 km). Such a large population can be randomly sampled to construct more reliable model for relative feature density. However, this experiment will be substantially more demanding in terms of computing time.

Additional shortcoming is that current study is tied to specific spatial data product and to only three levels of detail. Since each product and LoD is derived using a specific data selection and generalization rules, the effectiveness of the model should be assessed before its application. The same issue is true for specific data sources used for prediction. In particular, these data sources are not suitable for density assessment of detailed (large scale) spatial data due to their resolution. Also, each of the data sources has its own errors and limited precision, which inevitably affects the quality of results. However, assessment of error propagation is out of the scope of the current paper.

A more convoluted problem is hidden in the assumption that the relative feature density is similar for each fragment independent from LoD. However, as we've seen in the paper, the database fragment which is 2 times denser than the average in one LoD, can be less different from the average in another LoD. We cannot integrate such information directly in our model, since LoD is unknown in our case. In addition, it should be stressed that only density-based characteristics of LoD are considered in the current study. Surely, other LoD descriptors such as feature granularity must be investigated in a similar way.

Finally, more sophisticated methods of model building for LoD recognition such as deep learning (DL) can be used instead of a simple linear regression with PCA. This may potentially improve the reliability and robustness of the derived model. Application of DL is impractical on current sample, but can be feasible if thousands of data extracts comprise the sample.

CONCLUSIONS

Digital topographic maps are commonly represented as multiscale spatial databases with several levels of detail (LoDs) corresponding to map scales. A sequence of LoDs covering the same area is characterized by monotonous change of the detail properties such as granularity and density of features (spatial objects): the smaller is the desired map scale, the less detailed is the LoD. However, the properties of one LoD may differ significantly between locations. For example, elevation contours in a rugged terrain are naturally more complex than over the gently sloped areas. The spatially varying shape of individual objects and terrain surface as well as their arrangement in specific patterns results in heterogeneity of each LoD. Hence, the measures which describe the level of detail may vary significantly. This complicates the integration of topographic data fragments covering different areas into one database. There is a need for an automated method that will help to assess feature density of the fragments and their correspondence to the desired level of detail.

In this paper we approached this problem by statistical learning from multiscale topographic database constructed through manual generalization. For each of the three LoDs we analyze how much the density of points, lines and intersections in each fragment is higher or lower than the average LoD density. This ratio, called relative density, is then modeled as a function of location properties expressed in a number of spatial and non-spatial measures. Principal components derived from measures showed significant contributions both from landscape complexity measures, and from ratios of different land cover classes. Urban and natural, mountainous and flat, with less and more developed river network areas were effectively differentiated. Results showed that normalization of raw feature density on its predicted relative value provides the

measure close to the mean value of the desired LoD. Using normalized values, the error of LoD recognition is reduced several times. This proves the hypothesis that location properties can be used as effective predictors of relative feature density in topographic data.

Results obtained in this paper can be used in spatial data integration and generalization workflows which involve spatial partitions – either in collaborative generalization or merging the data obtained independently for different areas. A more representative and large data sample and different machine learning methods can be used in future investigations to improve the predictive power of the proposed approach.

REFERENCES

Biljecki F., Ledoux H., and Stoter J. (2016). An Improved LOD Specification for 3d Building Models. Computers, Environment and Urban Systems, 59, 25–37, DOI: 10.1016/j.compenvurbsys.2016.04.005.

Buchhorn M., Lesiv M., Tsendbazar N.-E., Herold M., Bertels L., and Smets B. (2020). Copernicus Global Land Cover Layers Collection 2. Remote Sensing, 12 (6), 1044, DOI: 10.3390/rs12061044.

Buchin K., Meulemans W., Van Renssen A., and Speckmann B. (2016). Area-Preserving Simplification and Schematization of Polygonal Subdivisions. ACM Transactions on Spatial Algorithms and Systems, 2(1), 1-36, DOI: 10.1145/2818373.

Burrough P.A. (1981). Fractal Dimensions of Landscapes and Other Environmental Data. Nature, 294 (5838), 240-42, DOI: 10.1038/294240a0.

Cheng X., Liu Z., and Zhang Q. (2021). MSLF: Multi-Scale Legibility Function to Estimate the Legible Scale of Individual Line Features. Cartography and Geographic Information Science, 48(2), 151-68, DOI: 10.1080/15230406.2020.1857307.

Cheng X., Wu H., Ai T., and Yang M. (2017). Detail Resolution: A New Model to Describe Level of Detail Information of Vector Line Data. In Advances in Geographic Information Science, edited by Chenghu Zhou, Fenzhen Su, Francis Harvey, and Jun Xu, Singapore: Springer Singapore, 167-77, DOI: 10.1007/978-981-10-4424-3_12.

De Floriani L., Marzano M., and Puppo E. (1996). Multiresolution Models for Topographic Surface Description. The Visual Computer, 12 (7), 317-45, DOI: 10.1007/s003710050068.

Douglas D.H. and Peucker T.K. (1973). Algorithms for the Reduction of the Number of Points Required to Represent a Digitized Line or Its Caricature. The Canadian Cartographer, 10(2), 112-22, DOI: 10.3138/FM57-6770-U75U-7727.

Haunert J.-H. and Wolff A. (2010). Area Aggregation in Map Generalisation by Mixed-Integer Programming. International Journal of Geographical Information Science, 24(12), 1871-97, DOI: 10.1080/13658810903401008.

Hesselbarth M. H. K., Sciaini M., With K.A., Wiegand K, and Nowosad J. (2019). Landscapemetrics : An Open-Source R Tool to Calculate Landscape Metrics. Ecography, 42 (10), 1648-57, DOI: 10.1111/ecog.04617.

Imhof E. (1982). Cartographic Relief Presentation, Berlin: Walter der Gruyter, 416.

Jones C.B. and Abraham I.M. (1986). Design Considerations for a Scale-Independent Database. In Proceedings of Second International Symposium on Spatial Data Handling, Seattle, 384-98.

Kilpeläinen T. (2000). Maintenance of Multiple Representation Databases for Topographic Data. The Cartographic Journal, 37(2), 101-7, DOI: 10.1179/0008704.37.2.p101.

Kolbe T.H., Gröger G., and Plümer L. (2005). CityGML: Interoperable Access to 3d City Models. In: Geo-Information for Disaster Management, edited by Peter van Oosterom, Siyka Zlatanova, and Elfriede M. Fendel, Berlin, Heidelberg: Springer Berlin Heidelberg, 883-99, DOI: 10.1007/3-540-27468-5_63.

Lemmens M. (2011). Quality of Geo-Information. In: Geo-Information, Dordrecht: Springer Netherlands, 211-27, DOI: 10.1007/978-94-007-1667-4_11.

Li Z. and Openshaw S. (1992). Algorithms for Automated Line Generalization Based on a Natural Principle of Objective Generalization. International Journal of Geographical Information Systems, 6(5), 373-89, DOI: 10.1080/02693799208901921.

Lin P., Pan M., Wood E. F., Yamazaki D., and Allen G. H. (2021). A New Vector-Based Global River Network Dataset Accounting for Variable Drainage Density. Scientific Data, 8(1), 28, DOI: 10.1038/s41597-021-00819-9.

Meijer J.R., Huijbregts M.A.J., Schotten K.C.G.J., and Schipper A.M. (2018). Global Patterns of Current and Future Road Infrastructure. Environmental Research Letters, 13(6), 064006, DOI: 10.1088/1748-9326/aabd42.

Meng L. and Forberg A. (2007). 3D Building Generalisation. In: Generalisation of Geographic Information: Cartographic Modelling and Applications, Elsevier, 211-31, DOI: 10.1016/B978-008045374-3/50013-2.

Military Topographic Service. (1978). Guide to cartographic and cartographic works. Part 1. Drafting and preparation for publication of 1:25 000, 1:50 000, and 1:100 000 scale topographic maps [in Russian]. Moscow: Editorial; Publishing Department of Military Topographic Service.

Military Topographic Service. (1980). Guide to cartographic and cartographic works. Part 2. Drafting and preparation for publication of 1:200 000 and 1:500 000 topographic maps [in Russian]. Moscow: Editorial; Publishing Department of Military Topographic Service.

Military Topographic Service. (1985). Guide to cartographic and cartographic works. Part 3. Drafting and preparation for publication of 1:1 000 000 scale topographic maps [in Russian]. Moscow: Editorial; Publishing Department of Military Topographic Service.

Nowosad J. and Stepinski T. F. (2019). Information Theory as a Consistent Framework for Quantification and Classification of Landscape Patterns. Landscape Ecology, 34(9), 2091-101, DOI: 10.1007/s10980-019-00830-x.

Phillips J. (1999) Earth surface systems : complexity, order and scale – Malden, Mass: Blackwell Publishers.

Riitters K.H., O'Neill R.V., Wickham J.D., and Jones K.B. (1996). A Note on Contagion Indices for Landscape Analysis. Landscape Ecology, 11(4), 197-202, DOI: 10.1007/BF02071810.

Riley S.J., De Gloria S.D., and Elliot R. (1999). A Terrain Ruggedness That Quantifies Topographic Heterogeneity. Intermountain Journal of Science, 5 (1-4), 23-27.

Ruas A., and Bianchin A. (2002). Echelle Et Niveau de Detail. In: Generalisation et Representation Miltiple, edited by Anne Ruas, Paris: Hermes Lavoisier, 25-44.

Russian Federal State Statistics Service. (2022). Database of Municipal Indicators. Available at: https://www.gks.ru/free_doc/new_site/bd_munst/munst.htm. [Accessed 10 June 2022].

Samsonov T. (2022). Granularity of Digital Elevation Model and Optimal Level of Detail in Small-Scale Cartographic Relief Presentation. Remote Sensing, 14(5), 1270, DOI: 10.3390/rs14051270.

Samsonov T. and Yakimova O. (2020). Regression Modeling of Reduction in Spatial Accuracy and Detail for Multiple Geometric Line Simplification Procedures. International Journal of Cartography, 6(1), 47-70, DOI: 10.1080/23729333.2019.1615745.

Töpfer F. and Pillewizer W. (1966). The Principles of Selection. The Cartographic Journal, 3(1), 10-16, DOI: 10.1179/caj.1966.3.1.10.

Touya G. and Brando-Escobar C. (2013). Detecting Level-of-Detail Inconsistencies in Volunteered Geographic Information Data Sets. Cartographica: The International Journal for Geographic Information and Geovisualization, 48(2), 134-43, DOI: 10.3138/carto.48.2.1836.

Touya G., Duchêne C., and Ruas A.. (2010). Collaborative Generalisation: Formalisation of Generalisation Knowledge to Orchestrate Different Cartographic Generalisation Processes. In: Theories and Methods of Spatio-Temporal Reasoning in Geographic Space, Berlin, Heidelberg: Springer Berlin Heidelberg, 264-78, DOI: 10.1007/978-3-642-15300-6_19.

Visvalingam M. and Whyatt J.D. (1993). Line Generalisation by Repeated Elimination of Points. The Cartographic Journal, 30(1), 46-51, DOI: 10.1179/caj.1993.30.1.46.

Yakimova O., Samsonov T., Potemkin D., Usmanova E. (2021). QGIS processing tool for spatial data detail assessment. InterCarto. InterGIS, 27(2), 260-279, DOI: 10.35595/2414-9179-2021-2-27-268-279.

Appendix

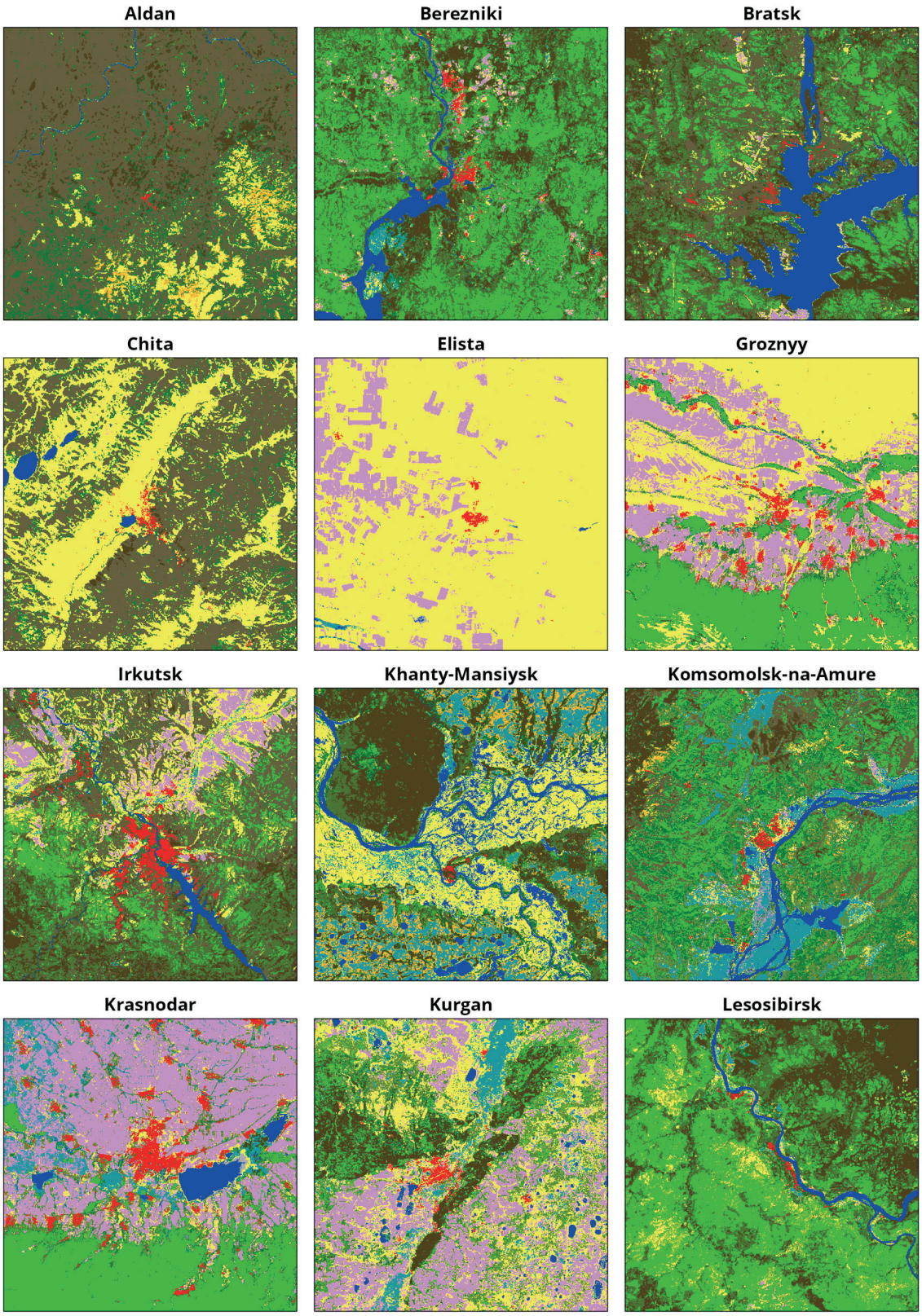

Fig. A.1. Land cover extracts for training fragments 1-12

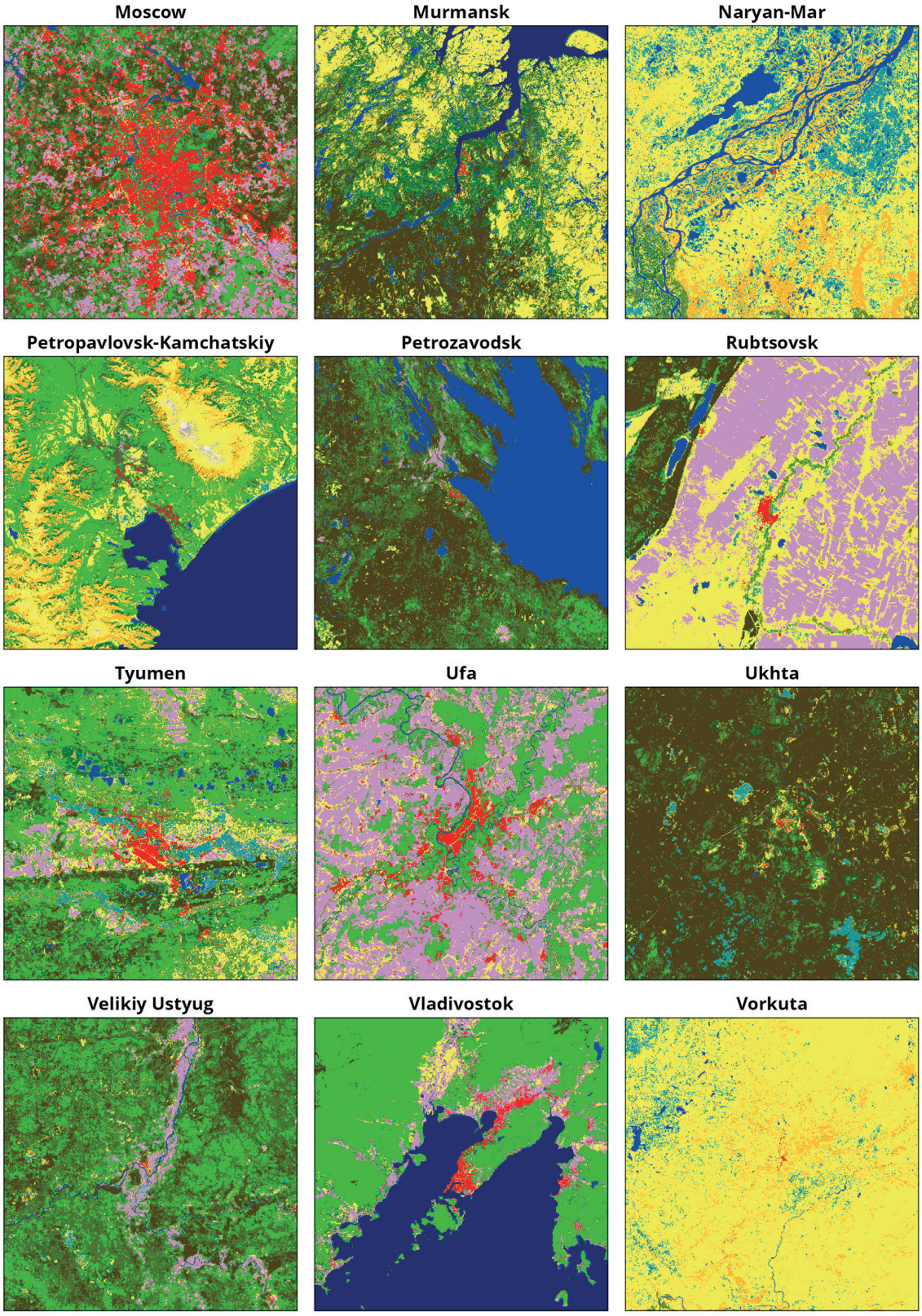

Fig. A.2. Land cover extracts for training fragments 13-24

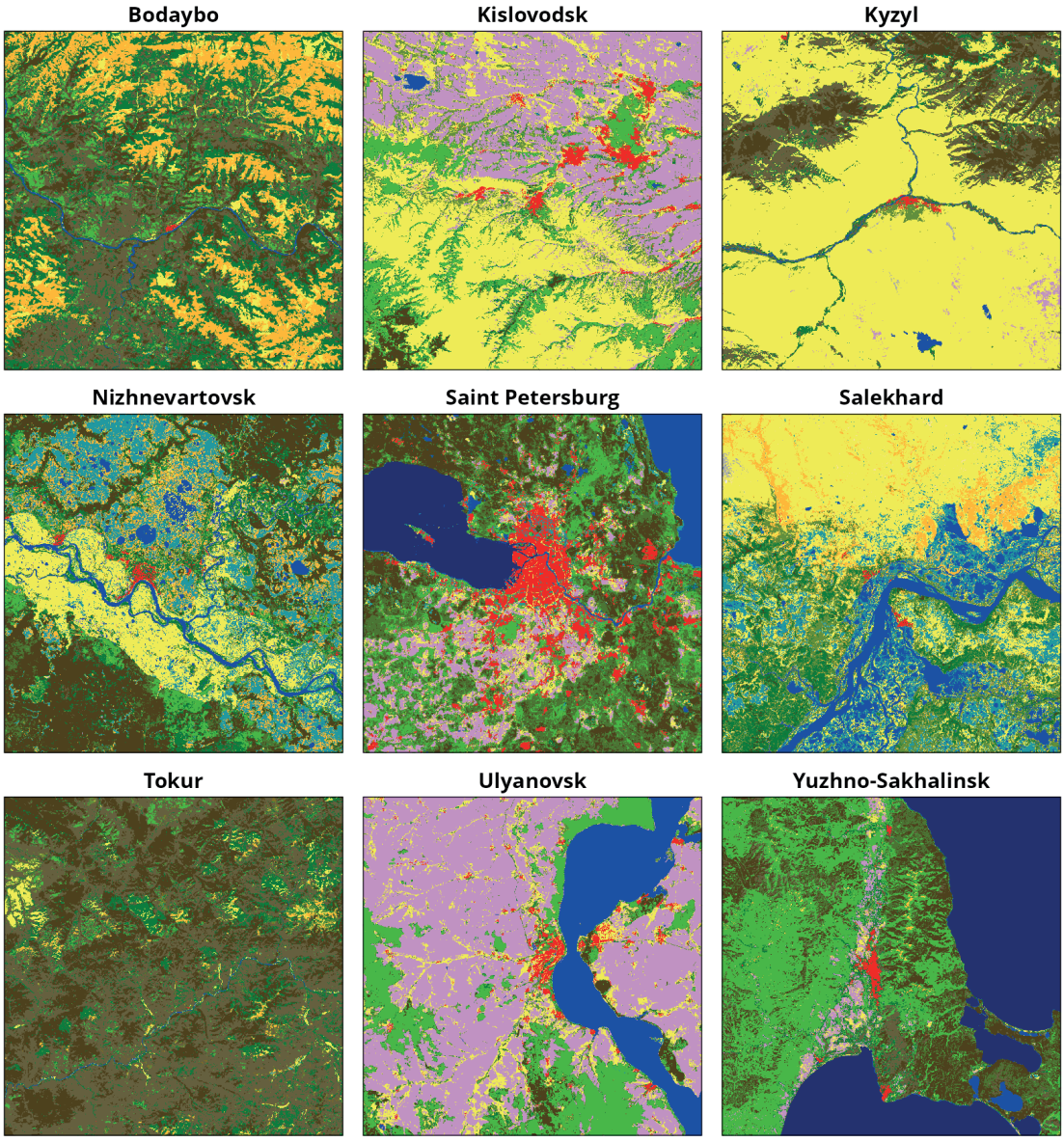

Fig. A.3. Land cover extracts for testing fragments

Table A.1. Copernicus Global Land Cover classes and colors

Type	Color	Description
0		No input data available
20		Shrubs
30		Herbaceous vegetation
40		Cultivated and managed vegetation/agriculture (cropland)
50		Urban / built up
60		Bare / sparse vegetation
70		Snow and Ice
80		Permanent water bodies
90		Herbaceous wetland
100		Moss and lichen
111		Closed forest, evergreen needle leaf
112		Closed forest, evergreen, broad leaf
113		Closed forest, deciduous needle leaf
114		Closed forest, deciduous broad leaf
115		Closed forest, mixed
116		Closed forest, unknown
121		Open forest, evergreen needle leaf
122		Open forest, evergreen broad leaf
123		Open forest, deciduous needle leaf
124		Open forest, deciduous broad leaf
125		Open forest, mixed
126		Open forest, unknown
200		Open sea

RESEARCH PAPER

MACROPHYTES AS INDICATORS OF THE ECOLOGICAL STATUS OF VALAAM ISLAND SMALL LAKES SYSTEM

Brenda B. Buenano[1], Nadezhda V. Zueva[2]

[1]Peoples' Friendship University of Russia, Institute of Ecology, Podol'skoye Shosse 8c5, 115093, Moscow, Russia

[2]Russian State Hydrometeorological University, Voronezhskay ul., 79, 192007, Saint-Petersburg, Russia

***Corresponding author:** 1042215057@pfur.ru, nady.zuyeva@ya.ru

Received: April 15th, 2022 / Accepted: February 15th, 2023 / Published: March 31st, 2023

https://DOI-10.24057/2071-9388-2022-056

ABSTRACT. The article evaluates the ecological status of five small lakes on Valaam Island (Igumenskoe, Chernoe, Ossievo, Nikonovskoe, Krestovoe) using macrophytes as bioindicators. The methods proposed by Finland, Sweden, and Norway were used, to assess the state of eutrophication, the change in the composition of specific species, the change in the water level, and the state of acidification, according to different indexes (Reference index (RI), Trophic Macrophyte Index (TMI), Trophic Index (TIc), the Proportion of Type–Specific Taxa (PTST), the Percent Model Affinity (PMA), Water level Index (WIc), and Acidification Index (SIc)). An analysis of the floristic composition for the period 2011 – 2020 was realized, including taxonomic analysis, ecogroup, and macrophyte diversity. The dominant taxon was *Elodea canadensis* Michx. in Igumenskoe, Chernoe, Ossievo lakes and *Calla palustris* L. in Nikonovskoe and Krestovoe lakes. The ecogroup hygrohelophyte was the most diverse in all lakes studied. The ecological status of the lakes according to each assessed parameter reflects that all lakes are characterized by a mesotrophic to eutrophic state, there is a variation in species composition of macrophyte and no water level change or acidification processes are presumed to occur in any of the lakes. In general, each method has its limitations, but it is suggested to continue studies for the RI, TMI, PTST, and PMA indices, and to integrate them with other national physicochemical or biological indices.

KEYWORDS: Aquatic flora, Bioindication, Biodiversity, Ecological status, Karelia, North-West of Russia

CITATION: Buenano B. B., Zueva N. V. (2023). Macrophytes As Indicators Of The Ecological Status Of Valaam Island Small Lakes System. Geography, Environment, Sustainability, 1(16), 103-110
https://DOI-10.24057/2071-9388-2022-056

Conflict of interests: The authors reported no potential conflict of interest.

INTRODUCTION

An ecosystem, like any system, is a set of different elements that interact with each other and behave as a unit. This close interaction between the elements of the ecosystem allows one element to be used as an indicator of the properties of another element (Brönmark and Hansson 2005; Lampert and Sommer 2007). In this study, macrophytes were used as bioindicators of the properties of the aquatic environment, specifically, as bioindicators of the ecological state of a group of small lakes in the Valaam archipelago.

The Valaam archipelago is located in the north of the Lake Ladoga and consists of more than 50 islands, of which the largest is Valaam Island, on which there are eleven small forest lakes characterized by low transparency (0,3 – 4,6 mSD), medium – high chromaticity (40 – 296°Pt-Co), medium – high content of organic matter (7,0 – 58,2 mgO/L) (Rumyantsev and Kondratiev 2013; Stepanova et al. 2016; Voyakina 2017).

The anthropogenic impact on the ecosystem has increased in recent years, especially since 2007, due to the construction of roads, new monastery hermitages, restoration and development of agricultural land, tourism, and recreational activities; further exacerbating concern about the disturbances of the natural environment, such as depletion of natural resources, change in the hydrological regime and the microclimate, accumulation of waste (municipal, agricultural, etc.), disappearance or reduction of species, chemical alteration of water, soil and air composition, erosion processes, and others (Litovka and Samokhin 1991; Stepanova et al. 2016). In the southern part of Ossievo and Chernoe lakes, pastureland improvement is developed; also, nearby is located the Valaam farm, which is expanding its production area. Since 2007, 15% of the Nikonevsky Lakes basin has been taking place in the process of meadows reclamation, which has affected the decrease in lake transparency (Stepanova et al. 2016).

The relevance of the study is linked to the contribution to the research being conducted in Valaam lakes, the evaluation of the implementation of assessment methods proposed by neighboring countries, the recognition of the importance of using bioindicators (as a complement to physicochemical assessments), the evaluation of the use of macrophytes as a good bioindicator (not limited to the more commonly used organisms such as phytoplankton and fish), the identification of a negative impact promptly to implement necessary actions to ensure a good condition, the integration and the comparison of the results obtained with the beginning of a future proposal for sampling, monitoring, and modeling.

The present study's main objective is to assess the ecological status of five small lakes in the Valaam archipelago, using methods with the macrophyte bioindicator. In accordance with the aim, an analysis of the floristic composition of macrophytes was also included, to have a more complete overview.

MATERIALS AND METHODS

Morphological and physicochemical characteristics of the studies of lakes

The present study involved the analysis of the characteristics of the Konevsky Lakes group (consisting of three lakes connected by channels: Igumenskoe, Chernoe, and Ossievo), Nikonovskoye, and Krestovoe Lakes (see Fig. 1). The five forest lakes are characterized by small areas (0,003 – 0,022 km^2), low – medium depth (1,3 – 4,5 m), humic – very humic (55 – 212 °Pt-Co), and slightly acid – neutral pH (5,6 – 8,6) (Stepanova et al. 2016; Voyakina 2017, Stepanova et al. 2021). The most important features of this group are given in Table 1 (Stepanova et al. 2021).

Macrophytes data for the period 2011 – 2020

In this study, the data corresponding to the period 2011 – 2018 was collected by N.V. Zueva. The data for 2020 were collected by B.B. Buenano and N.V. Zueva. The base for the fieldwork was the educational and scientific station of the Russian State Hydrometeorological University (RSUH).

Macrophyte sampling was carried out in all the lakes studied, during July and August, when the plants were well developed enough to be identified. Data for the years 2011 and 2018 are available for all studied lakes, while data for the year 2012 are available only for the Konevsky Lakes.

At the end of August 2020, according to the characteristics of lakes, especially their small size (<0,05 km^2), samplings were performed over the entire area of the lake (with special attention to the coastal zone), except for areas where there were no macrophytes (British Standards Institution 2007; European Commission, Joint Research Centre and Institute for Environment and Sustainability 2014; Kuoppala et al. 2008; Swedish Agency for Marine and Water Management 2015). The method of sampling and abundance measurement is presented in Table 2. Macrophyte species were identified in-situ by N.V. Zueva; when a confirmation in the determination of the specie was needed, it was taken to the RSHU scientific station, where after herbarium processing and microscopic identification was done, it was sent to the Herbarium of the Papanin Institute for Biology of Inland Waters Russian Academy of Sciences (IBIW) for storage. The identification of hydrophytes was confirmed by the expert of the Laboratory of Systematic and Geography of Aquatic Plants – A.A. Bobrov. Identification of mosses was performed by O.G. Grishutkin.

Taxonomic, ecogroup and biodiversity analysis of Macrophytes

Macrophytes were identified to the species level, and they were analyzed according to two parameters: taxonomic level (GBIF 2021) and lifestyle (ecogroup according to Table 3) (Papchenkov 2003). Macrophytes were identified exclusively up to the hygrophyte level (IV).

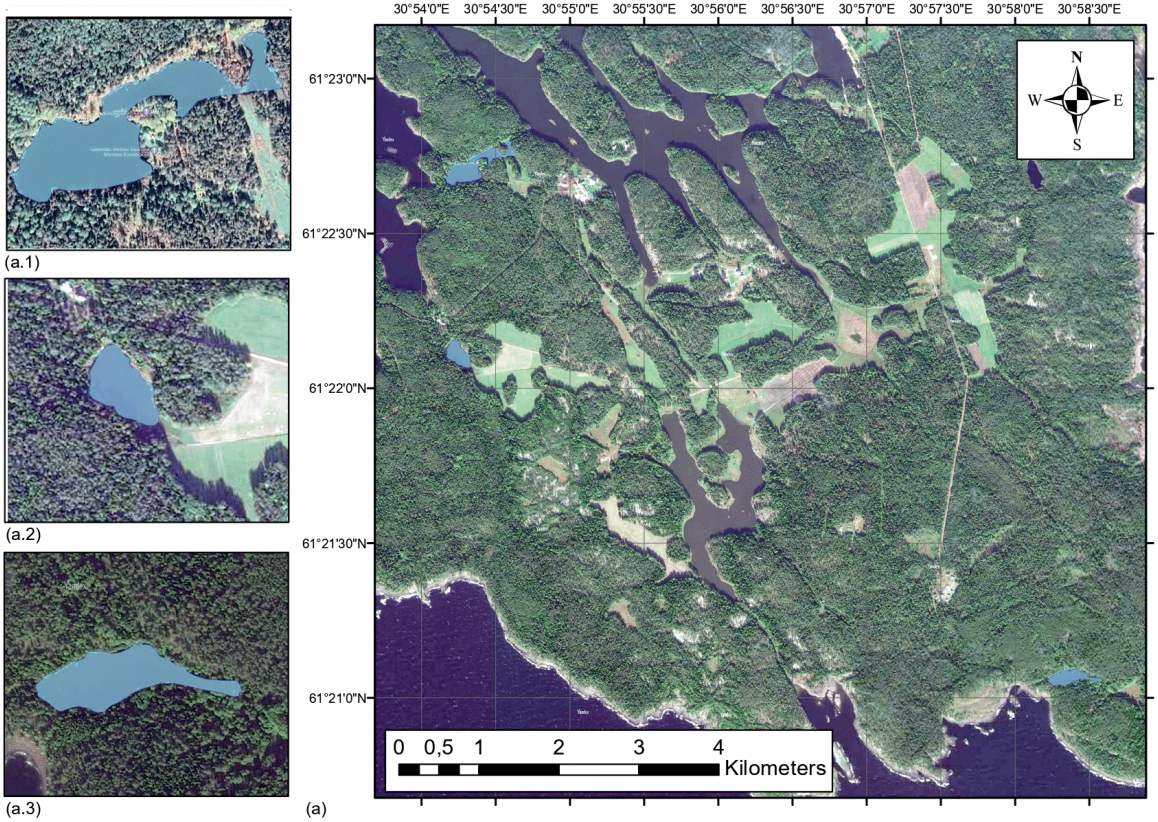

Fig. 1. (a) Location of the studied lakes on Valaam Island: (a.1) Konevsky Lakes (left to right: Igumenskoe, Chernoe, and Ossievo lakes), (a.2) Nikonovskoe lake, (a.3) Krestovoe lake

Table 1. General characteristics of the group of lakes studied

Characteristics	The Konevsky Lakes (Igumenskoe, Chernoe and Ossievo)	Nikonovskoe Lake	Krestovoe Lake
pH	5,6 – 7,5	5,8 – 7,6	7,3 – 8,6
Area [km^2]	0,003 – 0,022	0,011	0,014
Depth [m]	1,5 – 4,5	2,5	1,3
Humic [°Pt-Co]	55 – 110	90 – 260	80 – 212

Table 2. Description of the characteristics of the sampling carried out in 2020

Parameter	Description
Macrophytes	Any macrophyte that was in contact with water (hydrophytes and helophytes).
Method	Whole lake survey: longitudinal transect (maximum 100 m) divided into sub-transects of 10 m long, and from the shore to the maximum depth of macrophyte growth (perpendicular to the shore).
Abundance meters	Percentage scale (0,5 to 100%) and semi-quantitative (1 = rare, <1%; 2 = scattered, 1 – 10%; 3 = common or frequent, 10 – 25%; 4 = locally dominant or abundant, 25 – 75%; and 5 = dominant, > 75%).
Number of sampling sites	The number of transects sampled was 5 (Lake Igumenskoe), 3 (Lake Chernoe), 3 (Lake Ossievo), 5 (Lake Nikonovskoe) and 3 (Lake Krestovoe).
Criteria for reference lake	< 10% of the total catchment area with the presence of anthropogenic activity such as agriculture, grazing, deforestation, or land-use change; <0,1% with the presence of urban areas, no abrupt water level variations, no point sources of domestic or industrial water pollution.

For biodiversity analysis, specifically, the frequency of occurrence of species, the following indices were used (Death 2008; Fedor and Spellerberg 2013; Fedor and Zvaríková 2019; Ingram 2008): species richness (Margalef and Menhinik indices), diversity (Shannon – Wiener index), and equitability (Pielou and Berger – Parker index), according to Table 4. Furthermore, the verification of the species found in the lakes was realized according to the international and local red list (Republic of Karelia) (Artemyev et al. 2020; UICN 2021).

Assessment of ecological status using macrophytes

The ecological status is assessed as the degree of change of the lake in relation to its natural conditions (Brönmark and Hansson 2005; Kuoppala et al. 2008; Leka et al. 2008). The assessment of the ecological status can be analyzed by different methods, but, by the geographical location of the Valaam archipelago, methods developed in neighboring countries – Finland, Sweden and Norway (see Table 5) were used (European Commission, Joint Research Centre, Institute for Environment and Sustainability 2014; Leka et al. 2008; Norwegian Environment Directorate 2018; Swedish Maritime and Water Authority 2019). From the different indices available for assessing ecological status, it was decided to use six indices: three for assessing eutrophication status (RI, TMI, TIc), two for assessing change in species composition (PTST, PMA), and one for change in water level (WIc) and one for acidification process (SIc).

Table 3. Classification of macrophytes according to their life-form

Code	Ecogroup	
I.1	Hydrophyte	Hydrophyte 1. Macroalgae and aquatic mosses
I.2		Hydrophyte 2. Hydrophytes, freely floating in the water column
I.3		Hydrophyte 3. Submerged rooting hydrophytes
I.4		Hydrophyte 4. Rooting hydrophytes with leaves floating on the water
I.5		Hydrophyte 5. Hydrophytes, freely floating on the surface of the water
II.6	Helophyte	Helophyte 6. Short grass helophytes
II.7		Helophyte 7. Tall grass helophytes
III	Hygrohelophyte	
IV	Hygrophyte	
V	Hygromesophyte and mesophyte	

Table 4. Biodiversity indices

Parameter evaluated	Index	Equations	
Species richness	Margalef	$D_{Mg} = \frac{S-1}{\ln(N)}$	S – total number of species N – total number of individuals n_i – total number of species i $\log_2(S)$ – maximum diversity (H_{max}) N_{max} – number of individuals in the most abundant species (abundance of the dominant species)
	Menhinick	$D_{Mn} = \frac{S}{\sqrt{N}}$	
Species diversity (specific richness + uniformity)	Shannon – Wiener	$H = -\sum_{i=1}^{S}\left(\frac{n_i}{N} \times \log_2\left(\frac{n_i}{N}\right)\right)$	
Evenness vs equitability	Pielou	$J = \frac{H}{\log_2(S)}$	
	Berger – Parker	$d = \frac{N_{max}}{N}$	

Table 5. Ecological status parameters evaluated with the use of Macrophytes

Parameter assessed	Indices		
	Finland	Sweden	Norway
Eutrophication	Reference index (RI)	Trophic Macrophyte Index (TMI)	Trophic Index (TIc)
Change in species composition	The proportion of type–specific taxa (PTST) and the percent Model Affinity (PMA)	–	–
Water level change	–	–	Water level Index (WIc)
Acidification	–	–	Acidification Index (SIc)

Eutrophication. The trophic status of a water body is assessed based on a list of sensitive, tolerant, and indifferent species (specific in each country) to nutrient load and the effect of lake eutrophication on macrophytes, by the species found and identified (only hydrophytes in each country's lakes. The indices are calculated as shown in Table 6 (European Commission, Joint Research Centre, Institute for Environment and Sustainability 2014; Leka et al. 2008; Norwegian Environment Directorate 2018; Swedish Maritime and Water Authority 2019), the EQR value – (Ecological Quality Ratio) corresponds to the normalized value in base one of the indices.

Change in species composition. The PTST index considers the possible extinction of specific species and the emergence of new species, and the PMA index describes the composition and proportions of the number of species about the reference community of the specific lake type (equations in Table 7) (European Commission, Joint Research Centre, Institute for Environment and Sustainability 2014; Leka et al. 2008).

Water level changes and Acidification. The WIc index evaluates the water level change and reflects the impact on the coastal zone and biological conditions, the index uses a group of species (only hydrophytes) that are sensitive, tolerant, or indifferent to these changes. The SIc index evaluates the acidification, which is related to the carbon uptake preferences of some macrophyte (only hydrophytes) species, that are sensitive, tolerant, and indifferent to acidification, due to the content of dissolved CO_2 under acidic conditions (Norwegian Environment Directorate 2018). The equations for the calculation are in Table 8.

For the calculation of each index, the specific lists (for each country) of macrophyte species that are classified as sensitive, tolerant or indifferent, to nutrient loading and the effect of lake eutrophication (RI, TIc, and TMI), changes in the level of water and biological conditions in the coastal zone (WIc), acidification and the level of carbon uptake (SIc), were used (Joint website of Finland's environmental administration 2019; Norwegian Environment Directorate 2018; Swedish Maritime and Water Authority 2019). Likewise, each method establishes its limits into the five categories: excellent, good, satisfactory/regular, moderate and poor/bad.

Previously, the type of lake to which the five lakes studied correspond was defined, to compare the calculated values with the ranges established for each category as indicated. Thus,

Table 6. Equations of the assessment method for Reference index (RI), Trophic Index (TIc) and Trophic Macrophyte Index (TMI)

Index	Equations of RI, TIc, TMI		Equations of EQR	
RI (Finland)	RI and $TIc = \frac{N_s - N_r}{N} \times 100$	N_S – number of sensitive species N_T – number of tolerant species N – total number of species (sensitive, tolerant and indifferent)	$EQR = \frac{OV + 100}{RV + 100}$	*OV* – observed (calculated) value *RV* – reference value
TIc (Norway)				
TMI (Sweden)	$TMI = \frac{\sum_{i=1}^{n} (IV \times WF)}{\sum_{i=1}^{n} VF}$	*IV* – indicator value (1 to 10) *WF* – weight factor (0,1 to 1) Low values of *IV* and *WF* correspond to sensitive species	$EQR = \frac{OV - 1}{RV - 1}$	

Table 7. Equations for evaluation of PTST and PMA indices

Index	Equations of PTST and PMA	
PTST (Finland)	$PTST = \frac{\sum k_{ji}}{\sum k_j}$	k_{ji} – number of species specific to lake type k_j – total number of species in the lake (in the sampling)
PMA (Finland)	$PMA = 1 - 0,5 \sum \lvert a_i - b_i \rvert$	a_i – relative proportion (%) of taxon i in the reference community (data) b_i – relative proportion (%) of taxon i in the community assessed (in the sampling)

Table 8. Equations of the assessment method for Water level Index (WIc) and Acidification Index (SIc)

Index	Equations of PTST and PMA	
WIc (Norway)	WIc and $SIc = \frac{N_S - N_T}{N} \times 100$	*N_S – number of sensitive species* *N_T – number of tolerant species* *N – total number of species (sensitive, tolerant and indifferent)*
SIc (Norway)		

according to the methods in Finland, lakes Igumenskoe and Chernoe correspond to the "Ph" type (small and humic lakes: <5km^2, 30 – 90 mg Pt/L) and the rest of the lakes correspond to the "Mh" type (shallow and humic lakes: <3m, 30 – 90 mg Pt/L); according to the method in Sweden, all the lakes correspond to the type "Northern boundary of Limes Norrlandicus"; and according to the method in Norway, all the lakes correspond to the type "Humic (>30 mg Pt/L) lakes with low alkalinity (1 – 4 mg Ca/L)" (Joint website of Finland's environmental administration 2019; Norwegian Environment Directorate 2018; Swedish Maritime and Water Authority 2019).

According to the five lakes, Lake Krestovoe is the one that has the characteristics of a reference lake as mentioned in the methods used by the countries, mainly because of its low impact on anthropogenic activity (agriculture, livestock farming, urbanization, etc.), due to its location which makes it difficult to access easily in the island (European Commission, Joint Research Centre, Institute for Environment and Sustainability 2014).

RESULTS AND DISCUSSION

Taxonomic, ecogroup and biodiversity analysis of Macrophytes

The main results of sampling realized in 2020 are summarized in Table 9. The area occupied by macrophytes remains around 10 to 20%, except in the smallest lake, Lake Ossievo, where the macrophytes occupied about half of the lake area, even some macrophytes were found in the center of the lake. In comparison to the values reported in 2010 (Zueva 2010), the lake area occupied by the macrophytes has increased in the Konevsky Lakes and Nikonovskoe Lake from a range of 6 – 25% to 11 – 48%; likewise, it occurs in Krestovoe Lake from 5% to 16% (see Table 10), although there is a reduction in the number of species from 20 to 11 species. Suggesting a higher nutrient availability in lakes with surrounding anthropogenic activity (agriculture, livestock, and other) compared to the lake with the lowest of anthropogenic impact (Lake Krestovoe).

In general, in all lakes surveyed the taxonomic composition consists mainly of Tracheophyte (approx. 90%), followed by Bryophytes (approx. 10%, with two genus *Sphagnum* sp. and *Calliergon* sp.), and only in Chernoe Lake Charophyta phylum (*Nitella* sp.) was identified. A predominance of hydrophytes (44 – 73% of a total number of species, see Table 9) observed in 2020 is not recent, however, it increased compared to 2010 (Table 10) when values reported were within the range of 30 – 50% (in the Konevsky Lakes and Nikonovskoe Lake) and 45% (in Krestovoe Lake) were reported (Zueva 2010; Stepanova et al. 2021).

The composition and variation (in the years 2011, 2012, 2018, and 2020) of macrophyte ecogroups in the Konevsky Lakes are shown in Fig. 2, while the variation (in 2011 and 2020) for Nikonovskoe and Krestovoe is shown in Fig. 3. According to the period 2011 – 2020, ecogroup III was the most diverse in all lakes studied.

In Igumenskoe Lake, ecogroup I.1 was represented by genre *Calliergon* sp. and *Sphagnum* sp.; ecogroups I.2 (*Utricularia* sp.) and II.6 (*Alisma* sp., *Sparganium* sp.) were absent in 2012 and 2018, in ecogroup I.3 was identified a new species in 2020 (*Potamogeton alpinus* Balb.), ecogroups I.4 and I.5 have no variation, in ecogroup II.7 the specie *Typha latifolia* L. was observed only in 2009; and ecogroup IV was decreased to a single specie (*Lycopus europaeus* L.).

In Chernoe Lake, ecogroup I.1 and I.2 were stably represented by genre *Sphagnum* sp. and specie *Utricularia minor* L., respectively; in ecogroup I.3 were two genre (*Elodea* sp., *Potamogeton* sp.), ecogroup I.4 was represented only by specie *Nuphar lutea* (L.) Sm., in ecogroup I.5 was two species: *Hydrocharis morsus-ranae* L. and *Lemna minor* L., in ecogroups II.6 and II.7 *Sparganium minimum* Wallr. and *Naumburgia thyrsiflora* (L.) Rchb. were the species that were regularly observed, respectively; and ecogroup IV was represented by genres *Juncus* sp., *Lycopus* sp., *Lysimachia* sp., *Ranuculus* sp.

In Ossievo Lake, ecogroups I.1, I.2, I.3, I.4, I.5, II.6 do not show a considerable variation; in 2020, new species were identified for ecogroup I.1 (*Calliergon megalophyllum* Mikut., *Sphagnum squarrosum* Crome), ecogroup I.2 (*Utricularia vulgaris* L.), I.3 (*Callitriche cophocarpa* Sendtn., *Potamogeton berchtoldii* Fieber), I.4 (*Potamogeton natans* L.), I.5 (two species: *Hydrocharis morsus-ranae* L. and *Lemna minor* L.), II.7 (*Equisetum fluviatile* L., *Typha latifolia* L.), IV (*Bidens tripartita* L., *Juncus conglomeratus* L., *Juncus filiformis* L.).

Table 9. Taxonomic composition of lakes sampled in August 2020

Lake	Lake area occupied by macrophytes [%]	Maximum growth depth [m]	Total number of species (% hydrophytes)	Frequent and dominant species
Igumenskoe	11,1	1,8	24 (48%)	*Elodea canadensis* Michx., *Calla palustris* L., *Potamogeton alpinus* Balb; *Utricularia vulgaris* L., *Hydrocharis morsus-ranae* L., *Nuphar lutea* (L.) Sm.
Chernoe	21,5	1,5	29 (45%)	*Elodea canadensis* Michx., *Calla palustris* L., *Nuphar lutea* (L.) Sm.
Ossievo	47,8	1,8	36 (52%)	*Calliergon megalophyllum* Mikut., *Elodea canadensis* Michx., *Utricularia vulgaris* L., *Hydrocharis morsus-ranae* L.
Nikonovskoe	21,2	1,0	28 (44%)	*Calla palustris* L., *Cicuta virosa* L., *Potamogeton berchtoldii* Fieber
Krestovoe	16,5	1,5	11 (73%)	*Calla palustris* L., *Hydrocharis morsus-ranae* L.

Table 10. Comparison of floristic composition between 2010 and 2020

Lake	Lake area occupied by macrophytes [%]		Total number of species		Percentage of hydrophytes [%]	
	2010	2020	2010	2020	2010	2020
Konevsky and Nikonovskoe	5 – 25	11,1 – 47,8 (increase)	17 – 24	24 – 36 (increase)	30 – 50	44 – 52 (increase)
Krestovoe	5	16,5 (increase)	20	11 (decrease)	45	73 (increase)

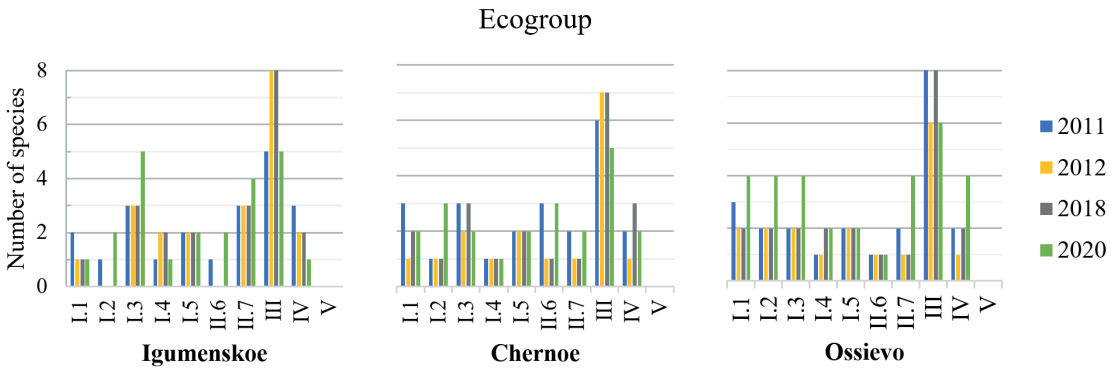

Fig. 2. Variation in the number of species by ecogroup in Igumenskoe, Chernoe, and Ossievoe Lakes in a period of 2011 – 2020

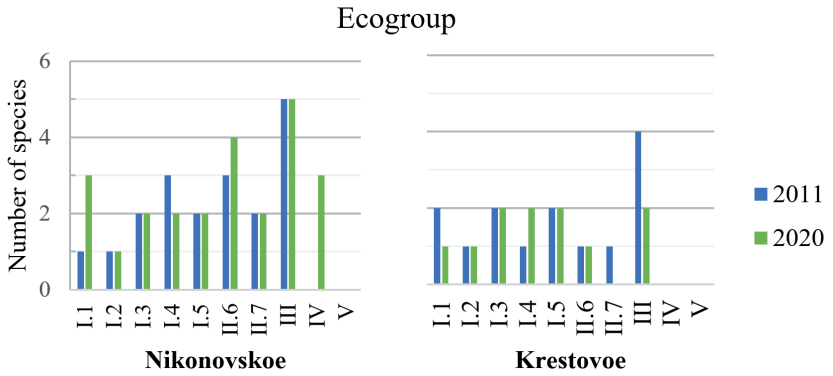

Fig. 3. Variation in the number of species by ecogroup in Nikonovskoe and Krestovoe in a period of 2011 – 2020

In the case of Nikonovskoe and Krestovoe lakes, only sampling data from 2011 and 2020 were available. In Nikonovskoe lake ecogroups I.2, I.3, I.5, II.7, III did not show a variation, in 2020 new species were identified for ecogroups I.1 (*Calliergon megalophyllum* Mikut., *Sphagnum squarrosum* Crome), II.6 (*Alisma plantago-aquatica* L.), II.7 (*Naumburgia thyrsiflora* (L.) Rchb.), III (*Cicuta virosa* L.), IV (*Bidens tripartita* L., *Lycopus europaeus* L., *Lysimachia vulgaris* L.), and other species were not observed for the ecogroups I.4 (*Nymphaea candida* J. Presl & C. Presl), II.7 (*Typha latifolia* L.), III (*Carex rostrata* Stokes). In Krestovoe lake ecogroups I.2, I.3, I.5, II.7, III did not show a variation, in 2020 some species were not observed for ecogroups I.1 (genre *Sphagnum* sp.), I.3 (*Potamogeton gramineus* L.), II.7 (*Sparganium emersum* Rehmann); and new species were identified for ecogroup I.1 (*Calliergon megalophyllum* Mikut.), I.3 (*Callitriche cophocarpa* Sendtn.), I.4 (*Nymphaea candida* J. Presl & C. Presl).

The calculated biodiversity values for the period of 2011 – 2020, in the Konevsky Lakes, show an increase of species richness (D_{Mg} and D_{Mn}) in the three lakes, but especially in Lake Ossievo, as it appreciated from the taxonomic and ecogroup analysis. The D_{Mg} index values were in a range 4,1 – 6,3, the maximum value correspond to Lake Ossievo in 2020; the D_{Mn} index values were in the range 2,3 – 3,1, with the same trend as the Margalef index. The diversity (H) of the Konevsky group has remained stable (4,2) with a slight tendency to increase in Ossievo Lake (4,9). Since 2011, equitability (J and d indices) has been high and stable in the community, with no major variations (0,98 and 0,10, respectively), despite an increase in the number of species.

Nikonovskoe Lake the species richness and biodiversity increased, while the uniformity remained low, which contributed to the dominance of some species over others; in Lake Krestovoye, species richness, uniformity and biodiversity were decreased.

Regarding the conservation status of the species identified in the lakes mentioned in this study, no species is on the Red List of the database for the Karelia region or UICN (Artemyev et al. 2020; UICN 2021).

Assessment of ecological status using macrophytes

Table 11 summarizes the results obtained for all the indices that use macrophytes as bioindicators, to assess eutrophication (RI, TMI and TIc), change in species composition (PTST and PMA), change in water level (WIc) and acidification (SIc) in 2020.

Eutrophication. When analyzing the trophic state, it should be considered that in all methods only hydrophytes species are used, so that the eutrophication state is associated with the aquatic environment. As a rule, in all Valaam lakes studied, tolerant species predominate, which determines the mesotrophic or eutrophic status.

According to the three indices used, the Norwegian TIc index is the one that rates the lowest status ("bad") for all lakes studied. Compared to lakes monitored for eutrophication in Norway, such as Lake Bergesvatnet (lowland, humus, shallow lake) which went through a process of eutrophication by agricultural activities in 1984 – 2001, where a moderate status (EQRTIc =0,84) was reported in 2016 and 2020 (Schartau et al. 2017; Schartau et al. 2021), it is suggested that it is perhaps not advisable to use this index for Valaam's lakes, because the list of species it uses is not in accordance; even because the reference lake (Lake Krestovoe) also obtained a low status.

Sweden's TMI index rates all lakes as moderate status, although it implements weight factors (WF) in the calculation, it remains to be considered whether the species list is in line with Valaam's lakes. While the species list used in Finland seems to be closer to the Valaam species list, it has also an important role to define correctly the type of lake (in our case Mh and Ph types), because according to the type of lake, will be the status ranges values, as it is observed the reference lake (lake Krestovoe) which is a more humic than the rest and has a lower status rating.

Table 11. Results of Eutrophication index (RI, TMI, TIc), Water level change index (WIc), Acidification index (SIc) and Species composition change index (PTST and PMA) in 2020

Lake	RI	TMI	TIc	WIc	SIc	PTST	PMA
Igumenskoe	0,48 Satisfactory	0,79 Moderate	0,41 Bad	70 Excellent	1,02 Excellent	0,52 Satisfactory	0,75 Good
Chernoe	0,44 Satisfactory	0,75 Moderate	0,50 Bad	65 Excellent	1,25 Excellent	0,36 Moderate	0,77 Good
Ossievo	0,44 Satisfactory	0,80 Moderate	0,37 Bad	64 Excellent	1,37 Excellent	0,35 Moderate	0,61 Good
Nikonovskoe	0,46 Satisfactory	0,70 Moderate	0,56 Bad	55 Excellent	1,26 Excellent	0,22 Moderate	0,42 Satisfactory
Krestovoe	0,38 Moderate	0,79 Moderate	0,56 Bad	33 Excellent	1,09 Excellent	0,55 Satisfactory	0,36 Moderate

Some of the lakes that are located in the Karelia region (on the border of Finland and Russia) and share the "moderate" status are Korpijärvi (Mh), Ylä-Tyrjä (Ph), Juurikkajärvi (Mh), Hanelinlampi (Mh), Puruvesi (Saimaa), Ristilahti (Ph), among others (SYKE, 2022).

Change in species composition. As mentioned, it is important to properly define the lake type in the method used in Finland. The overall species composition (relative percentage – PMA) reaches a "good" status in the Konevsky Lakes, however, for the case of Krestovoe lake the status is reduced to "moderate", even though it is considered that it has received the least anthropogenic disturbance. Also, the results obtained for the PTST index show no lake reaches a "good" status of species composition according to the species composition in the reference lakes of Finland (natural level), so, that indicates the species composition has had a great change (due to anthropogenic activities), or the possibility of better defining the lake type as was mentioned.

Water level changes and Acidification. According to the results of the WIc and SIc indices, all lakes have an "excellent" status, there is no concern for a process of water level variation or an acidification process.

Based on the precautionary principle of nature, the ecological status rating corresponds to the lowest rating obtained "bad" or "moderate". Despite the limitations of each method, it is recommended to follow the methodology of Finland and Sweden, and to implement the chemical status and other bioindicators, in order to have a complete overview. Regardless of the methodology used, it is recommended to continue with the monitoring program, preferably on an annual basis.

CONCLUSIONS

The aquatic flora has been varying over the years, but maintains a relative rich with a predominance of hydrophytes, which in 2020 represented between 44 and 73% of the total number of species.

The dominant taxon for all the studied lakes is Traqueophyte (90%). The families with the largest number of species overall in 2020 were Cyperaceae, Potamogetonaceae, Lentibulariaceae. The species with the highest occurrence were Elodea canadensis Michx. (in Igumenskoe, Chernoe and Ossievo lakes), Nuphar lutea (L.) (in Igumenskoe and Chernoe lakes), Calliergon megalophyllum Mikut. (in lake Ossievo), Calla palustris L. (in lakes Nikonovskoe and Krestovoe). The ecogroup III. Hygrohelophyte was the most diverse in all lakes studied.

All lakes can be attributed to mesotrophic and eutrophic types, because tolerant hydrophytes species are predominate in most lakes, even in the reference Krestovoe, therefore, it can be assumed that the studied lakes maybe naturally have a high level of trophic, but require additional research. No signs of changes in the water level on the banks or acidification processes were found.

In the future, it is proposed to conduct sampling in specific sectors of the lakes, and to classify macrophytes into zones of growth: helophytes, submerged hydrophytes and floating hydrophytes as proposed in the method of Finland, in order to better control and monitor the growth and change in the number and type of macrophytes.

REFERENCES

Artemyev A., Baryshev I., M.A. Boychuk, et al. (2020). The Red Book of the Republic of Karelia. Belgorod: Konstanta. [online] Available at: https://ecology.gov.karelia.ru/upload/iblock/b76/Krasnaya-kniga-Respubliki-Kareliya.pdf.

British Standards Institution (2007). BS EN 15460:2007. Water quality – Guidance standard for the surveying of macrophytes in lakes. EN 15460:2007: E.

Brönmark C. and Hansson L.-A. (2005). The Biology of Lakes and Ponds. 2nd ed. Oxford: Oxford University Press, 7, 73-75.

Death R. (2008). Margalef's Index. In: Encyclopedia of Ecology. Elsevier, 2209-2210, DOI: 10.1016/B978-008045405-4.00117-8.

European Commission. Joint Research Centre. Institute for Environment and Sustainability. (2014). Water Framework Directive Intercalibration Technical Report: Northern Lake Macrophyte Ecological Assessment Methods. Luxembourg: Publications Office of the European Union. DOI: 10.2788/75735.

Fedor P. and Zvaríková M. (2019). Biodiversity Indices. In: Encyclopedia of Ecology. Elsevier, 337-346, DOI: 10.1016/B978-0-12-409548-9.10558-5.

Fedor P.J. and Spellerberg I.F. (2013) Shannon–Wiener Index. In: Reference Module in Earth Systems and Environmental Sciences. Elsevier, DOI: 10.1016/B978-0-12-409548-9.00602-3.

GBIF (2021). GBIF. Free and open access to biodiversity data Facility. [online] Available at: https://www.gbif.org/ [Accessed 10 Mar. 2022].

Ingram J.C. (2008). Berger–Parker Index. In: Encyclopedia of Ecology. Elsevier, 332-334, DOI: 10.1016/B978-008045405-4.00091-4.

Joint website of Finland's environmental administration (2019). Species tables for assessment of Ecological Status. [online] Available at: https://www.ymparisto.fi/fi-FI/Vesi/Pintavesien_tila/Pintavesien_luokittelu/Lajitaulukot [Accessed 10 Mar. 2022] .

Kuoppala M., Hellsten S. and Kanninen A. (2008). Development of quality control in aquatic macrophyte monitoring. The Finnish environment 36/2008 36/2008, Environmental protection. Helsinki: Finnish Environment Institute SYKE. [online] Available at: http://hdl.handle.net/10138/38384.

Lampert W. and Sommer U. (2007) Limnoecology: The Ecology of Lakes and Streams. 2nd ed. New York: Oxford University Press, 234-235.

Leka J., Toivonen H., Leikola N., et al. (2008). Aquatic Plants as Indicators of the State of Finnish Lakes. Helsinki: Finnish Environment Institute.

Litovka O.P. and Samokhin Yu.A. (1991). The Valaam archipelago: problems and prospects. Soviet Geography 32(8), 566-571, DOI: 10.1080/00385417.1991.10640879.

Norwegian Environment Directorate (2018). Classification guide 02: 2018. Classification of environmental condition in water. Ecological and chemical classification system for coastal waters, groundwater, lakes and rivers. 02:2018. [online] Available at: https://www.vannportalen.no/veiledere/klassifiseringsveileder/#:~:text=I%20veileder%2002%3A2018%20Klassifisering,%22%2C%20i%20henhold%20til%20vannforskriften.

Papchenkov V.G. (2003). About the classification of plants of reservoirs and watercourses. In: Materials of the School of Hydrobotany, Rybinsk, Russia, 2003, 23-26. Rybinsk Printing House. [online] Available at: https://ibiw.ru/index.php?p=publ&id=430.

Rumyantsev V.A. and Kondratiev S.A. (2013). Ladoga. Saint Petersburg: Russian Geographical Society. [online] Available at: https://www.rgo.ru/sites/default/files/media/2013/08/ladoga.pdf.

Schartau A.K., Lyche Solheim A., Bongard T., et al. (2017). Surveillance monitoring of selected lakes 2016. Monitoring and classification of ecological status according to the WFD. M–758, Monitoring report, 27 June. Oslo: NINA, NIVA. [online] Available at: https://www.miljodirektoratet.no/publikasjoner/2017/juni-2017/okofersk-basisovervaking-av-utvalgte-innsjoer-2016/ [Accessed 10 Mar. 2022] .

Schartau A.K., Velle G., Bækkelie K.A.E., et al. (2021) Surveillance monitoring of selected lakes in Western Norway 2020. Monitoring and classification of ecological status. M–2053, Monitoring report, 21 September. Oslo: NINA, NORCE, NIVA. [online] Available at: https://www.miljodirektoratet.no/publikasjoner/2021/september-2021/okofersk--delprogram-vest-basisovervaking-av-utvalgte-innsjoer-i-2020/ [Accessed 10 Mar. 2022] .

Stepanova A.B., Babin A.B., Dmitricheva L.E., et al. (2016). Ecosystems of the Valaam Archipelago (Lake Ladoga) at the turn of the 20th and 21st centuries. Features of uniqueness and current state: Atlas. Saint Petersburg: RSHU. [online] Available at: http://valaam.rshu.ru/docs/rgo/Atlas_EHkosistemy%20Valaamskogo%20arhipelaga.pdf.

Stepanova A.B., Voyakina E.Yu., Zueva N.V., et al. (2021). Chapter 11. The Water System of the Valaam Archipelago. 11.3 Small forest lakes. In: Current state and problems of anthropogenic transformation of the Lake Ladoga ecosystem in a changing climate. Moscow: Russian Academy of Sciences, 477-484. [online] Available at: https://search.rsl.ru/ru/record/01010873128.

Swedish Agency for Marine and Water Management (2015). Survey: Macrophytes in lakes. [online] Available at: https://www.havochvatten.se/download/18.2a9deb63158cebbd2b44f0b4/1482842977748/makrofytersjoar.pdf.

Swedish Maritime and Water Authority (2019). Classification and Environmental Quality Standards regardingsurface water. HVMFS 2019:25. HVMFS 2019:25. [online] Available at: https://www.havochvatten.se/download/18.4705beb516f0bcf57ce1c145/1576576601249/HVMFS%202019-25-ev.pdf.

SYKE (n.d.) Water map – Water status of lakes in Finland. [online] Available at: https://paikkatieto.ymparisto.fi/vesikarttaviewers/Html5Viewer_4_14_2/Index.html?configBase=https://paikkatieto.ymparisto.fi/Geocortex/Essentials/REST/sites/VesikarttaKansa/viewers/VesikarttaHTML525/virtualdirectory/Resources/Config/Default&locale=fi-FI [Accessed 10 Mar. 2022].

UICN (2021). The UICN Red List of Threatened Species. [online] Available at: https://www.iucnredlist.org/ [Accessed 10 Mar. 2022].

Voyakina E.Yu. (2017). The Features of Production Processes in the Lakes of the Valaam Archipelago. Proceedings of the Zoological Institute RAS 321(1), 10–18, DOI: 10.31610/trudyzin/2017.321.1.10.

Zueva N.V. (2010). Aquatic flora of small forest lakes of Valaam archipelago. In: The I (VII) International conference on aquatic macrophytes 'Hydrobotany 2010', Borok, Russia, 9 October 2010, 130-131. Yaroslavl: 'Print House'. [online] Available at: https://ibiw.ru/index.php?p=publ&id=325.

RESEARCH PAPER

A NEW BACTERIOPHAGE OF THE FAMILY *SIPHOVIRIDAE* ISOLATED FROM THE SODDY-PODZOLIC SOILS OF THE PRIOKSKO-TERRASNY NATURE RESERVE

Alexandra N. Nikulina[1*], Natalia A. Ryabova[2], Yinhua Lu[3], Andrei A. Zimin[1*]

[1]Laboratory of Molecular Microbiology, G.K. Skryabin Institute of Biochemistry and Physiology of Microorganisms, Pushchino Scientific Center for Biological Research of the Russian Academy of Sciences, 142290, Pushchino, Russia

[2] Institute of Protein Research RAS, 142290, Pushchino, Russia

[3] College of Life Sciences, Shanghai Normal University, Shanghai, China

***Corresponding author:** a.karmanova@ibpm.ru, apollo66@rambler.ru

Received: April 14th, 2022 / Accepted: February 15th, 2023 / Published: March 31st, 2023

https://DOI-10.24057/2071-9388-2022-050

ABSTRACT. Bacteria of the genus *Streptomyces*, one of the main microorganisms of soils, and their bacteriophages are important inhabitants of soil ecosystems. Important though they are, not much is known about their functional patterns and population dynamics. A question of particular interest, which is still to be understood, is how bacteriophages regulate the population dynamics of *Streptomyces* and how this regulation affects the soil ecosystem as a whole. Isolation and study of new *Streptomyces* bacteriophages can help to understand these problems. In this paper, we describe isolation of a new bacteriophage from the soils of the Prioksko-Terrasny Reserve. The analysis of morphology of the new phage allows us to conclude that it belongs to the family *Siphoviridae*.

KEYWORDS: Streptomyces, phage, soddy podzolic soils, Prioksko-Terrasny Reserve

CITATION: Nikulina A. N., Ryabova N. A., Lu Y., Zimin A. A. (2023). A New Bacteriophage Of The Family Siphoviridae Isolated From The Soddy-Podzolic Soils Of The Prioksko-Terrasny Nature Reserve. Geography, Environment, Sustainability, 1(16), 111-118

https://DOI-10.24057/2071-9388-2022-050

ACKNOWLEDGEMENTS: This work was supported by grant of the Russian Science Foundation №22-25-00669 (https://rscf.ru/project/22-25-00669). We are thankful to our colleagues from the Electron Microscopy Core Facilities at ICB RAS (http://www.ckp-rf.ru/ckp/670266/) for the electron-microscopy analysis of samples and to the staff of Prioksko-Terrasny Nature Reserve for the opportunity to conduct the study.

Conflict of interests: The authors reported no potential conflict of interest.

INTRODUCTION

On the basis of their infection mechanism, bacteriophages, the viruses of bacteria, are divided into two groups. The first group is virulent bacteriophages, whose replication and propagation occurs via the lytic cycle (e.g., it involves lysis of the host bacterial cell as an obligatory step). The second group is temperate bacteriophages; their life cycle is lysogenic, meaning that they may incorporate in the bacterial genome in the form of a prophage. The prophage is not active; it does not cause lysis of the bacterial cell and can, therefore, be replicated along with the bacterial genome during the process of bacterial cell division (Abedon 2008). Bacteriophages are found in all the bacterial habitats. Some of the bacterial/phage ecosystems (e.g., aquatic and animal intra-intestinal habitats) are well-studied; others, like soil bacterial/phage communities, are not – the data on the latter are scarce.

Meanwhile, it is assumed that phage communities play a significant role in the soil ecosystems. For example, a metagenomic analysis of permafrost soils showed that bacteriophages could infect bacteria involved in the carbon cycle, thereby affecting biogeochemical processes (Truble et al. 2018; Emerson et al. 2018). The analysis of viriome of Chinese soils indicated that bacteriophages might also contribute to the cycle of phosphorus in the soil ecosystems (Han et al. 2022). In particular, quite a large number of agricultural-soil viruses were shown to have genes for the synthesis of phosphorus-containing compounds. The authors suggested that a part of soil phosphorus could be redirected to the synthesis of viral genomes, thereby affecting the strategies for acquiring phosphorus by plants and soil bacteria (Han et al. 2022).

The estimates based on direct counting indicate that soils can contain a large number of phage particles, up to ~10^{10} per gram of soil (Ashelford et al. 2003). It is suggested that in soils, the incidence of viral infection of bacteria is higher than in aquatic ecosystems (Kuzyakov and Mason-Jones 2018). The higher rate of infection may result from the adsorption of bacteriophages and their bacterial hosts on clays. In soil ecosystems, bacteriophage particles interact directly with the chemical components of the soil, and these interactions can have a great impact on the survival of phages. Depending on the phage and the clay type, the effect can be either negative or positive. In the case of actinophages, for example, the range of pH, in which they can survive, depends on the clay that the phage is adsorbed upon (Sykes and Williams 1978). As

active physical and chemical media, clays modulate the acts of host cell recognition and infection that occur on their surface. The negatively charged phages and bacteria bind to the clay cation groups, resulting in a stronger interaction between viral particles and the susceptible bacterial cells (Dashman and Stotzky 1984; Lipson and Stotzky 1984). On certain clays, the binding of phages to the clay particles was shown to be very strong (Sykes and Williams 1978). It was also demonstrated that clay binding could prolong the infectivity of eukaryotic viruses and reoviruses (Lipson and Stotzky 1985) – confirmed by a later observation that particles of infectious bacteriophages could persist in the soil for a long time (Williams et al. 1987). One could, therefore, argue that, in the absence of host bacteria, virulent phages can be preserved in the soil for relatively long periods and will resume their reproduction as the population of their hosts grows. Such a preservation was reported, for example, by Marsh and Wellington, who isolated virulent actinophages from a soil which was air-dried for several months and then rewetted with sterile distilled water (Marsh and Wellington 1994). The authors observed a spike in the number of phage particles after a 24-hour incubation, which could be either a gradual elution of phages tightly bound to the clay components or release of the new lysogenic and pseudolysogenic progeny. In the eluate, temperate phages, which produce turbid plaques on the indicator strain, were more numerous than virulent phages, producing clear plaques (Marsh and Wellington 1994). Evidently, bacteriophage particles are less protected outside the host, making lysogeny a more optimal strategy for the survival of phages in the soil ecosystems. Pseudolysogeny, which is observed in virulent bacteriophages, seems to contribute to the survival of phages as well.

There is only a small number of studies directly examining the in *situ* lytic activity of phages in soils. Pantastico-Caldas et al. (1992) reported that the presence of SP10C, a virulent phage of *Bacillus subtilis*, in the soil decreased the host population by an order of magnitude. On the other hand, the temperate actinophage KC301 did not affect the size of *Streptomyces* populations in both sterile and non-sterile soils (Marsh and Wellington 1992; Marsh et al. 1993). The experiments showed that the infectivity of KC301 was high enough to inhibit the vegetative growth of *Streptomyces lividans*, yet the inhibitory effect was compensated for by the sporulation of *Streptomyces* (Marsh and Wellington 1994). Other observations of the population dynamics of soil bacteria indicated that the effects of phages could be both adverse or beneficial. Many of the phage effects are related to the state of lysogeny in bacteria and the phenomenon of transduction, with the expression of phage genes or maintenance of lysogeny changing the metabolism of the host bacterial cell due to lysogen conversion.

Thus, soil bacteriophages are able to influence microbial mortality, food web dynamics, and biogeochemical cycling of soil elements (Emerson 2019).

This work examines bacteriophages from the soils of the Prioksko-Terrasny Biosphere Reserve, Moscow Region. The reserve is a semi-pure forest area (The Prioksko-Terrasny Nature Biosphere Reserve 2022), with brown forest, sod-weakly podzolic and sod-medium podzolic soil cover being the common soil types on the territory of the reserve (Kurganova et al. 2020). The reserve has a unique nursery of European bison, permanent dwellers of this area since the Middle Ages which are now listed in the Red Data Book of the Russian Federation (Zemlyanko et al. 2017). The soils of the Prioksko-Terrasny European bison nursery can, therefore, be considered as a model of native forest soils of ancient Eurasia. These forest soils are dominated by Actinomycetes; in particular, representatives of the genus *Streptomyces*. They are producers of various physiologically active substances and are able to effectively suppress the growth of other microorganisms (such as phytopathogenic fungi) within their econiche (Xu L.H et al. 1996; Pedziwilk 1995). The literature contains detailed data on the dynamics

Fig. 1. A paddock for young European bison where soil samples were collected (soil type, sod-podzolic)

and structure of soil *Streptomyces* populations, as well as their interactions with other bacteria (Dobrovol'skaya et al. 2015). At the same time, little is known on the modulation of soil *Streptomyces* populations by bacteriophages. How the communities of *Streptomyces* and their bacteriophages function as a whole, what the molecular mechanisms regulating their dynamics in particular soils are, and what role this bacterium/phage complex plays in the ecosystem – all these questions are still to be answered. In this paper, we have characterized the morphotype of new *Streptomyces* bacteriophages, which have been isolated from the soil samples taken on the territory of the Prioksko-Terrasny European bison nursery (Fig. 1).

MATERIALS AND METHODS

Bacterial Strains and Growth Conditions

Streptomyces venezuelae (Ac-589 type VKM) was used as the bacteriophage host. The strain was grown on a modified MS medium (mannitol, 10 g/L; peptone, 20 g/L; glucose, 2.5 g/L; agar, 20 g/L; tap water) at a temperature of 30°C. For agar double layers, MS was used with 0.5% and 1.5% agar for the top and bottom layers, respectively.

Sampling and processing

The sod-podzolic soil samples were collected from the top layer of soil cover in one of the paddocks of the young European bison nursery of the Prioksno-Terrasny Reserve (marked with orange crosses on the map of Figure 2). The samples (2 ml of soil) were collected into test tubes under sterile conditions and supplemented with 10 ml of a phage buffer (200 mM NaCl, 25 mM Tris-HCl (pH=8)). Extraction was carried out for two hours on a mini-rotator BioRS-24 (mini-rotator biosan) at a low rotation speed, followed by centrifugation of the samples (10,000 rpm; 90 seconds) to precipitate the soil particles. The supernatant was passed through a bacterial filter (0.2 µm); the filtrate was supplemented with a couple of drops of chloroform and stored is at 5-7°C.

Isolation and cultivation of phages

The phage filtrate (0.1 ml) was added to 2 ml of an overnight Streptomyces venezuelae culture (8–12 hours of growth), and the mixture was added to 0.5% MS agar (5 ml) melted in a water bath at 43°C. The inoculated agar was poured onto a layer of 1.5% MS agar solidified in a Petri dish (the double agar layer method; Kauffman and Polz 2018). After an overnight incubation at 30°C and visualization of plaques, phages from individual plaques were microbiologically purified by the three-passages-and-titration protocol according to Gracia. The overall scheme of procedures, from the soil sampling to the isolation of phages, is shown in Figure 3.

Preparing phage samples for the electron microscopy examination

To prepare samples for electron microscopy, bacteriophage particles were extracted with the phage buffer from fresh lawns of streptomycetes almost completely lysed by the phages. After incubation for a couple of days at 6°C, the phage extract was separated from the cell debris by centrifugation at 5000 rpm for 15 min and filtered through a bacterial filter (0.2 µm). The filtrate was concentrated using a vivaspim-500 concentrator, which increased the number of phage particles in the samples by a couple of orders of magnitude.

Electron Microscopy Examination of Phage Virions

The electron microscopy (TEM) examination was performed according to a standard technique. A sample aliquot was placed on a 400-mesh carbon-coated copper grid, washed with distilled water to remove unattached particles, and contrasted with an aqueous solution of 1% uranyl acetate. The samples were analyzed using a JEM-1200EX electron microscope (Jeol, Japan) at an accelerating voltage of 80 kV and magnification of 40–50 × 103. The results were micrographed on Kodak film SO-163 (Kodak, USA), 6.5 × 9 cm.

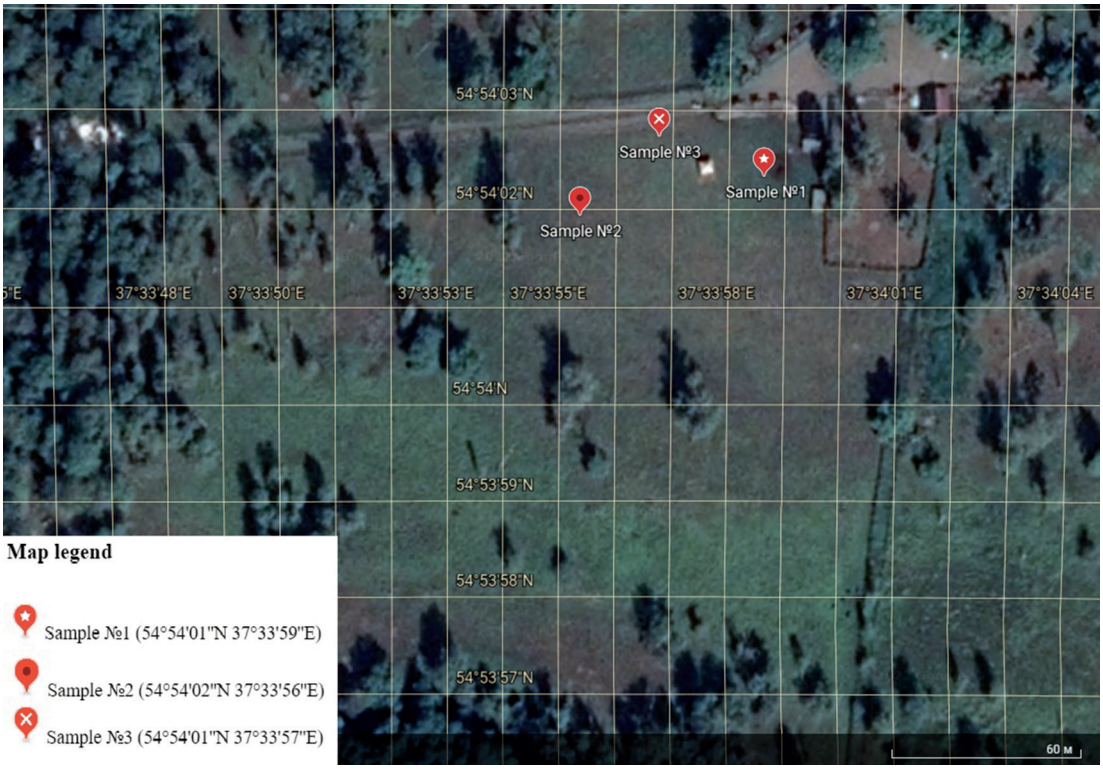

Fig. 2. The map of soil sampling sites. Sampling locations are marked with red label. Coordinates of sampling location are indicated in brackets on the map legend. The space image was taken from the Google Earth

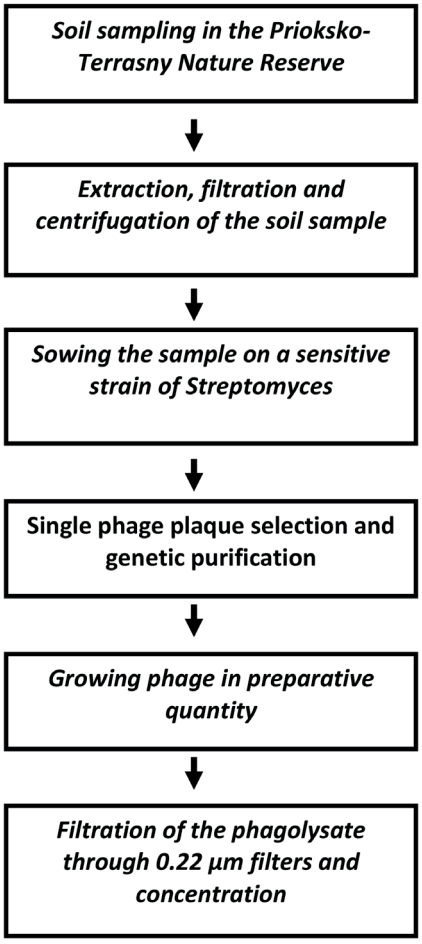

Fig. 3. A scheme of procedures for the isolation of Streptomyces phages from soils

RESULTS

As a result of the conducted experiments, we have isolated and microbiologically purified, through a series of successive titrations, an earlier unknown bacteriophage. The bacteriophage, which was isolated from a single plaque, was able to form new plaques within 12 hours since the moment of culture infection.

The maximal titer of the bacteriophage cultivated in large volumes (500 ml) under laboratory conditions was 10^{12} PFU/ml. When the phage was cultivated from a single plaque for 16 hours, the titer usually was in the range of 10^7-10^8 PFU/ml and could drop to 10^6 PFU/ml in the process of storage. The bacteriophage titer was calculated according to formula 1:

$$A = \frac{x \times 10^n}{v} \quad (1)$$

where x was the number of plaques on *a* Petri dish; *v*, the sample volume; n, the degree of sample dilution; *A*, the number of phage particles expressed in PFU/ml. The average titer was calculated as the arithmetic mean of the previously obtained titers (Table 1).

From the analysis of 100 bacteriophage plaques, we have described their characteristic morphology. The plaque diameter varied greatly: from 1 to 8 mm (diameter variability (CV) = 47.9%). The average diameter of bacteriophage plaques was calculated as 4.09 ± 2.08 mm (Table 2, Figure 3). More details on the variation of the plaque diameter are given in Table 2.

The plaques were transparent and had irregular edges, with the jags of viral infection protruding deeper into the field of bacterial culture. All over their perimeter, the plaques were interspersed with islets of phage-resistant colonies (Fig. 4-6).

Table 1. The quantitative parameters of bacteriophage cultivation

	Number of Streptomyces phage plaques on Petri dishes							
growing time and volume	n,V	12 h, 500 ml		16 h, 10 ml		16 h, 10 ml		16 h, 50 ml a month later
the degree of dilution of the sample cup no. 1 (n)	6	100000	2	10000	4	998	2	1350
the degree of dilution of the sample cup no. 2 (n)	6	100000	4	210	4	1115	2	1002
the degree of dilution of the sample cup no. 3 (n)	8	1215	4	230	4	1033	4	58
the degree of dilution of the sample cup no. 4 (n)	8	1250	6	6	6	14	4	51
the degree of dilution of the sample cup no. 5 (n)	10	12	6	1	6	10	6	0
V cup samples no. 1, ml	0,1		0,1		0,1		0,1	
V cup samples no. 2, ml	0,1		0,1		0,1		0,1	
V cup samples no. 3, ml	0,1		0,1		0,1		0,1	
V cup samples no. 4, ml	0,1		0,1		0,1		0,1	
V cup samples no. 5, ml	0,1		0,1		0,1		0,1	
number of phages of sample no. 1		$1{,}00\times10^{12}$		$1{,}00\times10^{7}$		$9{,}98\times10^{7}$		$1{,}35\times10^{6}$
number of phages of sample no. 2		$1{,}00\times10^{12}$		$2{,}10\times10^{7}$		$1{,}12\times10^{8}$		$1{,}00\times10^{6}$
number of phages of sample no. 3		$1{,}22\times10^{12}$		$2{,}30\times10^{7}$		$1{,}03\times10^{8}$		$5{,}80\times10^{6}$
number of phages of sample no. 4		$1{,}25\times10^{12}$		$6{,}00\times10^{7}$		$1{,}40\times10^{8}$		$5{,}10\times10^{6}$
number of phages of sample no. 5		$1{,}20\times10^{12}$		$1{,}00\times10^{7}$		$1{,}00\times10^{8}$		$0{,}00\times10^{6}$
average number of phages, PFU/ml		$1{,}13\times10^{12}$		$2{,}48\times10^{7}$		$1{,}11\times10^{8}$		$2{,}65\times10^{6}$

Table 2. Size characterization of the phage plaques

Plaque diameter, mm	Frequency, pi
1	15
2	12
3	12
4	15
5	25
6	6
7	7
8	8
The total number of plaques examined	100
Mean $\bar{x}$	4,09
Dispersion σ^2	4,34
Standard deviation σ	2,08
Coefficient of variation (CV)	47,99
Standard error (SE)	0,2

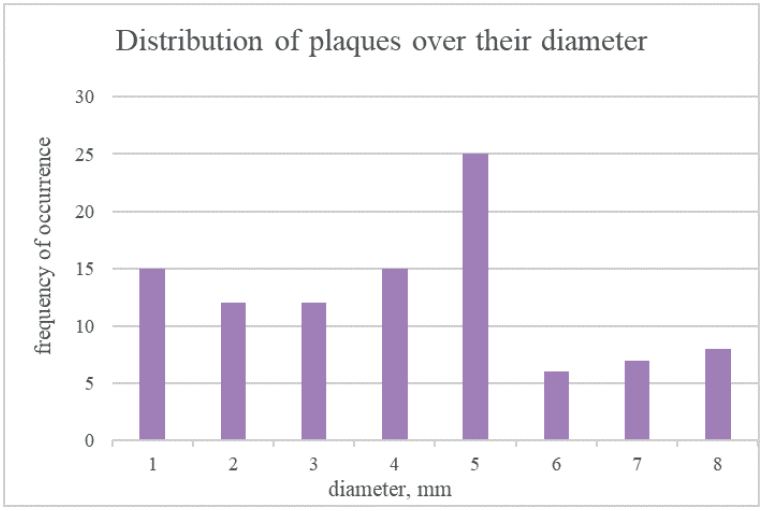

Fig. 4. The distribution of plaques of the new *Streptomyces* phage over their diameter

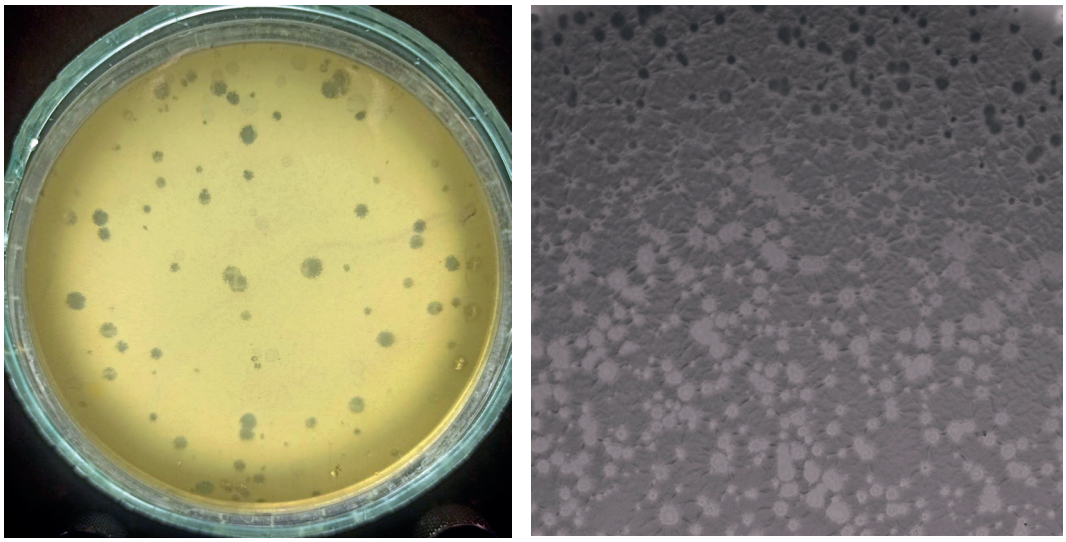

Fig. 5-6. Plaques of the new bacteriophage of *Streptomyces*

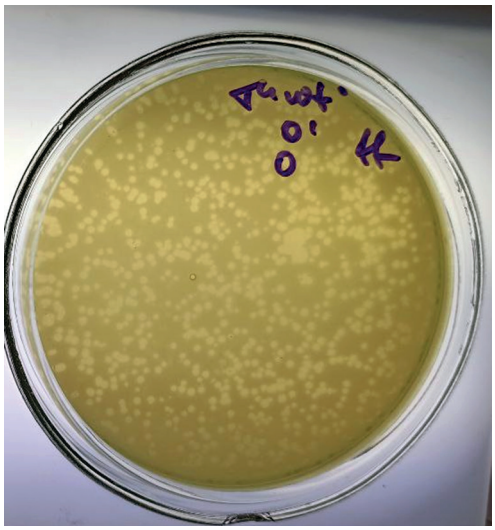

Fig. 7. Plaques of the lytic bacteriophage T4

Comparing the plaque morphology of the new bacteriophage with that of other phages (lysogenic phage λ and lytic phage T4; see Fig. 7) – as well as taking into account the character of the plaque overgrowth with the phage-resistant bacterial clones – we concluded that the new bacteriophage was, probably, lytic (Mitarai et al. 2016). There is, however, another possibility which cannot be write off. Some of the bacteriophages of *Streptomyces* are known to be plasmid-phages. In their prophage stage, plasmid-phages are not integrated into the host chromosome, but remain in the cytoplasm in the form of a plasmid (Zhong et al. 2010). Not much is known about the plaque morphology of plasmid-phages and how it differs from that of lytic phages. Therefore, an accurate assessment of the type of life cycle of the new phage can only be made after additional experiments.

The results of electron microscopy examination of the new phage are shown in Figure 8. The phage has an isometric icosahedral head, approximately 50 nm in size, and a seemingly non-contracting tail, approximately 110 nm long and 10 nm thick. According to Bradley's classification (Fig.9), the phage particle belongs to the B1 morphotype (Bradley 1967; Ackermann 2006; Ackermann 2012; Ackermann and Prangishvili 2012), which is characteristic of bacteriophages of the family *Siphoviridae*. The basal plate is quite thick (about ~15 nm) – and there should be 6 long fibrils extending from it (not visible on the micrograph).

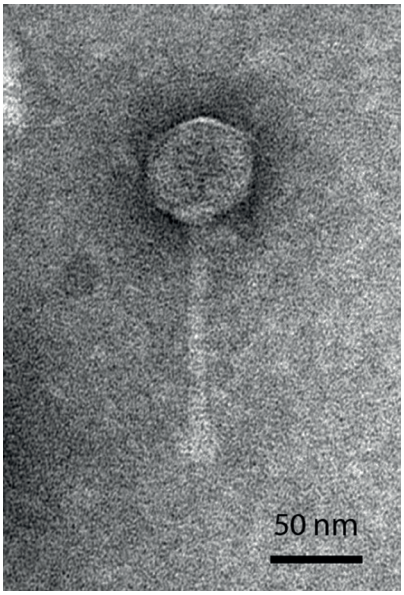

Fig. 8. An electron micrograph of the new bacteriophage of *Streptomyces*. The micrograph indicates that the phage belongs to the family *Siphoviridae*

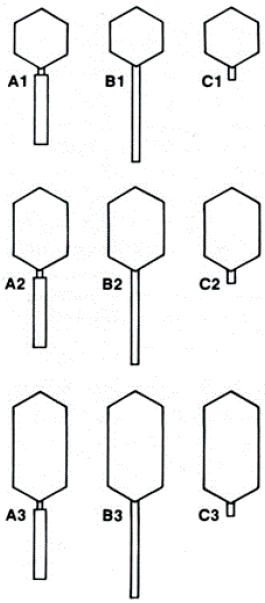

Fig. 9. Morphotypes of the families *Myoviridae* (A1 - A3), *Siphoviridae* (B1 - B3) and *Podoviridae* (C1 - C3) according to Bradley's classification (Bradley 1967)

DISCUSSION

The methods aimed at the study of soil viruses, which have been developed in this work, are the first step towards examining the role of viruses in soil ecosystems. In most soils, viruses are plentiful, reaching 10^{10} particles per gram of dry soil (Ashelford et al. 2003). This abundance, which is quite striking in comparison to other ecosystems, is likely a combined result of both replication of viruses and their accumulation over time. Determining the contribution of these two processes to the abundance of viruses in soils is a hot topic of research. The bacteriophage isolated and described in this paper can be used as a model object for studying preservation of bacteriophages in natural soils. Certain areas of the Prioksko-Terrasny Reserve are good testing grounds for such experiments. What is currently needed is modification and adaptation of the molecular-genetic methods for the analysis of viral and, more specifically, bacteriophage soil communities. Metagenomic projects aimed at the study of soil viruses are rare, despite the evidence that the genetic diversity of soil viruses may exceed that of marine ones. Soil viruses can control life activity of their bacterial hosts (through infection, lysis, lysogenization and lysogenic conversion), and might also affect their evolution (through horizontal transfer of genes by bacteriophages).

It has already been demonstrated that soil microbiocenoses are built on complex relationships between bacteria, fungi, and plants. Soil bacteriophages are also participants in these relationships (Ashfield-Crook et al. 2018, 2020). For example, *Streptomyces*, antagonists of fungi, are known to facilitate the development of the root system of plants by releasing fungicidal substances. In particular, the fungicidal activity of *Streptomyces* was reported to be crucial in the prevention of weight losses caused by the pathogenic fungus *Fusarium solani* in wheat shoots. Furthermore, inoculation of soil with phages had a negative effect on the growth of the shoots. Apparently, the phage-induced suppression of *Streptomyces* propagation may contribute to the opportunistic fungal infections in plants (Ashfield-Crook et al. 2018). The data of Ashfield-Crook et al. (2018) clearly demonstrated that a virulent phage of *Streptomyces* was capable to control the life activity of the bacterium: the experimental introduction of the phage into this system led to a decrease in the *Streptomyces* titer and provided conditions for an uncontrolled propagation of a parasitic fungus.

Similar to many other phages of *Streptomyces*, the new bacteriophage described in this paper may be polyvalent: rather than being specific to any particular strain of *Streptomyces*, it can infect various strains of this genus. The bacteriophage may, therefore, be capable of controlling the development of several or even many species of *Streptomyces*. By reducing their titer and facilitating the propagation of fungi, the bacteriophage could, therefore, contribute to the decomposition of plant residues in the forest podzolic soils of Central Russia, leading to their enrichment with nutrients necessary for the growth of trees.

In perspective, it seems promising to further study the newly discovered bacteriophage and the relative phages – both in the laboratory and natural setups. The isolated bacteriophage can be cultivated to high titers – and model experiments, in which the formation and dynamics of soil microbiocenoses could be studied under periodic inoculation of the soil with the phage filtrate (with monitoring the spontaneous emergence of resistant *Streptomyces* mutants), would be interesting. It would be also of interest to investigate the distribution of the new bacteriophage and the related phages in the soils of the Prioksko-Terrasny Reserve – both in the European bison nursery and other sectors of the reserve. The purpose of such studies could be to assess, by indirect methods, the influence of the European bison nursery on the development of forest soils, which would not only provide information on the rate and specifics of soil formation, but might also give an insight into the development of the soils in the future.

The methods of microbiological examination of *Streptomyces* bacteriophages, which were modified and adapted in this work for the analysis of soil samples, can be useful in further research in the field. The quantitative determination of phage titer in soil samples, for example, can be used to monitor the titer of bacteriophages (and, thus, to control the propagation of their *Streptomyces* hosts) in the soil. In the future, we plan to obtain data on the genome of the isolated phage, which would allow us to make a PCR-test – to replace microbiological methods for monitoring the phage in the reserve soils with genetic ones.

CONCLUSIONS

Based on the data obtained, we assume that the new bacteriophage of *Streptomyces* isolated and described in the paper belongs to the order *Caudovirales*. The bacteriophage has an isometric head in the shape of an icosahedron, approximately 50 nm in size, and a seemingly non-contracting tail, approximately 110 nm long and 10 nm thick. The phage forms transparent plaques with an average diameter of 4.09 ± 2.08 mm. A supposition is made that the phage belongs to the family *Siphoviridae*, representatives of which often infect *Actinomycetes*. Further studies of the phage and its genome, as well as the mechanisms and specifics of the infection process, will help to understand the relationships between the phage and its host bacteria and the role of these relationships in the natural ecosystems.

REFERENCES

Abedon S.T. (2008). Ecology of Viruses Infecting Bacteria. In Encyclopedia of Virology (Third Edition) 2008, Pages 71-77, DOI: 10.1016/B978-012374410-4.00745-7.

Ackermann H.W. (2006). Classification of bacteriophages. In: Calendar R., editor. The Bacteriophages. 2nd ed. Oxford University Press; New York, NY, USA, 8-17.

Ackermann H.W. (2012). Bacteriophage electron microscopy. Adv Virus Res.; 82:1-32, DOI: 10.1016/B978-0-12-394621-8.00017-0. PMID: 22420849.

Ackermann H.W., Prangishvili D. (2012). Prokaryote viruses studied by electron microscopy. Arch Virol. Oct;157(10):1843-9, Epub 2012 Jul 3. PMID: 22752841, DOI: 10.1007/s00705-012-1383-y.

Ashelford K.E., Day M.J., Fry J.C. (2003). Elevated abundance of bacteriophage infecting bacteria in soil. Appl Environ Microbiol, 69, 285-9.

Ashfield-Crook N.R., Woodward Z., Soust M., Kurtböke D.İ. (2021). Bioactive Streptomycetes from Isolation to Applications: A Tasmanian Potato Farm Example. Methods Mol Biol ;2232:219-249, DOI: 10.1007/978-1-0716-1040-4_18.

Ashfield-Crook N.R., Woodward Z., Soust M., Kurtböke D.İ. (2018). Assessment of the Detrimental Impact of Polyvalent Streptophages Intended to be Used as Biological Control Agents on Beneficial Soil Streptoflora. Curr Microbiol. Dec; 75(12), 1589-1601, Epub 2018 Sep 21, DOI: 10.1007/s00284-018-1565-2.

Bradley D.E. (1967). Ultrastructure of bacteriophage and bacteriocins." Bacteriological reviews vol. 31(4), 230-314, DOI: 10.1128/br.31.4.230-314.1967.

Dobrovol'skaya T.G., Zvyagintsev D.G., Chernov I.Y. et al. (2015). The role of microorganisms in the ecological functions of soils. Eurasian Soil Sc. 48, 959-967, DOI: 10.1134/S1064229315090033.

Dashman T. and Stotzky G. (1984). Adsorption and binding of peptides on homoionic montmorillonite and kaolinite. S. Biol. Biochem. 16, 51-55.

Emerson J.B., Roux S., Brum J.R., Bolduc B., Woodcroft B.J., Jang H.B., et al. (2018). Hostlinked soil viral ecology along a permafrost thaw gradient. Nat Microbiol., 3, 870-80.

Emerson J.B. (2019). Soil Viruses: A New Hope. mSystems, 4(3), e00120-19, DOI: 10.1128/mSystems.00120-19.

Han L.L., Yu D.T., Bi L. et al. (2022) Distribution of soil viruses across China and their potential role in phosphorous metabolism. Environmental Microbiome 17, 6, DOI: 10.1186/s40793-022-00401-9.

Herron P.R. and Wellington E.M.H. (1990). New method for the extraction of streptomycete spores from soil and application to the study of lysogeny in sterile amended and nonsterile soil. Appl. Environ. Microbiol. 56, 1406-1412.

Kauffman K.M., Polz M.F. (2018). Streamlining standard bacteriophage methods for higher throughput. MethodsX., 5,159-172, DOI: 10.1016/j.mex.2018.01.007.

Kurganova I.N., Lopes de Gerenyu V.O., Khoroshaev D.A. et al. (2020). Analysis of the Long-Term Soil Respiration Dynamics in the Forest and Meadow Cenoses of the Prioksko-Terrasny Biosphere Reserve in the Perspective of Current Climate Trends. Eurasian Soil Sc. 53, 1421-1436, DOI: 10.1134/S1064229320100117.

Kuzyakov Y., Mason-Jones K. (2018). Viruses in soil: nano-scale undead drivers of microbial life, biogeochemical turnover and ecosystem functions. Soil Biol Biochem, 127, 305-17.

Lipson S.M. and Stotzky G. (1984). Effect of proteins on reovirus adsorption to clay minerals. Appl. Environ. Microbiol. 48, 525-530.

Lipson S.M. and Stotzky G. (1985). Infectivity of reovirus adsorbed to homoionic and mixed-cation clays. Water Res. 19, 227-234.

Marsh P. and Wellington E.M.H. (1992). Interactions between actinophages and their streptomycete hosts in soil and the fate of phage borne genes. In: Gene Transfers and Environment (Gauthier, M.J., Ed.), 135-142. SpringerVerlag, Berlin.

Marsh P. and E.M.H. Wellington (1994). Phage-host interactions in soil. FEMS Microbiology Ecology 15, 99-108.

Marsh P., Toth I.K., Meijer M., Schilhabel M.B. and Wellington E.M.H. (1993). Survival of the temperate phage FiC31 and Streptomyces lividans in soil and the effects of competition and selection on lysogens. FEMS Microbiol. Ecol. 13, 13-22.

Mitarai N., Brown S., & Sneppen K. (2016). Population Dynamics of Phage and Bacteria in Spatially Structured Habitats Using Phage λ and Escherichia coli. Journal of bacteriology, 198(12), 1783–1793, DOI: 10.1128/JB.00965-15.

Pantastico-Caldas M., Duncan K.E., Istock C.A. and Bell J.A. (1992). Population dynamics of bacteriophage and Bacillus subtilis in soil. Ecologia 73, 1888-1902.

Pedziwilk Z. (1995) The numbers and the fungistatic activity actinomycetes in different soils supplemented with pesticides and organic substances. Pol. J. Soil Sci., 1995, 28, 45-52.

Sykes I.K. and Williams S.T. (1978) Interactions of actinopbage and clays. J. Gen. Microbiol. 108, 97-102.

The Prioksko-Terrasny Nature Biosphere Reserve (2022) Official Website. [online] Available at: http://www.mms.com/ [Accessed 14 Apr. 2022]. https://pt-zapovednik.org/

Trubl G., Jang H.B., Roux S., Emerson J.B., Solonenko N., Vik D.R., et al. (2018). Soil viruses are underexplored players in ecosystem carbon processing. mSystems [Internet], 3, DOI: 10.1128/mSystems.00076-18.

Williamson K.E., Fuhrmann J.J., Wommack K.E., Radosevich M. (2017). Viruses in soil ecosystems: an unknown quantity within an unexplored territory. Annu Rev Virol, 4, 201-19.

Williams S.T., Mortimer A.M. and Manchester L. (1987). The ecology of soil bacteriophage. In: Phage Ecology Goyal S.M., Gerba C.P. and Bitton G., Eds.), 157-179. John Wiley, New York.

Xu L.H., Li Q.R., Jiang C.L. (1996). Diversity of soil actinomycetes in Yunnan, China. Appl. Environ. Microbiol., 62, 244-248.

Zhong L., Cheng Q., Tian X., Zhao L., & Qin Z. (2010). Characterization of the replication, transfer, and plasmid/lytic phage cycle of the Streptomyces plasmid-phage pZL12. Journal of bacteriology, 192(14), 3747-3754, DOI: 10.1128/JB.00123-10.

Zemlyanko I.I., Zablotskaya M.M., Zimin A.A. (2017). Progress in breeding and scientific research in the central European bison nursery of M.A. Zablotsky Prioksky-Terrasny State Biosphere Reserve of the Ministry of Natural Resources of the Russian Federation – 2017. European Bison Conservation Newsletter, 10, 103-108.

RESEARCH PAPER

PATTERNS OF THE RED-LISTED EPIPHYTIC SPECIES DISTRIBUTION IN CONIFEROUS-DECIDUOUS FORESTS OF THE MOSCOW REGION

Tatiana V. Chernenkova[1*], Nadezhda G. Belyaeva[1], Elena G. Suslova[2], Ekaterina A. Aristarkhova[2], Ivan P. Kotlov[3]

[1] Institute of Geography of the Russian Academy of Sciences Staromonetniy pereulok, 29, 119017, Moscow, Russia
[2] M.V. Lomonosov Moscow State University, Faculty of Geography, Department of Biogeography, Leninskiye Gory, 1, 119991, Moscow, Russia
[3] A.N. Severtsov Institute of Ecology and Evolution of the Russian Academy of Sciences Leninsky Prospect, 33, 119071, Moscow, Russiaa
***Corresponding author:** chernenkova50@mail.ru
Received: May 27th, 2022 / Accepted: February 15th, 2023 / Published: March 31st, 2023
https://DOI-10.24057/2071-9388-2022-101

ABSTRACT. Epiphytes model the diversity of forest communities and indicate the integrity of natural ecosystems or the threat to their existence. The high sensitivity of epiphytic species to the environmental quality makes them good indicators in anthropogenic landscapes. The study deals with the distribution patterns of rare indicator epiphytic species at the border of their range in the broad-leaved–coniferous forest zone, in the central part of the East European Plain within the Moscow region. The distribution and abundance of eight lichen species *Anaptychia ciliaris, Bryoria fuscescens, B. implexa, Usnea dasopoga, U. glabrescens, U. hirta, U. subfloridana* and the epiphytic moss *Neckera pennata* were studied. The main environmental factors at the regional level were climate variables based on the Worldclim database, water indices based on Sentinel-2 multispectral remote sensing data, and the anthropogenic impact factor in terms of the Nighttime lights of the earth's surface based on the Suomi NPP satellite system. It was revealed that the vast majority of records were in the western and northern sectors of the region, i.e. in the broad-leaved–coniferous forest zone, while the vast majority of 0-records were in the southern and eastern sectors, in the area of broad-leaved and pine forests and extensive reclaimed wetlands. The association with different types of communities and biotopes, as well as tree species, was assessed at the ecosystem level, using field data. It has been established that the distribution of the studied species is governed by natural-geographic features of the territory. The principal limiting factors are air pollution, ecological restrictions (high humidity requirement of sites), cutting of mature forests and formation of local anthropogenic infrastructure. In perspective the study of ecology and living conditions of the studied rare species will help determine the optimal conditions contributing to biodiversity conservation in forests near large metropolitan areas and optimization of habitat diversity.

KEYWORDS: the red-listed epiphytic, forests, bioindicators, climate, anthropogenic impact, community ecology, biotope, urbanized landscapes, Moscow region

CITATION: Chernenkova T. V., Belyaeva N. G., Suslova E. G., Aristarkhova E. A., Kotlov I. P. (2023). Patterns of the red-listed epiphytic species distribution in coniferous-deciduous forests of the Moscow Region. Geography, Environment, Sustainability, 1(16), 119-131
https://DOI-10.24057/2071-9388-2022-101

ACKNOWLEDGEMENTS: The authors would like to thank the non-commercial Verkhovye Conservation Fund (www.verhovye.ru) for organizing field surveys and providing materials; and T.Yu.Tolpysheva, E.E. Muchnik, and I.N. Urbanavichene for identifying species of epiphytic lichens.

Conflict of interests: The authors reported no potential conflict of interest.

INTRODUCTION

The long-term transformation of forest cover is accompanied by a wide range of disturbances at the ecosystem and species levels of organization. Biodiversity change occurs mainly due to the reduction in the area and quality of sites, forest silviculture, decreasing number of native species, and introduction of alien species (Maron and Marler 2008; Aerts and Honnay 2011; Jönsson et al. 2011; Vilà et al. 2011; Lanta et al. 2013; "The Problem of Biodiversity Loss | Saving Earth | Encyclopedia Britannica," n.d.; "Threats to Biodiversity | GEOG 30N: Environment and Society in a Changing World," n.d.). The absence or declining numbers of rare organisms in suitable biotopes is a first sign of disturbance of native ecosystems (Barkman 1969; Case 1980; Folkeson and Andersson-Bringmark 1988; Hauck et al. 2013; Blackburn et al. 2019) indicating a certain threat to the integrity and the very existence of natural ecosystems (Hanski and Ovaskainen 2000).

For the forest community as a whole, the presence of epiphytic lichen and moss cover is very important, providing and maintaining biodiversity and «fullness» of the ecosystem. First of all, they indicate satisfactory air quality; then, their presence indicates the complexity and diversity of forest communities; and finally, such epiphytes fulfill certain ecosystem functions (Pettersson et al. 1995; Antoine 2004; Gunnarsson et al. 2004; Glime 2007).

Traditionally, many species of epiphytic mosses and lichens are considered as objects of indication and monitoring of air quality (Barkman 1969; LeBlanc et al. 1974; Scott and Hutchinson 1990; Byazrov 1994; Chernenkova 2002). More than half a century ago, it was noted that along with the higher pollution levels, the factor of drying, or aridization, could also increase the death of lichens and mosses in a large city (LeBlanc and Sloover 1970). The fact is that lichens and bryophytes are unable to regulate their water status by themselves with the help of a specialized system, available in vascular plants. Instead, they respond directly to environmental conditions, saturating their thalli or tissues with water when it is available, losing it also very quickly, and withstanding desiccation during dry periods. It is this flexibility to adapt to rapid environmental changes that makes such organisms well suited to epiphytic lifestyles (Kranner et al. 2008; Ellis et al. 2015). However, under high temperature and low air humidity, most lichen species seize their physiological activity. This happens at 20% or less saturation of the lichen thallus with moisture (Hawksworth and Rose 1970). Mosses are even worse adapted to droughts than lichens. The study of a wider range of distribution features of cryptogamic organisms makes it possible to assess the level of air pollution, as well as to identify the limiting ecological-coenotic conditions of the habitat, including the ecological state of forests, or inadequate forest management (Johansson and Gustafsson 2001; Boudreault et al. 2008).

Particular environmental features manifest themselves at different hierarchical levels, with dissimilar influence of physiographic (upper level) and biotopic (lower level) factors (Ellis and Coppins 2009; Ellis et al. 2015). For example, the most species of epiphytic lichens and bryophytes are recorded in the northern Holarctic and just sporadically to the south, along the large swamps on the Russian Plain, thereby indicating their obvious relationship with climatic parameters (Ignatov 1993; Shafigullina 2012). There is some evidence that a number of epiphytic lichens tend to open habitats (Halonen and Puolasmaa 1995; Suslova et al. 2017). At the same time, *Bryoria nadvornikiana* grows more slowly in the forests of Quebec under habitat openness of more than 40%, and for *Evernia mesomorpha* it happens under more than 70% openness (Boudreault et al. 2013). Studies of broad-leaved forests in the northwestern part of Germany found that the number of epiphytic lichens has significantly decreased over 100–150 years due to smaller numbers of over-mature and decay trees, lesser soil moisture, as well as deposition of sulfur and nitrogen compounds from the atmosphere (Hauck et al. 2013). The fact that some lichens give preference to certain tree species is also widely reported in the literature (Wirth 1995; Golubkova 1996a 1996b; Tolpysheva and Suslova 2019). Moreover, some species of epiphytes are thought to depend on microbiological habitats that are uniquely associated with the properties of the bark of old trees in late successional forests (Ellis 2012; Ellis et al. 2015; Notov and Zhukova 2015; Llewellyn et al. 2020). *Bryoria capillaris* in the UK (Rose 1976) and *B. nadvornikiana* in Sweden (Karström 1992) are thought to be indicators of mature indigenous forests. The presence of the rare lichens definitely proves the maturity of the stands and favorable environmental conditions for their growth.

An inventory of rare epiphytic cryptogamic organisms makes it possible to find out that the distribution of these organisms is closely associated with the remaining undisturbed forests, including those within the protected areas. This is particularly important for the natural environment of the Moscow region, in terms of the preservation of species and coenotic diversity of forest cover. The Red Data Book of the Moscow Region (2018) (*Red Data Book of the Moscow Region 2018*) includes 25 moss species and 40 rare lichen species out of 334 and 355 species, respectively, which were recorded in the region during the period of its study since the early 19th century. However, just few of them are characteristic of the least disturbed mature coniferous stands of the zonal type, as well as swamps and the margins of wetlands and peatlands. A number of studies deal with the distribution of certain species of epiphytic lichens and mosses in the Moscow region (Suslova et al. 2017; Tolpysheva et al. 2017; Tolpysheva and Suslova 2019); however, their ecological conditions have not been identified in full, and the patterns and factors of their distribution are not statistically confirmed.

The purpose of the study was to establish patterns of distribution of the red-listed epiphytic species on the southern border of the coniferous-deciduous forest zone in the East European Plain as in the case of the Moscow region. The following tasks were completed: 1) collection of data on the distribution and abundance of rare epiphytic forest species; 2) study of the influence of the principal environmental factors (climatic, coenotic, biotopic), explaining the variability in the distribution of species at different spatial levels; 3) assessment of the contribution of anthropogenic factor to the distribution patterns of the studied rare species; 4) identification of the preferability of the studied species in the indication of suitable habitats within an anthropogenic landscape.

MATERIALS AND METHODS

Study area

The Moscow region is a territory in the central part of the East European Plain with an area of 4.58 million hectares (Fig. 1). After the expansion of administrative boundaries in 2012, Moscow has moved from 11th to 6th place in the ranking of the world's largest cities in terms of the area, and the pressure on the region has increased significantly because of the transport infrastructure and construction. The diversity of forest cover in the study area has been formed over the past 100–150 years mainly through spontaneous natural succession within former arable lands or forest cuttings, as well as a result of pine and spruce planting. Silviculture has partially changed the ecological and coenotic features of zonal coniferous and broad-leaved-coniferous communities and the boundaries of their range.

The main part of the Moscow region is located within the zone of coniferous-deciduous forests; a border with the zone of deciduous forests goes through the south of the region (Petrov 1968; Kurnaev 1973). Despite the relatively high forest cover percentage (above 50%), the present-day forest cover is very mosaic and includes a large area of secondary forests with small-leaved species; most of the latter arose from forest plantations (Chernenkova et al. 2019). However, broad-leaved–coniferous, nemoral spruce, subnemoral and boreal forests, as well as broad-leaved forests close to natural zonal ones, have been preserved on

the territory due to the protection status of forests. Spruce (*Picea abies*), pine (*Pinus sylvestris*), birch (*Betula* spp.), aspen (*Populus tremula*), oak (*Quercus robur*), and linden (*Tilia cordata*) are the principal tree species in the forests near Moscow.

According to the schematic map of climatic provinces and regions of Europe, the Moscow region is classified as a temperate continental region (Rivas-Martínez et al. 2004). The mean annual air temperature is 2.7°-3.8° C, the annual precipitation is 479–644 mm. The relief of the territory is in general gently hilly, the heights vary slightly from 90 to 320 m a.s.l., on average 174 m a.s.l., the mean slope is 2.06° (0 to 30.9°). Variations of the main climatic characteristics within the physiographic provinces (PgP) of the Moscow region: 1 – Verkhnevolzhskaya, 2 – Moskovskaya, 3 – Smolenskaya, 4 – Moskvoretsko-Okskaya, 5 – Mescherskaya, 6 – Zaokskaya and 7 – Srednerusskaya (Annenskaya et al. 1997), are shown in Fig. 2. In general, the temperature and precipitation gradient is sub-latitudinal.

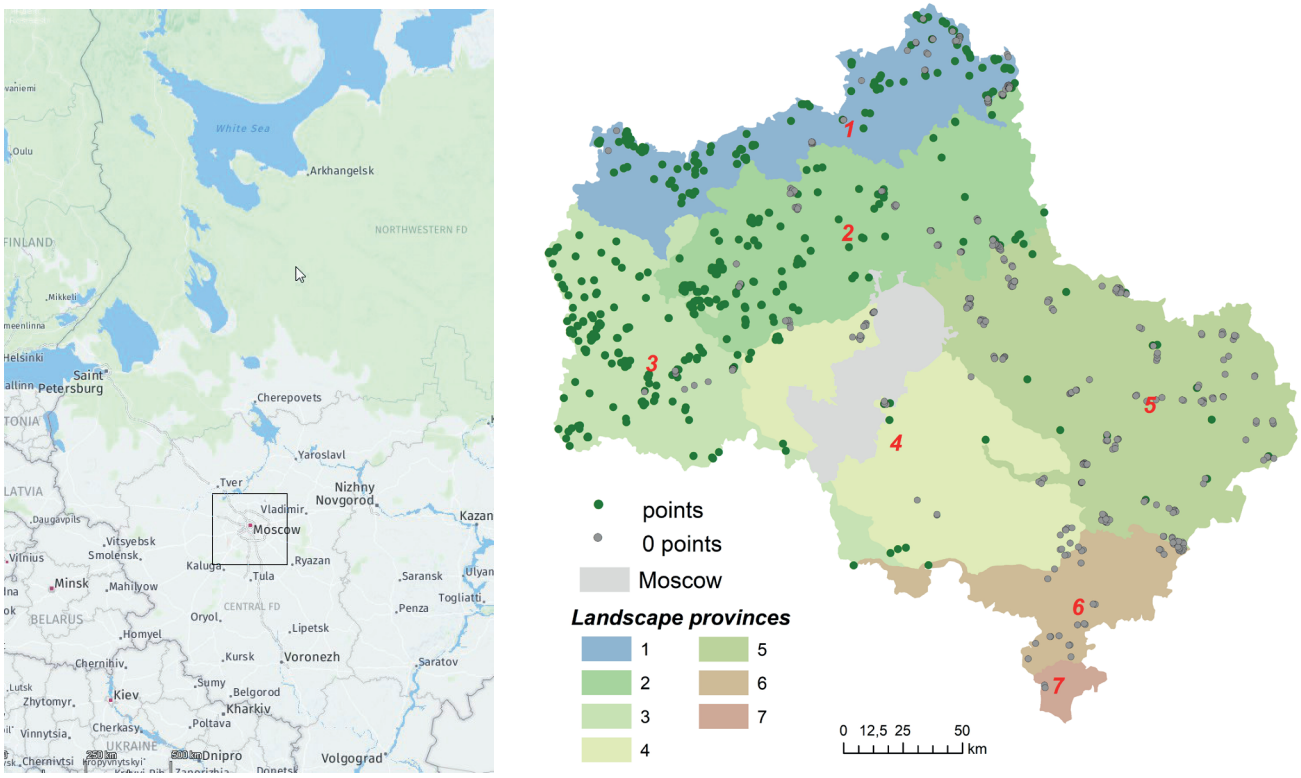

Fig. 1. Location of observation points within the physiographic provinces (PgPs) of the studied territory. 1 – Verkhnevolzhskaya, 2 – Moskovskaya, 3 – Smolenskaya, 4 – Moskvoretsko-Okskaya, 5 – Mescherskaya, 6 – Zaokskaya and 7 – Srednerusskaya (Annenskaya et al. 1997).

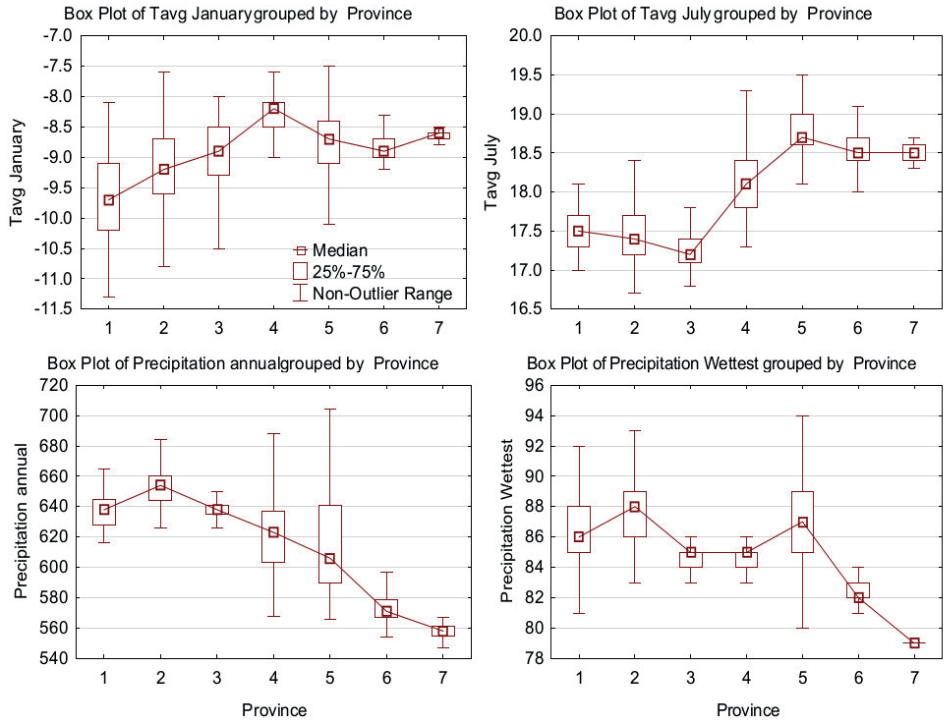

Fig. 2. Climatic characteristics of the Moscow region – the mean temperature of the coldest month ($T_{avg\ jan}$) (A) and the mean temperature of the warmest month ($T_{avg\ july}$) (B), annual precipitation (C) and precipitation of the warmest month (D)

Sampling methods

The following red-listed epiphytic lichen species: *Anaptychia ciliaris, Bryoria fuscescens, B. implexa, Usnea dasopoga, U. glabrescens, U. hirta, U. subfloridana*, as well as the epiphytic moss *Neckera pennata* were used as indicators of the state of forests. All these species are listed in the Red Data Book of the Moscow Region (2018) (*Red Data Book of the Moscow Region 2018*) (Figure 3). Compared to the rest of the red-listed epiphytic species, these species are noted not singly, which gave us reason to use them in statistical analysis in accordance with the objectives of the study.

The territory under study, including more than 150 Nature Protection Area (NPA), among them several newly organized ones, was surveyed by the route method. Surveys and sampling were carried out on the trunks and branches of trees at a height of 0-2 m from the ground. The territory of the city of Moscow was excluded from the survey.

When studied rare species were recorded, they were assessed in terms of the following characteristics: type of plant community, type of biotope, tree species, nature of anthropogenic disturbance, location within a SPNA. A scale for the abundance of particular species within the area of 1 km^2 was developed based on the expert assessment: 0 – the absence of species (378 sites in all), 1 – rarely and sporadically, 2 – occasionally in groups, 3 – very often and abundantly.

The total number of records of the above-mentioned eight species was 875, of which epiphytic lichens were found in 730 sites, and the moss *Neckera pennata* in 145 sites (Table 1).

The collected lichen samples were determined in the laboratory by standard lichenological methods (Golubkova 1996a 1996b; Muchnik et al. 2011) using a binocular and a set of chemicals. Samples of *Bryoria* spp. were confirmed basing of the analysis of secondary metabolites by thin layer chromatography (TLC) at the laboratory of lichenology and bryology of the BIN RAS.

Fig. 3. Photo of the red-listed epiphytic species. a – *Anaptychia ciliaris*, b – *Bryoria* spp., c – *Usnea* spp., d – *Neckera pennata (photo E.G. Suslova)*

Table 1. Numbers of records of the studied species (n)

n	Species	Species code
27	*Anaptychia ciliaris*	An cil
247	*Bryoria fuscescens*	Br fus
45	*Bryoria implexa*	Br imp
145	*Neckera pennata*	N pen
125	*Usnea dasopoga*	Us das
24	*Usnea glabrescens*	Us gla
202	*Usnea hirta*	Us hir
60	*Usnea subfloridana*	Us sub

Data analysis

The influence of principal environmental factors explaining the uneven distribution of cryptogamic epiphytic species was analyzed at different spatial levels, namely regional, coenotic, and biotopic. A hypothesis for the uniform distribution of species within the indicated spatial units was evaluated using the frequency analysis (observed frequencies were compared with expected uniform ones) according to the Chi-Square statistics (Statistica 12), taking into account critical values for probability level (0.05) and degrees of freedom.

Region level

The distribution of studied rare species was investigated over the entire geographic space of the Moscow region within the boundaries of seven PgPs (Figure 1).

To assess the influence of environmental factors, the correlation between species distribution and climatic characteristics was spatially analyzed using the Worldclim database with the spatial resolution of 1x1 km (Fick and Hijmans 2017). The autocorrelation analysis was applied to select the least correlated predictor variables (correlation level not more than 0.5) from a complete set of 48 monthly climatic characteristics; these are January temperature ($T_{avg\ jan}$), March temperature ($T_{avg\ march}$), May temperature ($T_{avg\ may}$), March precipitation ($P_{avg\ march}$), and April precipitation ($P_{avg\ april}$).

The NDWI spectral index (Normalized difference water index) (McFeeters 1996) was used as an ***indicator of environmental moisture*** (vegetation and soil). The index is calculated based on the cloudless Sentinel-2 multispectral mosaic compiled from images of June 18 and 20 2021.

$$NDWI = \frac{B03 - B08}{B03 + B08}$$

The ***anthropogenic impact*** factor was estimated using remote information on the nighttime brightness of the Earth's surface according to the VIIRS satellite data (VNP46A3/VJ146A3 Monthly and VNP46A4/VJ146A4 Yearly Moonlight-adjusted Nighttime Lights (NTL) Product) (Wang et al., n.d.). The nighttime brightness correlates well with the consumption of primary energy resources at the regional level (Tronin et al. 2014). It is assumed that Nighttime lights mark a number of anthropogenic pressure parameters, such as population density, recreational load, and atmospheric pollution. The following independent variables have been used:

- night illumination ($W \cdot cm^{-2} \cdot sr^{-1}$),
- distance to objects with illumination over 100 $W \cdot cm^{-2} \cdot sr^{-1}$,
- azimuth to the same objects with illumination over 100 $W \cdot cm^{-2} \cdot sr^{-1}$,
- distance and azimuth to the center of Moscow.

After excluding correlated variables, we chose from the above-listed three types of data, i.e. climate, NDWI, and nighttime luminosity, the variables that differentiate the studied rare species based on F-statistics (ANOVA). The multiple linear regression method (Statistica 12) was used to evaluate the most significant factors governing the occurrence and abundance of different species; the points where the species are absent were also taken into account.

Community level

The frequency analysis was applied to study the allocation of the studied rare species within various types of forests; 33 types of communities identified on the basis of the previously developed ecological-coenotic approach (Chernenkova et al. 2020) were analyzed. The type of community was determined according to the canopy composition (vertical column) and ground layers of vegetation, i.e. herb and moss layers (Table 2). The presence of species within four non-forest habitat types (Small leaf scrub, Cuts, Meadows and Open marshy habitat) was also taken into account.

Table 2. Forest community types

Tree layer	Ground layers								
	Dwarf shrubs–small herb–green moss	Small herb	Small herb–broad herb	Broad herb	Moist herb –broad herb	Grass-marsh	Meadow herb	Dwarf shrubs–herbal-sphagnum	Non-forest land cover types
Spruce	1	2	3	4					
Spruce – aspen/ birch	5	6	7	8					
Pine – spruce	9	10	11	12					
Pine	13	14	15	16			17	18	
Oak - spruce				19					
Broad leaf – spruce				20					
Linden				21					
Birch		22	23	24	25	26	27	28	
Aspen				29	30				
Grey alder					31				
Black alder					32	33			
Small leaf scrub									34
Cuts									35
Meadows									36
Open marshy habitats									37

Biotope level

Distribution of the studied rare species was assessed based on the frequency analysis within five main biotope types:

1 – forests of fresh habitats (mesotrophic forests) are groups of plant communities of sufficiently drained habitats with predominance of mesophytes. They are small herb, small herb–broad herb, broad herb spruce, and broad leaf–spruce, spruce–pine, and pine dwarf shrubs–small herb–green moss and spruce–aspen/birch forests. The shrubs, such as *Corylus avellana*, and *Lonicera xylosteum*, often form a well-defined layer. *Oxalis acetosella, Lamium galeobdolon, Carex pilosa, Asarum europaeum, Luzula pilosa, Vaccinium myrtillus*, etc. are typical plant species of the herb-shrub layer.

2 – forests of humid habitats (humid forests) are spruce, pine–spruce, pine, spruce–aspen/birch and small-leaved (aspen/birch/alder) moist herb–broad herb and fern–moist herb forests of shallow flat depressions with a water confining stratum. *Polytrichum commune* and *Sphagnum* spp. mosses are present in such coniferous forests in addition to *Bryidae* green mosses and *Vaccinium myrtillus* is abundant. The herb layer of small-leaved, aspen and alder, forests is dominated or co-dominated by hygromezophyte species (*Athyrium filix femina, Deschampsia cespitosa, Cirsium heterophillum, Crepis paludosa*) and some hygrophytes (*Filipendula ulmaria*).

3 – wetlands and peatlands with pine, birch, spruce undergrowth with *Carex* spp., *Sphagnum* spp., *Eriophorum vaginatum* and dwarf shrubs.

4 – opening in the forest, forest edge, clearing, road (marks the degree of illumination).

5 – local swampy depression, forest on the outskirts of a swamp, watercourse bed (marks the degree of moisture). This group of biotope types is represented by swamp *Polytrichaceae* moss, herbal-sphagnum and grass–marsh coniferous, coniferous–small-leaved and small-leaved forests of waterlogged depressions and the margins of wetland forests on the border with marshes, as well as forest-marsh complexes with alternation of willow-birch wetlands and wetlands with spruce, pine and grey or black alder. Floodplain coniferous-small-leaved and small-leaved moist herb and grass-marsh forests of small rivers and streams with spruce, black or grey alder, with *Padus avium*, and tree and shrub willows are also included in this type. Such habitats are found on the slopes and bottoms of forest ravines.

RESULTS

Region level

The frequency of records of the studied rare species under study varied considerably. *Anaptychia ciliaris, Bryoria implexa, Usnea subfloridana,* and *U. glabrescens* were the rarest among the listed lichen species (Table 1). Species abundance on the area of 1 km^2 also varied greatly in the range of 1.3 to 1.8 points. Such species of epiphytic lichens as *Anaptychia ciliaris, Bryoria fuscescens, Usnea dasopoga, U. hirta* and *U. subfloridana* in most cases form isolated groups with the abundance of more than 1.6 points. The rare and sporadic presence, or occasional in small groups, is characteristic of *Bryoria implexa, Usnea glabrescens* and *Neckera pennata* species (Fig. 4).

The distribution of species within the study area is extremely uneven (Fig. 1, 5). The overwhelming number of records was in the western and northern sectors, i.e. within

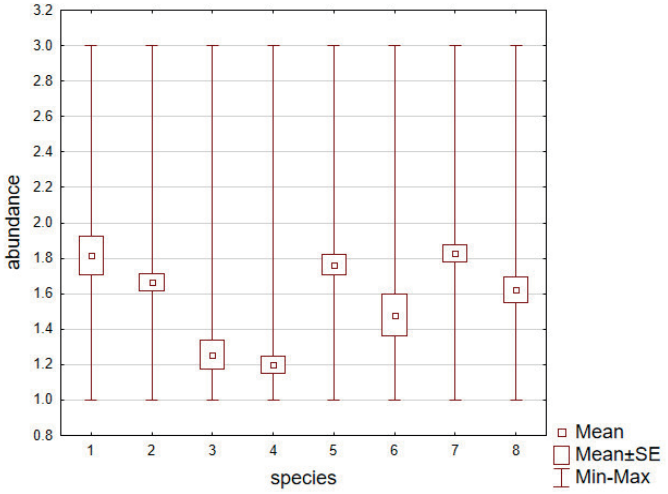

Fig. 4. Variations in the abundance of the studied rare species according to a three-point scale. The species codes are given in Table 1

#1-3 PgPs, very small number of occurrences in #4 and 5, and the absence in #6 and 7, which are characterized by increased mean annual temperatures and less precipitation (Fig. 2). Many habitats suitable for the studied rare species but lacking them totally (0-points) were recorded in the south and southeast sectors of the region (Fig. 1).

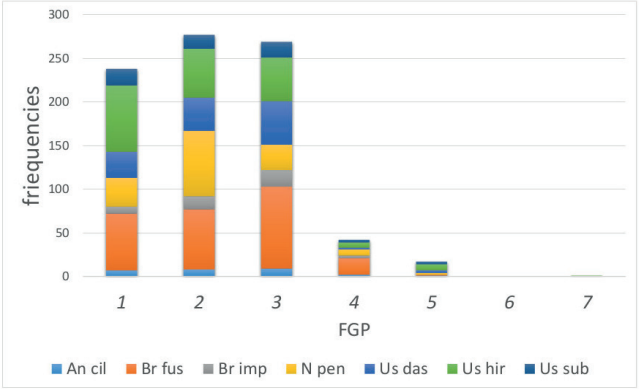

Fig. 5. Distribution of rare species within PgPs: 1 – Verkhnevolzhskaya, 2 – Moskovskaya, 3 – Smolenskaya, 4 – Moskvoretsko-Okskaya, 5 – Mescherskaya, 6 – Zaokskaya и 7 – Srednerusskaya (Annenskaya et al. 1997)

Specific distribution of particular studied rare species was noted (Fig. 5, Table 3). Thus, *Usnea hirta* and *U. subfloridana* are limited to the Verkhnevolzhskaya, Moskovskaya and Smolenskaya provinces (#1–3). Bryoria implexa is more common in the west of the region, i.e. in the Smolenskaya and Moskovskaya provinces (#2,3); *B. fuscescens* and *Usnea dasopoga* – in the Moskovskaya province (#2), and *Neckera pennata* in the Smolenskaya province (#3). Thus, a significant correlation was confirmed for almost all species, mainly with three PgPs (#1,2 and/or 3). Singular records of *Bryoria* and *Usnea* species in the SE part (the broad-leaved forests zone) were due to the absence of natural forest stands, where the studied species could be found. *Bryoria fuscescens* and *Usnea dasopoga* lichens were rarely recorded on isolated old birches.

To understand the nature of epiphyte distribution trends, independent climate variables with significant inter-group differences (ANOVA) were analyzed. As a result, we obtained significant climatic characteristics at the sites where epiphytic organisms were recorded, in addition to the average values of $T_{avg\ jan}$, $T_{avg\ july}$, Annual precipitation, and Precipitation of warmest month within PgPs. Such variables include temperatures in March ($T_{avg\ march}$) and May ($T_{avg\ may}$), and precipitation in March ($P_{avg\ march}$) and April ($P_{avg\ april}$) (Table 4).

Table 3. Results of frequency analysis of species distribution within PgPs

Species	χ^2	*p*	*df*	Class_number
Anaptychia ciliaris	9.851852	0.043001	4	1, 2, 3
Bryoria fuscescens	118.6129	0.00000	4	3
Bryoria implexa	13.57778	0.00354	3	2, 3
Neckera pennata	114.5479	0.00000	4	2
Usnea dasopoga	74.43902	0.00000	4	3
Usnea glabrescens	6.608696	0.036724	2	3
Usnea hirta	155.9796	0.00000	5	1, 2, 3
Usnea subfloridana	22.27119	0.000177	4	1, 2, 3

Table 4. Environment Variables (F-test, ANOVA)

	F	*df*	*p*
Climate Variables			
$T_{avg\ march}$	2.7784	7	0.0073
$T_{avg\ may}$	2.1190	7	0.0393
$P_{avg\ march}$	4.6633	7	0.00004
Pavg april	2.8001	7	0.0069
Water index			
NDWI	7.3821	7	0.00000
Anthropogenic pressure			
azim_0km	3.5788	7	0.0008
azim_light_100	2.4126	7	0.0189
dist_0km	3.4047	7	0.0014

To identify the importance of environmental moisture for epiphytic species, the values of the NDWI humidity index were involved in the analysis. The distribution of epiphytic organisms showed a significantly high level of correlation with the humidity index (Table 4).

Among the factors of anthropogenic pressure, the intergroup differences were revealed for azimuth to the center of Moscow (azim_0km), azimuth to objects with illumination over 100 $W \cdot cm^{-2} \cdot sr^{-1}$ (azim_light_100) and distance to the center of Moscow (dist_0km) (Table 4).

It is interesting, that no trend of recording rare species of epiphytic organisms within the existing network of NPA has been established. Moreover, Bryoria fuscescens was often recorded outside the boundaries of protected areas (Table 5).

Community level

When considering the total number of species records in different types of communities, in more than 70% of cases

Table 5. Results of frequency analysis of the NPA

Species	χ^2	*p*	*df*	Class_number
Anaptychia ciliaris	1.81481	0.177933	1	
Bryoria fuscescens	10.8160	0.001006	1	0 outside NPA
Bryoria implexa	1.08889	0.296718	1	
Neckera pennata	2.45578	0.117094	1	
Usnea dasopoga	0.968	0.325180	1	
Usnea glabrescens	1	0.317311	1	
Usnea hirta	0.32	0.571608	1	
Usnea subfloridana	0.26667	0.605577	1	

the preference is for spruce, pine and birch communities with a diverse composition of the ground layer, from boreal, subnemoral and nemoral to mesotrophic and oligotrophic types of community (Fig. 6).

At the same time, it is noticeable that certain types of epiphytic lichens are significantly more common in a limited range of forest types with highly humid habitat conditions. For example, *Anaptychia ciliaris, Bryoria fuscescens* and *Usnea dasopoga* are often found in birch grass-marsh forests (#26). *Bryoria fuscescens* and *Usnea dasopoga* are also characteristic of spruce small herb–broad herb forests (#3). *Usnea hirta* mostly grows in the peatlands with pine or birch (#18,28). The *Neckera pennata* epiphytic moss is most found in small herb–broad herb or broad herb spruce forests (#3,4) (Table 6).

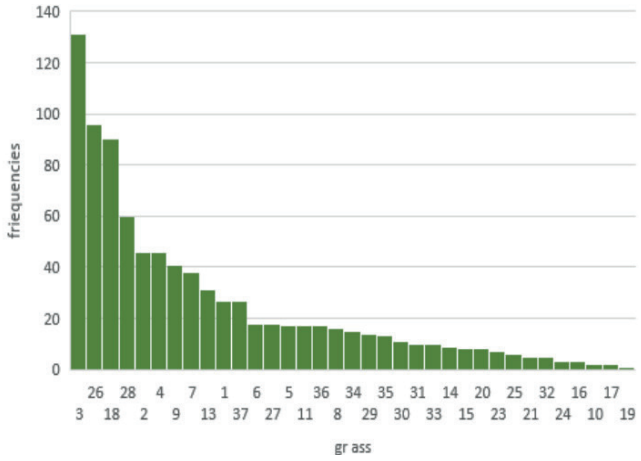

Fig. 6. Distribution of indicator species within different types of communities. Group numbers of community types are given in Table 2

Thus, the hypothesis for the uniform distribution of species in different types of communities was not confirmed in most cases. *Usnea glabrescens, Bryoria implexa* and *Usnea subfloridana* are not limited in their distribution to certain types of communities.

Biotope level

At the lowest spatial level (biotopes), all species of *Bryoria* genus and *Usnea dasopoga* are limited to humid forests (#2) and *U. hirta* to swamp forests (#3), while *Neckera pennata* grows in the least humid forest types of biotopes (mesotrophic forests) (#1). *U. subfloridana* was recorded evenly in all biotopes except for #5, where only one record was made (Fig. 7, Table 7).

Mesotrophic and humid forest biotopes (#1,2) rank first in the total number of records. This is obviously explained by a large area of these types of sites. The margins of peatlands and wetlands (#3) with spruce undergrowth are quite rich in epiphytic lichens; spruce branches host large numbers of *Usnea* spp. and *Bryoria* spp. *Anaptychia ciliaris* and *Neckera pennata* are absent from these sites.

The formation of biotope #4 can be logically assessed as a result of anthropogenic disturbance caused by the local forest cutting and creating ecotone conditions. Favorable conditions for the development of many epiphytic lichens, which urgently need sufficient light, are created within dampish and swampy forest edges, and also swampy glades, clearings, and power lines. Narrow forest roads and rather narrow clearings usually have higher numbers of individuals and species of *Usnea* spp. and *Bryoria* spp., which receive sufficient moisture and light there. Rarer occurrence of epiphytic species was observed at the edges of watershed forests and upland meadows, where epiphytic organisms are exposed to the desiccation factor because of excessive light and wind. Only *Usnea hirta* and *U. dasopoga* were sporadically recorded within such edges in the lower part of the trunks of old birches.

Despite favorable microclimate in habitats (#5), where both soil and atmospheric air are more humid, the frequency of occurrence of epiphytic lichens and mosses is low.

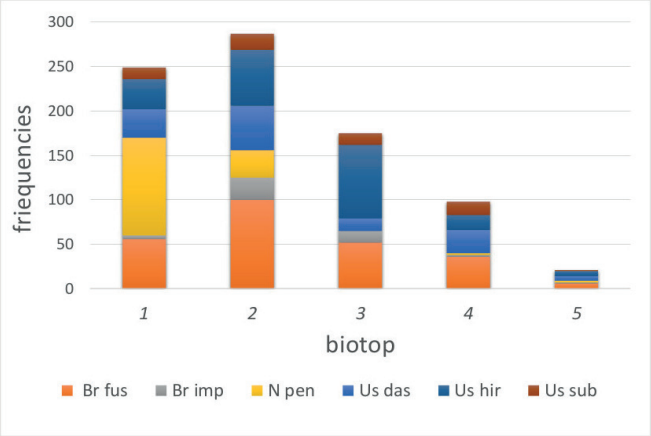

Fig. 7. Distribution of studied rare species in different types of biotopes

1 – fresh forest (mesotrophic forest), 2 – wet forest (humid forest), 3 – wetlands and peatlands, 4 – opening in the forest, forest edge, clearing, road (marks the degree of illumination), 5 – local swampy depression, outskirts of a swamp, watercourse bed (marks the degree of moisture).

Table 6. Results of frequency analysis within types of communities

Species	χ^2	*p*	*df*	Class number
Anaptychia ciliaris	54.63704	0.00000	7	26
Bryoria fuscescens	**341.408**	0.00000	26	3, 26
Bryoria implexa	25.51111	0.111482	18	
Neckera pennata	**217.6207**	0.00000	19	3, 4
Usnea dasopoga	133.2205	0.00000	23	3, 26
Usnea glabrescens	10.88	0.539231	12	
Usnea hirta	**373.7241**	0.00000	24	18, 28
Usnea subfloridana	28.93333	0.146786	22	

Table 7. Results of frequency analysis within biotopes

Species	χ^2	*p*	*df*	Class_number
Anaptychia ciliaris	8.222222	0.01639	2	2, 4
Bryoria fuscescens	93.44	0.00000	4	2
Bryoria implexa	45.55556	0.00000	4	2
Neckera pennata	215.5241	0.00000	3	1
Usnea dasopoga	7.05512	0.00000	4	2
Usnea glabrescens	9.4	0.024421	3	1, 2
Usnea hirta	100.9163	0.00000	4	3
Usnea subfloridana	14	0.007296	4	all except 5

Distribution of all epiphytes, except *Usnea glabrescens,* demonstrates that they are limited to a certain tree species (substrate type). Most of the studied rare species are found on the trunks and branches of spruce, and *Anaptychia ciliaris* and *Neckera pennata* prefer the trunks of old aspens 45-50 cm in diameter. Other tree species host far fewer studed epiphytic lichens and mosses (Table 8)

Discussion

The study focuses on identifying patterns in the distribution of rare epiphytic cryptogamic organisms within the territory of the Moscow region, the area of active development in recent decades. Variability in the distribution of different types of epiphytic lichens and mosses is well marked by the environmental features that correspond well to the original and published data.

4.1. Regional level

It is shown that distribution of the studied species within the territory of the Moscow region is extremely uneven and is clearly subject to natural patterns (Fig. 1, 5). It was revealed that the vast majority of records were in the western and northern sectors of the region, within the broad-leaved–coniferous forest zone, while the 0-point predominately concentrate in the southern and eastern sector, i.e. the area of broad-leaved forests. Based on the χ^2 criterion, a statistical correlation with three types of landscapes (#1–3) was confirmed, which have the lower temperatures of the coldest and warmest months and the maximum mean annual precipitation (Fig. 2). At the same time, one cannot deny the warming effect of the urban climate of the city of Moscow within landscape province #4, particularly in terms of the January temperature pattern, which was discussed in other publications (Varentsov et al. 2017). The fact of climate controlled distribution of lichens has been noted in other works (Cardós et al. 2017; Ellis 2019).

The analysis of 48 climate variables from the Worldclim database (Fick and Hijmans 2017) showed that distribution of the studied rare species is significantly determined by temperature and precipitation. The use of NDWI values for the summer period made it possible to link the points of species records with increased moisture content in habitats. This is another fact emphasizing the importance of the indicator, which during dry periods limits the existence of epiphytic organisms in the temperate zone (Hauck et al. 2013).

What is the **role of anthropogenic factor** in the distribution of epiphytic organisms within the forests of the region? A hypothesis for the principal importance of such indicators as the distance and direction from large urbanized systems, which determine the degree of air pollution, was confirmed. By applying the linear regression method, it was shown that the distribution and abundance of studied rare species is largely effected by the factor azim_0km - (direction to the city of Moscow); the factor showed the maximum coefficients of determination R2 for almost all species (Table 8). Obviously, the atmospheric transport of pollutants is determined by the prevailing SW winds in the region ("Weather in Moscow by months," n.d.), which results in the predominant distribution of epiphytes in the W, N, and N-W sectors of the region, in the "shadow" of the city of Moscow (Fig. 1). The factor of pollutant transfer from other large urban settlements (azim_osv_100) is no less significant. It was calculated using the original technique for assessing the level of anthropogenic pressure

Table 8. Results of frequency analysis in terms of substrate (tree species)

Species	χ^2	*p*	*df*	Tree species
Anaptychia ciliaris	16.33333	0.000053	1	*Populus tremula*
Bryoria fuscescens	1337.419	0.000000	8	*Picea abies*
Bryoria implexa	79.57143	0.000000	3	*Picea abies*
Neckera pennata	539.0884	0.000000	4	*Populus tremula*
Usnea dasopoga	550.1791	0.000000	9	*Picea abies*
Usnea glabrescens	10.96296	0.026985	4	
Usnea hirta	533.751	0.000000	7	*Picea abies*
Usnea subfloridana	114.8485	0.000000	7	*Picea abies*

through the night illumination index of large urban objects (Tronin et al. 2014). The proximity to the center of Moscow (dist_0km) showed lower coefficients of determination, which could be explained by specific features of species distribution due to natural factors in accordance with pronounced zoning (Petrov 1968; Kurnaev 1973).

The studied **rare species are different** in the response of their distribution to environmental factors. The results of the multiple linear regression analysis showed that the influence of a combination of factors at the regional level was most pronounced for *Usnea hirta* (R2=0.549), *Usnea dasopoga* (R2=0.453) and *Neckera pennata* (R2=0.428), while for other species the R2 determination value was less, from 0.323 to 0.131 (p=0.005) (Table 8).

As for particular variables, the highest values of the coefficient of determination were for *Anaptychia ciliaris* and *Neckera pennata* by dist_0km, which characterizes the distance to the center of Moscow (Table 8). Unlike other species, the moss *Neckera pennata* demonstrated the negative correlation with the effect of the variable dist_0km, and positive one with azim_0km, which could result from the substrate eutrophication due to the deposition of nitrogen compounds from the atmosphere near Moscow (Averkieva and Priputina 2011; Bednova 2017). Sporadic records of *Neckera pennata* are known even from several old parks in Moscow and the Moscow region (oral communication by E.G. Suslova). A high negative correlation with the azim_0km variable is characteristic of the distribution of epiphytic lichens *Anaptychia ciliari* and *Usnea* spp., indicating higher sensitivity of these lichen species to excessive levels of pollutants in the atmosphere in full compliance with the literature data (Carreras et al. 1998; Giordani et al. 2002; Otniukova and Sekretenko 2008). Generally low number of *Anaptychia ciliaris* and *Usnea subfloridana* records (Table 1) is obviously associated with high negative value of azim_0km, which confirms the transfer of suspended particles, carbon monoxide, nitrogen oxide and dioxide from the city of Moscow.

The temperatures of March and May, as well as the amount of precipitation in March, were significant for almost all types of rare epiphytic organisms.

The conservation significance of SPNAs for creating a favorable habitat for the studied rare species was not confirmed (Table 5). This suggests that under the current state of forest cover in the region the location within a SNPA is not so important in the distribution of species.

Community level

When analyzing the confinement of species to certain forest types, a stable correlation was found between the distribution of studied rare species and coniferous and small-leaved communities. It is quite obviously due to the distribution of coniferous forests in accordance with pronounced zoning (Kurnaev 1973; Petrov 1968). The connection between species and community types has rather different values. Thus, the highest value of χ^2=373.7241 was recorded for *Usnea hirta,* which is closely associated with the swamp type of dwarf shrubs–herbal-sphagnum communities (#18,28). The location of *Bryoria fuscescens* within nemoral spruce forests and birch forests of the grass-marsh group (#3,26) is confirmed by χ2=341.408. The distribution of *Neckera pennata* in the nemoral spruce communities (#3,4) is confirmed by the high correlation coefficient χ^2=217.6207 (Table 6). Low χ^2 values and no significant correlation with forest types are characteristic of *Bryoria implexa, Usnea glabrescens*, and *U. subfloridana*. It is quite obvious that in such case the conditions of biotopes within the considered types of communities are the most significant.

Biotope level

Considering a more detailed biotope level, we see that 80% of the records of epiphytic organisms are limited to three categories of humid habitat biotopes (#1–3). The critical importance of humidity and light for poikilohydric organisms has been repeatedly emphasized in other studies (Campbell and Coxson 2001; Nash 1996).

Lower number of the records of the studied rare species in biotope #4 (opening in the forest, forest edge, clearing, road) is directly related to anthropogenic disturbance and formation of the edge effect (Saunders et al. 1991). However,

Table 9. Results of multiple linear regression analysis of species distribution based on spatial environment factors (with due account of 0-points)

Environment factors	Anaptychia ciliaris	Bryoria fuscescens	Bryoria implexa	Neckera pennata	Usnea dasopoga	Usnea glabrescens	Usnea hirta	Usnea subfloridana
a	5.895	11.447	3.964	2.709	7.829	5.621	12.713	5.276
azim_osv_100	0.07	**0.154**	-0.01	0.038	**0.089**	0.079	0.006	0.032
dist_0km	**0.379**	**-0.18**	**0.149**	**-0.53**	**0.205**	**0.183**	**0.291**	**0.223**
azim_0km	**-0.57**	-0.2	**-0.33**	**0.3**	**-0.54**	**-0.43**	**-0.54**	**-0.56**
NDWI	-0.03	0.071	-0.06	**0.083**	-0.05	-0.05	**-0.08**	-0.02
$T_{avg\ march}$	**-0.27**	-0.05	**-0.21**	**-0.15**	**-0.22**	**-0.32**	**-0.27**	**-0.24**
$T_{avg\ may}$	**-0.27**	-0.13	**-0.36**	**-0.23**	**-0.31**	**-0.33**	**-0.41**	**-0.22**
$P_{avg\ march}$	**-0.18**	**-0.21**	**-0.17**	-0.01	**-0.17**	**-0.28**	**-0.17**	**-0.19**
$P_{avg\ april}$	-0.11	-0.15	0.113	-0.03	0.049	-0.03	-0.04	0.026
p	0.000	0.000	0.000	0.000	0.000	0.000	0.000	0.000
R2	0.289	0.131	0.323	0.428	0.453	0.222	0.549	0.316

a – intercept, *p* – p-level, *R2* – coefficient of determination

on the one hand, narrow forest roads and rather narrow clearings with additional illumination have higher numbers of individuals and species of *Usnea* spp. and *Bryoria* spp. On the other hand, the number of species is noticeably lower at the edges of watershed forests and upland meadows, where epiphytic organisms are exposed to the desiccation factor because of excessive light and wind. Similar data on the negative impact of undesirable gradients of light, humidity and wind at the edge of forest stands, where different microclimatic environmental conditions are formed, have been obtained in other studies (Esseen 2006; Hilmo and Holien 2002). The negative impact of linear cuts in managed forests has been analyzed in detail in relation to the distribution of epiphytic lichens *Bryoria* spp., *Usnea* spp. and *Evernia mesomorpha* (Boudreault et al. 2008).

In our study, the distribution of *Neckera pennata* in mesotrophic forest (#1) is confirmed by the highest correlation coefficient χ^2= 215.5241. Other species also have significant coupling coefficients. *Usnea glabrescens* is an exception, its distribution is not limited to any particular biotope type. It is a very rare species, and the validity of the sample is insufficient (Table 7). To clarify, it is desirable to increase the sample of records of the species in the future.

A large number of publications analyze the distribution and diversity of epiphytic cryptogamic organisms on different tree species (Nascimbene et al. 2009; Sales et al. 2016; Spier et al. 2010; Thor et al. 2010; Wirth 1995). In our study, a significant correlation of the habitats of the studied species with two tree species, i.e. spruce and aspen, was confirmed. It is important that the degree of connection with the substrate (tree species) is the closest in comparison with other biotic characteristics. Thus, the distribution of *Bryoria fuscescens* on spruce branches is confirmed with χ^2=1337.419, *Usnea dasopoga* with χ^2= 550.1791, *Usnea hirta* with χ^2=533.751. Location of *Neckera pennata* on mineral-rich, rather simple, cracked bark, mainly on old, free-standing aspen trunks, is confirmed with χ^2=539.0884. A small number of *Usnea glabrescens* records also did not allow establishing a reliable relationship with the tree species.

CONCLUSION

Epiphytes model the diversity of forest communities and fulfill certain ecosystem functions, despite their minor contribution to production processes in the temperate zone. The study is devoted to the patterns of distribution of rare epiphytic species at the border of the broad-leaved–coniferous forest zone. Identification of the limiting factors of the natural environment for such organisms at different spatial levels is a key to detailing natural boundaries over large geographic areas, and the ecological well-being of forests at the level of individual communities and biotopes. At the regional level we recorded edge effects on studied rare species at the gradient of climatic conditions and the transition of the broad-leaved-coniferous forest zone into the broad-leaved one. The distribution of studied rare species is synergistically superimposed by the influence of atmospheric transport of pollutants from the city of Moscow. The warming effect from Moscow remains possible but needs to be confirmed in the future. In general, the state and habitat feature of most forests outside the SPNA of the Moscow region do not differ significantly from those within the protected areas. This is confirmed by the absence of dependence of the studied rare species distribution on the areas with protection status.

Local ecological and coenotic conditions influencing light, temperature and humidity regimes are among the principal factors in the distribution of the rare species of epiphytic organisms at the level of habitats. Edge effects as represented by the decreasing number of species records are characteristic of the forest borders near major roads, as well as at the edge of watershed forests and upland meadows.

The narrow ecological compliance of epiphytic cryptogamous species and their sensitivity to air pollution make them good indicators of the environmental quality within anthropogenic landscapes. Subsequently, this will help in the best way determine the optimal conditions contributing to biodiversity conservation in forests near large metropolitan areas and optimization of optimal habitat diversity.

Funding

This study was conducted in the framework of the Institute of Geography RAS (№ 0148-2019-0007) and Severtsov Institute of Ecology and Evolution RAS.

REFERENCES

Aerts R., Honnay O. (2011). Forest restoration, biodiversity and ecosystem functioning. BMC Ecology 11, 29, DOI: 10.1186/1472-6785-11-29.

Annenskaya G.N., Zhuchkova V.K., Kalinina V.R., Mamai I.I., Nizovtsev V.A., Khrustaleva M.A., Tseselchuk Yu.N. (1997). Landscapes of the Moscow region and their current state. SGU, Smolensk, Russia.

Antoine M.E. (2004). An Ecophysiological Approach to Quantifying Nitrogen Fixation by Lobaria oregana. bryo 107, 82-87, DOI: 10.1639/0007-2745(2004)107[82:AEATQN]2.0.CO;2.

Averkieva V.Yu., Priputina I.V. (2011). Assessment of the impact of technogenic NOx emission on the nutrient regime of forest biogeocenoses of the Moscow region 51-57.

Barkman J.J. (1969). The influence of air pollution on bryophytes and lichens. Proc. First European Congress on the Influence of Air Pollution on Plants and Animals 197-209.

Bednova O.V. (2017). Indication of eutrophication in the forest ecosystems on urban areas. Forestry Bulletin 21, 4-14.

Blackburn T.M., Bellard C., Ricciardi A. (2019). Alien versus native species as drivers of recent extinctions. Frontiers in Ecology and the Environment 17, 203-207, DOI: 10.1002/fee.2020.

Boudreault C., Bergeron Y., Drapeau P., Mascarúa López L. (2008). Edge effects on epiphytic lichens in remnant stands of managed landscapes in the eastern boreal forest of Canada. Forest Ecology and Management 255, 1461-1471, DOI: 10.1016/j.foreco.2007.11.002.

Boudreault C., Coxson D., Bergeron Y., Stevenson S., Bouchard M. (2013). Do forests treated by partial cutting provide growth conditions similar to old-growth forests for epiphytic lichens? Biological Conservation 159, 458-467, DOI: 10.1016/j.biocon.2012.12.019.

Byazrov L.G. (1994). Species Composition and Distribution of Epiphytic Lichens in Moscow Forest Plantations. Lesovedenie, 45-54.

Campbell J., Coxson D.S. (2001). Canopy microclimate and arboreal lichen loading in subalpine spruce-fir forest. Can. J. Bot. 79, 537-555, DOI: 10.1139/b01-025.

Cardós J.L.H., Aragón G., Martínez I. (2017). A species on a tightrope: Establishment limitations of an endangered lichen in a fragmented Mediterranean landscape. American Journal of Botany 104, 527-537, DOI: 10.3732/ajb.1600338.

Carreras H.A., Gudiño G.L., Pignata M.L. (1998). Comparative biomonitoring of atmospheric quality in five zones of Córdoba city (Argentina) employing the transplanted lichen Usnea sp. Environmental Pollution 103, 317-325, DOI: 10.1016/S0269-7491(98)00116-X

Case J.W. (1980). The influence of three sour gas processing plants on the ecological distribution of epiphytic lichens in the vicinity of fox creek and Whitecourt, Alberta, Canada. Water Air Soil Pollut 14, 45-68, DOI: 10.1007/BF00291825.

Chernenkova T.V. (2002). Response of forest vegetation to industrial pollution, Nauka. ed. Moscow, Russia.

Chernenkova T.V., Kotlov I.P., Belyaeva N.G., Morozova O.V., Suslova E.G., Puzachenko M.Y., Krenke A.N. (2019). Sustainable Forest Management Tools for the Moscow Region. GEOGRAPHY, ENVIRONMENT, SUSTAINABILITY 12, 35-56.

Chernenkova T.V., Suslova E.G., Morozova O.V., Belyaeva N.G., Kotlov I.P. (2020). Forest biodiversity of Moscow region. Ecosystems: Ecology and Dynamics 4, 60-144, DOI: 10.24411/1993-3916-2021-10134.

Czerepanov S.K. (1995). Vascular plants of Russia and adjacent states (the former USSR), Cambridge: Cambridge university press, 516.

Ellis C.J. (2019). Climate Change, Bioclimatic Models and the Risk to Lichen Diversity. Diversity 11, 54, DOI: 10.3390/d11040054.

Ellis C.J. (2012). Lichen epiphyte diversity: A species, community and trait-based review. Perspectives in Plant Ecology, Evolution and Systematics 14, 131-152, DOI: 10.1016/j.ppees.2011.10.001

Ellis C.J., Coppins B.J. (2009). Quantifying the role of multiple landscape-scale drivers controlling epiphyte composition and richness in a conservation priority habitat (juniper scrub). Biological Conservation 142, 1291-1301, DOI: 10.1016/j.biocon.2009.01.036.

Ellis C.J., Eaton S., Theodoropoulos M., Elliott K. (2015). Epiphyte communities and indicator species: An ecological guide for Scotland's woodlands. Edinburgh: Royal Botanic Garden Edinburgh.

Esseen P.-A. (2006). Edge influence on the old-growth forest indicator lichen Alectoria sarmentosa in natural ecotones. Journal of Vegetation Science 17, 185-194, DOI: 10.1111/j.1654-1103.2006.tb02437.x

Fick S.E., Hijmans R.J. (2017). WorldClim 2: new 1-km spatial resolution climate surfaces for global land areas. International Journal of Climatology 37, 4302-4315, DOI: 10.1002/joc.5086

Folkeson L., Andersson-Bringmark E. (1988). Impoverishment of vegetation in a coniferous forest polluted by copper and zinc. Can. J. Bot. 66, 417-428, DOI: 10.1139/b88-067

Giordani P., Brunialti G., Alleteo D. (2002). Effects of atmospheric pollution on lichen biodiversity (LB) in a Mediterranean region (Liguria, northwest Italy). Environmental Pollution 118, 53-64, DOI: 10.1016/S0269-7491(01)00275-5

Glime J. (2007). Bryophyte ecology, vol 1. Physiological ecology. http://www.bryoecol.mtu.edu/.

Golubkova N.S. (1996a). Usnea. Key to lichens in Russia 62-107.

Golubkova N.S. (1996b). Bryoria. Key to lichens in Russia 18-32.

Gunnarsson B., Hake M., Hultengren S. (2004). A functional relationship between species richness of spiders and lichens in spruce. Biodiversity and Conservation 13, 685-693, DOI: 10.1023/B:BIOC.0000011720.18889.f7

Halonen P., Puolasmaa A. (1995). The lichen genus Usnea in eastern Fennoscandia. I. Usnea hirta. Annales Botanici Fennici 32, 127-135.

Hanski I., Ovaskainen O. (2000). The metapopulation capacity of a fragmented landscape. Nature 404, 755-758, DOI: 10.1038/35008063.

Hauck M., Bruyn U. de, Leuschner C. (2013). Dramatic diversity losses in epiphytic lichens in temperate broad-leaved forests during the last 150years. Biological Conservation 157, 136-145, DOI: 10.1016/j.biocon.2012.06.015

Hawksworth D.L., Rose, F. (1970). Qualitative Scale for estimating Sulphur Dioxide Air Pollution in England and Wales using Epiphytic Lichens. Nature 227, 145-148, DOI: 10.1038/227145a0

Hilmo O., Holien H. (2002). Epiphytic Lichen Response to the Edge Environment in a Boreal Picea abies Forest in Central Norway. The Bryologist 105, 48-56.

Ignatov M.S. (1993). Moss diversity patterns on the territory of the former USSR. Arctoa 13-47.

Johansson P., Gustafsson L. (2001). Red-listed and indicator lichens in woodland key habitats and production forests in Sweden. Can. J. For. Res. 31, 1617-1628, DOI: 10.1139/x01-091.

Jönsson M.T., Thor G., Johansson P. (2011). Environmental and historical effects on lichen diversity in managed and unmanaged wooded meadows. Applied Vegetation Science 14, 120-131, DOI: 10.1111/j.1654-109X.2010.01096.x.

Ignatov M.S., Ignatova E.A. (2003). Flora mkhov srednei chasti evropeiskoi Rossii (Moss flora of the Middle European Russia), Moscow: KMK, 1-2, 960.

Karström M. (1992). The project one step ahead — a presentation. Svensk Botanisk Tidskrift 86, 103-114.

Kranner I., Beckett R., Hochman A., Iii T.H.N. (2008). Desiccation-Tolerance in Lichens: A Review. bryo 111, 576-593, DOI: 10.1639/0007-2745-111.4.576.

Kurnaev S.F. (1973). Lesorastitel'noe rajonirovanie SSSR (Forest zoning of the USSR). Nauka, Moscow, Russia.

Lanta V., Hyvönen T., Norrdahl K. (2013). Non-native and native shrubs have differing impacts on species diversity and composition of associated plant communities. Plant Ecol 214, 1517-1528, DOI: 10.1007/s11258-013-0272-0.

LeBlanc F., Robitaille G., Rao D.N. (1974). Biological response of lichens and bryophytes to environmental pollution in the Murdochville copper mine area, Quebec. J. Hattori Bot. Lab.;(Japan) 38.

LeBlanc S.C.F., Sloover J.D. (1970). Relation between industrialization and the distribution and growth of epiphytic lichens and mosses in Montreal. Can. J. Bot. 48, 1485-1496, DOI: 10.1139/b70-224.

Llewellyn T., Gaya E., Murrell D.J. (2020). Are Urban Communities in Successional Stasis? A Case Study on Epiphytic Lichen Communities. Diversity 12, 330, DOI: 10.3390/d12090330.

Maron J.L., Marler M. (2008). Effects of Native Species Diversity and Resource Additions on Invader Impact. The American Naturalist 172, S18-S33, DOI: 10.1086/588303.

McFeeters S.K. (1996). The use of the Normalized Difference Water Index (NDWI) in the delineation of open water features. International journal of remote sensing 17, 1425-1432.

Muchnik E.E., Insarova I.D., Kazakova M.V. (2011). Training guide for lichens in Central Russia. Ryazan State University named after S.A. Yesenin, Russia, Ryazan.

Nascimbene J., Marini L., Nimis P.L. (2009). Influence of tree species on epiphytic macrolichens in temperate mixed forests of northern Italy. Can. J. For. Res. 39, 785-791, DOI: 10.1139/X09-013.

Nash T.H. (1996). Lichen Biology. Cambridge University Press.

Notov A.A., Zhukova L.A. (2015). Epiphytic lichens and bryophytes at different ontogenetic stages of Pinus sylvestris. Wulfenia 22, 245-260.

Otniukova T.N., Sekretenko O.P. (2008). Lichens on branches of Siberian fir (Abies sibirica Ledeb) as indicators of atmospheric pollution in forests. Izv Akad Nauk Ser Biol 479-490.

Petrov V.V. (1968). New scheme of botanical and geographical zoning of the Moscow region. Vestnik Moskovskogo gosudarstvennogo universiteta. Biologiya 44-50.

Pettersson R.B., Ball J.P., Renhorn K.-E., Esseen P.-A., Sjöberg K. (1995). Invertebrate communities in boreal forest canopies as influenced by forestry and lichens with implications for passerine birds. Biological Conservation 74, 57-63, DOI: 10.1016/0006-3207(95)00015-V.

Red Data Book of the Moscow Region, 2nd ed 2018. . KMK, Moscow, Russia.

Rivas-Martínez S., Penas A., Díaz T.E. (2004). Mapas bioclimáticos y biogeográficos [WWW Document]. URL https://www.globalbioclimatics.org/form/bi_med.htm (accessed 3.4.22).

Rose F. (1976). Lichenological indicators of age and environmental continuity in woodlands. Lichenology: Progress and problems 279-307.

Sales K., Kerr L., Gardner J. (2016). Factors influencing epiphytic moss and lichen distribution within Killarney National Park. Bioscience Horizons: The International Journal of Student Research 9, hzw008, DOI: 10.1093/biohorizons/hzw008.

Saunders D.A., Hobbs R.J., Margules C.R. (1991). Biological Consequences of Ecosystem Fragmentation: A Review. Conservation Biology 5, 18-32, DOI: 10.1111/j.1523-1739.1991.tb00384.x.

Scott M.G., Hutchinson T.C. (1990). The use of lichen growth abnormalities as an early warning indicator of forest dieback. Environ Monit Assess 15, 213-218, DOI: 10.1007/BF00394887.

Shafigullina N.R. (2012). Diversity, ecological features and distribution of brioflora on the territory of the republic of Tatarstan. Kazan, Russia.

Spier L., van Dobben H., van Dort K. (2010). Is bark pH more important than tree species in determining the composition of nitrophytic or acidophytic lichen floras? Environmental Pollution 158, 3607-3611, DOI: 10.1016/j.envpol.2010.08.008.

Suslova, E.G., Tolpysheva, T.Y., Rusanov, A.V., Rumyantsev, V.Y. (2017). Some rare and protected lichens current distribution in Moscow region. Ecosystems: Ecology and Dynamics 1, 93-118.

The Problem of Biodiversity Loss | Saving Earth | Encyclopedia Britannica [WWW Document], n.d. URL https://www.britannica.com/explore/savingearth/problem-biodiversity-loss (accessed 2.28.22).

Thor G., Johansson P., Jönsson M.T. (2010). Lichen diversity and red-listed lichen species relationships with tree species and diameter in wooded meadows. Biodivers Conserv 19, 2307-2328, DOI: 10.1007/s10531-010-9843-8.

Threats to Biodiversity | GEOG 30N: Environment and Society in a Changing World [WWW Document], n.d. URL https://www.e-education.psu.edu/geog30/node/394 (accessed 2.28.22).

Tolpysheva T.Yu., Suslova E.G. (2019). Species of Usnea Dill. Ex. Adans. (Lecanoromycetes, Ascomycota) in Protected Areas of Moscow Oblast. Lesovedenie 57-63.

Tolpysheva T.Yu., Suslova E.G., Rumyantsev V.Y. (2017). Bryoria species in Moscow region protected areas. Transactions of KarRC RAS 72-80.

Tronin A.A., Gornyy V.I., Kritsuk S.G., Latypov I.Sh. (2014). Nighttime lights as a quantitative indicator of anthropogenic load on ecosystems. Current problems in remote sensing of the Earth from space 11, 237-244.

Varentsov M.I., Samsonov T.E., Kislov A.V., Konstantinov P.I. (2017). Simulations of Moscow agglomeration heat island within the framework of the regional climate model COSMO-CLM. Vestnik Moskovskogo universiteta. Seriya 5. Geographiya 25-37.

Vilà M., Espinar J.L., Hejda M., Hulme P.E., Jarošík V., Maron J.L., Pergl J., Schaffner U., Sun Y., Pyšek P. (2011). Ecological impacts of invasive alien plants: a meta-analysis of their effects on species, communities and ecosystems. Ecology Letters 14, 702-708, DOI: 10.1111/j.1461-0248.2011.01628.x.

Wang Z., Shrestha R., Yao T., Kalb V., n.d. Black Marble User Guide (Version 1.2) [WWW Document]. URL https://ladsweb.modaps.eosdis.nasa.gov/missions-and-measurements/viirs/VIIRS_Black_Marble_UG_v1.2_April_2021.pdf (accessed 3.4.22).

Weather in Moscow by months [WWW Document], n.d. URL https://weatherarchive.ru/Pogoda/Moscow? (accessed 4.14.22).

Westberg M., Moberg R., Myrdal M., Nordin A., Ekman S. (2021). Santesson's Checklist of Fennoscandian Lichen-Forming and Lichenicolous Fungi. [WWW Document]. URL http://www.indexfungorum.org/ (accessed 14.06.22).

RESEARCH PAPER

BIODIVERSITY OF MARINE YEASTS ISOLATED FROM CORAL SAND IN TRUONG SA ARCHIPELAGO, KHANH HOA PROVINCE, VIETNAM

Hong T.T. Do[1*], Hoai T. Nguyen[1], Thang V. Le[1], Thanh T. K. Nguyen[1], Xuan T. Phan[2]

[1] Institute of Biotechnology, Vietnam Russia Tropical Center, Nguyen Van Huyen Street, Cau Giay District, Hanoi, Vietnam

[2] New technology transfer center, Vietnam Russia Tropical Center, Phan Van Tri Street, Ho Chi Minh city, Vietnam

***Corresponding author:** hongdt1009@gmail.com

Received: March 31st, 2022 / Accepted: February 15th, 2023 / Published: March 31st, 2023

https://DOI-10.24057/2071-9388-2022-034

ABSTRACT. Truong Sa archipelago of Vietnam are very diverse in microorganisms, however, compared to aquatic microorganisms (sea water, sediment, etc) terrestrial microorganisms (soil, coral sand, etc) has received little attention. This study focuses on assessing the biodiversity of marine yeasts in coral sand samples collected at some islands in Truong Sa archipelago. From nine coral sand samples collected at three islands: Song Tu island (three samples), Sinh Ton island (three samples), Truong Sa island (three samples), twenty – four strains of marine yeasts were isolated. The number of marine yeast strains isolated in Truong Sa island was the highest (ten strains). Sample CS9 had the highest number of strains. These strains were grouped into eight groups based on colony and cell morphology and fourteen groups by DNA fingerprinting. The results showed that there are strains in the same group according to morphology but belong to two different groups according to fingerprinting. Otherwise, some strains have different morphology but are grouped according to fingerprinting. The fourteen yeast strains representing groups by DNA fingerprinting were closely related to fourteen different yeast species and belong to ten yeast genera (*Yamadazyma, Candida, Trichosporon, Saccharomyces, Kodamaea, Rhodotorula, Rhodosporidium, Aureobasidium, Meyerozyma, Pichia*). Among them, the genus Candida accounted for the highest number. This is the first study on marine yeasts in coral sand in Truong Sa archipelago, Vietnam. This study can be a premise for further studies on marine yeast in different fields such as medicine, agriculture, environment, etc.

KEYWORDS: marine yeast, coral sand, DNA fingerprinting, Truong Sa archipelago

CITATION: Do Hong T. T., Nguyen H. T., Le Thang V., Nguyen Thanh T. K., Phan X. T. (2023). Biodiversity Of Marine Yeasts Isolated From Coral Sand In Truong Sa Archipelago, Khanh Hoa Province, Vietnam. Geography, Environment, Sustainability, 1(16), 132-139 https://DOI-10.24057/2071-9388-2022-034

ACKNOWLEDGEMENTS: This study is supported by the project "Research on the microflora distributed in the Truong Sa archipelago that has the ability to treat organic wastes that pollute the environment" (KCB-TS 05).

Conflict of interests: The authors reported no potential conflict of interest.

INTRODUCTION

Truong Sa archipelago belongs to Khanh Hoa province, Vietnam, it consists of islands, reefs, banks and shoals made up of biogenic carbonate. Truong Sa archipelago are located in a tropical climate with two seasons, divided into eight island clusters. In this study, three islands with high biodiversity representing the islands of Truong Sa archipelago (in the north – south direction) are selected including: Song Tu, Sinh Ton and Truong Sa. In which, we focus on studying marine yeast diversity in the coral sand ecosystem here. The actual surveys show that the coral sand ecosystem in the Truong Sa archipelago has differences compared to the coastal sandy ecosystems such as: sand grain structure, vegetation, natural and artificial factors. Sand in Truong Sa has diverse structure, which can be in the form of fine sand grains or larger coral fragments that are typical for each island each sampling site. Vegetation here is very limited, extreme weather conditions make it very difficult for natural plants to grow (only a few species have been recorded such as: *Canavalia maritima, Ipomoea pes-caprae* and *Passiflora foetida*) instead of plants grown by humans (mainly *Heliotropium foertherianum, Scaevola taccada, Casuarina equisetifolia, Cocos nucifera*). Due to these differences, microorganisms (including marine yeast) in the coral sand ecosystem in Truong Sa also have species differences. However, their role in the ecosystem may be similar to that of yeast in the soil, including: maintenance of sand structure, contribute to essential ecological processes such as the mineralization of organic material and dissipation of carbon and energy, some yeasts may also play a role in both the nitrogen and sulphur cycles and have the ability to solubilize insoluble phosphates (Botha A. 2011).

Studies on marine microorganisms in the Truong Sa archipelago (Vietnam), including marine yeasts, are limited. Studies on marine microorganisms in the Truong Sa archipelago (Vietnam), including marine yeasts, are limited. So far, there have been only a few studies by Vietnamese scientists on marine bacteria (Do Thi Tuyen et al. 2021), on marine yeasts (Chu Thanh Bình et al. 2019). Chu Thanh Binh et al. (2019) studied yeast in some marine animals of the genus Gastropoda. The yeast identification results showed that they consisted of four genera: *Meyerozyma,*

Aureobasidium, Pichia, Candida. Marine yeasts, defined as the yeasts that are isolated from marine environments, are able to grow better on a medium prepared using seawater rather than freshwater (Chi Z.M. et al. 2010). Marine yeasts were first reported by Fischer and Brebeck (1894) from Atlantic Ocean seawater and identified them as *Torula* sp. and *Mycoderma* sp.; subsequently yeasts have been observed in all oceans of the world, ranging from nearshore environments to oceanic surface waters and deep sea sediments (Kutty and Philip 2008). Many studies also show that marine yeast has very versatile applications. These include industrial, aquaculture, medical and environmental fields (Abdelrahman S. Z. et al. 2014; Anwesha S. and Bhaskar R. 2016; Sarkar et al. 2010, Long Y. et al. 2021, Skjermo J. 1999).

There are many methods to study yeast diversity, DNA fingerprinting is the method that allows to evaluate diversity with high reliability (Sam C. et al., 2014; Christopher D. C. et al., 2014; Konstantina A. et al. 2020;). Satellite DNA usually does not code for genes and is less prone to mutations and changes. Therefore, they are often used as powerful tools in classification. Using primers designed according to the sequence of satellite DNA in PCR reaction. The amplified satellite DNA fragments are then electrophoresed for size comparison (Mauricio Ramirez-Castrillon et al. 2014; Sam C. et al. 2014). The similarity of the band spectra represents the closeness of the yeast strains. Fingerprinting technique based on satellite DNA for taxonomy to species. Strains with the same band spectrum will belong to the same species, strains with different band spectrum will probably belong to different species depending on the degree of difference. Therefore, in this study, the morphological classification method combined with the DNA fingerprinting method will provide a more complete and reliable assessment of the diversity of yeast present in coral sands in the Truong Sa archipelago area, Khanh Hoa province, Vietnam.

MATERIALS AND METHODS

Materials

Sample

Nine coral sand samples were collected on three islands in the Truong Sa archipelago (three samples per each island (Table 1).

Samples were collected at locations spread around the sandy shores of the islands (Fig. 1.). GPS location coordinates were recorded from each sampling location.

Table 1. List of samples

No.	Place	Coral sand samples code	Time	Temperature
01	Song Tu island (11°25′55′′N 114°18′00′′E)	CS1, CS2, CS3	November 2021	32°C
02	Sinh Ton island (9°53′7′′N 114°19′46′′E)	CS4, CS5, CS6	November 2021	32°C
03	Truong Sa island (8°38′30′′N 111°55′55′′E)	CS7, CS8, CS9	October 2021	33°C
Total		9		

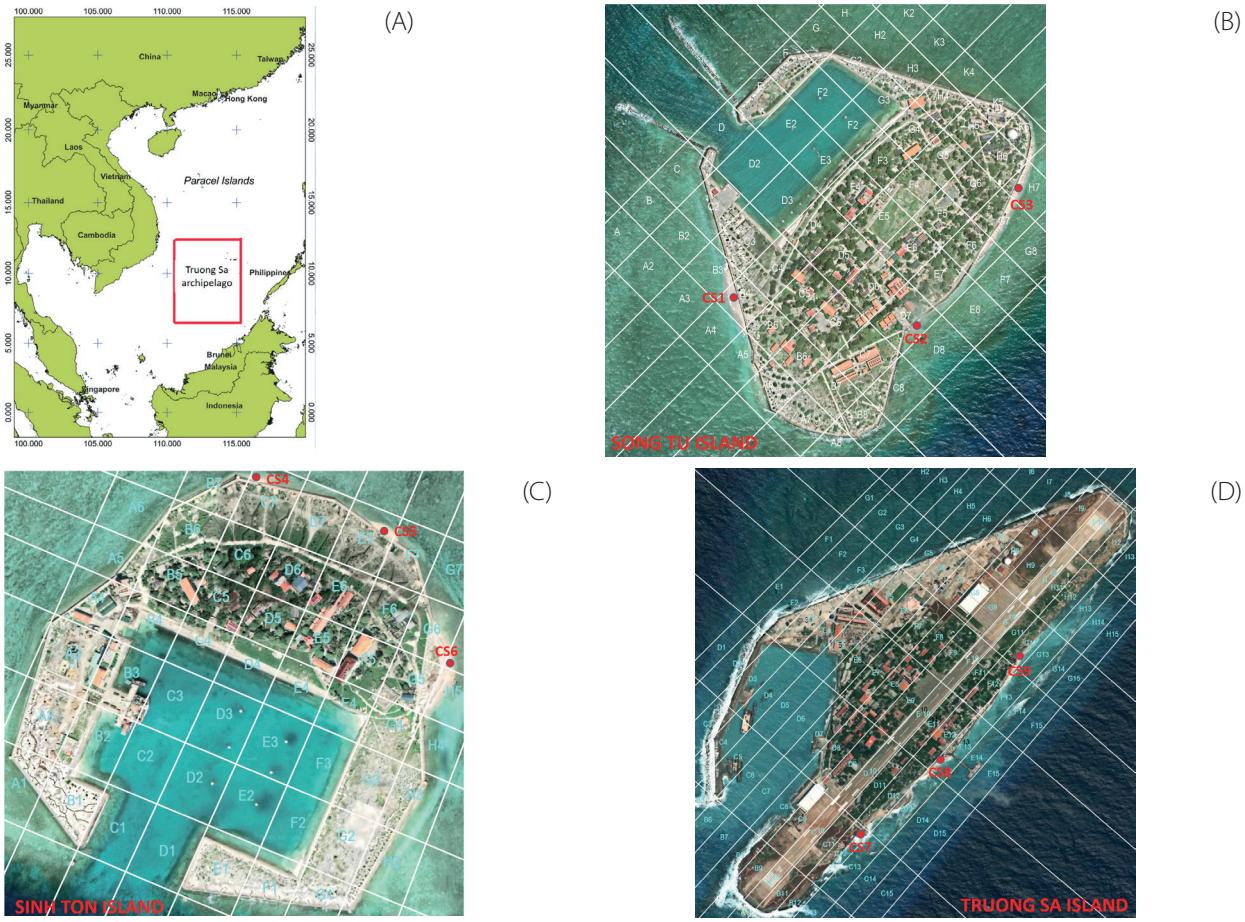

Fig. 1. (A) Map showing the location of Truong Sa archipelago in Vietnam; (B) Sampling locations at Song Tu island; (C) Sampling locations at Sinh Ton island; (D) Sampling locations at Truong Sa island

Fig. 2. Sampling in Truong Sa island (October 2021)

Media

Glucose Yeast Peptone Agar medium (GYPA medium, Glucose – 20g, Yeast extract – 5g, Peptone – 10g in 1000ml, pH 7.5 ± 0.2) with seawater. Sterilize by autoclaving at 121°C for 15 minutes. Mix well and pour into sterile Petri plates (Ausubel et al. 1994).

Methods

Sampling and physiochemical analysis: Coral sand samples were collected from the islands under conditions preventing the ingress of exogenous microbial contamination. Coral sand samples were scooped with a sterilized spoon at a depth of about 20 cm at the sandy shores of the islands. Then, the samples were stored in sterilized plastic boxes, sealed and stored at 4oC until transported to the laboratory for several weeks. The moisture and pH of the samples were measured in the laboratory using a moisture and pH meter (Tekamura DM15). The salinity of coral sand is determined by: (1) Drying 100g of sample in an oven at 105°C; (2) grind the sample; (3) Add deionized water to dissolve the sample; (4) Stir continuously with a magnetic stirrer for 5 minutes then allow to settle for 10 minutes; (5) Determine the salinity of the above solution using a hand-held refractometer.

Isolation method: The standard dilution method was used to count and isolate yeast in coral sand samples. A series of dilutions (using sterile 1.5 M NaCl solution) was prepared for each sample from the stock suspension, 1 g coral sand in 99 mL of 1.5M NaCl solution. Aliquots, 0.1 mL, from various dilutions (10–1 to 10–4) were spread on the surfaces of plates containing the GYPA medium. The plates were sealed and incubated at 30°C for a week. Three replicate plates were prepared for each dilution.

The total colony numbers were counted, and colony-forming units (CFU) per gram of sample were calculated. Three replicate plates of dilutions containing countable numbers of colonies (100–200) were pooled. Various colonies (colony shapes, sizes, colors, margins, texture, etc. and cell shapes and sizes) were sub-cultured, purified and maintained for further study (Kurtzman J.W. et al. 2011).

Grouping method: the strains were cultivated on GYPA medium, at 30°C in 5 days. Then they were differentiated by their macro and micro-morphologies according to Kurtzman J.W. et al. (Kurtzman J.W. et al. 2011)

DNA extraction: the experiment was carried out using Zymo Research Kit (USA). The genomic DNA is confirmed by gel electrophoresis by running it on 1% gel in 0.5 × TBE buffer. Gel images were observed by U-Genius 3 gel documentation system.

DNA fingerprinting: PCR reaction contained Master mix (Intron) 1x10µl, Primer MST1 (IDT) 5' – GTG GTG GTG GTG GTG – 3' 2 µl, H2O PCR (deionized water) 11 µl, DNA template 2 µl with 35 cycles. Amplification was programmed as follows: 2 min 94°C; 40s denaturation at 94°C; 60s at 52°C; 120s at 72°C; 10 min at 72°C (Mauricio Ramirez-Castrillon et al., 2014).

Amplification and sequencing of the D1-D2 region of the large-subunit RNA gene: Primers NL1 (5'-GCATATCAATAAGCGGAGGAAAAG-3') and NL4 (5'-GGTCCGTGTTTCAAGACGG-3') (Kurtzman C. P. and C. J. Robnett, 1997) were used to amplify this region. PCR was performed in a total reaction volume of 50 µl consisting of 10 mM Tris-HCl (pH 8.3), 50 mM KCl, 1.5 mM $MgCl_2$, 0.8 mM deoxynucleoside triphosphates (0.2 mM each), 1.2 U of *Taq* DNA polymerase, 0.4 µM (each) of the NL 1 primers and NL4 primers, 2 µl (1 to 5 ng) of DNA template, and add enough PCR water to 50 µl. PCR was carried out using the following conditions: initial denaturation at 94°C for 3 min; 30 cycles of denaturation (94°C for 1 min), annealing (60°C for 1 min), and extension (72°C for 1 min); and a final extension step at 72°C for 3 min. A negative control was performed with each run by replacing the template DNA with PCR water in the PCR mixture (Shiang N.L. et al. 2006).

Identification of yeast by the D1-D2 region of the large-subunit RNA gene: A total of 14 strains were examined. Species were identified by searching databases using the BLAST sequence analysis tool (http://www.ncbi.nlm.nih.gov/BLAST/).

RESULTS

Analysis of samples collected from Truong Sa archipelago

The results of moisture, salinity, and pH testing of coral sand samples are shown in Table 2.

Table 2. Moisture, salinity, and pH of coral sand samples

No.	Sample	Moisture	Salinity	pH
01	CS1	12,1%	9,7‰	7,78
02	CS2	10,9%	10,2‰	8,02
03	CS3	12,5%	10,2‰	7,57
04	CS4	11,7%	11,1‰	8,44
05	CS5	12,1%	11,0‰	8,12
06	CS6	11,8%	9,8‰	8,01
07	CS7	12,8%	10,0‰	7,85
08	CS8	12,3%	9,8‰	8,23
09	CS9	12,7%	9,9‰	8,25
	Average	*12,1%*	*10,2‰*	*8,03*

Isolation results

Twenty-four yeast strains were isolated from nine coral sand samples collected from Truong Sa archipelago (Table 3).

Grouping based on characteristics of colonies and cells

Colony and cells morphology showed marine yeasts of various colors (milky white, cream white, red, dark brown, black), colonies smooth or wrinkled, cells spherical or short rods, reproducing by budding. Accordingly, twenty-four yeast strains were divided into eight groups (Table 4).

DNA fingerprinting

DNA of twenty-four yeast strains was extracted and PCR with primer MST1 (primer sequences were given in the methods).

According to the results in Fig. 4, twenty-four yeast strains were divided into fourteen groups based on fingerprinting bands (Table 5).

On the basis of grouping by DNA fingerprinting, the study results are considered larger than the comparison at the island scale (Fig. 5).

Table 3. List of yeast strains

No.	Samples	Yeast strains code	Total per sample	Total per island
01	CS1	Y1	1	5
02	CS2	Y2, Y3,	2	
03	CS3	Y4, Y5	2	
04	CS4	Y6, Y7, Y8, Y9, Y10	5	9
05	CS5	Y11, Y12	2	
06	CS6	Y13, Y14	2	
07	CS7	Y15	1	10
08	CS8	Y16, Y17, Y18	3	
09	CS9	Y19, Y20, Y21, Y22, Y23, Y24	6	
Total			24	

Table 4. Grouping of yeasts by colonies and cells

Group	Strains code	Characteristic	
		Colony	Cell
01	Y1, Y2, Y3, Y6	Milky white, spongy	Spherical cells, separated, reproduce by budding
02	Y9, Y10, Y16	White, smooth	Spherical cells, separated, reproduce by budding
03	Y4, Y5, Y7	Creamy white, spongy	Spherical cells, arranged in chains
04	Y8, Y13, Y18	Red, wet, viscous	Spherical cells, reproduce by budding
05	Y11, Y12, Y22, Y23, Y24	Dark brown, wet, viscous	Rod and spherical cells, arranged in chains
06	Y14	Black, wet, viscous	Rod cells, arranged in chains
07	Y17, Y19, Y20, Y21	White, wrinkled surface	Rod cells, arranged in chains
08	Y15	Creamy white, spongy	Spherical cells, separated, reproduce by budding

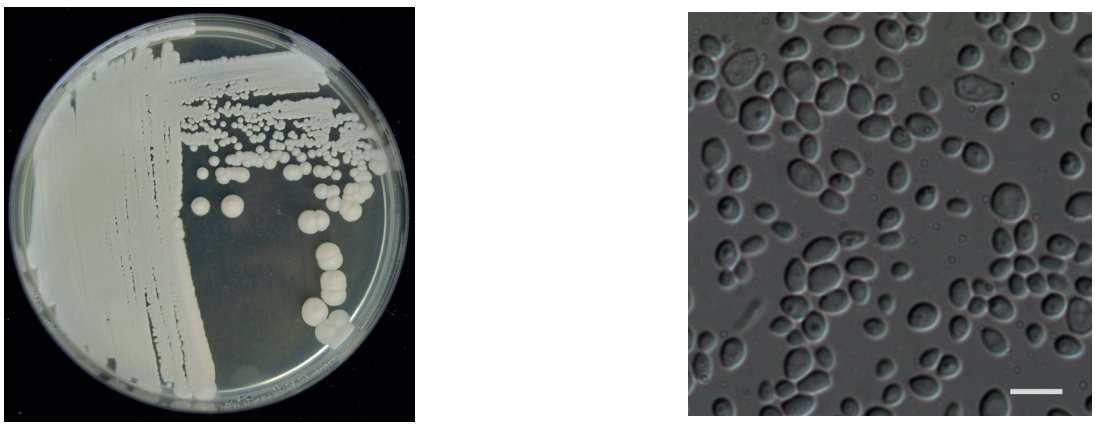

Fig. 3. Colony (left) and cell (right) of marine yeast strain Y10 (Cell images were taken under an optical microscope at 400x)

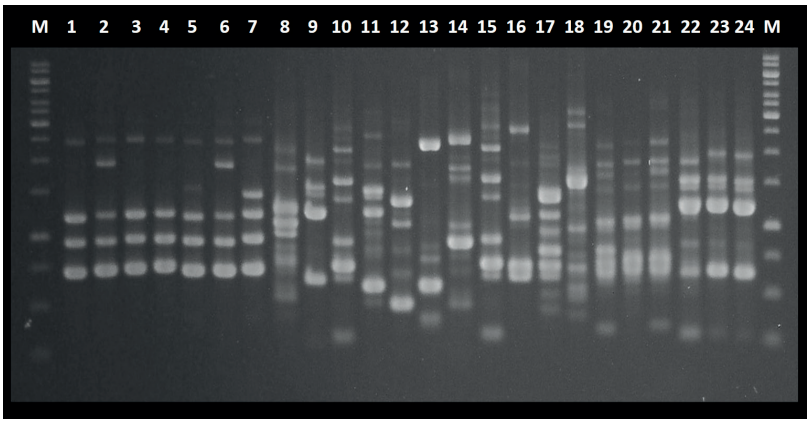

Fig. 4. Profile of fingerprinting of yeasts isolated from coral sand

Table 5. Grouping of yeasts by DNA fingerprinting

Group	Strains code	Group	Strains code
1	Y1, Y3, Y4	8	Y12
2	Y2, Y6	9	Y13
3	Y5, Y7	10	Y14
4	Y8	11	Y16
5	Y9, Y22, Y23, Y24	12	Y17
6	Y10, Y15	13	Y18
7	Y11	14	Y19, Y20, Y21

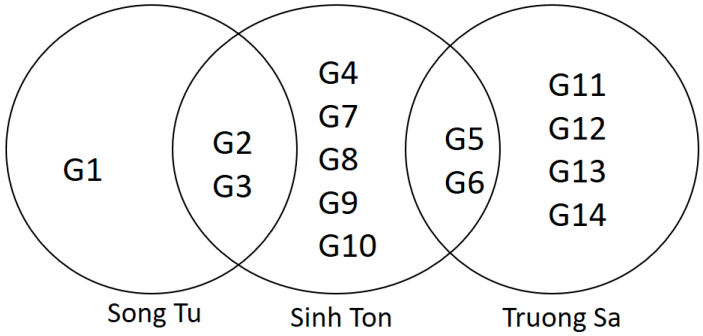

Fig. 5. Compare yeast groups among three islands

Identification of strains by the D1-D2 regions sequence analysis

Based on the results of DNA fingerprinting analysis, fourteen strains representing fourteen groups were selected for identification. BLAST search results have shown species closely related to yeast strains isolated in the study (Table 6).

DISCUSSION

Analysis of samples collected from Truong Sa archipelago

The average values of moisture, salinity, and pH of the samples serve as the basis for establishing the medium and conditions for isolating marine yeast. In this study, marine yeast strains were isolated under conditions similar to their natural habitat conditions. This makes the isolation of yeast more optimal, the assessment of yeast diversity in coral sand is more reliable. Cycil L. M. et al., when studying microorganisms in the Karak salt mine, Pakistan, also analyzed some natural elements of the samples as a basis for establishing the medium and microbial culture conditions (Cycil L. M. et al. 2020).

Isolation results

Table 3 showed that Song Tu island had the smallest number of yeasts, while yeasts in Truong Sa and Sinh Ton islands were similar. This can be partly explained by the geographical position of Song Tu island in the Truong Sa archipelago, which is located in the northern part of the archipelago, where the climatic conditions are harsh, frequent extreme weather events (strong storms, heavy rains, etc.) cause instability of ecosystems, including microorganisms. In contrast, Truong Sa Island is located in the southern part of the archipelago, with a more stable climate that makes the ecosystems here quite diverse. CS9 (in Truong Sa island) was the sample with the highest number of yeasts (six strains). However, these are only results recorded at the isolation step through differences in colony morphology. Cellular or genetic differences should be considered for higher confidence. In similar studies, marine yeasts were often isolated from seawater, sediments and animals (Corey A.H.A. and James B.M., 2019). Chutima K. et al. (2020) isolated forty yeast strains from twenty-five of the forty coral and zoanthid samples in Mu and Khram islands (Chutima K. et al. 2020). Thus, according to the results obtained from this study, the prevalence of yeast

Table 6. List of strains and species identification (% identity with sequences in GenBank)

No.	Yeast strains code	Species identification	% identity
1	Y4	Yamadazyma triangularis	99,67
2	Y2	Candida tropicalis	100
3	Y5	Kodamaea ohmeri	100
4	Y8	Rhodotorula paludigena	100
5	Y24	Trichosporon faecale	100
6	Y15	Candida oceani	99,61
7	Y11	Aureobasidium melanogenum	96
8	Y12	Meyerozyma amylolytica	99,62
9	Y13	Rhodotorula pacifica	98
10	Y14	Aureobasidium namibiae	98
11	Y16	Saccharomyces cerevisiae	100
12	Y17	Candida atlantica	99,62
13	Y18	Rhodosporidium sphaerocarpus	96
14	Y20	Pichia triangularis	99,44

in coral sand was much higher (twenty-four yeast strains in nine coral sand samples) than in marine animals in the study of Chutima Kaewkrajay et al. (forty yeast strains in forty marine animal samples). Vogel C. et al. (2007) studied yeast in the wet and dry sand of three recreational beaches in South Florida. A greater diversity of species (sixteen species) was found in the dry sand above the high tide mark compared with the wet sand in the intertidal zone (eleven species). Densities were also highest in the dry sand relative to wet sand (20-fold higher at Hobie beach, 6-fold higher at Fort Lauderdale Beach and 1.3-fold higher at Hollywood beach) (Vogel C. et al. 2007)

Yeast is a polymorphic microorganism group, characteristics of colonies (color, shape) and cells that can change in the life cycle (Pekka R. et al. 2014; Pincus D. H. et al. 2007; Roger S. et al. 2004). Therefore, it is necessary to use other classification methods (biochemical characteristics, molecular biology) to be able to more accurately assess the biodiversity of yeast.

Grouping based on characteristics of colonies and cells

According to the results of table 4, group 5, includes strains with dark brown, wet, viscous colonies rod and spherical cells, account for the most number (five strains). This is the typical morphology of the black yeast group (Seyedmojtaba S. et al. 2014; Connie F.C.G. 2018; Jerneja Z. et al. 2016). Black yeast is a group of yeasts that are highly adaptable to harsh conditions such as high salt concentration, low pH, high temperature, etc (Claudia S.K. et al. 2022; Vandewalle-Capo M. et al. 2020; Kreusch M.G. et al. 2021). Groups 6 and 8 include only one strain. With polymorphism, the classification of yeasts based on colony and cell morphology is only considered as the first step in classification. As mentioned, in order to have more reliable results, it is necessary to study biochemical and molecular characteristics. In this study, DNA fingerprinting was used to group yeasts at the molecular level.

DNA fingerprinting

From the results in Fig 4, it can be seen that the PCR product multiplied by the primer MST1 of yeast strains has different bands and is very diverse due to the distribution of copy number as well as the position of satellite DNA in the genome. The grouping technique uses satellite DNA-based primers for subspecies resolution. Strains with the same band will definitely belong to the same species, strains with different bands will probably belong to different species depending on the difference (Hilde N. et al. 2014; Dexi B. et al. 2021).

According to published studies, strains with the same bands when multiplied with primer MST1 will be similar in species name even subspecies when classified by 26S rDNA sequencing method (Baleiras Couto M.M. et al. 2005; Melissa L.I. et al. 2011). It can be said that the MST1 primer classification technique is an effective tool, giving the most accurate resolution of the electrophoresis bands. Grouping by fingerprinting makes reading sequences less expensive due to duplication.

Thus, the grouping of yeasts has been rearranged compared to the grouping by characteristics of colonies and cells. There were yeast strains with similar morphology (example Y10 and Y15) that were classified into the same group based on biological classification but had different fingerprinting bands, so they belong to two different groups according to PCR fingerprinting results. Besides, there were strains (example Y3 and Y4) with different morphology, so they were classified into two groups based on their characteristics, but the fingerprinting results showed that they could be in the same taxonomic group.
Considering yeast diversity at the molecular level, Sinh Ton island had the highest yeast diversity (nine yeast strains belonging to nine different groups). Five yeast strains isolated from Song Tu island belong to three different groups. There were groups of yeast that occur on both islands (example groups 2 and 3, groups 4 and 5) while there were groups that occur in only one island (example group 1). Song Tu island and Truong Sa island did not have the same group of yeasts. This can be explained by

geographical distance and differences in climate and soil between the two islands. Sinh Ton Island is located in the middle position compared to Truong Sa Island and Song Tu Island. The weather here is mild, with little volatility, favorable for the formation of sustainable ecosystems.

Identification of strains by the D1-D2 regions sequence analysis

The D1-D2 region gene sequence is commonly used in the identification and classification of yeasts (Shiang N. L. et al., 2006). In this study, the results of yeast identification based on the D1-D2 region gene sequences coincided with species predictions based on colony and cell morphology. The fourteen strains of yeast belonging to ten different genera include: *Yamadazyma, Candida, Trichosporon, Saccharomyces, Kodamaea, Rhodotorula, Rhodosporidium, Aureobasidium, Meyerozyma, Pichia*. In which, the genus Candida accounted for the highest number of species (3/14 species equivalent to 21.4%). Candida is a common yeast genus in marine environments because of its wide salt range and high tolerance to pH fluctuations (Jack W.F. 2012). *Rhodotorula, Rhodosporidium* and *Aureobasidium* were three genera of pigment-producing yeasts. According to many studies, the red pigment yeast group has the potential to biosynthesize many valuable biological compounds such as: squalene, exopolysaccharide, ... (Sara W. et al. 2021; Shakeri S. et. al. 2021).

Thus, the evaluation of yeast diversity by colony and cell morphology combined with DNA fingerprinting and sequencing methods has given a more complete and comprehensive view. Initial assessments have shown that yeast in coral sand in Truong Sa archipelago is diverse in both morphology and genetics. However, on the basis of this study, it is necessary to conduct biochemical studies as well as identify the isolated by other genes yeast strains to get more information about their taxonomy and phylogenetic origin. Thereby, it is possible to predict their roles and correlations in the ecosystem. In addition, this study can be a premise for further studies on marine yeast in many different fields such as medicine, agriculture, environment, etc.

CONCLUSIONS

Song Tu, Sinh Ton, Truong Sa are three representative islands of Truong Sa archipelago selected for research. Nine coral sand samples (three samples per island) were collected at different locations.

Twenty-four yeast strains isolated were morphologically diverse and grouped into eight groups based on their colony and cell morphology.

The results of grouping by DNA fingerprinting divided twenty-four yeast strains into fourteen groups.

The fourteen yeast strains representing groups by DNA fingerprinting were closely related to fourteen different yeast species and belong to ten yeast genera. Among them, the genus Candida accounted for the highest number.

Of the three islands considered in this study, Sinh Ton island has the highest yeast diversity, and Song Tu island has the least diversity. However, if we consider these 3 islands as representative of Truong Sa archipelago, we can evaluate Truong Sa as a place with high diversity of yeast in coral sand. Therefore, further research on biodiversity is needed here to give a fuller picture of the ecosystem.

REFERENCES

Abdelrahman S.Z., Gregory A.T., Zakaria Y.D., Chenyu D. (2014). Marine yeast isolation and industrial application. FEMS Yeast Research, 14, 813-825, DOI: 10.1111/1567-1364.12158.

Anwesha S., Bhaskar R. (2016). Marine yeast: A potential candidate for biotechnological applications – A review. Asian Journal of Microbiology, Biotechnology and Environmental Sciences, 627-634, DOI: 10.1111/1567-1364.12158.

Ausubel, Brent, Kingston, Moore, Seidman, Smith, Struhl (1994). Current Protocols in Molecular Biology, Current Protocols, Brooklyn, N.Y.

Baleiras Couto M.M., Reizinho R.G., Duarte F.L. (2005). Partial 26S rDNA restriction analysis as a tool to characterise non-Saccharomyces yeasts present during red wine fermentations. International Journal of Food Microbiology, 102(1), 49-56, DOI: 10.1016/j.ijfoodmicro.2005.01.005.

Botha A. (2011), The importance and ecology of yeasts in soil. Soil Biology and Biochemistry, 43(1), 1-8, DOI: 10.1016/j.soilbio.2010.10.001.

Chi Z.M., Liu G., Zhao S., Li J., Peng Y. (2010). Marine yeasts as biocontrol agents and producers of bio-products. Application Microbiology Biotechnology, 86, 1227-1241.

Chu Thanh Binh, Do Thi Thu Hong, Ngo Cao Cuong, Pham Thi Thu Huyen, Hoang Thi Thuy Duong, Nguyen Tai Tu, Britaev T.A. (2019). Biodiversity of microbial communities on some species in the class Gastropoda is distributed in coastal waters in the central of Vietnam. XX International scientific-practical conference «ACTUAL PROBLEMS OF ECOLOGY AND ENVIRONMENTAL MANAGEMENT», 2.

Chutima K., Thanongsak C., Savitree L. (2020). Assessment of Diversity of Culturable Marine Yeasts Associated with Corals and Zoanthids in the Gulf of Thailand, South China Sea, Microorganisms. 8(4), 474-490, DOI: 10.3390/microorganisms8040474.

Christopher D.C., Isak S.P. (2014). Genomic insights into the evolution of industrial yeast species Brettanomyces bruxellensis. Pubmed, 14(7), 997-1005, DOI: 10.1111/1567-1364.12198.

Claudia S.K., Lucero R.A., Luis D.A., Geovani L.O., Blanca M. C., Nayeli T.R., Georgina S., James G. (2022). Yeasts Inhabiting Extreme Environments and Their Biotechnological Applications. Microorganisms, 10(4), 794-818, DOI: 10.3390/microorganisms10040794.

Connie F.C.G., Nathan P.W. (2018). The Black Yeasts: an Update on Species Identification and Diagnosis. Current Fungal Infection Reports, 12, 59-65.

Corey A.H.A. and James B.M. (2019). Cell Biology: Marine Yeasts Deepen the Sea of Diversity. Current Biology, 29(20), 1083-1085.

Cycil L.M., DasSarma S., Pecher W., McDonald R., AbdulSalam M., Hasan F. (2020). Metagenomic insights into the diversity of Halophilic Microorganisms indigenous to the Karak Salt Mine, Pakistan. Front. Microbiol., 11(1567), 1-14.

Dexi B., Yin Z., Yaohui G., Hao L., Xingchen Z., Rong W., Ruting X., Qing W., Huanlong Q. (2021). A newly developed PCR-based method revealed distinct Fusobacterium nucleatum subspecies infection patterns in colorectal cancer. Microbial Biotechnology, 14(5), 1-11.

Do Thi Tuyen, Do Thi Thu Hong, Ngo Cao Cuong, Le Van Thang, Dang Thi Hong Phuong, Nguyen Thu Hoai (2021). Study of bacterial diversity in marine sediments in Truong Sa archipelago, Vietnam by traditional culture-dependent method in combination with denaturing gradient gel electrophoresis (DGGE). Tropical science and technology journal, 24, 131-143 (in Vietnamese with English summary).

Hilde N., Kurt W., Björn R. (2014). DNA fingerprinting in botany: past, present, future. Investigative Genetics, 5(1), 1-35, DOI: 10.1186/2041-2223-5-1.

Jack W.F. (2012). Yeasts in marine environments. https://www.researchgate.net/publication/288909618.

Jerneja Z., Monika N. B., Polona Z., Nina G. C. (2016). The Black Yeast Exophiala dermatitidis and Other Selected Opportunistic Human Fungal Pathogens Spread from Dishwashers to Kitchens. Plos one, 11(2), e0148166, DOI: 10.1371/journal.pone.0148166.

Konstantina A., Agapi I. D., Evanthia M., Athena G., Anthoula A. A., George-John E. N., Chrysoula C. T. (2020). Microbial Diversity of Fermented Greek Table Olives of Halkidiki and Konservolia Varieties from Different Regions as Revealed by Metagenomic Analysis, 8(8), 1241-1249, DOI: 10.3390/microorganisms8081241.

Kurtzman C.P., and C.J. Robnett. (1997). Identification of clinically important ascomycetous yeasts based on nucleotide divergence in the 5´ end of the large-subunit (26S) ribosomal DNA gene. J. Clin. Microbiol. 35, 1216-1223.

Kurtzman J.W., Fell T., Boekhout T. (2011). Definition, classification and nomenclature of the yeasts. In: The yeasts, a taxonomic study, 5th. Elservier, Amsterdam, 3-5.

Kutty S.N. and Philip R. (2008). Marine yeasts – a review. Yeast, 25, 465-483.

Kreusch M.G., Duarte R.T.D. (2021). Photoprotective compounds and radioresistance in pigmented and non-pigmented yeasts. Appl. Microbiol. Biotechnol, 105, 3521-3532.

Long Y., Wei W., Yingying Li., Mei X., Ting C., Chaoqun Hu., Peng L., Daning L. (2021), Potential application values of a marine red yeast, Rhodosporidiums sphaerocarpum YLY01, in aquaculture and tail water treatment assessed by the removal of ammonia nitrogen, the inhibition to Vibrio spp., and nutrient composition. PLOS ONE, 16(2), 1-15, DOI: 10.1371/journal.pone.0246841

Mauricio Ramirez-Castrillon, Sandra D. C. M., Mario Inostroza-Ponta, Patricia V. (2014). (GTG)5 MST-PCR Fingerpriting as a Technique for Discrimination of Wine Associated Yeasts. PLOS ONE, 9(8), 1-8, DOI: 10.1371/journal.pone.0105870.

Melissa L.I., Trevor G.P. (2011). Detection and identification of microorganisms in wine: a review of molecular techniques. Journal of Industrial Microbiology and Biotechnology, 28(10), 1619-1634, DOI: 10.1007/s10295-011-1020-x.

Pekka R., Jake L., Adrian C. S., Zhihao T., Saija S., Aleksi K., Matti N., Olli Yli-Harja, Ilya S., Aimée M.D. (2014). Quantitative analysis of colony morphology in yeast. BioTechniques, 56, 18-27, DOI: 10.2144/000114123.

Pincus D.H., Orenga S., Chatellier S. (2007). Yeast identification — past, present, and future methods. Medical Mycology, 45(2), 97-121, DOI: 10.1080/13693780601059936.

Roger S. (2004), Genetics, Molecular and Cell Biology of Yeast, Yeast Genetics. Universitas Friburgensis.

Sam C., Bo Z., Jan S., Pieter B., Gorik D. S., Kathleen M., Kris A. W., Kevin J. V., Bart L. (2014). Assessing Genetic Diversity among Brettanomyces Yeasts by DNA Fingerprinting and Whole-Genome Sequencing. American Society for Microbiology, Applied and Environmental Microbiology, 80 (14), 4398-4413, DOI: 10.1128/AEM.00601-14.

Sara W., Lucie D., Marine L., Julie M., Amelie V. C., Laura F., Joana C., Isabelle M. P. (2021). Population dynamics and yeast diversity in early winemaking stages without sulfites revealed by three complementary approaches. Applied sciences, 11, 2494-2516.

Sarkar S., Pramanik A., Mitra A. Mukherjee J. (2010). Bioprocessing data for the production of marine enzymes. Mar Drugs, 8, 1323-1372.

Seyedmojtaba S., Mihai G.N., Johan W.M., Willem J.G.M., Paul E.V., G.S.H. (2014). Black Yeasts and Their Filamentous Relatives: Principles of Pathogenesis and Host Defense. Clin Microbiol Rev, 27(3), 527-542, DOI: 10.1128/CMR.00093-13.

Shakeri S., Khoshbasirat F., Maleki M. (2021). Rhodosporidium sp. DR37: a novel strain for production of squalene in optimized cultivation conditions. Biotechnol Biofuels, 14(95), DOI: 10.1186/s13068-021-01947-5.

Shiang N.L., Hsien C.C., Hsiao F.S., Richard B., Jean-Philippe B., and Tsung C.C. (2006). Identification of Medically Important Yeast Species by Sequence Analysis of the Internal Transcribed Spacer Regions. J Clin Microbiol., 44(3), 693-699, DOI: 10.1128/JCM.44.3.693-699.2006.

Skjermo J., Vadstein O. (1999). Techniques for microbial control in the intensive rearing of marine larvae. Aquaculture, 177(1-4), 333-343.

Vandewalle-Capo M., Capo E., Rehamnia B., Sheldrake M., Lee N.M. (2020). The biotechnological potential of yeast under extreme conditions. Biotechnol. Appl. Extrem. Microorg, 313-356.

Vogel C., Rogerson A., Schatz S., Laubach H., Tallman A., Fell J. (2007). Prevalence of yeasts in beach sand at three bathing beaches in South Florida. Water Reseach, 41(9), 1915-1920, DOI: 10.1016/j.watres.2007.02.010.

RESEARCH PAPER

CHANGES IN THE MODERN RANGE OF THE GREAT BUSTARD *OTIS TARDA* IN UZBEKISTAN UNDER THE INFLUENCE OF AGRICULTURAL TRANSFORMATION OF LANDSCAPES AND CLIMATE

Roman D. Kashkarov[1,2*], Anna Ten[1,2], Yuliya O. Mitropolskaya[1], Valentin Soldatov[1]

[1] Institute of zoology, Bogi-Shamol Str., 232 B, Tashkent, 100053, Republic of Uzbekistan

[2] Uzbekistan Society for the protection of birds, Bogi-Shamol Str., 232 B, Tashkent, 100053, Republic of Uzbekistan

***Corresponding author:** roman.kashkarov@iba.uz

Received: May 16th, 2022 / Accepted: February 15th, 2023 / Published: March 31st, 2023

https://DOI-10.24057/2071-9388-2022-091

ABSTRACT. Previously, there was no special study of the Great Bustard (*Otis tarda*) in Uzbekistan. The first Bustard survey was conducted within the Winter Bustards Census Programme of the Eurasian Bustard Alliance in 2019. The discovery of a Great Bustards aggregation of 96 individuals in Jizzakh region showed that the wintering grounds are more stable than was expected before and that there is no information about the wintering grounds of this species in the country. The aim of this work was to find other wintering grounds, estimate the number of wintering Great Bustards and assess threats. The identification of potential wintering grounds was carried out using satellite images in Q-GIS 3.0 based on published records of the Great Bustard in the winter season. The field survey of the Great Bustard was carried out using two methods. The first one was based on car transects, which is suitable for natural habitats. The second method that we used on open rain-fed fields, was point count from higher locations. Both methods give the actual number of birds, and could not be used for extrapolation as this species' distribution is fragmented. In 2020-2021 we covered a considerable part of the foothill plains of the central part of Uzbekistan. As a result, two wintering grounds were identified in which about 500 Great Bustards were concentrated. The surveys also made it possible to identify the main threats, which are poaching and collision with power lines. The results highlighted wintering grounds which required conservation.

KEYWORDS: the Great Bustard, wintering grounds, rare species, conservation

CITATION: Kashkarov R. D., Ten A., Mitropolskaya Y. O., Soldatov V. (2023). Changes In The Modern Range Of The Great Bustard Otis Tarda In Uzbekistan Under The Influence Of Agricultural Transformation Of Landscapes And Climate. Geography, Environment, Sustainability, 1(16), 140-149
https://DOI-10.24057/2071-9388-2022-091

ACKNOWLEDGEMENTS: The study was conducted within the framework of the programme "Conservation of Wintering Great Bustard (VU) in Uzbekistan" by the Uzbekistan Society for the Protection of Birds (UzSPB), with the support of the Mark Constantine international conservation foundation and Eurasian Bustard Alliance (headed by Dr. Aimee Kessler).

We thank Timur Abduraupov from the Institute of Zoology and Jurabek Tulaev – a UzSPB member, for participating in the fieldwork. Special thanks to Abdurasul Khaydarov (local guide) for his active role in this survey and the worries of Great Bustards.

Conflict of interests: The authors reported no potential conflict of interest.

INTRODUCTION

The Great Bustard (*Otis tarda* Linnaeus 1758) is a rare species listed in the Red Data Book of Uzbekistan (Lanovenko and Filatova 2019) with status 1 (CR) – critically endangered, a migratory European subspecies. It is included in the IUCN Red List as vulnerable (VU) (BirdLife 2022). The first inclusion of the Bustard in the Red Data Book of the Uzbek SSR was in 1983 (Salikhbaev 1983), when it was listed as an extinct breeding and very rare passage and wintering bird. In the subsequent four editions of the Red Data Book of Uzbekistan in 2003, 2006, 2009, and 2019, the Great Bustard was assessed as critically endangered – a migratory European subspecies on the verge of complete extinction.

The global population of the Great Bustard is estimated to be between 44,000 and 57,000 individuals (Alonso and Palacín 2010; Alonso 2014). Most of it (57-70%) inhabits the Iberian Peninsula, and the second largest (15-25%) habitat in terms of population is the south-west of Russia. Here populations are declining in most of this species' range (Oparin et al. 2013; Oparina et al. 2022). Over the past fifty years, its numbers have declined sharply in the eastern half of the Great Bustard's range, where this species has completely disappeared from a number of regions (Kessler and Batbayar 2014; Kessler 2016).

Historically, Great Bustards in Kazakhstan and Tajikistan used to migrate southwards, to Uzbekistan, Turkmenistan, Afghanistan, and Pakistan for wintering (Bostanjoglo 1911; Gubin 2010). Prior to the development of Kazakhstan's

virgin lands, the Great Bustard was mainly a passage bird in Uzbekistan, with smaller numbers staying in the country for the winter and on very rare occasions – to breed in steppe areas (Meklenburtsev 1990). As the steppes in Jizzakh, Tashkent, and Syrdarya regions of Uzbekistan had been developed, the species completely stopped breeding there (Meklenburtsev 1990; Kreuzberg-Mukhina 2003). In the 1970s and 1980s, individual passage birds were recorded in Uzbekistan (Meklenburtsev 1990). That period, when the development of agriculture peaked in the USSR, proved to be the most critical for the Great Bustard (Kashkarov et al. 2022). R. Meklenburtsev (1990) associated the decrease in the numbers of the Great Bustard in wintering grounds in Uzbekistan with a sharp decline in the Great Bustard population in Kazakhstan and its disappearance from Tajikistan.

After the disintegration of the Soviet Union and changes in the land use system in Kazakhstan, when a large portion of developed steppe territories became neglected, the situation changed somewhat for the better (Berezovikov et al. 2002). Based on her personal records and interviews with hunters, rangers, and colleagues, E. Kreuzberg-Mukhina (2003) came to the conclusion that the numbers of migrating and wintering Great Bustards in Uzbekistan have increased slightly in recent decades. The modern data on the distribution of Great Bustards in Uzbekistan during migration and in winter are very scarce and comprise rare and occasional records or oral reports from hunters. These data were brought together in a paper on the specification of the Great Bustard's status in Uzbekistan completed by Kashkarov et al. (2022). These studies have shown that the area of land suitable for the habitation of the species has decreased more than 15 times. The current estimate of the number of wintering and migratory birds in Uzbekistan – up to 500 individuals in severe winters – is also very rough and inaccurate.

No special census of the Great Bustard has been made in the country in recent decades (Kreuzberg-Mukhina 2003; Kashkarov et al. 2022). Only in 2019, with the support of the Eurasian Bustard Alliance, probably, the first targeted survey of Great Bustards was conducted, which confirmed them wintering in the foothills of the Pistalitau Range area (Forish District, Jizzakh region) (Ten et al. 2020).

This article presents the results of the study of the Great Bustard's wintering grounds in 2020-2021 conducted within the framework of the programme 'Conservation of the wintering Great Bustard in Uzbekistan' by the Uzbekistan Society for the Protection of Birds (UzSPB).

MATERIALS AND METHODS

Identification of biotopes

The Great Bustard is the most typical species for open steppes. It breeds in the steppes and desert steppes of Eurasia, as well as in some parts of North Africa. Today, agricultural fields in some areas are the only available breeding habitats for Great Bustards (Kessler and Batbayar, 2014). These birds use active, fallow and abandoned grain fields, where they feed mainly on insects and non-cereal vegetation (Bravo et al. 2012). Wintering sites are similar to breeding biotopes. In winter, Great Bustards feed on stubble or alfalfa in agricultural fields (Lane et al. 2001).

Before starting surveys in winter 2019–2020, we made effort to identify potential wintering sites for Great Bustards. Based on the results of the study in January 2019 and on the analysis of the Great Bustard records from literature sources, we managed to identify the main biotopes preferred by the Great Bustard in winter: 1) clayey or gravelly foothills or piedmonts, mostly flat and gently rolling, covered mainly with sagebrush associations, more rarely without any shrub; 2) non-irrigated rain-fed lands planted with traditional winter wheat and other winter crops. Great Bustards do not visit irrigated lands, perhaps, because of various agricultural activities, including the soil washing of fields in winter.

Potential wintering biotopes were identified based on the study of literature data and comparison of satellite images in Google Pro, as well as by satellite images. The mapping was carried out in QGIS 3.0 and Google Pro.

Suitable sites were identified in Jizzakh region (Pistalitau, Gallaaral, Arnasay, Zaamin) and Samarkand region (near Kattakurgan and Juma); the survey also covered Karnabchul, located in the territories of Bukhara, Samarkand and Kashkadarya regions. Many of them were visited and inspected in 2020 and 2021. As a result, the aggregations of Great Bustards were recorded on a site near the villages of Yangikishlak (Forish district) and Gallaaral (Gallaaral district).

Survey methods

The Great Bustard is a rare species, which is hard to record due to its behaviour, extremely low numbers, and fragmented distribution. This is the reason why experts recommend to count its numbers in situ without extrapolation. The survey was carried out following the recommendations by Dr. Mimi Kessler (co-chief IUCN Bustard Specialist Group), it was most comprehensively standardized in Spain (Alonso et al. 1990) and is generally applicable across the range of the species. The field survey of

Fig. 1. The small group of Great Bustards flying from the rain-fed fields planted with winter wheat (Jizzakh region, Gallaaral district) Photo by V. Soldatov

the Great Bustard was carried out using two methods. The first one was line auto transects (Alonso et al. 1990). In this method, observers are driving through the survey area slowly (max. 30 km/h) following an established uninterrupted zigzag route with frequent stops (about once every 1 km, but this depends on the weather, terrain, density of birds, and vegetation structure). We used it for natural habitats, covered with bushes. The potential territory was combed using a 4x4 vehicle UAZ 2206, which stopped every 2-3 km, depending on the landscape and viewing range. The second method was point count from elevated spots. This method was suitable for survey on open rain-fed fields. Our experience of the Great Bustard survey in Jizzakh region has shown that in open rain-fed fields, where visibility is 3-5 km, it is possible to count birds from higher points (with a telescope) at a distance of 1-2 km. This approach helps to not disturb birds and minimizes the possibility of a double count. The survey method was chosen based on visibility condition in the survey area.

We used 60x magnification telescopes and 8-10x magnification binoculars. The Great Bustard surveys require observers who can detect the species and determine the age and sex of the observed birds. Routes and locations were recorded with the use of a mobile application for outdoor navigation.

It is recommended to identify the social and age composition of the group because these data allow to assess the structure of the population, but also to differentiate groups from each other to prevent the counting of the same groups. However, in 2019–2021, we observed the birds from an average distance of 800-1,000 m, which made it difficult to identify the sex and almost impossible to identify the age.

The studies took 9 days in January and February of 2020 (January 6-10, January 31-February 3), as well as 19 days in the winter of 2020-2021 (December 23-27, 2020, January 25-29, 2021, February 18-22, 2021). The total length of the transect over 28 field days was 3,350 km, (Fig. 2).

The data on population size presented in the article include the total number of individuals in all groups of Great Bustards recorded during one trip to a certain site (no more than 1 day). Based on the movements of these groups of birds, some groups were excluded from the count so that they could not be erroneously recorded for the second time. That was why in 2021 we preferred not to disturb groups and count from a considerable distance, which affected the identification of the social and age composition of groups. The surveys were carried out within a short period of time, and although they were not in fact a one-time survey, they can probably be treated like this. It is also worth noting that in January and February 2021, with a difference of 1-2 days, the surveys were carried out in both Gallaaral and Forish Districts.

Weather during the survey was generally satisfactory, in winter, fog is the most common factor that impacts the efficiency of counting and is difficult to predict.

Interviewing local people

The local population was interviewed using standard methods of collecting information on rare species, including the demonstration of photographic materials for comparison with other similar species.

RESULTS

Wintering grounds

The search for wintering grounds confirmed the data by E. Kreuzberg-Mukhina (2003) about the Great Bustard wintering in the Aydar Lake area. In addition to the 2019 data (Ten et al. 2020), our studies in 2020 and 2021 showed that Great Bustards winter regularly in this part of Forish District. Further research revealed a wintering ground near the town of Gallaaral. These two sites were surveyed several times in 2020 and 2021 (Fig. 3). Also, based on interviews, potential wintering sites were identified in the Zaamin area in Jizzakh region, near the village of Jum (Samarkand region) and the village of Krasnogorsk (Tashkent region), but the data were not confirmed due to a lack of surveys. As a result, the most significant regular wintering sites for the Great Bustard in Uzbekistan were identified in Forish District (near Pistalitau) and in Gallaaral District (near the village of Gallaaral) (Fig. 3).

Population size

In winter 2019–2020, the number of Great Bustards on the site near Yangikishlak ranged from 11 to 28 individuals, while the population near Gallaaral consisted of 107 individuals. The total number of Great Bustards in Jizzakh region in winter 2019–2020 was estimated at 107. In winter 2020–2021, surveys revealed 3-42 wintering individuals in Forish District, and 42-455 individuals near Gallaaral. The total number of wintering Great Bustards was estimated at 455 individuals (Table 1).

Detailed information is presented in Table 2.

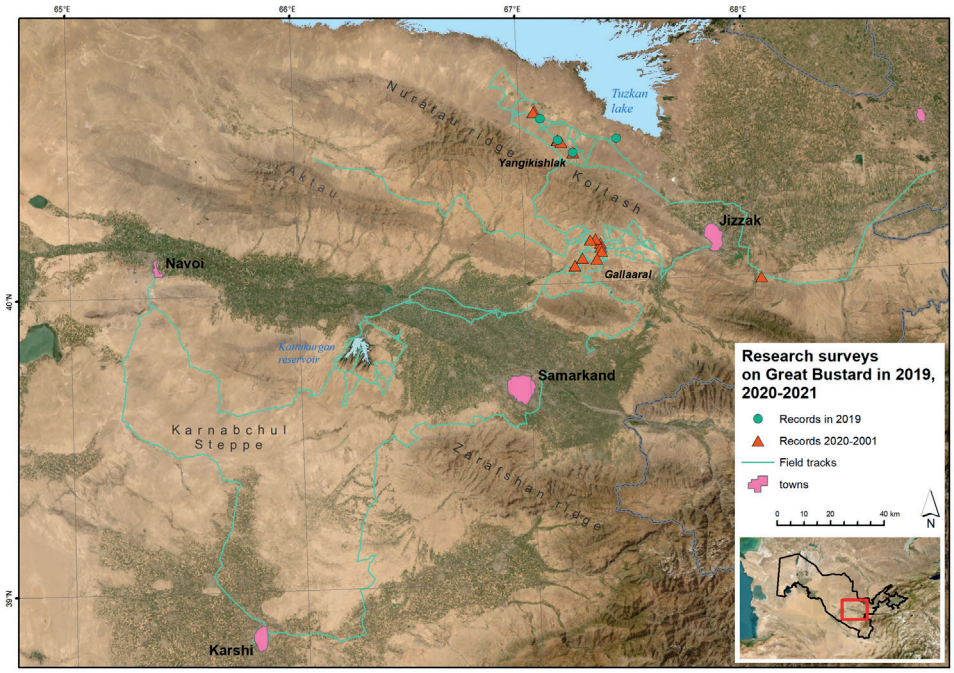

Fig. 2. Field survey of the Great Bustard in Jizzakh, Samarkand, Bukhara, Navoi, and Kashkadarya regions, 2020–2021

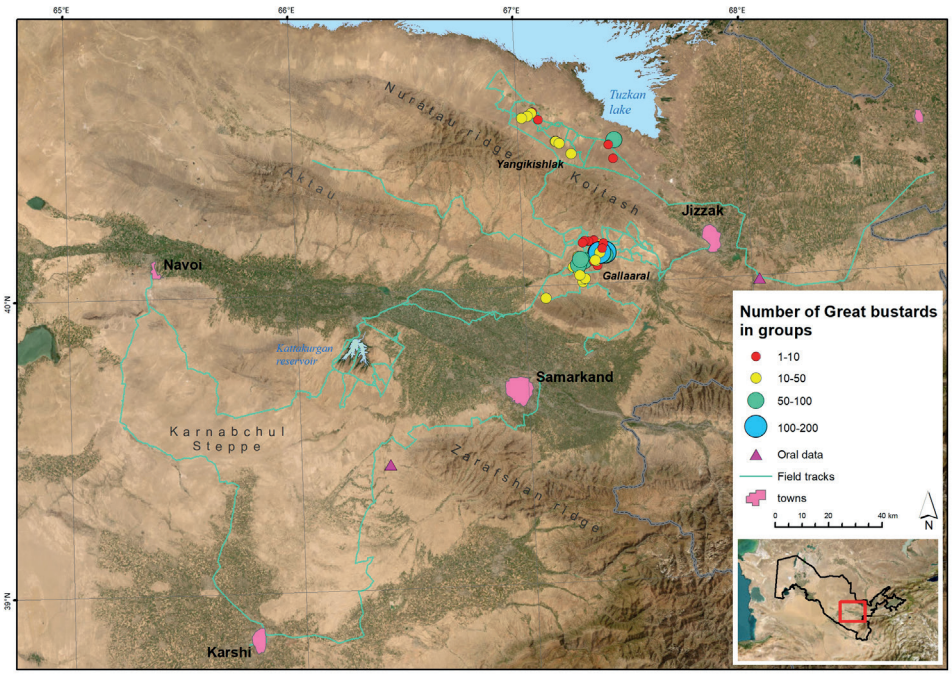

Fig. 3. Number of Great Bustards in flocks in winter 2020–2021

Table 1. Numbers of the Great Bustard on 2 wintering sites from 2019 to 2021

Year	Forish	Gallaaral	Total number
2019	105	No data	105
2019-2020	1-40	107	107
2020-2021	3-42	42-455	455

Table 2. Great Bustards records in 2019–2020

Date	Place	Natural habitats	Rain-fed fields	Total number
12.01.2019	Forish (Jizzakh region)	2	96	98
13.01.2019	Forish (Jizzakh region)	7	0	7
24.12.2019	Forish (Jizzakh region)	40	0	40
07.01.2020	Forish (Jizzakh region)	1	-	1
09.01.2020	Forish (Jizzakh region)	11	0	11
13.01.2020	Forish (Jizzakh region)	20	0	20
14.01.2020	Forish (Jizzakh region)	17	-	17
22.01.2020	Forish (Jizzakh region)	21	-	21
01.02.2020	Gallaaral (Jizzakh region)	-	30+77	107
03.02.2020	Malguzar (Jizzakh region)	0	0	oral data
15.02.2020	Forish (Jizzakh region)	28	-	28
14.11.2020	Bogaty (Tashkent region)	14 (oral data)		14
15.12.2020	Forish (Jizzakh region)	3	0	3
21.12.2020	Forish (Jizzakh region)	22	0	22
24.12.2020	Gallaaral (Jizzakh region)	-	20+30+1+1+3+6	61
25.12.2020	Gallaaral (Jizzakh region)	-	42	42
26.01.2021	Gallaaral (Jizzakh region)	-	4+6+161+105+72+7+80+20	455

28.01.2021	Gallaaral (Jizzakh region)	-	33+13+26+70+8+18+179+33+6+4	390
03.02.2021	Forish (Jizzakh region)	27+15	0	42
06.02.2021	Forish (Jizzakh region)	12+1+8	0	21
10.02.2021	Forish (Jizzakh region)	3+10	0	13
09.02.2021	Jam (Samarkand region)	-	0	oral data

The areas of the Great Bustard aggregations in the survey territory showed that these birds are more frequently found in rain-fed fields than in natural biotopes, which is associated with rich food resources (Fig. 1). Birds also used some slopes for rest (Fig. 4).

The survey showed that the first birds appear in December after a long period of cold weather in Kazakhstan, which confirms the reports of wintering in Kazakhstan (Shakula et al. 2016) and the assumptions of E. Kreuzberg-Mukhina (2003) that the arrival of Great Bustards in Uzbekistan is the result of winter short-distance migration. However, according to our data, this wintering is regular. Birds begin to move back to the north in early-mid-February. We also assume that the Gallaaral and Forish sites are interconnected and represent a single wintering aggregation (Fig. 5), in which birds move depending on the level of disturbance (possibly hunting pressure), food resources, and weather conditions.

The boundaries of the "Forish" and "Gallaaral" wintering grounds were identified based on suitable habitat. The total area was estimated at 166,000 hectares (Fig. 4). The number of Great Bustards wintering in these sites was 107 birds in 2020 and 455 in 2021 (Table 1). This means, that the population of wintering Great Bustards in Uzbekistan could be close to the KBA criteria A1b – ≥1% of the global population size of a VU species (IUCN 2016), or 440-570 individuals according to Alonso and Palacín (2010).

Fig. 4. Great Bustards resting in Gallaaral
Photo by V. Soldatov

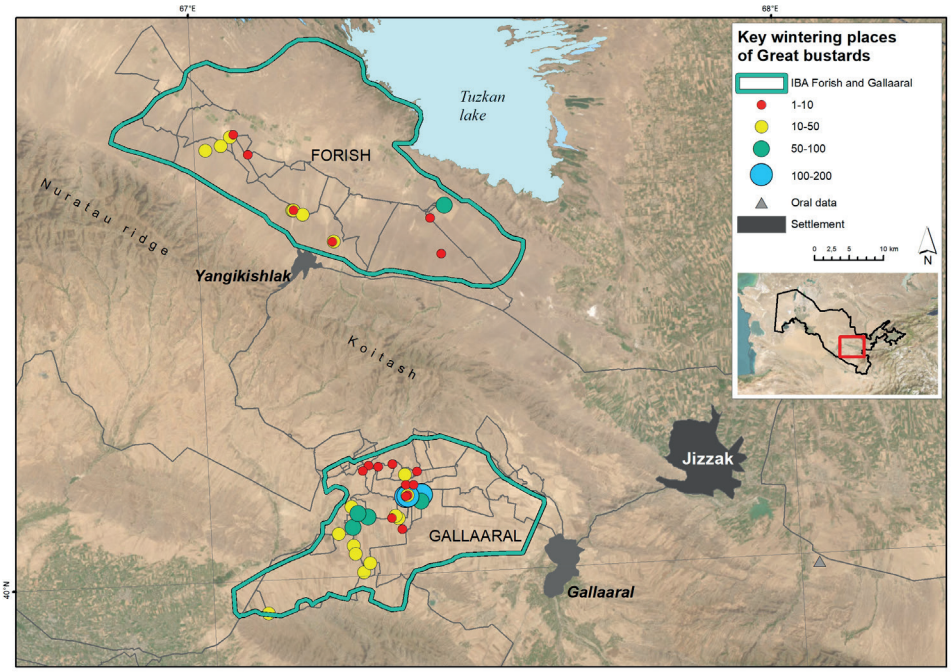

Fig. 5. Forish and Gallaaral – regular wintering sites for the Great Bustard

Work with the local community

The work conducted with the local community was key to identifying the wintering grounds of the Great Bustard. Local people, mainly shepherds, know all 3 Bustard species (Asian Houbara, Little Bustard, and Great Bustard). Local people - shepherds, hunters, farmers - were interviewed all across the survey sites. A total of 48 local residents were interviewed, 6 of them near the village of Yangikishlak, 3 in the Zaamin area, 16 near the village of Gallaaral, 6 near the village of Jush, 7 near the village of Jum, 5 near Kattakurgan and 5 in Karnabchul.

The interviewees were divided into groups:

- Shepherds who know the Great Bustard well and remember well when, where, and how many individuals they have seen – 11 people
- Shepherds who do not know the Great Bustard – 15 people. Only one knew the name.
- Farmers who know the Great Bustard (forestry workers) – 8 people.
- Farmers who do not know the Great Bustard – 1 person.
- Local residents who do not know the Great Bustard – 11 people.
- Hunters – 2 people. One of them knew the Great Bustard but attempted to mislead us, saying there were no Great Bustards in the Gallaaral area. The other said he used to hunt the Great Bustard.

The interview results suggest that shepherds are the most informed group of local residents familiar with Great Bustards. Moreover, they not only know the birds but also remember their numbers, where they stay and when. The age of shepherds also matters, so the best informed are middle-aged and old shepherds. Young shepherds do not see these birds, apparently, because of their small numbers.

In general, locals know that all Bustards are included in the Red Data Book and protected by the state. About 44% of respondents know and have seen the Great Bustard, the rest know Macqueen's Bustard or do not know about Bustards at all. Raising the awareness of local residents about threats to Bustards requires a careful approach, which should primarily include fostering a sense of pride in their native land. This species also rarely occurs near relatively large human settlements, in 2019 we recorded Great Bustards 3 km from the village of Yangikishlak

Threats

Threats in this article are presented in the format of the Great Bustard MOU – Action Plan 2018. Except for threats related to breeding, since the Great Bustard no longer breeds on the territory of Uzbekistan. The main reason for the disappearance of Great Bustards from their nesting grounds is the transformation of habitats caused by agricultural modification (Kashkarov et al. 2022).

Collision with power lines. One of the largest and heaviest birds with low maneuverability in flight, the Great Bustard is very prone to collisions with overhead power lines (Janss & Ferreer 2000; Raab et al. 2012). Collision mortality is recorded throughout the species' range and is expected to increase in Asia as infrastructure and industry develop (Kessler and Batbayar, 2014).

On 6 February 2021, Abdurasul Khaydarov recorded a Great Bustard that died from a collision with a power line during a survey in Forish District.

There are plans to develop power infrastructure at well-known wintering sites (UzAtom project, solar power station, and others). These projects involve the creation of power lines or long-term construction work, which will increase disturbance at wintering sites.

Hunting. Hunting for Great Bustards is prohibited almost throughout their entire range. However, over the past fifty years, uncontrolled illegal hunting has become the main reason for the reduction and even extinction of local populations of this slow-breeding species in the central and eastern parts of its range (Chan and Goroshko 1998; Heunks et al. 2001). Poaching, in either breeding or wintering grounds, is a grave threat to the survival of the Great Bustard population breeding in Turkey, Kazakhstan, south-eastern Russia, and Mongolia. The development of a network of paved roads in rural Asia has made it easier for urban hunters to reach rural areas (Kessler and Batbayar 2014; Kessler 2016). Some researchers note that the abolition of many anti-poaching departments and the atmosphere of lawlessness and chaos after the disintegration of the Soviet Union have contributed to the rise of illegal hunting (Berezovikov and Levinsky 2005; Khokhlov et al. 2010). Hunting in the Great Bustard wintering grounds in the south of Kazakhstan and Uzbekistan is a special problem as it is particularly common due to the proximity of these territories to capital cities. This poaching, apparently, caused a 30% reduction in the number of wintering Great Bustards in eastern Kazakhstan in 2012 (Berezovikov and Levinsky 2012) and the destruction of a wintering aggregation of at least 200 birds in Uzbekistan (Kreuzberg-Mukhina 2003).

The Great Bustard – is a state-protected, Critically Endangered, migratory European subspecies. According to Resolution No. 290 by the Cabinet of Ministers of the Republic of Uzbekistan, the fine for illegal hunting is 100 times the reference calculation value (27 million Uzbek soums or 2,480 USD).

Our survey did not record any death of a Great Bustard through hunting. Nevertheless, there is a lot of data confirming poaching, which is especially important for the key wintering sites we have identified. According to R. Meklenburtsev (1953), "during migration, Great Bustards fly

Fig. 6. Great Bustard that died as a result of collision with a power line
Photo by A. Khaydarov

at a height of 40 m above the ground; they are not capable of manoeuvring quickly and are thus extremely vulnerable. Great Bustards are sold at bazaars in Tashkent". Illegal hunting was mentioned as one of the gravest threats when Kh. Salikhbayev and M. Ostapenko (1964) wrote: "The numbers of wintering birds in the lower reaches of the Surkhandarya river have significantly decreased because hunters chase birds in cars". E. Kreuzberg-Mukhina (2003) confirms that poaching remains the main threat to the species in Uzbekistan. According to A.S. Nuridjanov, in the winter of 1999, about 200 Great Bustards appeared near Aydar Lake after cold weather had settled. Within a few days, almost all the birds were shot by poachers (Kreuzberg-Mukhina, 2003). In February 2015, after a heavy snowfall, 30-40 Great Bustards were spotted in the same area, and 6 of them were later killed by hunters (Asif Khan, oral report). Regular mass wintering of Great Bustards in the Zeravshan River valley is well known to local hunters (survey data, 2010). Besides purposeful poaching, some Great Bustards die because of the ignorance of local people. Local residents admitted that Great Bustards were shot by mistake instead of geese and pheasants in the Keles valley in 2008 and in the Karnabchul steppe in 2009 due to poor visibility (oral data by A. Ten).

Our research confirmed the high pressure from poachers. The first indicator was the distance, at which the birds left, scared. It was not smaller than 500 m. In our survey, we had to record Great Bustards at a distance of 800-1,000 m. The second one was the interviews with hunters. Hunters with a Niva car interviewed on 28 January 2021 in Gallaaral told they came to hunt Great Bustards. On 10 February 2021, a farmer told poachers shot a bird weighing 9 kg in 2020 (Gallaaral).

Interviews with local residents on poaching gave a mixed picture. We could not gain reliable information from a local hunter, since he said there were no Great Bustards in Gallaaral (we came across a group of birds 15 km from his village of Lalmikor) and that all hunters went to Aydar Lake (Forish District) for Great Bustards.

Habitat quality decrease. The use of agricultural machinery at inappropriate times and the intensification of agricultural production are the main threats to the quality of breeding habitats. For Great Bustards inhabiting natural pastures, overgrazing reduces the quality of food and increases the risk of destroying nests.

This threat is significant in Uzbekistan, where crops on the Great Bustard's wintering grounds, including those in Gallaaral, are sown in winter. In February 2021, large-scale agrotechnical activities (ploughing and sowing) in Gallaaral led to a sharp decline in the Great Bustard population, while in Forish District it grew somewhat. Probably, the wintering aggregation, disturbed by tractors and larger numbers of people, moved to the Forish area.

Disturbance. Great Bustards are extremely cautious and sensitive to disturbance from humans, and run away when one approaches them to a distance of 500 to 1,500 m (Gewalt 1959). This is particularly so in areas where they are hunted by people. An inappropriate level of even harmless human activity may cause Great Bustards to leave a suitable habitat (Kessler and Batbayar 2014).

The birds that we encountered on the wintering grounds were extremely cautious and did not allow us to observe them from a smaller distance than 800-1,000 m. This behaviour confirms the high sensitivity of this species to various kinds of disturbances and should be taken into account in implementing further protection measures.

Climate change. Large and heavy, male Great Bustards are sensitive to high temperatures (Alonso et al. 2009). Climate modelling suggests that most of the Great Bustard's current range in Europe would become unusable by the late 21st century. Huntley et al. (2007) found that suitable habitats will move from Western Europe to some parts of Eastern Europe and Sweden, currently uninhabited by this species. It is unclear how this highly philopatric species will adapt to climate change (Kessler and Batbayar 2014).

It is likely that this threat may indirectly affect the state of food resources on rain-fed farmlands in Uzbekistan, which are one of the important wintering habitats (Fig. 7). The low precipitation in autumn often leaves land dry, which does not allow farmers to plough it and sow crops in the usual time and forces them to do it at the end of the cold season, when first warm days set in. It is possible that the active ploughing of fields in Gallaaral in February 2021 forced the birds out of this area. Our interviews in other regions showed that in some areas of Kashkadarya region, similar foothills are much less often used for agricultural purposes

Fig. 7. A group of Great Bustards foraging in a wheat rain-fed field (Jizzakh region, Gallaaral district) Photo by V. Soldatov

because winter precipitation has decreased heavily. All this may lead, on the one hand, to a decrease in food resources, on the other hand, to a higher disturbance in the fields associated with agricultural activities in winter (December-February).

Threats associated primarily with migration and movements. The long flyways of the Asian subspecies, which include several stopovers and the crossing of international borders, as well as its nomadic behaviour on wintering grounds, expose them to special risk. Tagged females in a group of Asian Great Bustards died through all kinds of causes on their migration route and in wintering grounds (Kessler and Batbayar 2014). Most likely, Great Bustards that remain for the winter in Forish and Gallaaral breed in the central part of Kazakhstan. According to the study of wintering in the south of Kazakhstan, on the border with Uzbekistan (Shakula et al. 2016), the birds most likely migrate to the south as unfavourable conditions, such as lack of food resources and unsuitable weather, develop in the region. Wintering in Uzbekistan, they also face various threats. Increased agricultural activities in Gallaaral in February 2021 made the birds abandon their wintering grounds in that region. It is not clear where the birds have moved to. The population in Forish has increased slightly, but it is likely that the birds migrated not only to Forish, but also to other less favourable areas.

National and international use. In the past, international trade in the Great Bustard feathers led to the inclusion of this species in Appendix II and then in Appendix I of the Convention on International Trade in Endangered Species of Wild Fauna and Flora (CITES). This trade has largely been overcome. Great Bustard hunting is prohibited in Uzbekistan.

DISCUSSION

The legal protection of the Great Bustard in Uzbekistan is at the highest national and international levels. In addition, the species is protected by international conventions ratified in Uzbekistan. The Great Bustard is included in Appendix II to the Convention on International Trade in Endangered Species of Wild Fauna and Flora (CITES). It is also listed in Appendix I to the Convention on the Conservation of Migratory Species of Wild Animals (CMS): within the framework of this convention, according to the Action Plan for the Central Asian Flyway, migratory birds must be protected throughout their year-round range in Central Asia. In addition, the Great Bustard is included in Appendix I of the European Commission Birds Directive. Importantly, this list also provides a mechanism to share knowledge about advanced methods of protecting Great Bustards (for example, methods to equip power lines with bird-protective devices, and development of cooperation agreements with farmers) through EU projects with non-EU range states (Kessler and Batbayar, 2014). This means that Uzbekistan should take into account the significance of the species for the territories in which EU-supported projects will be implemented, including those funded by the European Bank for Reconstruction and Development (EBRD). According to Kreuzberg-Mukhina (2003), nowadays, effective protection of the Bustard populations, including those of the Great Bustard, is possible through the development of multilateral treaties and agreements under the CMS and CITES, as well as through the development of a special action plan that would enhance the legal protection of the species and creation of strictly protected natural areas to ensure the protection of species within their ranges.

Observations made in recent years arouse hope that the Great Bustard will not disappear from Central Asia. However, the recorded population growth is insignificant, rapid changes are taking place in the region and the species remains very vulnerable. In order to conserve its population, it is necessary to immediately improve the situation with poaching and low reproduction (Kessler 2016). Habitat protection should be formalized and strengthened with more steps to combat poaching and reduce disturbance.

To prepare an Action Plan for the conservation of the Great Bustard in Uzbekistan, it is important to obtain a full picture of the ecology of the species in winter, including its distribution, abundance, mortality, threats, migration routes, wintering grounds, and other information. This requires various kinds of studies, including sociological ones, since winter grounds are located in close proximity to human settlements. Therefore, the preparation of the plan remains a long-term activity. Since wintering sites are currently under threat, urgent measures must include an immediate action plan to conserve Great Bustards, which should include priority steps to protect already known wintering sites and reduce known threats – combating poaching, supplying power lines with bird protection devices, informing energy infrastructure development projects and so on.

One of the main goals of such a plan we think is creating natural protected areas on the key wintering sites – Forish and Gallaaral with a regime prohibiting hunting in the winter period. As the area is mainly used by farmers, the optimal category for this area is an ornithological 'zakaznik' – IV category of the IUCN protected areas – with enhanced protection and prevention of any disturbance during the winter period.

The second is reducing the risks of collision with power lines on key sites and flyways. The main areas of Great Bustards' movements (between roosting and foraging sites, short-distance flyways) should be identified, and the sections of power lines that have already caused deaths should be spotted. Power lines should be equipped with bird-protective equipment or, ideally, diverted from sensitive areas to reduce mortality (Raab et al. 2012). The potential danger of constructing power lines should be taken into account when large-scale industrial projects are implemented in the Great Bustard habitats. This action seems to us to be quite realistic. Several experienced experts, including the authors of this article, have in recent years carried out environmental impact assessments for large power plant and transmission line projects. Recommendations have already been made to reduce the risks for the Great Bustard.

Information campaigns should also contribute to developing in people a sense of pride in the preservation of this species. Taking into account that some hunters come from urban settlements, such campaigns should be implemented not only at the local, but also at the national level (Kessler 2016).

One of the possible long-term steps is to develop a Great Bustard - friendly farming system, e.g. protecting some areas with natural food from ploughing and reducing disturbance by farmers in places where Great Bustards aggregate.

CONCLUSION

Surveys in Jizzakh, Samarkand, Kashkadarya, and, partially, Bukhara regions show that key wintering sites for the Great Bustard species are located in Forish and Gallaaral

Districts of Jizzakh region. In these sites we recorded 455 individuals in winter 2020-2021 (Fig.3, Fig.5). This number is close to the KBA criteria A1b – ≥1% of the global population size of a VU species (IUCN 2016), as the total global number is estimated at 44,000-57,000 individuals (Alonso and Palacín 2010).

48 local residents were interviewed and shepherds were identified as a key group as they are the most aware of the distribution of these birds. Hunters are aware of the status of the Great Bustard and purposefully hunt this species on its wintering grounds in Forish and Gallaaral Districts of Jizzakh region. Constant structural changes taking place in the State Committee for Ecology of the Republic of Uzbekistan lead to a weakening of the protection, which is carried out by state inspectors.

We found all signs of poaching (from interviews with hunters and local people, literature data, and Bustard behaviour), and found a bird dead due to the collision with a power line. There are also other non-direct threats, such as climate change, which is already negatively affecting traditional farming in the southern regions of Uzbekistan, in recent years farmers have been unable to sow due to the low precipitation in the winter period. And in 2021, for the same reason, farmers started to plow in February while traditionally they do this in late November - December.

The results of this study show the need to conserve the Great Bustard wintering grounds (Forish and Gallaaral) through the creation of a protected area.

REFERENCES

Alonso J.C. and Palacín C.A. (2010). The world status and population trends of the great Bustard (Otis tarda). Chinese Birds, 1, 141-147.

Alonso J.A., Alonso J.C., Hellmich J. (1990). Metodología propuesta para los censos de avutardas. In: Alonso, J.C., Alonso, J.A. eds., Parámetros demográficos, selección de hábitat y distribución de la Avutarda en tres regiones españolas, 1st ed. Madrid: Icona, 86-98

Alonso J. C., Palacín, C. A., Alonso, J. A. and Martín, C. A. (2009). Post-breeding migration in male Great Bustards: low tolerance of the heaviest Palaearctic bird to summer heat. Behav. Ecol. Sociobiol., 63, 1705-1715.

Alonso J.C. (2014). The Great Bustard: past, present and future of a globally threatened species. Ornis Hungarica 22(2), 1-13.

Beresovikov N.N., Anisimov E.I., Levinskiy Yu.P., Zinchenko Yu.K., Kovalenko A.V., Gavrilov E.I., Gavrilov A.E., Belyalov O.V., Gubin B.M., Levin A.C., Karpov F.F. (2002). Great Bustard. Kazakhstan ornithological bulletin, 1, 74-77 (in Russian).

Berezovikov N.N., Levinskii Y.P. (2005). Overwintering of Great Bustards in the Alakol' Basin in 2004–2005, Russian Ornithological Journal, 289, 489-491 (in Russian).

Berezovikov N.N., Levinskii Y.P. (2012). Overwintering of the Great Bustard in the Alakol' depression form 2011–2012, Russian Ornithological Journal №758, 1153–1155 (in Russian)

BirdLife International (2022). Available at: http://datazone.birdlife.org/species/factsheet/great-Bustard-otis-tarda/text.

Bostanzhoglo V.N. (1911). Ornithological fauna of the Aral-Caspian steppes. Moscow, Russia (in Russian).

Bravo C., Ponce C., Palacín C.A., Alonso J.C. (2012). Diet of young Great Bustards Otis tarda in Spain: sexual and seasonal differences. Bird Study, 59(2), 243-251.

Chan S., Goroshko O.A. (1998). Action plan for conservation of the Great Bustard. BirdLife International, Tokyo, Japan.

Gewalt W. (1959). Die Großtrappe (Great Bustard). Die neue Brehm-Bücherei. Wittenberg Lutherstadt, Germany.

Gubin B.M. (1996). Great Bustard. In: A. Kovshar, ed., Red Book of Kazakhstan, 3st ed. Almaty: Konjyk, 168-169 (in Russian)

Heunks C., Heunks E., Eken G., Kurt B. (2001). Distribution and current status of Great Bustard Otis tarda in the Konya Basin, central Turkey. Sandgrouse 23, 106-111.

Huntley B., Green R.E., Collingham Y.C., Willis S.G. (2007). A climatic atlas of European breeding birds. Barcelona: Durham University, the RSPB and Lynx Edicions.

IUCN (2016). A Global Standard for the Identification of Key Biodiversity Areas, Version 1.0. 1 ed. Gland, Switzerland: IUCN

Janss G.F.E. and Ferrer M. (2000). Common crane and great Bustard collision with power lines: collision rate and risk exposure. Wildlife Society Bulletin, 28(3), 675-680.

Kashkaro R.D., Mitropolskaya Yu.O., Ten A.G. (2022). The historic and current status of the Great Bustard Otis tarda tarda in Uzbekistan and prospects for its conservation. Sandgrouse, 44(1), 26-34

Kessler M. (2016). Modern status of Great Bustard in Cental Asia and steps for conservation. Steppe Bulletin, 46, 61-69. (in Russian)

Kessler M., Batbayar N. (2014). Proposal to list the global population of Great Bustard on Appendix I, submitted by the Government of Mongolia to the Convention on Migratory Species in 2014. UNEP/CMS/ScC18/Doc.7.2.4: Proposal 1

Khokhlov A.N., Il'yukh M.P., Shevtsov A.S., Khokhlov N.A. (2010). On the significant decreases in migratory and wintering Great Bustards in Stavropol Krai. Ornithology in Northern Eurasia. Materials of the 13th International Ornithological Congress of Northern Eurasia. Orenburg, 319 (in Russian)

Kreuzberg-Mukhina E.A. (2003). The current status of Bustard species in Uzbekistan. Bustards of Russia and adjacent countries, 2. Saratov, 64-75 (in Russian)

Lane S.J., Alonso J.C., Martín C.A. (2001). Habitat preferences of Great Bustard Otis tarda flocks in the arable steppes of central Spain: are potentially suitable areas unoccupied? J. Appl. Ecol., 38, 193-203

Lanovenko E.N., Filatova E.A. (2019). Great Bustard. In: The Red Data Book of the Republic of Uzbekistan. Vol. II. Animals. Tashkent, Uzbekistan: Chinor ENK publishing house. (in Russian with English summary)

Meklenburtsev R.N. (1953). Fauna of the Uzbek SSR. Vol 2: Birds, Part 1. Tashkent, Uzbek SSR: FAN publishing house. (in Russian)

Meklenburtsev R.N. (1990). Order Gruiformes. In: N. Matchanov, A. Sagitov, ed., Birds of Uzbekistan, 2. Tashkent, Uzbek SSR: FAN publishing house, 7-10 (in Russian)

Oparin M.L., Oparina O.S., Kondratenkov I.A., Mamaev A.B., Piskunov V.V. (2013). Factors causing long-term dynamics in the abundance of the Trans-Volga Great Bustard (Otis tarda L.) population. Biol. Bull., 40, 843-853 (in Russian).

Oparina O.S., Oparin M.L., Kudryavtsev A.Yu., Oparina A.M. (2022). Characteristics of the Great Bustard (Otis tarda) (Otididae, Aves) habitats in the Trans-Volga region according to food availability during the chick rearing period. Povolzhskiy Journal of Ecology, (1), 34-54 (in Russian)

Raab R., Schütz C., Spakovszky P., Julius E., Schulze C.H. (2012). Underground cabling and marking of power lines: conservation measures rapidly reduced mortality of West -Pannonian Great Bustards Otis tarda. Bird Conservation International, 22, 299-306, DOI: 10.1017/S0959270911000463.

Salikhbaev H.S. (1983). Great Bustard. In: Red Data Book of Uzbek SSR. Rare and endangered species of animals and plants. Vol. I. Vertebrates. Sadykov A. S. ed. Tashkent, Uzbek SSR: FAN publishing house (in Russian)

Salikhbaev H.S., Ostapenko M.M. (1964). Birds. In: Ecology and economic value of vertebrate animals of Southern Uzbekistan (Surkhandarya Basin). Bogdanov O. P. ed. Tashkent, Uzbek SSR: FAN publishing house (in Russian)

Shakula G., Baskakova S., Shakula D., Shakula S. (2016). Great Bustard (Otis tarda) on the southern Kazakhstan. Ornithol. conf. « Birds and agriculture: current state, problems and prospects for study». Moscow, 313-318. (in Russian)

Ten A.G., Tulayev J.A., Soldatov V.A., Khaydarov A. (2020). Wintering grounds of Great Bustard Otis tarda in the Jizzakh region and threats. Zoological science of Uzbekistan: modern problems and development prospects. Materials of II national science conf., 281-283. Tashkent, Uzbekistan: FAN publishing house (in Russian with English summary).

RESEARCH PAPER

DISTRIBUTION OF ICINGS IN THE NORTHERN (RUSSIAN) PART OF THE SELENGA RIVER BASIN AND THEIR ROLE IN THE FUNCTIONING OF ECOSYSTEMS AND IMPACT ON SETTLEMENTS

Vladimir N. Chernykh[1*], Alexander A. Ayurzhanaev[1], Bator V. Sodnomov[1], Endon Zh. Garmaev[1], Bair Z. Tzydypov[1], Andrey N. Shikhov[2], Margarita A. Zharnikova[1], Bair O. Gurzhapov[1], Andrey G. Suprunenko[1], Avirmed Dashtseren[3]

[1] Baikal Institute of Nature Management of the Siberian Branch of RAS, 6 Sakhyanovoi St., 670047, Ulan-Ude, Russia
[2] Perm State National Research University, 614990, Perm, Russia
[3] Institute of Geography and Geoecology, Mongolian Academy of Sciences, Ulaanbaatar, Mongolia
***Corresponding author:** geosibir@yandex.ru
Received: April 15th, 2022 / Accepted: February 15th, 2023 / Published: March 31st, 2023
https://DOI-10.24057/2071-9388-2022-052

ABSTRACT. Icing is an integral part of the landscape in areas with permafrost. It is formed in winter in river valleys, along stream beds, in places of groundwater discharge and, unlike other objects of the cryosphere, is characterized by active dynamics. The main objective of this study is to identify the role and significance of icings in the functioning of natural systems of Russian part of the Selenga River basin, as well as their impact on settlements.

The first map of icings distribution was created based on Landsat imagery. In total, more than 15,500 icings were found. The highest concentration of icings is observed for forest landscapes. Icings in the forest-steppe belt are distinguished by their morphometric characteristics. They are often formed in giant areas of more than 1 km^2. Steppe icings account for about 8 % of all objects of the study area. Icings play an important role in the functioning of forest and, in particular, forest-steppe ecosystems, as they largely determine the redistribution of water flow in small watersheds.

During the period of increasing total water content, icings become a factor contributing to emergency situations. The potential risk of inundation has been established for 65 settlements in the Russian part of the Selenga River basin.

KEYWORDS: Icings, the Selenga River basin, runoff, mapping, NDSI, natural systems, anthropogenic systems, landscape

CITATION: Chernykh V. N., Ayurzhanaev A. A., Sodnomov B. V., Garmaev E. Zh., Tzydypov B. Z., Shikhov A. N., Zharnikova M. A., Gurzhapov B. O., Suprunenko A. G., A. Dashtseren (2023). Distribution Of Icings In The Northern (Russian) Part Of The Selenga River Basin And Their Role In The Functioning Of Ecosystems And Impact On Settlements. Geography, Environment, Sustainability, 1(16), 150-156
https://DOI-10.24057/2071-9388-2022-052

ACKNOWLEDGEMENTS: The work was carried out within the framework of the state task of the Baikal Institute of Nature Management SB RAS (AAAA-A21-121011990023-1)

Conflict of interests: The authors reported no potential conflict of interest.

INTRODUCTION

Icings formed in river valleys in the areas of permafrost distribution have been studied by scientists and research teams for more than a century. There are many publications devoted to the regularities of ice field formation and destruction (Podyakonov 1903; Tolstikhin 1974; Koresha 1981; Kravchenko 1985) the impact of icings on the river flow (Socolow 1975; Aufeis of Siberia 1981), spatial and temporal dynamics (Topchiev 1981; Alekseev 1973, 2007, 2016; Morse P.D 2015; Epsom T. et al. 2020), and other aspects. However, to a lesser extent, icings are studied in terms of their ecosystem significance, especially in regions where, at first glance, the role of icings in the functioning of the landscape sphere is insignificant. This includes Transbaikalia, including that part of the Selenga River basin. Icings and the processes associated with them have not been studied in the paper in as much detail as, for example, in the North-East of Russia or in the Baikal-Amur Mainline, because they do not cover large areas and volumes, but their role in the moisture turnover and some other processes of hydroclimatic nature is significant here.

The main goal of this paper is to assess the mapping of icings, taking into account the landscape approach with the study of their role in the ecosystems of the territory and their impact on the economic infrastructure and the environment. At the same time, making large-scale maps of the icings distribution is an important part of the work, since there are no available ones for the territory in question. Having a cartographic basis and databases containing the main morphometric characteristics of objects, it is possible to carry out a spatial analysis, to reveal regularities of icings distribution, its confinement to natural landscapes and location in relation to man-made objects.

The icings in the permafrost areas of are an integral part of the landscapes and, to some extent, markers of the

climatic changes occurring in the cryosphere (Alekseev 2016). At the same time, the natural processes occurring in continuous permafrost areas are different from those manifested in areas where the permafrost has a sporadic, intermittent development (Chalov et al. 2017). In the areas of continuous permafrost, stretching in a wide belt across the northern continents from Alaska to Chukotka, icings are formed in the conditions of forest, swamp forest, and tundra landscapes. This is not the case at the southern border of the cryolithozone. Here, the range of natural complexes is considerably extended, up to semi-deserts and deserts. In Western Transbaikalia, in the Selenga River basin, significant areas of icing fields are ubiquitous in steppes (Chernykh et al. 2022). In Eastern Transbaikalia, icings are adjacent to the centers of desertification in the Chara River valley (Alekseev 2008). In different natural complexes, ice processes manifest themselves with their own specificity and the greater the diversity of facies, the greater the variations. In this respect, the Selenga River basin is considered to be a particularly interesting study area. Giant icings of river water and small spring icings — taryns — are formed here. There are great number of objects to study.

Another distinctive feature of the northern (Russian) part of the Selenga River basin is the relative development and settlement of the area. The icings are affecting economic activities and the population of the area. According to open sources, 13 cases of flooding of settlements and some infrastructure facilities (roads) by thawed icings were recorded in 2022. Therefore, when studying the role and significance of ice, it is necessary to pay attention to the aspects of ensuring safety of the population living in areas with intensive formation of icings.

MATERIALS AND METHODS

Study Area

The northern, Russian part of the Selenga River basin was chosen as the study area (Fig. 1). The total area is 148,060 km^2. The study area includes, fully or partially, the watersheds of the major tributaries, the rivers of Dzhida, Chikoi, Khilok, Temnik, and Uda. It is a combination of intermountain depressions and low- to medium-altitude mountain ranges. The peculiarity of the study area is a well-developed hydrographic network with a large number of small rivers and streams (Chernykh et al. 2021). The study area is typically characterized by the distribution of different types of permafrost rocks (permafrost). Thus, the central part, including the Selenga River valley and the adjacent areas with thick sandy and sandy loam sediments, is characterized by predominantly thawed soils. Insular permafrost is typical of the basins of the Dzhida (southern part), Khilok, Tugnui, Uda and other rivers in areas with mountain dissected terrain. Continuous permafrost is widespread everywhere in the mountainous parts of the Chikoi and Dzhida River basins (northern part of the basin). The diversity of cryogenic geological conditions in the area with a dense hydrographic network and harsh, sharply continental climate determines the specific features of the intensity of ice formation processes.

Satellite images

Multispectral satellite images from Landsat 4-5, Landsat 8 and Sentinel were used as input data for the process of icings mapping. Landsat 8 and Sentinel images were used to determine the current location of objects in river valleys and to prepare maps of their current state. Twenty Landsat 8 scenes and ten Sentinel scenes were acquired from the servers of the US National Geological Service (https://earthexplorer.usgs.gov/). The images were selected so that the area of snow cover on them was minimal, and the imaging dates should not be far from the beginning of the icing fields thawing. For the lowland areas of the central part of the Selenga River basin it is late March – early April, for the middle mountains of the Dzhida and Chikoi Rivers basins, it is late April – early May. Under these conditions, even small ice fields with the size of 1-2 pixels (with the resolution of 60 m per point) are visually distinguishable on the obtained images. We used images from 2020, in some cases, when there were no images of proper quality from 2020, we used scenes from 2019. Comparison of the same scenes shows the similarity of natural and climatic conditions in spring 2019 and 2020, which in general satisfies the mapping tasks.

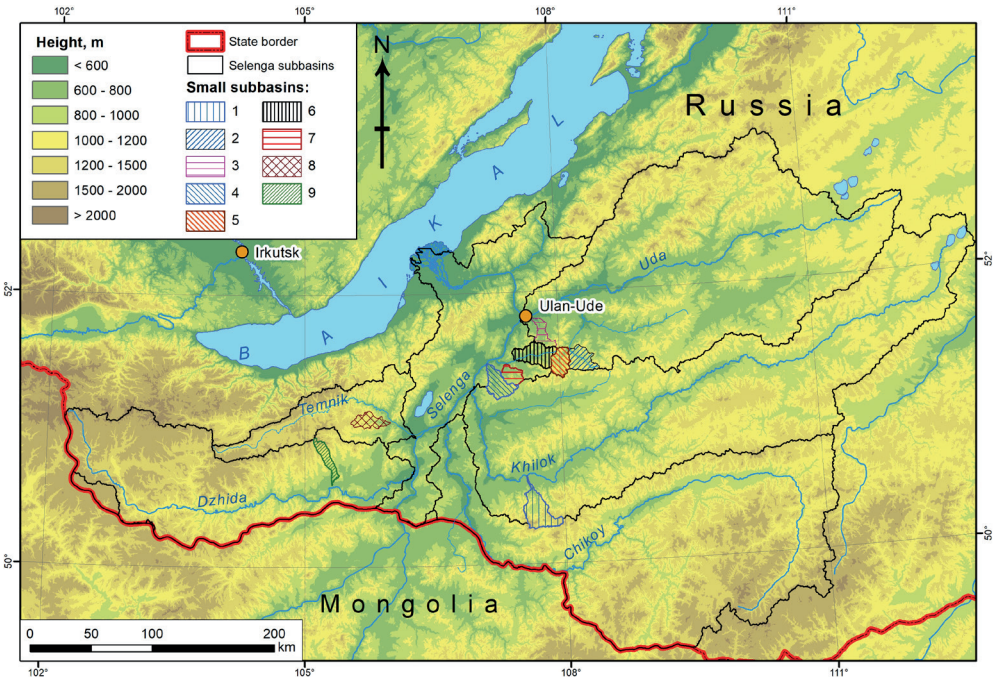

Fig. 1. Study area. Numbers indicate key sites (small watersheds): 1 - Vorovka, 2 - Kuytun, 3 - Kokytey, 4 - Shabur, 5 - Tarbagatai, 6 - Zhirim, 7 - Bichura, 8 - Urma 9 - Tsagatuy

Data analysis

The study used the NDSI index to determine the localization of the icings. The Normalized-Difference Snow Index, or NDSI, is an index for the interpretation of snow-ice objects (Hall 1995; Gagarin 2020; Brittney 2021). Its calculation is based on the difference in the reflection of radiation between the visible green (Green) and shortwave infrared (SWIR) parts of the spectrum. The index can be calculated in various GIS with a built-in algorithm for raster images (Raster Calculator). NDSI is calculated using the formula NDSI = (Green-Swir1)/(Green+Swir1).

This index is widely used by researchers in the interpretation of snow-ice objects, including icings, from multispectral satellite images. To facilitate the search process, various algorithms are used, allowing more or less automation of the process. In most cases, a buffer zone is pre-determined around watercourse thalwegs, within which calculations are performed, an output mask by NDSI threshold values and the reflection coefficient in the infrared range (Makarieva et al. 2019) are created, which allows to successfully distinguish ice from snow in watersheds later on. The above approach can be effectively applied to detect large ice deposits in those areas where they are formed on medium or large rivers. With the overwhelming majority of watercourses being small rivers and streams, the very process of buffer definition already becomes a complex and laborious work.

The results of the analysis of various publications indicate that semi-automatic methods of icings interpretation in combination with expert assessment are mostly used in large-scale icings mapping (Shikhov et al. 2020). For territories with complex, dissected topography, where the vast majority of icing fields are relatively small in size, such interpretation methods are the most suitable and give the most reliable results.

Field data

Individual icings located in different, small watersheds were studied by field expedition methods. Detailed investigations, which included ice field surveys from an unmanned aerial vehicle (UAV) with additional ground referencing, ice measurement surveys, ice drilling and ice volume counts, photographic recording, etc., covered 15 medium and large ice fields in 9 small watersheds (Fig. 1). Geological and geomorphological features of the study area, the role of icings in the ecosystems of the territory, and potential risks of minor flooding of settlements and infrastructure facilities were taken into account as criteria for selecting key sites. Meteorological data and quantitative runoff characteristics (for the key site in the Kuitunka River basin) were obtained from the Tarbagatai meteorological station (hydrological post).

RESULTS

Creation of thematic maps of hydrological processes is an important part of the study of water resources (Kortney et al. 2020). The icings mapping within the northern, Russian part of the Selenga River basin was performed with the use of Landsat and Sentinel satellite images. The 2019 and 2020 imagery was used in the study process, so the resulting map of the icings (Fig. 1) reflects the current location of the ice fields. The original map (GIS layer) is a set of polygons showing the actual position and morphometry of the icing fields.

There are 15547 objects marked on the map (in the vector layer), and attribute tables contain their basic planned morphometric characteristics. The total area of the icings as of 2020 is 364.79 km^2. Table 1 shows the distribution of the icings in the basins of the major rivers of Selenga tributaries.

According to the main morphometric characteristics, 6,117 objects belong to small and medium icings (S = 0.1 – 10 thousand m^2), 8,878 – large (10 – 100 thousand m^2), 429 – very large icings (100 – 1000 thousand m^2). Very small icings, with an area of less than 100 m^2, are definitely present within the territory, but their interpretation on medium resolution space images, especially in the forest belt, is complicated. We recorded one giant icing (Dzhida River basin).

Ice measurement surveys to determine ice thickness were conducted in the key study areas. The results of measurements show that the thickness of ice fields can vary from 0.45 to 3.5 m, depending on the valley structure and intensity of the icings processes. The average thickness of the icings in the study area ranges from 0.8 to 1.3 m.

Taking into account the experience of colleagues who have performed icings mapping within a region similar in area and number of objects (Brombierstäudl et al. 2021), we developed an icings map based on the «Icing» layer, which is a generalized image for the convenience of presentation. All the icing deposits in a 10 × 10 km cell are united by one scale symbol, denoting the icing coverage (S of the icing cover to S of the area ratio) for each specific cell. This allowed, on the one hand, to preserve the ideas about the localization of objects within the study area and on the other hand, to avoid "blurring" the correct perception of the information about the mapped objects.

Cartographic methods have been used to determine the difference in the icings coverage in the study area. It is highest in the Dzhida River basin, the territory of which is characterized by dissected relief and the presence of a large number of watercourses. Here this indicator can

Table 1. Icings by the basins of major tributaries of the Selenga River

	Rivers	Basin area, km^2	Number, pcs.	Total area, km^2	Volume, km^3	Ice coverage, %
1	Selenga*	16,926	69	2.8	0.003	0.016
2	Uda	34,800	2,929	88.41	0.079	0.254
3	Khilok	38,500	4,484	86.52	0.095	0.224
4	Chikoy	34,700	5,462	107.71	0.118	0.310
5	Dzhida	18,894	2,383	74.75	0.097	0.395
6	Temnik	4,240	220	4.6	0.003	0.108
	Total	148,060	1,5547	364.79	0.395	0.217

*- Russian part of the catchment basin (without the basins of major tributaries).

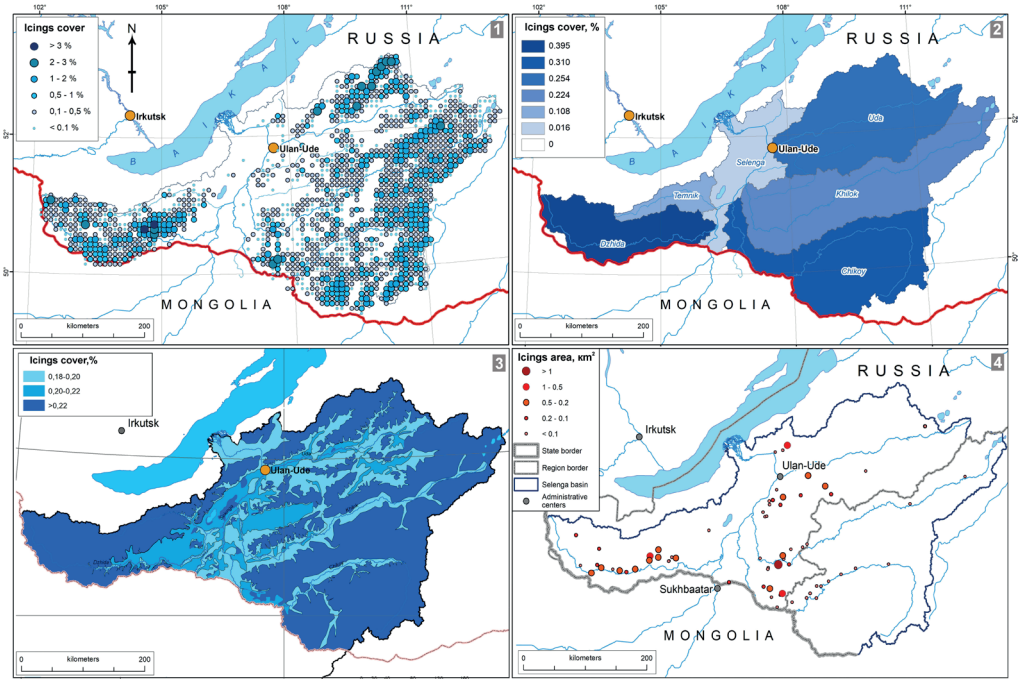

Fig. 2. Icings in the northern (Russian) part of the Selenga River basin: 1 - location card, 2 - icings coverage by the Selenga River tributary basins, 3 - icings coverage by landscape (altitude) belts, 4 - potentially dangerous icings

reach 0.4 %. The minimum icing coverage (0.01%) is observed in the central part of the Selenga River basin (not including basins of major tributaries), where icing is typical only for valleys of small rivers of Tsagan-Daban range spurs. Individual, small objects were observed during field studies in deep ravines and gullies in Medvedchikovo, Oditsar, Mengei and some other hollows.

Comparison with landscape maps (Atlas of Transbaikalia 1967; The ecological atlas... 2015) allowed us to establish quantitative characteristics of the icings distribution in different natural complexes by altitudinal belts. The forest belt (up to 12.2 thousand) is distinguished by the greatest amount of the icings, as it occupies the largest area. There are many facies in the Selenga River basin, depending on the absolute height, steepness and exposure of the slope, and the nature of vegetation. Icings are formed in narrow gaps almost everywhere in mountain-taiga and sub-taiga landscapes. Here they have small areas, 5–10 thousand m^2, with a thickness of 1–2 m. In the forest-steppe belt of low mountains, in intermountain depressions, where mouth parts of small and middle river beds are located, at least 2.2 thousand icing deposits are formed. They are larger than those in forests, and in some cases are up to 4–5 m thick. About 1 thousand icing deposits are distinguished in steppe landscapes of the territory. Ice-covered steppes are not exactly a typical phenomenon, but icings are ubiquitous, although not very large, in South Siberia and Mongolia. The distribution of the icings over natural complexes determines the differences in icings coverage (Fig. 2, 3).

Here, the icings are formed in valleys of numerous small rivers and along streams. At the same time, areas and volumes of the icings in river valleys, flowing in the forest-steppe conditions, are much larger than those in the forest belt. The icings are also observed in the steppes of the northern (Russian) part of the Selenga River basin, but they are of limited development. These are mainly spring icings.

DISCUSSION

The cartographic analysis established the similarities and differences in icing cover in the basins of the major tributaries of the Selenga River. They are determined by physical and geographical conditions. In the Uda and Khilok River basins, which are similar in size, the icings areas and the icing coverage coefficients are approximately the same. In the Chikoi River basin, which is approximately the same size as the Uda and Khilok Rivers within the territory of Russia, the total area of the icings is 20 km^2 larger.

The most important factor determining the intensity of ice formation is the type of permafrost rock characteristic of the territory. This is confirmed by the comparison of the permafrost distribution maps (Geocryology of the USSR 1989; Bazhenova 2018) with the obtained map of the icing coverage of the territory. The greatest number and the maximum total area of the icings (relative to the basin area) is observed in the Dzhida River basin, where continuous permafrost is widespread. The number of icings increases in the southeastern part of the Chikoi River basin, which is characterized by the same type of permafrost, in the mountainous part of the Uda River basin. In the head watershed of the Selenga River, in the estuaries of the valleys of large tributaries, the concentration of the icings is minimal, since thawed soils are common here.

As part of natural complexes with traces of the lower boundary of the cryosphere in their lithogenic base, the icings perform important habitat-forming and habitat-protecting ecosystem functions. At the same time, the ecosystem significance of icings is more pronounced in the forest belt and floodplain landscapes of the mountain forest-steppe. Thus, with an average thickness of 1.5 – 2 m, the icings in floodplains and on low terraces of small rivers in the Selenga middle mountains may persist until early June. Observations in the key area, where sensors were installed to record the main climatic parameters of the environment, showed that under current climatic conditions the process of icing formation starts at the end of December and ends at the end of March. For example, in 2022, the icings in the upper reaches of the Vorovka River, the beginning of formation of which was recorded on December 23 at air temperatures below – 20 °C, had an area of 0.074 km^2 and a volume of 100 thousand m^3 by the beginning of thawing on March 30. Thus, the ice fields mid-mountain forest-steppe landscapes exist up to 5 months, 2 of which are at maximum area with a constant increase

in volume. In addition, the spatial and temporal dynamics are characterized by a year-to-year shift of ice fields along stream channels within a wide range, and characteristic icing glades are well defined in the topography and recorded in floodplain vegetation.

The impact of icings on forest ecosystems, including mountain taiga, is even more pronounced. There, they are actually formed everywhere in narrow, often V-shaped valleys with permanent watercourses, rivers or streams. In the forest belt, in the Selenga River basin, where the upper boundary of spring icings spreads up to 1550 – 1600 m, even small in thickness icings may persist until the end of June. This determines a special microclimate, topography and hydrological features. The icing glades in the depressions are usually waterlogged, and the vegetation period of herbaceous vegetation starts belatedly.

The icings in the northern (Russian) part of the Selenga River basin play an important role in supplying river runoff. During the mapping process, 1,400 small rivers (3rd order) and more than 3,300 streams were identified within the territory. The runoff of these watercourses from April till June depends almost entirely on the thawing of the ice fields in their valleys. Icings accumulate a whole winter runoff. Calculations of the icing runoff, made using Landsat satellite images, data from a gauging station and Tarbagatai weather station (2000) through the example of small catchment area of Kuitunka River show that by the middle of April about 1540 thousand m^3 of ice is contained in the icings fields, which makes 8.4% of annual flow of Kuitunka River. Similar values were obtained by calculation for other small watersheds in the key study areas. Thus, in total, not less than 0.6 km^3 of ice is contained in the icings of the territory by spring. Part of this melting water flows further into medium and large rivers, but part of the runoff, which is very important, is taken for the agriculture needs. The water of small rivers and streams is actively used by the local population and agricultural enterprises for irrigation of cultivated meadows in the river valleys. For this purpose, entire networks of irrigation systems, which allow transferring water over distances of dozens of kilometers, were created using traditional technologies as far back as the last century. Due to the melting of the icings, providing almost uninterrupted flow of small rivers and streams during the period when precipitation is very limited (Garmaev at el. 2020).

Along with the important ecological significance, the icing processes under consideration are also the factors of geo-ecological risks associated with the threats of flooding. The potential threats of flooding in this case should be understood as the probability of excessive development of the ice field of an icing, in which case residential houses, buildings on household plots, infrastructure facilities, etc. are affected by the natural process. A total of 350 settlements, including towns, villages, large summer houses (farms) included in municipalities, were considered in the Russian part of the Selenga River basin, including the Republic of Buryatia (RB) and Zabaykalsky Krai. When identifying the icing threats, not only the territory included in the settlement's boundaries, but also infrastructure facilities adjacent to the settlement, farms, roads, railroads, power lines, etc. were taken into account. The risk was determined by the actual proximity or presence of the icings in the boundaries of the settlement.

Potential threats of underflooding by icings have been established for 65 localities within the Selenga River basin (Fig. 2, 4), of which 51 are in the RB, including 3 cities (Fig. 3). In Ulan-Ude, the capital of the Republic of Buryatia, residential houses in Arshan, Verkhnyaya Berezovka, Divizionnaya Station, Zabaikalsky and Erhirik settlements (part of the agglomeration) are flooded by the icings. Zakamensk, located in the Dzhida River basin and characterized by unfavorable environmental conditions (Garmaev et al. 2016), is also affected by the icings. The Icings are also formed in the center of the bordering town of Kyakhta. In Zabaikalsky Krai, the potential threats of underflooding by the icings have been established for 14 settlements. A study of the dynamics of individual the icings over the period from 2000 to 2020 in small watersheds within the Russian part of the territory showed that, depending on the climatic cycle, the areas of the icings can vary by 6 times (Chernykh et al. 2021). Thus, the current location of the potentially hazardous icings determines the risks of underflooding both in the current natural-climatic situation and with further increase in the total water content.

Combating icings and protecting settlements from underflooding is becoming an increasingly urgent task in the region due to the onset of a high-water climatic cycle.

Fig. 3. Icings in the settlements: 1 – Nikolaevsky, 2 – Burnashevo, 3 – Petropavlovka, 4 – Bichura
Photo images from an unmanned aerial vehicle

The long period of drought in Transbaikalia has led to the dilapidation and partial destruction of a number of icing protection structures (dams with sluices), which requires their inventory, repair and restoration, and the construction of new ones. The experience of 2022 has shown that it is necessary to purchase special equipment, which allows reducing the risks of underflooding where the icings have already reached significant volumes. In these cases, sawing ice to create ditches to divert water is almost the only way to protect against flooding, and it must be done until the ice fields begin to melt.

The main hazard of icings is that forecasting the intensity of their development and location in relation to populated areas and infrastructure objects is an extremely difficult task, since a large number of factors, from precipitation to tectonics, must be taken into account (Romanovskii 1973; Shesternev and Verkhoturov 2006). As studies show, the spatial and temporal dynamics of icings is expressed in their extreme variability (Alekseev 1987). Therefore, it is necessary to scientifically substantiate and create a modern monitoring system for icings potentially hazardous for settlements and infrastructure objects.

Thus, the icings formed in the northern (Russian) part of the Selenga River basin play an important role in balancing natural and anthropogenic-transformed systems, as well as in maintaining a favorable environmental situation in the territory, which differs in its characteristics from the hard-to-reach areas of the North or Northeast Russia, where giant icings are formed, which have been studied by various researchers for many years.

CONCLUSIONS

Icings are fascinating objects of the cryosphere. In the northern (Russian) part of the Selenga River basin, they are formed in forest, forest-steppe, steppe and even, in fact, semi-desert (dry-steppe) landscapes. This is one of the peculiarities of Transbaikalia — the formation of so-called permafrost or cryoarid landscapes (Taisaev 2004). Cryogenic processes are observed throughout the region, especially during high-water climatic cycles. It should be noted that large-scale GIS mapping of the icings has not been conducted in this part of the territory before, which is one of the factors explaining the novelty of this work.

The results of the study:

1. The first large-scale map of the location of the icings in the northern (Russian) part of the Selenga River basin has been compiled. The peculiarity of the map is that it shows the maximum number of objects for this mapping scale — more than 15.5 thousand. With a frequency of the icings formation is 75% and higher, which is typical for the study area according to the analysis of multi-temporal satellite images, the map is relevant not only for the specific and nearest years, but can be used for long-term observations and research of icings.

2. Vector data and basic, planned morphometric characteristics of the icings in the transects of the vast area have been obtained. These data can be used in studying icing dynamics, identifying the dependence of icing formation intensity on various environmental factors, as well as in applied activities, for example, in planning the organization of the economic activity within an area.

3. The landscape approach to the study of icings allowed us to determine their place, role and significance in the natural systems of the study area. New up-to-date views on the areas of the icings formation for varying altitudinal belts were obtained. The Icings in the taiga and sub-taiga landscapes form the microclimatic features of the mountainous areas. The Icings in the forest-steppe belt contain maximum water reserves. Up to 8 % of the icings are confined to steppe landscapes of the territory. Icings play an important role in providing and maintaining the runoff of small rivers and streams, numbering least 5 thousand within the study area.

4. Icings have a negative impact on the man-made systems of the territory, primarily on the settlements and infrastructure facilities. This impact is expressed in the form of underflooding, which occurs during the cold season in early spring and is therefore difficult to remedy. In the northern (Russian) Selenga Basin, flooding risks have been identified for 65 communities and numerous infrastructure facilities.

The study of icings, in various aspects, remains urgent. This is especially true of the areas on the southern border of permafrost distribution. In the past, there has been little attention paid to icings, but there is little research at present. At the same time, interest in these objects of the Earth's cryosphere is growing, and modern technical capabilities, including the use of space images and drones, bring the study of icing processes to a new level.

REFERENCES

Alekseev V.R. (1973). Aufeis as a factor of river valley morpholithogenesis. In: Regional Geomorphology in Siberia. Novosibirsk: Nauka, 89-134. (in Russian).

Alekseev V.R. (1987). Aufeis. Novosibirsk: Nauka, 256. (in Russian).

Alekseev V.R. (2007). Aufeis Science: Dictionary-Reference Book. Novosibirsk: SB RAS Publishing house, 438. (in Russian).

Alekseev V.R. (2008). Cryology of Siberia: selected works / V.R. Alekseev. Novosibirsk: Academic edition «GEO». 483.

Alekseev V.R. (2016). Long-term variability of the spring taryn-aufeises. Ice and Snow, 56(1), 73-92, DOI: 10.15356/2076-6734-2016-1-73-92. (In Russian).

Atlas of Transbaikalia (Buryat ASSR and Chita region). GUGK. Moscow-Irkutsk. 1967, 176 (in Russian).

Aufeis of Siberia and the Far East (1981). Nauka, Novosibirsk, 244. (in Russian).

Bazhenova O.I. (2018). Modern denudation of foothill steppe plains. Novosibirsk: Academic publishing house «Geo», 259.

Brombierstäudl D., Schmidt S., Nüsser M. (2021). Distribution and relevance of aufeis (icing) in the Upper Indus Basin. Science of The Total Environment, 780, 146604.

Brittney K. Glass, David L. Rudolph, Claude Duguay, Andrew Wicke. (2021). Identifying groundwater discharge zones in the Central Mackenzie Valley using remotely sensed optical and thermal imagery. Canadian Journal of Earth Sciences, 58, 105-121

Chalov S., Golosov V., Tsyplenkov A., Theuring P., Zakerinejad R., Märker M., Mikhail Samokhin M. (2017). A toolbox for sediment budget research in small catchments. Geography, Environment, Sustainability, 10(4), 43-68, DOI-10.24057/2071-9388-2017-10-4-43-68.

Chernykh V.N., Sodnomov B.V., Ayurzhanaev A.A., Tsydypov B.Z., Dabaeva D.B., Suprunenko A.G. (2021). Aufeis in the mountainous areas of the northwestern part of the Selenga River basin. IOP Conference Series: Earth and Environmental Science, 885(1), 012034.

Chernykh V.N., Sodnomov B.V., Ayurzhanaev A.A., Batotsyrenov E.A. (2022). Ice in the steppes of Western Transbaikalia // Issues of steppe science, 3, 4-11, DOI: 10.24412/2712-8628-2022-3-4-11 (in Russian).

Endon Zh. Garmaev, Anatoly I. Kulikov, Bair Z. Tsydypov, Bator V. Sodnomov, Alexander A. Ayurzhanaev (2019). Environmental Conditions of Zakamensk Town (Dzhida River Basin Hotspot). Geography, Environment, Sustainability, 12, 3, 224-239, DOI-10.24057/2071-9388-2019-32.

Ensom T., Makarieva O., Morse P., Kane D., Alekseev, V., Marsh P. (2020). The distribution and dynamics of aufeis in permafrost regions. Permafrost and Periglacial Processes, 31, 383-395.

Gagarin L., Wu Q., Melnikov A., Volgusheva N., Tananaev N., Jin H., Zhang Z, Zhizhin V. (2020). Morphometric Analysis of Groundwater Icings: Intercomparison of Estimation Techniques. Remote Sensing, 12, 692.

Garmaev E.Zh., Ayurzhanaev A.A., Tsydypov B.Z., Alymbaeva Zh.B., Sodnomov B.V., Andreev S.G., Zharnikova M.A., Batomunkuev V.S., Mandakh N., Salikhov T.K., Tulokhonov A.K. (2020). Assessment of the Spatial and Temporal Variability of Arid Ecosystems in the Republic of Buryatia. Arid Ecosystems, 10, 2, 114-122.

Geocryology of the USSR (1989). Eastern Siberia and the Far East. eds. by Ershov E.D. Moscow, Nedra Publisher, 516. (in Russian).

Hall D.K., Riggs G.A., Salomonson V.V. (1995). Development of methods for mapping global snow cover using Moderate Resolution Imaging Spectroradiometer data // Remote Sens. Environ, 54, 127-140.

Koresha M.M. (1981). The methods of aufeis research. In: Alekseev VR, ed. Aufeis of Siberia and Far East. Novosibirsk, Russia: Nauk, 38-52. (in Russian).

Kravchenko V.V. (1985). Regularities of formation and distribution of aufeis at rivers in the southern regions of East Siberia. In: Glaciological Studies in Siberia. Irkutsk, Russia: Institute of Geography SB RAS, 19-38. (in Russian).

Leonid M. Kortney, Olga V. Gagarinova, Elena A. Ilyicheva, Natalya V. Kichigina (2020). A Geographical Approach to Water Resource Mapping for Atlases. Geography, Environment, Sustainability, 13(2), 96-103, DOI-10.24057/2071-9388-2019-171.

Lyytimäki Jari. (2014). Ecosystem disservices: Embrace the catchword. Ecosystem Services. 12, DOI: 10.1016/j.ecoser.2014.11.008.

Makarieva O.M., Shikhov A.N., Ostashov A.A., Nesterova N.V. (2019). Historical and recent aufeis in the Indigirka River basin (Russia). Earth System Science Data, 11(1), 409-420. (in Russian).

Morse P.D., Wolfe S.A. (2015) Geological and meteorological controls on icing (icings) dynamics (1985 to 2014) in subarctic Canada. Journal of Geophysycal Research: Earth Surface, 120, 1670-1686.

Podyakonov S.A. (1903). Aufeis in Eastern Siberia and the causes of their occurrence. Izvestiya RGO [Bull. of Russian Geographical Society], 39, 305-337. (in Russian).

Romanovskii N.N. (1973). About geological role of aufeis. In: Permafrost Studies, 13. Moscow, Russia: Moscow State University, 66. (in Russian).

Shesternev D.M, Verkhoturov A.G. (2006). Aufeis in Transbaikalia. Institute of Natural Resources, Ecology and Cryology: Chita, Russia. (in Russian).

Shikhov A.N., Gerasimov A.P., Ponomarchuk A.I. (2020). Thematic interpretation and interpretation of space images of medium and high spatial resolution: a tutorial. Perm State National Research University. Perm, 192.

Socolow B.L. (1975). Naleds and river runoff. Gidrometeoizdat, Leninrgad, 190 (in Russian).

Taysaev T.T. (2004). The phenomenon of cryobiogenesis and self-organization of permafrost geochemical landscapes. Successes of modern natural sciences, 1, 20-24.

The ecological atlas of the Baikal basin (2015). Irkutsk. Ulanbaatar. Ulan-Ude. 145.

Tolstikhin N.I. (1974). Instructions on aufeis studies. In: Tolstikhin ON, ed. Digest of instructions and program directions on the investigation of frozen ground and permafrost - Aufeis and Underground Water in the North-Eastern Regions of the USSR. Novosibirsk, Russia: Nauka, 64. (in Russian).

Topchiev A.G., Gavrilov A.V. (1981). Satellite methods of studies and mapping of icings (South Yakutia). In: Icings in Siberia and the Far East. Nauka, Novosibirsk, 64-71 (in Russian).

Yu W.B., Lai Y.M., Bai W.L., et al. (2005). Icing problems on road in DaHinggangling forest region and prevention measures. Cold Regions Science and Technology, 42(1), 79-88.

RESEARCH PAPER

MAGNETIC PARTICLES IN SOILS AND EPIPHYTES IN THE ZONE OF INFLUENCE OF A FERROUS METALLURGY FACTORY IN THE CITY OF PERM

Anastasiia V. Bobrova[1*], Andrey A. Vasil'ev[1]

[1]Federal State Budgetary Educational Institution of Higher Education «Perm State Agro-Technological University named after Academician D.N. Pryanishnikov», 23 Petropavlovskaya street, 614045, Perm, Russian Federation

***Corresponding author:** pet508nas@mail.ru**

Received: April 10th, 2022 / Accepted: November 11th, 2022 / Published: December 31st, 2022

https://DOI-10.24057/2071-9388-2022-058

ABSTRACT. The intensification of industrial production leads to an increase in the technogenic impact on the environment. Minerals containing iron are sensitive to many environmental processes and analysis of the composition of magnetic particles is relevant in the study of environmental pollution. This study focused on urban soils of near-trunk circles and epiphytic mosses on *Populus nigra* L. in the territory of Motovilikhinsky district of Perm, where a metallurgical plant is located. In this work, using electron probe microanalysis and scanning electron microscopy, we analyzed the magnetic susceptibility (MS), morphology, and chemical composition of magnetic particles isolated from urban soils and epiphytic mosses. The content of heavy metals in the studied soils exceeds the clarkes of chemical elements (CCE) in the upper continental crust: Cr - 286 times, Mn - 15 times, Fe - 11 times, Ti - 4 times, Mg - 4 times. The study of the chemical composition of epiphytes made it possible to assess the contribution of aerial sources to soil pollution. The concentrations of metals in the magnetic particles of epiphytes also exceed the Clarke values: Cr - 3257 times, Fe - 8 times, Ti - 7 times, Mg - 4 times. The similarity of the morphology and chemical composition of the magnetic particles of soils and epiphytes indicate common sources of pollution. A comprehensive assessment of the state of the territory may include magneto-geochemical monitoring of the soil cover and monitoring of the magnetic state of epiphytes on *Populus nigra* L.

KEYWORDS: magnetic susceptibility, heavy metals, urban soils, epiphytic mosses, aerial pollution, electron microscopic analysis

CITATION: Bobrova A.V., Vasil'ev A.A. (2023). Magnetic Particles In Soils And Epiphytes In The Zone Of Influence Of A Ferrous Metallurgy Factory In The City Of Perm. Geography, Environment, Sustainability, 1(16), 157-162
https://DOI-10.24057/2071-9388-2022-058

Conflict of interests: The authors reported no potential conflict of interest.

INTRODUCTION

The soils of industrial cities are often polluted with technogenic magnetic particles (TMP), including technogenic magnetite (Fe_3O_4) - iron oxide, the content of which in urban soils can reach more than 3-4% (Vodyanitskii 2010), while in the background uncontaminated sod-podzolic soils it does not exceed 1% (Babanin et al 1995). Aerial magnetic pollution of soils is caused by emissions from ferrous and non-ferrous metallurgy plants, thermal power plants, exhaust gases and particles of braking elements of cars (Sheshukov, Mikheenkov, Nekrasov, Yeghiazaryan 2020; Winkler 2020; Kirana et al. 2021; Narayana 2021; Wang et al. 2021). The value of MS in urban soils polluted with TMP increases significantly. During high-temperature technogenic processes, some of the Fe ions in the lattice of technogenic magnetite are replaced by other cations, which makes it possible to identify the increase in the magnetic susceptibility of soils with an increase in the degree of their contamination with heavy metals (Vasiliev, Lobanova 2015; Bobrova 2021; Narayana 2021; Zhang et al. 2022).

Pollution of the environment with toxic chemical elements that comprise TMP determines high levels of ecologically conditioned diseases (Kopylov 2013) and can be identified through epiphytic mosses (Varduni 2015; Sukhareva 2018; Ananyan 2020; Mostalygina 2020; Bobrova 2021).

Biomonitoring methods are widely introduced into the practice of ecological and geochemical research in urban areas (Varduni 2015; Gatziolis et al. 2016; Jiang et al. 2018; Koroleva 2020; Messager et al. 2021; Kropova et al. 2022; Zhang et al. 2022). The study of the elemental composition of epiphytes is often used to assess the degree of aerial pollution of ecosystems with heavy metals (Tarkhanov 2016; Ananyan 2020; Mostalygina 2020; Evseev et al. 2021; Kataeva, Belyaeva 2021; Nuguyeva, Mammadov 2021).

The city of Perm is home to Motovilikhinsky plants, the oldest industrial metallurgical enterprise in the Urals. Emissions of this enterprise have a negative impact on the environment primarily in Motovilikhinskiy district. However, the similarity of magnetic particles in the composition of soils and epiphytes of the city of Perm has not been assessed. Data on the content, morphology, and chemical and mineralogical composition of magnetic particles in epiphytes are also still missing. This information will make it possible to assess the contribution of technogenic magnetic particles to the aerial pollution of urban soils, which determines the relevance of the performed research.

The goal of the study was to assess the content, morphology, and ecological and geochemical state of magnetic particles in the composition of soils and epiphytic mosses of the black poplar in Motovilikhinsky district of Perm. The research focused on the soils of near-stem circles of *Populus Nigra* L. and epiphytic mosses *Pleurozium schreberi* (Brid.) Mitt.

MATERIALS AND METHODS

Magnetic susceptibility of soils was measured in sections of 100-150 m long and 5-7 m wide, located parallel to Vosstaniya Street (st.) at a distance of 500-540 m from Motovilikhinsky plants (Fig. 1).

Samples of epiphytes were taken from the surface of the *Populus Nigra* L. trunks at a height of 1.5 m using a plastic knife. At the same time, soil samples were taken in 10 locations around the trunks from a depth of 0-5 cm. The collected samples were dried at room temperature. Soil samples were ground in an agate mortar and passed through a sieve (diameter 1 mm), and moss samples were mechanically dispersed to the state of dust in double polyethylene bags using fingers.

The MS of soils was determined using a kappameter KT-6 manufactured by SATISGEO (Czech Republic) with the instrument sensitivity of 1×10^{-5}SI. The magnetic phase of the samples was extracted with a permanent ferrite magnet (Vasiliev et al. 2020).

The microstructure of the magnetic phase particles was studied using an FEI Quanta 650 FEG high-resolution scanning electron microscope with an EDAX Octane Elite energy dispersive spectrometer (Thermo Fisher Scientific, USA). The microscope is characterized by a 5-1000000 magnification and can operate in variable pressure (pressure range 10-200 Pascal) and high vacuum (10^{-2}-10^{-4} Pascal) modes. The resolution of the spectrometer is 125 electron volts (Gordeev 2017).

The ecological and geochemical assessment of the elemental composition of soils and particles of the magnetic phase was carried out by comparing the content of the element in the sample with geochemical constants, represented by the average content of elements in the upper continental crust (Wedepohl 1995). The MS of the studied soils was compared with the background values for the territory of the city of Perm, which are in the range of 0.43-0.62×10^{-3} SI (Vasil'ev, Lobanova 2015).

RESULTS AND DISCUSSION

Very high median values of MS are typical for the soils of streets with heavy traffic located at a distance of 500 m from Motovilikhinsky plants. Soil MS values vary over a wide range, from 3.13 to 11.2×10^{-3} SI, with an average median value of 5.6×10^{-3} SI and a coefficient of variation of 40 percent.

The volumetric magnetic susceptibility of soils is more than 10 times higher than the local background (0.43-0.62×10^{-3} SI), which indicates soil contamination with magnetic particles.

Clastic particles ranging from 1 μm to 600 μm in size dominate in the highly magnetic phase of the soil near

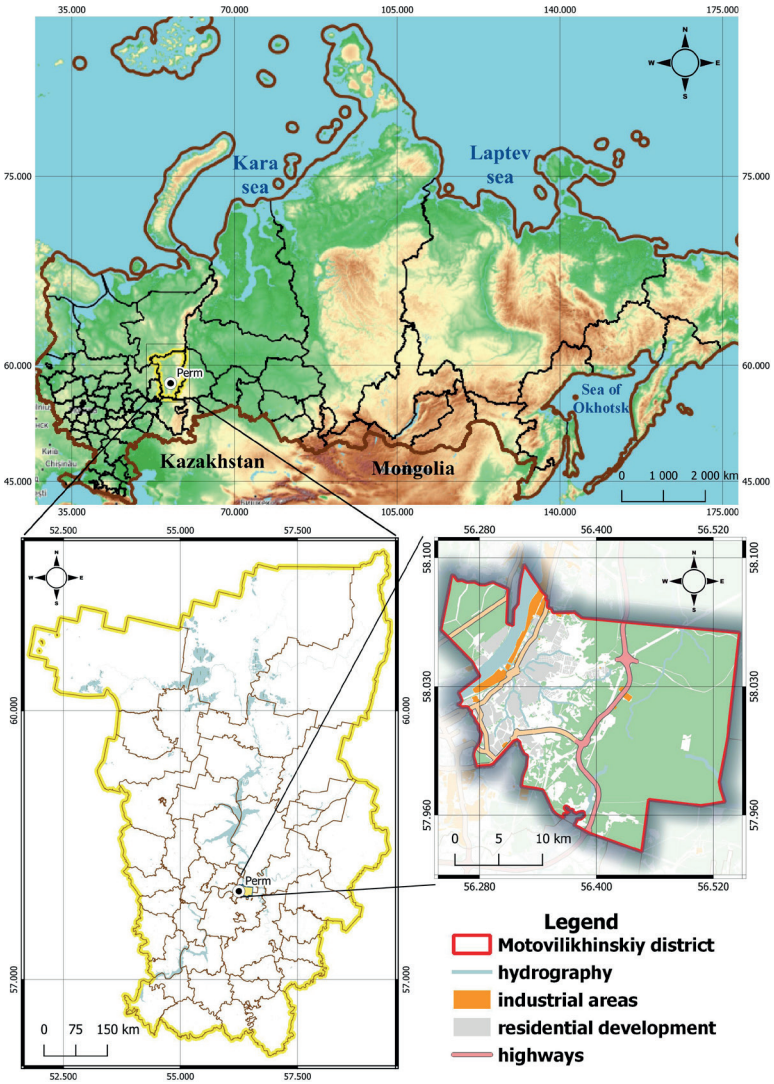

Fig. 1. Study area map

the trunks of black poplar on Vosstaniya street. Some particles are spherical (Selected Area 3, Fig. 2). The areas of energy dispersive analysis are indicated in the figures by squares. Magnesium ferrites in the form of spherules are usually found in dusty emissions from ferrous metallurgy enterprises (Makarov, Osovetsky, Antonova 2017; Vasiliev et al. 2020).

The peaks of Fe^{+2} and Fe^{+3} atoms on the energy dispersive spectra correspond to magnetite- maghemite (Fig. 3).

Individual sections of the sample are characterized by Fe content from 6.5 to 49.9%. Some elements such as Ti, Cr and Mn are not present in all particles (Table 1).

The concentration of metals in the composition of magnetic particles exceeds CCE in the upper continental crust according to K.H. Wedepohl (1995): Cr - 286 times, Mn - 15 times, Fe - 11 times, Ti - 4 times, Mg - 4 times (Fig. 4).

Magnetic particles in the composition of the soil along Vosstaniya street in Motovilikhinskiy district are characterized by an intensive accumulation of Cr (CC = 1209 units). Some magnetic particles are enriched in Ti. The content of Fe at all points of the energy-dispersive analysis of magnetic particles is above CCE.

The heterogeneous content of Mn in the composition of magnetic phase particles allows us to consider this metal as a soil pollutant. The accumulation of Mn in soils

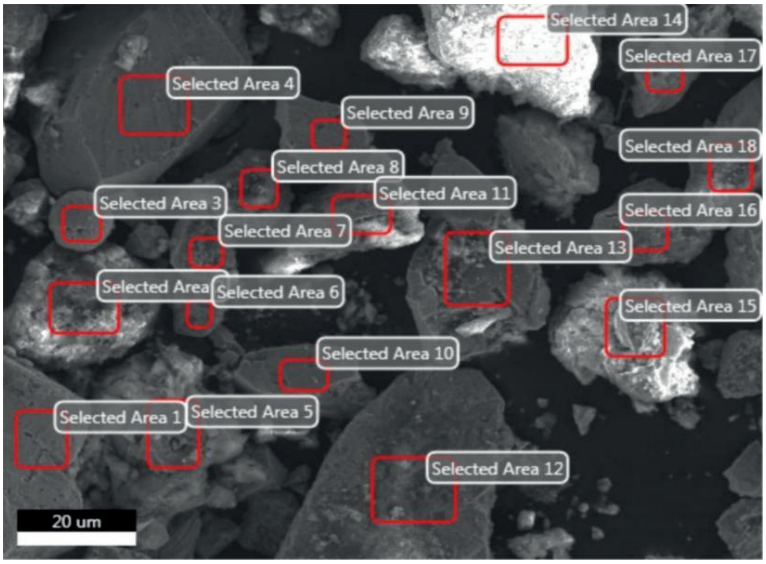

Fig. 2. Microphotograph of the highly magnetic phase particles in the soil on Vosstaniya street

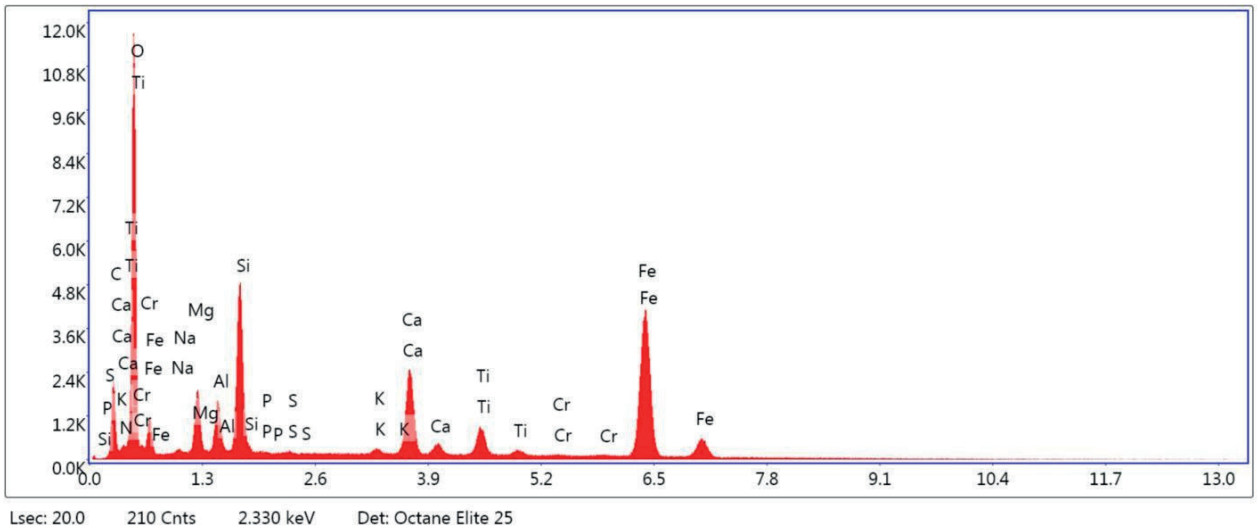

Fig. 3. Energy-dispersive spectrum of the magnetic phase particles in the soil on Vosstaniya street, point number 13

Table 1. Chemical composition of the magnetic phase particles in the soil on Vosstaniya street

Chemical element	CCE, %	Spectrum number																	
		№1	№2	№3	№4	№5	№6	№7	№8	№9	№10	№11	№12	№13	№14	№15	№16	№17	№18
Fe	3.089	48.5	15.9	44.8	44.4	17.4	46.7	25.7	8.1	43.6	49.9	23.7	17.8	24.2	6.5	26.3	38.7	24.8	15.1
Mg	1.351	2.6	3.4	2.1	2.5	4.0	2.3	2.6	1.1	2.5	2.5	7.7	6.2	4.4	7.7	3.1	5.3	6.4	5.2
Mn	0.0527	–	–	0.5	–	0.5	–	–	–	–	–	0.6	1.1	–	–	–	–	–	–
Ti	0.3117	1.5	0.2	–	0.8	2.8	0.9	2.7	0.1	1.0	–	0.6	0.1	2.4	0.1	0.3	–	–	0.2
Cr	0.0035	0.1	0.1	–	0.1	0.1	2.4	–	0.0	–	–	4.2	–	0.1	–	–	0.6	–	–

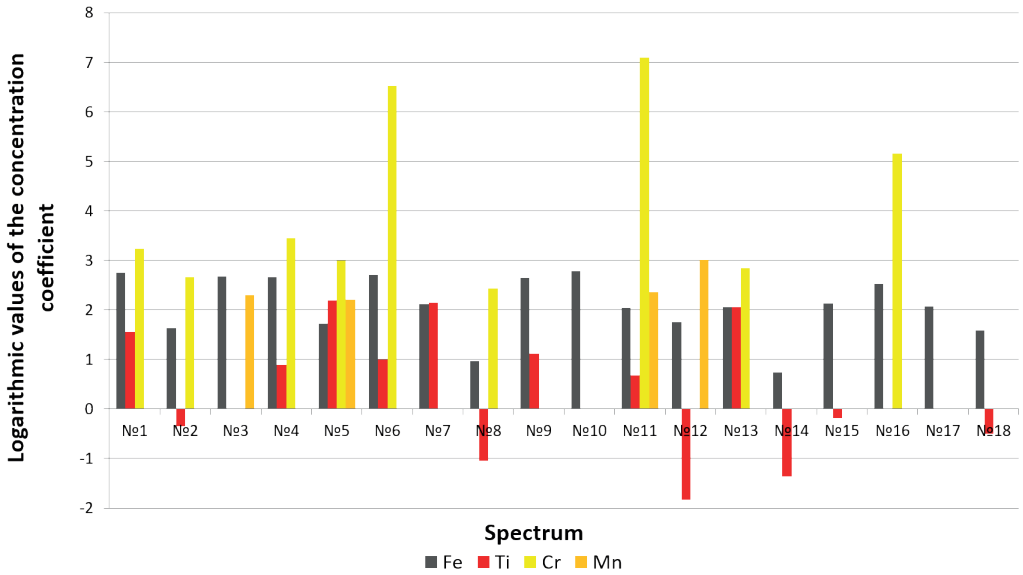

Fig. 4. Logarithmic values of the concentration coefficient (CC) of Fe and heavy metals in the soil, Perm

near metallurgical enterprises is a characteristic feature of the negative impact of this industry on environmental components, including soils.

Particles of detrital and spherical shapes ranging in size from 1 μm to 700 μm dominate in the highly magnetic phase of the moss sample from Vosstaniya street (Fig. 5).

Microprobe analysis of the highly magnetic phase of the epiphyte samples from Motovilikha district of the city of Perm revealed the content of Fe ranging from 4.9 to 38.0%, and Mg from 1.9 to 18.9%, while Ti and Cr also accumulated in some particles (Table 2).

The average concentrations of metals in the composition of magnetic particles exceed CCE in the upper continental crust: Cr - 3257 times, Fe - 8 times, Ti - 7 times, Mg - 4 times (Fig. 6).

The CC values for Mg in all cases are above 1.0, which indicates the presence of magnesium ferrites (Vasiliev, Lobanova 2015). The values of CC for Fe in all particles of the magnetic phase are high with the CC ranging from 1.6 to 12.3 units.

Thus, the accumulative role of the magnetic phase of epiphytes is confirmed by the high CC for heavy metals, particularly Ti (CC up to 6.7 units) and Cr (CC up to 8217.1 units). These elements are not found in all particles of the magnetic phase, which indicates their anthropogenic technogenic origin.

The concentration of Cr, Fe, Mg, Ni, and Ti in the magnetic phase particles is several times higher than CCE in the upper continental crust, which characterizes soil pollution as a polyelemental one.

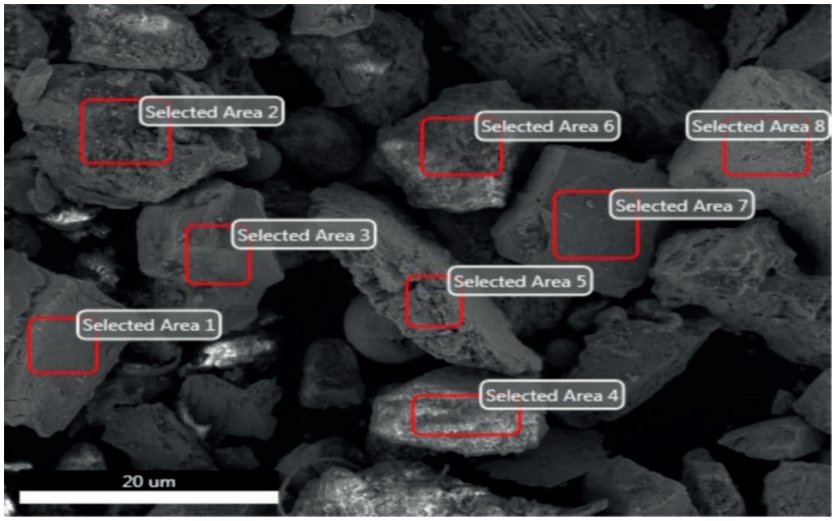

Fig. 5. Micrograph of the highly magnetic phase particles of epiphytes on Vosstaniya street

Table 2. Chemical composition of the magnetic phase particles in the composition of epiphytes on Vosstaniya street

Chemical element	CCE, %	Spectrum number							
		№1	№2	№3	№4	№5	№6	№7	№8
Fe	3.089	37.12	17.88	32.16	4.86	31.10	11.70	38.04	7.98
Mg	1.351	1.98	5.07	2.76	18.87	1.90	5.73	1.98	3.04
Ti	0.3117	1.91	–	–	–	–	–	2.09	–
Cr	0.0035	0.45	–	–	1.10	28.76	0.00	–	–

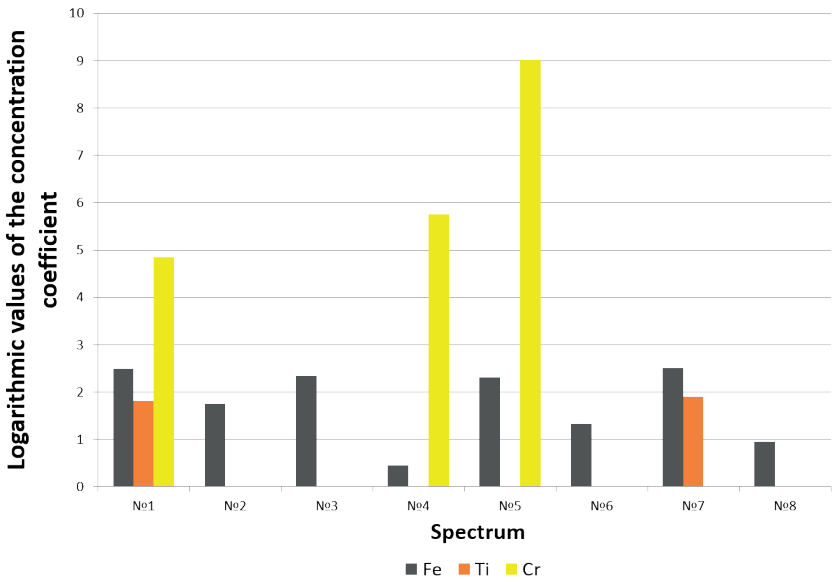

Fig. 6. Logarithmic values of the CC of Fe and heavy metals in epiphytes, Perm

The analysis of the chemical composition of epiphytes demonstrates similarity with the composition of the studied soils. The pollutants in the samples are represented by the same elements (Fe, Ti, and Cr) and contamination of both epiphytes and soils is highest near industrial enterprises, which suggests that epiphyte mosses can act as indicators of aerial pollution of the environment.

The results of our research coincide with the data obtained earlier. Foreign scientists have found that in epiphytic mosses and lichens, part of the internal volume of thalli consists of loose long-cell biogenic parts that form a cottony layer with a very high internal air space, which makes it easy to absorb and retain TMP for a long time. This was demonstrated using scanning electron microscopy and magnetic measurements (Winkler et al. 2019; Chaparro 2021). The concentrations of metals in moss pseudotissues are not so affected by local fluctuations in the level of metals in the soil (Jiang et al. 2018). Mosses have been widely used in several countries in Europe and China as biological monitors of metal pollution for decades because they easily accumulate pollutants over time, reflecting their long-term levels (Fernández et al. 2015; Zhang et al. 2022). As a result, numerous studies have successfully used elemental analysis of mosses to estimate the spatial distribution and sources of metals associated with urban and vehicular traffic. Also, epiphytic mosses were used to map metal pollution in urban areas (Gatziolis et al. 2016).

CONCLUSIONS

The soils near the streets of Motovilikhinsky district, located close to the territories of industrial enterprises (Motovilikhinsky plants), concentrate particles of a magnetite-like mineral complex – magnetite-maghemite, magnesium ferrites, etc. The magnetic susceptibility of soils in Motovilikhinsky district significantly exceeds the background values for the soil cover of the city of Perm. The content of Cr, Fe, Mg, Ni, and Ti in the composition of magnetic soil particles and epiphyte mosses significantly exceeds CCE in the upper continental crust.

Epiphytic mosses living on the bark of trees passively accumulate TMP. They are ubiquitous in the study area of the city and can be found even in the most polluted areas near factories. Epiphytic mosses have an advantage over urban soils as they are well dispersed in urban areas, which allows to use them for biomonitoring of environmental pollution where urban soils can be covered with asphalt, concrete, or fresh soil in the surface layer.

REFERENCES

Ananyan A.S., Koroleva Yu.V., Alekseyonok Yu.V. (2020). Biomonitoring of heavy metals in the territory of the Kaliningrad region // International Scientific Research Journal. № 12-2 (102), 25-31, DOI: 10.23670/IRJ.2020.102.12.038

Babanin V.F., Truhin V.I., Karpachevskij L.O., Ivanov A.V., Morozov V.V. (1995). Soil magnetism // Yaroslavl: YaGTU, 223.

Bobrova A.V., Vasil'ev A.A. (2021). Heavy metals in soils and mosses-epiphytes of the Leninsky district of the city of Izhevsk // [Electronic resource] // AgroEcoInfo:

Electronic scientific and production journal. №4. – URL: http://agroecoinfo.ru/STATYI/2021/4/st_402.pdf, DOI: 10.51419/20214402.

Chaparro M.A.E. (2021). Airborne particle accumulation and loss in pollution-tolerant lichens and its magnetic quantification // Environmental Pollution, 288, 117807, DOI: 10.1016/j.envpol.2021.117807

Evseev A.V., Shakhpenderyan E.A., Sultygova Kh.S. (2021). Aerosol income of man-made pollutants into environment components in the central-kola impact region // Ecosystems: ecology and dynamics, 5(1), 74-93.

Fernández J.A., Boquete M.T., Carballeira A., Aboal J.R. (2015). A critical review of protocols for moss biomonitoring of atmospheric deposition: sampling and sample preparation // Science of the Total Environment, 517, 132-150, DOI: 10.1016/j.scitotenv.2015.02.050

Gatziolis D., Jovan S., Donovan G., Amacher M., Monleon V. (2016). Elemental atmospheric pollution assessment via moss-based measurements in Portland, Oregon // Gen. Tech. Rep. PNW-GTR-938. Portland, OR: US Department of Agriculture, Forest Service, Pacific Northwest Research Station, 938, 55, DOI: 10.2737/PNW-GTR-938

Gordeev K., Shakhnovich I., Shishkin A. (2016). From production control to cell cultivation. Advanced solutions at Analytica // Analytics. 2017, 2(33), 38-65, DOI: 10.22184/2227-572X.2017.33.2.38.65

Jiang Y., Fan M., Hu R., Zhao J., Wu Y. (2018). Mosses are better than leaves of vascular plants in monitoring atmospheric heavy metal pollution in urban areas // International journal of environmental research and public health, 15(6), 1105, DOI: 10.3390/ijerph15061105

Kataeva M.N., Belyaeva A.I. (2021). Accumulation of heavy metals in epiphytic liches of the Middle Taiga subzone of the spruce // International Journal of Applied and Fundamental Research, 7, 17-21.

Kirana K.H., Apriliawardani J., Ariza D., Fitriani D., Agustine E., Bijaksana S., Nugraha M.G. (2021). Frequency Dependent Magnetic Susceptibility in Topsoil of Bandung City, Indonesia // IOP Conference Series: Earth and Environmental Science. IOP Publishing, 873(1), 012016, DOI: 10.1088/1755-1315/873/1/012016

Kopylov I.S. (2013). Anomalies of heavy metals in soils and snow cover of the city of Perm as manifestations of factors of geodynamics and technogenesis // Fundamental Research. 2013, 1-2, 335-339.

Kropova Yu.G., Khovrin A.N., Vyrodov I.V. (2022). Influence of the transport and road complex on the pollution of soils and plants with heavy metals // Vestnik NSAU (Novosibirsk State Agrarian University), 4, 36-44, DOI: 10.31677/2072-6724-2021-61-4-36-44

Makarov A.B., Osovetsky B.M., Antonova I.A. (2017). Magnetic spherules from soils near the slag dump of the Nizhny Tagil Metallurgical Plant // Bulletin of the Ural State Mining University, 4(48), 42-45, DOI: 10.21440/2307-2091-2017-4-42-45

Messager M.L., Davies I.P., Levin P.S. (2021). Low-cost biomonitoring and high-resolution, scalable models of urban metal pollution // Science of The Total Environment, 767, 144280, DOI: 10.1016/j.scitotenv.2020.144280

Mostalygina L.V., Elizarova S.N., Kostin A.V. (2020). Sorption ability of mosses and lichens of the Trans-Urals in relation to lead ions // Chemistry of vegetable raw materials, 3, 315-321, DOI: 10.14258/jcpim.2020035605

Narayana A.C., Ismaiel M., Priju C.P. (2021). An environmental magnetic record of heavy metal pollution in Vembanad lagoon, southwest coast of India // Marine Pollution Bulletin. T. 167, 112-344, DOI: 10.1016/j.marpolbul.2021.112344

Nuguyeva Sh.S., Mammadov E.A. (2021). Investigation of the content of heavy metals in atmospheric precipitation of the Goygol, Dashkesan and Gedabek regions of Azerbaijan // Bulletin of science and practice, 7(6), 60-66, DOI: 10.33619/2414-2948/67

Sheshukov O.Y., Mikheenkov M.A., Nekrasov I.V., Yeghiazaryan D. K. (2020). Negative effect of ferrous metallurgy new technologies on the environment and possible ways to overcome them // Journal of Chemical Technology and Metallurgy, 3(55), 592-597.

Sukhareva T.A. (2018). Elemental composition of green mosses in background and technogenically disturbed territories // Uchenye zapiski Petrozavodskogo gosudarstvennogo universiteta, 3(172), 89-96, DOI: 10.15393/uchz.art.2018.130

Tarkhanov S.N. (2016). Influence of aerotechnogenic pollution on the coverage of tree trunks by epiphytic lichens in forest plantations of the North Dvina basin and the Belomorsko-Kuloi plateau // Forest magazine, 1 (349), 37-47, DOI: 10.17238/issn0536-1036.2016.1.37

Varduni T.V., Minkina T.M., Gorbov S.N., Mandzhieva S.S. (2015). Analysis of the content of heavy metals in Pylaisia polyantha growing in Rostov-on-Don // Scientific journal of KubGAU, 2, 1-14.

Vasiliev A., Gorokhova S., Razinsky M. (2020). Technogenic magnetic particles in soils and ecological–geochemical assessment of the soil cover of an industrial city in the Ural, Russia // Geosciences (Switzerland), 10(11), 1-34, DOI: 10.3390/geosciences10110443

Vasiliev A.A., Lobanova E.S. (2015). Magnetic and geochemical assessment of the soil cover of the urbanized territories of the Cis-Urals on the example of the city of Perm // Perm: FGBOU VPO «Perm State Agricultural Academy», 243.

Vodyanitskii Yu.N. (2010). Iron minerals in urban soils // Soil Science, 12, 1519-1526.

Wang B., Zhang X., Zhao Y., Zhang M., Jia J. (2021). Spatial and temporal distribution of pollution based on magnetic analysis of soil and atmospheric dustfall in Baiyin city, northwestern China // International Journal of Environmental Research and Public Health, 18(4), 1681, DOI: 10.3390/ijerph18041681

Wedepohl K.H. (1995). The composition of the continental crust // Geochim. Cosmochim. Acta, 59(7), 1217-1232.

Winkler A., Caricchi C., Guidotti M., Owczarek M., Macrì P., Nazzari M., Amoroso A., Di Giosa A., Listran S. (2019). Combined magnetic, chemical and morphoscopic analyses on lichens from a complex anthropic context in Rome, Italy // Science of the Total Environment, 690, 1355-1368, DOI: 10.1016/j.scitotenv.2019.06.526

Winkler A. (2020). Magnetic Emissions from Brake Wear are the Major Source of Airborne Particulate Matter Bioaccumulated by Lichens Exposed in Milan (Italy) // Applied Sciences, 10(6), 2073, DOI: 10.3390/app10062073

Zhang J., Lin Q., Liu B., Guan Y., Wang Y., Li D., Zhou X., Kang X. (2022). Magnetic Response of Heavy Metal Pollution in Soil of Urban Street Greenbelts // Polish Journal of Environmental Studies, 31(2), 1923-1933, DOI: 10.15244/pjoes/141339

RESEARCH PAPER

HYDROCHEMICAL AND BACTERIAL PROPERTIES OF WATER BODIES OF THE EAST EUROPEAN PLAIN DURING LOW WATER PERIOD

Vladimir V. Tikhonov[1*], Diana R. Koriytchuk[1], Andrey V. Yakushev[1], Vladimir S. Cheptsov[1], Mikhail M. Karpukhin[1], Ruslan A. Aimaletdinov[1], Olga Yu. Drozdova[1]

[1]Lomonosov Moscow State University, Leninskie Gory 1, 12, 119991, Moscow, Russia

***Corresponding author:** vvt1985@gmail.com

Received: April 15th, 2022 / Accepted: November 11th, 2022 / Published: December 31st, 2022

https://DOI-10.24057/2071-9388-2022-061

ABSTRACT. This paper is devoted to the study of the chemical and biological properties of river waters and the relationship between them. We examined the hydrochemical and bacterial properties of surface water in 3 waterbodies: the Mezha River, a pond in Zapovedny village (Central Forest Nature Reserve, Tver Oblast) and the lower reaches of the Don River (Rostov Oblast). The biodiversity of bacteria was determined based on their growth on dissolved organic matter (DOM). Among bacterioplankton capable of growing on DOM as the only source of carbon, the predominant species in the Don River were *Pseudomonas* and *Deinococcus*, in the Mezha River – *Pseudomonas* and *Janthinobacterium*, in the pond – *Arcicella*. In terms of sanitary and microbiological indicators, none of the waterbodies complied with the Sanitary Rules and Regulations 1.2.3685-21 for surface waters. The content of most of the studied elements and heterotrophic bacteria in stagnant waterbodies was lower than in flowing streams. The concentration and activity of heterotrophic bacteria in the studied waters correlated positively with the content of biophilic elements in them and negatively with the absence of a current. We showed that there is a strong correlation between bacterial and chemical indicators due to common factors: eutrophication, features of the physical and geographical conditions of the territory, and the presence of a current or animal waste products.

KEYWORDS: surface waters, heterotrophic bacteria, DOM, elements, biodiversity

CITATION: Tikhonov V. V., Koriytchuk D. R., Yakushev A. V., Cheptsov V. S., Karpukhin M. M., Aimaletdinov R. A., Drozdova O. Yu. (2023). Hydrochemical And Bacterial Properties Of Water Bodies Of The East European Plain During Low Water Period. Geography, Environment, Sustainability, 1(16), 163-171
https://DOI-10.24057/2071-9388-2022-061

ACKNOWLEDGEMENTS: Water sampling and chemical analysis were carried out with the support of the Russian Science Foundation, project No. 21-77-10028. Identification of microorganisms was carried out as part of the Federal Program "Soil microbiomes: genomic diversity, functional activity, geography and biotechnological potential", No. 121040800174-6 and Ministry of Science and Higher Education of the Russian Federation, project No. the 075-15-2021-1396. The authors express their gratitude to the staff of the Azovo-Chernomorsk Branch of the Federal State Budgetary Scientific Institution «VNIRO» and personally to Dr. Barabashin T.O.

Conflict of interests: The authors reported no potential conflict of interest.

INTRODUCTION

There are many papers devoted to the study of sanitary and microbiological indicators (Dolgonosov et al. 2006; Sorokovikova et al. 2013; Lartseva et al. 2015; Obukhova et al. 2017) and geochemical characteristics (Lobbes et al. 2000; Grishantseva et al. 2020; Drozdova et al. 2021; Pakusina et al. 2022) of lowland rivers in Russia. However, only a few of them investigate the relationship between the abundance and properties of microorganisms, their activity and the chemical composition of water (Judd et al. 2006; Tanentzap et al. 2019). Moreover, despite the constant monitoring of sanitary conditions in waterbodies, there is little data on the autochthonous microbiome and its functioning, especially for the rivers of the Russian Federation (Belkova et al. 2003; Kopylov and Kosolapov 2011). At the same time, the role of heterotrophic bacterioplankton in the biogeochemical cycle is extremely high (Fasching et al., 2014; Amado and Roland 2017; Cai et al. 2021; Yang et al. 2021), since it is the most important trophic link in the nutrient network of waterbodies. Previously, Azam et al. (1983) formulated the concept of a "microbial loop", according to which most of the matter created by phytoplankton in the form of intravital secretions and mortmass represented by dissolved organic matter (DOM) serves as food for planktonic heterotrophic bacteria which then become food for larger organisms. The "microbial loop" is an alternative to the well-known phytoplankton-zooplankton-fish pathway for the transfer of matter and energy through trophic networks. The DOM of natural waters differs significantly: in the southern rivers, autochthonous DOM prevails due to their high production, while in the northern rivers, allochthonous DOM originating from the watershed is predominant. In this study, we examined surface water samples from two natural zones: the large steppe river Don (in the area of the Tsimlyansk Reservoir)

and the Mezha River, particularly a section of the river in the taiga zone, a dam on the Mezha River and a small pond in the Mezha River basin (Tver Oblast). Our hypothesis was that the chemical and bacterial properties of surface waters are closely interrelated and this relationship determines the differences in the functioning of waterbodies as aquatic ecosystems. The aim of this study was to identify the relationship between the concentration and activity of various groups of heterotrophic bacteria and the chemical composition of stagnant (river dam, pond) and flowing (rivers) waters of the taiga and steppe zones of the East European Plain, as well as to identify bacterial dominants capable of using DOM as the only source of carbon.

MATERIALS AND METHODS

Water sampling was carried out in mid-August of 2021 at four locations: the Don River, the Mezha River (2 points) and a pond in Zapovedny village (Fig. 1). The characteristics of the studied waterbodies are given in Table 1. For microbiological analyses, water samples were collected into sterile 15 mL flacons and transported in a thermal bag; for chemical analyses, water was collected into 5 L plastic bottles. The sampling was carried out in triplicate and the samples were delivered to the laboratory within 24 h.

Isolation of culturable bacteria. Isolation of bacteria was carried out using the dilution method onto the following agar media: nutrient agar (Himedia, M001), MacConkey agar with crystal violet and 0.15% bile salts (Himedia, M081), bile esculin agar with sodium azide (Himedia, M493), Ashby agar with mannitol (Himedia, M706), medium for the isolation of iron bacteria (Himedia, M622), peptone-yeast extract-glucose (PYG) agar (10 g/L peptone, 5 g/L yeast extract, 2 g/L glucose, 15 g/L agar), copiotrophic (oligotrophic) agar (Semenov et al. 1991) (2.5 g (25 mg/L) glucose, 0.2 g/L casein hydrolysate, 0.5 g/L $MgSO_4 \times 7H_2O$, 0.5 g/L KH_2PO_4, 0.06 g/L $Ca(NO_3)_2$), as well as agar with the DOM of a waterbody as the only source of carbon. For the latter medium, we used sterile water from a waterbody (filtered through a 0.2 μm filter) mixed with the mineral base of the 2x Czapek-Dox medium. Incubation on PYG, copiotrophic/oligotrophic agar, Ashby medium, and agar for the isolation of iron bacteria was carried out at 28 °C. Colony counting was conducted after 5 days of incubation. Incubation on MacConkey agar and bile esculin agar was conducted at 37 °C, colony counting was conducted after 1.5 days. Incubation on nutrient agar was conducted at 22 °C and 37 °C and colony counting was conducted after 5 and 1.5 days, respectively. All experiments were performed in triplicate.

Identification of bacteria: Bacterial strains were identified based on the 16S rRNA gene sequences as described previously in Belov et al. (2018). The resulting sequences were checked for chimeras using the DECIPHER 2.20.0 program (Wright et al. 2012) and deposited into GenBank under accession numbers OM763864-OM763869.

Comprehensive structural and functional approach. To study the bacterial complex of the waterbodies, we used a comprehensive structural and functional approach described by Yakushev (2015). The approach is based on the analysis of the total concentration of bacteria cells that have grown on a selection of liquid nutrient media containing biopolymers (or Tween 20) as the only carbon source after their inoculation with water from the studied waterbodies. The concentration of

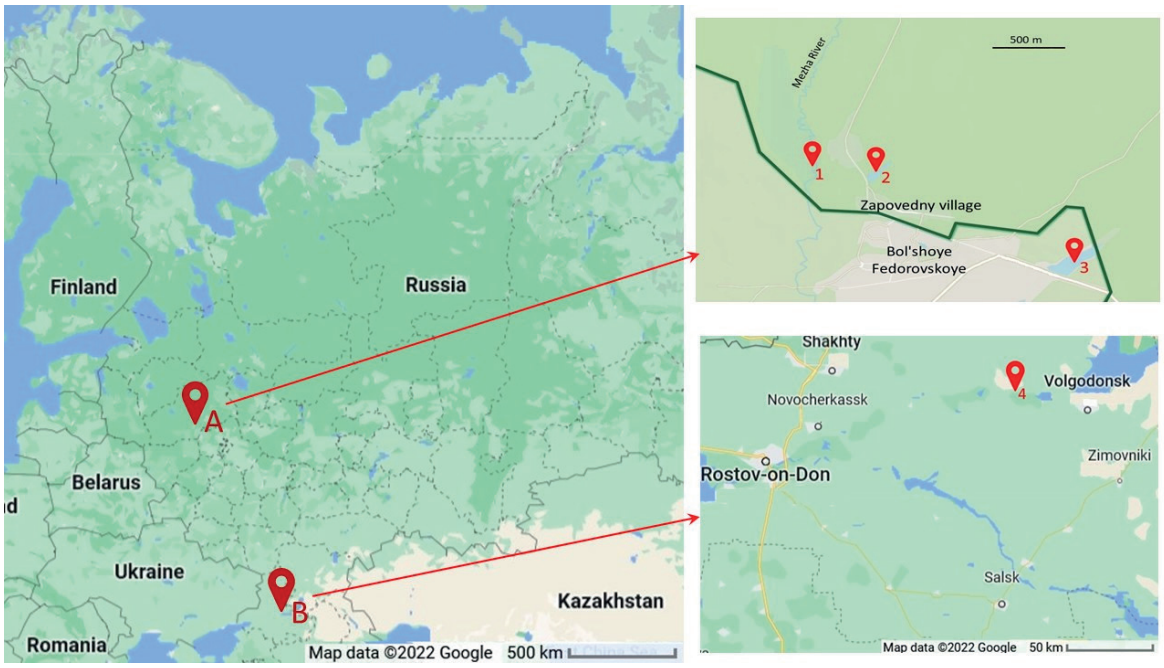

Fig. 1. Sampling scheme: 1 - the Mezha River, 2 - the pond, 3- the Mezha River ('Old dam') (Tver region – A), 4 - the Don River (Rostov region - B)

Table 1. Characteristics of sampling points

Object	Geographical coordinates	River length, km/surface area, m^2	Water temperature, °C	Air temperature, °C
Don River	47.55898N, 41.99808E	1870/	26	32
Mezha River (taiga zone)	56.45525N, 32.96316E	259/	15	15
Mezha River ('Old dam')	56.45006N, 32.98901E	/25000	19	
Pond in Zapovedny village ('Prudka')	56.45637N, 32.97012E	/7000	16	

bacteria in nutrient media was determined by measuring the dynamics of their optical density at 620 nm in 96-well culture plates. The approach was modified for water objects as follows: (i) the number of media was reduced to 8 (media with chitin, cellulose, xylan, agarose, keratin, inulin, dextran, Tween 20); (ii) 100 µL of water from a waterbody and 100 µL of a liquid medium with a polymer at a concentration of 5 g/L were added to the wells of 96-well culture plates; (iii) changes in the concentration of bacteria in liquid media were registered over 260 h; (iv) the intensity of the bacterial community growth on polymers was characterized using the area under the growth curve as an integral parameter.

Chemical analysis of water. The content of anions was determined using ion chromatography on a Dionex ICS-1100 chromatograph. The content of metals and metalloids was determined using inductively coupled plasma optical emission spectrometry on an Agilent 5110 ICP-OES instrument. The content of the ammonium ions was determined using spectrophotometry with the indophenol blue dye formed as a result of the reaction of ammonium ions with sodium hypochlorite and sodium salicylate in the presence of sodium nitroprusside at a wavelength of 655 nm. The content of dissolved organic carbon and total nitrogen was determined using a LiquiTOCtrace analyzer (Elementar, UK).

Statistical data processing. Statistical data processing was carried out using the Statistica 8 program. The arithmetic mean and standard error values of the studied parameters were calculated and a correlation analysis was carried out to preliminarily establish the relationship between the chemical and bacterial indicators of waterbodies. To identify the most significant correlations, we carried out a multiple linear regression analysis of the indicators that showed strong correlation during the correlation analysis. To evaluate the relationship between the chemical and bacterial indicators of waterbodies in general, we used the principal component analysis (PCA). The reliability of the principal components was determined based on the cross-validation data, the values of the Kaiser criterion and the scree plot. The analysis was performed separately for bacterial culture chemistry data and for the comprehensive method. In the case of the comprehensive method and chemical indicators, the principal component analysis was first carried out for all indicators, and then only for those that had a correlation coefficient with the principal components (PC) greater than 0.7 in order to improve the accuracy of the analysis and exclude the influence of non-informative indicators.

RESULTS AND DISCUSSION

The sanitary and microbiological state of waterbodies was assessed using 3 indicators: the concentration of enterococci in water (the medium with esculin), the concentration of total coliform bacteria (TCB, the MacConkey medium) and the ratio between the number of colonies grown on nutrient agar at 22 °C and the number of colonies grown at 37 °C (self-purification index, Sanitary and Epidemiological Guidelines 4.2.1884-04). Based on these three indicators, the waterbodies were ranked according to the increasing level of pollution as follows (the self-purification index is inversely proportional to pollution): the Mezha River (dam area), the pond, the Mezha River (stream), the Don River (Fig. 2, Table 2). According to enterococci and TCB indicators, none of the objects complied with the Sanitary Rules and Regulations 1.2.3685-21 for surface waters for any of the possible uses (recreation, sport, and water supply). The high values of sanitary indicators in the Don River can be explained by the discharge of sewage into the river and the intensification of agriculture (the inflow of sewage into the river with farm animal waste) (Zhuravlev et al. 2010), while in the Mezha River the high abundance of TCB and enterococci can be explained by the activity of beavers (Skinner et al., 1984) and waterfowl (Standridge et al. 1979; Moriarty et al. 2011). In the dam area, sedimentation of suspended matter and colloids takes place, which can also reduce the abundance of the considered microorganism groups (Kepkay 1994). A similar series can be observed for the total abundance of bacteria grown on nutrient agar at 37 °C and on the Ashby agar. When bacteria were grown on the DOM of waterbodies, nutrient agar at 22 °C and PYG, the abundance of microorganisms in stagnant water (the Mezha River near the dam and the pond) was lower than in flowing water. Perhaps, this is due to the feeding activity of planktonic filter-feeding crustaceans, which leads to a reduction in bacterioplankton (Richardson and Mackay 1991). A large concentration of autochthonous microbiome in the Mezha River compared to the Don River was clearly seen through the growth of microorganisms on polymers (Table 3): for all the medium options, except for Tween 20, the growth was more intense in the Mezha River than in the Don River. There was also a trend of weaker growth of microbial complexes in conditionally stagnant waterbodies compared to flowing watercourses (chitin, cellulose, agarose, Tween 20).

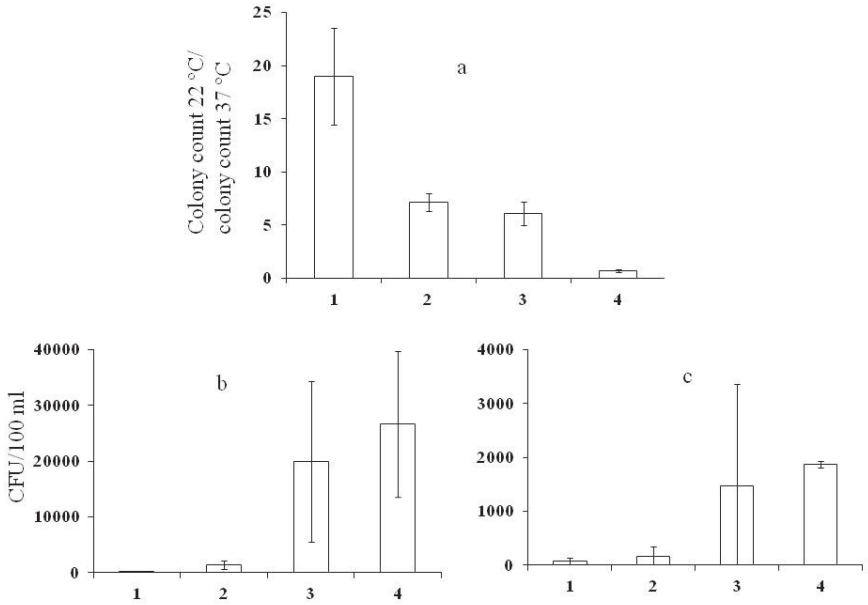

Fig. 2. The ratio of Colony count at 22°C to Colony count at 37°C (a), the abundance of coliform bacteria (b) and enterococci (c) in (1) the Mezha River ('Old dam'), (2) the pond, (3) the Mezha River and (4) the Don River

Table 2. Concentration of culturable bacteria

Medium	Concentration of bacteria in waterbodies, CFU/mL			
	Don River	Dam on the Mezha River	Mezha River	Pond
Peptone yeast extract glucose agar	1,150±321	1,133±44	9,166±833	1,233±120
Ashby's Glucose Agar	5,000±243	783±142	3,800±1,200	1,066±384
Nutrient Agar 37°C	1,733±233	61±6	1,500±75	71±3
Nutrient Agar 22°C	1,250±230	1,133±44	9,166±833	506±29
MacConkey Media	266±66	2.0±0.5	199±73	14±3
Oligotrophic media	933±381	1,866±550	3,333±763	2,033±450
Copiotrophic media	783±202	883±600	1,666±288	1,333±288
Dissolved organic matter	108,000±80,804	63,000±30,512	143,000±39,887	41,000±34,394
Medium for Isolation of Iron Bacteria	124,000±27,184	70,333±65,574	163,33±73,050	11,800±6,557
Bile Esculin Azide Agar	18±0.6	0.6±0.6	14±5	1.6±1.3

Table 3. Growth of bacterioplankton on polymers (comprehensive approach)

Liquid medium containing polymer	Area, optical units×h			
	Don River	Dam on the Mezha River	Mezha River	Pond
Keratin	2,340±780	1,820±260	4,160±1,300	2,600±260
Chitin	4,160±1,560	2,340±1,040	5,980±520	2,600±260
Cellulose	598±208	390±208	1,742±234	702±104
Agarose	192±78	75±26	465±156	286±78
Inulin	3,900±780	2,080±1,040	5,200±260	4,618±780
Xylan	2,912±624	2,418±780	2,418±520	1,924±520
Tween 20	7,124±520	2,080±520	6,214±520	5,200±780
Dextran-500	208±130	468±104	1,716±442	598±156

Species composition of bacteria growing on DOM. The dominant bacteria utilizing DOM in the Don River represented the *Pseudomonas* genus with a share of up to 64% of the cultivated bacteria; 25% represented Deinococcus (Table 4). Pseudomonas dominated in the Mezha River as well (70%), while representatives of *Janthinobacterium* comprised the second largest group (20 %). The pond was dominated by the representatives of *Arcicella* (92%). Representatives of these genera are often found in surface waterbodies, and the studied strains had a high similarity of the 16S rRNA gene sequences to those of water strains (Van Horn et al. 2011; Baltrus et al. 2014; Tuohy et al. 2018; Friedrich et al. 2020).

The analysis of Table 5 indicates that there are fundamental differences between the studied waters in terms of chemical indicators. For instance, it shows that the surface and groundwater runoff leads to the enrichment of the rivers with Si, Ca, Mg, Sr, K, and Na compared to stagnant waterbodies (the pond and the dam on the Mezha River), in which suspended and colloidal particles are removed from solution and accumulate in bottom sediments. The water of the more southern region has certain features in the chemical composition: the content of the main inorganic anions and cations in the Don River is much higher than in the waters of the Tver Oblast. Greater content of biophilic elements and

Table 4. Percentage of dominant bacteria growing on DOM as the only carbon source

Object	Bacterial strain [GenBank accession number]	Percentage, %
Don River	*Pseudomonas* [OM763864]	33
	Pseudomonas [OM763866]	31
	Deinococcus [OM763865]	25
Mezha River	*Pseudomonas* [OM763868]	70
	Janthinobacterium [OM763867]	20
Pond	*Arcicella* [OM763869]	92

better aeration of the Don River with oxygen promotes intensive mineralization of organic matter. In the Mezha River and the pond, the content of organic carbon is 2.3–2.9 times higher than in the Don River. Lower values of the C/N indicator in the Don River indicate a greater predominance of autochthonous organic matter compared to the Mezha River. The hydrological regime of the Central Forest Nature Reserve is significantly affected by swamps, which leads to an increased content of Fe, Mn and Corg in surface waters. An increase in the concentrations of NO3- and NO2- indicates more intense eutrophication of the Mezha River compared to the Don River and stagnant waterbodies due to animal activity.

Thus, it is possible to identify the differences between the studied objects based on the interrelated chemical and bacterial indicators, particularly the features of the physical and geographical conditions of the territory, the presence of a current and eutrophication.

This relationship is confirmed by the correlation between microbiological and chemical indicators (Table 6,7). There is a direct correlation of the CFU of bacteria with the content of biophilic elements (Ca, Fe, K, Mg, P, S, N) and an inverse correlation with the content of organic matter. This can be explained by the fact that the content of biophilic elements in water limits the abundance and activity of bacteria, while DOM, as the main source of nutrition for bacteria, undergoes rapid mineralization. The highest number of correlations between microbiological and chemical indicators is observed for an easily accessible polymer Tween 20, while for a medium with Fe, there is no significant correlation with chemical properties.

Based on Tables 2, 3, and 5, we carried out a multiple correlation analysis which showed the most interconnected chemical and microbiological indicators. These indicators are marked in Table 6 with an asterisk. We found that bacterial indicators are primarily associated with the content of

Table 5. Concentrations of chemical elements and ions in water (± mean error)

Elements and ions	Concentration, mg/L			
	Don River	Mezha River ('Old dam')	Mezha River	Pond
Al	n.d.	0.082±0.005	0.026±0.007	0.052±0.006
B	0.103±0.001	0.003±0.001	0.016±0.0001	0.010±0.0001
Ba	0.0250±0.0002	0.0100±0.0002	0.107±0.005	0.0250±0.0003
Ca	32.8±0.2	9.1±0.2	37.6±0,05	17.2±0.1
Co	n.d.	n.d.	0.0035±0.0001	n.d.
Fe	0.028±0.003	0.88±0.02	3.0±0.1	1.84±0.06
Cu	n.d.	0.0006±0.0001	n.d.	0.014±0.002
K	4.99±0.05	0.18±0.07	1.79±0.01	0.747±0,007
Li	0.0250±0,0001	n.d.	n.d.	n.d.
Mg	28.1±0,1	1.7±0,3	9.51±0,04	3.19±0,02
Mn	0.059±0.007	0.213±0.009	5.5±0.3	0.79±0.03
Na	77.4±0.2	2±1	4.27±0.02	1.32±0.02
P	0.068±0.006	0.032±0.002	0.047±0.003	0.052±0.001
Si	2.70±0.02	0.49±0.01	3.64±0.01	1.081±0.02
Sr	0.690±0.005	0.041±0.009	0.385±0.002	0.065±0.001
F	0.340±0.002	0.052±0.001	0.182±0.002	0.040±0.001
Ti	n.d.	0.002±0.001	n.d.	n.d.
Zn	0.005±0.002	0.01±0.001	0.002±0.001	0.006±0.005
Cl	94±1	0.4±0.2	1.91±0.02	0.83±0.03
NO_2	n.d.	n.d.	0.17±0.02	0.01±0.01
NO_3	n.d.	n.d.	0.34±0.07	0.09±0.05
SO_4	131.9±0.6	0.8±0.3	2.56±0.03	0.32±0.03
NH_4	0.35±0.04	0.19±0.04	0.510±0.006	0.217±0.009
C_{org}	6.2±0.5	17.85±0.09	14.1±0.1	18.2±0.2
N_{org}	1.6±0.1	1.2±0.1	1.1±0.1	1.3±0.1
C/N	3.8±0.2	15±1	13±1	14±1

n.d.-not detected

Table 6. Values of the correlation coefficient between microbiological (microbiological culturing) and chemical indicators. Only indicators with significant correlation are shown

Chemical indicators	Concentration of bacteria in water taken into account on media								
	Peptone yeast extract glucose agar	Ashby's Glucose Agar	Oligotrophic media	Copiotrophic media	Nutrient Agar 37°C	Nutrient Agar 22°C	Dissolved organic matter	MacConkey Media	Bile Esculin Azide Agar
Al	-0.25	**-0.83**	0.16	-0.12	-0.87	-0.27	-0.47	**-0.83**	-0.58
B	-0.24	**0.73**	-0.6	-0.4	**0.71**	-0.19	0.25	0.68	0.59
Ba	**0.97**	0.4	**0.74**	0.61	0.54	**0.96**	0.55	0.37	0.42
Ca	0.66	**0.81**	0.23	0.29	**0.91**	0.68	0.62	**0.78**	0.7
Fe	**0.81**	-0.12	**0.86**	0.72*	-0.02	**0.76***	0.21	-0.12	-0.02
K	-0.04	**0.82**	-0.46	-0.28	0.83	0	0.35	**0.76**	0.67
Mg	-0.06	**0.81**	-0.48	-0.3	0.82	-0.01	0.35	**0.76***	0.66
Mn	**0.97***	0.26	**0.81**	0.63	0.4	**0.96***	0.49	0.24	0.32
Na	-0.3	0.69	-0.64	-0.46	0.67	-0.25	0.21	0.65	0.55
P	-0.13	0.56	-0.45	-0.18	0.55	-0.13	0.16	0.44	0.5
S	-0.32	0.68	-0.66	-0.47	0.65	-0.27	0.2	0.63	0.54
Si	**0.75**	**0.78**	0.32	0.34	**0.9**	**0.77**	0.64	**0.75**	0.67
Sr	0.19	**0.88***	-0.27	-0.15	**0.93**	0.24	0.49	**0.83**	**0.73***
Zn	-0.32	-0.21	-0.26	-0.23	-0.34	-0.31	-0.16	-0.31	-0.25
F	0.13	**0.87**	-0.32	-0.21	**0.91**	0.19	0.48	**0.82**	**0.72**
Cl	-0.32	0.68	-0.65	-0.46	0.66	-0.27	0.19	0.64	0.55
NO_3	**0.89**	0.23	**0.85**	0.61	0.31	**0.87**	0.32	0.17	0.42
SO_4	-0.32	0.68	-0.65	-0.47	0.66	-0.27	0.21	0.63	0.54
NH_4	**0.82**	0.68	0.52	0.52	**0.83**	**0.84**	**0.71***	**0.7**	**0.59**
C_{org}	0	**-0.83**	0.43	0.29	**-0.86***	-0.05	-0.35	**-0.79***	-0.69
N_{org}	0.08	**0.74**	-0.17	-0.01	**0.7**	0.13	0.52	**0.74**	0.5
C/N	0.17	**-0.77**	0.53	0.33	**-0.72**	0.13	-0.24	**-0.74**	-0.54

Note: Correlation coefficients values that are significant according to the data of correlation analysis (p=0.95) are highlighted in bold; * marks correlation coefficients that are significant according to the data of multiple linear regression

Table 7. Values of the correlation coefficient between microbiological (comprehensive approach) and chemical indicators. Only indicators with significant correlation are shown

Chemical indicators	Area under curve describing the concentration of bacterial communities on media with polymers							
	Keratin	Chitin	Cellulose	Agarose	Inulin	Xylan	Tween 20	Dextran-500
Al	-0.23	-0.34	-0.32	-0.34	**-0.9**	0.06	**-0.96**	-0.11
B	-0.11	-0.19	-0.18	-0.13	**0.74**	-0.08	**0.8**	-0.39
Ba	**0.79**	**0.97**	**0.94**	**0.82***	0.49	0.28	0.31	**0.93**
Ca	0.58	**0.71**	**0.7**	0.63	**0.91**	0.16	0.82	0.54
Fe	0.68	**0.81**	**0.81**	**0.76**	-0.03	0.18	-0.12	**0.88**
K	0.04	0.01	0.02	0.04	**0.85**	-0.02	**0.87***	-0.2
Mg	0.02	-0.02	-0.02	0	**0.83**	-0.02	**0.85***	-0.22
Mn	**0.78**	**0.96**	**0.93**	**0.8**	0.35	0.28	0.15	**0.96**
Na	-0.17	-0.26	-0.25	-0.2	0.69	-0.08	**0.74**	-0.44

P	0.01	-0.06	0.08	0.2	**0.76**	-0.21	**0.81**	-0.14
S	-0.19	-0.28	-0.28	-0.22	0.67	-0.09	**0.73**	-0.46
Si	0.62	**0.78**	**0.76**	0.66	**0.87**	0.19	**0.74**	0.63
Sr	0.19	0.23	0.22	0.18	**0.92**	0.07	**0.87**	0.03
Zn	-0.34	-0.34	-0.28	-0.48	-0.54	**0.71**	-0.38	-0.34
F	0.14	0.16	0.14	0.11	**0.9**	0.05	**0.84**	-0.04
Cl	-0.18	-0.28	-0.27	-0.21	0.68	-0.11	**0.74**	-0.46
NO_3	**0.83***	**0.89**	**0.81***	**0.82**	0.32	0.23	0.13	**0.86***
SO_4	-0.18	-0.28	-0.27	-0.21	0.68	-0.1	**0.74**	-0.46
NH_4	**0.7**	**0.86***	**0.75**	**0.72**	**0.72***	0.14	**0.63**	**0.71**
C_{org}	-0.06	-0.03	-0.03	-0.02	**-0.85**	0.02	**-0.83**	0.16
N_{org}	0.14	0.21	0.07	0.11	0.63	0.13	**0.75***	-0.14
C/N	0.09	0.12	0.11	0.14	**-0.71**	-0.01	**-0.76***	0.36

Note: Correlation coefficient values that are significant according to the data of correlation analysis (p=0.95) are highlighted in bold; * marks correlation coefficients that are significant according to the data of multiple linear regression

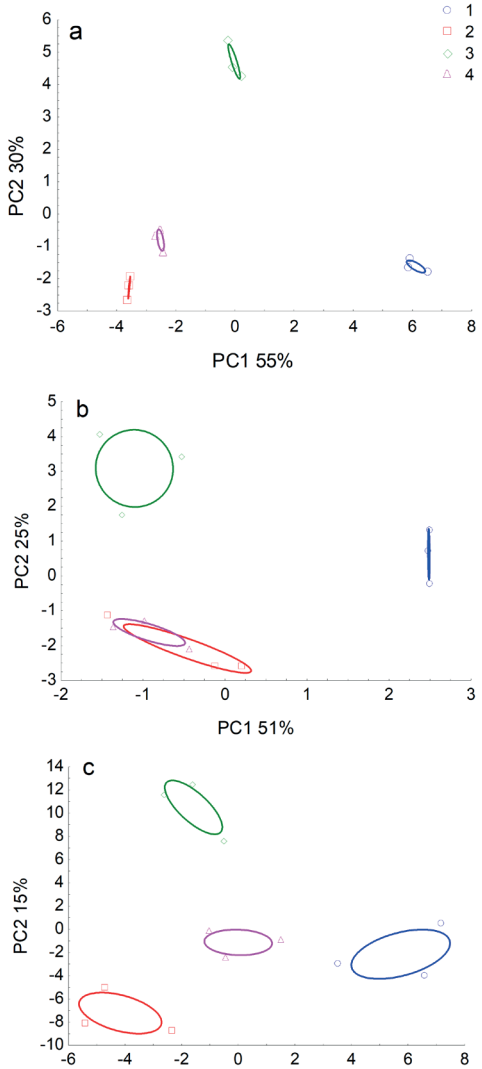

Fig. 3. Relative position of the studied waterbodies in the PC1 and PC2 factor space constructed according to chemical indicators (a), microbiological culturing (b) and the comprehensive approach (c). Correlation ellipses limit the area with p=0.95. 1 – bacterial complex of the Don River, 2 – the dam on the Mezha River, 3 – the Mezha River, 4 – the pond

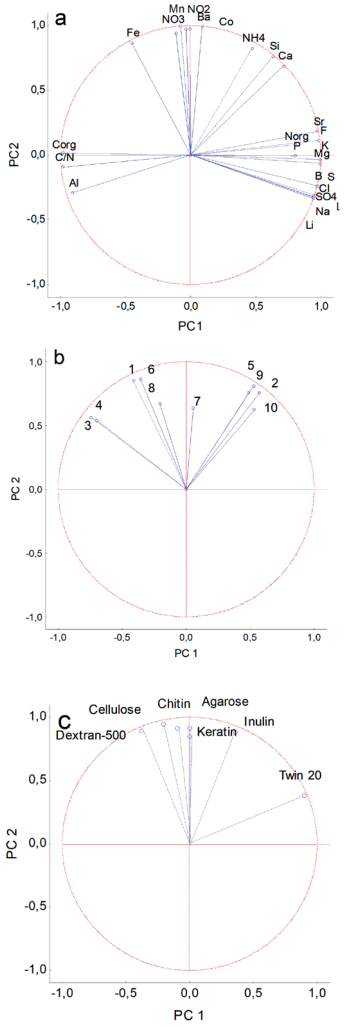

Fig. 4. Values of the correlation coefficient between PC1 and PC2 according to chemical indicators (a), microbiological culturing (b), and indicators of the comprehensive approach (c). 1- Glucose peptone yeast extract agar, 2- Ashby's Glucose Agar, 3- Oligotrophic media, 4- Copiotrophic media, 5- Nutrient Agar 37°C, 6- Nutrient Agar 22°C, 7- Soluble organic matter, 8- Isolation Medium for Iron Bacteria, 9- MacConkey Media, 10- Bile Esculin Azide Agar

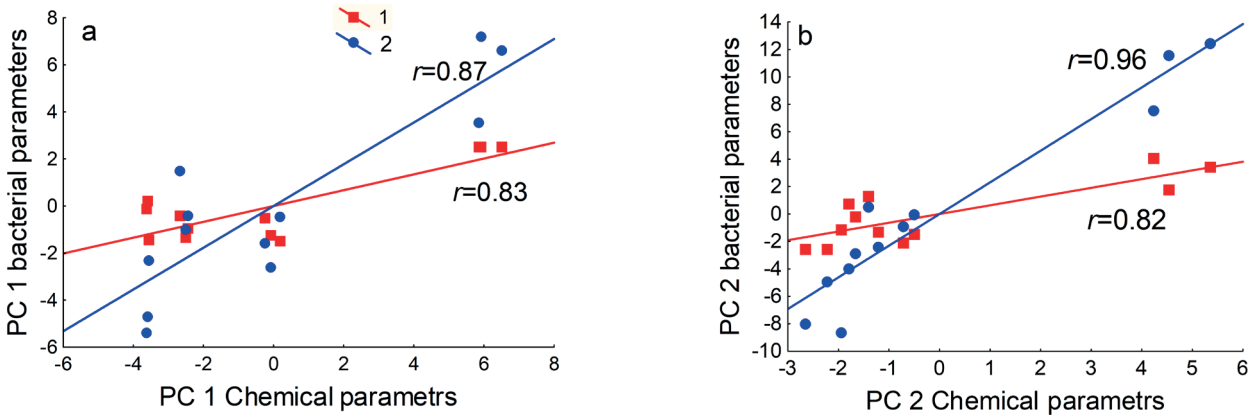

Fig. 5. Correlation between PC1 (a) and PC2 (b) of the chemical and microbiological indicators. 1 – Bacterial culture on agar plates, 2 – Comprehensive approach

biophilic elements (Mg, Mn, Fe) and macroelements (N, C_{org}). At the same time, only CFU on nutrient agar at 22 °C and the area under the growth curve of the bacterial community on the Tween 20 medium were found to depend on two or more indicators.

The PCA showed that the relative position of the studied waterbodies in the space of PC1 and PC2 calculated from chemical and bacterial indicators are similar (Fig. 3).

Data on the correlation between PCs and the studied water indicators (Fig. 4) fully confirmed the data obtained from the analysis of Tables 2, 3 and 5. This indicates the reliability of the identified patterns and suggests the existence of a general relationship between chemical and bacterial indicators of water. In order to prove this relationship, we examined the correlation between PCs calculated from chemical and bacterial indicators and found that it is strong (Fig. 5).

Thus, either there is a causal relationship between bacterial and chemical indicators, or the same environmental factors affect both chemical and bacterial indicators.

CONCLUSIONS

Based on the results of the work, we established that differences in the functioning of the studied waterbodies are related to the differences in both hydrochemical and bacterial properties of water. It can be assumed that there is either a causal relationship between the hydrochemical and microbiological indicators of water or an indirect mechanism of correlation through the independent action of the same factors on both hydrochemical and bacterial indicators. We identified three factors that determine the specifics of the studied waterbodies. The most important factor is the presence or absence of current as it affects both bacterial and chemical indicators. The second most important factor is the geochemical features of the region from where water flows into the waterbody. This factor affects the studied hydrochemical indicators. The third most important factor in terms of the impact on the studied waterbodies is eutrophication which affects the concentration of mineral forms of nitrogen in the water, the total concentration of heterotrophic bacterioplankton and sanitary-indicative microorganisms. The influence of seasonal and yearly variation was not examined in this study. Further studies will expand the list of factors affecting water indicators. The established relationships suggest that methods of bacterial bioindication of the hydrochemical properties of water in waterbodies could be developed in the future.

REFERENCES

Amado A. and Roland F. (2017). Microbial role in the carbon cycle in tropical inland aquatic ecosystems. Frontiers in Microbiology, 8, 20, DOI: 10.3389/fmicb.2017.00020

Azam F., Fenchel T., Field J., Gray J., Meyer-Reil L. and Thingstad F. (1983). The ecological role of water-column microbes in the sea. Mar. Ecol. Prog. Ser.,10, 257-263.

Baltrus D., Yourstone S., Lind A., Guilbaud C., Sands D. C., Jones C. D. and Dangl J. (2014). Draft genome sequences of a phylogenetically diverse suite of Pseudomonas syringae strains from multiple source populations. Genome Announcements, 2(1), 01195-13, DOI: 10.1128/genomeA.01195-13

Belkova N.L., Parfenova V.V., Kostornova T.Ya., Denisova L.Ya. and Zaichikov E.F. (2003). Microbial biodiversity in the water of lake Baikal. Microbiology, 72, 203-213

Belov A., Cheptsov V. and Vorobyova E. (2018). Soil bacterial communities of Sahara and Gibson deserts: Physiological and taxonomical characteristics. AIMS microbiology, 4(4), 685-710, DOI: 10.3934/microbiol.2018.4.685

Cai W., Li Y., Hu J. and Cheng H. (2021). Exploring the Microbial Ecological Functions in Response to Vertical Gradients in a Polluted Urban River. CLEAN–Soil, Air, Water, 49(9), 2100004, DOI: 10.1002/clen.202100004

Dolgonosov B.M., Korchagin K.A. and Messineva E.M. (2014). Model of fluctuations in bacteriological indices of water quality.Water Resources, 2014, 33(6), 637-650, DOI: 10.1134/S0097807806060054

Drozdova O.Yu., Karpukhin M.M., Dumtsev S.V. and Lapitskiy S.A. (2021). The forms of metals in the water and bottom sediments of the Malaya Sen'ga river (Vladimir oblast). Moscow University Geology Bulletin,76(3), 336-342, DOI: 10.3103/S0145875221030030

Wright E., Yilmaz L. and Noguera D. (2012). DECIPHER, A Search-Based Approach to Chimera Identification for 16S rRNA Sequences. Applied and Environmental Microbiology,78(3), 717-725, DOI: 10.1128/AEM.06516-11

Fasching C., Behounek B., Singer G. and Battin T. (2014). Microbial degradation of terrigenous dissolved organic matter and potential consequences for carbon cycling in brown-water streams. Scientific Reports, 4(1), 1-7, DOI:10.1038/srep04981

Friedrich I., Hollensteiner J., Schneider D., Poehlein A., Hertel R. and Daniel R. (2020). First complete genome sequences of Janthinobacterium lividum EIF1 and EIF2 and their comparative genome analysis. Genome Biology and Evolution, 12(10), 1782-1788, DOI: 10.1093/gbe/evaa148

Grishantseva E.S. Alekhin Yu.V., Drozdova O.Yu, Demin V.V and Zavgorodnyaya Yu.A. (2020). Experimental studies of organic matter in natural waters of lakes in Vladimir region using a set of analytical methods. Experiment in GeoSciences, 26(1), 126–129

Judd K., Crump B. and Kling G. (2006). Variation in dissolved organic matter controls bacterial production and community composition. Ecology, 87, 2068–2079. DOI: 10.1890/0012-9658(2006)87[2068:VIDOMC]2.0.CO;2

Kepkay P. (1994). Particle aggregation and the biological reactivity of colloids. Mar. Ecol. Prog. Ser., 109, 293–304

Kopylov A. I. and Kosolapov D.B. (2011). Microbial Loop in Plankton Communities of Marine and Freshwater Ecosystems. Izhevsk: Knigograd, 332 (In Russian)

Lartseva L.V., Obuhova O.V. and Istelueva A.A. (2015). The geoecological aspects of bacteriocoenosis in Volga delta in conditions of anthropogenic load. South of Russia: ecology, development, 4(4), 170-173. (In Russian), DOI: 10.18470/1992-1098-2009-4-170-173

Lobbes J., Fitznar H. and Kattner G. (2000). Biogeochemical characteristics of dissolved and particulate organic matter in Russian rivers entering the Arctic Ocean. Geochimica et Cosmochimica Acta, 64(17), 2973-2983, DOI: 10.1016/S0016-7037(00)00409-9

Moriarty E., Karki N., Mackenzie M., Sinton L., Wood D. and Gilpin B. (2011). Faecal indicators and pathogens in selected New Zealand waterfowl. New Zealand Journal of Marine and Freshwater Research, 45(4), 679-688, DOI: 10.1080/00288330.2011.578653

Obukhova O.V., Lartseva L.V., Volodina V.V. and Vasilyeva L.M. (2017). Dynamics of potentially pathogenic microflora of the water and pike perch in the Volga Delta.Contemporary Problems of Ecology, 10(5), 563-574, DOI: 10.1134/S1995425517050109

Pakusina A.P., Tsarkova M.F., Platonova T.P., Kolesnikova T.P. (2022). Characteristics of the Zavitaya River in terms of hydrochemical and microbiological indicators during the flood of 2021. IOP Conference Series: Earth and Environmental Science, 981, 4, 042068, DOI: 10.1088/1755-1315/981/4/042068

Richardson J. and Mackay R. (1991). Lake outlets and the distribution of filter-feeders: An assessment of hypotheses.Oikos., 62, 370-380, DOI:10.2307/3545503

Semenov A. M. (1991). Physiological Bases of Oligotrophy of Microorganisms and Concept of Microbial Community. Microb. Ecol., 22, 239-247. DOI: 10.1007/BF02540226

Skinner Q., Speck J., Smith M. and Adams J. (1998). Stream water quality as influenced by beaver within grazing systems in Wyoming. Journal of Range Management Archives, 37(2), 142-146

Sorokovikova L.M., Popovskaya G.I., Tomberg I.V., Sinyukovich V.N., Kravchenko O.S., Marinaite, I.I., Bashenkhaeva N.V. and Khodzher T.V. (2011). The Selenga River water quality on the border with Mongolia at the beginning of the 21st century. Russian Meteorology and Hydrology, 38(2), 126-133, DOI: 10.3103/S1068373913020106

Standridge J., Delfino J., Kleppe L. and Butler R. (1979). Effect of waterfowl (Anas platyrhynchos) on indicator bacteria populations in a recreational lake Madison, Wisconsin. Applied and Environmental Microbiology, 38(3), 547-550, DOI: 10.1128/aem.38.3.547-550.1979

Tanentzap A., Fitch A., Orland C., Emilson E., Yakimovich K., Osterholz H. and Dittmar T. (2019). Chemical and microbial diversity covary in fresh water to influence ecosystem functioning. Proc. Natl. Acad. Sci. U.S.A., 116, 24689–24695, DOI: 10.1073/pnas.1904896116

Tuohy J., Mueller-Spitz S., Albert C., Scholz-Ng S., Wall M., Noutsios G. and Sandrin, T. R. MALDI-TOF MS affords discrimination of Deinococcus aquaticus isolates obtained from diverse biofilm habitats//Frontiers in Microbiology.2018. 2442. DOI: 10.3389/fmicb.2018.02442

Van Horn D., Sinsabaugh R., Takacs-Vesbach C., Mitchell K. and Dahm C. (2011). Response of heterotrophic stream biofilm communities to a gradient of resources. Aquatic Microbial Ecology,64(2), 149-161. DOI:10.3354/ame01515

Yakushev A. V. (2015). Integral structural–functional method for characterizing microbial populations. Eurasian Soil Science, 48(4), 378–394. DOI: 10.1134/S1064229315040110

Yang N., Zhang C., Wang L., Li Y., Zhang W., Niu L., Zhang H. and Wang, L. (2021). Nitrogen cycling processes and the role of multi-trophic microbiota in dam-induced river-reservoir systems.Water Research, 206, 117730. DOI: 10.1016/j.watres.2021.117730

Zhuravlev P.V., Aleshnya V.V., Golovina S.V., Panasovets O.P., Nedachin E.A., Talaeva Yu.G., Artemova T.Z., Gipp E.K., Zagaynova A.V. and Butorina N.N. (2010). Monitoring bakterial'nogo zagryazneniya vodoemov Rostovskoy oblasti. Gigiena i Sanitariya, 5, 33-36 (in Russian)

RESEARCH PAPER

FEATURES OF THE FIRST HAZARD CLASS ELEMENTS ACCUMULATION BY PLANTS OF THE *PAEONIA* L. GENUS

Antonina A. Reut[1*], Svetlana G. Denisova[1]

[1]South-Ural Botanical Garden-Institute of Ufa Federal Research Centre of Russian Academy of Sciences, Mendeleev Street, Ufa, 450080, Russia

***Corresponding author:** cvetok.79@mail.ru

Received: April 13th, 2022 / Accepted: November 11th, 2022 / Published: December 31st, 2022

https://DOI-10.24057/2071-9388-2022-049

ABSTRACT. Heavy metals are generally recognized as primary soil pollutants. The most active pollutants are their mobile forms, which can migrate from a solid state into soil solutions and become absorbed by plants. The aim of this work was to study the features of heavy metal accumulation in the aboveground and underground parts of the *Paeonia* L. genus representatives in the urbanized environment of Ufa. The research considered four species and three varieties of hybrid paeony. The elemental composition of the aboveground and underground parts was analyzed using the method «Determination of As, Pb, Cd, Sn, Cr, Cu, Fe, Mn and Ni in samples of food products and food raw materials by the atomic absorption method with electrothermal atomization». Eight elements were studied for each raw material group and their concentrations were determined in mmol/kg of air-dry raw material. The minimum concentrations of arsenic, chromium, manganese, and iron were observed in the roots; lead, cadmium, and copper – in the leaves; nickel – in the flowers of the studied paeonies. The maximum content of arsenic and chromium was found in leaves; lead, nickel, manganese, and iron – in stems; cadmium and copper – in flowers. The results of the correlation analysis showed that there is a moderate or strong relationship between the concentrations of the studied elements in the considered taxa of paeonies.

KEYWORDS: *Paeonia*, heavy metals, aboveground organs, underground mass, Republic of Bashkortostan.

CITATION: Reut A. A., Denisova S. G. (2023). Features Of The First Hazard Class Elements Accumulation By Plants Of The *Paeonia* L. Genus. Geography, Environment, Sustainability, 1(16), 172-180
https://DOI-10.24057/2071-9388-2022-049

ACKNOWLEDGEMENTS: The work was carried out under the Program of Basic Research of the Praesidium of the Russian Academy of Sciences «Biodiversity of Natural Systems and Plant Resources of Russia: Assessment of the State and Monitoring of Dynamics, Problems of Conservation, Reproduction, Increase and Rational Use» and within the framework of the state assignment of the SUBGI UFRC RAS on the topic No. FMRS-2022-0072.

Conflict of interests: The authors reported no potential conflict of interest.

INTRODUCTION

Currently, a lot of attention all over the world is paid to the protection of the external and internal human environment from the increasing influence of chemicals (in particular, heavy metals and soluble forms of their toxic compounds) of anthropogenic and natural origin (Bashmakov and Lukatkin 2009; Kaloev and Kumsiev 2014). Ufa is the capital of the Republic of Bashkortostan, a city of republican significance, and the administrative center of Ufa district. The environmental conditions in the city are determined not only by natural, but also by man-made factors, the role of which increases every year. Ufa ranks 8th in terms of pollution among major Russian cities and has more than 700 enterprises that operate in the city, polluting the natural environment in various ways. The leading industrial sectors of the city are oil refining, engineering, and chemical industries. The main contribution to emissions from stationary sources is made by the oil refining industry – 48% (Bashneftekhim) and the electric power industry – 21% (Ufa heating networks). Vehicle emissions into the atmosphere, such as sulfur dioxide, nitrogen oxide, and ash elements, also have a great influence on the environment, contributing around 53% to the total emissions in the city. On the other hand, it is known that plants have a positive effect not only on the ecological conditions due to the accumulation of toxic substances, but also serve as a health factor for residents of urbanized environments. Many of them play a phytomeliorative role in the landscaping of many cities in the Altai Territory, Bashkiria, Crimea, the Urals, and the European part of Russia (Sedelnikova and Tsandekova 2021).

With the growth in urbanization, a significant transformation of the natural environment takes place. A common feature of urbanized areas is the contamination of soil with heavy metals, which also have a toxic and mutagenic effect on plants (Davydova and Tagasov 2002; Bityutsky 2005). Heavy metals are particularly important compared to other toxic technogenic elements because they do not undergo biogenic and physicochemical decay processes and thus can concentrate in the fertile soil layer, changing its properties (Titov et al. 2011). As a result, pollutants remain available for absorption by plant roots for a long time, and can subsequently move along the food

chain of a biogeocenosis (Sedelnikova and Chankina 2016; Mikhalchuk 2017).

With an increase in the content of metals in the soil, its general biological activity decreases. This has a considerable effect on the growth and development of plants, which can have a different reaction to the excess of metals (Chirkova 2002; Titov et al. 2014). Metals are distributed throughout the plant organs unevenly, as they are primarily accumulated in leaves (Uzakov 2018).

Also, it was found that vegetable crops can accumulate significantly more heavy metals than tubers and root crops, which is particularly important for their cultivation (Ilyinsky 2020; Dinu et al. 2020). Ornamental flower cultures, meanwhile, firmly occupy their ecological niche and are almost never considered from this point of view (Mazhaisky et al. 2016; Elagina et al. 2016). However, representatives of the *Paeonia* L. genus are widely used in the landscaping of cities and towns of the Republic of Bashkortostan and can potentially be used as indicators for assessing the ecological state of the environment.

Therefore, the purpose of this research was to study the features of heavy metal accumulation in the aboveground and underground organs of *Paeonia* L. genus representatives in the urban environment of the city of Ufa.

MATERIALS AND METHODS

The study was conducted at the South-Ural Botanical Garden Institute of Ufa Federal Research Center of the Russian Academy of Sciences (hereinafter referred to as SUBGI UFRC RAS) during the growing seasons of 2018-2021 based on the collection of the laboratory of introduction and breeding of flowering plants (Abramova et al. 2019).

A combined soil sample was taken from the experimental plot during the same period. It consisted of 25 point samples, the sampling depth was 1–25 cm and the mass of the combined sample was 1 kg. These soil samples were later used to determine the content of mobile forms of heavy metals.

The research focused on four species: *Paeonia peregrina* Mill., *P. lactiflora* Pall., *P. lactiflora f. rosea* Pall., and *P. delavayi* Franch. (*Paeoniaceae* family). From P. *lactiflora* Pall., three varieties of paeony, particularly 'Appassionata', 'Mustai Karim', and 'Jeanne d'Arc' (Fig. 1), were introduced and grown at the SUBGI UFRC RAS facilities (Mironova and Reut 2017; Reut and Mironova 2018).

The study of the microelement composition of raw plant material (flowers, stems, leaves, and roots) was carried out at the analytical laboratory of the Research Institute of Agriculture. The phases of the raw material collection are defined by pharmacopoeia based on the dynamics of the accumulation of biologically active compounds. For example, grass should be collected from the regrowth phase to fruiting, flowers – in the phase of mass flowering, and roots – in the phase of death of aboveground organs (Demidenko 2020). For analysis, 10 middle-aged cultivars of

Paeonia delavayi Franch. *Paeonia peregrina* Mill. *P. lactiflora* Pall.

P. lactiflora f. rosea Pall. *P. lactiflora 'Mustai* Karim'

P. lactiflora 'Jeanne d'Arc'

P. lactiflora 'Appassionata'

Fig. 1. Studied *Paeonia* L. Species

each taxon of the generative stage of development in the flowering phase (May–June) were used. The collection of aboveground parts (flowers, leaves, stems) of the studied plants was carried out in the morning. The roots were dug in late September – early October (before the first frosts) and were washed first with regular water, and then with distilled water. For quantitative analysis, the raw material was dried to an air-dry state and then crushed to a particle size passing through a 1 mm sieve (Wang et al. 2016; Fotev et al. 2021).

The elemental composition of the samples was analyzed using the method «Determination of As, Pb, Cd, Sn, Cr, Cu, Fe, Mn and Ni in samples of food products and raw food materials by the atomic absorption method with electrothermal atomization» (Simonova et al. 2020; Reut et al. 2021).

Mathematical data processing was carried out using the general statistical methods implemented in the AgCStat Excel add-in and the AGROS 2.09 statistical and biometrical genetic analysis software package (Gonchar-Zaikin and Chertov 2012; Chekin and Nikiforov 2016; Nesterov et al. 2016; Budko et al. 2018; Zakharov and Mishenkina 2020).

RESULTS

The analysis showed that the content of heavy metals in the studied soil samples does not exceed the established maximum permissible concentrations.

The study of the trace element content in flowers, leaves, stems, and roots was carried out for seven different taxa of paeonies ('Appassionata', 'Mustai Karim', 'Jeanne d'Arc', *P. delavayi, P. lactiflora, P. lactiflora f. rosea, P. peregrina*.) and eight elements. The obtained quantitative estimates of their concentration are given below in mmol/kg of air-dry raw material (Fig. 2–5).

The analysis revealed a relatively high content of copper in all types of raw material and all studied plants with concentrations 4.15–2520.00 times higher compared to other elements. The maximum content of copper was noted in the roots, and the minimum – in the leaves of the plants.

It was also found that the minimum concentrations of arsenic, chromium, manganese, and iron correspond to the roots; lead, cadmium, and copper – to the leaves; nickel – to the flowers of the studied paeonies. The maximum content of arsenic and chromium was found in leaves; lead, nickel,

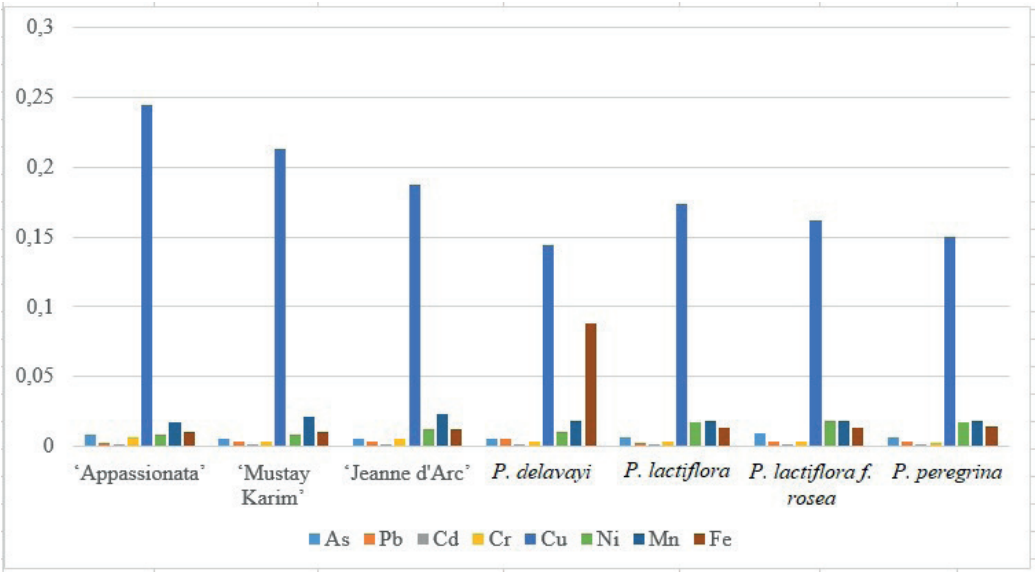

Fig. 2. The content of heavy metals in flowers of the Paeonia genus representatives (mmol/kg)

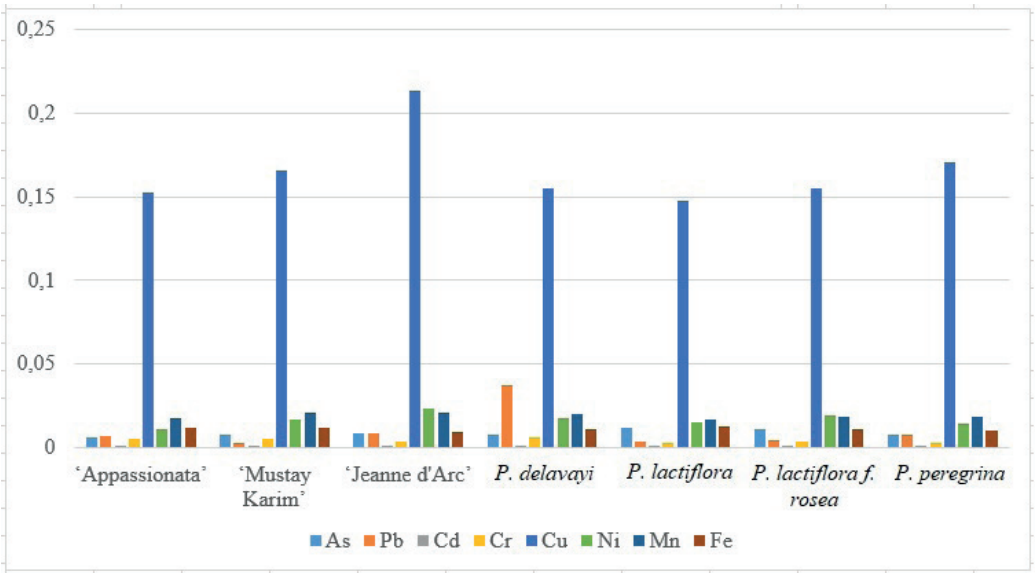

Fig. 3. The content of heavy metals in leaves of the Paeonia genus representatives (mmol/kg)

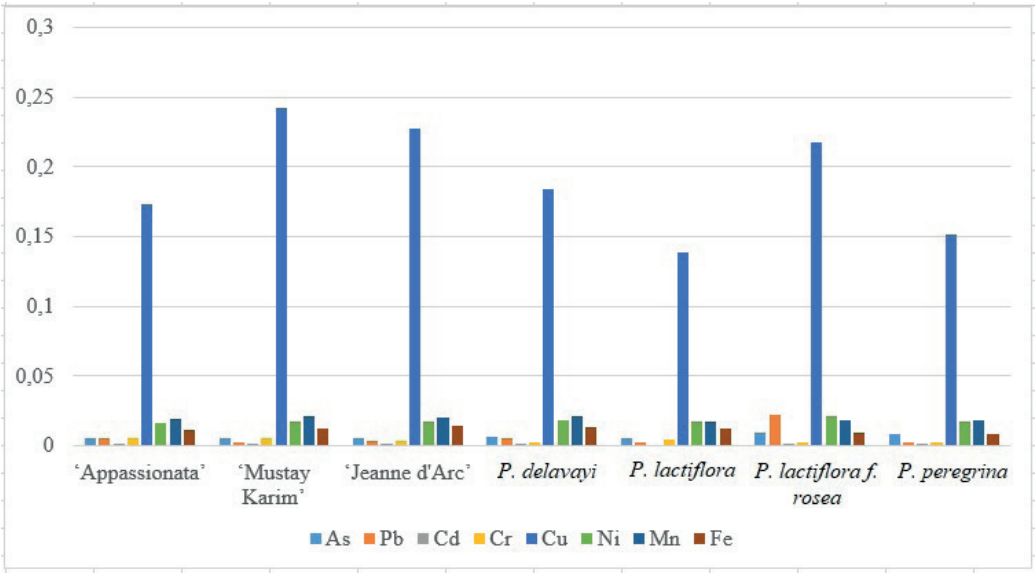

Fig. 4. The content of heavy metals in stems of the Paeonia genus representatives (mmol/kg)

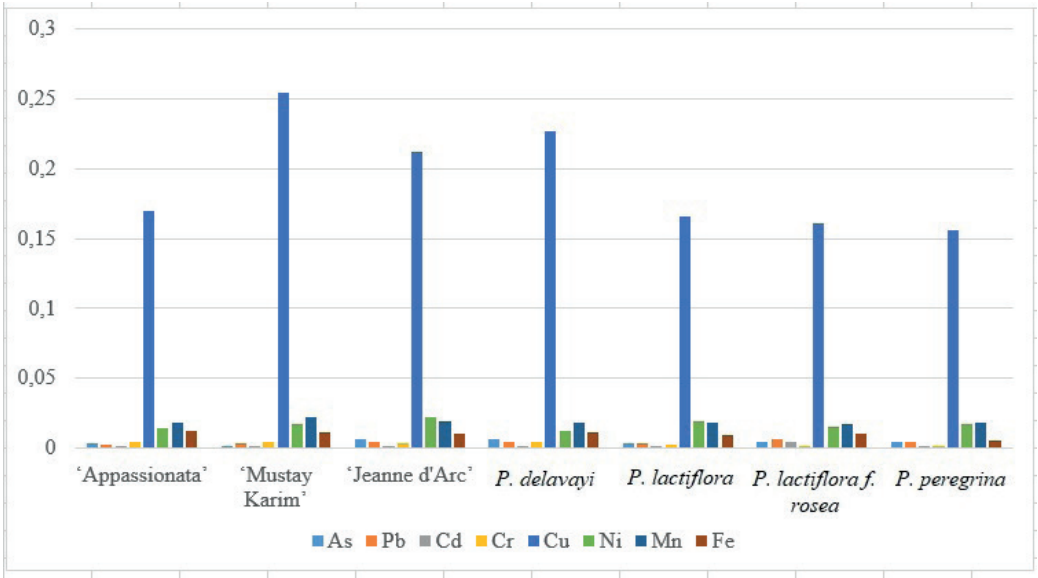

Fig. 5. The content of heavy metals in roots of the Paeonia genus representatives (mmol/kg)

manganese, and iron – in stems; cadmium and copper – in flowers.

For the convenience of the two-way analysis of variance, the concentration values were converted into logarithms. The results of this analysis showed significant differences in the content of heavy metals in different taxa and plant parts. It was revealed that the taxon has the most influence on the content of cadmium, chromium, and manganese, with an influence share of 56.45–70.83%; the second most important factor is the part of the plant, which accounts for 2.37–14.87%; the contribution of the taxon – plant part interaction is 17.11–29.23% (Table 1). The main contribution to the content of arsenic, lead, copper, nickel, and iron is made by the taxon – part of the plant interaction (41.16–68.87%); the share of the first factor accounts for 14.43–44.19%, while the share of the second one is 9.19–33.22% (Table 1).

As a result of the correlation analysis, relationships between the content of the studied elements in different plant parts were revealed (Tables 2–5). It was found that the amount of lead and cadmium in stems, as well as cadmium in flowers is directly dependent on the content of arsenic with a correlation in the range of 0.62–0.74. An inverse relationship between the amount of arsenic and the content of chromium in leaves, lead and manganese in flowers, manganese in roots, and chromium in stems was also revealed with a correlation in the range of 0.49–0.83.

Table 1. Results of the two-way analysis of variance of the elemental composition of paeonies

Element	Sources of variation	SS	Df	ms	Ffact	Share, %
Arsenic (As)	General	34.57	83.00	-	-	-
	Taxon (A)	7.74	6.00	1.29	1605.87	22.39
	Part of the plant (B)	11.48	3.00	3.83	4764.83	33.22
	Interaction (AB)	15.30	18.00	0.85	1057.89	44.26
	Random	0.04	54.00	0.0008	-	-

Lead (Pb)	General	30.67	83.00	-	-	-
	Taxon (A)	9.21	6.00	1.53	5353.04	30.01
	Part of the plant (B)	5.74	3.00	1.91	6678.85	18.72
	Interaction (AB)	15.71	18.00	0.87	3044.60	51.21
	Random	0.02	54.00	0.0003	-	-
Cadmium (Cd)	General	36.95	83.00	-	-	-
	Taxon (A)	21.32	6.00	3.55	51.83	57.71
	Part of the plant (B)	5.49	3.00	1.83	26.71	14.87
	Interaction (AB)	6.32	18.00	0.35	5.12	17.11
	Random	3.70	54.00	0.0686	-	-
Chromium (Cr)	General	10.06	83.00	-	-	-
	Taxon (A)	5.68	6.00	0.95	709.62	56.45
	Part of the plant (B)	1.36	3.00	0.45	339.60	13.51
	Interaction (AB)	2.94	18.00	0.16	122.48	29.23
	Random	0.072	54.00	0.00133	-	-
Copper (Cu)	General	2.68	83.00	-	-	-
	Taxon (A)	1.18	6.00	0.20	668.02	44.19
	Part of the plant (B)	0.25	3.00	0.08	277.82	9.19
	Interaction (AB)	1.23	18.00	0.07	231.78	46.00
	Random	0.016	54.00	0.00030	-	-
Nickel (Ni)	General	5.48	83.00	-	-	-
	Taxon (A)	1.66	6.00	0.28	421.16	30.25
	Part of the plant (B)	1.53	3.00	0.51	777.33	27.92
	Interaction (AB)	2.25	18.00	0.13	191.00	41.16
	Random	0.035	54.00	0.00066	-	-
Manganese (Mn)	General	0.50	83.00	-	-	-
	Taxon (A)	0.35	6.00	0.06	836.37	70.83
	Part of the plant (B)	0.01	3.00	0.00	55.97	2.37
	Interaction (AB)	0.13	18.00	0.01	102.48	26.04
	Random	0.004	54.00	0.00007	-	-
Iron (Fe)	General	2.95	83.00	-	-	-
	Taxon (A)	0.43	6.00	0.07	21.20	14.43
	Part of the plant (B)	0.30	3.00	0.10	30.25	10.30
	Interaction (AB)	2.03	18.00	0.11	33.73	68.87
	Random	0.181	54.00	0.00335	-	-

Table 2. Correlation matrix of the content of elements in flowers of paeony

Indicators	As	Pb	Cd	Cr	Cu	Ni	Mn	Fe
As	1.00							
Pb	-0.49*	1.00						
Cd	0.63**	-0.03	1.00					
Cr	-0.05	-0.26	-0.61**	1.00				
Cu	0.09	-0.48*	-0.41	0.78**	1.00			
Ni	0.32	-0.32	0.50*	-0.63**	-0.66**	1.00		
Mn	-0.65**	0.15	-0.36	0.33	0.16	-0.29	1.00	
Fe	0.21	-0.60**	0.25	-0.34	-0.31	0.84**	0.04	1.00

Note: * – significant at the 5% level; ** – significant at the 1% level; the absence of * indicates that the correlation is not significant

Table 3. Correlation matrix of the content of elements in leaves of paeony

Indicators	As	Pb	Cd	Cr	Cu	Ni	Mn	Fe
As	1.00							
Pb	-0.34	1.00						
Cd	0.38	-0.18	1.00					
Cr	-0.66**	0.65**	-0.02	1.00				
Cu	-0.14	-0.09	-0.14	-0.27	1.00			
Ni	-0.02	-0.03	-0.10	-0.27	0.17	1.00		
Mn	-0.39	0.29	0.08	0.40	0.53*	-0.01	1.00	
Fe	0.30	-0.13	-0.20	0.02	-0.78**	-0.14	-0.47*	1.00

Note: * – significant at the 5% level; ** – significant at the 1% level; the absence of * indicates that the correlation is not significant

Table 4. Correlation matrix of the content of elements in stems of paeony

Indicators	As	Pb	Cd	Cr	Cu	Ni	Mn	Fe
As	1.00							
Pb	0.74**	1.00						
Cd	0.62**	0.77**	1.00					
Cr	-0.83**	-0.60**	-0.32	1.00				
Cu	-0.03	0.27	0.64**	0.12	1.00			
Ni	-0.13	-0.05	-0.04	-0.00	0.26	1.00		
Mn	-0.38	-0.22	0.01	0.23	0.66**	0.13	1.00	
Fe	-0.20	-0.08	-0.20	0.38	-0.08	-0.06	0.10	1.00

Note: * – significant at the 5% level; ** – significant at the 1% level; the absence of * indicates that the correlation is not significant

Table 5. Correlation matrix of the content of elements in roots of paeony

Indicators	As	Pb	Cd	Cr	Cu	Ni	Mn	Fe
As	1.00							
Pb	0.39	1.00						
Cd	0.02	0.48*	1.00					
Cr	-0.26	-0.64**	-0.33	1.00				
Cu	-0.25	-0.17	-0.28	0.61**	1.00			
Ni	0.08	-0.08	-0.13	-0.43*	-0.04	1.00		
Mn	-0.64**	-0.19	-0.07	0.35	0.62**	-0.04	1.00	
Fe	-0.19	-0.27	-0.06	0.80**	0.52*	-0.35	0.26	1.00

Note: * – significant at the 5% level; ** – significant at the 1% level; the absence of * indicates that the correlation is not significant

DISCUSSION

It is known that heavy metals can migrate between different tissues and that their content can also change during the growing period of plants (Nan et al. 2019).

In previous studies, it was found that the highest amounts of arsenic are recorded in the leaves and roots of plants (Meshkinova et al. 2006). In this study, however, the highest concentration of this element was observed in the flowers and stems of P. lactiflora f. rosea.

Lead in natural populations is present in all plants, while its role in metabolism has not been established (Kabata-Pendias and Pendias 1989). The present research showed that the maximum content of lead in most samples corresponds to the leaves, while minimum concentrations are found in different types of raw materials.

According to literature data, the highest concentrations of cadmium in contaminated plants are always found in roots and leaves (Seregin and Ivanov 2001). In this study, the stems, leaves, flowers, and roots of *P. lactiflora* f. rosea were characterized by the high content of this element.

Some plants, mainly from areas near serpentinite or chromite deposits, can accumulate chromium up to 0.3% of their dry weight (Seregin and Kozhevnikova 2006). The highest levels of chromium in this study were found in different parts of plants – flowers, leaves, and stems. The lowest values were observed in the roots of most of the samples.

As a result of this study, a hypothesis can be made that cutting peonies in the autumn before retiring can help to avoid the accumulation of heavy metals in the soil. In addition, according to other researchers, harvesting plants that accumulate heavy metals is a potential method to prevent toxic pollutants from entering the food chain and conserve biodiversity (Parveen et al. 2022).

CONCLUSIONS

During this study, it was found that the content of mobile forms of heavy metals in the soil of the experimental site does not exceed the maximum permissible concentrations. Analysis of the content of eight elements in different samples of the Paeonia genus representatives revealed that the minimum concentrations of arsenic, cadmium, chromium, manganese, and iron are observed in the roots; lead and nickel – in flowers; copper – in the leaves of the studied paeonies. The maximum content of arsenic, lead, and chromium was found in the leaves; cadmium, nickel, and manganese – in stems; iron – in flowers. It was shown that all studied plants are characterized by relatively high concentrations of copper (4.15–2520.00 times higher compared to other elements) in all types of raw materials. The maximum content of copper was observed in the roots, while the minimum values corresponded to the leaves of plants. Certain patterns in the content of elements in the aboveground and underground plant parts were also identified.

Based on the accumulation in the phytomass of the studied cultivars, the metals were ranked in an ascending series as follows: Cd < Cr < Pb < As < Fe < Ni < Mn < Cu. The highest accumulation of heavy metals among the studied cultivars was observed in the species of *P. lactiflora f. rosea*, while the lowest was found in P. lactiflora.

The obtained data can be used as an indicator for monitoring and assessing the state of plants in an urbanized environment.

The results of the correlation analysis showed that there is a moderate to strong correlation between the concentrations of the studied elements in the considered taxa of Paeonia. A strong positive relationship was found for the following combinations: chromium and copper (0.78), and nickel and iron (0.84) in flowers; arsenic and lead (0,74), and lead and cadmium (0.77) in stems; chromium and iron in roots (0.80). A strong negative relationship was identified between iron and copper (–0.78) in leaves, and arsenic and chromium (–0.83) in stems.

Correlation study makes it possible to reveal the presence or absence of synergy in the accumulation of elements, which corresponds to the results of other studies.

In most of the studied samples, the highest concentration of heavy metals was found in the aboveground phytomass rather than in the roots. This is especially pronounced in *P. lactiflora f. rosea, P. delavayi*, and *P. peregrina*, which makes it possible not only to consider them as bioindicators of the pollution of aboveground ecosystems but also to use them in the phytoremediation method of removing heavy metals from soils.

REFERENCES

Abramova L.M., Anishchenko I.E., Vafin R.V., Golovanov Ya.M., Zhigunov O.Yu., Zaripova A.A., Kashaeva G.G., Lebedeva M.V., Polyakova N.V., Reut A.A., Shigapov Z.Kh. (2019). Plants of the South Ural Botanical Garden-Institute of the Ufa Federal Research Center of the Russian Academy of Sciences. Ufa: World of Printing (in Russian).

Bashmakov D.I., Lukatkin A.S. (2009). Ecological and physiological aspects of accumulation and distribution of heavy metals in higher plants. Saransk: Publishing House of the Mordovian University (in Russian).

Bityutsky N.P. (2005). Essential micronutrients for plants. St. Petersburg: DEAN Publishing House (in Russian).

Budko E.V., Yampolsky L.M., Zhukov I.M., Chernikova D.A. (2018). Concentration correlations of the elemental organization of hemostatic plants. International Journal of Applied and Fundamental Research, 7, 95-100 (in Russian with English summary).

Chekin G.V., Nikiforov V.M. (2016). Development of the root system of spring wheat at the early stages of ontogenesis during pre-sowing treatment of seeds with chelate preparations. Actual problems of agricultural technologies of the XXI century and the concept of their sustainable development: materials of the national correspondence scientific and practical conference / Ministry of Agriculture of the Russian Federation; Department of Science and Technology Policy and Education; Voronezh State Agrarian University named after Emperor Peter I; under total ed. N.I. Bukhtoyarova, N.M. Derkanosova, V.A. Gulevsky. Voronezh, 34-38 (in Russian with English summary).

Chirkova T.V. (2002). Physiological bases of plant resistance. St. Petersburg: Publishing House of St. Petersburg State University (in Russian).

Davydova S.L., Tagasov V.I. (2002). Heavy metals as supertoxicants of the XXI century: Proc. allowance. Moscow: RUDN University (in Russian).

Demidenko G.A. (2020). Phytomedicinal resources. Tutorial. Krasnoyarsk: Krasnoyarsk State Agrarian University (in Russian).

Dinu C., Vasile G.G., Buleandra M. (2020). Translocation and accumulation of heavy metals in Ocimum basilicum L. plants grown in a mining-contaminated soil. J. Soils Sediments, 20, 2141-2154, DOI: 10.1007/s11368-019-02550-w.

Elagina D.S., Arkhipova N.S., Sibgatullina M.Sh. (2016). Study of the features of the accumulation of heavy metals by plants of Amaranthus retroflexus L. Young scientists and pharmacy of the XXI century. Moscow: Nauka, 189-195 (in Russian with English summary).

Fotev Yu.V., Shevchuk O.M., Syso A.I. (2021). Study of the variability of the elemental composition of seeds of the cultivars Vigna unguiculata (L.) Walp. in the south of Western Siberia and Crimea. Chemistry of vegetable raw materials, 2, 217-226 (in Russian with English summary), DOI: 10.14258/JCPRM.2021027543.

Gonchar-Zaikin P.P., Chertov V.G. (2012). Excel add-in for statistical evaluation and analysis of the results of field and laboratory experiments [online] (in Russian with English summary). Available at: http://vniioh.ru/nadstrojka-k-excel-dlya-statisticheskoj-ocenki-i-analiza-rezultatov-polevyx-i-laboratornyx-opytov/ [Accessed 28 October 2021].

Guanjun Nan, Liying Guo, Yuqiong Gao, Xianxin Meng, Lina Zhang, Ning Song & Guangde Yang. (2019). Speciation analysis and dynamic absorption characteristics of heavy metals and deleterious element during growing period of Chinese peony. International Journal of Phytoremediation, 21(14), 1407-1414, DOI: 10.1080/15226514.2019.1633261.

Ilyinsky A.V. (2020). Analysis of biological absorption coefficients of heavy metals for fodder beet. Eurasian Union of Scientists, 2-6 (71), 9–12 (in Russian with English summary).

Kabata-Pendias A., Pendias H. (1989). Microelements in soils and plants. M.: Mir (in Russian).

Kaloev B.S., Kumsiev E.I. (2014). Accumulation and distribution of heavy metals in plants under natural geochemical conditions. Bulletin of the Gorsky State Agrarian University, 51(3), 97-102 (in Russian with English summary).

Mazhaisky Yu.A., Galchenko S.V., Guseva T.M., Cherdakova A.S. (2016). Accumulation of heavy metals by decorative flower crops. Successes of modern science and education, 9(3), 203-205 (in Russian with English summary).

Meshkinova S.S., Elchininova O.A., Shakhovtseva E.V. (2006). Trace elements in plants of Northern Altai. Polzunovskiy vestnik, 2, 291-295 (in Russian with English summary).

Mikhalchuk N.V. (2017). Heavy metals and microelements in background soils and agricultural landscapes in southwestern Belarus. Agroekological journal, 3, 27-31 (in Russian with English summary).

Mironova L.N., Reut A.A. (2017). Peonies. Collections of the Botanical Garden-Institute of the Ufa Scientific Centre of the Russian Academy of Sciences. Ufa: Bashk. Encycl. (in Russian).

Nesterov M.I., Krivokhizhina L.V., Ermolaeva E.N., Kantyukov S.A. (2016). Influence of the degree and duration of blood loss on the level of triglycerides, phospholipids, total cholesterol, cholesterol in lipoproteins. Modern Problems of Science and Education, 6, 101 (in Russian with English summary).

Parveen S., Bhat I.U.H., Khanam Z., (...), Yusoff H.M., Akhter M.S. (2022). Phytoremediation: In situ alternative for pollutant removal from contaminated natural media: A brief review. Biointerface Research in Applied Chemistry, 12(4), 4945-4960, DOI: 10.33263/BRIAC124.49454960.

Reut A.A., Biglova A.R., Allayarova I.N. (2021). Comparative analysis of the chemical composition of plant materials of some representatives of the genera Narcissus L. and Camassia Lindl. Agrarian Bulletin of the Urals, 2 (205), 79-90 (in Russian with English summary), DOI: 10.32417/1997-4868-2021-205-02-79-90.

Reut A.A., Mironova L.N. (2018). Rare species of the genus Paeonia L. cultivated in the Bashkir Urals. Agrarian Russia, 2, 30-34 (in Russian with English summary).

Sedelnikova L.L., Chankina O.V. (2016). The content of heavy metals in the vegetative organs of the hybrid Krasodnev (Hemerocallis hybrida) in an urbanized environment. The Bulletin of KrasGAU, 2(113), 34-43 (in Russian with English summary).

Sedelnikova L.L., Tsandekova O.L. (2021). On the specifics of the content of ash content and some biogenic elements (n, s, p) in the leaves of herbaceous plants in the conditions of the city of Iskitim, Novosibirsk Region. Chemistry of plant raw materials, 1, 213-218, DOI 10.14258/jcprm.2021018413 (in Russian with English summary).

Seregin I.V., Ivanov V.B. (2001). Physiological aspects of the toxic effect of cadmium and lead on higher plants. Plant Physiology, 48(4), 606-630 (in Russian with English summary).

Seregin I.V., Kozhevnikova A.D. (2006). Physiological role of nickel and its toxic effect on higher plants. Plant Physiology, 53(2), 285-308 (in Russian with English summary).

Simonova O.A., Simonov M.V., Tovstik E.V. (2020). Varietal features of bioaccumulation of iron in barley plants. Taurida herald of the agrarian sciences, 3 (23), 142-150 (in Russian with English summary), DOI: 10.33952/2542-0720-2020-3-23-142-151.

Titov A.F., Kaznina N.M., Talanova V.V. (2014). Heavy metals and plants. Petrozavodsk: Karelian Scientific Centre of the Russian Academy of Sciences (in Russian).

Titov A.F., Talanova V.V., Kaznina N.M. (2011). Physiological bases of plant resistance to heavy metals: textbook; Institute of Biology KarRC RAS. Petrozavodsk: Karelian Research Center RAS (in Russian).

Uzakov Z.Z. (2018). Heavy metals and their effect on plants. Symbol of Science, 1-2, 52-53 (in Russian).

Yanjie Wang, Chunlan Dong, Zeyun Xue, Qijiang Jin, Yingchun Xu. (2016). De novo transcriptome sequencing and discovery of genes related to copper tolerance in Paeonia osti. Gene, 576 (1), 126-135, DOI: 10.1016/j.gene.2015.09.077.

Zakharov V.G., Mishenkina O.G. (2020). Adaptive properties of new varieties of oats in the Middle Volga region. Vestnik of Ulyanovsk state agricultural academy, 4(52), 100-107 (in Russian with English summary).

RESEARCH PAPER

COMBINATION OF SUPERABSORBENT POLYMER AND VETIVER GRASS AS A REMEDY FOR LEAD-POLLUTED SOIL

Tran Quoc Toan[1], Tran Thi Hue[1], Nguyen Quoc Dung[1], Nguyen Thanh Tung[2], Nguyen Trung Duc[2], Nguyen Van Khoi[2], Dang Van Thanh[3], Ha Xuan Linh[4*]

[1]Faculty of Chemistry, Thai Nguyen University of Education, Thai Nguyen, Vietnam
[2]Institute of Chemistry, Vietnam Academy of Science and Technology, Ha Noi, Vietnam
[3]Faculty of Basic Sciences, Thai Nguyen University of Medicine and Pharmacy, Thai Nguyen, Vietnam
[4]International School-Thai Nguyen University, Thai Nguyen, Vietnam
***Corresponding author:** haxuanlinh@tnu.edu.vn

Received: April 15th, 2022 / Accepted: November 11th, 2022 / Published: December 31st, 2022
https://DOI-10.24057/2071-9388-2022-054

ABSTRACT. Heavy metal pollution in the soil environment is a worldwide environmental problem as it has negative effects on both human health and the environment. Remediation of heavy metal-contaminated soil is essential to improve soil quality, provide land resources for agricultural production, and protect human and animal health and the ecological environment. There is the possibility of remediating these contaminated soils through the use of several heavy metal absorbing plants and Superabsorbent polymers. Superabsorbent polymers (SAPs) are 3D polymer networks having hydrophilic nature, which can swell, absorb and hold a large amount of water or aqueous solutions in their network. This study evaluates the effect of superabsorbent polymer on Pb absorption capacity of Vetiver (*Vetiveria zizanioides.L*) that was grown on contaminated soil in Trai Cau iron ore dumpsite, Dong Hy district, Thai Nguyen province. The experiment was designed with five recipes and three replicates. The contents of SAP studied were 0, 0.6, 0.8, and 1.0 g/kg of soil. Uncontaminated soil was used as the control treatment. In the supplemented recipe of SAP, Vetiver showed better Pb treatment efficiency than the recipes without adding polymers. After 120 days of planting, SAP increased the tolerance and Pb absorption of Vetiver, improving soil properties. The best Pb treatment efficiency is achieved when using SAP with content from 0.8-1.0 g/kg soil.

KEYWORDS: Superabsorbent polymers, Vetiver (Vetiveria zizanioides L.), lead, absorption, soils

CITATION: Tran Q. Toan, Tran T. Hue, Nguyen Q. Dung, Nguyen T. Tung, Nguyen T. Duc, Nguyen V. Khoi, Dang V. Thanh, Ha X. Linh (2023). Combination of Superabsorbent Polymer And Vetiver Grass As A Remedy For Lead-Polluted Soil. Geography, Environment, Sustainability, 1(16), 181-188
https://DOI-10.24057/2071-9388-2022-054

Conflict of interests: The authors reported no potential conflict of interest.

INTRODUCTION

Heavy metal pollution in the soil is a global environmental problem (Liuwei Wang et al. 2021; Sarwar et al. 2017) and has been increasing as a result of various human activities as well as the process of industrialization and urbanization (Hong-Giang Hoang et al. 2018; Rama Karna et al. 2021) etc. Among all kinds of heavy metals, lead (Pb) is considered as one of the most toxic substances and a major cause of environmental pollution (Kumar 2015). Pb has many toxic effects on human health as it disrupts many bodily functions, such as nervous, cardiovascular, hematological, and reproductive systems (Pal et al. 2015). In pregnant women, the exceeding amount of lead in the body can cause miscarriage (Amadi et al. 2017). In the case of plants, high concentrations of lead can slow down plant growth, inhibit photosynthesis, disturb water balance, blacken roots, and cause other symptoms. Lead toxicity is one of the most hazardous metal toxicities after arsenic (Bikash Debnath et al. 2019).

Soils contaminated with lead or other heavy metals mainly come from human activities such as mining (Shah V et al. 2020), metallurgy, metal production, recycling, use of chemical fertilizers, and use of leaded gasoline (Indah Lestari 2018). Many studies have shown that Pb contamination in soil occurs around non-ferrous metal mining areas (Amjad Alia et al. 2017; Nicolae Cioica et al. 2019). Soil heavy metal pollution from non-ferrous metal mining has been an important and increasing problem in Vietnam. Thai Nguyen is a mountainous province in the North of Vietnam, where there are many mineral mines with large reserves. Studies have shown that in some mining areas of Thai Nguyen province, the concentration of heavy metals such as Cd, Pb, As in the soil after mining is exceeded the allowed criteria (Bui Thi Kim Anh et al. 2011; Takashi Fujimori et al. 2016; Dang et al. 2011).

There are many methods to treat heavy metals in the soil, such as: washing the soil, fixing heavy metals by chemical methods, treating plants, etc. (Liuwei Wang et al. 2021; Nan Lu et al. 2021). The technology of plant treatment (Phytoremediation) is widely applied to treat metal pollution in industrial and mining zones (M. Lambert et al. 2021; Bouzid Nedjimi 2021). Compared with other treatment methods, plant treatment technology is more environmentally friendly. This technology has advantages such as stabilizing the surface soil structure, improving soil nutrition, and significantly reducing the content of metallic pollutants (S. Haq et al. 2020). In addition, pollution

remediation and ecological restoration can be carried out in a mining area simultaneously. Plant remediation of lead pollution has been carried out early in many parts of the world, such as the United States, Germany, China, etc. *Thlaspi rotundifolium (L.), Brassica juncea (L.), Artemisia capillaris, Taraxacum mongolicum, Phragntic australis, Medicago sativa, Plantago asiatica L (Zahra Derakhshan* et al. 2018), *Phragntic australis* (Tran Thi Pha et al. 2014) Hardy 'Limelight' Hydrangea (*Hydrangea paniculata*) and the common sunflower (*Helianthus annuus*) (Forte J et al. 2017), Sunflower (*Helianthus annuus L.*), Sorghum (*Sorghum bicolor L.*) and Chinese Cabbage (*Brassica chinensis*) (Rodrick Hamvumba et al. 2014), etc. have been used to absorb Pb with promising efficacy.

Superabsorbent polymers (SAPs) with superabsorbent and water-holding capacity have been applied to improve agricultural water use efficiency, help maintain soil moisture and reduce irrigation water (Q. Guiwei et al. 2008) thanks to their large amount of hydrophilic groups and a three-dimensional network structure with cross-linking. These characteristics ensure their ability to store a large amount of water even under certain pressures (Luq man AliShah et al. 2018; Mohammad et al. 2008). They also have the ability to cross-link with metallic ions. When added to the soil, it will increase the water-holding capacity of the soil, reduce the toxicity of metals to plants, and stimulate the growth of plants (Guiwei et al. 2009; Liangyu et al. 2021).

Therefore, the combination of superabsorbent polymers and metal-tolerant plants offers a new prospect for the restoration and remediation of heavy metal-contaminated soils (Tran Quoc Toan et al. 2021). In this research, we present the results of studying the effects of superabsorbent polymers on Pb absorption capacity of Vetiver grass grown on contaminated soil at Trai Cau iron ore dumpsite, Dong Hy district, province Thai Nguyen. Vetiver grass (*Vetiveria zizanioides. L*) is an easy-to-grow plant, appearing commonly in areas after mining (Luu Thai Danh et al. 2009; Ha Xuan Son et al. 2018). Vetiver grass gives high biomass, has the ability to absorb and accumulate heavy metals, and can live in environments polluted by toxic metals. So it has been widely used in the world to stabilize vegetation, and handling heavy metals (Suelee et al. 2017; Truong, P., & Danh, L. T. 2015; Norbert Ondo Zue Abaga et al. 2021).

MATERIALS AND METHODS

Materials

- Superabsorbent polymers (Vietnam): opaque white solids with a water absorption capacity of 350 mL of water per 1 g of polymer.
- HNO_3 solution (Merk)
- $HClO_4$ solution (Merk)
- Experimental soil was taken according to TCVN 7538-2:2005 on soil quality - sampling. Soil samples were taken from the surface layer, with a depth of 0-20cm. Pb-contaminated soil samples were taken at different locations around Trai Cau iron ore mine waste dump, Dong Hy district, Thai Nguyen province. Unpolluted soil samples were taken from a garden in Dong Hy district, Thai Nguyen province. The physicochemical properties and Pb content of the studied soil samples are presented in Table 1, in which the allowed limit of Pb is 70 mg/kg dried soil was demonstrated in accordance to QCVN 03-MT:2015/BTNMT, the Vietnam national technical regulation on the allowable limits of heavy metals in the soils
- Vetiver grass (*Vetiveria zizanioides. L*) was selected as the grass in the period of strong growth (3-4 months old), cut the stem 25 cm long and the root 5 cm long. Grasses are rooted in moist sand for two weeks before planting. Each pot planted three cloves of grass, daily watering for moisturizing to create conditions for the plants to grow well.

Experiments

- Vetiver grasses were grown in Polyethylene (PE) nursery posts with a height of 20cm, a top diameter of 26cm, and a bottom diameter of 22 cm. The experiments were arranged in a completely randomized block design with five treatments, and each of them was replicated three times. The experimental formulas are as follows:

+ Treatment 1 (CT1- Control): Grass was grown on unpolluted soil.

+ Treatment 2 (CT2): Grass was grown on contaminated soil without SAP

+ Treatment 3 (CT3): Grass was grown on contaminated soil with 0.6 g SAP/kg soil

+ Treatment 4 (CT4): Grass was grown on contaminated soil with 0.8 g SAP/kg soil

+ Treatment 5 (CT5): Grass was grown on contaminated soil with 1.0 g SAP/kg soil

- In the treatment using SAP, we mix the soil with a determined amount of SAP.

- Experiment time: from August 15, 2021 to December 15, 2021.

Sample processing method

- Vetiver grass: the grasses after being harvested will be washed, then rinsed with distilled water, separated the leaves and roots, dried at 80oC until completely dry, crushed, and stored in a clean plastic bag with a tight seal for metal analysis.

- Soil sample: After being collected, it is necessary to remove the roots and impurities in the soil, dry it in the air at room temperature, then grind it into small pieces and sieve it through a 1mm sieve. The soil samples were stored in clean plastic bags with a tight seal to determine the chemical composition of the soil.

Analytical methods

a. *Determination of heavy metals in soil and grass samples:* Soil and Vetiver grass samples after being crushed were automatically digested in the Velp DKL. Pb metal contents were analyzed by atomic absorption spectroscopy (AAS) on an Analytik Jena novAA 400P instrument.

Table 1. Some physicochemical properties of the soil samples studied

Soil samples	pH_{KCl}	CEC	OM	Pb concentration	Pb according to QCVN 03-MT:2015/BTNMT
		(meq/100g)	*(%)*	*mg/kg*	*mg/kg*
Unpolluted soil	5.12	11.84	3.12	16.13	
Polluted soil	6.12	7.3	2.03	441.75	70

b. *Determination of Vetiver grass biomass:* After being harvested, the grass was washed, dried, and weighed on a Mettler Toledo analytical balance to determine the weight of leaves and roots of a cluster in grams.

c. *Data processing:* The biomass indicators and analysis results of heavy metal content in soil samples and Vetiver grass were processed using SAS 9.1 software and Excel 2016.

RESULTS AND DISCUSSION

Effect of SAP on Vetiver grass biomass formation

Even though Vetiver grass has the ability to absorb heavy metals not as high as some super-accumulators of heavy metals, Vetiver grass is one of the species that is widely used to treat heavy metal pollution present in the world due to its high biomass and strong regenerative capacity. In this study, the effect of SAP on biomass (weight of stems, leaves, roots) of Vetiver grass grown on lead-contaminated soil is presented in Table 2 - 3. The results showed that after 30 days of planting, the biomass of Vetiver grass was not high because it began to adapt to the new soil environment. Over time, the biomass of grass increased sharply because lead has a positive effect on the growth and development of the grass, helping the number of branches/ clusters, leaf height, length, and biomass higher than the non-polluted soil treatment (CT1). The treatment using SAP for biomass (mass of leaves and roots) was higher than that of CT2 without SAP, in which CT3 gave the highest biomass at 95% statistical significance. SAP has increased the water-holding capacity of the soil, and optimized the metabolism of nutrients in the soil (including heavy metal ions) to help plants grow and develop well with high biomass. In the treatments using SAP with a high content (CT4, CT5), the biomass of grass increased sharply, in which CT5 gave the highest biomass parameters (weight of leaves: 56.14 g/clump, the weight of roots: 23.66 g/clump) compared with formula CT1, CT2 at 95% statistical significance after 120 days of planting.

Effect of SAP on the ability to accumulate Pb in leaves and roots of Vetiver

The ability to accumulate heavy metals in the parts of the Vetiver (stems and roots) is the main route of metal removal from the soil (Ha Xuan Son et al. 2018). The results of determining the ability to accumulate Pb in the leaves and roots of Vetiver over time are presented in Table 4-5.

Table 2. Effect of SAP on Vetiver leaf weight

Treatment	Time			
	30 days	60 days	90 days	120 days
	Leaf weight (g/cluster)	Leaf weight (g/cluster)	Leaf weight (g/cluster)	Leaf weight (g/cluster)
CT1	$10.96^{bc} \pm 1.07$	$17.63^{c} \pm 1.18$	$23.87^{c} \pm 1.69$	$39.52^{c} \pm 1.34$
CT2	$10.42^{c} \pm 1.19$	$19.27b^{c} \pm 1.43$	$28.66^{b} \pm 1.87$	$40.82^{c} \pm 2.09$
CT3	$13.16^{a} \pm 1.11$	$21.15^{b} \pm 1.40$	$33.10^{a} \pm 2.12$	$49.36^{b} \pm 1.27$
CT4	$13.64^{a} \pm 1.26$	$24.70^{a} \pm 1.49$	$34.27^{a} \pm 1.76$	$55.47^{a} \pm 1.50$
CT5	$12.91^{ab} \pm 1.14$	$26.32^{a} \pm 2.18$	$32.45^{a} \pm 1.77$	$56.14^{a} \pm 2.74$
$LSD_{0.05}$	2.09	2.86	3.36	3.02
CV%	9.42	7.20	6.05	3.44

Note: $LSD_{0.05}$ is the smallest statistically significant difference. CV% is the coefficient of variation. The letters a, b, and c are significant differences at the 95% level.

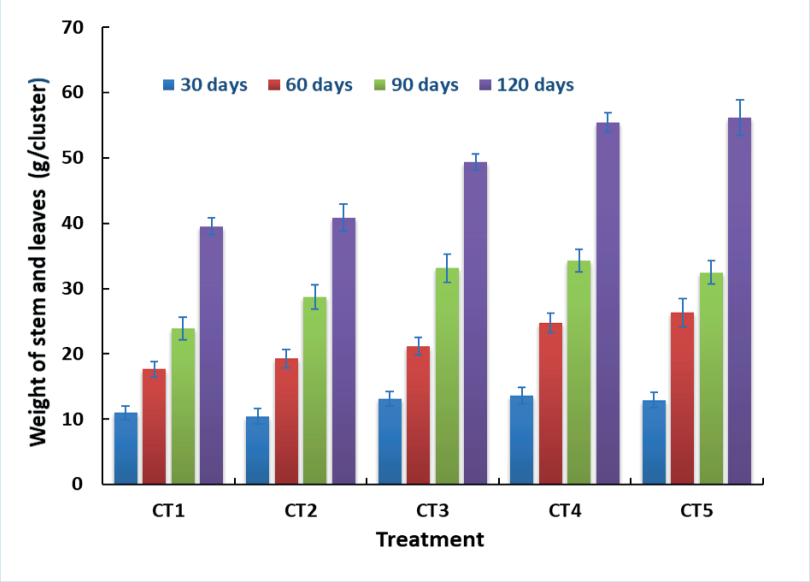

Fig. 1. Effect of SAP on Vetiver leaf weight

Table 3. Effect of SAP on Vetiver root weight

Treatment	Time			
	30 days	60 days	90 days	120 days
	Root weight (g/cluster)	Root weight (g/cluster)	Root weight (g/cluster)	Root weight (g/cluster)
CT1	$3.13^{c}\pm 0.35$	$6.65^{b}\pm 0.85$	$13.66^{b}\pm 1.60$	$20.26^{c}\pm 1.36$
CT2	$3.64^{bc}\pm 0.56$	$7.41^{b}\pm 1.12$	$14.37^{ab}\pm 1.17$	$22.52^{b}\pm 2.42$
CT3	$5.12^{a}\pm 0.55$	$9.56^{a}\pm 1.10$	$17.21^{a}\pm 1.46$	$25.65^{a}\pm 1.96$
CT4	$4.66^{ab}\pm 0.81$	$8.33^{ab}\pm 1.14$	$16.65^{a}\pm 1.53$	$23.73^{a}\pm 1.85$
CT5	$4.27^{abc}\pm 0.76$	$8.25^{ab}\pm 0.86$	$15.87^{ab}\pm 2.04$	$23.66^{a}\pm 1.28$
$LSD_{0.05}$	1.36	1.86	2.88	3.25
CV%	17.89	12.67	10.18	7.72

Note: $LSD_{0.05}$ is the smallest statistically significant difference. CV% is the coefficient of variation. The letters a, b, and c are significant differences at the 95% level.

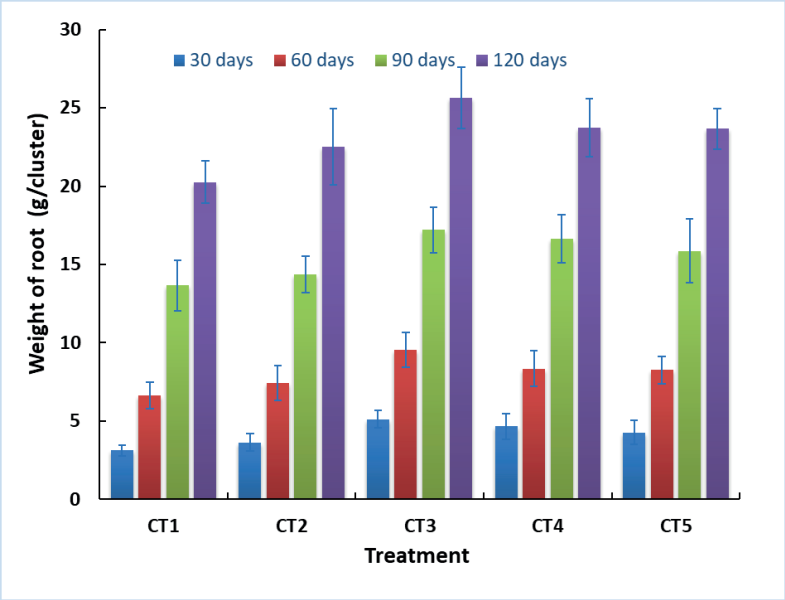

Fig. 2. Effect of SAP on Vetiver root weight

Table 4. Effect of SAP on Pb content in Vetiver leaves (n = 3, mean± SD)

Treatment	Pb content before treatment (mg/kg)	Pb content in leaves after treatment (mg/kg)			
		30 days	60 days	90 days	120 days
CT1	1.03	$1.15^{d}\pm 0.03$	$1.48^{d}\pm 0.04$	$1.86^{d}\pm 0.28$	$2.94^{d}\pm 0.11$
CT2		$4.94^{c}\pm 0.24$	$5.82^{c}\pm 0.32$	$8.91^{c}\pm 0.71$	$14.35^{c}\pm 1.05$
CT3		$6.32^{b}\pm 0.25$	$9.83^{b}\pm 0.35$	$15.82^{b}\pm 1.02$	$21.12^{b}\pm 1.36$
CT4		$8.56^{a}\pm 0.48$	$14.45^{a}\pm 0.55$	$20.35^{a}\pm 1.25$	$26.45^{a}\pm 1.25$
CT5		$9.13^{a}\pm 1.02$	$15.63^{a}\pm 0.93$	$21.55^{a}\pm 1.12$	$27.57^{a}\pm 1.44$
$LSD_{0.05}$		1.16	1.41	1.53	1.71
CV%		10.55	8.20	6.16	5.07

Note: $LSD_{0.05}$ is the smallest statistically significant difference. CV% is the coefficient of variation. The letters a, b, c, and d are significant differences at the 95% level.

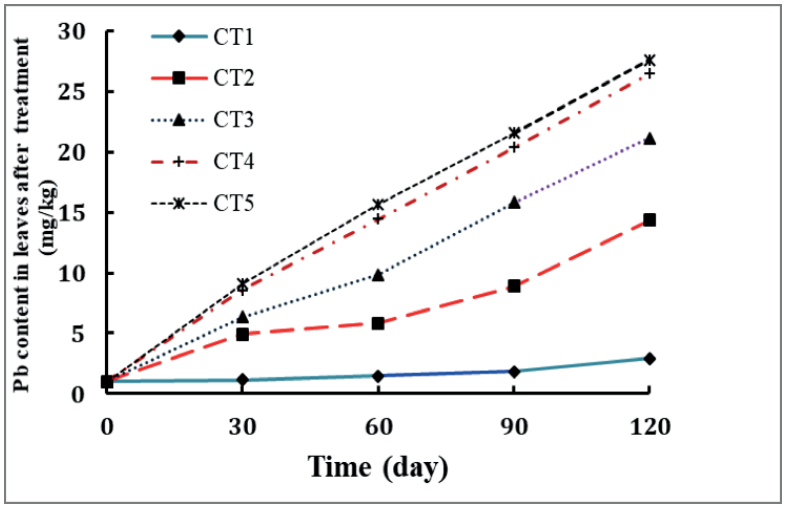

Fig. 3. Effect of SAP on Pb content in Vetiver leaves

Table 5. Effect of SAP on Pb content in Vetiver roots (n = 3, mean± sd)

Treatment	Pb content before treatment (mg/kg)	Pb content in roots after treatment (mg/kg)			
		30 days	60 days	90 days	120 days
CT1	1.98	2.88^{e}± 0.11	4.59^{e}± 0.25	6.62^{e}± 0.22	7.05^{e}± 0.31
CT2		18.78^{d}± 1.24	34.12^{d}± 2.35	53.93^{d}± 2.15	76.64^{d}± 2.85
CT3		39.68^{c}± 1.45	82.17^{c}± 2.67	122.63^{c}± 4.65	134.12^{c}± 5.12
CT4		56.39^{b}± 3.15	113.45^{b}± 5.52	149.62^{b}± 5.52	210.57^{b}± 6.32
CT5		71.25^{a}± 3.18	144.72^{a}± 5.54	186.55^{a}± 6.82	236.44^{a}± 8.25
$LSD_{0.05}$		1.82	2.23	2.55	2.91
CV%		2.65	1.61	1.35	1.20

Note: $LSD_{0.05}$ is the smallest statistically significant difference. CV% is the coefficient of variation. The letters a, b, c, and d are significant differences at the 95% level.

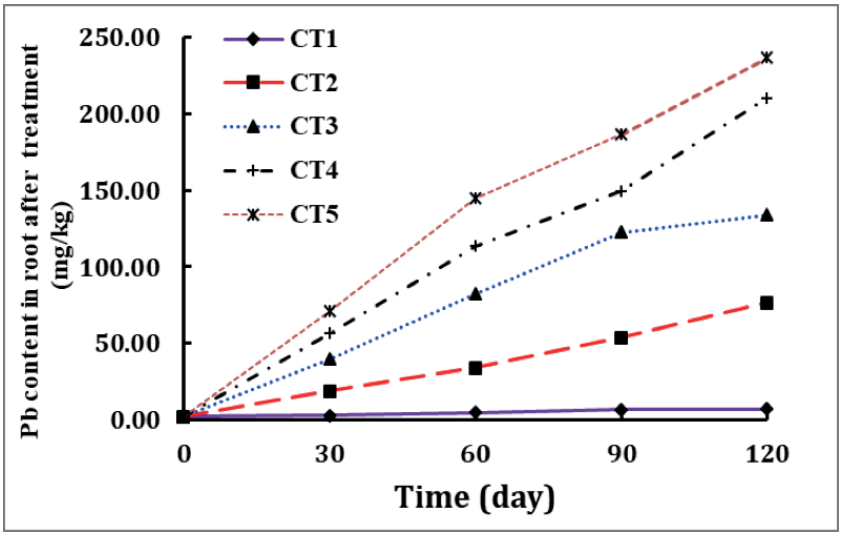

Fig. 4. Effect of SAP on Pb content in Vetiver roots

Research showed that the accumulated Pb content in leaves and roots is proportional to SAP content and experimental time. In the first 30 days, the ability to accumulate Pb of Vetiver grass increased slowly. They increased faster after 90 days of planting, then gradually slowed down in the next 30 days. In the treatments involving using SAP (CT3, CT4, CT5), the ability to accumulate Pb in leaves and roots was much higher than that of CT1 and CT2, in which CT5 gave the highest Pb accumulation value at a statistically significant level. Pb accumulation in grassroots is also proportional to Pb content in soil and experimental time. However, Pb accumulation in roots is much higher than in leaf stems. In CT1 and CT5, after 120 days of planting grass, the accumulated lead content in leaf stems increased by 2.85 times and 26.77 times, respectively, while these numbers in roots subsequently were 3.56 times and 119.41 times.

Table 6. Results of analysis of Pb content in the soil before and after the experiment

Treatment	Pb content before treatment (mg/kg)	Pb content after treatment (mg/kg)			
		30 days	60 days	90 days	120 days
CT2	441.75	387.34[a]± 2.42	298.65[a]± 3.25	225.29[a]± 4.15	132.13[a]± 2.16
CT3		345.23[b]± 6.25	236.71[b]± 5.52	175.10[b]± 3.62	119.65[b]± 2.31
CT4		305.67[c]± 4.55	216.54[c]± 4.72	152.83[c]± 3.85	100.42[c]± 3.15
CT5		286.80[d]± 5.10	193.25[d]± 5.15	141.64[d]± 2.84	97.34[c]± 2.10
$LSD_{0,05}$		7.74	7.05	6.52	5.80
CV%		1.24	1.58	1.99	2.74

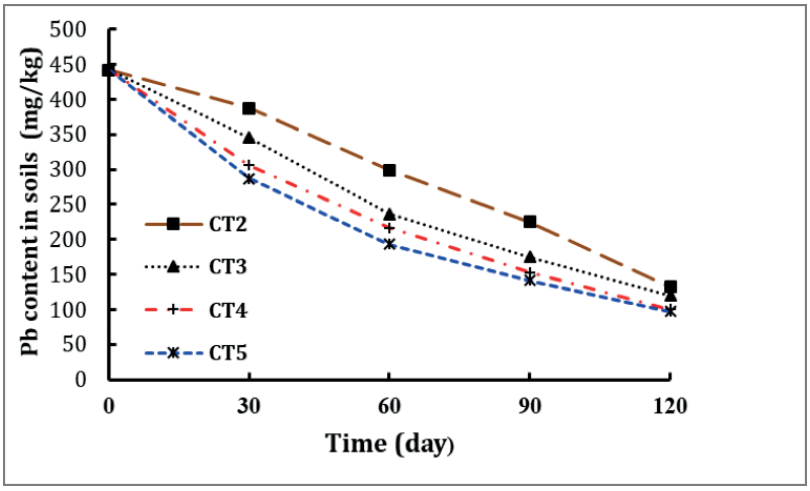

Fig. 5. Pb content in the soil before and after the experiments

Research results demonstrate that Pb first accumulated in the roots and then transported to the leaves. The higher the Pb content in the soil, the more Pb was accumulated in the plant parts. Vetiver grass not only can grow and develop well in soil contaminated with Pb, but also has the ability to absorb and accumulate Pb in its biomass. The results of this study are consistent with those of other authors (Luu Thai Danh et al. 2009; Ha Xuan Son et al. 2018).

Effect of SAP on the change of Pb content in the soil before and after the experiment

The results in Table 6 show that the Pb content in contaminated soil (CT2-CT5) tended to decrease sharply after 120 days of growing Vetiver grass in all experimental treatments, in which the formulas used SAP showed a faster decrease in Pb content compared to CT2. When combining Vetiver with SAP, the efficiency of Pb removal in contaminated soil is higher than when using Vetiver alone. After 120 days of planting Vetiver grass, the ability to treat Pb in the soil reached its highest in CT4 and CT5. However, there is no statistical difference between CT4 and CT5 at the 95% confidence level. This can be explained because SAP has increased the water-holding capacity of the soil, reduced the toxicity of metals to plants, and stimulated the growth and development of plants, thus increasing the tolerance and Pb uptake.

CONCLUSION

Vetiver grass can tolerate and grow on lead-contaminated soils due to mining activities. Vetiver grass demonstrates the ability to uptake and accumulate Pb in its leaves and roots. The amount of uptake and accumulated Pb in the biomass of Vetiver grass is directly proportional to SAP content and Pb content in the soil as well as experimental time.

Better Pb treatment efficiency was observed in the treatment with the SAP supplement than in the one without it. The presented data have also proved that SAP increased the tolerance and Pb absorption capacity of Vetiver grass after 120 days of planting. The highest Pb treatment efficiency and fastest Pb removal from contaminated soil were obtained when adding SAP with the content from 0.8-1.0 g/kg soil.

The results of this study show the high feasibility of removing Pb in contaminated soil with a combination of plants and superabsorbent polymers. It is a promising and "green" solution that can be applied not only for Pb but also for other heavy metals in polluted soil.

REFERENCES

Amadi C.N., Igweze Z.N., Orisakwe O.E. (2017). Heavy metals in miscarriages and stillbirths in developing nations. Middle East Fertility Soc J, 22, 91-100.

Amjad Ali, Di Guo, Amanullah Mahar, Wang Ping, Fazli Wahid, Feng Shen, Ronghua Li, Zengqiang Zhang. (2017). Phytoextraction and the economic perspective of phytomining of heavy metals. Solid Earth Discussions, 75, 3-13, DOI:10.5194/SE-2017-75.

Bikash Debnath, Waikhom Somraj Singh, Kuntal Manna. (2019). Sources and Toxicological Effects of Lead on Human Health. Indian Journal of Medical Specialities, June 4.

Bouzid Nedjimi (2021). Phytoremediation: a sustainable environmental technology for heavy metals decontamination. SN Applied Sciences, 3, 286, DOI: 10.1007/s42452-021-04301-4.

Bui Thi Kim Anh, Dang Dinh Kim, Tran Van Tua, Nguyen Trung Kien, Do Tuan Anh. (2011). Phytoremediation potential of indigenous plants from Thai Nguyen province, Vietnam. J. Environ. Biol, 32, 257-262.

Dang V.M., Bui T.H., Dao V.N. and Nguyen D.H. (2011). Evaluation of soil quality after mining in Thai Nguyen province. Vietnam Soil Science Journal, 36, 153-157.

Forte J., Mutiti S. (2017). Phytoremediation Potential of Helianthus annuus and Hydrangea paniculata in Copper and Lead-Contaminated Soil. Water Air Soil Pollut, 228, 77, DOI:10.1007/s11270-017-3249-0.

Guiwei Qu, Amarilis de Varennes & C. Cunha-Queda. (2008). Remediation of a mine soil with insoluble polyacrylate polymers enhances soil quality and plant growth. Soil Use and Management, 25, 350-356, DOI: 10.1111/j.1475-2743.2008.00173.x.

Guiwei Qu, Amarilis de Varennes. (2009). Use of Hydrophilic Insoluble Polymers in the Restoration of Metal – Contaminated Soils. Applied and Environmental Soil Science, 1-8, DOI: 10.1155/2009/790687.

Ha Xuan Son, Nguyen Thi Kim Ngan, Le Duc Manh, Dang Van Thanh, Do Tra Huong, Ha Xuan Linh. (2018). Study using Vetiver (Vetiveria Zizanioides (L.) Nash), Ferns (Marattiopsida (P. Calomelanos) Pteris Vittata L and Eleusine Indica (L.) Gaertn treatment of the lead (Pb) contamination in soil around the lead and zinc mine of Hich Village, Dong Hy district, Thai Nguyen province. TNU Journal of Science and Technology, 185(09), 111-116.

Haq S., Bhatti A. A., Dar Z. A. and Bhat S. A. (2020). Phytoremediation of Heavy Metals: An Eco-Friendly and Sustainable Approach. Bioremediation and Biotechnology, Chapter 10, 215 - 226.

Hong-Giang Hoang, Tzung-Yuh Yeh, Chitsan Lin. (2018). Overview of Integrated Phytoremediation for HeavyMetals Contaminated Soil. Sustainable Forestry, Volume 1, DOI: 10.24294/sf. v1i4.931.

Indah Lestari, Tri Edhi Budhi Soesilo, and Haruki Agustina. (2018). The Effects of Lead Contamination in Public Health Case: Pesarean Village, Tegal District, Indonesia. E3S Web of Conferences, 68, 03012.

Kumar G.H., Kumari J.P. (2015). Heavy metal lead influative toxicity and its assessment in phytoremediating plants – A review. Water Air Soil Pollut, 226, 324.

Lambert M., Leven B.A., Green and R.M. (2011). New Methods of Cleaning Up Heavy Metal in Soils and Water. Environmental Science and Technology briefs for citizens, 1-3.

Liangyu Chang, Liju Xu, Yaohu Liu, Dong Qiu. (2021). Superabsorbent polymers used for agricultural water retention. Polymer Testing, 94, 1-7, DOI: 10.1016/j.polymertesting.2020.107021.

Liuwei Wang, Jörg Rinklebe, Filip M. G. Tack, Deyi Hou. (2021). A review of green remediation strategies for heavy metal contaminated soil. Soil Use and Management, 37(4), 1-28, DOI: 10.1111/sum.12717.

Luq man Ali Shah, Majid Khan, Rida Javed, Murtaza Sayed, Muhammad Saleem Khan, Abbas Khan, Mohib Ullah. (2018). Superabsorbent polymer hydrogels with good thermal and mechanical properties for removal of selected heavy metal ions. Journal of Cleaner Production, 201, 78-87.

Luu Thai Danh, Paul Truong, Raffaella Mammucari, Tam Tran, Neil Foster. (2009). Vetiver grass, Vetiveria zizanioides: A choice plant for phytoremediation of heavy metals and organic wastes. International Journal of Phytoremediation, 11(8), 664-691, DOI: 10.1080/15226510902787302.

Mohammad J., Zohuriaan-Mehr and Kourosh Kabiri. (2008). Superabsorbent Polymer Materials: A Review. Iranian Polymer Journal, 17(6), 451-477.

Nan Lu, Gang Li, Yingying Sun, Yang Wei, Lirong He and Yan Li. (2021). Phytoremediation Potential of Four Native Plants in Soils Contaminated with Lead in a Mining Area. Land, 10, 1129

Nicolae Cioica, Cătălina Tudora, Dorin Iuga, György Deak, Monica Matei, Elena Mihaela Nagy, and Zoltan Gyorgy. (2019). A review on phytoremediation as an ecological method for in situ clean up of heavy metals contaminated soils. E3S Web of Conferences, 112(4), 03024, DOI: 10.1051/e3sconf/201911203024.

Norbert Ondo Zue Abaga, Sylvie Dousset, Colette Munier-Lamy. (2021). Phytoremediation Potential of Vetiver Grass (Vetiveria Zizanioides) in Two Mixed Heavy Metal Contaminated Soils from the Zoundweogo and Boulkiemde Regions of Burkina Faso (West Africa). Journal of Geoscience and Environment Protection, 9(11), 73-88, DOI: 10.4236/gep.2021.911006.

Pal M., Sachdeva M., Gupta N., Mishra P., Yadav M., Tiwari A. (2015). Lead exposure in different organs of mammals and prevention by curcumin-nanocurcumin: A review. Biol Trace Elem Res, 168, 380-391.

Rama Karna, Nishita Ojha, Sadiqa Abbas, Sonal Bhugra. (2021). A review on heavy metal contamination at mining sites and remedial techniques. IOP Conf. Series: Earth and Environmental Science, 796, 012013, DOI: 10.1088/1755-1315/796/1/012013.

Rodrick Hamvumba, Mebelo Mataa & Alice Mutiti Mweetwa. (2014). Evaluation of Sunflower (Helianthus annuus L.), Sorghum (Sorghum bicolor L.) and Chinese Cabbage (Brassica chinensis) for Phytoremediation of Lead Contaminated Soils. Environment and Pollution, 3(2), DOI: 10.5539/ep.v3n2p65.

Sarwar N., Imran M., Shaheen M.R., Ishaque W., Kamran M.A., Matloob A., Rehim A., Hussain S. (2017). Phytoremediation strategies for soils contaminated with heavy metals: Modifications and future perspectives. Chemosphere, 171, 710-721.

Shah V., Daverey A. (2020). Phytoremediation: A multidisciplinary approach to clean up heavy metal contaminated soil. Environ Technol Innov, 18, 100774.

Suelee A.L., Hasan S.N.M.S., Kusin F.M., Yusuff F.M., & Ibrahim Z.Z. (2017). Phytoremediation Potential of Vetiver Grass (Vetiveria zizanioides) for Treatment of Metal-Contaminated Water. Water Air and Soil Pollution, 228(4), 158, DOI: 10.1007/s11270-017-3349-x.

Takashi Fujimori, Akifumi Eguchi, Tetsuro Agusa, Nguyen Minh Tue, Go Suzuki, Shin Takahashi, Pham Hung Viet, Shinsuke Tanabe. (2016). Lead contamination in surface soil on roads from used lead-acid battery recycling in Dong Mai, Northern Vietnam. Journal of Material Cycles and Waste Management, 18(4), 599-607, DOI: 10.1007/s10163-016-0527-7.

Tran Thi Pha, Dang Van Minh, Dam Xuan Van and Le Duc. (2014). Growth and Absorbance of Heavy metals of reed plants (phragmites australis) in soil after mineral mining in Thai Nguyen province of Viet Nam. ARPN Journal of Agricultural and Biological Science, 9(8), August 2014.

Tran Quoc Toan, Nguyen Thi Yen, Nguyen Quoc Dung, Tran Thi Hue, Nguyen Thanh Tung, Nguyen Trung Duc, Vu Thi Thuy, Nguyen Xuan Hoa, Dang Van Thanh. (2021). Effects of Superabsorbent Polymers AMS-1 on Cadmium Absorption of Vetivers grown on contaminated soils. Journal of Analytical Sciences, 26(4B), 151-156.

Truong P., & Danh L.T. (2015). The Vetiver System for Improving Water Quality: Prevention and Treatment of Contaminated Water and Land (2nd ed.). The Vetiver Network International. https://www.vetiver.org/TVN_Water_quality%202%20ed.pdf.

Zahra Derakhshan Nejad Myung Chae Jung, Ki-Hyun Kim. (2018). Remediation of soils contaminated with heavy metals with an emphasis on immobilization technology. Environ Geochem Health, 40(3), 927-953, DOI: 10.1007/s10653-017-9964-z.

RESEARCH PAPER

ASSESSMENT OF ANTHROPOGENIC IMPACT ON FOREST ECOSYSTEM: A CASE STUDY OF KUMBHALGARH WILDLIFE SANCTUARY, INDIA

Bhanwar Vishvendra Raj Singh[1*], Anjan Sen[2], Ravi Mishra[1], Ritika Prasad[3]

[1]Department of Geography, Faculty of Earth sciences, Mohanlal Sukhadia University, Udaipur-313001, India,
[2]Department of Geography, Delhi School of Economics, University of Delhi, Delhi-110007, India,
[3]Department of Geography, University of Lucknow-226,007, India
***Corresponding author:** bhanwarsa28@gmail.com

Received: April 5th, 2022 / Accepted: November 11th, 2022 / Published: December 31st, 2022
https://DOI-10.24057/2071-9388-2022-047

ABSTRACT. In the era of the modern world, natural resources are continuously diminishing and simultaneously the human population is also increasing, which is alarming for the present and future world. Global biodiversity is playing a pivotal role in all ecosystem services, meanwhile, anthropogenic activities and encroachment are the main drivers for the widespread loss of local biodiversity. In India, Kumbhalgarh Wildlife Sanctuary is situated in the world's oldest Aravali Mountain range. Near protected areas of this wildlife sanctuary have an entire concentration of rural populations, which are interdependence with this forest ecosystem. The key objective of the research study is to measure the anthropogenic impact on Kumbhalgarh Wildlife Sanctuary. It's a micro-level study based on primary and secondary data through GIS mapping as well as Socio-Economic & Physical factors to inter-connect with forest habitats. Especially, core and periphery LULC have been obtained from the Multispectral images from ETM+ and OLI sensors of Landsat satellites. This study examines the spatial and temporal patterns of LULC change along the boundary of Kumbhalgarh from 2000 to 2020. The research also describes land use and land cover pattern, forest cover and vegetation index, and human encroachment, Eventually, the situation would be alarming for the local biodiversity and habitat due to the high pressure of anthropogenic activities and encroachment.

KEYWORDS: Forest Ecosystem; Forest Cover; Land use and land cover; Biodiversity Conservation

CITATION: Bhanwar V. R. Singh, Anjan Sen, Ravi Mishra, Ritika Prasad (2023). Assessment Of Anthropogenic Impact On Forest Ecosystem: A Case Study Of Kumbhalgarh Wildlife Sanctuary, India. Geography, Environment, Sustainability, 1(16), 189-199
https://DOI-10.24057/2071-9388-2022-047

ACKNOWLEDGEMENTS: It is my proud privilege to release the emotions of gratitude to many persons who helped me directly or indirectly to conduct this scientific research work. I express my heart full indebt Ness and owe a deep sense of gratitude to my colleagues and my well-wishers for their encouragement. I am extremely thankful to Prof. R B Singh, Prof. Anjan Sen, Mr. Ravi Mishra, Ritika Prasad, and every member of my life for their sincere guidance and inspiration in completing this project. I also thank all my friends who have more or less contributed to the preparation of this project report. I will be able to be always indebted to them. The Kumbhalgarh Wildlife Sanctuary has a diversity of biodiversity resources which is the source of the development of flora and fauna in the region. With the passage of time people's trends are also changing and they are becoming the most dangerous source of degradation of the forest ecosystem. The results of the study emphasized that a thorough and comprehensive approach can reduce anthropogenic pressure by increasing the use of eco-friendly techniques and raising the awareness level of local people. The study has indeed helped me to explore more knowledgeable avenues associated with my topic and I am sure it'll help me to grow more in the future.

Conflict of interests: The authors reported no potential conflict of interest.

INTRODUCTION

The man-environment relationship is interconnected from the beginning of human civilization. From the Palaeolithic to the modern technological age relationship has been changed. Then, man was depended on their adjacent environment for food, water, and shelter with eco-friendly behaviours. Now, the sustainability of the environment is reliant on humans and the risk of survival of humankind is emerging with environmental degradation (UNEP 2014; Akpan et al. 2010).

There are several natural and artificial phenomena occurring on a global to local scale such as climate change, environmental degradation, deforestation, overpopulation, genetic engineering, pollution, resources depletion, industrialization, urbanization, etc. The earth is facing high rates of biodiversity loss and corrosion which are escorted by ecosystem degradation. It's impacting human well-being through the loss of benefits ("ecosystem services") that ecosystems provide (Bhagabati et al. 2014). As a result, degradation, fragmentation, and loss of natural habitats (Hososuma et al. 2005), depletion of prey animals, and poaching to supply a large illegal global trade in their body

parts have pushed wild animals and their landscapes to the brink of extinction. These threats are exacerbated by the limited capacity for conservation action. Anthropogenic activities are major threats to providing various forest ecosystem services to people (Millennium Ecosystem Assessment (MA) 2005).

People derive direct and indirect benefits from forest ecosystem services in terms of support, provision, regulation and cultural services (Benzes et al. 2020; Manning et al. 2018). But cultural services are the strongest of them all. The increasing demand for these services has put enormous pressure on the forest ecosystem, and in such a scenario, eco-tourism is another additional stress (Holting et al. 2019). Meanwhile, conservation of forests has numerous advantages viz. promotion of cultural services, increase in carbon storage and sequestration, reduction in greenhouse gasses emission (Houghton, 2012; Ravindranath, 2008; Asner et al. 2010), watershed protection, natural hazard regulation, sustaining food security and cultivation services, improvement of medical services and ecotourism (Sierra et al. 2013; Wasserstrom et al. 2013; Fagua et al. 2019; Foley et al. 2007). Therefore, the forest ecosystem services defiantly mitigate climate change such as conserving the habitat, water quality, quality of life, global carbon cycle, economic growth, demographics, agriculture, and forest products, regional and planning policies through sustainable practices (FAO, Global Forest Resources Assessment, 2020; Kissinger et al. 2012).

Across the world, the forest ecosystem is rapidly decreasing due to the greediness of humans. Various species of flora and fauna have been extinct and various are near threatened. There is a positive correlation between population growth and decreasing forests (Corvalan et al. 2005; McMichael 2013). Global to local scale, humans use forests to fulfill the demand for commercial and household goods and services (Thomas et al. 2006; He GM et al. 2009; Salerno et al. 2010; Swanson et al. 2011; Pan et al. 2012).

India is a treasure trove of different vegetation and fauna. There was a blistering decline in the figures of numerous species. Severe reductions in flora and fauna can be get ecological imbalances, affecting numerous aspects of the climate and ecosystem. The most recent exertion in this regard passed during the British period was the Protection of Wild Birds and creatures, 1935. This demanded to be upgraded because the corrections given to nimrods and dealers of wildlife products weren't in proportion to the huge fiscal benefits they entered. Before the enactment of this Act, there were only five public premises in India.

The Act also provides for the protection of a listed species of creatures, catcalls, and shops and also for the establishment of a network of ecologically important defended areas in the country. For the first time, a comprehensive list of exposed wildlife in the country was prepared. The act banned the stalking of exposed species. Trade in listed creatures is banned as per the vittles of the Act. The Act provides for licenses for the trade, transfer, and possession of certain wildlife species. It provides for the establishment of wildlife sanctuaries, public premises, etc (Wildlife Protection Act 1972).

Wildlife Sanctuaries are present areas where species are protected against poaching, hunting, and hunting. Here animals don't seem to be reared for commercial exploitation. The species is shielded from any disturbance. Catching or killing of animals isn't allowed inside the sanctuaries. A wildlife sanctuary is said by the government by a notification. The boundaries are often changed by a resolution of the state legislature. Human activities like timber harvesting, the gathering of minor forest products, and personal ownership rights are permitted as long as they are doing not interfere with the well-being of the animals. Limited act is permitted. they're hospitable the overall public. But people aren't allowed without protection. There are restrictions on who can enter and/or reside within the bounds of the sanctuary. Only public servants, persons having immovable property inside, etc. are allowed. People using the highways passing through the sanctuaries also are allowed inside (Wildlife Protection Act, 1972).

MATERIALS AND METHODS

Study Area

The Kumbhalgarh Wildlife Sanctuary is chosen as the study area (Fig. 1). It is situated in the most fragile ecosystem of the world's oldest mountain range Aravali, Rajasthan, India. It is 80k.m. in the North of the world's famous tourist city Udaipur. Geographically this sanctuary is located between 25^0 North to 25^{0}40′ North Latitudes and 73^{0}2′ East to 73^{0}30′ East Longitude. The core area of the sanctuary is 610.528 Sq. km.

The Sanctuary was a natural tiger habitat till 70s and declared as wildlife sanctuary in 1988 (RajRAS. 2019). The sanctuary is spread over the entire Aravalli range covering parts of the Rajsamand, Udaipur, and Pali districts, at an altitude of 500 to 1,300 meters (1,600 to 4,300 ft). It is part of the Khathiyar-Gir dry deciduous forests ecoregion. It is named after the impressive historical fort of Kumbhalgarh. The wildlife sanctuary covers a core area of 224.890 km (87 sq. mi) and a buffer area of 385.638 km (149 sq. mi). It includes the four hills and mountain ranges of the Aravallis: The Kumbhalgarh Range; Sadri Range; Desuri Range and Bokhada Range. Twenty-two villages are located inside the sanctuary. The soil in this area is generally thin, mostly sandy loam (Bohra & Sultana 2013).

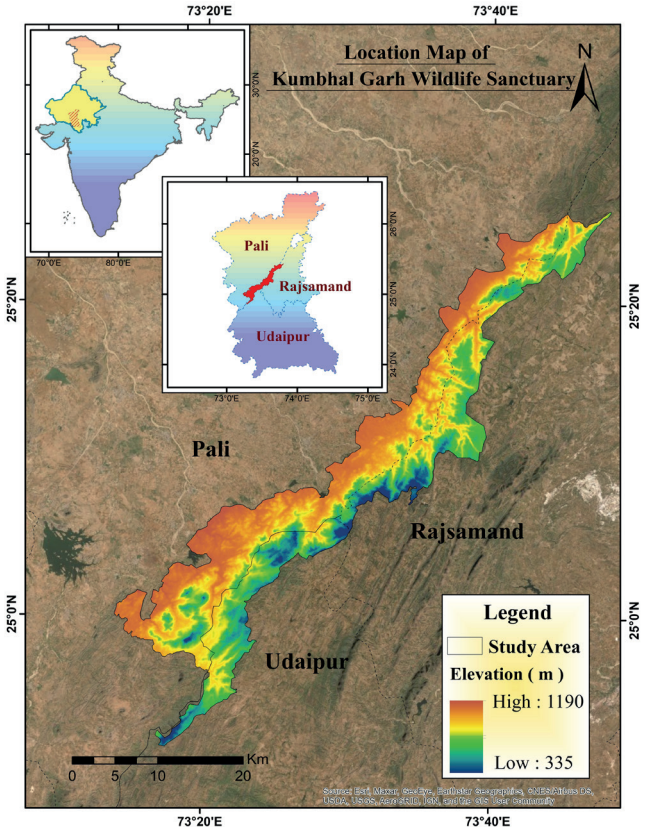

Fig. 1. Kumbhalgarh Wildlife Sanctuary (Source: DFO Office, Rajsamand 2019)

The natural environment of Kumbhalgarh is very attractive and captivating as well as this sanctuary is home to a variety of wildlife, some of which are endangered species. The wildlife found here includes the Indian wolf, Indian leopard, sloth bear, striped hyena, golden jackal, wild cat, sambar, nilgai, chausingha (four-horned antelope), chinkara, and Indian hare. The leopard is the supreme predator in the sanctuary (Bohra & Sultana 2013). The birds of Kumbhalgarh include the normally shy and unreliable gray wildebeest. Peacocks and pigeons can also be often seen here. Birds like the red bird, parrot, golden oriole, gray pigeon, bulbul, pigeon, and white-breasted kingfisher are also seen near the water holes. Kumbalgarh Sanctuary was one of the places which were considered for the reproduction of the Asiatic lions (BOHRA 2013). Biodiversity flourishing in this sanctuary is moderate and the status of threatened species in different blocks is also moderate. Central and Southern parts of the sanctuary have a high level of anthropogenic disturbance (FES report 2010). In this research, the prime objective was to assess the anthropogenic pressure on the forest ecosystem of the Kumbhalgarh Wildlife Sanctuary. The result shows that anthropogenic pressure is chronically changing. The South and south-west part of the sanctuary has maximum anthropogenic pressure due to the maximum population in this area but the dependency on forest resources of these people is decreasing because of the availability of alternative resources which is a good indicator for this sanctuary. The climate of this sanctuary is sub-tropical with extremely hot summer and relatively moderate winter. The three main seasons is summer, winter, and rainy season. The average rainfall is 752 mm. The number of rainy days is approx. 25 on average. The highest rainfall was observed in July (Chhangani 2002).

Dataset and Methodology

The methodology is presented on the Fig. 2

Dataset

The satellite images were sorted and classified for analysis and interpretation. Landsat images are among the widely used satellite remote sensing data and their spectral, spatial, and temporal resolution made them useful input for mapping and planning projects (Singh and Sen 2018). Landsat Thematic Mapper 5 and 8 were used for land use and land cover classification in 2000, 2010, and 2020. Landsat-5 was used for the years 2000 and the year 2010 and 2020 Landsat-8 was used. The resolution of both datasets is 30m. These datasets were downloaded from the USGS (United States Geological Survey) site. For the calculating height of the study area, SRTM DEM was used at a resolution of 30m. For data preparation, Erdas Imagine and ArcGIS software were used. Satellite data sets were imported into the ERDAS Imagine software to create a false-colour composite (FCC). The FCC images were layer-

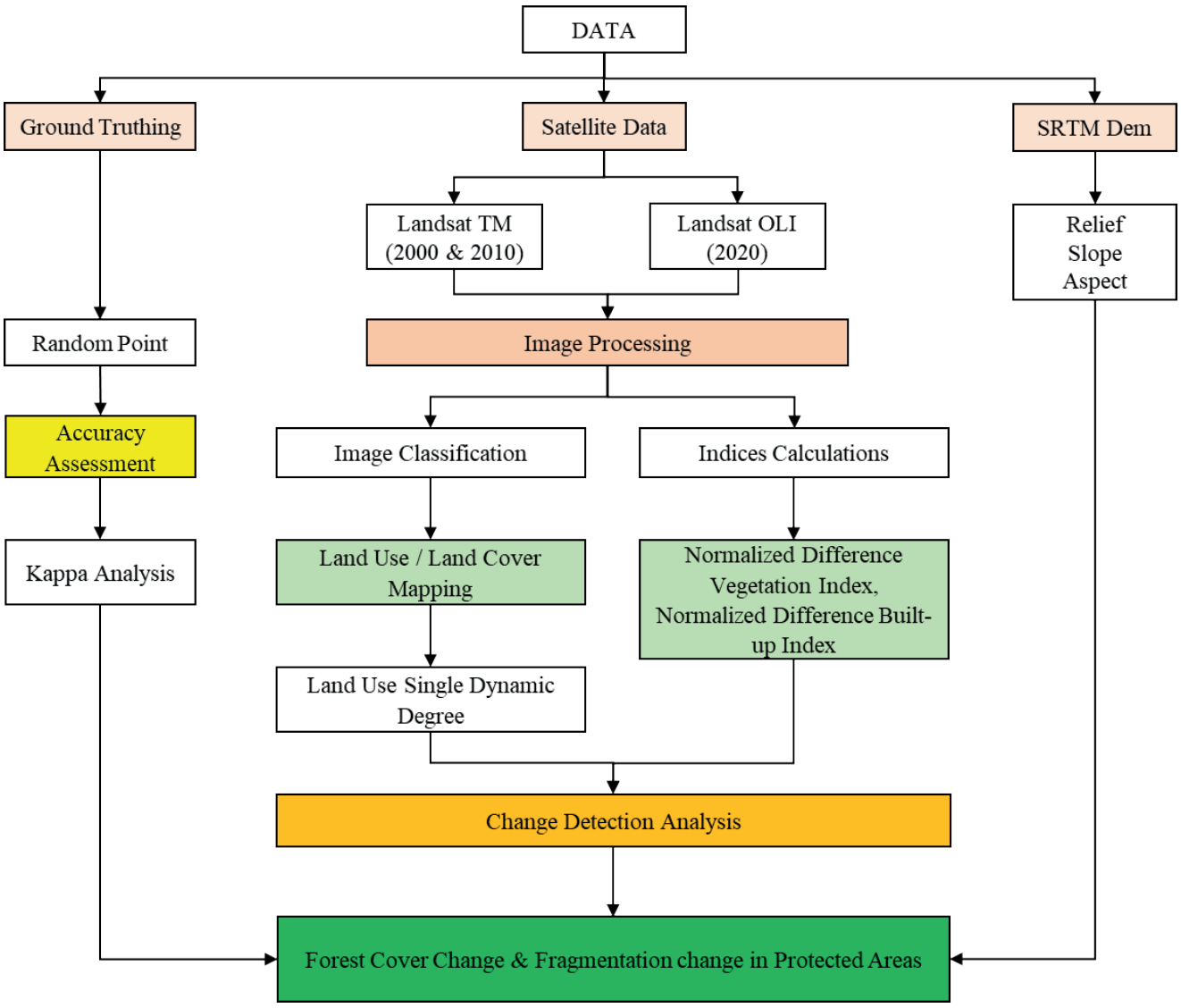

Fig. 2. Research Methodology Chart

stacked and then all data sets were mosaicked. Other work and analysis were done using Arc GIS software using geo-referenced shapefiles of the study area collected from the DFO Office, Rajsamand, 2019.

Land use and land cover change analysis

Supervised Classification: To analyse the land use and land cover change of the Kumbhalgarh Wildlife Sanctuary, a Supervised classification method was applied in the ERDAS imagine software. This classification method is used Maximum Likelihood Classifier algorithm (Singh and Sen, 2018; Singh et.al., 2021). The images were classified into 7 respective classes (Table 1).

Calculation of the Accuracy Assessment or Error Matrix: Accuracy Assessment is an important part of any classification project. Accuracy Assessment or error matrix compares the classified image to the ground truth data. For calculating the Accuracy of the classified image create a set of random points and these points are verified in a Google Earth computer program.

Kappa Coefficient: Kappa Coefficient essentially evaluates how well the classification performed as compared to the randomly assigned values. The Kappa Coefficient ranges from -1 to 1. A value of 0 indicates that the classification is no better than a random classification. A negative value signifies that the classification is worse than random. If the value is close to 1 then the classification is signified classification is better than random. This is defined by the small "k" (1).
This is calculated as:

$$k = \frac{OA - AC}{1 - AC} \quad (1)$$

Here, k = kappa coefficient, OA= Overall accuracy, AC= Expected by chance agreement,
1 = Constant value

Create Random Point: After classifying all the images, create an equalized random point in the Arc GIS and then these points are saved as a KML (Keyhole Markup Language) layer to collect the ground-truth value of all classified imageries with the help of Google Earth.

Table 1. Description of the land use and land cover

Land use/land cover class	Description
Water Bodies	Includes the rivers, ponds, streams, etc.
Fellow Land	all piece of land that is normally covered with vegetation but that is left with no crops on it for a season
Barren Land	Includes the Barren Land and Hilly Area.
Arable Land	Agriculture Land, Sown area
Sparse Vegetation	Includes the all-small plants, grassland, and shrubs.
Dense Vegetation	Includes the areas which are covered by the trees.
Settlement	Includes the areas of construction, roads, bridges, houses, etc.

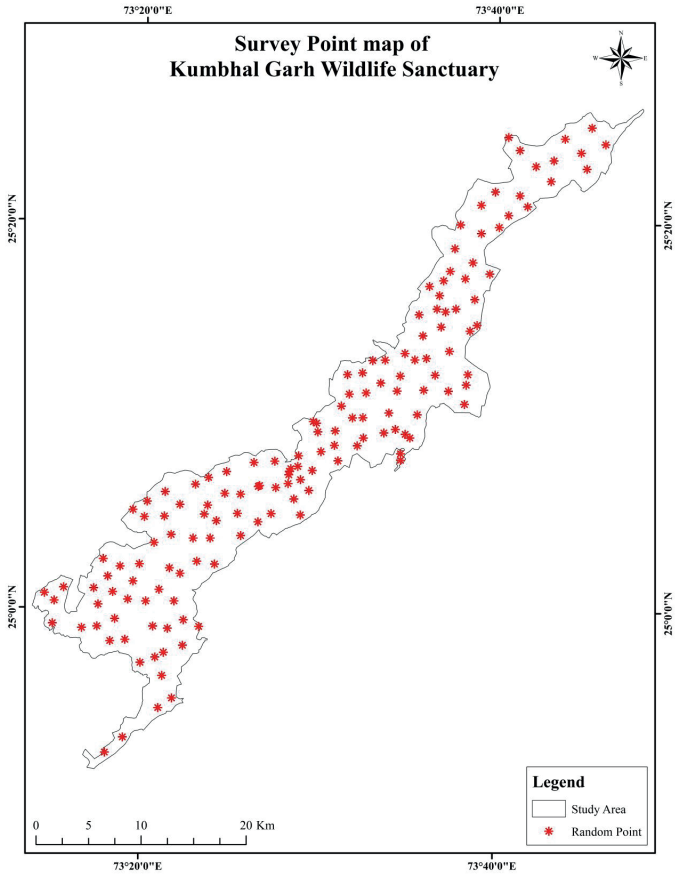

Fig. 3. Random Points

Single Land uses dynamic degree: The Single Land Use Dynamic Degree Index has been chosen for this study to measure the temporal and spatially changing characteristics of land use. The dynamic degree of land use refers to the total amount of changes in certain types of land use over a given period in the study area (Hong-zhi, et al. 2002).

This can be calculated as:

$$LC(K) = \frac{u_b - u_a}{u_a} \times \frac{1}{T} \times 100\% \quad (2)$$

In this formula, u_b is the area of a certain land use category at the last year of the research period, and u_a, is the area of a certain land-use type at the initial year of the research period. T is the length of the research period respectively (2). LC represents the dynamic degree of certain types of land use within the study period or at one time.

Built-up Index Indices: Normalized Difference Built-up Index (NDBI) is used to extract the built-up features and it ranges from +1 to -1. It is calculated by formula (3):

$$NDBI = (SWIR - NIR)/(SWIR + NIR) \quad (3)$$

Here, SWIR is Short Wave Infrared and NIR is Near Infrared

Normalized Vegetation Index: Normalized Difference Vegetation Index (NDVI) is calculated from the visible and near-infrared light reflected by vegetation. Healthy vegetation absorbs most of the visible light that hits it and reflects a large portion of the near-infrared light. Unhealthy or sparse vegetation reflects more visible light and less near-infrared light (earthobservatory.nasa.gov). The NDVI values lie between 1 to -1.

The formula of NDVI is:

$$NDBI = \frac{(Near\ Infrared) - (Red\ Band)}{(Near\ Infrared) + (Red\ Band)} \quad (4)$$

Weighted Overlay Analysis: The weighted overlay is a standard GIS analysis technique that is often used for solving multi-criteria problems such as generating surfaces representing site suitability and travel cost. The weighted overlay is used when several factors of varying importance should be considered to arrive at a final decision (Singh et.al., 2021).

Weighted overlay is calculated by (5):

$$*Weighted\ Overlay = LULC(25) + NDVI(45) + NDBI(30)... \quad (5)$$

Three input Rasters have been reclassified to a common measurement scale of 1 to 3 for the Study area (Fig. 8a, b, c). Each raster is assigned a percentage influence. The cell values are increased by their proportion effect, and the results are added composed to create the output raster.

RESULTS

Terrain Maps: By using SRTM Dem data, these terrain maps are created in Geospatial Software. A slope map provides a colorized representation of the slope (Fig. 4a). The degree of slope steepness is depicted by light to dark color - flat surfaces as green, shallow slopes as yellow, moderate slopes as light orange, and steep slopes as Red. An aspect-slope map instantaneously displays the aspect (direction) and degree (sharpness) of slope for a topography (or another continuous surface) (Fig. 4b). Relief maps depict the contours of landmarks and terrain, based on shape and height (Fig. 4c).

Land use /Land cover change analysis: The land use and land cover (LULC) of the Study Area has been slightly changed by anthropogenic pressure, deforestation, agricultural and subsidiary activities, and unplanned or unprofessional slope cutting for infrastructure developments (Fig. 5). In agricultural areas and grassland found in areas of high population density, especially along economic corridors, soil degradation has increased in low lands areas.

From 2000 to 2020 all the land use/ land cover types are changed dynamically. Fellow Land and Barren Land was Dramatically decreased in the 2000 - 2010 period and again increased in 2020. In 2000, Fellow Land and Barren land covered an area of about 19263.15 Hectares and 7455.18 Hectares but it decreased in 2010 by 387.54 and 2226.29 Hectares. The total area of Barren land again increased to 1637.64 and 5382.26 Hectares in 2020. Settlement was increased over the past 20 years but it's quite low. In 2000, 7.62 Hectares areas were covered by Settlement and it increased in 2010 by 27.13 hectares and 95.68 Hectares in 2020. On the other hand, the Sparse and Dense Vegetation area increased in the 2000-2010 period and slightly decreased in the recent decade. In 2000, Sparse and Dense Vegetation covered an area of 9396.90 Hectare and 1905.30 Hectare but it increased by 23427.54 and 22613.4 Hectare in 2010 and again its slight decreases in 2020, by 21332.16- and 12027.69-Hectare area. Arable land has covered 19737.27 Hectare areas in 2000 and was decreased in 2010 by 8953.65 Hectare but again it increased in 2020 and covered an area of 17043.66 Hectare due to decreasing Vegetation cover in the recent period (Table 2).

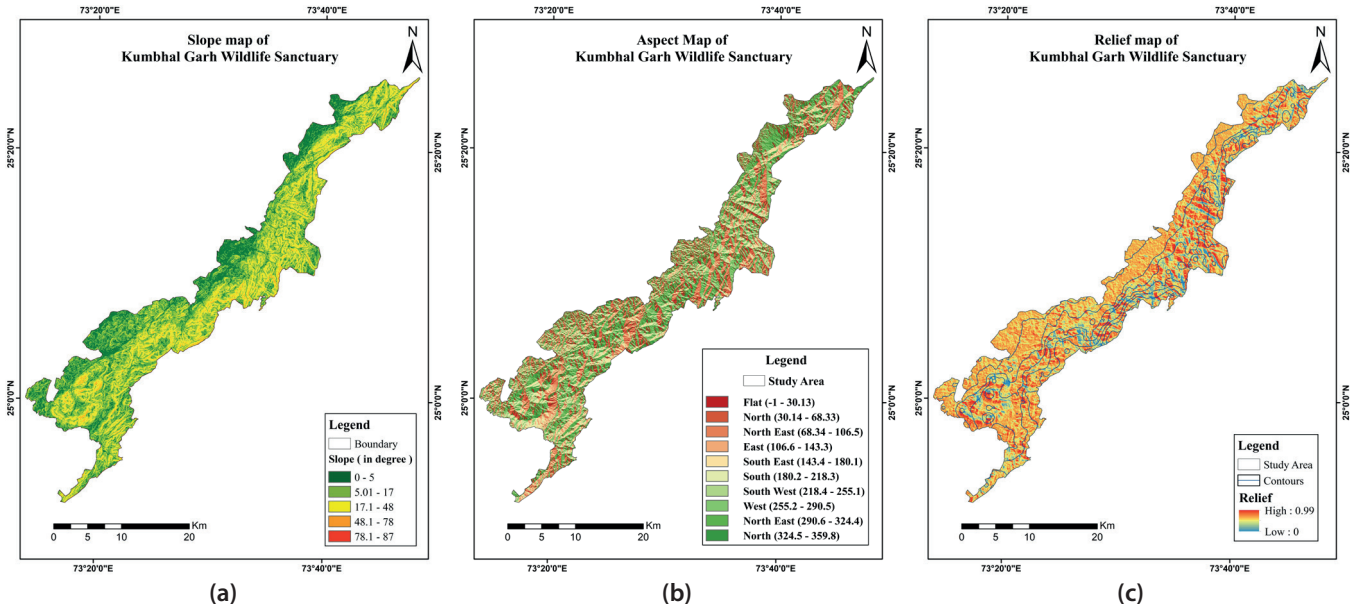

(a) (b) (c)

Fig. 4. Terrain Features a. Slope, b. Aspect & c. Relief Maps

Table 2. land use and land cover area in Hectare

Land use/cover categories	Area, 2000 (Ha)	Area, 2010 (Ha)	Area, 2020 (Ha)
Water Bodies	27.36	157.23	273.69
Fellow Land	19263.15	387.54	1637.64
Barren Land	7455.18	2226.29	5382.26
Arable Land	19737.27	8953.65	17043.66
Sparse Vegetation	9396.90	23427.54	21332.16
Dense Vegetation	1905.30	22613.4	12027.69
Settlement	7.62	27.13	95.68

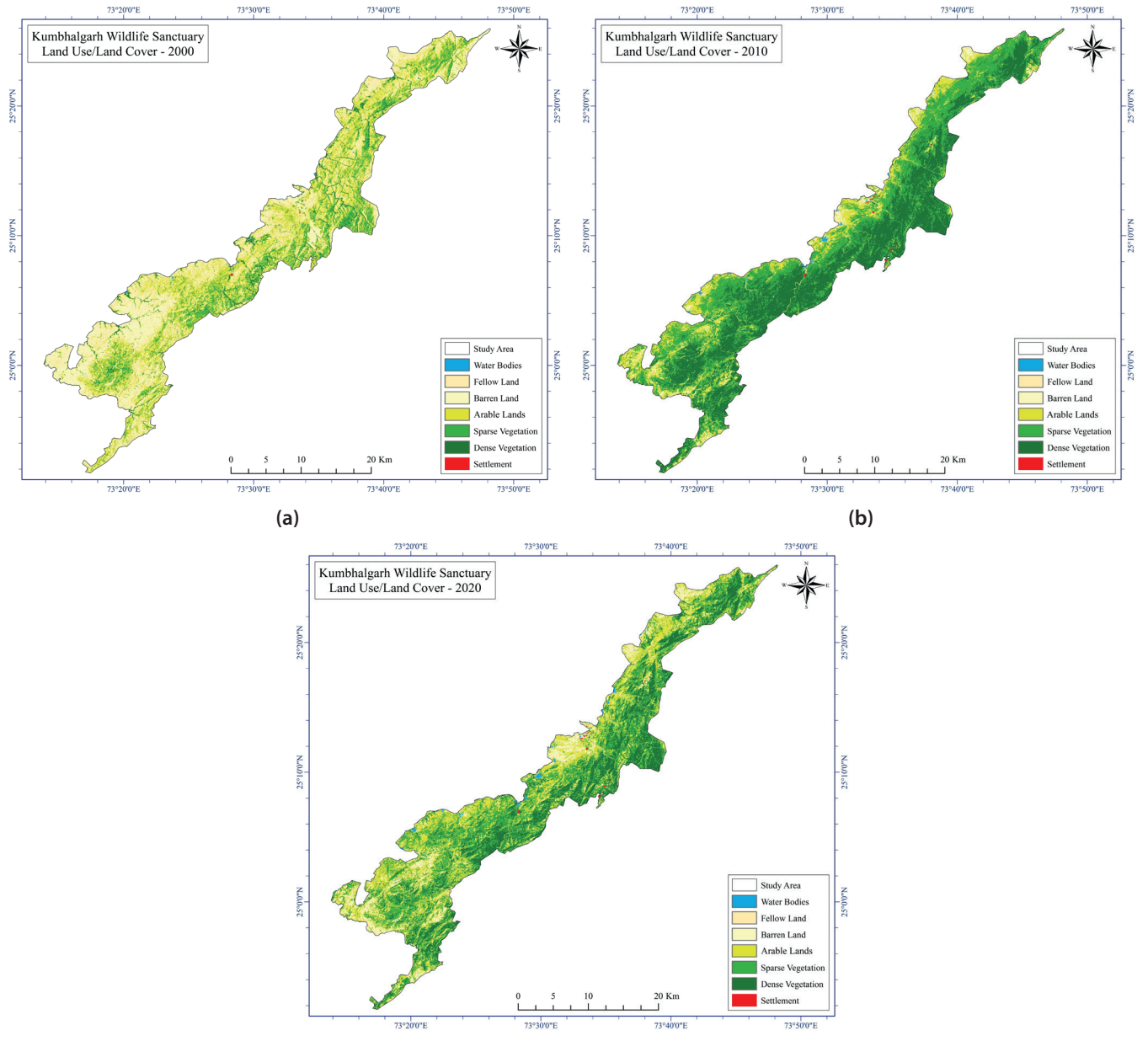

(a) (b)

(c)

Fig. 5. Land Use & Land Cover Maps a. LULC 2000, b. LULC 2010, c. LULC 2020

Land Use Land Cover Change (LULCC) % and Single Land Use Dynamic Degree (SLUDD): From 2000 to 2010, the area of the Water bodies, Settlement, Dense Vegetation, and Sparse Vegetation increased by 474.67%, 255.85%, 1086.87%, and 19.31% respectively. On the other hand, the other three classes have witnessed decreasing pattern in these years (Table 3). From 2010-to 2020 the area of the most classes seen an increase such as Water bodies, Fellow land, Barren land, Arable land, and Built-up land by 74.07%, 322.57%, 141.76%, 90.35%, and 252.67%. On the other hand, Sparse and Dense Vegetation cover decreased by 8.94% and 46.81%. Overall, from 2000-to 2020, most of the lands were witnessed increasing patterns such as Water bodies, Sparse and Dense Vegetation along with Settlement. The increasing percentages were 900.33, 127.01, 531.28, and 1154.98% respectively. Fellow Land, Barren Land, and

Arable land witnessed decreasing patterns during these periods with 91.50%, 27.81% and 13.65% respectively. (Table 3).

From table 3 of Single Land Use Dynamic Degree, we can find out that the water bodies were increased by 45.02% each year from 2000 to 2020. From 2000 to 2020 highly increased LULC classes were built-up land. It increased each year by 57.75% from 2000 to 2020. The Barren lands were decreasing slightly in these years by 1.39%. The annual increasing rate of Sparse and Dense Vegetation is quite impressive with 6.35 and 26.56%. Followed by the Arable land is slightly decreasing by 0.68% annually from 2000 to 2020.

Human and natural interventions can be attributed to these changes. Around the year 2000, a wide area of Rajasthan experienced severe drought, its effect is clearly visible in all the maps of the year 2000. It can be seen in Figure 5A and Table 2 that all the attractive classes with vegetation have very low value and the value of fallow land or barren land is very high. After that till the year 2010, there has been considerable improvement in the vegetation. In this, where water bodies are increasing, the same sparse vegetation and dense vegetation are also increasing (Figure 5b). The main reason for these changes can be attributed to changes in people and strict actions of the government with regard to biodiversity conservation, such as in 2002, the Supreme Court of India, following the advice of its Central Empowered Committee, declared that all the sanctuaries in the country It was decided to impose a complete ban on all types of human uses, the main one being the ban on grazing, harvesting and timber harvesting. But in the year 2020 map 5c, it can be seen that again there has been a negative change in the vegetation cover, the amount of sparse vegetation and dense vegetation has decreased as compared to the year 2010. The main reason for which is also clear from this map and table that how settlement and farming have taken their place. The movement of people again increased a lot, which has to be controlled, otherwise, the decrease in vegetation in the sanctuary will continue to increase.

Accuracy Assessment and Kappa Coefficient: Accuracy assessment of the LU/LC classification results obtained showed an overall accuracy of 84% for 2000, 80.67% for 2010, and 88% for 2020. Kappa coefficients for these imageries were 0.81 for 2000, 0.77 for 2010, and 0.86 for 2020 (Table 4).

Normalized Differential Built-up Index

NDBI method is used to map built-up areas in the study area. All three maps of NDBI are highly comparable to one another. The NDBI value for the Study Area is -0.26 to 0.49 for the year 2000 (Fig. 6a), -0.42 to 0.39 for the year 2010 (Fig. 6b), and -0.34 to 0.13 for the year 2020 (Fig. 6c). In comparison with supervised classification, NDBI enables built-up areas to be mapped at a better degree of accuracy and objectivity. The absence of coaching samples from the mapping makes subjective intervention from the human

Table 3. lland use and land cover area change in % and Single Land Use Dynamic Degree

Sr. No.	Land Use Land Cover	2000 - 2010		2010 - 2020		2000 - 2020	
		LULCC	SLUDD	LULCC	SLUDD	LULCC	SLUDD
1	Water Bodies	474.67	23.73	74.07	3.70	900.33	45.02
2	Fellow Land	-97.99	-4.90	322.57	16.13	-91.50	-4.57
3	Barren Land	-70.14	-3.51	141.76	7.09	-27.81	-1.39
4	Arable Land	-54.64	-2.73	90.35	4.52	-13.65	-0.68
5	Sparse Vegetation	149.31	7.47	-8.94	-0.45	127.01	6.35
6	Dense Vegetation	1086.87	54.34	-46.81	-2.34	531.28	26.56
7	Settlement	255.85	12.79	252.67	12.63	1154.98	57.75

Table 4. Accuracy Assessment Table for year 2000, 2010 & 2020

Years	2000		2010		2020	
LULC	Producer Accuracy	User Accuracy	Producer Accuracy	User Accuracy	Producer Accuracy	User Accuracy
Water Bodies	86.36	90.48	84.21	94.12	90.48	95.00
Fellow Land	88.46	85.19	82.61	90.48	91.30	87.50
Barren Land	82.76	80.00	77.78	72.41	80.95	80.95
Arable Land	86.36	79.17	73.91	68.00	92.00	85.19
Sparse Vegetation	77.27	85.00	80.00	80.00	88.89	88.89
Dense Vegetation	86.36	82.61	85.19	82.14	82.14	85.19
Settlement	71.43	100.00	81.82	90.00	92.86	100.00
Overall Accuracy	**84.00**		**80.67**		**88.00**	
Kappa Coefficient	**0.81**		**0.77**		**0.86**	

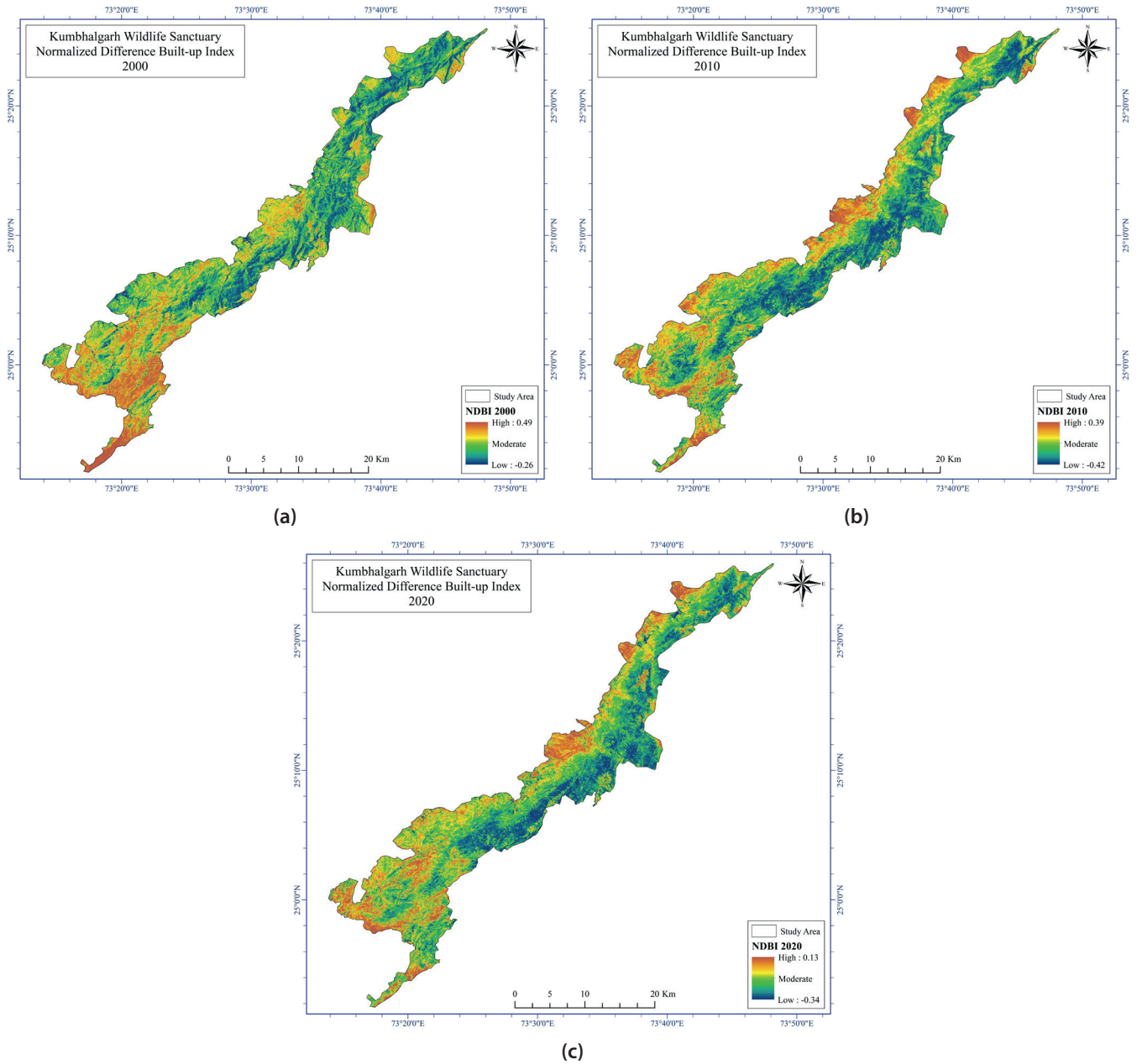

Fig. 6. Normalized Difference Built-up Index Maps a. NDBI 2000, b. NDBI 2010, c. NDBI 2020

analyst redundant. this suggests that identical results are derived no matter the analyst or what percentage of times the mapping is repeated.

Normalized Differential Vegetation Index

For the Study Area, NDVI maps have been used to assess different types of vegetation health and their uses. The NDVI value for the Study Area is -0.22 to 0.52 for the year 2000 (Fig. 7a), -0.11 to 0.71 for the year 2010 (Fig. 7b), and -0.052 to 0.57 for the year 2020 (Fig. 7c). NDVI values are in the middle of 0.2 and 0.4 and linked to areas with bare vegetation, the NDVI value of moderate vegetation inclines to lie between 0.4 and 0.6, and the NDVI value above 0.6 shows the highest possible density of greeneries. There are very small patches of forest that can be found in the year 2000, most areas are full of grass and shrubs. But there are increased values in the year 2010, Whereas in the year 2020, there are some good patches that can be seen in the whole part of the map (Fig. 7).

Therefore, in the period between 2000 and 2020, land cover change in the Kumbhalgarh Wildlife Sanctuary, whether in the direction of increase or decrease in density, is likely to be greater in areas relatively closer to human access. Therefore, some areas of mixed density are likely to be highly exploited during this period, while other areas of similar coverage have little or no impact, progressively moving into higher levels of vegetation density. Humans in Kumbhalgarh seem to be agents of change, but potentially in many directions.

Weighted Overlay Analysis

Weighted Overlay analyses were used to identify the site selection or suitability of the area and to determine the foremost effective place or site related to anthropogenic Impact. The results were categorized into five parts, from Very Low to Very High from the sight of vulnerability (Fig. 8). The sites in the Very High category have the most anthropogenic sites and are vulnerable to animals and human encounters. The very Low, Low & Moderate categories have very rare points for this kind of activity as this area is not at the point of interaction between humans and wildlife.

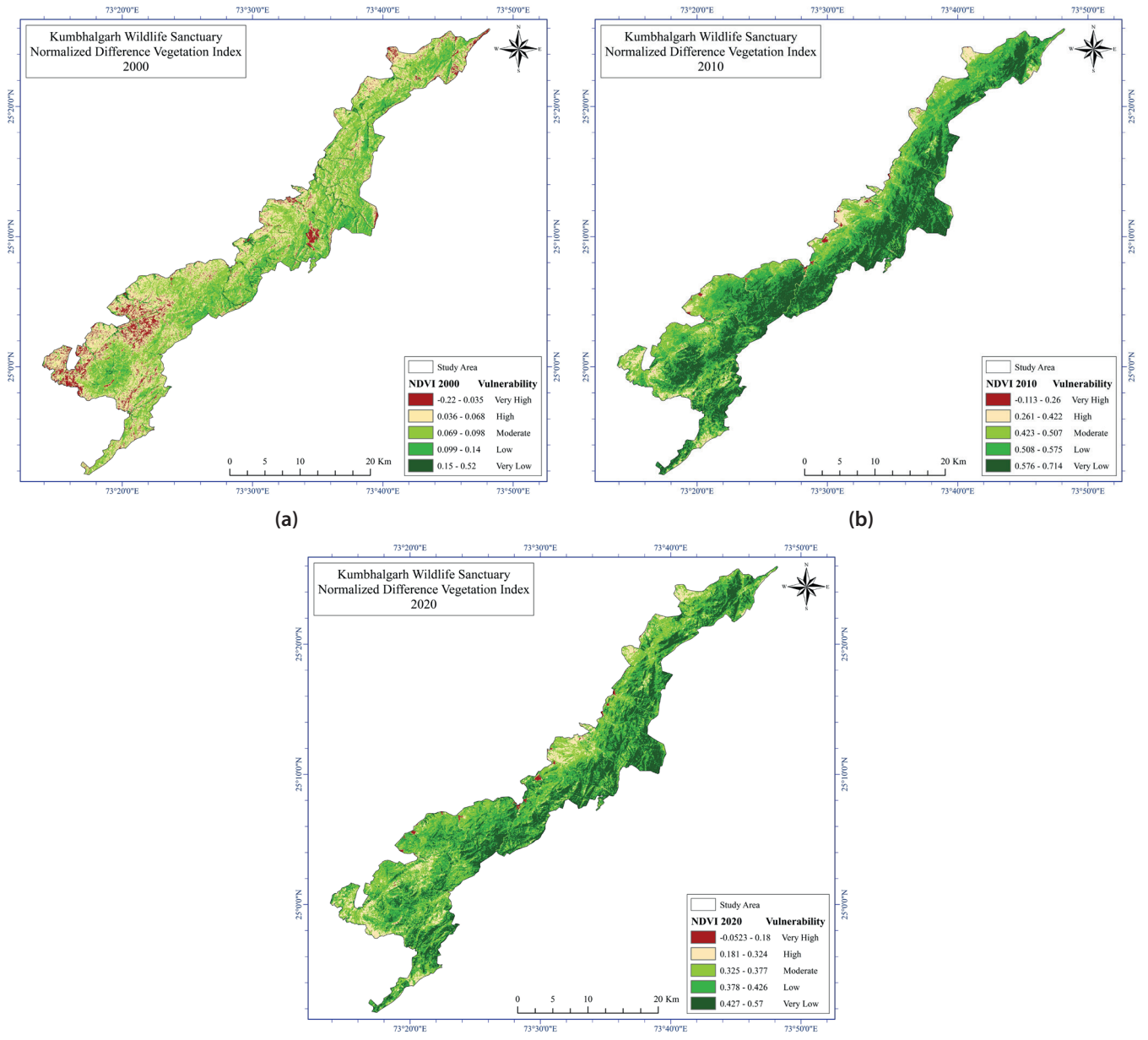

Fig. 7. Normalized Difference Vegetation Index Maps a. NDVI 2000, b. NDVI 2010, c. NDVI 2020

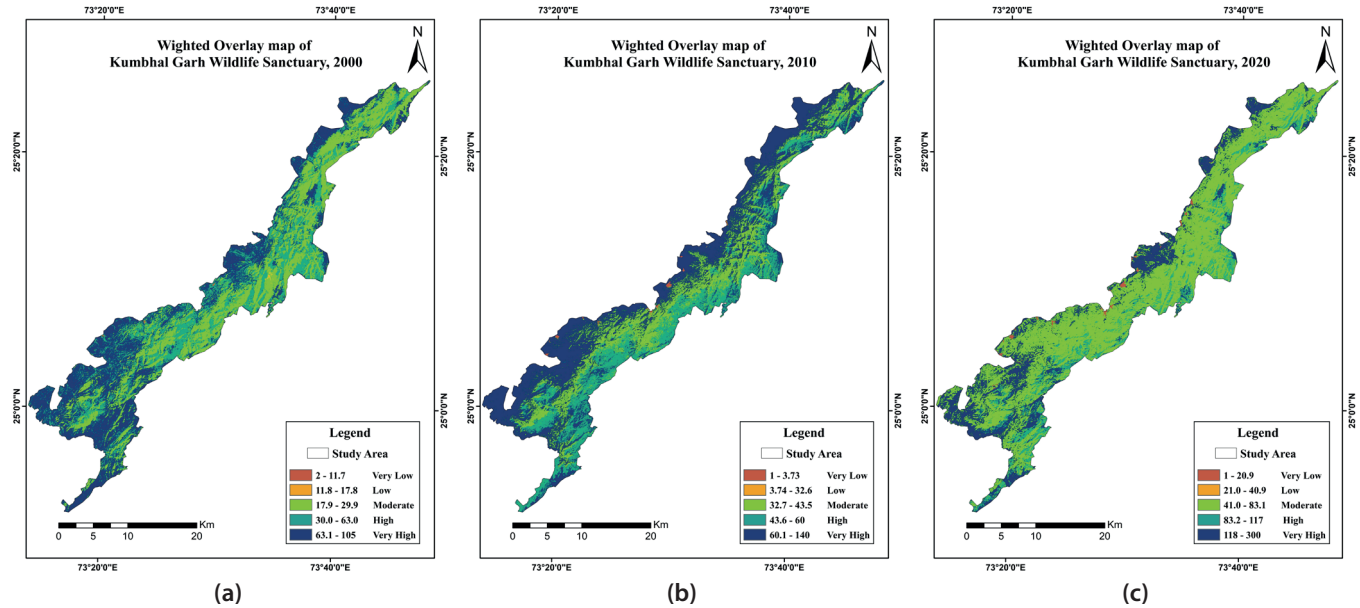

Fig. 8. Weighted Overlay Analysis Maps, the a. year 2000, b. the year 2010, c. the year 2020

DISCUSSIONS

This research study documented the anthropogenic impacts on the forest ecosystem of the Kumbhalgarh Wildlife Sanctuary, India. Anthropogenic pressure has highly negative results in this sanctuary viz. degradation of forest resources, fragmentation, loss of natural habitats, depletion of prey animals, poaching, illegal trade of body parts of wild animals (Hososuma, N. et al. 2005). The results of the research study showed that the lower and southwest part of the study area has maximum vulnerability due to high anthropogenic pressure while the other parts are less vulnerable.

The study results emphasized that a complete and comprehensive approach can minimize the anthropogenic pressure by the use of eco-friendly techniques and increasing the awareness level of local people. The ecosystem services of this sanctuary are constantly decreasing day by day and future generations will get depleted biodiversity resources. And, threats are increasing with climate change and anthropogenic pressure on the forest resources. Therefore, the forest ecosystem degradation shows that in the coming 40 to 50 years' biodiversity and ecosystem services can no longer be treated as endless and free goods. People of the surrounding areas obtained direct and indirect benefits from the forest ecosystem of this wildlife sanctuary which includes different types of services in terms of supporting, provisioning, regulating, and cultural services.As the results indicate that in the year of 2000 A.D. anthropogenic pressure shows a high interrelationship between local people and forest resources because they were dependent on it to fulfill their basic requirements. They expanded their agricultural land, built-up area or residential area, roads, and other physical structures on the forest land through deforestation. Hence the pressure level has been increased in this forest ecosystem of the Kumbhalgarh Wildlife Sanctuary. The map for the year 2020 A.D. clearly shows that the area of maximum anthropogenic pressure has been increased in the form of low vegetation areas which is a negative indicator for forest resources.

CONCLUSION

The Kumbhalgarh Wildlife Sanctuary has a diversity of biodiversity resources which is the source of the development of flora and fauna in the region. With time the trend of people is also changing and they are becoming the most dangerous source of degradation of the forest ecosystem. Research studies have found that anthropogenic impact varies from region to region according to the size of the population of the surrounding areas. The forest ecosystem of this sanctuary and the tribal community are intertwined, so this is a positive factor as well as a negative one. Domestic use of wood for cooking is one of the major factors of deforestation and others are grazing, collection of food and fodder, expansion of agricultural activities, habitat loss, climate change, development of the built-up areas, transportation routes, and poaching of wild animals, etc.

The southern and southwest part of this wildlife sanctuary has a higher density of human population than other areas. Therefore, the anthropogenic impact is also high in this area as compared to other parts of the sanctuary. There is less anthropogenic pressure on the forest ecosystem in the core areas and northern and north-eastern parts of this sanctuary, hence forest resources and wildlife are thriving in these areas. Due to anthropogenic pressure, the forest cover is decreasing day by day and it is a threat to the wildlife. Biodiversity issues suffer from inadequate integration into broad policies and rigorous strategies and programs at the local level and globally.

Protected areas must be designated and effectively managed to protect the ecosystem and hence the organisms that live there. Today, protected areas around the world cover about 15 percent of our land, about 10 percent of coastal and marine areas under national jurisdiction, and 3.4 percent of our oceans. While their effectiveness varies from country to country, it is important to continue efforts to advance protected areas. The study is a testimony to the need for comprehensive interventions to holistically tackle environmental problems caused by anthropogenic pressure in this sanctuary. This research study relied on satellite imagery data, LULC, NDBI, NDVI, etc., and statistical data collected by the Census and Forest Department, which may slightly limit this result, for extensive research, on other factors of deforestation. Like climate and soil also have to be used. This will make research more efficient.

REFERENCES

Akpan G.P., Bashar A.K., & Zamare U.S. (2012). An Overview of the Impact of Man-Environment Relationship on Human Health in Nigeria. Int. J. Geography and Environmental Management, 1(8), 1-8.

Asner G.P., Powell G.V., Mascaro J., Knapp D.E., Clark J.K., Jacobson J., ... & Hughes R.F. (2010). High-resolution forest carbon stocks and emissions in the Amazon. Proceedings of the National Academy of Sciences, 107(38), 16738-16742.

Benz J.P., Chen S., Dang S., Dieter M., Labelle E.R., Liu, G., ... & Fischer A. (2020). Multifunctionality of forests: A white paper on challenges and opportunities in China and Germany. Forests, 11(3), 266.

Bhagabati N.K., Ricketts T., Sulistyawan T.B.S., Conte M., Ennaanay D., Hadian O., ... & Wolny S. (2014). Ecosystem services reinforce Sumatran tiger conservation in land use plans. Biological Conservation, 169, 147-156.

Bhuyan P., Khan M.L., & Tripathi R.S. (2003). Tree diversity and population structure in undisturbed and human-impacted stands of tropical wet evergreen forest in Arunachal Pradesh, Eastern Himalayas, India. Biodiversity & Conservation, 12(8), 1753-1773.

Blignaut J., & Moolman C. (2006). Quantifying the potential of restored natural capital to alleviate poverty and help conserve nature: a case study from South Africa. Journal for Nature Conservation, 14(3-4), 237-248.

Bohra P.A.D.M.A., & Sultana R.A.Z.I.A. (2013). Plant and soil nematodes. Zoological Survey of India, Kumbhalgarh Wildlife Sanctuary, Conservation Area Series, 7-29.

BOHRA P. (2013). KUMBHALGARH WILDLIFE SANCTUARY: AN OVERVIEW. Faunal Exploration of Kumbhalgarh Wildlife Sanctuary Rajasthan, 1.

Carpenter S.R., DeFries R., Dietz T., Mooney H.A., Polasky S., Reid W.V., & Scholes R.J. (2006). Millennium ecosystem assessment: research needs. Science, 314(5797), 257-258.

Chételat J., Kalbermatten M., Lannas K.S., Spiegelberger T., Wettstein J.B., Gillet F., ... & Buttler A. (2013). A contextual analysis of land-use and vegetation changes in two wooded pastures in the Swiss Jura Mountains. Ecology and Society, 18(1).

Chhangani A.K. (2002). AVIFAUNA OF KUMBHALGARH WILDLIFE SANCTUARY. Zoos print journal, 17(4), 764-768.

Clark J.A., & Covey K.R. (2012). Tree species richness and the logging of natural forests: A meta-analysis. Forest Ecology and Management, 276, 146-153.

Corvalan C., Hales S., & McMichael A core writing team (2005). Ecosystems and Human Well-being: Health Synthesis (A Report to the Millennium Ecosystem Assessment) WHO Press; Geneva, Switzerland, 53.

De Groot R., Brander L., Van Der Ploeg S., Costanza R., Bernard F., Braat L., ... & van Beukering P. (2012). Global estimates of the value of ecosystems and their services in monetary units. Ecosystem services, 1(1), 50-61.

Fagua J.C., Baggio J.A., & Ramsey R.D. (2019). Drivers of forest cover changes in the Chocó-Darien Global Ecoregion of South America. Ecosphere, 10(3), e02648.

FAO, Global Forest Resources Assessment. Terms and Definitions FRA 2020; Working Paper Series; Food and Agriculture Organization of the United Nations: Rome, Italy, 2020, 1-26.

FES final report (2010). Assessment of Biodiversity in Kumbhalgarh Wildlife Sanctuary: A Conservation Perspective. (Foundation for Ecological Security P.B. No. 29, Jahagirpura, P.O. Gopalpura, Vadod 388 370, Anand, Gujarat).

Foley J.A., Asner G.P., Costa M.H., Coe M.T., DeFries R., Gibbs H.K., ... & Snyder P. (2007). Amazonia revealed: forest degradation and loss of ecosystem goods and services in the Amazon Basin. Frontiers in Ecology and the Environment, 5(1), 25-32.

Garbarino M., Lingua E., Weisberg P.J., et al. (2013). Land-use history and topographic gradients as driving factors of subalpine Larix decidua forests. Landscape Ecology. 28:805–817, DOI: 10.1007/s10980-012-9792-6.

He G.M., Chen X.D., Bearer S., et al. (2009). Spatial and temporal patterns of fuelwood collection in Wolong Nature Reserve: Implications for panda conservation. Landscape and Urban Planning.92:1–9, DOI: 10.1016/j.landurbplan.2009.01.010.

Hölting L., Beckmann M., Volk M., Cord A. (2019). Multifunctionality assessments—More than assessing multiple ecosystem functions and services? A quantitative literature review. Ecol. Indic., 103, 226-235.

Hong-zhi W.A.N.G., Ren-Dong L.I., & He-Hai W.U. (2002). Bilateral change dynamic degree model for land use and its application to the land use study of in suburban areas of Wuhan. Remote Sensing for Land & Resources, 14(2), 20-22.

Hososuma N., Herold M., De-Sy V., De-Fries R., Brockhaus M., Verchot L., Angelsen A., & Romijn E (2012). An assessment of deforestation and forest degradation drivers in developing countries. Environ. Res. Lett., 7, 1-12.

Houghton R.A. (2012). Carbon emissions and the drivers of deforestation and forest degradation in the tropics. Current Opinion in Environmental Sustainability, 4(6), 597-603.

Kissinger G.M., Herold M., & De Sy V. (2012). Drivers of deforestation and forest degradation: a synthesis report for REDD+ policymakers. Lexeme Consulting.

Kumar R., & Shahabuddin G. (2005). Effects of biomass extraction onvegetation structure, diversity and composition of forests in Sariska Tiger Reserve, India. Environmental Conservation, 32:248–259, DOI: 10.1017/S0376892905002316.

Kumbhalgarh Wildlife Sanctuary - RajRAS. (2019). Retrieved 22 July 2022, from https://www.rajras.in/kumbhalgarh-wildlife-sanctuary/#:~:text=The%20area%20was%20a%20natural,the%20good%20density%20of%20leopards.

Manning, P.; van-der-Plas, F.; Soliveres, S.; Allan, E.; Maestre, F.; Mace, G.; Whittingham, M.; & Fischer, M (2018). Redefining ecosystem multifunctionality. Nat. Ecol. Evol., 2, 427–436.

McMichael A.J. (2013). Globalization, climate change and human health. New England Journal of Medicine, 368, 1335-1343, DOI: 10.1056/NEJMra1109341.

Millennium Ecosystem Assessment (MA) (2005). Ecosystems and Human Well- Being: Synthesis. Island Press, Washington DC.

Pan Y., Zhen L., Yang L., et al. (2012). Ecological consequences of changing fuelwood consumption patterns in remote villages of Northwestern China. [9 September 2013]; Applied Ecology and Environmental Research. 10, 207-222.

Ravindranath N.H., & Ostwald M. (2007). Carbon inventory methods: handbook for greenhouse gas inventory, carbon mitigation and roundwood production projects (Vol. 29). Springer Science & Business Media.

Sagar R., & Singh J.S. (2006). Tree density, basal area and species diversity in a disturbed dry tropical forest of northern India: Implications for conservation. Environmental Conservation. 33:256–262, DOI: 10.1017/S0376892906003237.

Salerno F, Viviano G, Thakuri S, et al. (2010). Energy, forest, and indoor air pollution models for Sagarmatha National Park and buffer zone, Nepal. Mountain Research and Development. 30(2), 113-116.

Sharma C.M., Gairola S., Ghildiyal S.K., et al. (2009). Forest resource use patterns in relation to socioeconomic status: A case study in four temperate villages of Garhwal Himalaya, India. Mountain Research and Development. 29, 308-319, DOI: 10.1659/mrd.00018.

Sierra R. & Patrones Y. (2013). Factores De Deforestación En El Ecuador Continental, 1990–2010. Y un Acercamiento a Los Próximos 10 Años. Conservación Internacional Ecuador Y Forest Trends; GeoIS: Quito, Ecuador, 1-57.

Singh B.V.R., Sen A., Verma L.M., Mishra R., & Kumar V. (2021). Assessment of potential and limitation of Jhamarkotra area: A perspective of geoheritage, geo park and geotourism. International Journal of Geoheritage and Parks, 9(2), 157-171.

Singh B.V.R., Sen A. (2018). Geo-Spatial Mapping of Land Use and Land Cover Changes in the Core and Periphery Area of Ranthambore Tiger Reserve, Rajasthan, India, 1975–2015. Annals of Valahia University of Targoviste, Geographical Series, 18(1), 62-67.

Swanson M.E., Franklin J.F., Beschta R.L., et al. (2011). The forgotten stage of forest succession: early-successional ecosystems on forest sites. Frontiers in Ecology and the Environment. 9, 117-125, DOI: 10.1890/090157.

TEEB Foundations (2010). In: Kumar P. (Ed.), The Economics of Ecosystems and Biodiversity: Ecological and Economic Foundations. Earthscan, London, Washington.

TEEB in Policy (2011). In: ten Brink., P. (Ed.), The Economics of Ecosystems and Biodiversity in National and International Policy Making. Earthscan, London, Washington.

TEEB Synthesis (2010). Mainstreaming the Economics of Nature: A Synthesis of the Approach Conclusions and Recommendations of TEEB. Earthscan, London, Washington.

Thomas J.W., Franklin J.F., Gordon J., et al. (2006). The Northwest Forest plan: origins, components, implementation experience, and suggestions for change. Conservation Biology. 20, 277-287, DOI: 10.1111/j.1523-1739.2006.00385. x.

United Nation Environment Programme (UNEP) Annual Report, (2014). Publication: UNEP 2014 Annual Report ISBN: 978-92-807-3442-3 Job Number: DCP/1884/NA

Wasserstrom, R.; & Southgate, D. (2013). Deforestation, Agrarian Reform and Oil Development in Ecuador, 1964–1994. Nat. Resour. 4, 31-44.

Wildlife Protection Act, 1972 - Salient Features, Provisions & Issues for UPSC Exam. (2022). Retrieved 22 July 2022, from https://byjus.com/free-ias-prep/wildlife-protection-act-1972/#:~:text=The%20Act%20prohibited%20the%20hunting,sanctuaries%2C%20national%20parks%2C%20etc.

ges.rgo.ru/jour/

ISSN 2542-1565 (Online)